

Characterization of *PRL1* and
its paralogue *PRL2* in
Arabidopsis thaliana

Inaugural-Dissertation
zur Erlangung des Doktorgrades
der Mathematisch-Naturwissenschaftlichen Fakultät
der Universität zu Köln



vorgelegt von
Nicolas F. Villacorta
aus Oviedo, Spanien

Köln, 2011

Berichterstatter: Prof. Dr. George Coupland
Prof. Dr. Wolfgang Werr

Tag der Disputation: 8. Juni 2010

Die vorliegende Arbeit wurde am Max-Planck-Institut für Pflanzenzüchtungsforschung (MPIPZ) in Köln in der Abteilung Entwicklungsbiologie der Pflanzen (Direktor: Prof. Dr. George Coupland) in der Arbeitsgruppe von Dr. Csaba Koncz angefertigt. Diese Arbeit wurde teilweise durch das sechste Forschungsrahmenprogramm (FP6) der Europäischen Kommission finanziert. Außerdem erhielt Nicolas F. Villacorta als Mitglied des *ADONIS* Early Stage Research Training-Netzwerkes (MEST-CT-2005-020232) einen Vertrag im Rahmen der Marie-Curie-Maßnahmen.



MAX-PLANCK-GESELLSCHAFT

Imagination will often carry us to worlds that never were. But without it we go nowhere.

Carl Sagan (*Cosmos*, 1980)

Zusammenfassung

Das *Arabidopsis*-Gen *PLEIOTROPIC REGULATORY LOCUS 1 (PRL1)* kodiert für ein Protein, das ein Mitglied einer konservierten WDR-Protein-Familie in Eukaryoten ist. *PRL1*-Mutationen führen zu Zucker-Überempfindlichkeit, verursachen zahlreiche pleiotrope Veränderungen bei der Wurzel-, Blatt- und Blütenentwicklung und lösen Antworten auf abiotische und biotische Stress-Reize aus, indem sie die Pflanzenhormon-Homöostase verändern.

Im Gegensatz zu anderen Eukaryoten enthält das *Arabidopsis*-Genom mit *PRL2* ein *PRL1*-Paralog, das mit *PRL1* eine hochkonservierte C-terminale WDR-Domäne teilt. Verglichen mit *PRL1* besitzt *PRL2* jedoch unterschiedliche N-terminale Sequenzen. Nichtsdestotrotz weisen die N-terminalen Bereiche von *PRL1* und *PRL2* eine für die Evolution im Pflanzenreich außergewöhnlich hochkonservierte Struktur auf. Untersuchungen an Hefen und Säugetieren zeigten, dass *PRL1* eine Schlüsselrolle bei der Aktivierung des Spliceosoms spielt. Dennoch impliziert die Divergenz der N-terminalen *PRL1*-Region in *Arabidopsis* pflanzenspezifische Funktionen beim Spleißen.

Ein Ziel dieser Arbeit war es, Einblicke in regulatorische Funktionen von *PRL1* zu ermöglichen. Affymetrix ATH1-Arrays und Tiling-Arrays bestätigten zusammen mit der RNA-Seq-Analyse die im gesamten Genom vorhandenen Veränderungen der *prl1* Mutante. Darüber hinaus legt die Hochregulierung der Transposons zusammen mit der Hochregulierung von vielen weiteren Genen nahe, dass *PRL1* ebenfalls an der Kontrolle des Gen-Silencing beteiligt ist. Zudem konnte durch die Verwendung von veränderten *PRL1*-Konstrukten gezeigt werden, dass *PRL1*-Transkription und *PRL1*-Stabilität stressabhängig sind und dass *PRL1* nicht in die Proteasom-Aktivität eingreift. Ein weiteres Ziel war, das Ausmaß der funktionellen Übereinstimmung von *PRL1* und *PRL2* zu beurteilen. Ein Transkriptionsvergleich von *PRL1* und *PRL2* ergab, dass *PRL2* in den meisten Gewebeteilen auf einem signifikant niedrigeren Niveau transkribiert wird. So wird *PRL2* in Blüten speziell im männlichen Reproduktionsgewebe, in Pollenkörnern, im Endosperm und in der Zygote exprimiert, wohingegen *PRL1* in sich entwickelnden Samenanlagen und im Integument der sich entwickelnden Samen aktiv ist. Die *prl2*-Mutationen sind embryoletal, während somatische *prl2*-Mosaikere einen *prl1*-ähnlichen Phänotyp zeigen.

Durch den Austausch der unterschiedlichen N-terminalen Domänen zwischen *PRL1* und *PRL2* konnte die Subfunktionalisation von *PRL1* und *PRL2* gezeigt werden. Die N-terminale Domäne von *PRL2* komplementiert den *prl1*-Wurzelpheänotyp nur teilweise. Sie kann jedoch die von *prl2* verursachte embryonale Letalität wiederherstellen. Zudem ersetzt die N-terminale *PRL1*-Domäne zusammen mit der C-terminalen *PRL2*-Domäne den *prl1*-Phänotyp, aber nicht den embryoletalen *prl2*-Phänotyp. Zusätzlich zu der unterschiedlichen Transkription, die man bei *PRL1* und *PRL2* beobachtet, hat die Diversifikation der N-terminalen Domänen zu der Subfunktionalisation von *PRL1* und *PRL2* in *Arabidopsis* beigetragen. Die in dieser Arbeit vorgelegten Ergebnisse weisen zudem darauf hin, dass *PRL1* und *PRL2* eine spezielle Funktion bei der Kontrolle des Gen-Silencing in *Arabidopsis* spielen.

Abstract

The *Arabidopsis* gene *PLEIOTROPIC REGULATORY LOCUS 1 (PRL1)* encodes a protein that has been identified as a member of a conserved WDR protein family in eukaryotes. Mutations of *PRL1* result in hypersensitivity to sugars, cause a wide range of pleiotropic alterations in root, leaf and flower development and activate responses to abiotic and biotic stress stimuli by modifying the plant hormone homeostasis.

In contrast to other eukaryotes, the genome of *Arabidopsis* encodes a *PRL1* paralogue, *PRL2*, which shares a highly conserved C-terminal WDR domain with *PRL1*. However, *PRL2* carries divergent N-terminal sequences when compared to *PRL1*. Nevertheless, the N-terminal domains of *PRL1* and *PRL2* show an exclusive evolutionary conservation in the plant kingdom. Studies in yeast and mammals revealed that *PRL1* plays a pivotal role in spliceosome activation. However, the divergence of the *PRL1* N-terminal region in *Arabidopsis* implies plant-specific functions in splicing.

One aim of this work was to provide insights into the regulatory functions of *PRL1*. Affymetrix ATH1 arrays and Tiling arrays, together with RNA-Seq analysis, confirmed genome-wide alterations of the *prl1* mutant. Moreover, the up-regulation of transposable elements, together with the up-regulation of other genes suggests that *PRL1* is involved in the control of gene silencing. Furthermore, it was shown by using modified *PRL1* constructs that *PRL1* transcription and *PRL1* stability are stress-dependent and that *PRL1* does not interfere with the proteasome activity. Another aim was to assess the degree of functional complementarity of *PRL1* and *PRL2*. Therefore, the *PRL2* transcription was compared to the one of *PRL1*, showing that *PRL2* is transcribed in most organs at a significant lower level. In flowers, *PRL2* is expressed specifically in male reproductive tissues, pollen grains, endosperm and the zygote, whereas *PRL1* is active in developing ovules and in the integuments of developing seeds. The *prl2* mutations cause embryo lethality, whereas somatic *prl2* mosaics show a *prl1*-like phenotype.

PRL1 and *PRL2* sub-functionalization was revealed by the replacement of the divergent N-terminal domains of *PRL1* with *PRL2*. The N-terminal domain of *PRL2* rescues the root phenotype of *prl1* only partially. However, it complements the embryonic lethality caused by *prl2*. Moreover, the N-terminal domain of *PRL1* in combination with the C-terminal domain of *PRL2* complements the phenotype of *prl1*, but not the embryo lethal phenotype of *prl2*. In addition to the different expression observed for *PRL1* and *PRL2*, the diversification of the N-terminal domains has contributed to the sub-functionalization of *PRL1* and *PRL2* in *Arabidopsis*. The results presented in this work also suggest that *PRL1* and *PRL2* perform a specific function in the control of gene silencing in *Arabidopsis*.

Contents

Zusammenfassung	vii
Abstract	ix
Abbreviations	xxi
1 Introduction	1
1.1 PRL1	2
1.1.1 <i>Arabidopsis prl1</i> mutant	2
1.1.2 Orthologues of <i>PRL1</i>	2
1.1.3 Function and conservation	4
1.2 Splicing	4
1.2.1 The Prp19-associated complex	5
1.2.2 Alternative splicing	7
1.2.3 Co-transcriptional splicing	7
1.3 The proteasome	7
1.3.1 Ubiquitin signalling	8
1.4 Gene duplication in evolution	9
1.4.1 Homology of sequences	9
1.4.2 Mechanisms of gene duplication	9
1.4.3 Functional connotations	10
1.5 Stress situations in plants	10
1.5.1 Energy homeostasis	10
1.5.2 Reactive Oxygen Species	11
1.5.3 Pathogen response	11

1.5.4	Programmed cell death	12
1.5.5	Genotoxic stress	12
1.6	DNA repair in plants	12
1.6.1	DNA damage	12
1.6.2	Repair mechanisms	13
1.7	Transposable elements in plants	13
1.7.1	Classification	14
1.7.2	Life cycle of LTR retro-transposons	15
1.7.3	Retro-transposons in the context of a host genome	15
1.8	Mechanisms of gene silencing in plants	16
1.8.1	Pre-transcriptional control	16
1.8.2	Post-transcriptional control	16
1.9	Development of reproductive structures in plants	17
1.9.1	Flower development in <i>Arabidopsis</i>	17
1.9.2	Gametophyte development	17
1.10	Genetic exchange in <i>Arabidopsis</i>	19
1.10.1	From pollination to fertilization	19
1.10.2	Double fertilization	20
1.11	Early development of the sporophyte	20
1.11.1	Processes in zygote formation	20
1.11.2	Pattern formation in the <i>Arabidopsis</i> embryo	21
1.11.3	Endosperm role	21
1.11.4	Genomic imprinting	22
1.11.5	Reproductive interplay in seed development	23
1.12	New technologies in gene expression profiling	23
1.12.1	Microarrays	23
1.12.2	Next generation sequencing	24
1.12.3	Data analysis development	25
1.13	Aims of this work	26

2 Results	27
2.1 Characterization of <i>PRL1</i> functions	27
2.1.1 <i>PRL1-PIPL</i> complements the <i>prl1</i> phenotype	27
2.1.2 <i>PRL1</i> transcription is sucrose-independent	29
2.1.3 <i>PRL1</i> accumulation is sucrose-dependent	30
2.1.4 <i>PRL1</i> depletion does not affect the proteasome catalytic activity	31
2.1.5 <i>PRL1</i> is highly conserved in the kingdom plantæ	33
2.1.6 Isolated <i>PRL1</i> domains fail to complement <i>prl1</i>	33
2.2 Studies of <i>PRL1</i> target regulation by transcript profiling	37
2.2.1 Tiling arrays show a genome-wide transcription alteration in <i>prl1</i>	37
2.2.2 RNA-Seq analysis also reveals multiple transcriptional changes	42
2.2.3 Tiling and RNA-Seq results have small overlap	42
2.2.4 ATH1 arrays reveal multiple changes during <i>PRL1</i> depletion	43
2.2.5 QPCR partially validates the transcript profiling data of <i>prl1</i>	52
2.3 RNA-Seq analyses	54
2.3.1 Only Open Source tools allow flexible analyses	54
2.3.2 Data pre-processing	54
2.3.3 Mapping suggests an over-representation of exon sequences in <i>prl1</i>	54
2.3.4 Transcription of transposable elements is altered in <i>prl1</i>	55
2.4 Characterization of <i>PRL2</i>	56
2.4.1 The <i>prl2</i> T-DNA mutant has an atypical segregation	56
2.4.2 The <i>prl2</i> mutation results in embryo lethality	56
2.4.3 The <i>prl1</i> × <i>prl2</i> /+ mutant shows a more severe phenotype	56
2.4.4 <i>PRL2</i> transcription differs from <i>PRL1</i>	58
2.4.5 <i>PRL2</i> is localized in nuclei and translated in reproductive organs	58
2.4.6 Conditional genetic mosaics of <i>prl2</i> reveal defects in reproductive organs	61
2.4.7 Ectopic over-expression of <i>PRL1</i> complements <i>prl2</i> and vice versa	68
2.4.8 Chimeric <i>PRL1-PRL2</i> proteins complement both <i>prl1</i> and <i>prl2</i>	72

3	Discussion	75
3.1	Transcriptional regulatory effects of <i>prl1</i>	75
3.1.1	PRL1 function has a direct impact in gene regulation	75
3.1.2	RNA-Seq is a powerful tool for revealing alternative splicing	82
3.1.3	Tiling arrays and RNA-Seq analyses provide different resolution	83
3.1.4	Transposable element loci show differential expression in <i>prl1</i>	84
3.2	Characterization of PRL1 functions	85
3.2.1	<i>PRL1-PIPL</i> is expressed in native conditions	85
3.2.2	<i>PRL1</i> transcription and PRL1 accumulation are sucrose-dependent	85
3.2.3	PRL1 does not affect the proteasome catalytic activity	87
3.2.4	PRL1 could be involved in gene silencing	88
3.3	Functional comparison of PRL2 with PRL1	88
3.3.1	Ectopic expression of <i>PRL1</i> or <i>PRL2</i> complement mutual phenotypes	88
3.3.2	PRL1 and PRL2 are required in the nucleus	89
3.3.3	However, mutant phenotypes differ due to gene sub-functionalization	90
3.3.4	Induced <i>prl2</i> somatic phenotype is similar to <i>prl1</i>	90
3.3.5	<i>prl1</i> × <i>prl2</i> /+ suggests asymmetrical and functional redundancy	91
3.3.6	Differential expression during development reflects sub-functionalization	91
3.3.7	Embryo lethality of <i>prl2</i> could be linked to gene silencing	91
3.4	Final conclusions	93
4	Experimental	95
4.1	Materials	95
4.1.1	Plant material	95
4.1.2	Bacterial strains	95
4.1.3	General consumables	96
4.1.4	Plasmid vectors and constructs	99
4.1.5	Oligonucleotides	100
4.1.6	Enzymes	100
4.1.7	Antibodies	101
4.1.8	Culture media	101

4.1.9	Antibiotics	104
4.1.10	Hormones	104
4.1.11	Microarrays	104
4.1.12	Computational resources	105
4.2	Methods	106
4.2.1	Plant methods	106
4.2.2	DNA handling methods	108
4.2.3	General cloning techniques	112
4.2.4	Gateway [®] cloning	114
4.2.5	Transformation of bacteria and <i>Arabidopsis</i>	115
4.2.6	Construction of binary vectors for transformation	116
4.2.7	RNA methods	121
4.2.8	RNA-Seq methods	123
4.2.9	Microarray methods	127
4.2.10	Protein analytical methods	128
4.2.11	Imaging methods	132
4.2.12	<i>In silico</i> methods	133
Appendices		137
A Sequences		139
A.1	Insertional mutants	139
A.2	Aligned sequences	140
A.3	Oligonucleotides	151
B Scripts for microarray analysis		155
C Transcript profiling tables		159
Bibliography		273
Agradecimientos		297
Lebenslauf		303

List of Figures

1.1	Pleiotropic phenotype of <i>prl1</i>	3
1.2	Schematic overview of the splicing process	5
1.3	Schematic overview of the proteasome structure	8
1.4	Classification of transposable elements	14
1.5	Schematic overview of micro-sporogenesis	18
1.6	Schematic overview of the mega-gametophyte	19
1.7	Schematic overview of <i>Arabidopsis</i> embryo patterning	21
2.1	Confirmation of PRL1-PIPL translation in cell suspensions	28
2.2	<i>PRL1-PIPL</i> expression in <i>planta</i> during the day	29
2.3	Accumulation of PRL1-PIPL in <i>planta</i> during the day	30
2.4	Schematic overview of the ER-PRL1/ <i>prl1</i> system	31
2.5	Activity-based profiling of the proteasome	32
2.6	Alignment of N-terminal region of PRL1 orthologues	34
2.7	Phenotype of PRL1-N-HA/ <i>prl1</i> line #3-1 compared to WT and <i>prl1</i>	35
2.8	Phenotype of PRL1-C-HA/ <i>prl1</i> line #6-11 compared to WT and <i>prl1</i>	36
2.9	Venn diagrams of tiling analyses	38
2.10	Venn diagrams comparing RNA-Seq and tiling analyses	43
2.11	Validation of ER-PRL1/ <i>prl1</i> samples from the time-course experiment	44
2.12	Genes with altered expression of ER-PRL1/ <i>prl1</i> samples during the time-course	45
2.13	Clusters of the time-course experiment	50
2.14	Phenotype of <i>prl2/+</i>	57
2.15	<i>prl1</i> × <i>prl2/+</i> double mutant phenotype	59
2.16	Transcription of <i>PRL2</i> compared to <i>PRL1</i> in different organs	60

2.17	Subcellular localization of over-expressed PRL2 fused to YFP	60
2.18	Comparison of <i>PRL1::GUS</i> and <i>PRL2::GUS</i> in young seedlings	62
2.19	Comparison of <i>PRL1::GUS</i> and <i>PRL2::GUS</i> during flower development	63
2.20	Comparison of <i>PRL1::GUS</i> and <i>PRL2::GUS</i> during ovule and embryo development	64
2.21	Localization of GFP in PRL2-HS/ <i>prl2</i>	66
2.22	PRL2-HS/ <i>prl2</i> genetic mosaic plants	67
2.23	<i>prl1</i> flower phenotype in SD	68
2.24	<i>prl2</i> -induced phenotype of stems in PRL2-HS/ <i>prl2</i> plants	68
2.25	Phenotype of PRL1-HA/ <i>prl1</i> line #10-8 compared to WT and <i>prl1</i>	69
2.26	Phenotype of PRL2-HA/ <i>prl1</i> line #2-9 compared to WT and <i>prl1</i>	70
2.27	<i>PRL2</i> cDNA over-expression in <i>prl2</i> plants	71
2.28	<i>PRL1</i> cDNA over-expression in <i>prl2</i> plants	71
2.29	Phenotype of pPAMpat-1N2C-HA line #7-3 compared to WT and <i>prl1</i>	73
2.30	Phenotype of pPAMpat-2N1C-HA line #8-8 compared to WT and <i>prl1</i>	74
2.31	<i>2N1C-HA</i> cDNA over-expression in <i>prl2</i> plants	74
4.1	Schematic structure of the pPCV002-PRL1-PIPL construct	117
4.2	Schematic structure of over-expression and chimeric constructs for <i>PRL1</i> and <i>PRL2</i>	118
4.3	Partial nucleotide alignment of <i>PRL1</i> and <i>PRL2</i> CDSs	119
4.4	Schematic structure of pPCV812-PRL2::GUS	120
4.5	Schematic structure of pCB1-PRL2::PRL2gDNA in <i>HS-CRE</i> background	121
4.6	Chemical structure of MVB072	132
A.1	Insertional mutants of <i>PRL1</i> used in this work	139
A.2	Insertional mutants of <i>PRL2</i> used in this work	139
A.3	Nucleotide alignment of <i>PRL1</i> and <i>PRL2</i> gDNAs	140
A.4	Complete nucleotide alignment of <i>PRL1</i> and <i>PRL2</i> CDSs	141
A.5	Complete amino acid alignment of <i>PRL1</i> and <i>PRL2</i>	144
A.6	Alignment of <i>PRL1</i> orthologues with yeast and hominidæ	146
A.7	Alignment of <i>PRL1</i> orthologues from plants and algae	147

List of Tables

2.1	Up-regulated pathways in <i>prl1</i>	39
2.2	Down-regulated pathways in <i>prl1</i>	40
2.3	Genes from up-regulated pathways in <i>prl1</i>	41
2.4	Genes from down-regulated pathways in <i>prl1</i>	41
2.5	<i>PRL1</i> transcription in the time-course experiment of ER- <i>PRL1/prl1</i>	46
2.6	Enriched GO terms for genes co-regulated with <i>PRL1</i> in the time-course	47
2.7	Significantly co-regulated pathways with <i>PRL1</i>	47
2.8	Significantly up-regulated pathways	48
2.9	Enriched GO terms for genes in cluster #5 in the time-course	49
2.10	Significantly down-regulated pathways	51
2.11	QPCR validation from the ER- <i>PRL1/prl1</i> experiment	51
2.12	QPCR validation from the tiling and mRNA-Seq experiments	52
2.13	Summary of RNA-Seq alignment with Bowtie	55
4.1	Accessions of <i>Arabidopsis thaliana</i> used in this work	95
4.2	Chemicals and reagents used in this work	96
4.3	Plasmid vectors used in this work	99
4.4	Plasmid constructs used or designed in this work	100
4.5	Secondary antibodies used in this work	101
4.6	Antibiotics used in this work	104
4.7	Hormones used in this work	104
A.1	Oligonucleotides used for plant genotyping	151
A.2	Oligonucleotides used in PCR-based cloning and sequencing	151

A.3	Oligonucleotides for transcript profiling data validation	152
A.4	Oligonucleotides used for preparing the Illumina library	153
C.1	Enriched GO terms from the tiling array up-regulated gene-list	159
C.2	Enriched GO terms from the tiling array down-regulated gene-list	162
C.3	Enriched GO terms from the RNA-Seq up-regulated gene-list	162
C.4	Enriched GO terms from the RNA-Seq down-regulated gene-list	166
C.5	Altered transposable elements in <i>prl1</i>	169
C.6	Up-regulated genes in <i>prl1</i> from the tiling array analysis	172
C.7	Down-regulated genes in <i>prl1</i> from the tiling array analysis	181
C.8	Up-regulated genes in <i>prl1</i> from the RNA-Seq analysis	186
C.9	Down-regulated genes in <i>prl1</i> from the RNA-Seq analysis	198
C.10	Miss-regulated genes in the the ER-PRL1/ <i>prl1</i> samples	206

Abbreviations

C _t	threshold cycle
L	Avogadro constant
°C	degree Celsius
A	ampere
BAP	6-benzylaminopurine
bp	base pair
cDNA	complementary DNA
chDNA	chloroplast DNA
Col-0	ecotype Columbia-0 of <i>Arabidopsis thaliana</i>
cRNA	complementary RNA
DMSO	dimethyl sulfoxide
DNA	deoxyribonucleic acid
dNTPs	deoxyribonucleotides
DSB	double-strand break
ds cDNA	double strand complementary DNA
DTT	dithiothreitol
E	einstein
EB	elution buffer
ECL	enhanced chemiluminescence
EDTA	ethylenediaminetetraacetic acid
EMS	ethyl methanesulfonate
FC	fold change

gDNA	genomic DNA
H3	histone 3
HA	peptide derived from the haemagglutinin protein of the human influenza virus
HTE	high Tris-EDTA
LB	lysogeny broth medium
LN	liquid nitrogen
LTE	low Tris-EDTA
LTR	long terminal repeat
M	molar
MMS	methyl methanesulfonate
mtDNA	mitochondrial DNA
NAA	1-naphthaleneacetic acid
NEB	New England Biolabs
NER	nucleotide excision mechanism
NIB	nuclear isolation buffer
NLB	nuclear lysis buffer
NLS	nuclear localization signal
nt	nucleotide
NTC	Nineteen complex
NWB	nuclear washing buffer
OD	optical density
PCR	polymerase chain reaction
PE	pair-end
PIC	plant protease inhibitor cocktail
PNK	polynucleotide kinase
PRL1	Pleiotropic Regulatory Locus 1
PRL2	Pleiotropic Regulatory Locus 2
QPCR	quantitative real-time PCR
RAM	random access memory

RNA	ribonucleic acid
RNase A	ribonuclease A
ROS	reactive oxygen species
rpm	revolutions per minute
RT	room temperature
RT-PCR	reverse transcription polymerase chain reaction
SDS	sodium dodecyl sulphate
SDS-PAGE	sodium dodecyl sulphate polyacrylamide gel electrophoresis
TBE	Tris-borate-EDTA buffer
TE	Tris-EDTA buffer
TE	transposable element
TF	transcription factor
TUB	tubulin
U	unit of enzymatic activity
Ub	ubiquitin
UDGase	uracil-N-glycosylase
UV	ultra-violet
V	volt
X-Gluc	5-bromo-4-chloro-3-indolyl-1- β -D-glucuronic acid
Y2H	yeast two hybrid system
YEB	yeast extract broth medium
YFP	yellow fluorescent protein

Amino acids

A	Ala	Alanine
C	Cys	Cysteine
D	Asp	Aspartic acid
E	Glu	Glutamic acid
F	Phe	Phenylalanine
G	Gly	Glycine
H	His	Histidine
I	Ile	Isoleucine
K	Lys	Lysine
L	Leu	Leucine
M	Met	Methionine
N	Asn	Asparagine
P	Pro	Proline
Q	Gln	Glutamine
R	Arg	Arginine
S	Ser	Serine
T	Thr	Threonine
V	Val	Valine
W	Trp	Tryptophan
Y	Tyr	Tyrosine
X	xxx	any amino acid

A mis padres
Für Marcus

1. Introduction

Barbara McClintock already speculated with the idea of dynamic genomes when she discussed her findings in heterochromatin behaviour in Maize (McClintock, 1950). This discovery, together with many others, including genetic transformation via *Agrobacterium*, made plants, and especially *Arabidopsis thaliana*, interesting model organisms to be studied and understood. New emerging high-throughput sequencing technologies have shown how complex and dynamic genomes are (Lister et al., 2009), and how many processes in gene regulation still remain to be understood in plant development.

This work deals with the functional analysis of two mutations in *Arabidopsis thaliana*, *prl1* and *prl2*, which affect a multitude of regulatory processes. *Arabidopsis prl1* shows a *pleiotropic* phenotype. Pleiotropy is defined as the effect of a mutation in a single gene, which influences multiple phenotypic traits. The pleiotropy showed by *prl1* suggests the impossibility of carrying precise genetic studies. However, for geneticists, the pleiotropic nature of a mutation also means that the affected gene could perform a central regulatory function. The study of the gene may reveal new pathways and disciplines. For readers of this thesis biased by these contrasting views, the work described here tries to prove that the latter opinion is correct, and pleiotropic regulatory functions and pathways affected by genes can be precisely defined, both by classical genetics and by modern genome-wide transcription analysis technologies.

To provide the necessary background for understanding and qualifying of results described below, the introduction starts presenting the *prl1* mutant and the known functions of *PRL1*. Splicing mechanisms and the proteasome system are introduced due to previous studies in orthologue systems and in *Arabidopsis*, respectively. The implications of gene duplication are introduced to support the sub-functionalization of *PRL1* and *PRL2*. Stress situations in plants where *PRL1* seems to be involved are also introduced. DNA repair in plants is explained as a mechanism used to face certain kind of stresses in which *PRL1* could be associated through its interaction with the DDB1-CUL4 and Prp19-PSO4 complexes involved in DNA damage signalling. Transposable elements are described as a stress response together with silencing mechanisms. Development processes related to plant reproduction, in which *PRL1* and *PRL2* show a sub-functionalization, are explained before finishing with presenting new technologies in gene expression profiling and the aims of the present work.

1.1 PRL1

1.1.1 *Arabidopsis prl1* mutant

Németh et al. (1998) identified and characterized the *prl1* mutant in *A. thaliana*. This mutant was found in the Koncz T-DNA collection in a screen designed to identify factors involved in sugar signalling pathways. 1 200 T-DNA lines were analysed in this screen for growing defects in media containing 0,1, 0,5, 2, 4, 6, 8 and 10 % of sucrose or glucose.

The *prl1* mutant was found in this T-DNA screen as a mutant that showed arrested development when grown on high sucrose-containing medium (Németh et al., 1998). When grown on soil, *prl1* presented a semi-dwarf phenotype (Figure 1.1a). Furthermore, the leaf size was smaller, with edges in a serrated shape and a higher chlorophyll and anthocyanin content. Flowers are also smaller than the WT (Figure 1.1b), with a petal length similar to the length of the sepals which exposed the style and stigma earlier in the flower development than in the WT. One very useful phenotypic trait of the *prl1* mutant, that was used as a phenotypic marker, is the root length phenotype. In *in vitro* culture, the root length of the *prl1* mutant is smaller than the WT (Figure 1.1c). In addition, the *prl1* mutant was shown to be hypersensitive to plant growth regulators in the *in vitro* medium, including auxins, cytokinins, abscisic acid, salicylic acid, gibberellins and ethylene. Furthermore, *prl1* showed a slower development in low temperature conditions (Németh et al., 1998). The complex and pleiotropic phenotype shown by the mutant, due to the disruption of a single locus, reflects the miss-regulation of many metabolic and developmental processes. This was the reason for naming the locus *PLEIOTROPIC REGULATORY LOCUS 1 (PRL1)*.

The T-DNA insertion was found in the annotated unit AT4G15900 between exons 15 and 17 (Németh et al., 1998). The transcribed region of *PRL1* is 3,94 kb long, covering a small 5' UTR sequence (38 bp), 17 exons and a 3' UTR region of 222 bp. *PRL1* CDS is 1461 bp long and encodes for a protein of 54 kDa with seven WD40 repeats in its C-terminal region. Whereas, no known domains were identified in the N-terminal region. *PRL1* was found to be a conserved protein with potential identified orthologous genes (Németh et al., 1998), but no function could be assigned. Further studies found that *PRL1* was higher transcribed in actively-dividing organs, and that sequences from the two first introns were needed for the correct gene expression. Furthermore, it was shown that the protein is accumulated in the nucleus (Szakonyi, 2006) and interacts *in vitro* with AKIN10 and AKIN11 (Bhalerao et al., 1999), regulators of glucose signalling. *PRL1* was also suggested to influence the proteasome activity through its interaction with SnRK1 (Farrás et al., 2001).

In *Arabidopsis* there is another gene sharing a high identity with *PRL1*: it is a paralogue coded AT3G16650 and named *PRL2*. *PRL2* was first described by Németh et al. (1998) and the insertional mutant was isolated by Ríos et al. (2002). *PRL2* shows a 79,6 % amino acid identity with *PRL1*, this identity is specially higher between the C-terminal region of both proteins.

1.1.2 Orthologues of *PRL1*

After the characterization of *PRL1* published by Németh et al. (1998), studies in yeast were published where the function of orthologous genes of *PRL1* were dissected.



Figure 1.1: Pleiotropic phenotype of *prl1* (right) compared to WT (left). The phenotypical effects include (a) semi-dwarfism, (b) smaller flowers and (c) shorter root compared to WT.

Prp5, the potential orthologous gene of *PRL1* in fission yeast (*Schizosaccharomyces pombe*), was identified in a screen for mutants defective in mRNA splicing under certain temperature conditions (Potashkin et al., 1998). The phenotype shown by the *prp5* mutant were general defects in cell division and cell cycle. Further analyses showed that the *prp5* phenotype was caused by a reduced or abolished ATPase activity of Prp5p at non permissive conditions (Dayyeh et al., 2002). In budding yeast (*Saccharomyces cerevisiae*), Prp46 was identified in a two-hybrid screen for splicing factors which interacted with the DExH box RNA helicase Prp22p (Albers et al., 2003). Prp46p was identified as a protein associated to the spliceosome and essential for pre-mRNA splicing, furthermore, the *prp46* knock-out is not viable. Other studies specified that *PRL1* activity in the spliceosome could be associated to the Nineteen complex (NTC, Ohi and Gould, 2002) which is required for spliceosome activation (Chan et al., 2003).

In mice, *PLRG1* deficiency provokes embryo lethality 1,5 days after fertilization. *PLRG1* deficiency causes enhanced p53 phosphorylation and stabilization in the presence of increased γ -H2AX immuno-reactivity, indicating an activated DNA damage response. Moreover, the down-regulation of p53 rescues lethality in both *PLRG1*-deficient embryonic tissue culture and zebrafish *in vivo*, suggesting that the apoptosis resulting from *PLRG1* deficiency is p53-dependent

(Kleinridders et al., 2009). This result links PLRG1 with programmed cell death in response to DNA damage.

PRL1 was found to be part of the splicing machinery in humans (Ajuh et al., 2000). Furthermore, PRL1 was unequivocally associated with the spliceosome through its presence in the CDC5L complex –or NTC– which impairs the spliceosome activity but not its assembly *in vitro*.

1.1.3 Function and conservation

The conservation of orthologue genes of *PRL1* lie in the repeated WD40 motifs. Neer et al. (1994) defined the WD40 motif as a repeating polypeptide unit of variable length, starting in a Gly-His (GH) and ending with Trp-Asp (WD). The distance between the GH and WD points was found to be somehow fixed in 23–41 residues, whereas the distance of the WD point with the GH point from the next repeated unit was found to be much more variable in length. In this study it was already proposed that the WD40 repeats domain (WDR) could serve as an interaction surface for other proteins. Furthermore, they found different proteins carrying the WDR domains with different functions, meaning that carrying the WDR domain is not a synonym of a conserved function (Neer et al., 1994).

However, the sequence conservation in the WDR is not high across members of different sub-families, Jawad and Paoli (2002) proposed that the three-dimensional structure in which the WDR is more important than the amino acid sequence. They found that different sub-families of proteins, with different sequences between the WD residues, generated super-imposable structural models. The 7 WD40 motifs of *PRL1* could be folded in a β -propeller structure which is used as a protein-protein interaction region, as modelled for Bub3p by Larsen and Harrison (2004).

The super-family of WDR proteins was studied in *Arabidopsis* (van Nocker and Ludwig, 2003), discovering members involved in different processes. From those results, 113 proteins were identified to have a clear homology with proteins from other analysed eukaryotes. It was suggested that the conservation across organisms not only could be linked to different basic cellular mechanisms, but also to plant-specific processes.

1.2 Splicing

In eukaryotes, the RNA transcribed as pre-messenger RNA (pre-mRNA) needs to be processed in order to produce the protein with the right amino acid sequence. These immature transcripts contain amino acid-coding sequences (exons) with non-coding sequences (introns) in between. The maturation processes of the mRNA includes the removal of intron sequences from the immature transcript, and the ligation of the exon sequences. This process is accomplished by the spliceosomal machinery, a huge complex comprising five non-coding RNAs and about 200 proteins. The machinery is present in every eukaryote organism and has undergone evolution parallel to intron length in different lineages (Collins and Penny, 2005).

Spliceosomal introns contain a short conserved GU sequence in the 5' side, followed by a larger and lesser conserved sequence. The 3' side of the spliceosomal introns contain almost an invariant AG sequence, preceded by a poly-pyrimidine region. The branch point inside the intron is an adenine residue found in direction 3' of the poly-pyrimidine region. The spliceosome

processes the introns and consists in an RNA-protein complex composed of the U1, U2, U4, U5, and U6 small nuclear ribo-nucleoproteins (snRNPs). In addition, a number of proteins and associated complexes, including the Prp19-associated complex (Nineteen Complex, NTC), are required for the activity of the spliceosome (Jurica and Moore, 2003).

The biochemical process (Figure 1.2) takes place as follows: U1 binds to the GU sequence at the 5' splice site (E complex). Subsequently, the U2 snRNP binds to the branch site, and ATP is hydrolyzed (complex A). Once U1 and U2 are on place, the U5, U4/U6 tri-snRNPs bind forming the pre-catalytic spliceosome (B complex). Specifically U5 binds the exon at the 5' site, and U6 binds to the U2 snRNP. The complex B* is activated when U1 and U4 are released, U5 shifts from the exon to the intron sequence, and U6 binds at the 5' splice site. The C complex is formed when U6 and U2 catalyse the trans-esterification reaction, U5 shifts from the intron to the 3' exon. This results in the 5' splicing site to be cleaved, and the 3' side of this break, by nucleophilic attack, binds covalently to the adenine in the branching point, resulting in the formation of the lariat. In complex C2, U2, U5 and U6 remain bound to the lariat, the 3' splicing site is cleaved and both exons are ligated. The spliced RNA is released and the lariat de-branches (Wahl et al., 2009).

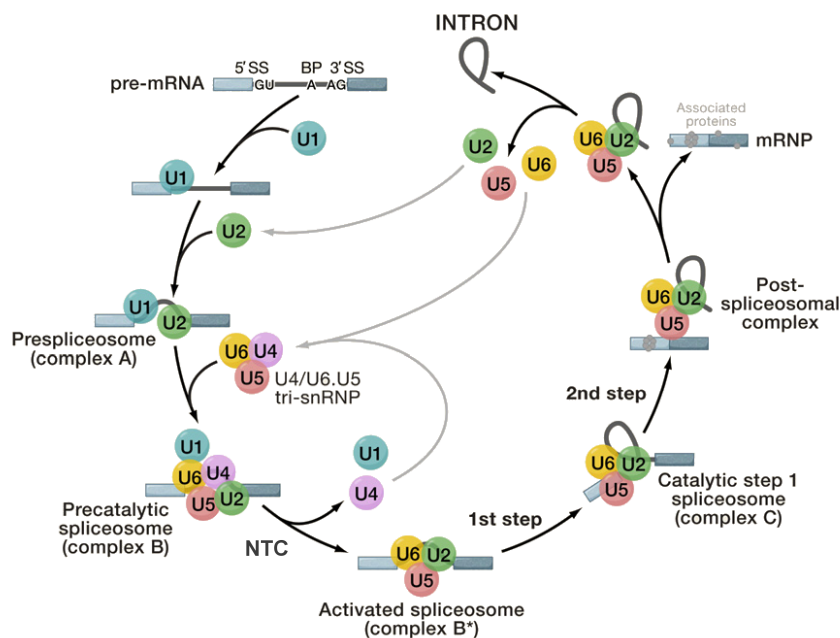


Figure 1.2: Schematic overview of the biochemical reactions in the splicing process. The Prp19-associated complex (NTC) stabilizes the B* complex. Adapted from Wahl et al. (2009).

1.2.1 The Prp19-associated complex

Orthologue genes of *PRL1* have been placed in the so called Prp19-associated complex or Nineteen complex (NTC). In yeast, the relationship of NTC with the spliceosome was already described by Ohi et al. (2002) and Ohi and Gould (2002). The human NTC (or CDC5L complex) was identified by Ajuh et al. (2000). Further studies revealed the stoichiometry and composition of the human complex *in vitro*, revealing a core formed by four units of hPrp19 and one unit of PRL1, CDC5L

and SPF27 (Grote et al., 2010). In *Arabidopsis* the existence of this complex was suggested by Palma et al. (2007) and further studied in Monaghan et al. (2009), confirming that the Prp19-associated complex is present in *Arabidopsis*.

It has been reported that the Prp19-associated complex is required for the stabilization of U5 and U6 snRNPs after release of the U4 snRNP in order for the trans-esterification reaction to take place (Chan et al., 2003). Moreover, the NTC specifies the interaction of U5 and U6 with the 5' splice site (Chan and Cheng, 2005).

1.2.1.1 PRP19

PRP19 is the core protein of NTC, called Prp19p in yeast, was first described by Henriques et al. (1989). It was named PSO4 and associated with the pathway of error-prone recombinatorial repair of DNA. Later on, Cheng et al. (1993) identified the protein as a novel splicing factor and Grey et al. (1996) linked its function to both processes. The PRP19 protein in yeast consists of a U-box domain with E3 ubiquitin ligase activity, a coiled-coil domain used for tetramerization, and a WDR domain for protein-protein interaction (Ohi et al., 2005). In humans, hPrp19 has been shown to homo-oligomerize in human models (Grillari et al., 2005). In mice, where it is called SNEV, it was shown to be non-redundant and indispensable for embryo development (Fortschegger et al., 2007). Further studies in mice also reflected the connection of PRP19 with the proteasome degradation machinery through the direct cytoplasmic interaction with SUG1, a regulatory sub-unit of the 26S proteasome (Sihn et al., 2007). In *Arabidopsis*, two orthologues were identified by Monaghan et al. (2009) that share a 83 % of identity.

1.2.1.2 CDC5

CDC5 is a Myb-related protein (Ohi et al., 1998), it was also found to be part of the NTC in yeast (Ohi and Gould, 2002) and human (Burns et al., 1999). Previously, the *cdc5* mutant in *S. pombe* was found to be defective in cell cycle progression (Ohi et al., 1994). The conservation of CDC5 function was studied by Ohi et al. (1998) when *CDC5* genes from several other species could complement the cell cycle phenotype in *S. pombe*. Subsequently, the orthologous gene was identified in *A. thaliana* and found to be also able to complement the *S. pombe cdc5* phenotype (Hirayama and Shinozaki, 1996). Also in humans, CDC5 was found to be part of the spliceosome, and specifically part of the NTC complex (Ajuh et al., 2000).

1.2.1.3 MOS4

MOS4, also known as SPF27 in humans or Snt309p in *S. cerevisiae*, was first identified in a genetic screen as a mutant with a worse *prp19* phenotype (Chen et al., 1998). Snt309p was found to be associated with the spliceosome at the same time as Prp19p (Chen et al., 1998). It was previously co-purified with Prp19p by Tarn et al. (1994) and the interaction with Prp19p was further analysed by Chen et al. (1999), observing that the presence of Snt309p was necessary for the stability of the Prp19-associated complex. Recent studies in *Arabidopsis* confirmed the presence of MOS4 in the Prp19-associated complex (Monaghan et al., 2009).

1.2.2 Alternative splicing

After several genomes were sequenced, it became clear that the complexity seen at the organism level, did not keep a linear relationship with the number of predicted genes. Whereas the genome of the nematode *Caenorhabditis elegans* is thought to have 20 100 genes (*C. elegans Sequencing Consortium, 1998*), the human genome contained *only* 23 000 genes (*Human Genome Sequencing Consortium, 2004*). Furthermore, the 8th release of the *Arabidopsis* annotation project (TAIR8) contains a similar number of genes (27 379, *Swarbreck et al., 2008*).

A recent study reported how the exon-intron architecture is reflected in the chromatin structure of the genes. *Schwartz et al. (2009)* have shown that the enrichment of methylated histone-3 proteins in exons –compared to introns– is due to the higher presence of nucleosomes in exons.

The alternative splicing process increases transcriptome and proteome diversification. The *alternate* ways of splicing mRNA include the skip of an exon, the use of alternative 5' or 3' splice sites or intron retention. Interestingly, the predominant process for alternative splicing in humans is exon skipping, whereas in plants, intron retention is more frequent (*Barbazuk et al., 2008*).

For some years, it has been shown that stress situations affect the splicing of several genes in plants. These stresses can be of biotic –pathogen-induced–, or abiotic origin –drought or salt– (*Kazan, 2003*). A current example studies the abundance of two transcripts of *DREB2* in rice, where the isoform with the complete third exon is more prevalent under low and high temperature conditions (*Matsukura et al., 2010*). The *stress* isoform was shown to contain a putative nuclear localization signal, and an AP2/ERF DNA-binding domain, whereas the short isoform not.

1.2.3 Co-transcriptional splicing

The synthesis of mRNA has long seen to be a co-ordinated process where the 5' capping, intron splicing and polyadenylation take place in the nascent mRNA (*Neugebauer, 2002*).

Co-transcriptional splicing was discovered in genes coding for long sequences, where it seems logical to envision active splicing as a mechanism which takes place at the same time the RNA polymerase II transcribes the sequence (*Tennyson et al., 1995*). Later studies in *Drosophila* supported this finding (*Beyer and Osheim, 1988*). Furthermore, it has been shown how spliceosomal snRNPs can enhance elongation of the mRNA in human cells, when splicing signals are included in a transcript (*Fong and Zhou, 2001*) and that the spliceosomal machinery is actively recruited to intron-containing transcripts. However, in yeast, the 90 % of the genes are spliced post-transcriptionally (*Tardiff et al., 2006*) due to the association of some splicing factors in a later stage, one of this late-factors is specifically, Prp19 (*Moore et al., 2006*). The situation in plants on co-transcriptional splicing it is still unknown.

1.3 The proteasome

The proteasome is a large protein complex (Figure 1.3) which main function is to degrade poly-ubiquitylated proteins for its turn-over. The proteasome can be found in all eukaryotes where it is located in the nucleus as well as in the cytoplasm. The better studied form is the 26S proteasome,

a multi-subunit complex that is composed of two sub-complexes with different sedimentation coefficients, 20S and 19S (Ciechanover, 2005).

In *Arabidopsis*, several isoforms of the core particle (20S) can be found. But generally, 20S has a cylindrical shape and is composed by four stacked rings. The two outer rings are formed by α -subunits and the two inner rings are formed by β -subunits, with seven subunits in each ring. The proteolytic activity is located on the inner side of the cylindrical structure formed by the β -subunits (Yang et al., 2004).

The 19S subunit is composed by a base that interacts with the 20S subunit and a lid that selects poly-ubiquitylated proteins to be translocated into the 20S particle. The lid is responsible of recognizing the substrate (Glickman et al., 1999), whereas the base is responsible of unfolding the targeted protein (Glickman et al., 1998). The access to the central chamber is regulated by a narrow channel, which opening is controlled by interactions with the α -subunits of the 20S particle.

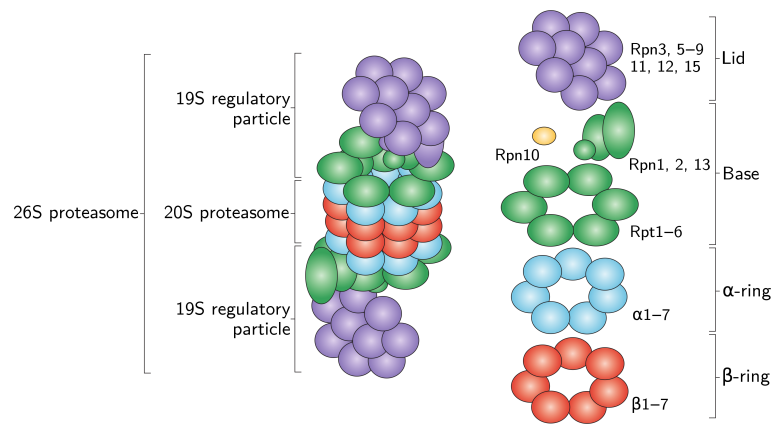


Figure 1.3: Schematic overview of the proteasome structure. The 26S proteasome is composed of the 19S and 20S complexes. The 20S particle is composed of four rings, two outer rings with 7 α -subunits and two inner rings composed of 7 β -subunits. The 19S particle is divided in the base and lid complexes. Adapted from Murata et al. (2009).

Apart from the proteolytic function of the proteasome, for example, the 19S has been shown to be involved in chromatin remodelling, with implications in DNA repair and transcription (Sikder et al., 2006). Farrás et al. (2001) observed in *Arabidopsis* the nuclear interaction of SnRK1 with the α -subunits of the 20S proteasome. This interaction could have implications in the re-programming of transcription processes by SnRK1 as energy homeostasis sensor (Baena-González and Sheen, 2008).

1.3.1 Ubiquitin signalling

The best known function of the proteasome is the degradation of proteins after being poly-ubiquitylated. Ubiquitin is a small conserved protein that not only targets proteins to be degraded, but also has roles in signalling. Poly-ubiquitylation of proteins via the residue Lys 48 of the ubiquitin units serves as a signal for proteasomal degradation of target proteins. There are many examples of ubiquitylation in several signalling processes, independent of protein

degradation (Sun and Chen, 2004), including DNA repairing (Bergink and Jentsch, 2009), and direct transcriptional regulation (Hochstrasser, 2004).

Poly-ubiquitylation of proteins targeted to degradation involves an ATP-dependent enzymatic cascade of three different enzymes: 1. A ubiquitin activating enzyme (E1), 2. A ubiquitin conjugating enzyme (E2) and 3. A ubiquitin protein ligase (E3). The ubiquitin moieties are transferred one by one to the target protein following the E1-E2-E3 cascade. Several cycles of the cascade result in the poly-ubiquitin chain (Hershko and Ciechanover, 1998) that is recognized by the lid of the 19S particle of the proteasome. A ubiquitin chain of at least four moieties serves as a signal for degradation. The release of attached ubiquitin moieties is mediated by de-ubiquitinating enzymes (DUBs). DUBs cleave the ubiquitin monomers from the precursor protein, recycling ubiquitin moieties during the breakdown of the ubiquitin-protein conjugates (Wilkinson, 1997).

1.4 Gene duplication in evolution

Gene duplication is the consequence of duplication of a DNA region that contains the gene. This process generates *raw* material, useful in adaptative evolution (Bodt et al., 2005). Much of the plant diversity may be explainable by duplication and adaptative specialization or sub-functionalization of pre-existing genes.

1.4.1 Homology of sequences

Homology, in this case, refers to similarity of DNA or protein sequences. These sequences are usually similar, but not identical. When an evolutionary scenario is taken into account, the homologous relationship can be specified. Orthologue genes are similar genes separated by speciation, whereas parologue genes are similar genes in an organism arisen by a duplication event (Koonin, 2005).

The definition of orthology does not mention the relationship of biological function, whereas the definition of paralogy contains major functional implications. The *PRL* gene family in *Arabidopsis* is a typical example for a paralogous relationship.

1.4.2 Mechanisms of gene duplication

The two most common processes of gene duplication are unequal cross-over and retro-position (Zhang, 2003). Moreover, Morgante et al. (2005) suggested that transposable elements could also be the cause for gene duplication and exon shuffling in plants. Another perspective of gene duplication is the scale of the duplication. An extreme example is the polyploidy, when the whole genome is duplicated. Lower scales include segmental and tandem duplication of genes and trans-duplication by DNA transposons (Flagel and Wendel, 2009).

As an example, in *Arabidopsis* there are several clusters of snRNA: 7 clusters containing U1 and U4 and two tandem duplications for both U2 and U5. The case of the large number of U1-U4 clusters arose after sequential duplications (Wang and Brendel, 2004).

1.4.3 Functional connotations

The functional connotations of the comparison of two paralogue genes take a relevant role in opposition to an orthologous situation. In some cases, paralogues may have the same function. A classic example of it is the amplification in the genome of the rRNA genes. More frequently, paralogue genes exhibit a sub-functionalization during evolution (Flagel and Wendel, 2009). An interesting example is the evolution of the ancestral RNA polymerase from archaea, contrasted to two of the three RNA polymerases in eukaryotes (Pühler et al., 1989). RNA polymerase I is responsible of the transcription of the rRNA genes, whereas RNA polymerase II transcribes the protein-coding genes and RNA polymerase III is in charge of the tRNA genes.

Another example is provided by the *U2 AUXILIARY FACTOR (U2AF)* that promotes the binding of the U2 snRNP subunit to the intron branch-point. In *Arabidopsis* there are two *U2AF* genes with a slight sub-functionalization: one gene is strongly expressed in young roots and root tips, whereas the other gene is limited to root vascular tissue. Furthermore, reduced expression of *U2AF* show a pleiotropic phenotype in *Arabidopsis* (Wang and Brendel, 2006).

1.5 Stress situations in plants

Developmental and environmental signals can trigger adaptative processes in plants. Rapid changes in plant metabolism and transcription, in order to be adapted to the new conditions, are regarded as stress responses. Stress responses have a heavy epigenetic-based regulation (Chinnusamy and Zhu, 2009). The *prl1* mutant has been recently shown to have a reduced expression of stress-responsive genes (Baruah et al., 2009).

1.5.1 Energy homeostasis

Plants belong to one of the few kingdoms able to transform electro-magnetic energy –sunlight– and low-energy compounds into chemical potential energy, i.e. biomolecules like glucose which contain high chemical potential energy. This process is called photosynthesis and takes place in a specialized organelle inside plant cells called chloroplast.

When glucose is abundant, the chemical energy, present in the bounds of the molecule, is transformed by the glycolysis process. Through several enzymatic reactions ATP, a molecule extensively used in energy exchange processes, is synthesized. In energy-deprivation conditions, like in the absence of glucose, the mobilization of stored energy is favoured. This energy is released from polysaccharides like starch or fatty acids. The mobilization of this energy stored as biomolecules is seen as a form of cellular stress.

Plants can sense the energy deficiency or its fluctuations. These changes in energy are associated with stress situations including alterations of the photoperiod and carbon hijack done by pathogens. To get adapted to stress situations, the plant must re-programme the transcriptional machinery. A general view is emerging in which, the adaptation to stress or energy deficiency and the restoration of the homeostasis is regulated by SnRK1 (SNF1-related kinase 1). SnRK1 is seen as a sensor of the energy homeostasis which is evolutionary conserved (Baena-González and Sheen, 2008). In more detail, Baena-González et al. (2007) found that over-expression of AKIN10 enhances tolerance to starvation, altering architectural and developmental processes. Moreover,

AKIN10 and AKIN11 deficiency hampers the transcriptional switch to mobilize starch at night. In rice, SnRK1 it has been shown to regulate seed germination and seedling growth (Lu et al., 2007).

1.5.2 Reactive Oxygen Species

One by-product of energy conversion in living organisms is the generation of reactive oxygen species (ROS). Specially in plants, because of the high-energetic reactions that take place during photosynthesis. Normally ROS are directly scavenged after its generation by anti-oxidative compounds. Different factors, including high light intensity, high and low temperature or drought can perturb this equilibrium, affecting either the mechanisms for ROS production or detoxification (Apel and Hirt, 2004).

High light stress leads to the production of ROS in chloroplasts and peroxisomes. In normal light conditions there are two electron sinks in the photosynthetic systems: one causes the reduction of oxygen by photosystem I and generates superoxide and H₂O₂. The other sink is composed by the Rubisco oxygenase reaction and the photo-respiratory pathway that lead to H₂O₂ generation within the peroxisome. Under intense light stress, increasing amounts of singlet oxygen (O₂^{•-}) are produced by photosystem II (Hideg et al., 1998).

Scavenging of ROS is done enzymatically or non-enzymatically through the reduction of antioxidant compounds, mainly including glutathione (GSH), as well as ascorbate, carotenoids and flavonoids. In the case of glutathione, a high ratio of reduced to oxidized GSH is essential for ROS scavenging. The level of reduced GSH is maintained by glutathione reductase (GR) using NADPH as reducing agent (Asada, 2006). Furthermore, the overall balance among different antioxidants must be tightly controlled. This balance is evident in chloroplasts of cells with enhanced glutathione biosynthesis: paradoxically, the chloroplasts show oxidative stress damage, which is very likely caused by changes in its overall redox state (Creissen et al., 1999).

1.5.3 Pathogen response

Pathogen attack elicits stress responses in plants. Doke (1985) already observed the oxidative burst when potato was inoculated with an avirulent pathovar of *Phytophthora infestans*, whereas a virulent pathovar virulent failed to induce O₂^{•-} generation.

Plants have developed different strategies to counteract the effect of pathogens, whereas pathogens have evolved in parallel in order to divert these strategies. One good example of this is the high polymorphism found in resistance (*R*) loci in plants. These *R* proteins are activated indirectly –or directly– by pathogen-encoded effectors (*E*). Effectiveness of *R* proteins vary among the different *E* proteins which leads to a *weapon race* between the plant and pathogen populations (Jones and Dangl, 2006).

R-genes are normally located in clusters with several copies of paralogues which arose either from a single gene family, or from several unrelated families. The number of *R*-genes in the clusters can vary from two to several genes. The repeated sequences within the clusters arose by duplications and transposon insertions via recombinatorial mispaired cross-overs (Friedman and Baker, 2007). Interestingly, the mispaired cross-overs seem to be more frequent in infected plants (Kovalchuk et al., 2003).

1.5.4 Programmed cell death

Programmed cell death (PCD) is an extreme response to stress that can be triggered by external or internal factors. The main forms of PCD recognized in plants are apoptotic-like PCD, autophagy and necrosis (Reape et al., 2008).

PCD is defined as a sequence of events, genetically controlled, leading to the death of the cell. In plants, PCD can be found during senescence (Lim et al., 2007), in the hypersensitive response (HR) after pathogen attack and in several developmental processes including the formation of tracheary elements or gametophyte development.

Classically, the mitochondrion has been regarded as a main player in PCD through a permeability change of in the membrane and translocation of cytochrome *c* into the cytosol (Tiwari et al., 2002). In plants it has also been observed that ROS generated in the chloroplast can collaborate in the execution of the HR (Liu et al., 2007).

1.5.5 Genotoxic stress

Genotoxic stress is defined as the response of an organism to damage to the genome resulting from the chemical action of a molecule.

Plants must sense this situation and relay the signal to the protective and repair mechanisms. This kind of stress is sensed, like many other stresses (Tena et al., 2001), by the mitogen-activated protein kinase (MAPK) cascades. Holley et al. (2003) observed how a MAPK was specifically activated after UV-B treatment in tomato. In *Arabidopsis*, the *mcp1* mutant was identified in a T-DNA mutant screening looking for hypersensitive lines to methyl methanesulfonate (MMS). This isolated mutant was also found to be hypersensitive to UV-C radiation (Ulm et al., 2001). Further studies linked the *mcp1* hypersensitivity to genotoxic stress to an elevated resistance to salt-induced stress (Ulm et al., 2002).

Brown et al. (2005) presented the *Arabidopsis UV RESISTANCE LOCUS 8 (UVR8)* as a component in UV-B signalling, controlling the expression of several genes with functions in UV protection. Specifically they showed the regulated expression of the transcription factor *HY5* by UVR8 in exposure to UV-B. *HY5* is required for plant viability in high UV-B irradiation conditions.

1.6 DNA repair in plants

Damage to the genome occurs very frequently in every cell. Efficient cellular mechanisms should sense, recognize and eliminate this damage. The fact that plants do not keep a reserve germ line, accentuates this problem. Furthermore, plants are very exposed to UV light, a major mutagen.

1.6.1 DNA damage

Damage to DNA can be of several types depending whether is caused by a chemical or an electro-magnetic agent. Damages by chemical agents include hydrolytic damage (a base detaches from the DNA chain), alkylation damage –like the effects of ethyl methanesulfonate (EMS)–, or oxidative damage by ROS. Electro-magnetic agents include ionizing radiation, which provokes unspecific

damages by ROS or nick generation, UV light specifically induces base dimers. The lesions include mismatched bases, double-strand breaks and chemically-modified bases (Britt, 1996).

1.6.2 Repair mechanisms

There are different mechanisms of DNA repair, including the direct reversal of damage, the repair mechanism by excision and the repair mechanisms of double-strand breaks (Bray and West, 2005).

Cyclobutane pyrimidine dimer (CPD) photolyases can directly reverse the main damage caused by UV-light exposure in a process called photo-reactivation. In rice, it has been shown that photo-reactivation is the preferential repairing mechanism in non-dividing tissues (Kimura et al., 2004). Furthermore, Kaiser et al. (2009) demonstrated that the over-expression of the CPD photolyase *At-PHR1* (Ahmad et al., 1997) increased plant fitness under elevated UV-light radiation.

Repair mechanisms undergoing base or nucleotide excision are repaired using the information of the complementary strand. The existence of this repair mechanism in plants has been tested in cell extracts, suggesting that gap filling and ligation may proceed either through insertion of just one nucleotide or several nucleotides (Córdoba-Cañero et al., 2009). The complex CUL4-DDB1A, through its E3 ubiquitylation activity (Hu et al., 2004), is involved in the nucleotide excision repair (NER) mechanism. The deletion of DDB1 in mice has effects in cell cycle, cell death and embryonic development (Cang et al., 2006). The complex CUL4-DDB1A in *Arabidopsis* (Bernhardt et al., 2006) has also been shown to be involved in this repairing mechanism (Molinier et al., 2008). Furthermore, WDR proteins interact with this complex, and specially PRL1 seems to be one of this interacting partners in *Arabidopsis* (Lee et al., 2008).

Double-strand break (DSB) repair uses information from identical or very similar DNA sequences. The repair mechanisms can make use of homologous recombination and non-homologous end joining (Bleuyard et al., 2006). A single non-repaired DSB in a dispensable artificial chromosome can produce cell death in yeast (Bennett et al., 1996). PSO4 (Prp19) was already associated with this repair mechanism (Henriques et al., 1989). Furthermore, hPRP19, together with hCDC5L, hPLRG1 and hSPF27 have been found to be related to the event of double-strand breaks caused by DNA inter-strand cross-links (Zhang et al., 2005). However, the ubiquitylated state of hPRP19 is critical: when ubiquitylated, hPRP19 has been shown to fail in interacting with either hCDC5L or hPLRG1 indicating that DNA damage can induce changes in the hPRP19 core complex (Lu and Legerski, 2007).

1.7 Transposable elements in plants

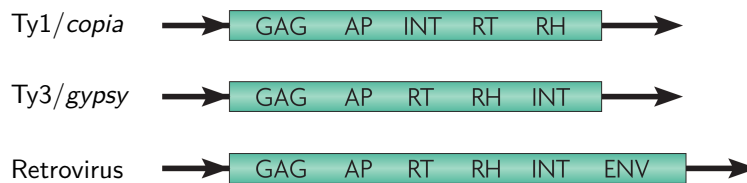
Transposable elements (TE) were first discovered in plants. In the work published by McClintock (1950) in maize, they were named as *controlling* elements, elements that could control the action of neighbouring genes. One of this elements, termed *Dissociator*, was found to cause the break of the chromosome upon dissociation. In general, these elements were found to move from one position to another in the linkage unit. Terms like variegation, mosaicism, mutable loci or positional effect could be explained by studying the function of various transposable elements.

1.7.1 Classification

TEs are classified into two categories which differ in the transposition process. Class I are RNA transposons or retro-transposons, whereas class II are DNA transposons (Feschotte et al., 2002).

Class I transposons (retro-transposons) replicate in the host genome by a *copy and paste* mechanism. The original element is not excised from the host genome and its mRNA is transformed into a new element upon integration elsewhere. Two groups of retro-transposons are distinguished by the presence or absence of flanking long terminal repeats (LTRs). To the LTR sub-group belong the Ty1/*copia* and the Ty3/*gypsy* families which have a similar organization to retro-viruses. The second sub-group does not exhibit LTRs but a polyadenylation site at the 3' end, the LINE (long interspersed nuclear elements) and SINE (short interspersed nuclear elements) families belong to this group (Figure 1.4, Wicker et al., 2007).

Class I (retro-transposons)



Class II (DNA transposons)

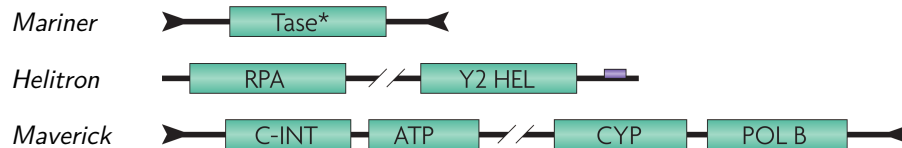


Figure 1.4: Classification of transposable elements families. \longrightarrow : long terminal repeat; --- : coding region; $\blacktriangleright \blacktriangleleft$: terminal inverted repeats; --- : non-coding region; $\text{---}/\text{---}$: region containing additional ORF(s); --- --- : diagnostic feature in non-coding region. GAG: capsid protein; AP: aspartic proteinase; INT: integrase; RT: reverse transcriptase; RH: RNase H; ENV: envelope protein; Tase*: transposase; RPA: replication protein A; Y2 HEL: helicase; C-INT: cysteine protease; POL B: DNA polymerase B. Adapted from Wicker et al. (2007).

Class II transposons (DNA transposons) are not transcribed like class I. Instead, they are excised and reinserted somewhere else in the genome. This class includes three groups (Feschotte and Pritham, 2007): 1. The classic DNA transposons which are transposed by *cut and paste* mechanism by an element-encoded transposase, are transposed as double strand DNA and have, generally, terminal inverted repeats. After transposition they leave a characteristic repeated sequence from the flanking host sequence. 2. The group of *Helitrons*, originally discovered in plants (Kapitonov and Jurka, 2001), which have a different transposition system –rolling-circle– that showed to have implications in capturing host gene fragments (Hollister and Gaut, 2007). 3. The group of *Maverick*-like transposons has no examples described in plants. Class II transposons

can only increase their number during DNA replication. When the transposon is in one DNA area that has already been replicated and jumps to other area which has not undergone replication.

1.7.2 Life cycle of LTR retro-transposons

LTR retro-transposons are the main components of higher plant genomic DNA and by far, the best studied examples (Kumar and Bennetzen, 1999). Retro-transposition involves four steps: transcription, translation, reverse transcription of mRNA to cDNA and integration of the cDNA in the host genome.

First, the retro-transposon is transcribed into RNA by the host RNA polymerase II using the promoter placed in the 5' LTR. The poly-cistronic mRNA is translated into the proteins that from the virus-like particle, reverse-transcribe the RNA and integrate the cDNA. Two RNA molecules are usually packed into the virus-like particle and are transcribed subsequently into double strand cDNA (dsDNA). Priming for dsDNA synthesis is done by tRNA and the 5' and 3' LTR RNA sequences. Finally, the dsDNA is integrated into the host DNA, adding another copy of the transposable element to the genome (Havecker et al., 2004).

This process is tightly controlled, involving functions encoded by the element itself and by the host. One of the major control steps is transcription, which determines both the production of the template RNA required in the reverse transcription and the synthesis of mRNAs for translation. In LTR retro-transposons, transcriptional control involves *cis*-regulatory sequences that are normally found in the LTR region of the element (Casacuberta and Santiago, 2003). Promoter sequences of the 5' LTR region have been shown to be similar to plant defence promoters, moreover, proteins induced by pathogen-related stresses interact *in vivo* with this sequences (Vernhettes et al., 1997).

1.7.3 Retro-transposons in the context of a host genome

Many studied plant retro-transposons are normally silent during plant development but activated by stresses, like pathogen attack, energy-depriving conditions, wounding, or *in vitro* culture (Grandbastien, 1998). McClintock already proposed that this process may reflect a plant strategy to increase the genomic diversity, being the retro-transposons the direct generators of this diversity (McClintock, 1950).

Already Grandbastien et al. (1997) observed the connection of stress responses in plants with the activation of retro-transposon transcription, especially stresses caused by pathogen attack. It was already observed that regulatory *cis*-elements of several known retro-transposons share similarities with a motif involved in the activation of several plant defence genes (Vernhettes et al., 1997). More recently, Maumus et al. (2009) made the connection of stress conditions with genome re-arrangement due to LTR retro-transposon activity: they showed that in the diatom algae (*Phaeodactylum tricornutum*), LTR retro-transposons are very abundant and are activated in several stress conditions. Furthermore, different accessions from around the world show different insertion patterns, which suggest the generation of intra-specific genetic variability through genome re-arrangement.

Retro-transposons are widespread in plant genomes in high copy number, representing a 4–8 % of the genome of *Arabidopsis* to a 50–80 % in the case of maize (Kumar and Bennetzen, 1999). The example of the *Ty1/copia* Hunk-2 has an estimated copy number of 200 000 in maize

(Meyers et al., 2001). However, they discuss that elements with high-copy number are not expressed, whereas elements with low-copy number are usually transcriptionally active. A cause of –endogenous– activation of transposons is DNA methylation. Mutants of *Arabidopsis* deficient for DNA methylation were shown to have a higher number of integrated copies of one class of retro-transposons (Miura et al., 2001).

1.8 Mechanisms of gene silencing in plants

Gene silencing involves epigenetic processes. They can be classified depending on the level they reduce –or completely switch off– gene expression: at the pre-transcriptional or at the post-transcriptional level. These mechanisms also protect the plant genome from transposons and viruses. It could be seen as an ancient immune system protecting from several infectious DNA.

1.8.1 Pre-transcriptional control

Mechanisms silencing gene expression at the pre-transcription stage include DNA methylation and histone modifications that create a heterochromatic environment in which the transcriptional machinery cannot enter. This process has major effects in development (Kwon and Wagner, 2007).

The *ddm1* mutant of *Arabidopsis*, impaired in DNA methylation, was isolated from a raw screen from EMS-mutagenized plants with hypo-methylation in centromeric repeats (Vongs et al., 1993). Later on, Jeddeloh et al. (1998) observed that the DDM1 locus is required for maintaining gene silencing in *Arabidopsis*. Another mutant impaired in methylation, *met1* (MET1 encodes a cytosine-DNA-methyl-transferase gene), was characterized by Kankel et al. (2003). They suggested that MET1 has a direct role in cytosine methylation. A *met1* background can release retro-transposition of certain elements, which later decays, suggesting that not only there is a transcriptional suppression, but also tailored silencing mechanisms in retro-transposon life-cycle (Mirouze et al., 2009).

Lister et al. (2008) presented a comprehensive map of *Arabidopsis* methylome, studying mutants defective in maintenance, establishment and demethylation. They found altered transcription of many genes, transposons and non-annotated transcripts, related with extensive changes in methylation. Furthermore, they directly linked the biogenesis of small RNA molecules with a decreased methylation state.

1.8.2 Post-transcriptional control

Post-transcriptional mechanisms involve the degradation of the mRNA of the target gene through several RNA silencing pathways (Brodersen and Voinnet, 2006). RNA silencing refers to the inhibition, sequence-specific, of gene expression at the transcriptional, mRNA stability or translational levels.

The pathway of double-strand RNA (dsRNA) involves the generation of short interfering RNAs (siRNA). These siRNAs are the product of juxtaposed *cis*-antisense (trans)gene pairs. 21 nt siRNAs are mainly involved in mRNA cleavage, whereas 24 nt siRNAs mediate, exclusively, chromatin modifications. RNA-dependent RNA polymerases were found to be involved in this

post-transcriptional silencing (Dalmay et al., 2000) in trans-gene silencing, and also as a response to virus defence (Mourrain et al., 2000).

Another type of interfering small RNAs are the microRNAs (miRNAs). They are usually 20–24 nt-long and originate in a non-coding transcript with an intricate fold-back structure. miRNAs induce targeting transcript degradation by cleavage (Bartel, 2004). Many of them have been found in *Arabidopsis*, with roles in development, physiology and stress responses. Specifically, Jones-Rhoades and Bartel (2004) found that plant miRNAs are well conserved between *Arabidopsis* and *Oriza sativa*, and miR395 was found to be up-regulated under sulphate deprivation conditions.

1.9 Development of reproductive structures in plants

Different reproductive structures have evolved in parallel since evolution proved to plants that protecting the gametophyte, specially the mega-gametophyte and the early stages of sporophyte development, is an advantage in reproduction. Some of the latest evolutionary examples include seeds and flowers. Interestingly, whereas these structures have gained in complexity, the gametophytic structures, directly used for exchanging genetic material between individuals, have been extremely simplified.

1.9.1 Flower development in *Arabidopsis*

Smyth et al. (1990) presented a comprehensive and detailed study of early flower development in *A. thaliana*. They defined *early* as the development processes in between bud formation and anthesis and divided the development in 13 different stages: during stages 1 and 2, the flower buttress arises and the flower primordium is formed; stages 3 to 6 limit the sepal formation and the coverage of the meristem by the sepals, during these stages, petal and stamen primordia are formed; stages 7 to 10 review the stamen development; stages 11 to 12 represent the growth of the gynœcium and elongation of stamens and petals; in stage 13, petals can be already seen between sepals meanwhile the gynœcium continues growing until the stigma is fully formed. During stage 14, anthesis takes place.

1.9.2 Gametophyte development

Plants, in contrast to animals, do not set aside a germ-line, instead, the cells that undergo meiosis produce a haploid structure called gametophyte which differentiates in the adult plant during flower development (Walbot, 1985). In angiosperms, the gametophyte is basically reduced to a minimalistic structure (embryo sac and pollen grains) which are always protected by structures from the sporophyte. Two kinds of gametophytes exist in angiosperms, the mega-gametophyte or embryo sac, and the micro-gametophyte or pollen grain.

1.9.2.1 Micro-sporogenesis and micro-gametogenesis in *Arabidopsis*

For the formation of the male spore, a sporophytic diploid cell (mother cell) is divided by meiosis into four microspores forming the tetrad (Figure 1.5). Each microspore undergoes an asymmetrical division, where the vegetative cell takes most of the cytoplasm and the generative cell only a small

fraction. Subsequently, the generative cell is absorbed by the vegetative cell and undergoes a mitosis forming the two sperm cells (McCormick, 1993). Recently, it was reported that *DDM1* and many siRNAs related to silencing of transposable elements are down-regulated in the vegetative cell, which re-activates TE expression in pollen. Furthermore, they found that siRNAs produced in TE biogenesis in the vegetative cell, are used for triggering siRNA-mediated silencing of TE elements in the sperm cells. Combined with the expression of *DDM1* in the sperm cells, the genetic integrity of the sperm cells is secured (Slotkin et al., 2009). After pollination, the vegetative cell migrates through the stigma as the pollen tube grows. The sperm and vegetative nuclei lead this migration (McCormick, 1993). The development of pollen grains –or micro-gametophyte– only finishes when the two sperm cells are released into the embryo sac. The genetic control of this processes is tightly regulated (McCormick, 2004).

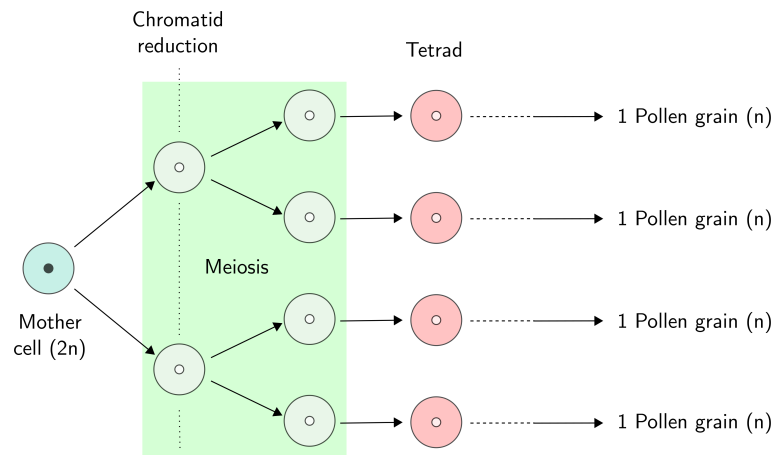


Figure 1.5: Schematic overview of micro-sporogenesis. One mother cell undergoes meiosis to form 4 microspores that will undergo two more asymmetrical mitoses to give rise to the mature pollen grain. Modified from the [original design](#) of Emmanuel Boutet. Released under the Creative Commons Attribution and ShareAlike (CC-BY-SA v2.5) license.

1.9.2.2 Mega-sporogenesis and mega-gametogenesis in *Arabidopsis*

The mega-sporogenesis process is very similar to the process observed for the male spore, with the only difference that, apart from taking place in the ovule and not in the anther, from the four female spores obtained by meiosis, only one survives and the other three undergo cell-death (Yadegari and Drews, 2004).

The mega-gametophyte or female gametophyte development is somehow more complex than the micro-gametogenesis. In this case, the surviving megaspore undergoes 2 subsequent mitoses without cellularization. These two mitoses generate 8 nuclei. Four of them are closer to the micropylar structure of the developing ovule and give rise to the egg cell, the two synergid cells and one polar nucleus. The other four nuclei, placed opposite the synergid cells and egg cell in the embryo sac, produce the three antipodal cells, that eventually undergo cell death before fertilization. In each of the poles of the gametophyte there is a polar nucleus that fuse together giving rise to the homo-diploid central cell (Yadegari and Drews, 2004).

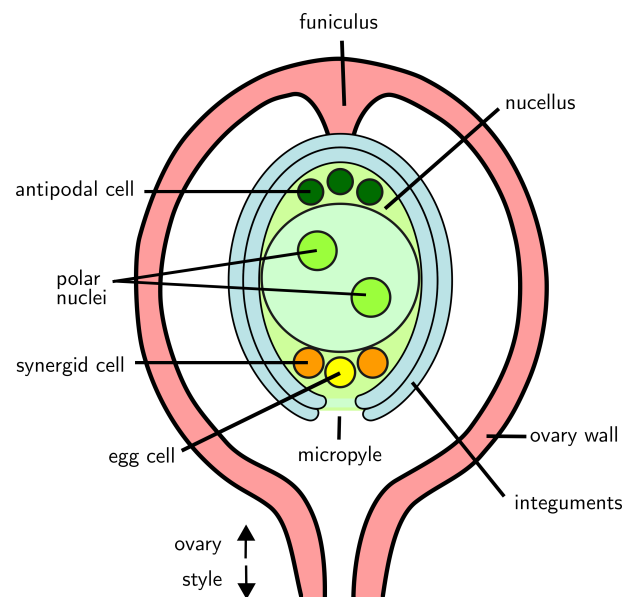


Figure 1.6: Schematic overview of the mega-gametophyte in the ovary. The egg cell is located in the micropylar pole together with the two synergid cells. Opposite in the embryo sac are located the antipodal cells and in the central area of the embryo sac the two polar nuclei are located. The two polar nuclei fuse just before fecundation to form the central cell.

The development of the gametophyte takes place in the developing ovule. Maternal tissues develop synchronously during spore and gametophyte development (Robinson-Beers et al., 1992). Specifically, the inner integument cell layer covers the nucellus (future embryo sac) after the sporogenesis, and before the gametophyte development is complete (Figure 1.6). In this same study, the authors framed the different developmental stages of the mega-gametophyte in the flower developmental stages already described by Smyth et al. (1990).

1.10 Genetic exchange in *Arabidopsis*

Genetic exchange between individuals of the same species is a powerful tool for adaptation and evolution. Plants have developed strategies to overcome the fact that they are sessile organisms.

1.10.1 From pollination to fertilization

Pollination is the process of transferring pollen grains between different plant structures or different plants from the same species, allowing genetic information exchange and thus, sexual reproduction. In *Arabidopsis*, the process of self-pollination is favoured in the species. Whereas this fact hinders the genetic exchange between different individuals, it makes easier the study of the species as a model organism (Meinke et al., 1998). Fertilization in plants is the actual process of gamete fusion.

Pollination starts with the adhesion of the pollen grains to the receptive stigma. At this point, the pollen grain is recognized by the stigma that releases water in order for the pollen grain to be able to germinate (Pruitt and Hülskamp, 1994). The germination of the pollen grain continues with the formation and elongation of the pollen tube. The pollen nuclei lead the growth of this tube and the process is controlled by the surrounding female structures, since the masculine gametes are not mobile (Pruitt and Hülskamp, 1994). In the last phases, the pollen tube grows in the funiculus, and prior to fertilization, seems to be directly guided by precise cross-talk between the two gametophytes. Specifically, factors from the synergid cells and the central cell (Chen et al., 2007) are essential for the micropylar pollen tube guidance. When the pollen tube enters the micropyle, it discharges its contents in the space left by one of the two synergid cells that undergo cell death (Dresselhaus and Márton, 2009).

1.10.2 Double fertilization

Fertilization in *Arabidopsis*, like in most angiosperms, consists not only in the fertilization of the egg cell by one sperm cell to form the zygote, but also in the fusion of the other sperm nucleus from the pollen grain with the homo-diploid central nucleus (Berger et al., 2008). Thus, in *Arabidopsis*, the endosperm has two copies of the maternal information coming from the homo-diploid central cell and only one copy of information of paternal origin.

The evolutionary significance of the double fertilization was taken from embryo studies in *Gnetum*, an extant gymnosperm genus, close-related to angiosperms. In this species, a rudimentary double fertilization was observed (Carmichael and Friedman, 1995) in which only one embryo completes development, whereas the other embryo is used as nourishment. This was taken as a proof for the supra-numerary embryo origin of the endosperm (Friedman, 2001).

1.11 Early development of the sporophyte

The main tissue types of *Arabidopsis* and the architectural axis of the plant-to-be, are already present shortly after the formation of the new zygote (Nawy et al., 2008).

1.11.1 Processes in zygote formation

Once the sperm cells are discharged into one of the synergid cells inside the embryo sac, several processes occur. Faure et al. (2002) made a comprehensive study of the changes from the moment the paternal genetic information enters the embryo sac. First, they observed that both synergid cells had the ability to receive the contents from the pollen tube. They also observed how the polarity of the egg cell changed, as the nucleus moved closer to the micropyle from its original place, closer to the central cell boundary.

Although fertilization seems to occur first in the egg cell followed by the central cell (Ingouff et al., 2007), divisions start earlier in the fertilized central cell –to form a syncytium– than in the zygote that only enlarges its shape (Faure et al., 2002). Both sperm cells are exchangeable for fertilizing either the egg cell or the central cell (Ingouff et al., 2009).

Divisions start in the fertilized zygote in an asymmetrical way: the basal cell, that will give rise to the embryo suspensor, contains more cytoplasm –and is longer– than the apical cell that will produce the embryo. The basal cell divides transversally and the daughter cells grow longitudinally. Whereas the apical cell divides longitudinally and transversally to form the globular embryo (Mayer et al., 1991).

1.11.2 Pattern formation in the *Arabidopsis* embryo

From the first division, the zygote shows a polarity that is established by auxin flux, as reported by Friml et al. (2003), where they showed that the globular embryo receives auxin from the suspensor cells. This polarity is reflected in the subsequent development of the embryo.

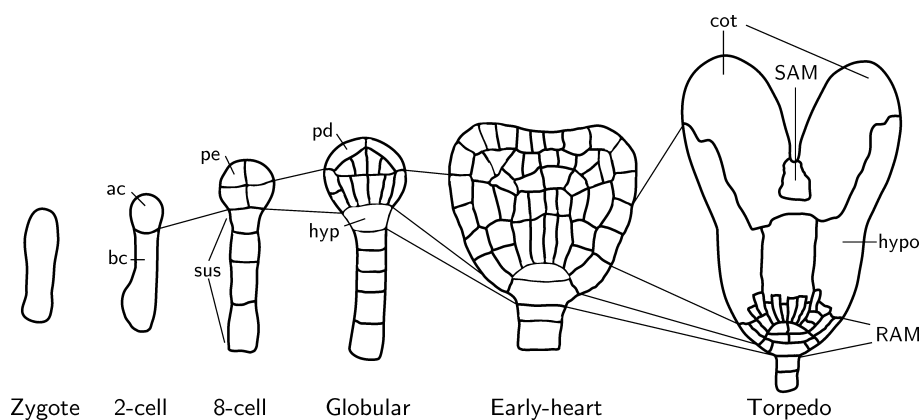


Figure 1.7: Schematic overview of *Arabidopsis* embryo patterning. ac: apical cell, bc: basal cell, pe: pro-embryo cell, sus: suspensor cells, pd: protoderm cell, hyp: hypophysis cell, cot: cotyledons, hypo: hypocotyl, SAM: shoot apical meristem, RAM: root apical meristem. Adapted from Möller and Weijers (2009).

Jürgens et al. (1991) described for the first time the pattern formation in the *Arabidopsis* embryo (Figure 1.7), which was very similar to previous studies from other dicotyledonous plants. The classification divides the embryo development based on the morphological shapes –patterns– the embryo attains. The classification starts with the *octal* embryo, composed by only 8 cells. Continues with the *globular* stage, when the embryo has more than 16 cells and a round shape. The name of the *heart*-shaped embryo remembers the shape of the developing gametophyte in ferns. As the cotyledons grow, and the hypocotyl expands, the embryo attains a *torpedo* shape. Later on, following more cell divisions, the growing cotyledons bend over lying next to the hypocotyl and conforming the mature embryo. Jürgens et al. (1991) introduced a *triangle* stage just before the heart shape stage to reflect the symmetry change at that time-point.

1.11.3 Endosperm role

The endosperm is the second fertilization product in the ovule sac which transmits nutrients to the embryo, but does not contribute with its genome to the next generation. Furthermore, it plays a central role in seed development: a successful double fertilization is required for complete seed

and fruit development. The seed containing the embryo and a fertilized endosperm has exclusively evolved in angiosperms, although in gymnosperms a rudimentary mechanism exists: the embryo sac in gymnosperms contains several egg cells which are fertilized and form a poly-embryonic seed. However, only one embryo survives whereas the rest are used as nutrient provision for the surviving embryo (Buchholz, 1920).

Development of the endosperm is tightly regulated through nuclear and cell division, differentiation and parental dosage (Berger, 2003). Development of the endosperm starts when the central cell starts dividing. This division takes place earlier than the divisions of the zygote. The divisions in the endosperm are not followed by cellularization, instead, a syncytium is formed. Only later on, the endosperm starts to cellularize in the area in contact with the developing embryo. More specifically, Boissard-Lorig et al. (2001) showed that the control of the cell cycle creates mitotic domains in different areas of the endosperm after observing the accumulation pattern of *CYCLINB1*;1. Furthermore, the cellularization process was observed to be genetically controlled, since *AGL62* reduces its expression after endosperm cellularization (Kang et al., 2008).

1.11.4 Genomic imprinting

Genomic imprinting is the expression of genes in a parent-of-origin-specific manner. Only mammals and angiosperms have been shown to develop genomic imprinting. It involves an inheritance process which is independent of the classical mendelian inheritance: it depends on differential DNA methylation of the two alleles (Scott and Spielman, 2006). In plants, the endosperm is the only known place where genomic imprinting plays a role in plant development. The mechanism of imprinting in plants involves differences in chromatin structure and DNA methylation between paternal and maternal alleles which are differentially expressed (Gehring et al., 2004).

Imprinting is seen in the endosperm through a balanced amount of maternal and paternal genetic information (two copies from the mother, one copy from the father). It was observed that when the maternal and paternal dosage is not balanced, a miss-expression of imprinted PcG genes like *MEDEA* takes place, producing aberrant seeds (Erilova et al., 2009).

Another example of genomic imprinting has been found by Bayer et al. (2009). They showed that specific paternal transcripts, which are delivered with the sperm cells, are transiently translated in the zygote and endosperm. Translation of the paternal transcripts triggers the transcription of *YODA* (*YDA*), a mitogen-activated protein kinase involved in the early-elongation of the embryo and the differentiation of the suspensor and embryo cells.

Recently, Gehring et al. (2009) found that fragments from transposable elements are extensively de-methylated in the endosperm. Through association of genes preferentially expressed and hypo-methylated in the endosperm new imprinted genes were identified. The authors also suggested that the whole mechanism of imprinting in plants arose, in the evolutionary process, from methylation of transposable elements in the neighbourhood of genic regulatory elements (Gehring et al., 2009).

1.11.5 Reproductive interplay in seed development

The seed itself consists of three basic units representing three different organisms: the embryo, which is the new sporophyte generated by the fusion of the egg cell and the sperm cell; the endosperm that is the fertilization product of a second sperm cell and the homodiploid central cell; and the integuments which are part of the sporophyte. In order to form one functionally-integrated whole, these three organisms have to tightly coordinate their growth and development through feed-back signalling events (Berger, 2003).

A recent study reflects the interdependency of embryo and endosperm through a signal from the fertilized egg cell that triggers the endosperm development (Unguru et al., 2008). Furthermore, the authors reviewed later on (Nowack et al., 2010) that specifically, the globular embryo needs a signal from the endosperm in order continue with the development. Interestingly, when a *fis* mutant is fertilized by *cdka;1* pollen (only the egg-cell is fertilized and no nuclei fusion takes place for the central cell), it can complete seed development (Nowack et al., 2010). In these *fis* × *cdka;1* seeds, the fertilized embryo develops next to a diploid endosperm lacking the paternal information. This is an indication that the embryo can trigger not only the differentiation of the endosperm, but also –directly or indirectly– communicate with the integuments that sustain the seed development and survival.

1.12 New technologies in gene expression profiling

Determination of the nucleotide sequence of the bacteriophage ϕ X174 by Sanger et al. (1978) started the race for genome sequencing. Nowadays, the genomic sequence of 41 eukaryotic organisms is *complete*, whereas 322 have been assembled and 388 more are in progress. Specifically in plants, 7 genomes are *completed*, 21 have been assembled and 85 are in progress (Entrez Genome Project). The race for genome sequencing is reaching an unprecedented level of detail, going towards the aim of making the sequencing of personal genomes a commodity (Venter, 2010).

For expression profiling, not only the genome sequence should be known, but also the genome of new-sequenced organisms must be annotated with gene models. Some strategies have arisen, like using RNA-Seq for building *de novo* gene models in grapevine (Denoeud et al., 2008). However, an accurate functional and biochemical annotation needs complex computational strategies: prediction and annotation of gene function must be based, not only in homology methods, but also in a combination of chromosomal gene clustering, phylogenetic and gene fusion information (Hsiao et al., 2010).

Only an accurate gene annotation together with the knowledge of the genomic sequence make it possible to study gene expression in an organism from a genome-wide perspective.

1.12.1 Microarrays

Fifteen years ago, the development of the cDNA arrays (Schena et al., 1995) allowed the simultaneous expression measurement of thousand of genes. At the same time, the oligo-nucleotide microarrays were developed by Affymetrix which are based in a photo-lithographic synthesis of the different oligo-nucleotide probes (Lipshutz et al., 1995, 1999).

In 2000 Affymetrix –in collaboration with Syngenta– developed the AtGenome1 array before the *Arabidopsis* sequence was completed, this first design contained 7 000 probe sets designed with several EST databases (Zhu and Wang, 2000). Later on, it was shown that the array had a different coverage of the different chromosomes (Borevitz et al., 2003).

After the completion of the sequencing of the *Arabidopsis* genome, Affymetrix released the ATH1 array which contains probe sets for identifying 24 000 genomic features (Redman et al., 2004). This array is based in the TIGRv2 annotation and sequence assembly release. Both arrays, despite the different order of magnitude in identifying miss-regulated genes, correlate globally well for expression data, with only a few exceptions (Hennig et al., 2003).

In 2007 and based on the TIGRv5 assembly, Affymetrix released the Tiling 1.0F and Tiling 1.0R arrays. Each of them contain 3,2 million probe pairs (perfect match and mismatch) tiled through the complete –non-repetitive– *Arabidopsis* genome. The Tiling 1.0F array –whose production was discontinued– contains one DNA strand, whereas the Tiling 1.0R array contains the complementary strand. The probes are 25 nt-long and are tiled at an average of 35 bp resolution, leaving a gap of approximately 10 bp between probes. Several papers described the use of this arrays, not only for measuring genome-wide gene expression in *Arabidopsis* (Naouar et al., 2009; Jones-Rhoades et al., 2007), but also for conducting pioneering studies in protein interactions with the genome (ChIP-on-chip, Ren et al., 2000) or for novel transcript identification (Shoemaker et al., 2001) in other species.

The latest development of Affymetrix for *Arabidopsis* is the AGRONOMICS1 array. The design is based on the sequence assembly of TAIR8 and contains the tiled sequence of both DNA strands in form of perfect match probes. The probes are 25 nt-long with a separation of 7 nt between probes of the same strand, and a separation of 16 nt between the centre points of partially-overlapping complementary probes. No mismatch probes were included due to the difficulties in data interpretation. In addition, all the perfect match probes from the ATH1 array were added. Custom definition files (CDFs) for quantitative transcriptome profiling in R/Bioconductor were made available, not only based on the TAIR8 annotation release, but also on TAIR9 (Rehrauer et al., 2010).

In this work, ATH1 and Tiling 1.0R arrays were used to analyse the transcription profile in an estradiol-regulated conditional complementation system and in the *prl1* mutant, respectively.

1.12.2 Next generation sequencing

Further developments of the polymerase chain reaction (PCR) for complementary DNA synthesis, allowed the process to be monitored in real time, retrieving the DNA sequence information during the synthesis process (Bentley, 2006; Shendure and Ji, 2008). Novel technologies, still in development (Peng and Ling, 2009), include techniques that do not rely on DNA complementary synthesis, but rather in the long-known property of DNA and RNA strands to sequentially modify an applied-electric field as they pass through a nano-pore (Kasianowicz et al., 1996).

The different commercialized technologies (as for 2009–2010) include the Illumina’s Genome Analyzer (based on the works of Fedurco et al., 2006; Turcatti et al., 2008), Roche’s 454 (based on pyro-sequencing, Ronaghi et al., 1998; Margulies et al., 2005), Applied Biosystems’ SOLiD (adapted from Shendure et al., 2005) and Helicos Biosciences’ HeliScope (Harris et al., 2008). These technologies are able to read thousands of millions of bases arranged in sequences in days. The

generated sequences are relatively short, typically from a few tens to a few hundred nucleotides in length, with an inverse relation between the total number of read sequences and the read length.

These technologies have allowed the re-sequencing of the genome of the Col-0 accession of *Arabidopsis thaliana* for the last TAIR release (v9) which introduced deep changes in already known gene-models, especially in its location in the genome (Ossowski et al., 2008). Furthermore, the 1001 Genomes Project is making use of these technologies in order to sequence the genome of several *Arabidopsis thaliana* accessions in a short time-frame.

The production of an incredible amount of data with these technologies, not only has risen concerns over effective analyses (Pop and Salzberg, 2008), but also over data storage and availability (Shumway et al., 2010) and visualization (Nielsen et al., 2010).

For this work the Illumina platform was used to sequence the *whole* transcriptome (RNA-Seq) of the *prl1* and *cdc5* mutants.

1.12.3 Data analysis development

The development of the different microarray and sequencing platforms also involves the parallel development of new techniques for a proper data analysis.

The case of the Affymetrix microarrays it is worth to note, since this was the first array platform widely used by the scientific community: the default expression measures performed with the Microarray Affymetrix Suite (MAS v5.0) could be significantly improved (Irizarry et al., 2003b). The new analysis work-flow and algorithms were published as an R package (Irizarry et al., 2003a; Gautier et al., 2003) which was the origin of Bioconductor (Gentleman et al., 2004): an Open Source project focused on the analysis of genetic data that runs on top of the R environment for statistical computing (Ihaka and Gentleman, 1996).

Pop and Salzberg (2008) commented the challenges that data analysis of next-generation sequencing may need to overcome. Two years later, the situation has developed to a point where many tools are available to perform multiple analyses. Due to the highly dynamic field of next-generation sequencing technologies, only Open Source solutions keep pace in order to perform a reliable data analysis (Richter and Sexton, 2009). Examples like Bowtie (Langmead et al., 2009), BFAST (Homer et al., 2009) or BWA (Li and Durbin, 2010) can efficiently map short reads against known genome sequences. Other Open Source tools are specific for studying gene structure, like TopHat (Trapnell et al., 2009), QPalma (Bona et al., 2008) or mGene (Schweikert et al., 2009). Furthermore, Open Source tools for *de novo* assembly of genomes use state-of-the-art algorithms (Miller et al., 2010). These tools include WGA Assembler/CABOG (Myers et al., 2000), MIRA (Chevreux et al., 2004) and Velvet (Zerbino and Birney, 2008; Zerbino et al., 2009).

Many commercial solutions are being developed nowadays. However, privative software does not use the most up-to-date algorithms, licenses are expensive and restrictive, programmes perform poorly and do not keep pace with the latest developments in sequencing technologies. Therefore, in this work Open Source tools were used to analyse the sequenced transcriptome of the *prl1* mutant of *Arabidopsis thaliana* Col-0.

1.13 Aims of this work

The major aim of this work was to further characterize the functions of *PRL1* and its paralogue *PRL2* in *Arabidopsis thaliana*. Therefore, the following questions were addressed: (1) the characterization of *PRL1* function, (2) the impact of the absence of *PRL1* at the level of transcription regulation and (3) the characterization of mutations in the *PRL2* locus.

The results will start with the characterization of *PRL1* functions. For this purpose, different approaches were followed, including the design of a genomic construct to express *PRL1* under native conditions and study its expression and *PRL1* accumulation under sucrose-deprivation conditions. The proteasome activity was monitored in the *prl1* mutant, as well as during a time-course with *PRL1* ectopic expression and depletion by activity-based protein profiling. *PRL1* was compared to its orthologues from several plant and non plant species.

Subsequently, to have a broader view on the regulatory functions of *PRL1*, multiple transcript profiling analyses were performed, involving tiling arrays, RNA-Seq of *prl1* and ATH1 arrays with an ectopic expression of *PRL1* in time-course experiment where *PRL1* accumulation decreases during time.

Following this, the results describing the characterization of *PRL2* are explained. This characterization was addressed through the phenotypic analysis of the *prl2/+* and *prl1 × prl2/+* mutants. In addition, the sub-cellular localization of *PRL2* and the transcription pattern of *PRL2* during plant development were studied. Due to the embryo-lethal phenotype of *prl2*, *prl2* conditional mosaics were generated in order to characterize the somatic phenotype of *prl2*.

Finally, to support the hypothesis of *PRL1* and *PRL2* sub-functionalization, *PRL1* and *PRL2* were ectopically expressed in *prl1* and *prl2* to characterize the complementation of the mutual phenotypes. Furthermore, chimeric constructs of *PRL1* and *PRL2* were designed and transformed into *prl1* and *prl2* mutants to study the phenotype complementation and to add some knowledge on this sub-functionalization.

The thesis is closed by a general discussion of the results to answer the specific questions posed above and to contribute to understand the regulatory mechanism controlled by *PRL1* and *PRL2* in *Arabidopsis*.

2. Results

2.1 Characterization of *PRL1* functions

PRL1 has been one of the first general regulatory factors described in *Arabidopsis*, which influences the transcript levels of numerous genes involved in the control of well defined hormonal and stress responses pathways (section 1.1.1). *PRL1* was found to be a member of a highly conserved class of eukaryotic nuclear WDR proteins, which have been associated to spliceosome-activating complexes, from yeast to humans (section 1.2.1). Purification and functional analysis of plant-spliceosomal components lag much behind compared to other systems, so far no *in vitro* splicing assays could be developed in plants due to difficulties in isolation of the spliceosome and the associated regulatory factors. To facilitate the isolation of nuclear protein complexes, our laboratory has developed a novel combined affinity tag (section 4.2.6.1), which has been used in this work to assay expression and stability of the *PRL1* protein in genetically-complemented *prl1* mutant plants.

2.1.1 *PRL1*-PIPL complements the *prl1* phenotype

The pPCV002-*PRL1*::*PRL1*-PIPL construct (section 4.2.6.1) which carries the triple affinity tag developed by Horváth (2008) is a suitable tool to analyse native expression of *PRL1* and also, to detect protein-protein interactions in transient expression assays performed with *Agrobacterium*-infected plant tissues or with *Arabidopsis* cell cultures.

2.1.1.1 Expression analysis

Correct expression of the pPCV002-*PRL1*::*PRL1*-PIPL construct and production of the tagged *PRL1* protein was first assayed in *Agrobacterium*-transformed light-grown photosynthetic *Arabidopsis* (Col-0) cell suspension by Western blot analysis with a monoclonal α -HA and a polyclonal α -*PRL1* antibody (Figure 2.1).

As a control, a sample from plants expressing a *PRL1* cDNA construct was used. In this construct, *PRL1* is tagged with the HA peptide and its expression is driven by a 2 \times CaMV35S promoter-controlled expression cassette (pPAMpat-*PRL1*-HA, section 4.2.6.2).

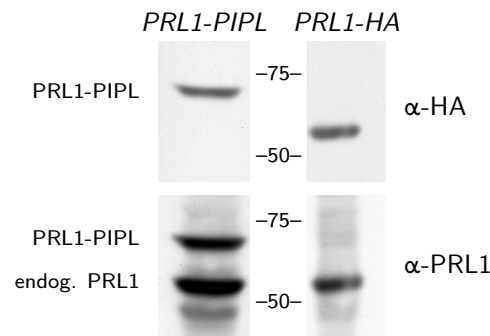


Figure 2.1: Western blot comparison of SDS-PAGE migration properties of PRL1-PIPL and PRL1-HA in protein extracts prepared from pPCV002-PRL1::PRL1-PIPL-transformed cell suspensions and pPAMpat-PRL1-HA transformed plants using α -HA and α -PRL1 antibodies. Size markers are indicated in kDa.

Comparison of the mobility of the PIPL-tagged and the HA-tagged PRL1 protein isoforms indicated that the C-terminal PIPL tag causes a shift in the apparent molecular mass of the tagged PRL1 protein. This shift in migration is larger than the inferred difference in size. Addition of the PIPL tag (6,73 kDa) increased the apparent molecular mass of the PRL1 protein (54 kDa) to about 70 kDa. However, detection of the same PRL1-PIPL protein band, which cross-reacted with both α -HA and α -PRL1 antibodies, indicated that this unexpected migration of the PRL1-PIPL protein is conferred by structural features of the PIPL tag. By contrast, the HA-labelled (1,1 kDa) PRL1 protein co-migrated with the endogenous PRL1 protein produced in both cell suspensions and plants. Confirmatory DNA sequencing of the pPCV002-PRL1::PRL1-PiPL construct also excluded that this aberrant migration behaviour of PRL1-PIPL on SDS-PAGE gel would be caused by an unexpected cloning error. Similar alteration in the expected SDS-PAGE migration behaviour has been also observed with other PIPL-tagged proteins (M. Horvath, T. Sarnowski, unpublished).

2.1.1.2 Complementation analysis

To demonstrate that the C-terminal fusion of the PIPL tag did not alter the functionality of PRL1, the pPCV002-PRL1::PRL1-PiPL construct was transformed by *Agrobacterium* into the *prl1* (Koncz) mutant and control wild type (Col-0) plants using the floral-dip method. From both transformations, 20 T1 seedlings were selected on MSAR plates containing kanamycin. All 20 T1 plants in the *prl1* mutant background showed a wild type root length phenotype as control Col-0 transformants. In contrast, the *prl1* mutant displays a characteristic defect in root elongation and growth (Németh et al., 1998). This result demonstrated that the addition of PIPL did not alter the functionality of PRL1, whose expression conferred the genetic complementation of the *prl1* mutation. Upon self-pollination of T1 plants, T2 seeds were germinated on kanamycin to identify lines showing a 3:1 segregation ratio of resistant:sensitive progeny with wild type root elongation. Single insertion-complemented lines of pPCV002-PRL1::PRL1-PiPL T-DNA were identified. By assaying the germination of the T3 seed progeny on kanamycin or hygromycin (marker of the *prl1* insertion mutation, Németh et al., 1998) containing media, PRL1-PIPL/*prl1* lines carrying the complementing T-DNA construct in homozygous form were identified.

2.1.2 *PRL1* transcription is sucrose-independent

Németh et al. (1998) demonstrated that the *prl1* mutation enhances the sensitivity to added sucrose or glucose in the germination medium. To assess whether *PRL1* would act as a primary regulator in a sugar-regulated signalling cascade, *PRL1* transcription was measured in a genetically complemented *PRL1-PIPL/prl1* line. Seedlings from this line were germinated and grown on solid MSAR solid media containing either 0,1 % or 3 % of sucrose under short day (SD) conditions. Samples from three biological replicates were harvested every 4 hours during 2 days. Dr. Femke de Jong helped with the sowing, harvesting and grinding processes.

RNA was extracted from the samples using the QIAGEN RNeasy Plant Mini Kit (QIAGEN) and converted to cDNA for QPCR analysis as described in sections 4.2.7.2 and 4.2.7.3. Abundance of the *PRL1-PIPL* transcript was measured by QPCR using the PiPL-F and PiPL-R primers (Table A.2). For normalization of the amounts of cDNA template across the samples and replicates, the ubiquitin (*UBQ5*, AT3G62250) UBQ-F and UBQ-R primers were used. The efficiency of both PIPL and UBQ primer pairs was compared by regression analysis of a dilution series using one control sample. As the efficiencies of PIP-L and UBQ primers proved to be equal, the $\Delta\Delta C_t$ method (section 4.2.7.3) was used for comparing the different time-points and treatments.

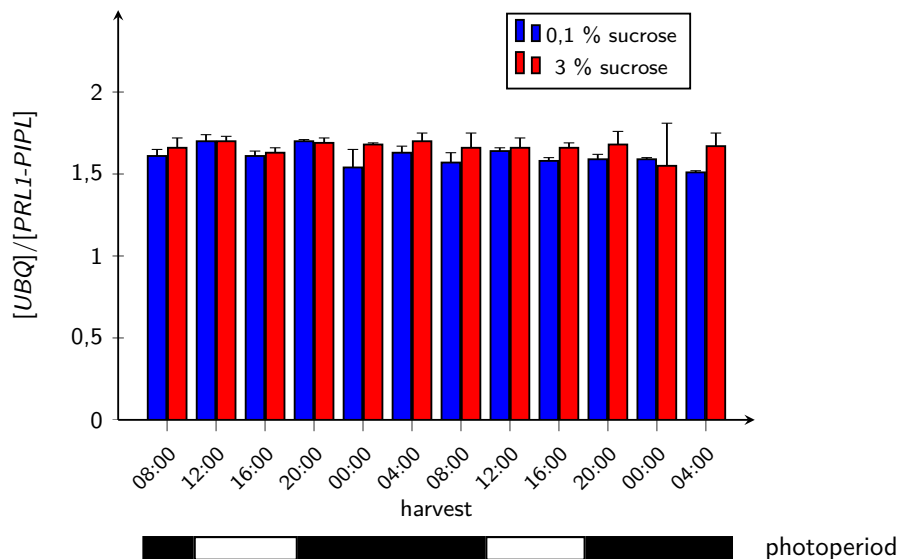


Figure 2.2: QPCR measurement of *PRL1-PIPL* transcript levels during the day-night cycle in *PRL1-PIPL/prl1* plants grown in the presence of 0,1 % and 3 % sucrose. Transcript levels of ubiquitin were used as reference to normalize *PRL1-PIPL* expression across samples and replicates.

As illustrated in Figure 2.2, no difference was detected in *PRL1* transcript levels between the studied time-points of the day-night cycle and between seedlings grown in the presence of 0,1 % and 3 % sucrose.

2.1.3 PRL1 accumulation is sucrose-dependent

To analyse whether the accumulation of PRL1 is affected by the availability of external sucrose during the day-night cycle, the PRL1-PIPL/*prl1* samples harvested for section 2.1.2 were subjected to a nuclear extraction protocol with the help of Dr. Femke de Jong, as described in section 4.2.10.2. Protein samples were size-separated by SDS-PAGE and subjected to Western blot analysis with α -HA and α -H3 IgGs (section 4.1.7.1). To perform a quantitative evaluation of reaction signals, the primary α -HA signal was visualized with a 680 nm-fluorescent dye-conjugated secondary antibody (Goat Alexa Fluor 680 α -rat IgG), whereas the α -H3 cross-reacting band was visualized with a 800 nm-emitting fluorescent dye-conjugated secondary antibody (Goat IRDye800 Conjugated α -rabbit IgG, Table 4.5). Both fluorescence signal intensities were quantitatively measured by scanning the membranes in an Odyssey Infrared Imaging System (Licor Biosciences). PRL1-PIPL amount across samples was measured with the α -HA signal and normalized across samples with the α -H3 signal.

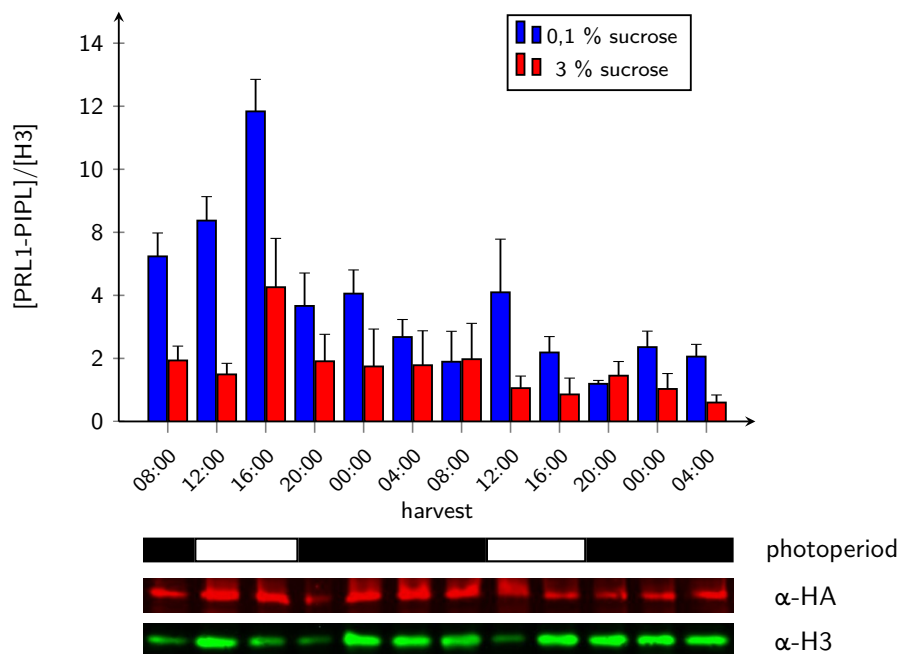


Figure 2.3: Comparison of PRL1-PIPL accumulation during the day-night cycle in PRL1-PIPL/*prl1* seedlings grown in the presence of either 0,1 % or 3 % sucrose. Measurement of Histone 3 (α -H3) levels was used as internal reference.

The results showed that in the majority of samples, PRL1-PIPL levels were at least 2-fold higher in seedlings grown in the presence of 0,1 % sucrose compared to samples grown with 3 % sucrose (α -HA). Whereas little variation was observed between sampling time-points in seedlings grown on 3 % sucrose during the day-night cycle. Seedlings grown in the presence of 0,1 % sucrose showed a tendency of higher PRL1-PIPL accumulation during the day compared to samples harvested at night. Nevertheless, these differences were not repeated during the second day, indicating that this technology has an inherent error in quantitative measurement of PRL1-PIPL protein levels. Therefore, in connection to the time-course transcript profiling experiments described

in section 2.2.4, it remains necessary to use a β -estradiol-dependent complementation system, in which *PRL1* expression can be silenced in the *prl1* mutant. This would help in determining precisely the kinetics of both *PRL1* transcript and product.

2.1.4 *PRL1* depletion does not affect the proteasome catalytic activity

Farrás et al. (2001) demonstrated that *PRL1* reduces the interaction of SKP1/ASK1 with the SnRK1 kinase catalytic subunits that target SCF (SKP-Cullin1-F-box protein) E3 ubiquitin ligases to the $\alpha 7$ -subunit of the 20S proteasome subunit. As *PRL1* was shown to act as inhibitor of SnRK1 kinase activity and compete with SKP1 and proteasome binding of SnRK1 enzymes in vitro, it appeared plausible that the catalytic activity of the proteasome could be affected by the *prl1* mutation.

To test this possibility, the β -estradiol-dependent conditional genetic complementation system was used. This system allows the study of the effects caused by timely depletion of *PRL1* levels in a *prl1* background. For this purpose, a *prl1* line (named ER-*PRL1/prl1*) transformed with the pER8(Km)-*PRL1*cDNA vector was used. In this line, *PRL1* is only expressed by the presence of β -estradiol in the culture medium (Szakonyi, 2006). The T-DNA of pER8(Km)-*PRL1*cDNA vector carries a minimal 35S promoter, which is fused to the *LexA* operator. In addition, it includes a constitutive promoter-driven hybrid gene that encodes a fusion protein carrying the *LexA* DNA binding domain fused to the VP16 transcription activator and human receptor of β -estradiol. In the presence of β -estradiol, the hybrid β -estradiol receptor is activated and binds as a dimer to the *LexA* operator site, driving the transcription of *PRL1* in the *prl1* mutant (Figure 2.4). Conversely, removal of plants from the β -estradiol-containing medium causes a depletion of the hormone content, which results in a stop of *PRL1* transcription followed by a decay of both *PRL1* transcript and product. The *prl1* phenotype is then manifested (Szakonyi, 2006).

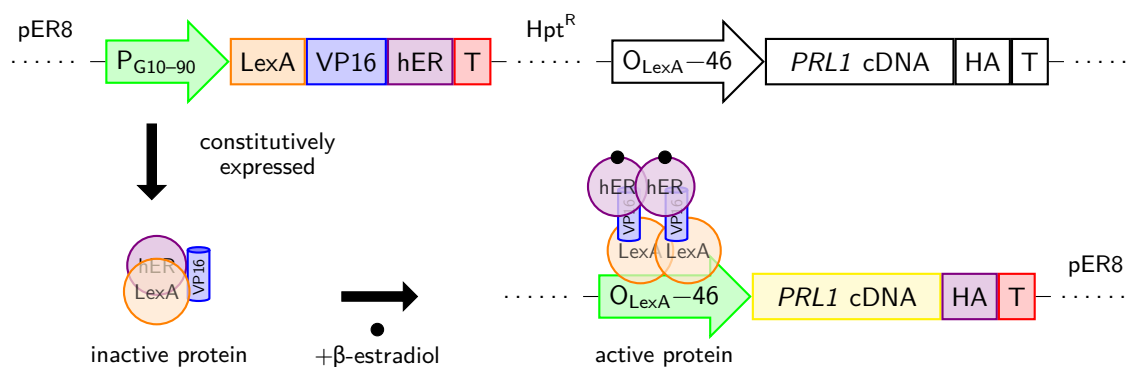


Figure 2.4: Schematic representation of pER8(Km)-*PRL1*cDNA-HA construct (Szakonyi, 2006) used for the β -estradiol-dependent complementation. *PRL1* is only expressed in the presence of β -estradiol. Details in section 2.1.4.

The activity-based proteasome profiling assay is based on the use of a fluorescent probe (MVB072, kindly provided by R. van der Hoorn) which specifically targets the active $\beta 1$, $\beta 2$ and $\beta 5$ subunits of the 20S proteasome complex. Thereby, the proteasome activity can be monitored both qualitatively and quantitatively by SDS-PAGE analysis as described in section 4.2.10.4.

Seeds from the complementing ER-PRL1/*prl1* line #5 (Szakonyi, 2006), Col-0 WT and *prl1* were germinated and grown on solid MSAR medium containing 4 μ M of β -estradiol. Following 2 weeks, seedlings were transferred to solid MSAR medium without β -estradiol. Samples were harvested at the day of transfer (d0), three (d3) and five (d5) days after transferring the seedlings to medium without β -estradiol.

Protein extraction for activity-based profiling of the proteasome was performed as described in section 4.2.10.6 with the help of Johana Misas Villamil. Following size separation of the extracted proteins by SDS-PAGE, the gels were subjected to the measurement of the amount of active proteasome-binding MVB072 probe. In addition, depletion of PRL1 and the changes in the levels of the α 1-3, 5-7 and Rpn6 proteasome subunits were measured during the time-course by Western blot. Due to the conferred expression of an HA-tagged PRL1 protein (PRL1-HA) by the pER8(Km)-PRL1cDNA conferred expression, PRL1 accumulation could be monitored using α -PRL1 and α -HA antibodies.

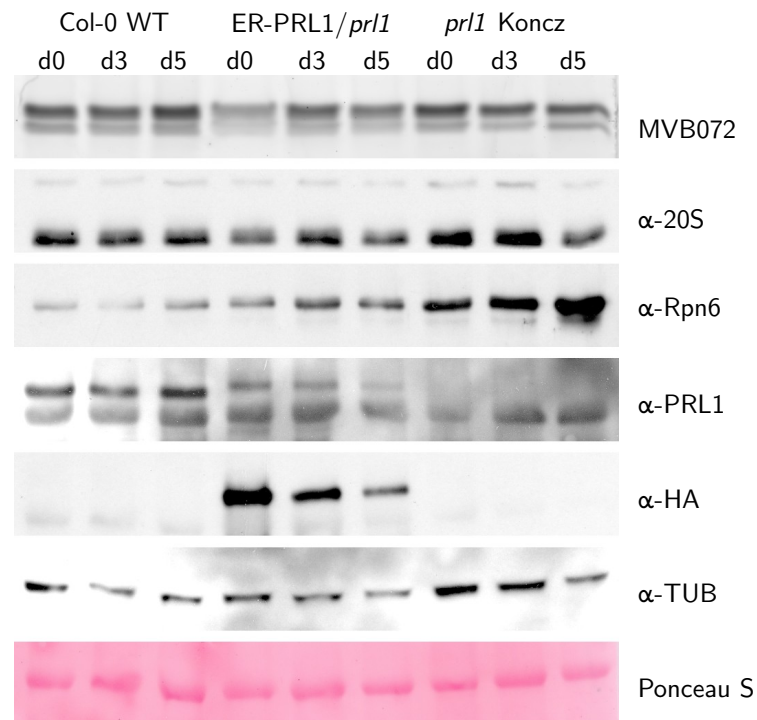


Figure 2.5: Activity-based profiling of the proteasome measured with the MVB072 fluorescent probe. Samples were harvested in complementation-induced conditions (d0), three days (d3) and five days (d5) after transferring to medium without β -estradiol. The fluorescent probe MVB072 was used to detect the proteasome activity, whereas α -20S and α -Rpn6 antibodies were used to monitor the levels of proteasomal subunits. Changes in PRL1 levels were detected with α -PRL1 and α -HA antibodies. Equal loading of protein samples was normalized using α -TUB antibody and Ponceau S staining.

As shown by Figure 2.5, β -estradiol-treatment of WT plants did no affect PRL1 accumulation. Similarly, no PRL1 was detected in the *prl1* mutant at any time point of the analysis. The Western

blot of both α -PRL1 and α -HA indicated that following the β -estradiol removal, the levels of PRL1 gradually decreased in the conditionally-complemented ER-PRL1/*prl1* line. At day 5 (d5) this level reached about 10–15 % of day 0 (d0) value. Depletion of PRL1 did not cause a significant change in the levels of the α -subunits detected by the α -20S proteasome antibody. In addition, the levels of these proteasome subunits were also comparable to those in the WT and *prl1* samples. Although at d0, somewhat less MVB072 binding was detected in the ER-PRL1/*prl1* sample, no significant effect of PRL1 depletion during the time-course was found, and total cellular proteasome activities detected in WT and *prl1* samples were comparable at all examined time-points. However, the results showed that the level of the Rpn6 proteasome-regulatory subunit (α -Rpn6, Figure 2.5) was increased in response to PRL1 depletion. In addition, Rpn6 accumulation is significantly higher in the *prl1* mutant compared to the partly PRL1-depleted sample d5 of ER-PRL1/*prl1* and WT samples.

2.1.5 PRL1 is highly conserved in the kingdom plantæ

Alignment of PRL1 amino acid sequence with several other species was already published by Németh et al. (1998) comparing *Arabidopsis* PRL1 to yeast, human and *Caenorhabditis elegans* orthologues, to make the case for an evolutionary conserved function. Specifically, the C-terminal region, containing 7 WD40 motifs, showed the highest identity score, whereas the N-terminal regions were divergent (Figure A.6 on page 146).

For this work, the phylogenetic analysis of PRL1 and PRL2 was extended with sequences of recently-sequenced plants and algae, including *Populus trichocarpa*, *Vitis vinifera*, *Oriza sativa*, *Zea mays*, *Physcomitrella patens*, *Chlamydomonas reinhardtii* and *Ostreococcus tauri* (Figure A.7 on page 148).

The results from this alignment show that PRL1 is very conserved in the kingdom plantæ (Figure 2.6). However, *Ostreococcus tauri* and *Chlamydomonas reinhardtii* orthologues show considerable divergence, suggesting that the functions of PRL1/PRL2 orthologues may differ in unicellular algae. Interestingly, in *C. reinhardtii*, the whole N-terminal region is missing (Figure A.7). This assumption is in accordance with the result of alignments with sequences from even more distant species. The N-terminal region of *A. thaliana* PRL1 shows minimal identity with orthologues in budding and fission yeast, chimpanzee and human (Figure A.6).

The alignment of the first 146 amino acids of *Arabidopsis* PRL1 with orthologues across plants, yeast and hominidæ (Figure 2.6) reveals a completely different sequence with only few common amino acids. Using the N-terminal sequence of *A. thaliana* PRL1 (amino acids 1 to 146) as query in the UniProtKB database found only orthologues from higher plants like rice and maize. However, no hit was found for organisms outside the kingdom plantæ. Furthermore, when the amino acid sequence was analysed with the InterPro database, no domain with known function was identified. Together, these results reveal an evolutionary divergence of N-terminal sequences that can have an impact in the function of the different orthologues. Specifically, this divergence can bias the decision on assigning a conserved function to PRL1 in *Arabidopsis*.

2.1.6 Isolated PRL1 domains fail to complement *prl1*

To determine whether evolutionary divergent N-terminal sequences of PRL1 are functionally essential and required for genetic complementation of the *prl1* mutation, D. Szakonyi developed

P. trichocarpa	MPGPTVEMEPTEPQSVKKLSFKSLKRTSDLFSPTHQAQLAPPDPESKKIRM	50
V. vinifera	MPGPTVEMEPVPEPQSLKKLSFKSLKRALDLFSP IHGHFAPPDPESKKIRL	50
A. thaliana	MPAPTTEIEPIEAQSLKKLSLKS LKRSLELFSPVHGQFPFPDPPEAKQIRL	50
O. sativa	...MATAEPVPEPQSLKKLSLKS LKRSRSHDLFAPTHSLLFTPDPESKQVRV	46
Z. mays	MATAAADGPPVEPQSLKKLSLRS LKRSLELFAPAHALLFTPDAESKRIRT	50
P. patens	GGGSTEVLEAVEPQSLKKLSLKS LKRALDLFAPTHGDRNGAMPESCKIRI	54
C. reinhardtii	0
O. tauri	SALRNADVMFGADRALDRGGGSNWRARDGSDGSAEAAARTSLRVKIANEYA	64
P. troglodytes	FVADNGKPVPLDEESHKRRKMAIKLRNEYGPVLHMPTSKENLKEKGPQNT	74
H. sapiens	FVADNGKPVPLDEESHKRRKMAIKLRNEYGPVLHMPTSKENLKEKGPQNT	74
S. pombeMTEAKNISDDTDVLSLTTNSLRRTSKTLFGAEFG	33
S. cerevisiaeMDGNDHKVE	9
P. trichocarpa	NHKINLEYKGIKSTCEPQQVN...SATTEASGPSNVLALPGSGDSSVS	95
V. vinifera	SHKIQLLEYGGIKSATNPNQANST.QPDGNSQASAPSNALALPGTENS KDP	99
A. thaliana	SHKMKVAFGGVEPVVSQPPRQ...PDRINEQPGPSNALSLAAPEGS KST	96
O. sativa	GCKVNAEYS AVKKNLPTDQGRG...QVKSA AAP..STALALPGTQDV KDA	90
Z. mays	GCKVSAEYGA VKDLTPEQGRG...GQKGPAPPSSTALALPGTQD KDA	96
P. patens	SCKVND EYAAVKDMPAASTRENVGAKPGDNGLQSLRVPGSEQPTT NAGPA	104
C. reinhardtii	0
O. tauri	SVRTLARENELAGSKGEDGGRGRS SGRGSAAAAEAPVKAERKRKKEP SDIA	114
P. troglodytes	DSYVHKQY PANQQQEVEYFVAG.....VALTADTKIQRMPSE SAAQ	115
H. sapiens	DSYVHKQY PANQQQEVEYFVAGTHPYPPGPGVALTADTKIQRMPSE SAAQ	124
S. pombe	SVTSFDDTVAQNLKRTRYKEHLEYGSVLGGTVGKRKNRHYEEDTIGSNALT	83
S. cerevisiae	NLGDVDKFFYSRIRWNNQFSYMATLPPHLQSEMEGQKSLLMRYD TYRKESS	59
P. trichocarpa	QKSGAQNALVVGPSLQS...KARSDGGVSGKSTAVITA.SGSSERNFST	140
V. vinifera	QTGGTQNALVVGPSVQQ...KGLNDVGHLGKSTAVVSS.SGP SERNLST	144
A. thaliana	QKGATESAIVVGP TLLRPILPKGLNYTGSSGKSTTIIPANVSSYQRNLST	146
O. sativa	DNKGSSTAIVPAPHMLP...KAPDSTIPGKNTTITIP...GSSDRFST	132
Z. mays	HGEGSRNAIVPAPLMLP...KAPESTIPGKNTTILSIP...GSSDRFST	138
P. patens	SGKGGGKQLALVPARAQQPPVPAPVVGAAAPAAPAVDR TSTAIASDRHQPS	154
C. reinhardtiiSS	2
O. tauri	SMIDSIDEQDVRDGGAGAGPSTALAPFRGEDAKKNLPVSI FGRHANANIG	164
P. troglodytes	SLAVALPSQTKADANRTAPSGSEYRHPGASDRPQP TAMNSIVMETGNTKN	165
H. sapiens	SLAVALPLQTKADANRTAPSGSEYRHPGASDRPQP TAMNSIVMETGNTKN	174
S. pombe	VRADSENPSQVITKFSDPNKKIAGQVSMQSLEKIKGVPEAAHRIAGE SQ	133
S. cerevisiae	SFSGEGKKVTLQHVPTDFSEASQAVISKKDHDTHASAFV NKFQPEVAEE	109

Figure 2.6: Alignment of N-terminal region of *PRL1* orthologues performed with the emma package from the EMBOSS suite and functionally shaded with `TeXshade` (functional legend in Figure A.5). The N-terminal region of *Arabidopsis* *PRL1* shows significant divergence compared to non-plant orthologues.

two constructs which are suitable for the expression of truncated *PRL1* proteins that lack either the divergent N-terminal or the conserved C-terminal regions (pPAMpat-*PRL1*-N-HA and pPAMpat-*PRL1*-C-HA, respectively). The design details are described in section 4.2.6.3 on page 117 and the schematic view is depicted in Figure 4.2 on page 118.

2.1.6.1 Complementation analysis

The two constructs carrying the N-terminal or C-terminal regions of *PRL1* were transformed into *prl1* K. plants (Németh et al., 1998) via *Agrobacterium*. Twenty primary transformants for each construct were selected on selective solid MSAR medium. These *PRL1*-N-HA/*prl1* and

PRL1-C-HA/*prl1* lines were analysed for a unique trans-gene insertion by segregation analysis. Subsequently, T3 lines carrying the pPAMpat-*PRL1*-N-HA and pPAMpat-*PRL1*-C-HA T-DNA inserts in a homozygous state were identified. Three selected lines for each trans-gene were grown on vertical plates to measure the root length (section 4.2.1.4).

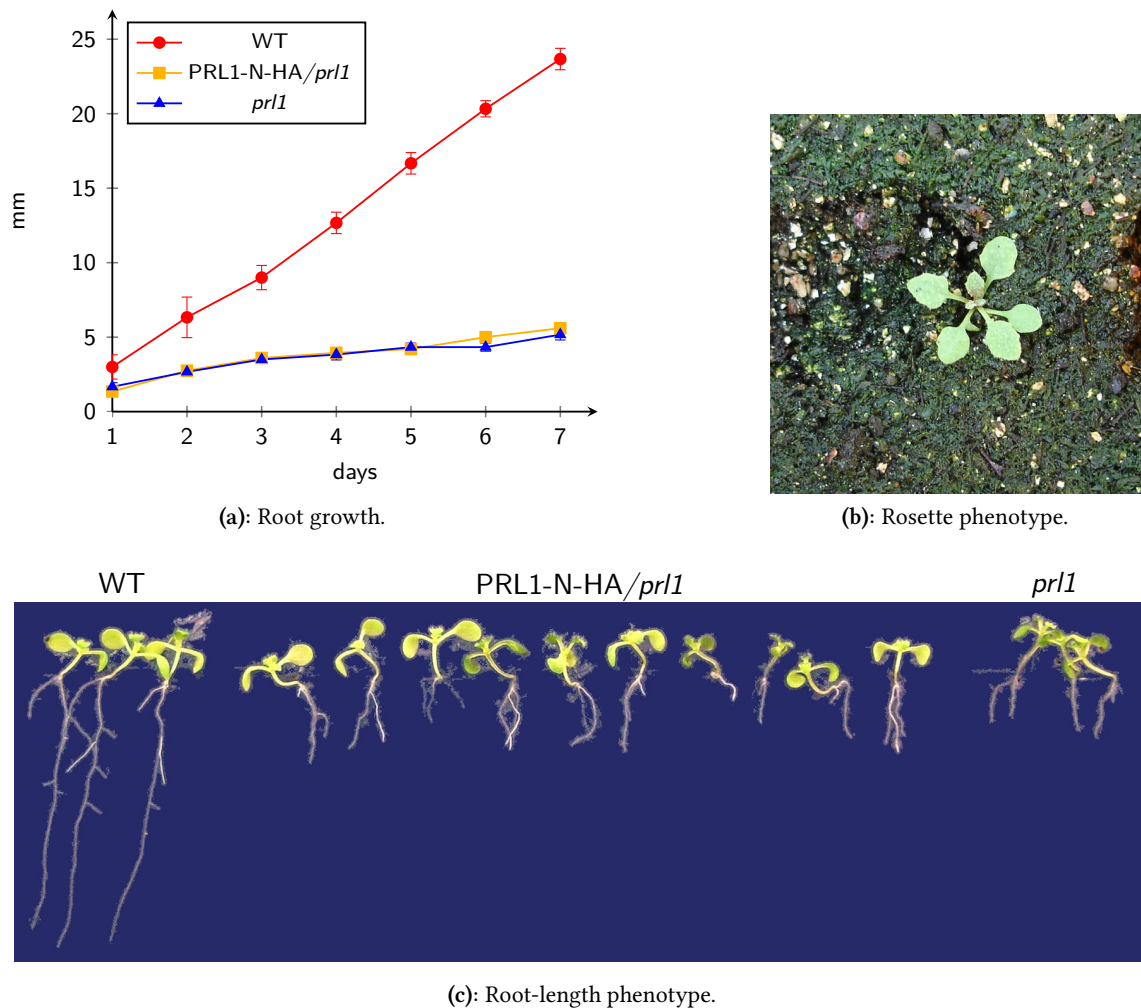


Figure 2.7: Phenotype of *PRL1*-N-HA/*prl1* line #3-1 compared to WT and *prl1*. The measured root length (a) showed a *prl1* phenotype (c), in addition, plants showed a *prl1*-like rosette phenotype (b).

For both constructs, the measured root length in the analysed T3 lines was similar to the root length of the *prl1* control (Figures 2.7 and 2.8). Moreover, lines with more than one T-DNA insertion were unsuccessfully screened for long root phenotype. This result suggest that the over-expression of only the C-terminal or N-terminal regions of *PRL1* alone, can not confer genetic complementation of the *prl1* phenotype.

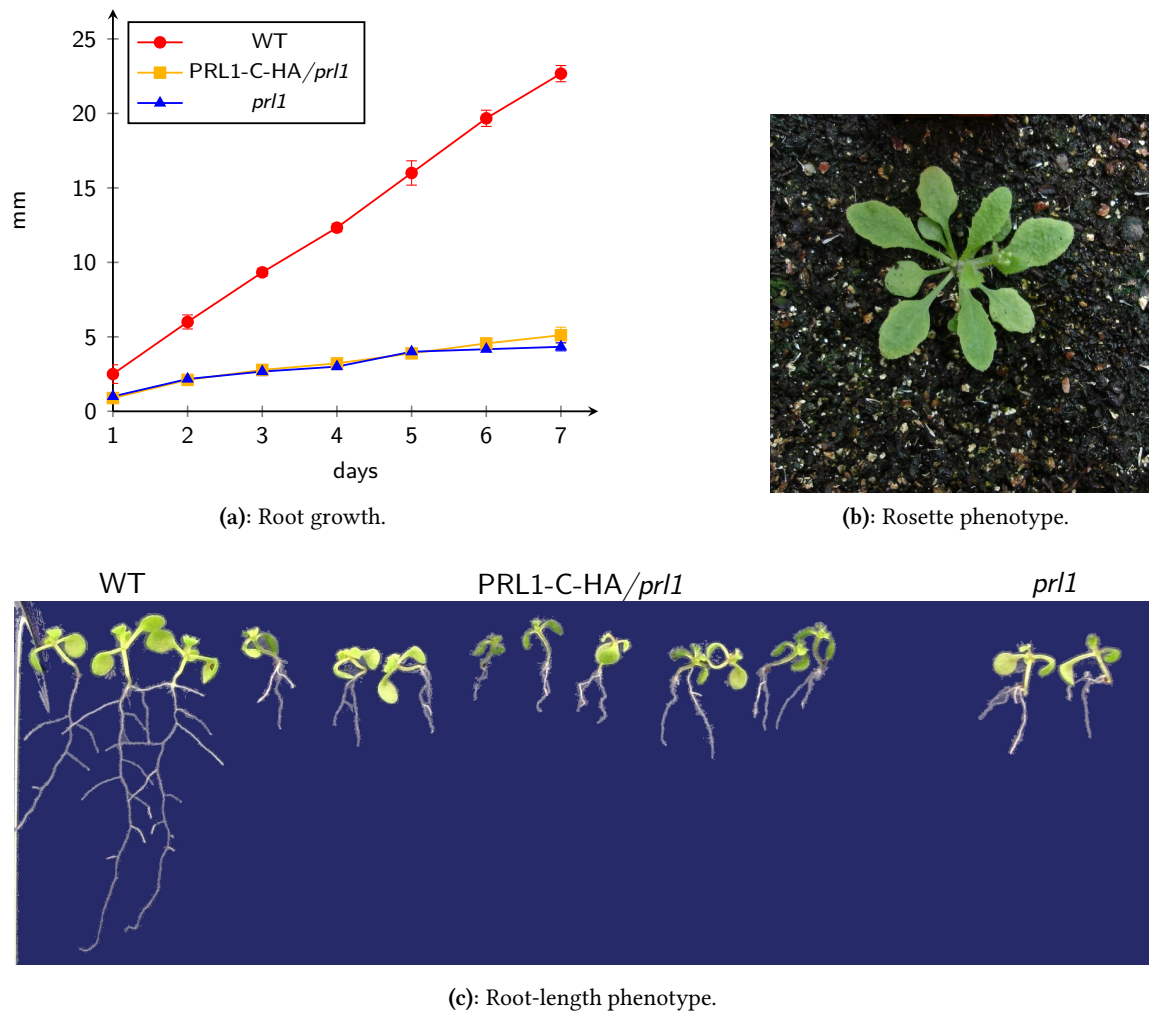


Figure 2.8: Phenotype of *PRL1-C-HA/prl1* line #6-11 compared to WT and *prl1*. The measured root length (a) showed a *prl1* phenotype (c), in addition, plants showed a *prl1*-like rosette phenotype (b).

2.2 Studies of PRL1 target regulation by transcript profiling

To study the effects of the *prl1* mutation on the regulation of transcript levels in *Arabidopsis*, and to obtain more insight into the cellular functions of *PRL1*, three different transcript profiling technologies were tested. Two of them involved microarrays (ATH1 and tiling arrays), the third approach was based on RNA-Seq analysis.

2.2.1 Tiling arrays show a genome-wide transcription alteration in *prl1*

As explained in section 4.1.11, the design of tiling arrays is independent of the available gene annotation, making them useful to study gene regulation, while applying the most up-to-date *Arabidopsis* annotation. Furthermore, tiling arrays allow the study of non-annotated, inter-genic regions or strand-specific transcription. In this work, the Arabidopsis Tiling 1.0R arrays were used in combination with the TAIR7 annotation for identifying the miss-regulated genes and metabolic pathways in the *prl1* mutant. Application of this tiling array for transcript profiling purposes was originally reported by Naouar et al. (2009), who compiled a description file with the TAIR7 annotation release to be used with R/Bioconductor.

2.2.1.1 Sample processing

To identify which genes are miss-regulated in the *prl1* mutant, two week-old Col-0 WT and *prl1* K. plants were grown on solid MSAR medium and ground in liquid nitrogen.

RNA was extracted with the ultra-centrifugation method as described in section 4.2.7.1 (page 121) and DNA contamination was monitored by PCR using the purified RNA templates with the PRL1-F, PRL1-HA and PRL1-F, PRL2-HA primer pairs. RNA quality and concentration was measured with a Bioanalyzer (Agilent Technologies, Waldbronn). RNA samples were processed and hybridized to the tiling arrays by Bruno Huettel at the MPIPZ (section 4.2.9.2 on page 127). A total of 6 Affymetrix Tiling 1.0R arrays were hybridized from three different biological replicates.

2.2.1.2 Core analysis

The CEL files containing the raw data were quality-checked with the `affyQCReport` package for R/Bioconductor and analysed using the `limma` (Smyth et al., 2005) package for R/Bioconductor.

The statistical analysis was performed using a linear model specifically set up for this experiment with the `limma` package using the annotation file provided by Naouar et al. (2009). The results of the `limma` package were compared to the results from the `RankProd` (Hong et al., 2006) package. For both packages, the confidence value for identifying a gene showing an altered regulation was set to 95 % and the cut-off fold-change (FC) was set to 1.5. With these settings, 354 up-regulated genes (Table C.6 on page 172) and 172 down-regulated genes (Table C.7, page 181) were found using `limma`. By contrast, only 158 up-regulated genes and 33 down-regulated genes were found using `RankProd`. This result suggest that the altered processes reflected in the *prl1* phenotype are caused mainly by gene over-expression.

2.2.1.3 Comparison of the limma and RankProd statistical approaches

The two statistical packages used for these analyses (RankProd and limma), are based on very different statistical approaches. RankProd uses a classical non-parametric rank test for assessing significance, whereas limma fits samples to an *ad hoc* linear model. To identify genes that show a common change in transcription with both statistical approaches, the overLapper.R script available from R/Bioconductor was used for comparing the results using Venn diagrams.

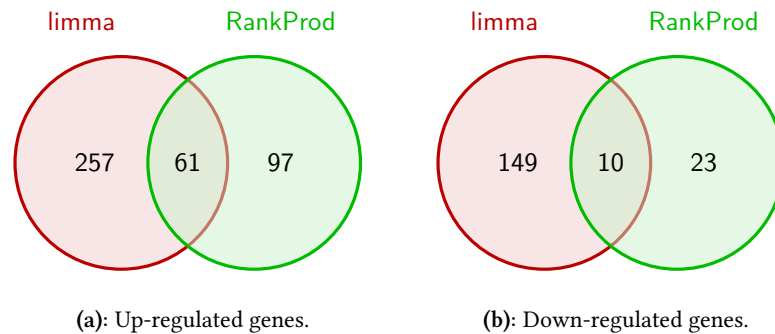


Figure 2.9: Venn diagrams from the analyses performed with the tiling arrays showing the overlap between the results from the limma package and the RankProd package in the up- and down-regulated subsets of genes.

This analysis resulted in a small overlap between the two statistical methods. Only 61 up-regulated and 10 downregulated genes were found in common in the two analysis approaches. (Figure 2.9).

2.2.1.4 Enrichment analyses

Plant MetGenMAP and AgriGO (section 4.1.12.5) were used to sort genes showing altered regulation in *prl1* compared to WT to metabolic pathways and GO terms. Plant MetGenMAP provides a physiological perspective since metabolic pathways are built based on hormone, metabolite, secondary metabolite biosynthesis and degradation.

After identifying the miss-regulated genes, the up- and down-regulated genes identified with limma were segregated into up- and down-regulated subsets (Tables C.6 and C.7, respectively). These two subsets of genes were analysed for enriched GOterms with AgriGO. The results showed by AgriGO revealed that many processes are differently regulated in the *prl1* mutant compared to WT. These differentially regulated processes include different responses to stimuli and stress, responses hormones like salicylic acid and ethylene and hormone signalling. Different RNA-related processes, such as transcription and regulation of RNA metabolism. Immune response and developmental processes are also included in this list (Tables C.1 and C.2 on page 159 and 162, respectively). These results fit well with the pleiotropic and stress-related phenotype observed in the *prl1* mutant.

Table 2.1: Significant up-regulated pathways in the *prl1* mutant. The tiling array results were post-processed with Plant MetGenMAP.

Pathway name	p-value
phenylpropanoid biosynthesis	0,0000
superpathway of flavones and derivatives biosynthesis	0,0001
suberin biosynthesis	0,0001
flavonoid biosynthesis	0,0011
de novo biosynthesis of purine nucleotides	0,0011
flavonol biosynthesis	0,0011
scopoletin biosynthesis	0,0011
homogalacturonan degradation	0,0011
jasmonic acid biosynthesis	0,0011
simple coumarins biosynthesis	0,0011
sphingolipid biosynthesis (plants)	0,0011
superpathway of proto- and siroheme biosynthesis	0,0011
superpathway of heme biosynthesis	0,0011
monolignol glucosides biosynthesis	0,0171
sucrose degradation to ethanol and lactate (anaerobic)	0,0171
chlorophyllide a biosynthesis	0,0171
superpathway of ribose and deoxyribose phosphate degradation	0,0171
glucosinolate biosynthesis from tryptophan	0,0171
cytokinins-O-glucoside biosynthesis	0,0171
glucosinolate biosynthesis from tetrahomomethionine	0,0171
hydroxycinnamic acid tyramine amides biosynthesis	0,0171
glucosinolate biosynthesis from homomethionine	0,0171
ferulate and sinapate biosynthesis	0,0171
phospholipases	0,0171
methionine salvage pathway	0,0171
(deoxy)ribose phosphate degradation	0,0171
serine biosynthesis	0,0171
glucosinolate biosynthesis from pentahomomethionine	0,0171
pyruvate fermentation to ethanol	0,0171
free phenylpropanoid acid biosynthesis	0,0171
tetrapyrrole biosynthesis	0,0171
salicylic acid biosynthesis	0,0171
very long chain fatty acid biosynthesis	0,0171
ethylene biosynthesis from methionine	0,0171
trehalose biosynthesis	0,0171
cutin biosynthesis	0,0171
glucosinolate biosynthesis from hexahomomethionine	0,0171
sterol biosynthesis	0,0171
glucosinolate biosynthesis from dihomomethionine	0,0171
abscisic acid glucose ester biosynthesis	0,0171
phenylpropanoid biosynthesis, initial reactions	0,0171

continued on next page

Table 2.1 – continued from previous page

Pathway name	p-value
heme biosynthesis from uroporphyrinogen	0,0171
tRNA charging pathway	0,0171
glycolipid desaturation	0,0171
glucosinolate biosynthesis from phenylalanine	0,0171
glucosinolate biosynthesis from trihomomethionine	0,0171
quercetin glucoside biosynthesis	0,0171
coniferin metabolism	0,0171
leucopelargonidin and leucocyanidin biosynthesis	0,0171
leucodelphinidin biosynthesis	0,0171
triacylglycerol degradation	0,0171

Plant MetGenMAP helped to sort the differentially regulated genes into physiological pathways (p-value < 0,05). Among these, the analysis identified genes acting in the biosynthesis pathways of flavonoids and chlorophyllide *a*, as well as in the biosynthesis and degradation of gibberellins, jasmonic acid, cytokinins, salicylic acid and abscisic acid. In addition, genes related to sucrose signalling and energy homeostasis were identified with the Plant MetGenMAP analysis (Table 2.1 and Table 2.2).

 Table 2.2: Significant down-regulated pathways in the *prl1* mutant. The tiling array results were post-processed with Plant MetGenMAP.

Pathway name	p-value
phosphatidylglycerol biosynthesis I (plastid)	0,0064
removal of superoxide radicals	0,0064
superpathway of flavones and derivatives biosynthesis	0,0064
phenylpropanoid biosynthesis	0,0064
gibberellin inactivation	0,0064
phosphatidylglycerol biosynthesis II	0,0064
oxidative branch of the pentose phosphate pathway	0,0064
ascorbate biosynthesis I (L-galactose pathway)	0,0064
GDP-D-mannose biosynthesis	0,0064
homogalacturonan degradation	0,0064
riboflavin and FMN and FAD biosynthesis	0,0064
superpathway of oxidative and non-oxidative branches of pentose phosphate pathway	0,0064
CDP-diacylglycerol biosynthesis I	0,0064
CDP-diacylglycerol biosynthesis II	0,0064
folate polyglutamylolation II	0,0064
triacylglycerol biosynthesis	0,0064
phospholipid biosynthesis	0,0064
methyl indole-3-acetate interconversion	0,0064
Fe(III)-reduction and Fe(II) transport	0,0064
flavonol biosynthesis	0,0064
cellulose biosynthesis	0,0064

When focusing on hormone biosynthesis pathways, the analysis revealed that genes belonging to the jasmonic and salicylic acid biosynthesis pathways were up-regulated in *prl1* (Table 2.3), whereas, one gene belonging to the GA2-oxidase family, active in the gibberellin inactivation pathway is down-regulated in *prl1* (Table 2.4). A deeper analysis of the obtained data is provided in the discussion section 3.1.

Table 2.3: Genes from significantly up-regulated hormone biosynthesis pathways in the *prl1* mutant. The tiling array results were post-processed with Plant MetGenMAP.

Gene ID	FC	p-value	Description
Jasmonic acid biosynthesis			
AT5G42650	2	0,04	AOS (ALLENE OXIDE SYNTHASE); hydro-lyase/ oxygen binding
AT1G20510	2,04	0,04	OPCL1 (OPC-8:0 COA LIGASE1); 4-coumarate-CoA ligase
Chlorophyllide a biosynthesis			
AT5G13630	1,55	0,04	GUN5 (GENOMES UNCOUPLED 5)
Salicylic acid biosynthesis			
AT2G37040	1,88	0,03	PAL1 (PHE AMMONIA LYASE 1); phenylalanine ammonia-lyase
Cytokinins-O-glucoside biosynthesis			
AT1G22360	1,8	0,03	UDP-glycosyltransferase
Abscisic acid glucose ester biosynthesis			
AT3G21780	2,19	0,03	UGT71B6 (UDP-glucosyl transferase 71B6); UDP-glycosyltransferase/ abscisic acid glucosyltransferase/ transferase, transferring glycosyl groups

Table 2.4: Genes from significant down-regulated pathways in the *prl1* mutant. The tiling array results were post-processed with Plant MetGenMAP.

Gene ID	FC	p-value	Description
Removal of superoxide radicals			
AT1G08830	-1,9	0,04	CSD1 (copper/zinc superoxide dismutase 1)
Gibberellin inactivation			
AT3G46500	-1,81	0,02	oxidoreductase, 2OG-Fe(II) oxygenase family protein

Furthermore, transcription of genes implicated in the removal of superoxide radicals was also down-regulated in the *prl1* mutant. Altered regulation of this pathway could explain the stress-related phenotype of *prl1*.

2.2.2 RNA-Seq analysis also reveals multiple transcriptional changes

An RNA-Seq experiment was performed in order to obtain complementary data on changes in transcript levels and potential alterations of pre-mRNA splicing patterns at a genome-wide level in the *prl1* mutant. For this analysis, the whole transcriptome from the Col-0 WT and *prl1* samples harvested for the tiling experiment (section 2.2.1.1), including a sample from the *cdc5* mutant was sequenced with the Illumina Genome Analyzer 2 (Illumina UK, Little Chesterford, UK).

For this analysis, total polyA⁺ RNA samples were prepared from 15 day-old WT, *prl1* and *cdc5* mutant seedlings and converted to cDNA as described in section 4.2.8. As PRL1 has been demonstrated to directly interact with CDC5 in the spliceosome-activating complex (Palma et al., 2007; Monaghan et al., 2009), the use of the *cdc5* mutant in this analysis intended to provide additional information on the mutation of two interacting subunits that could produce analogous changes.

The RNA samples were extracted as described in section 4.2.7.1. DNA contamination was checked by PCR and RNA quality and concentration was measured with a Bioanalyzer (Agilent Technologies, Waldbronn). Samples were further processed and sequenced at the Max Planck Institute for Molecular Genetics in Berlin as described in section 4.2.8 (page 123 and following).

The Illumina raw sequence data was transferred through the network to the MPIPZ and all the analyses were carried out on the computer described in section 4.1.12.1. Details of the *in silico* work-flow are described in section 4.2.12.7.

2.2.2.1 Read alignment

As a first step, TopHat was run specifying the parameters for minimum and maximum intron size and the distance between the sequence pairs (section 4.2.12.7). The output coverage file provided by TopHat was converted and uploaded to the MySQL database for its visualization with a local installation of GBrowse at the MPIPZ.

2.2.2.2 Core analysis

Subsequently, the mapped reads from TopHat were post-processed with Cufflinks for performing the actual transcript profiling analysis. Using a cut-off of 2-fold change and a p-value of 0,05, 435 annotated units in TAIR9 were found to be up-regulated (Table C.8 on page 186) and 268 down-regulated (Table C.9 on page 198).

Afterwards, all genes showing altered regulation in the *prl1* mutant were grouped using functional GO terms (Table C.3 on page 162 for up-regulated genes and Table C.4 on page 166 for down-regulated genes). These enriched GO terms include responses to other organisms and defence, stress responses by ROS and heat, phosphorylation and kinase activity. A deeper analysis of the obtained data is provided in the discussion section 3.1.

2.2.3 Tiling and RNA-Seq results have small overlap

The tiling array and RNA-Seq samples were prepared from similar material using the same extraction procedure. This allowed the results of the two performed transcript profiling experiments by

both platforms to be compared. Nevertheless, the data processing of the tiling array and RNA-Seq data was quite different. The transcript profiling from the tiling arrays was performed with the only tool available, which is based on the TAIR7 assembly and annotation (description file by Naouar et al., 2009), whereas the analysis of the RNA-Seq data was performed with Cufflinks which is based on the *Arabidopsis* TAIR9 assembly and annotation.

For comparison of the results from the tiling experiment and the mRNA-Seq experiment, the two subsets of up- and down-regulated genes from the two experiments with a $|FC| > 1,5$ and a p-value $< 0,05$ were analysed for overlapping.

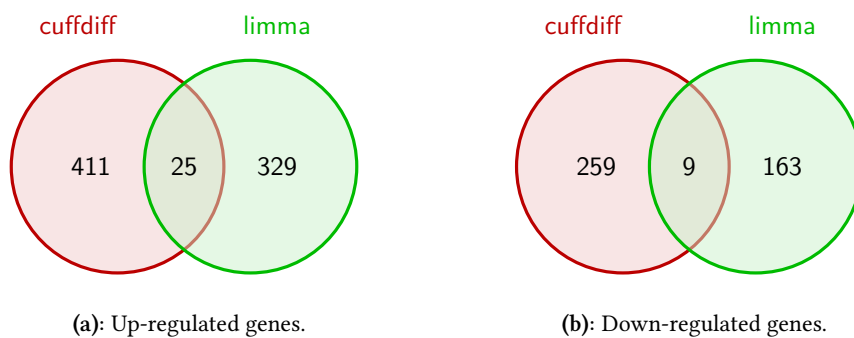


Figure 2.10: Venn diagrams from the RNA-Seq and tiling analyses showing the overlap between cuffdiff output and the limma package in the up- and down-regulated subsets of genes.

The overlap between the genes identified by both approaches is rather small. For the subset of up-regulated genes, only 25 genes overlap in the two analyses, whereas from the down-regulated genes, only 9 genes are common between the tiling and RNA-Seq analysis data. The reason for this inconsistency could lie in the fact that RNA-Seq analysis takes account of different transcript isoforms in the TAIR9 annotation release, whereas the description file compiled by Naouar et al. (2009) only relies on gene models from TAIR7.

2.2.4 ATH1 arrays reveal multiple changes during PRL1 depletion

A conditional complementation system developed by Szakonyi (2006) provided a suitable tool to study transcriptional changes in the timely depletion of PRL1 in the *prl1* mutant. This system allows the study of the early changes taking place from a PRL1-complemented situation to a *prl1*-like situation.

To identify the genes that are directly miss-regulated by a down-regulation or absence of PRL1, two analyses were performed: a pair-wise analysis and a time-course analysis. For these analyses, the conditionally-complemented ER-PRL1/*prl1* plants from Szakonyi (2006) were used.

2.2.4.1 Sample processing

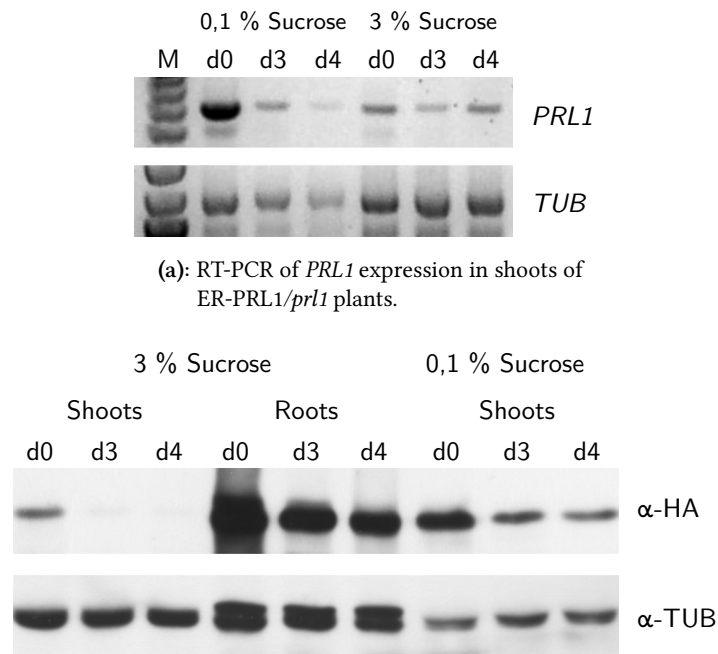
ER-PRL1/*prl1* plants were grown on solid MSAR medium with either 3 % or 0,1 % of sucrose and 4 μM β -estradiol. Two week-old plants were transferred to medium without β -estradiol. Samples

were harvested at the day transfer took place (d0), three (d3) and four (d4) days after transferring the plants to medium without β -estradiol. Dr. D. Szakonyi helped in harvesting shoots and roots samples, which were processed separately. In addition, samples from roots and shoots of Col-0 WT and *pr1* K. seedlings grown for 15 days in MSAR medium with either 3 % or 0,1 % of sucrose in the absence of β -estradiol were harvested and used as control samples.

RNA extracted from the samples using the QIAGEN RNeasy Plant Mini Kit (QIAGEN) was processed and hybridized in the Affymetrix CoreLab at the Westfälische Wilhelms-Universität in Münster. For each sample, two arrays were used, making a total of 28 ATH1 hybridized arrays.

2.2.4.2 *A priori* validation

Down-regulation of *PRL1* in d3 and d4 samples compared to d0 was confirmed at both transcript and protein level by RT-PCR and a Western blot analysis, respectively (Figure 2.11).



(a): RT-PCR of *PRL1* expression in shoots of ER-*PRL1/pr1* plants.
(b): Western blot of *PRL1* from ER-*PRL1/pr1* plants in shoots and in roots from MSAR medium with 3 % sucrose and only shoots in 0,1 % sucrose concentration.

Figure 2.11: RT-PCR assay of *PRL1* transcript levels and Western blot analysis of *PRL1* accumulation during the time-course experiment performed with ER-*PRL1/pr1* plants grown in 0,1 % and 3 % sucrose-containing media. Samples were taken at the end of the inductive period (d0), and three days (d3) and four days (d4) after transferring the seedlings onto medium without β -estradiol.

Protein and mRNA content decreased in shoots during the time-course, with a sharper decrease of mRNA levels in plants grown on 0,1 % sucrose than on 3 % sucrose medium. Furthermore, the stability of the *PRL1* transcript appeared higher in plants grown on 3 % sucrose medium (Figure 2.11a). However, at d0 the transcript level was lower in shoots growing on 3 % sucrose

compared to plants on 0,1 % sucrose medium. In addition, samples grown on 3 % sucrose show a higher accumulation of PRL1-PIPL in roots than in shoots (Figure 2.11b).

2.2.4.3 Transcription profiling

Pair-wise comparison of d3 and d4 samples to d0 was done by Dr. Csaba Koncz by applying unpaired t-tests with the GeneSpring GX v10.0 Expression Analysis suite (Agilent Technologies, Waldbronn). The genes showing a differential expression of 1,5 in FC at a p-value < 0,05 were sorted to GO terms and then manually sorted into pathway-related functional groups (Table C.10 on page 206 and following) based on the current information available in the PubMed and TAIR databases regarding literature.

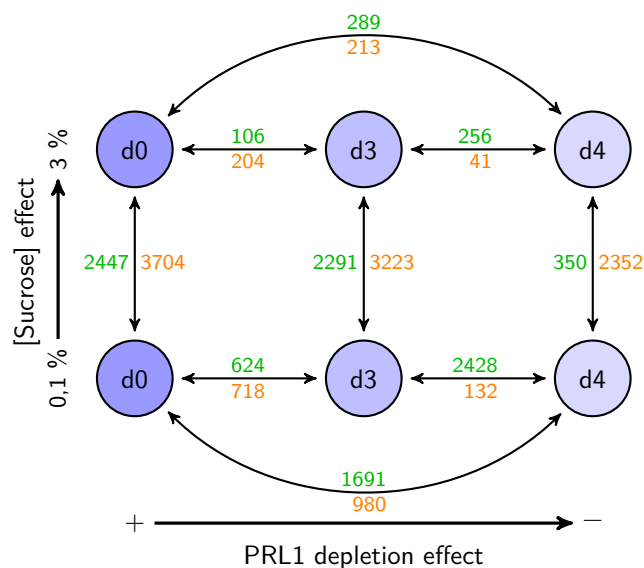


Figure 2.12: Schematic overview of pair-wise-compared data of the ER-PRL1/*prl1* samples during the time-course experiment. Number of genes with altered expression is shown in shoots (green) and in roots (orange). Data was generated with the GeneSpring GX v10.0 Expression Analysis suite (Agilent Technologies, Waldbronn) by Dr. Csaba Koncz.

Many genes were affected by changes in expression between samples. Interestingly, there were more genes changing in expression in plants grown on 0,1 % sucrose medium than in plants grown on 3 % sucrose medium. The FC in gene expression in shoots between samples d0 and d4 is one order of magnitude bigger in plants grown on 0,1 % sucrose medium (Figure 2.12). Furthermore, it was observed that in roots, the highest number of genes with altered expression were found between sample d0 and d3. Whereas in shoots, the biggest difference in number of altered genes was between samples d0 and d3. Whereas in shoots, the biggest difference in number of genes with altered expression was found between samples d3 and d4 (Figure 2.12). In addition, a large number of differently-regulated genes was also observed between the samples of the two different sucrose concentrations (Figure 2.12). This suggested that sucrose availability, or the energetic state of the plant, is affecting gene expression when *PRL1* is down-regulated.

2.2.4.4 Considerations on *PRL1* transcription

To have a better idea on how this artificial system behaves, *PRL1* expression levels in the ER-*PRL1/prl1* samples were analysed by the limma package (Smyth et al., 2005) under R/Bioconductor. In summary, the first and last time-points (d0 and d4) of the time-course experiment were pair-wise compared with root samples from WT and *prl1* K. grown under similar conditions (Table 2.5).

Table 2.5: Comparison of *PRL1* transcription in the ER-*PRL1/prl1* time course experiment to control samples, between different time-points and treatments. Values are in fold change.

Treatment	d0	d4	d0/WT	d4/WT	d4/ <i>prl1</i>	<i>prl1</i> /WT	WT
Roots							
Sucrose 3 %	0,75	1,45	12,64	1,22	2,46	0,49	1,05
Sucrose 0,1 %			17,69	0,89	1,55	0,57	
Shoots							
Sucrose 3 %	0,09	1,00					
Sucrose 0,1 %							

As expected from an over-expression situation, *PRL1* expression was higher in sample d0 compared to the WT, but surprisingly, *PRL1* transcription in roots at day four (column d4/WT in Table 2.5) was very similar to the expression observed for the WT, for both sucrose-containing media. Furthermore, when *PRL1* transcription in the last time-point is compared to the *prl1* sample (column d4/*prl1* in Table 2.5), *PRL1* is still over-expressed in both sucrose conditions. From this results, it is worth to mention that these changes in the time-course experiment reflect an artificial situation: *PRL1* transcription is strikingly high at d0 to be reduced to WT-similar levels at d4. Most importantly, d4 is not a completely *prl1*-like situation.

The results from these arrays were not compared to the transcript profiling done with the tiling arrays or RNA-Seq transcript profiling due to this artificial situation. Furthermore, the ATH1 array design is based on the out-dated TIGRv2 annotation which was released on 2001. This two facts were considered for not to perform a data comparison with these arrays.

2.2.4.5 Time-course and gene clustering analyses

Gene clustering analysis groups the miss-expressed genes in expression profiles, making it easier to identify co-regulated genes. To have a better insight of the changes observed at the transcript level in the ER-*PRL1/prl1* time-course experiment, samples from roots grown on 0,1 % sucrose were subjected to a proper time-course analysis. This selected time-series was chosen, since it showed the greatest difference in *PRL1* transcription (Table 2.5, columns d0/WT and d4/WT) between the time-points.

Raw microarray data was analysed with the limma package under R/Bioconductor using a time-course-fitted linear model. In this linear model, the contrast matrix only contains the comparisons between consecutive time-points. The obtained transcription profiles were post-processed with the Mfuzz package (Kumar and Futschik, 2007) under R/Bioconductor. Details on

the analysis set up can be found on the method section 4.2.12.3 and the *ad hoc* written code for this analysis on page 156.

The gene clustering analysis showed that 218 genes were co-regulated with *PRL1* during the time-course (cluster #3, Figure 2.13). In addition, 51 genes were up-regulated (cluster #5, Figure 2.13) and 42 genes were down-regulated (cluster #6) during *PRL1* depletion.

2.2.4.6 Enrichment analyses

Following the same work-flow as in the case of tiling arrays (section 2.2.1.4), AgriGO and Plant MetGenMAP were used for grouping the genes from the previously selected clusters (clusters #3, #5 and #6).

The GO enrichment analysis was performed taking into account that the ATH1 array is based on the TIGRv2 annotation. From the 218 genes co-regulated with *PRL1*, AgriGO revealed that there was an enrichment of genes involved in responses to various stresses, including temperature, chemical and abiotic stimuli (Table 2.6).

Table 2.6: Enriched GO terms for genes co-regulated with *PRL1* (cluster #3) in the time-course experiment. Enrichment was performed with AgriGO using only the annotated genes in the ATH1 microarray as reference.

GO term	Ontology	Description	p-value
GO:0009266	P	response to temperature stimulus	$1,40 \times 10^{-006}$
GO:0009408	P	response to heat	$1,30 \times 10^{-006}$
GO:0006950	P	response to stress	$3,40 \times 10^{-005}$
GO:0042221	P	response to chemical stimulus	0
GO:0006979	P	response to oxidative stress	0
GO:0050896	P	response to stimulus	0
GO:0009628	P	response to abiotic stimulus	0

The Plant MetGenMAP analysis revealed that the co-regulated genes with *PRL1* are involved in pathways of hormone biosynthesis, including brassinosteroids and polyamines, energetic pathways including the Calvin cycle and photosynthesis. Sugar-related pathways including glycolysis and gluconeogenesis were also co-regulated with *PRL1* depletion (Table 2.7).

Table 2.7: Significantly co-regulated pathways with *PRL1* (cluster #3). Genes belonging to this cluster were post-processed with MetGenMAP.

Pathway name	p-value
Calvin cycle	$4,41611 \times 10^{-05}$
photosynthesis	$4,41611 \times 10^{-05}$
superpathway of flavones and derivatives biosynthesis	0,00691489
spermine biosynthesis	0,00691489
superpathway of geranylgeranyldiphosphate biosynthesis II (plastidic)	0,00691489

continued on next page

Table 2.7 – continued from previous page

Pathway name	p-value
brassinosteroid biosynthesis II	0,00691489
superpathway of polyamine biosynthesis	0,00691489
non-oxidative branch of the pentose phosphate pathway	0,00691489
brassinosteroid biosynthesis I	0,00691489
methylglyoxal degradation	0,00691489
flavonol biosynthesis	0,00691489
thiamine biosynthesis	0,00691489
superpathway of oxidative and non-oxidative branches of pentose phosphate pathway	0,00691489
glycolipid desaturation	0,00691489
glycolysis II (plant plastids)	0,00691489
superpathway of starch degradation to pyruvate	0,00691489
sinapate ester biosynthesis	0,00691489
monolignol glucosides biosynthesis	0,00691489
phospholipases	0,00691489
Rubisco shunt	0,00691489
sorbitol degradation	0,00691489
coniferin metabolism	0,00691489
gluconeogenesis	0,00691489
methylerythritol phosphate pathway	0,00691489

Additionally, Plant MetGenMAP and AgriGO were also used to analyse up-regulated genes, such as the ones from cluster #5. The group of 51 genes in this cluster include genes acting in photosynthesis, Calvin cycle, gluconeogenesis, glycolysis and hormone biosynthesis pathways, including jasmonic and abscisic acid biosynthesis (Table 2.8). The GO term analysis revealed that from the genes contained in cluster #5, there is an enrichment of genes related to the chloroplast compartment (Table 2.9).

Table 2.8: Significant up-regulated pathways from cluster #5. Genes in this cluster were post-processed with MetGenMAP.

Pathway name	p-value
photosynthesis	$3,45202 \times 10^{-15}$
Calvin cycle	$1,08531 \times 10^{-07}$
photosynthesis, light reaction	$1,08531 \times 10^{-07}$
glycolysis II (plant plastids)	$2,54776 \times 10^{-05}$
superpathway of sucrose degradation to pyruvate	$2,54776 \times 10^{-05}$
sucrose degradation to ethanol and lactate (anaerobic)	$2,54776 \times 10^{-05}$
superpathway of starch degradation to pyruvate	$2,54776 \times 10^{-05}$
gluconeogenesis	$2,54776 \times 10^{-05}$
superpathway of cytosolic glycolysis (plants), pyruvate dehydrogenase and TCA cycle	$2,54776 \times 10^{-05}$
glycolysis I (plant cytosol)	$2,54776 \times 10^{-05}$

continued on next page

Table 2.8 – continued from previous page

Pathway name	p-value
scopoletin biosynthesis	0,00531915
Rubisco shunt	0,00531915
13-LOX and 13-HPL pathway	0,00531915
phenylpropanoid biosynthesis	0,00531915
oxidative ethanol degradation III	0,00531915
simple coumarins biosynthesis	0,00531915
oxidative ethanol degradation I	0,00531915
jasmonic acid biosynthesis	0,00531915
aliphatic glucosinolate breakdown	0,00531915
flavonoid biosynthesis	0,00531915
abscisic acid glucose ester biosynthesis	0,00531915
pyrimidine salvage pathway	0,00531915

Table 2.9: Enriched GO terms for genes in cluster #5 (up-regulated) in the time-course experiment. Enrichment was performed with AgriGO using only the annotated genes in the ATH1 microarray as reference.

GO term	Ontology	Description	p-value
GO:0034357	C	photosynthetic membrane	0,00001
GO:0009579	C	thylakoid	0,00001
GO:0010287	C	plastoglobule	0,00001
GO:0044435	C	plastid part	0,00013
GO:0044434	C	chloroplast part	0,00041
GO:0055035	C	plastid thylakoid membrane	0,00160
GO:0009535	C	chloroplast thylakoid membrane	0,00160
GO:0042651	C	thylakoid membrane	0,00160
GO:0009534	C	chloroplast thylakoid	0,00210
GO:0031976	C	plastid thylakoid	0,00210
GO:0031984	C	organelle subcompartment	0,00210
GO:0044436	C	thylakoid part	0,00210
GO:0009536	C	plastid	0,01600
GO:0009507	C	chloroplast	0,02400
GO:0044446	C	intracellular organelle part	0,02400
GO:0044422	C	organelle part	0,02400

Subsequently, Plant MetGenMAP and AgriGO were used to analyse the down-regulated genes in cluster #6. The group of 42 genes in this cluster showed an over-representation of genes related to glucosinolate biosynthesis (Table 2.10). No enriched GO term could be found for this cluster.

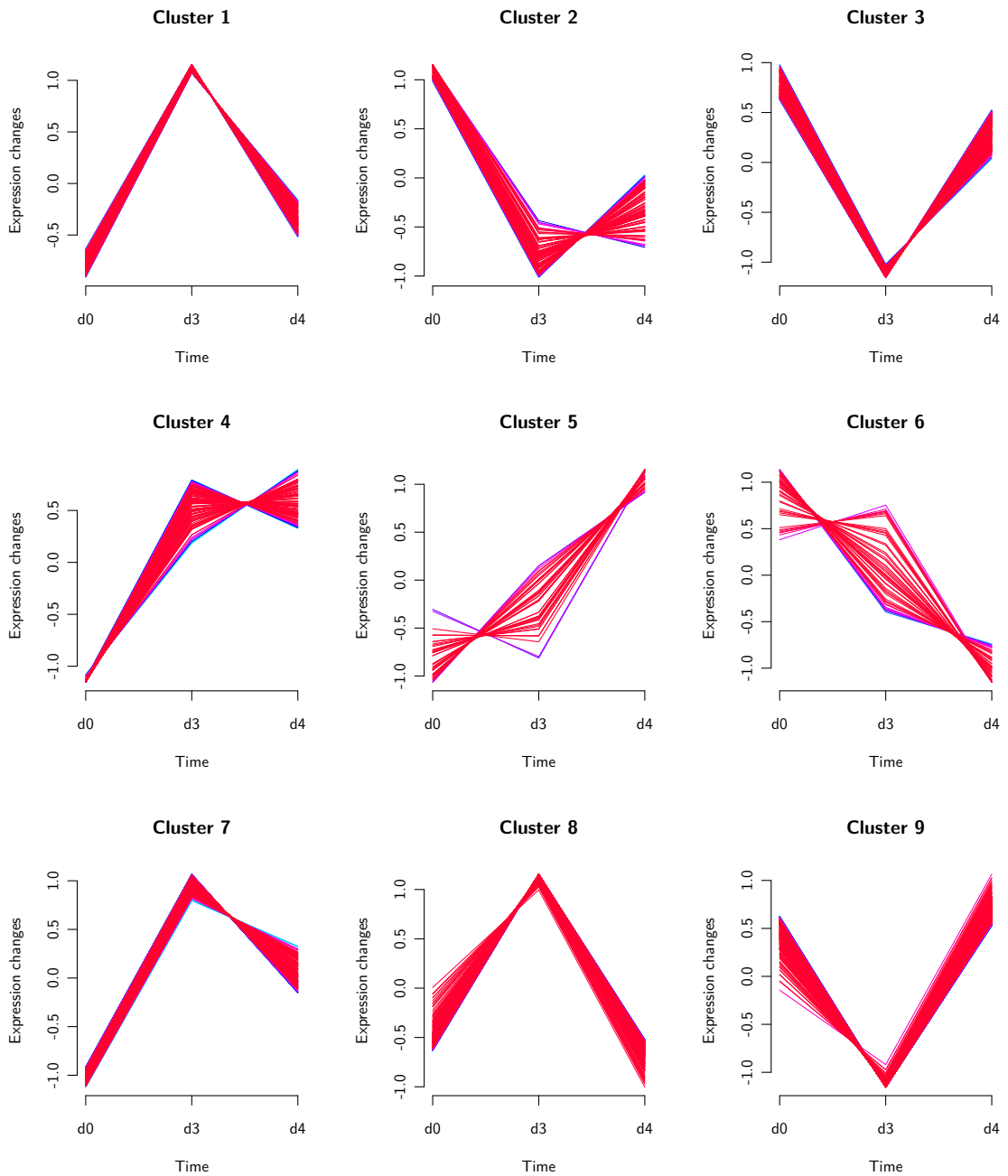


Figure 2.13: Similarly-regulated gene clusters for the time-course experiment in root samples of seedlings grown in the presence of 0,1 % sucrose. *PRL1* is found in cluster #3. Mfuzz under R/Bioconductor was used to build the clusters.

Table 2.10: Significant down-regulated pathways from cluster #6. Genes in this cluster were post-processed with Plant MetGenMAP.

Pathway name	p-value
purine nucleotide metabolism (phosphotransfer and nucleotide modification)	0,00106
glucosinolate biosynthesis from pentahomomethionine	0,00106
glucosinolate biosynthesis from homomethionine	0,00106
glucosinolate biosynthesis from hexahomomethionine	0,00106
glucosinolate biosynthesis from dihomomethionine	0,00106
glucosinolate biosynthesis from trihomomethionine	0,00106
glucosinolate biosynthesis from tetrahomomethionine	0,00106

2.2.4.7 QPCR validation of transcriptional changes

Validation of the microarray results for the ER-PRL1/*prl1* samples was done by QPCR. First, a melting curve analysis was performed with a control cDNA template to test the suitability of the primer pairs for the QPCR analysis. A primer pair is suitable for QPCR when only one amplicon is produced and the PCR efficiency for the primer pair is the same as for the house-keeping gene used as control in the experiments (UBQ in this case). From the 32 assayed primer pairs (Table A.3 on page 152 and following), 26 primer pairs were suitable for the QPCR analysis of the ER-PRL1/*prl1* samples.

Not every ER-PRL1/*prl1* sample was used for this validation, only shoot samples from seedlings grown in 0,1 % of sucrose. In addition, only time-points d0 and d4 were analysed since the pairwise analysis indicated that this comparison showed the highest number of differentially regulated genes during the time-course analysis (Figure 2.12 and Table C.10).

Table 2.11: QPCR validation from the ER-PRL1/*prl1* experiment. Values (in fold change, FC) are shown in red for up-regulated genes and in green for down-regulated genes. Missing values in the ATH1 experiment represent genes showing no differential regulation.

AGI code	Gene symbol	QPCR	ATH1
AT2G46830	CCA1	2,15	1,9
AT1G01060	LHY	4,23	2,68
AT2G21660	CCR2	1,11	3,56
AT5G02810	PRR7	1,07	2,61
AT1G22770	GI	1,13	2,2
AT1G19180	JAZ1	5,7	2,26
AT1G55020	LOX1	3,91	2,26
AT2G06050	OPR3	4,15	1,6
AT1G65480	FT	1,61	2,06
AT3G07650	COL9	1,71	2,78
AT5G15850	COL1	1,72	
AT3G02380	COL2	2,08	1,54

continued on next page

Table 2.11 — continued from previous page

AGI code	Gene symbol	QPCR	ATH1
AT2G02820	MYB88	1,01	1,96
AT4G39950	CYP79B2	12,15	1,69
AT5G39660	CDF2	20,18	1,9
AT3G09150	HY2	2,31	2,32
AT3G17609	HYH	2,83	
AT1G69440	AGO7	7,81	2,73
AT5G46700	TRN2	3,22	1,67
AT1G24260	SEP3	1,48	2,05
AT5G20240	PI	1,57	6,19
AT1G14350	FLP	2,91	2,07
AT1G49720	ABF1	2,66	4,2
AT4G24540	AGL24	1,58	3,71
AT4G28190	ULT1	1,48	2,07
AT5G58140	PHOT2	7,62	1,64

From these 26 assayed genes (Table 2.11), the measurement of transcript levels by QPCR confirmed the data observed in the ATH1 transcript profiling for 18 genes. The fold-change value for these 18 genes was comparable, except for *CDF2* and *CYP79B2*, where there is a difference of one order of magnitude in the fold-change measurement. Six of the analysed genes showed an opposite regulation by QPCR when compared to the ATH1 result, but in most of the cases, both fold-change measurements were close to one. The case of *JAZ1* is worth to mention, since in the ATH1 experiment is down-regulated at d4 by 2,26 fold when compared to d0, whereas the QPCR result shows an up-regulation of 5,7 fold. These different measurements between the two techniques could be based on the fact that genes expressed at low level are falsely classified by the ATH1 transcript profiling. Furthermore, the QPCR technique does not have the inherent saturation effect of the ATH1 arrays.

2.2.5 QPCR partially validates the transcript profiling data of *prl1*

The tiling array data and the RNA-Seq data were validated by QPCR using the same primer pairs as for the ER-PRL1/*prl1* samples. As in section 2.2.4.7, 26 primer pairs (Table A.3 on page 152) were used for the validation of the transcription data.

Table 2.12: Combined QPCR validation from the tiling and mRNA-Seq experiments. For the RNA-Seq experiment, significant changes are shown in red for up-regulated genes and in green for down-regulated genes. Asterisks in the RNA-Seq column indicate statistical significance. Missing values in the RNA-Seq represent genes with several isoforms and different abundances.

AGI code	Gene symbol	QPCR	tiling	RNA-Seq
AT2G46830	CCA1	2,43		1,69
AT1G01060	LHY	2,23		1,63*

continued on next page

Table 2.12 – continued from previous page

AGI code	Gene symbol	QPCR	tiling	RNA-Seq
AT2G21660	CCR2	1,45		1,52*
AT5G02810	PRR7	1,37		1,20*
AT1G22770	GI	1,26		1,04*
AT1G19180	JAZ1	3,05		1,54
AT1G55020	LOX1	2,63		1,38*
AT2G06050	OPR3	1,79		
AT1G65480	FT	1,29		1,60
AT3G07650	COL9	1,01		1,41
AT5G15850	COL1	1,13		1,26
AT3G02380	COL2	1,27		1,08
AT2G02820	MYB88	1,01		1,14
AT4G39950	CYP79B2	8,73		2,74*
AT5G39660	CDF2	1,18		1,14
AT3G09150	HY2	1,31		
AT3G17609	HYH	1,7		
AT1G69440	AGO7	1,21		1,04
AT5G46700	TRN2	1,04		1,08
AT1G24260	SEP3	1,43		1,05
AT5G20240	PI	2,91	2,41	1,62*
AT1G14350	FLP	1,07		
AT1G49720	ABF1	1,53		1,02
AT4G24540	AGL24	2		2,08*
AT4G28190	ULT1	1,54		1,38*
AT5G58140	PHOT2	1,52		1,09*

Unfortunately, from the QPCR analysed genes, only *PISTILLATA (PI)* could be found in the list of differentially regulated genes from the tiling array experiment after the analysis with limma (section 2.2.1.2). *PI* transcription, measured by QPCR and the limma package, was down-regulated in the *prl1* mutant. However, when analysed by RNA-Seq, *PI* was slightly over-expressed, this over-expression of *PI* was statistically significant.

Validation tests of RNA-Seq by QPCR identified 12 genes out of the 26 tested, which showed the same up- or down-regulation trend in both experiments. From these 12 genes, 7 showed significantly altered regulation in *prl1* (values with asterisks in Table 2.12). In particular, *CCR2*, *PI* and *AGL24* deserved special attention since the differential regulation observed in the RNA-Seq experiment was the opposite as the expression measured by QPCR. This could be explained by the fact that the primers for the QPCR experiment were not designed for detecting the occurrence of different transcript isoforms, whereas the performed RNA-Seq transcript profile analysis was aware of this fact.

2.3 RNA-Seq analyses

The pleiotropic phenotype showed by *prl1* suggested that processes controlling the transcription could be affected in the *prl1* mutant. Previous transcription data from RNA hybridization by northern published by Németh et al. (1998) showed that the *prl1* mutation affects the transcriptional regulation of several genes. Moreover, the transcript profiling performed with the tiling arrays for the *prl1* mutant (section 2.2.1.2) and the ATH1 arrays for the ER-PRL1/*prl1* samples (section 2.2.4.3) clearly indicated an affected transcriptional regulation of hundreds of genes.

RNA-Seq data provides information on transcription of intergenic and non-annotated units. In addition, RNA-Seq provides information on transcription of different gene isoforms. To study the hypothesis that *prl1* phenotype could be explained by alterations of pre-mRNA splicing patterns at a genome-wide level, the PE-sequenced samples in section 2.2.2 were subjected to more detailed analyses.

2.3.1 Only Open Source tools allow flexible analyses

After evaluating different commercial and Open Source options for data analysis, only Open Source approaches proved to be flexible enough for performing such specialized analyses. In addition, commercial solutions including NextGENe, the Genomatix Mining Station, the Partek Genomics Suite and the web-based GeneSifter Suite were tested. The Open Source solutions used in this work include the short-read aligner Bowtie, the junction mapper TopHat and the transcript assembler Cufflinks (section 4.1.12.4). Specifically, Cufflinks can assemble *de novo* transcripts to study alterations in the splicing process or in start codon selection.

2.3.2 Data pre-processing

First, the raw-data files containing the sequencing data and the quality data were pooled and converted into the FASTQ format (section 4.2.12.4). The resultant file from each sample was split into two, in order to separate the sequences coming from the two rounds of the PE sequencing.

2.3.3 Mapping suggests an over-representation of exon sequences in *prl1*

The segregated FASTQ files were used to align the sequenced data against different *ad hoc*-created *Arabidopsis thaliana* indices (based on TAIR9) with the Bowtie aligner. The sequences were aligned against the index representing the whole genome, and also against indices representing only cDNA, CDS, exon, intron, 5' and 3' UTRs, transposable elements and intergenic sequences. The fact that the pair of segregated FASTQ files have complementary information was not taken into consideration for these analyses.

The WT and *prl1* samples provided around 50 million of useful sequences, whereas the *cdc5* sample provided 40 million of useful reads. The percentage of aligned reads versus not aligned reads was similar in the three samples for the alignment against most of the indices (Table 2.13). One remarkable exception was found. For the exon index, 60,27 % of the reads from the *prl1* sample were mapped, in contrast to the WT sample where only a 54,66 % was successfully aligned. This difference was even bigger for the *cdc5* mutant, where a 62,93 % of the reads mapped to the

exon-derived index. Contrarily, WT, *prl1* and *cdc5* samples provided a very similar percentage of reads mapping against the intron index (Table 2.13). This suggests that there is not a remarkable number of intron retention events in the *prl1* and *cdc5* mutants. No difference in percentage was observed in the three samples when the reads were mapped against the transposable element index.

Table 2.13: Summary of the RNA-Seq alignment performed with Bowtie allowing a maximum of 3 mismatches in a seed-length of 35 nt. Numbers represent aligned or discarded reads for each index.

Reference		wt		<i>prl1</i>		<i>cdc5</i>	
genomic	aligned	29063037	59,68 %	31945708	65,94 %	28683056	67,76 %
	discarded	19634035	40,32 %	16501528	34,06 %	13645700	32,24 %
cDNA	aligned	29742330	61,08 %	32367251	66,81 %	29828629	70,47 %
	discarded	18954742	38,92 %	16079985	33,19 %	12500127	29,53 %
CDS	aligned	18644186	38,29 %	18666747	38,53 %	18083485	42,72 %
	discarded	30052886	61,71 %	29780489	61,47 %	24245271	57,28 %
exon	aligned	26619597	54,66 %	29200334	60,27 %	26637882	62,93 %
	discarded	22077475	45,34 %	19246902	39,73 %	15690874	37,07 %
intron	aligned	658466	1,35 %	613200	1,27 %	516264	1,22 %
	discarded	48038606	98,65 %	47834036	98,73 %	41812492	98,78 %
5' UTR	aligned	174741	0,36 %	216008	0,45 %	199196	0,47 %
	discarded	48522331	99,64 %	48231228	99,55 %	42129560	99,53 %
3' UTR	aligned	8399776	17,25 %	10398392	21,46 %	9068198	21,42 %
	discarded	40297296	82,75 %	38048844	78,54 %	33260558	78,58 %
intergenic	aligned	1157201	2,38 %	1516482	3,13 %	1039953	2,46 %
	discarded	47539871	97,62 %	46930754	96,87 %	41288803	97,54 %
transposable elements	aligned	148945	0,31 %	153637	0,32 %	156486	0,37 %
	discarded	48548127	99,69 %	48293599	99,68 %	42172270	99,63 %

2.3.4 Transcription of transposable elements is altered in *prl1*

Results from the tiling array data analysis (section 2.2.1.2) already suggested the alteration in transcription of transposable elements and pseudogenes in the *prl1* mutant. Based on this observation, the tiling and RNA-Seq analyses were inspected in more detail for an altered transcriptional regulation of transposable elements.

This analysis revealed that for both datasets, several annotation units belonging to the retro-transposon type (class I transposable elements) showed significantly altered transcription in the *prl1* mutant compared to WT (Table C.5). Specifically, in the RNA-Seq dataset, several copia-like transposons were found to be differentially expressed. However, upon comparison of the tiling array and RNA-Seq data, it was observed that the overlap between both experiments was inconsistent. Nevertheless, this altered expression of retro-transposons observed in both experiments suggests an alteration of silencing mechanisms in the *prl1* mutant.

2.4 Characterization of *PRL2*

Compared to other eukaryotes, numerous subunits of the Prp19-associated complex (or NTC) are encoded by pairs of paralogue genes in *Arabidopsis*. *Arabidopsis* genome has also annotated the *PRL2* gene, the sequence of which is closely related to *PRL1*. The amino acid sequence *PRL1* and *PRL2* aligned with the needle package from the EMBOSS suite indicates a 79,6 % of identity. In their C-terminal regions, which carry seven highly conserved WD40 motifs, *PRL1* and *PRL2* sequences share 88,3 % identity, whereas the N-terminal regions are more divergent (68,8 % sequence identity, Figure A.5).

The sections below focus on elucidating whether *PRL1* and *PRL2* perform overlapping cellular functions in *Arabidopsis*.

2.4.1 The *prl2* T-DNA mutant has an atypical segregation

In this work, two already identified and isolated insertion mutations of *PRL2* were used (*prl2-1* Koncz 16136-4 and *prl2-2* GABI 228D02, Figure A.2), one derived from the Koncz collection (Ríos et al., 2002) and the other one from the GABI-Kat collection (Rosso et al., 2003).

For both insertional alleles, the segregation ratio in selective media was 2:1 (resistant:sensitive, Szakonyi, 2006), although reciprocal crosses between mutants and WT yielded a 1:1 segregation ratio in both directions. This indicates that the male and female transmission –or gametogenesis– is fully normal and the mutation affects the embryo development following fertilization.

2.4.2 The *prl2* mutation results in embryo lethality

The *Arabidopsis* T-DNA mutants of *PRL2* (Koncz and GABI) show a different phenotype compared to *prl1*. The *prl1* mutant has a pleiotropic phenotype, reflecting changes in numerous developmental, hormonal and signalling processes, whereas the *prl2* insertional mutations are recessive and different. Plants resistant to the selection marker, and positive by PCR for the T-DNA insertion in *PRL2*, do not show any macroscopic difference with WT. However, the *prl2*/₊ flowers are 10 % smaller compared to WT (Figure 2.14).

In fact, upon opening of the siliques of T2 *prl2*/₊ mutant plants, a 3:1 segregation of viable:aborted seeds was observed (Szakonyi, 2006). This indicates that the *prl2* mutation causes early embryo lethality. To analyse in more details at which stage the *prl2* mutation leads to an arrested embryo development, siliques from *prl2*/₊ GABI plants were inspected at different stages of development. The siliques were open on a microscope slide, fixed in acetone and cleared with chloral hydrate (section 4.2.1.8). Observation of over 500 aborted and non-aborted seeds from siliques at different developmental stages, indicated that the non-developed seeds carried either no embryo at all, a globular- stage embryo or, an early heart-shaped stage embryo (Figure 2.14).

2.4.3 The *prl1* × *prl2*/₊ mutant shows a more severe phenotype

To test whether the *prl2* mutation would reveal any phenotype that indicates haploid insufficiency in the *prl1* background, the two mutants were crossed. Specifically, *prl2*/₊ GABI was crossed with a homozygous *prl1* SALK insertion mutant (Figure A.1). Hybrid T1 seeds were germinated



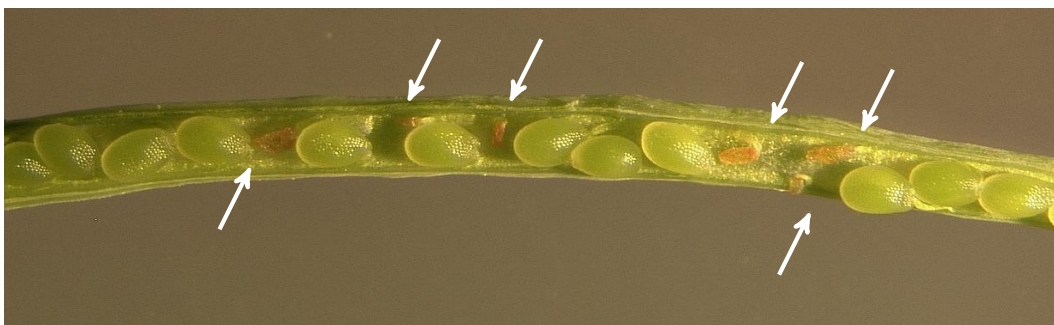
(a): General view of 6 week-old *prl2/+* mutant (right) and control WT (left) plants.



(b): Flower of *prl2/+* mutant (right) and control WT (left).



(c): Cleared *prl2/prl2* embryo (left) and *prl2/+* embryo (right) from a *prl2/+* plant.



(d): Silique of a *prl2/+* plant showing the aborted *prl2* embryos (arrows).

Figure 2.14: Phenotype of *prl2/+*. Whereas the mutant shows a WT-like phenotype (a), flowers show a reduced size (b) and siliques contain aborted seeds (d) that carry arrested embryos (c).

by selecting for the GABI resistance (sulfadiazine) and self-pollinated to obtain T2 seeds. The T2 progeny was analogously selected for the presence of the GABI T-DNA insertion, and then screened for the short root phenotype conferred by the homozygous status of the *prl1* mutation. Selected seedlings were subjected to confirmatory PCR assays to validate the *prl1/plr1*; *prl2/+* genotype. Upon self-pollination of this plants, the expected 2:1 segregation ratio showed a significant change (1:1,5) suggesting that the stress hypersensitivity conferred by the *prl1* mutation increased the embryonic phenotype of *prl2/+*. Specifically, this result suggest a genetic interaction between the two loci.

The phenotype of the double mutant (*prl1/pr1* × *prl2/+*) is highly pleiotropic and similar to that of *prl1*. At 6 week-old stage, the single *prl1* mutant is indistinguishable from the double mutant (Figure 2.15a). At 3 month-old stage, the mutant *prl1* is twice as taller as the double mutant, reflecting a more severe phenotype (Figure 2.15b). In addition, the flowers of the double mutant show an enhancement of *prl1* phenotype, specifically, petals and sepals are shorter compared to WT (Figure 2.15c).

2.4.4 *PRL2* transcription differs from *PRL1*

To study the spatial control of *PRL2* transcription, a semi-quantitative RT-PCR experiment was performed. *PRL2* expression was monitored in roots, rosette leaves, stems, cauline leaves, flowers, and in whole 2 week-old seedlings. *PRL2* cDNA was found in every analysed organ, except for roots. Interestingly, the expression of *PRL2* was at least one order or magnitude lower, compared to *PRL1* (Figure 2.16). Specifically, the *PRL2* transcript required 30 PCR cycles for producing a visible band of *PRL2* cDNA, whereas 25 cycles sufficed for visualizing *PRL1* and *UBQ* cDNAs.

2.4.5 *PRL2* is localized in nuclei and translated in reproductive organs

To analyse the subcellular localization of the *PRL2* and the spatial expression of *PRL2*, two strategies were followed. *PRL2* fused to the yellow fluorescent protein (YFP) was expressed by a 35S promoter construct in cell suspensions, whereas the developmental regulation of the *PRL2* promoter was studied *in planta* using a *PRL2::GUS* reporter gene construct.

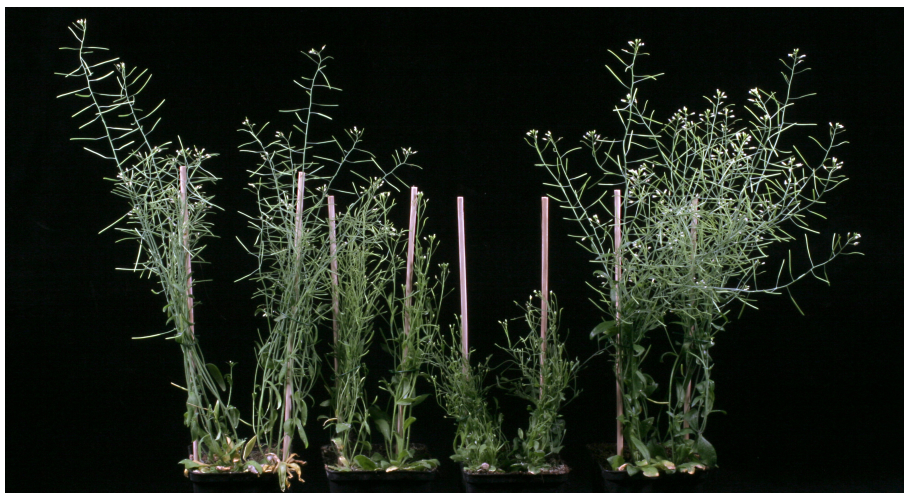
2.4.5.1 Subcellular localization of *PRL2*

To study the cellular localization of the *PRL2* protein, the coding sequence from *PRL2* cDNA was cloned into the pEarlyGate-YFP vectors for the expression of N- and C-terminal YFP fusion of *PRL2* in plant cells (section 4.2.6.5 on page 118). These constructs were transformed into root-derived dark-grown *Arabidopsis* cell suspensions. Following the selection of stably-transformed cell lines, aliquots from the transformed cell suspension cultures were counter-stained with propidium iodide and analysed for *PRL2* localization by confocal microscopy.

The YFP-*PRL2* fusion protein showed an exclusive nuclear localization, whereas *PRL2*-YFP could also be detected in the cytoplasm, in addition to nuclei (Figure 2.17). This indicates that YFP fused to the C-terminus of *PRL2* interferes with proper nuclear localization of the fusion protein. This finding correlated well with the observation of Németh et al. (1998) who identified a potential nuclear localization signal (NLS) in C-terminal sequences of *PRL1*, also conserved in *PRL2*.



(a): Comparison of 1,5 month-old plants.



(b): Comparison of 3 month-old plants.



(c): Detail of flowers.

Figure 2.15: Phenotype of (from left to right) WT, *prl1* SALK, *prl1* × *prl2*+, and *prl2* GABI. The double mutant shows a more severe *prl1*-like phenotype in pigmentation (a), height (b) and flower structure (c). Furthermore, embryo lethality was also observed.

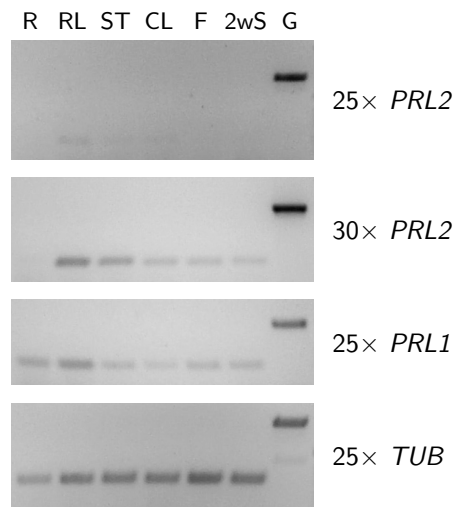


Figure 2.16: Transcription levels of *PRL2* compared to *PRL1* and *TUB* in different organs. *R*: root, *RL*: rosette leaf, *ST*: stem, *CL*: cauline leaf, *F*: flower, *2wS*: 2 week-old seedlings, *G*: gDNA.

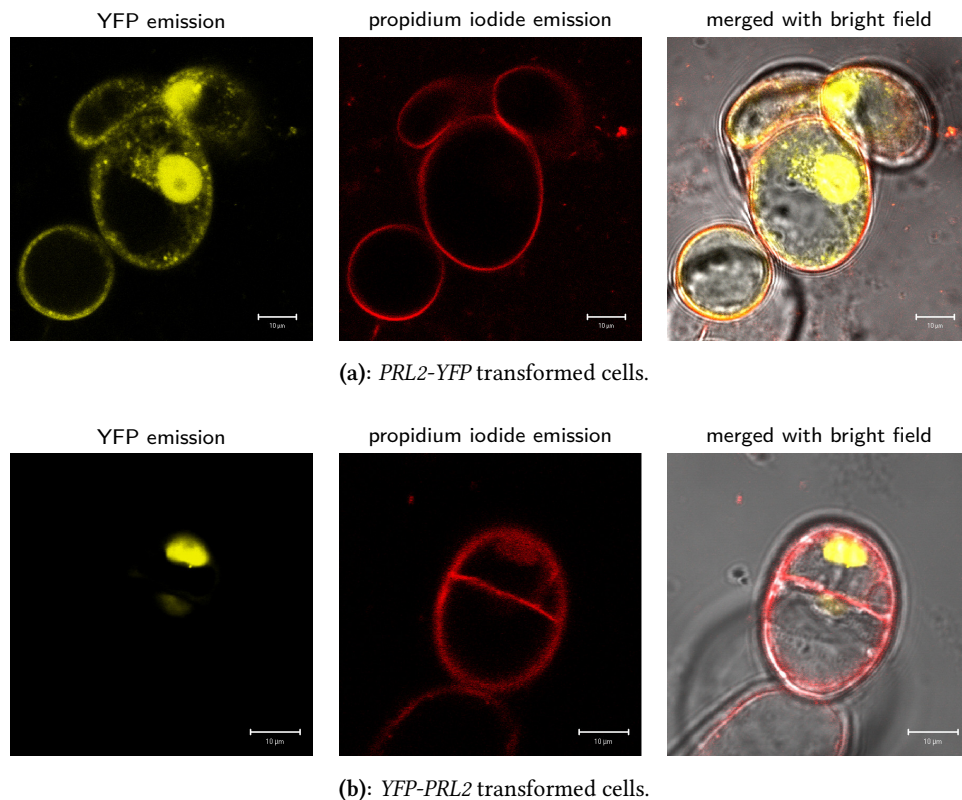


Figure 2.17: Subcellular localization of *PRL2* carrying either C- (a) or N-terminal (b) YFP fusion protein in root-derived dark-grown cell suspensions. Cells were counter-stained with propidium iodide to visualize membranes and nuclei.

2.4.5.2 Developmental regulation of *PRL2* transcription

To study the developmental regulation of *PRL2* transcription, D. Szakonyi generated the pPCV812-*PRL2*::*GUS* construct which carries the 5' UTR region and coding sequences of *PRL2* extending to the 3rd exon in fusion with an *uidA* gene for monitoring *GUS* expression in plants. The design of this construct implied the assumption that, analogously to *PRL1*, essential promoter elements of *PRL2* are localized in the second intron (Szakonyi, 2006).

pPCV812-*PRL2*::*GUS* (section 4.2.6.6) was transformed into WT (Col-0) plants with *Agrobacterium* using the floral-dip method. Subsequently, 20 hygromycin-resistant primary transformants were selected and self-pollinated to obtain T2 lines. These lines were screened for a 3:1 segregation ratio of single T-DNA insertions to obtain T3 families carrying the T-DNA of pPCV812-*PRL2*::*GUS* in homozygous form. The selected T3 lines were used to monitor the expression of the *GUS* reporter during plant development in various organs and tissues.

To compare the developmental regulation of the *PRL2* promoter with that of its *PRL1* paralogue, the expression pattern of *PRL2*::*GUS* was compared to that of a *PRL1*::*GUS* reporter construct which carried the promoter region of *PRL1* (pPCV812-*PRL1*-PROM, Szakonyi, 2006).

In two and four week-old seedlings, *PRL1*::*GUS* was detected in tissues showing active cell division, including young primary leaves, apical meristem, vascular tissue, and axillary and apical meristem regions in roots. In comparison, no expression of *PRL2*::*GUS* was detected in any organ of two and four week-old seedlings (Figure 2.18), even upon prolonged incubation in X-Gluc solution for 24 h.

In inflorescences of mature plants, *PRL2*::*GUS* expression was only detected in fully developed anthers, where the expression was exclusively localized in pollen grains. By contrast, *PRL1*::*GUS* expression was observed both during early and late stages of flower development in tissues with active cell division, in both masculine and feminine floral organs (Figure 2.19). However, *PRL1*::*GUS* expression gradually declined during anther maturation, but persisted through pistil development, where in later stages was localized in developing ovules. Thus, just before anthesis, *PRL1*::*GUS* expression showed an exclusive localization in ovules, whereas *PRL2*::*GUS* expression was detected only in pollen grains and in the already-pollinated stigma.

A detailed analysis of *PRL1*::*GUS* expression during ovule and embryo development revealed that the *PRL1* promoter was active in developing, but not in mature ovules. By contrast, *PRL2*::*GUS* expression could only be detected in fertilized ovules, developing zygote and in endosperm nuclei. During embryo development, *PRL2*::*GUS* expression extended to the endosperm, whereas *PRL1*::*GUS* expression was detected in the seed coat and connecting tissue to the ovary (Figure 2.20).

2.4.6 Conditional genetic mosaics of *prl2* reveal defects in reproductive organs

To be capable to examine the effect of *PRL2* inactivation in developing plants, despite the fact that the *prl2* mutation causes an early embryonic lethality, the conditional complementation system established by Heidstra et al. (2004) was used. This approach allows the generation of genetic mosaics by exploitation of the CRE/*lox* site-specific recombination properties. First, the *prl2* mutant was complemented with a construct (pCB1-*PRL2*::*PRL2*gDNA, section 4.2.6.7) carrying the wild type *PRL2* between two *lox* sites that interrupt the expression of a 35S promoter-driven *Gal4VP16*. The presence of *PRL2* between the *lox* sites prevents the expression of the

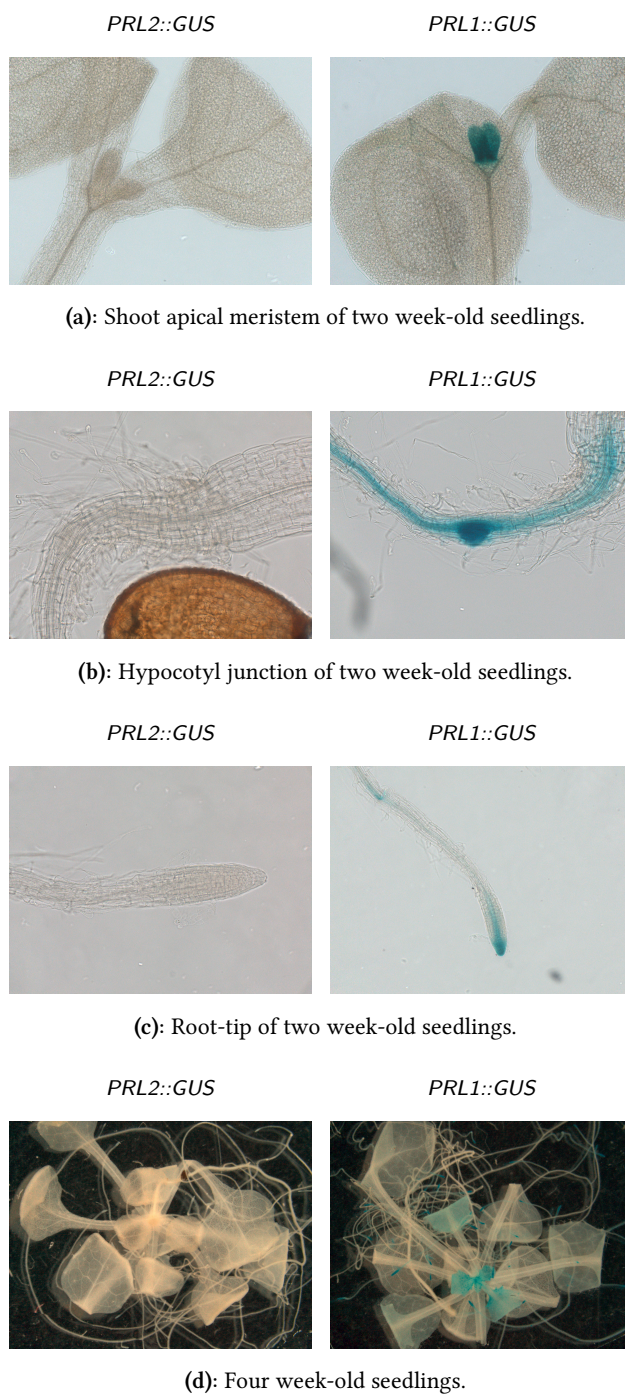


Figure 2.18: Comparison of *PRL1::GUS* and *PRL2::GUS* expression patterns in young seedlings. Only *PRL1-GUS* was observed in cell-dividing tissues, whereas *PRL2-GUS* not.

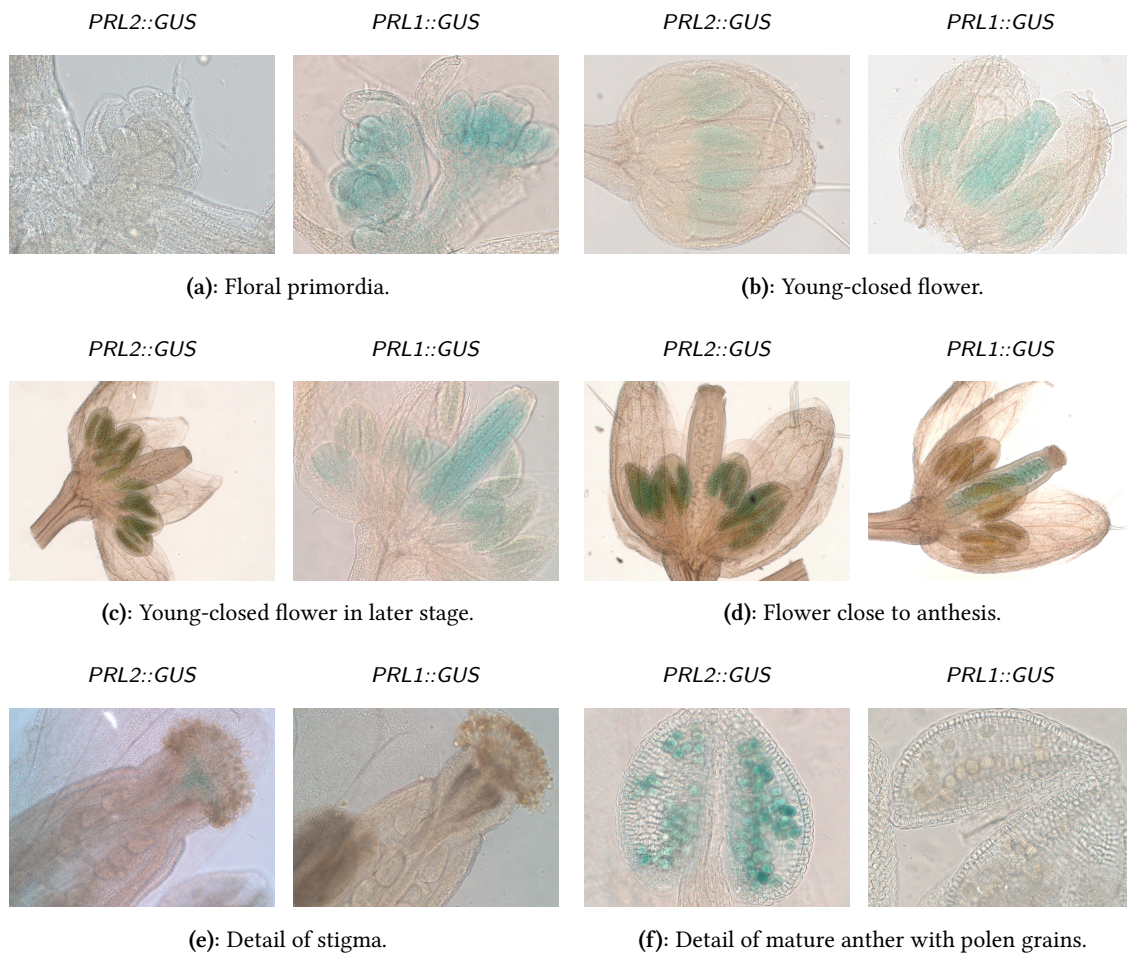


Figure 2.19: Comparison of *PRL1::GUS* and *PRL2::GUS* expression patterns flower development. *PRL1::GUS* was observed in early stages of flower development (a, b and c), and later only in the ovary (d). *PRL2::GUS* was only observed in late development of anthers (d), specifically in pollen grains (f) and pollinated stigma (e).

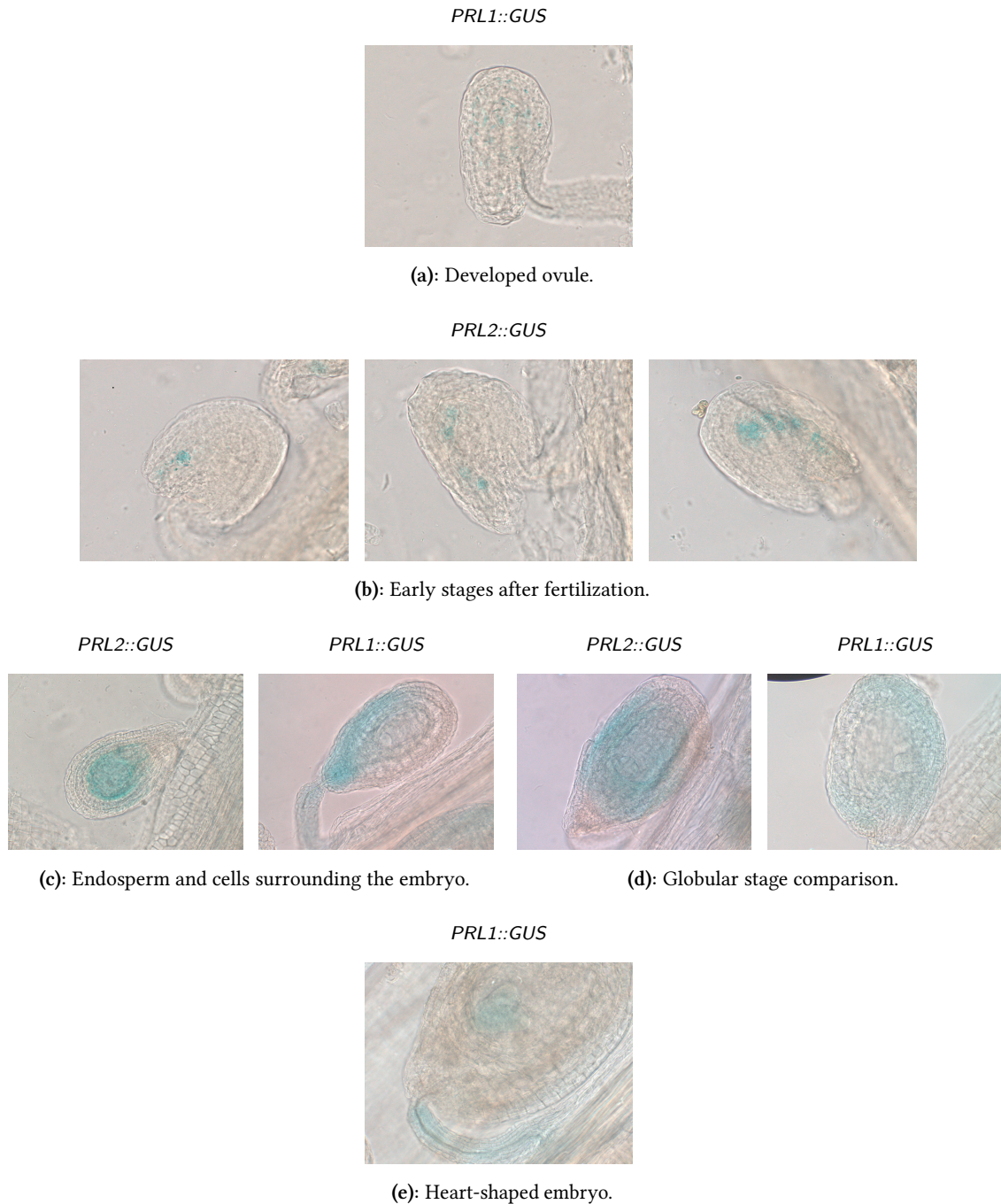


Figure 2.20: Comparison of *PRL1::GUS* and *PRL2::GUS* expression patterns during ovule and embryo development. Only *PRL1-GUS* was observed during ovule development (a), whereas an exclusive *PRL2-GUS* localization was observed in the early stages of embryo development following fecundation (b), including the endosperm (c and d). During this early development, *PRL1-GUS* was only observed in the integuments (c and d). Heart-shaped embryos (e) showed accumulation of *PRL1-GUS* exclusively.

Gal4VP16-regulated *GFP* reporter in cells of genetically-complemented *prl2* plants. Subsequently, a construct carrying a heat-shock driven CRE recombinase (pGII227-HS::CRE) was introduced in the complemented *prl2* background.

Heat-shock treatment results in the activation of the CRE recombinase, which mediates the excision of the complementing *PRL2* by *lox* site recombination. Cells losing wild type *PRL2* display the accumulation of GFP and manifest the traits conferred by the *prl2* mutation (section 4.2.6.7).

2.4.6.1 Construction of inducible *prl2* genetic mosaics

To create the *prl2* genetic mosaic, first *prl2/+* GABI plants were transformed with the pCB1-PRL2::PRL2gDNA construct. Subsequently, 20 DL-phosphinothricin (ppt)-resistant T1 lines carrying a single T-DNA insertion were selected by segregation analysis and the T-DNA insertion was brought to a homozygous state. Additionally, the same lines were screened for segregation on sulfadiazine-containing medium, the resistance marker of the *prl2* GABI line, and subjected to self-pollination to obtain the T3 offspring. Homozygous T3 lines carrying the T-DNA of the pCB1-PRL2::PRL2gDNA (*PRL2gDNA*) in homozygous state were isolated and subjected to diagnostic PCR to detect the *PRL2gDNA* and *prl2* T-DNA insertions. In this PCRs, the PRL2-5' + PRL2-3', PRL2-3' + FISH2 and 2PR-R + Gal4VP16-R primer pairs were used (Table A.1 and A.2 on page 151).

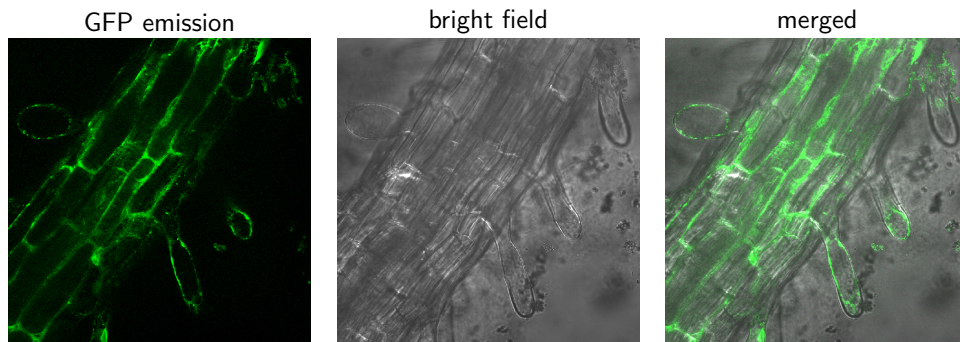
The results showed that in plants carrying the complementing *PRL2gDNA* sequence in a homozygous state, also the *prl2* GABI T-DNA insertion was detected in a homozygous state. This result proves that the *prl2* mutation is complemented by the *PRL2gDNA* insertion.

Subsequently, these *PRL2gDNA* plants were crossed with *prl2/+* GABI plants which were previously transformed with pGII227-HS::CRE in a homozygous form. The F2 lines from this cross were screened for the presence of the *prl2* GABI allele in homozygous form, in addition to the presence of the *PRL2gDNA* and pGII227-HS::CRE by segregation analysis using selection markers (ppt and kanamycin, respectively). Lines carrying all the three T-DNA insertions in a homozygous state were designated as *PRL2gDNA-HS*.

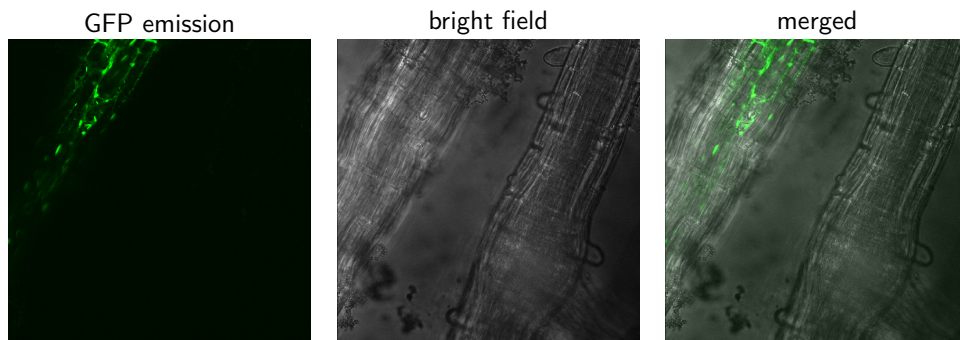
2.4.6.2 Generation of genetic mosaics by heat shock

PRL2gDNA-HS and *PRL2gDNA* plants were grown on MSAR medium for four days after germination. At this point, plants were heat shocked by placing the petri dishes for 30 min at 37 °C. *PRL2gDNA-HS* plants not subjected to heat shock were used as additional control. Following a few days of growth recovery, *PRL2gDNA-HS* plants were observed under the confocal microscope to monitor the expression of the *GFP* reporter, activated upon heat shock by the excision of the *lox*-flanked *PRL2gDNA*.

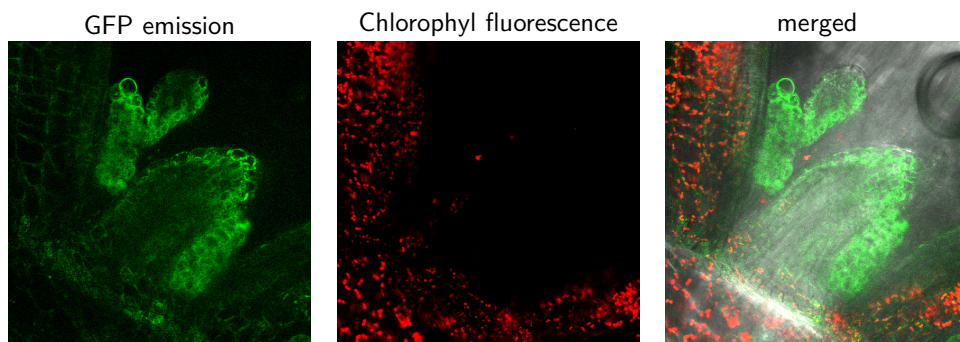
Expression of the *GFP* reporter in heat shock-treated *PRL2gDNA* seedlings (Figure 2.21) indicated that in some cells the *PRL2gDNA* lying between the *lox* sequences was successfully excised. However, GFP was also detected in roots of the control plants (not heat shocked *PRL2gDNA-HS* plants), although only in very restricted root sectors (Figure 2.21). GFP emission also detected in shoot apical meristems of several lines and confirmed by λ -scanning to clearly distinguish it from auto-fluorescence. Heat shocked and untreated control *PRL2gDNA-HS*



(a): Root from heat-shocked line #2.



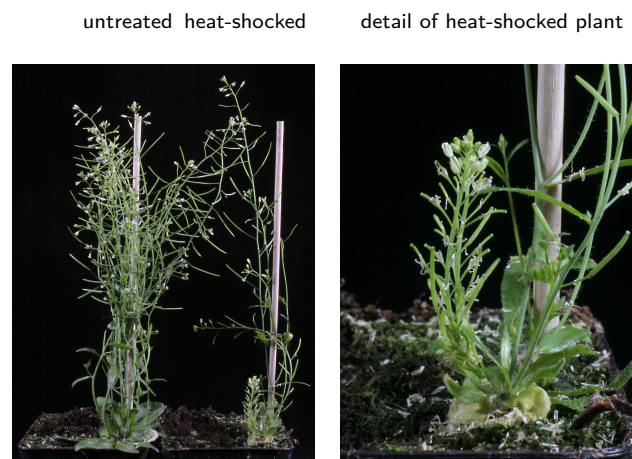
(b): Roots from untreated control line #2.



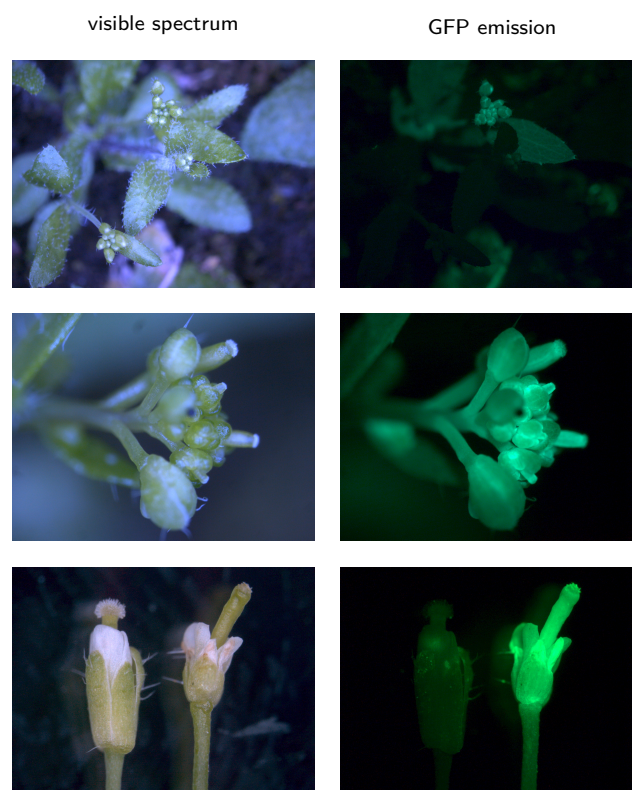
(c): SAM from heat shocked line #10.

Figure 2.21: Localization of GFP in heat-shocked and untreated control in *PRL2*-HS/*prl2* seedlings. GFP marks the cells where the excision of *PRL2* took place in roots (a) and apical meristem (c). However, untreated lines show discrete sectors with GFP fluorescence (b).

plants were transferred into soil and grown in LD conditions. Subsequent analysis showed that several heat-shocked *PRL2*gDNA-HS plants exhibited dwarfism and an early-flowering phenotype, compared to the untreated control (Figure 2.22a). Flowers from these dwarf plants were analysed under the stereo microscope and all of them displayed GFP fluorescence (Figure 2.22b). The flower phenotype of *prl2* resembled the flower phenotype observed earlier by Gergely Molnár in *prl1* plants grown under SD conditions (Figure 2.23).



(a): Phenotype of heat-shocked *PRL2*-HS/*prl2* plants.



(b): Visualization of GFP-expressing sectors in heat-shocked *PRL2*-HS/*prl2* plants.

Figure 2.22: *PRL2*-HS/*prl2* genetic mosaic plants show defects in development following *PRL2*gDNA excision upon heat shock treatment (a). GFP marks the aberrant organs where *PRL2* excision took place (b).

Another heat shock experiment was performed to *PRL2*gDNA-HS plants when they were already bolting on soil. As expected, the effect of the heat shock treatment was much less dramatic. The aberrant flower phenotype conferred by the *prl2* mutation was only observed in few isolated

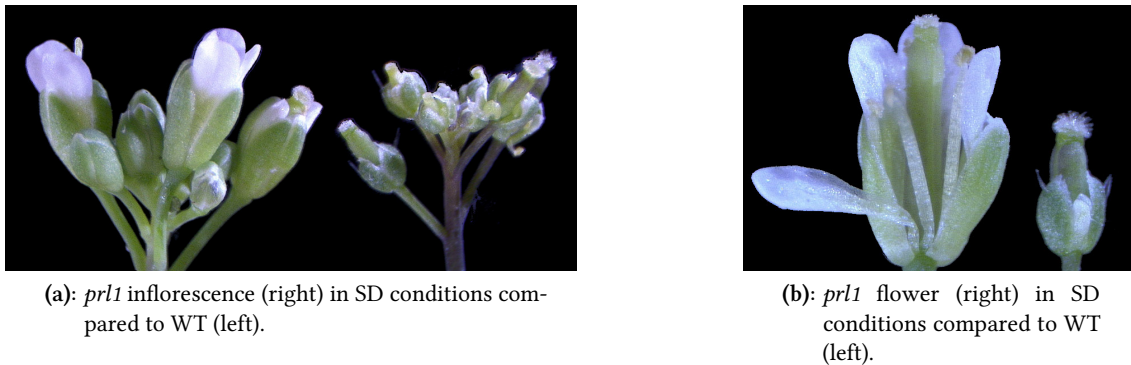


Figure 2.23: Stereo microscope image of *prl1* inflorescence (a) flower (b) phenotype compared to WT in short day conditions. This picture was kindly provided by Gergely Molnár.

flowers which developed after the heat-shock treatment (Figure 2.24). These flowers showed an arrested development and displayed a failure of subsequent silique development.



Figure 2.24: *prl2* phenotype of stems in *PRL2*-HS plants. Plants were heat-shocked when grown on soil for 10 weeks. The defects in development do not affect the whole plant since the excision event did not occur in every cell. Pictures represent (from left to right) the same stem with increasing magnification.

2.4.7 Ectopic over-expression of *PRL1* complements *prl2* and vice versa

To study the functional redundancy of *PRL1* and *PRL2*, Dr. D. Szakonyi developed two different constructs in which the *PRL1* and *PRL2* cDNAs are driven by a double 35S promoter to express fusion proteins labelled with a C-terminal HA tag.

2.4.7.1 Cross-complementation analyses

The *PRL1-HA* and *PRL2-HA* constructs (section 4.2.6.2) were transformed into *prl1* K. and *prl2/+* K. plants via *Agrobacterium*.

Transformed *prl1* plants with *PRL1-HA* and *PRL2-HA* (*PRL1-HA/prl1* and *PRL2-HA/prl1* plants respectively) were identified, and the trans-genes were brought into a homozygous state by segregation analysis. To analyse the rescue of the *prl1* phenotype, seedlings from four selected T3 lines carrying the T-DNA of either the *PRL1-HA* or *PRL2-HA* constructs were grown on vertical MSAR plates along with seedlings of WT Col-0 and *prl1* K. mutant. Root elongation was measured through 7 days following germination (section 4.2.1.4).

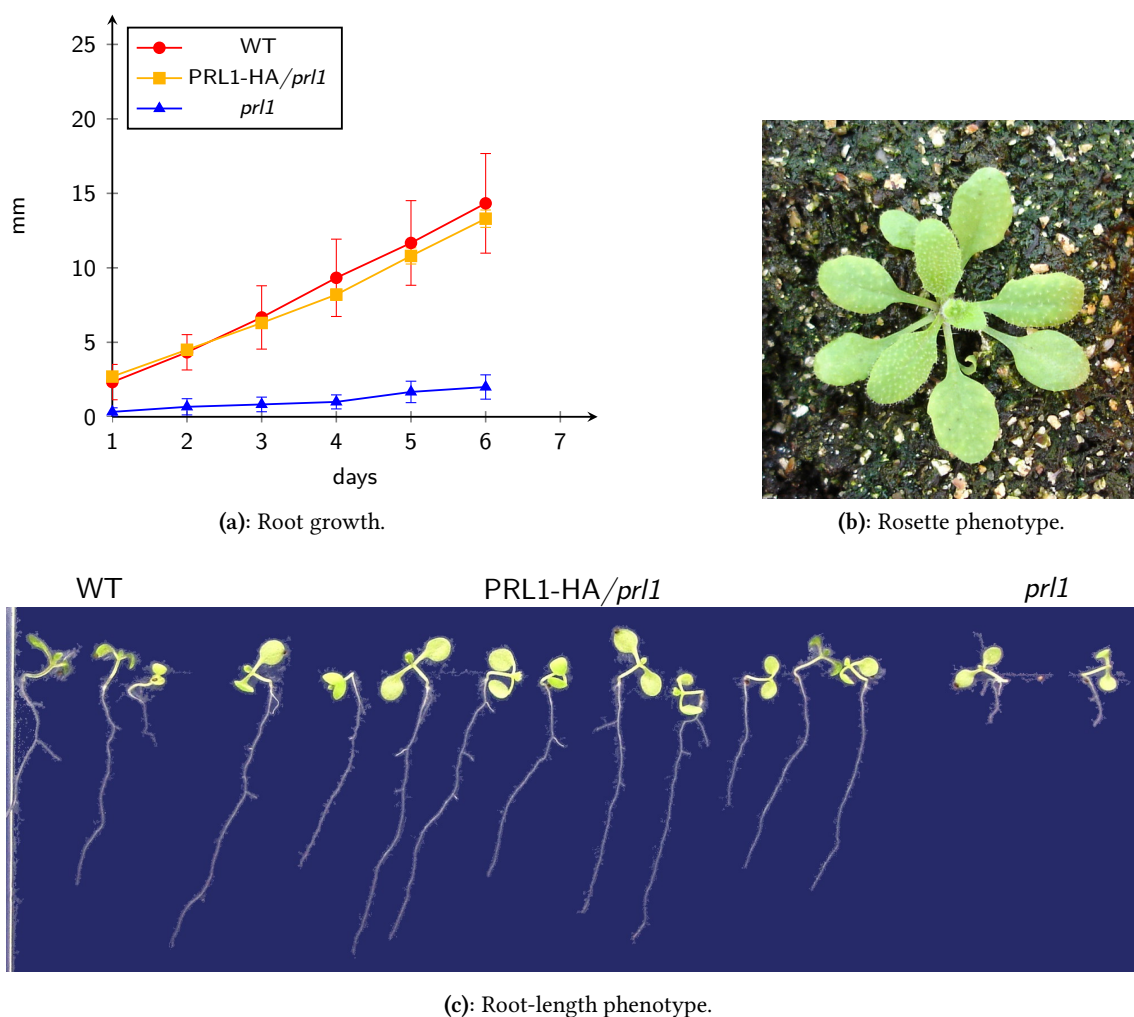


Figure 2.25: Phenotype of *PRL1-HA/prl1* line #10-8 compared to WT and *prl1*. The measured root length (a) showed a WT phenotype (c), in addition, plants showed a WT rosette phenotype (b).

Remarkably, *prl1* plants carrying both *PRL1-HA* or *PRL2-HA* constructs displayed a wild type rosette phenotype when grown in soil. However, measurement of root elongation indicated that

PRL1-HA/*prl1* lines showed a complete rescue of root length (Figure 2.25), whereas *PRL2*-HA/*prl1* lines displayed only a partial rescue in root elongation (Figure 2.26).

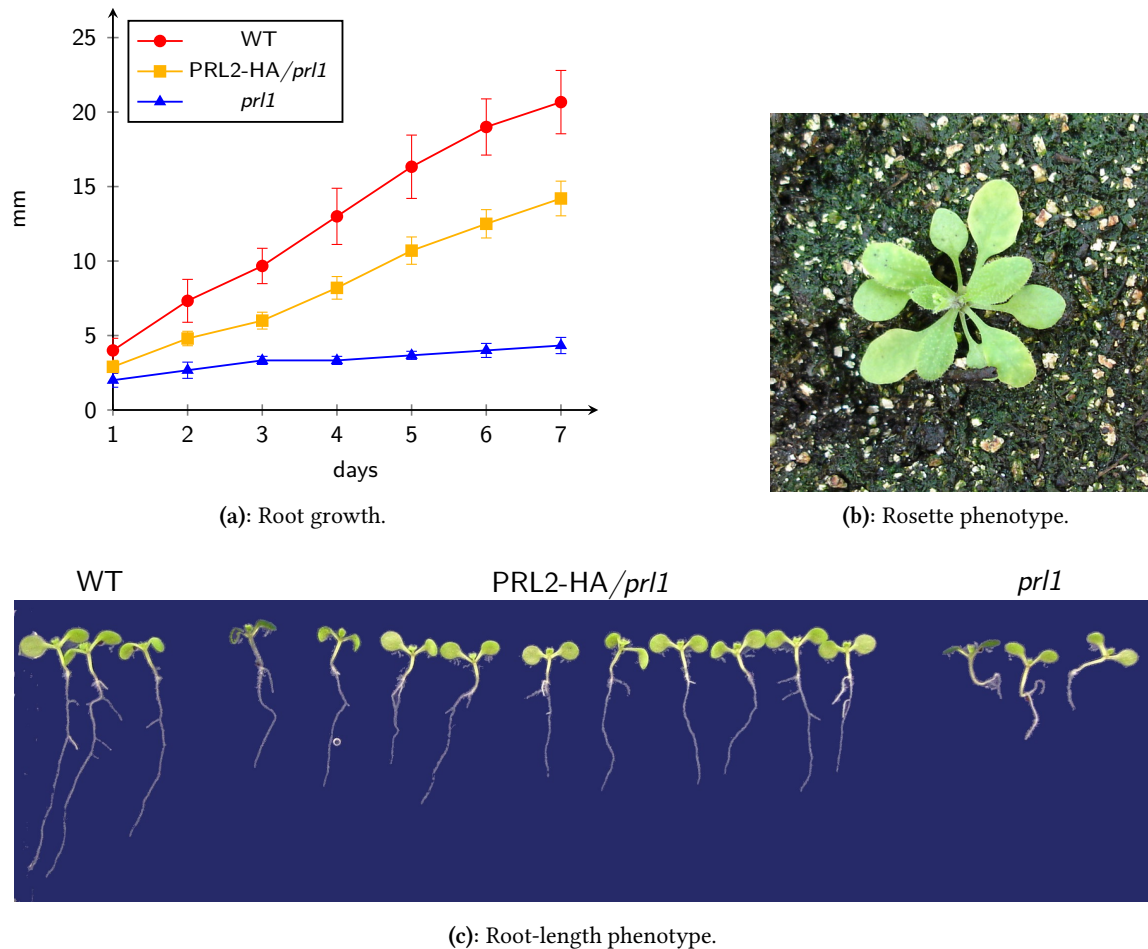


Figure 2.26: Phenotype of *PRL2*-HA/*prl1* line #2-9 compared to WT and *prl1*. The measured root length (a) showed a partially-rescued phenotype (c), in addition, plants showed a WT rosette phenotype (b).

To analyse the complementation of the *prl2* mutation, the *PRL2*-HA and *PRL1*-HA were also introduced in *prl2*+ K. plants (*PRL2*-HA/*prl2* and *PRL1*-HA/*prl2* plants, respectively). Therefore, 40 lines of T2 seeds for each construct were grown in hygromycin (hyg), as well as in ppt. Those lines carrying only one insertion of either *PRL1*-HA or *PRL2*-HA, and the Koncz T-DNA insertion in the native *PRL2* were selected. To analyse the *prl2* phenotype rescue, a segregation analysis was carried out with the T3 seeds. Several lines of *PRL1*-HA and *PRL2*-HA with all seedlings resistant to either ppt and hyg, were identified. This result indicated that when *PRL1*-HA or *PRL2*-HA are in a homozygous state, the Koncz T-DNA insertion can also be in a homozygous state, in contrast to what happens in the *prl2*+ K. mutant.

To place this result in a genetic perspective, 3 T3 lines with a complemented *prl2* phenotype were genotyped together with lines where the *prl2* T-DNA insertion was segregating. Diagnostic PCRs were performed for this confirmation. The primer pairs PRL2-5' + PRL2-3' (*PRL2* gDNA) and PRL2-3' + FISH2 (T-DNA) were used for confirming the presence of the T-DNA insertion

in the native *PRL2*. In addition, the primer pair PRL2-F + PRL2-HA (*PRL2* cDNA) was used for confirming the presence of *PRL2-HA*. The primer pairs PRL1-F + PRL1-HA (*PRL1* cDNA) and PRL1-5' + PRL1-3' (*PRL1* gDNA) were used for confirming the presence of *PRL1-HA*.

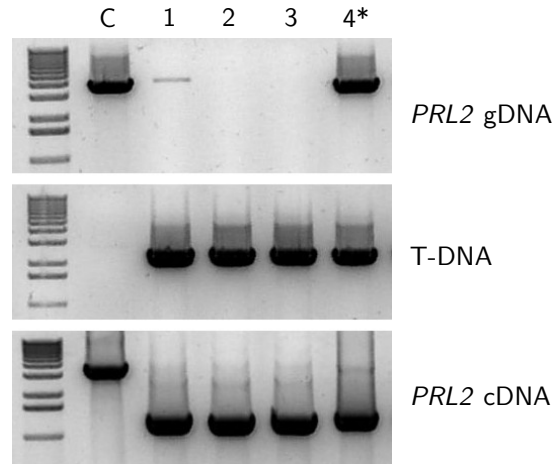


Figure 2.27: *PRL2* cDNA over-expression in the *prl2* mutant (absence of band in *PRL2* gDNA PCR) allows the maintenance of the T-DNA insertion (presence of band in T-DNA PCR) in a homozygous state in the *PRL2* locus. Line #4* is a *prl2*/+ control which segregates for the *PRL2* cDNA construct.

Figure 2.27 shows the PCR assay DNA from 4 different *PRL2-HA/prl2*. The absence of PCR product for the native *PRL2* gene (*PRL2* gDNA PCR) and the presence of PCR product for the T-DNA insertion of *prl2* in lanes 1, 2 and 3 indicated that the *prl2* mutation can be maintained in a homozygous state when the complementing *PRL2* cDNA is present and not segregating. Lane 4* represented a non-complemented *PRL2-HA/prl2* line in which the T-DNA insertion still segregated.

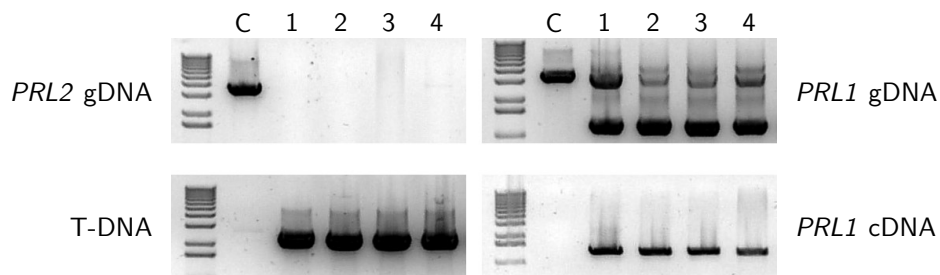


Figure 2.28: *PRL1* cDNA over-expression (presence of band in *PRL1* cDNA PCR) in the *prl2* mutant (absence of band in *PRL2* gDNA PCR) allows the T-DNA insertion (presence of band in T-DNA PCR) to be retained in a homozygous state in the *PRL2* locus, complementing the embryo lethal phenotype.

Similar PCR assays were performed with 4 complementing *PRL1-HA/prl2* lines (Figure 2.28). The PCR results showed that the native *PRL2* (*PRL2* gDNA product) can be absent when *PRL1* cDNA

is present, allowing the T-DNA insertion in *PRL2* to be in a homozygous state. From these results, it can be concluded that both ectopic over-expression of homologous *PRL2*-HA and heterologous *PRL1*-HA proteins can confer genetic complementation of the embryo lethal *prl2* mutation.

2.4.8 Chimeric *PRL1*-*PRL2* proteins complement both *prl1* and *prl2*

To study the functional complementarity of N- and C-terminal domains of *PRL1* and *PRL2*, two alternative constructs *1N2C-HA* and *2N1C-HA* were designed by Dr. D. Szakonyi in which the N-terminal part of *PRL1* was fused to the C-terminal WDR domain of *PRL2* and vice versa.

2.4.8.1 Complementation analyses

1N2C-HA and *2N1C-HA* (section 4.2.6.4) were transformed into the *prl1* K. and *prl2*/+ K. mutants via *Agrobacterium*. Lines carrying a T-DNA insertion of both constructs were identified by segregation analysis, and the T-DNAs were brought into a homozygous state. To analyse the complementation of the *prl1* mutation, the rescue of the short root phenotype was examined by measuring root elongation as described in section 4.2.1.4.

In *1N2C-HA/prl1* plants expressing a fusion protein with the N-terminal domain from *PRL1* and the C-terminal domain from *PRL2*, the root length phenotype was complemented to the same degree as observed in *PRL1*-HA/*prl1* plants (Figure 2.29 and Figure 2.25, respectively). However, *2N1C-HA/prl1* plants, expressing a fusion protein with the N-terminal domain of *PRL2* and the WDR domain from *PRL1*, showed only a partial complementation of the *prl1* short root phenotype. The root length was comparable to that of *PRL2*-HA/*prl1* plants (Figure 2.30 and Figure 2.26, respectively). These results indicated that the N-terminal domain of *PRL1* is required for proper genetic complementation of the root elongation defect caused by the *prl1* mutation.

The constructs *1N2C-HA* and *2N1C-HA* were also transferred into *prl2* K. plants via *Agrobacterium* to examine the genetic complementation of the *prl2* mutation. Only 2 lines from 40 primary transformants of *2N1C-HA*, which express a fusion protein with the N-terminal domain of *PRL2* and the WDR domain of *PRL1*, were identified to complement the *prl2* lethal phenotype. However, no complementing *1N2C-HA/prl2* line, expressing a fusion protein with the N-terminal domain of *PRL1* and the WDR domain of *PRL2*, was identified after analysing the offspring of 40 primary transformants. This result suggests that the divergent N-terminal domain of *PRL2* is functionally essential for complementing the embryo lethal phenotype caused by the *prl2* mutation.

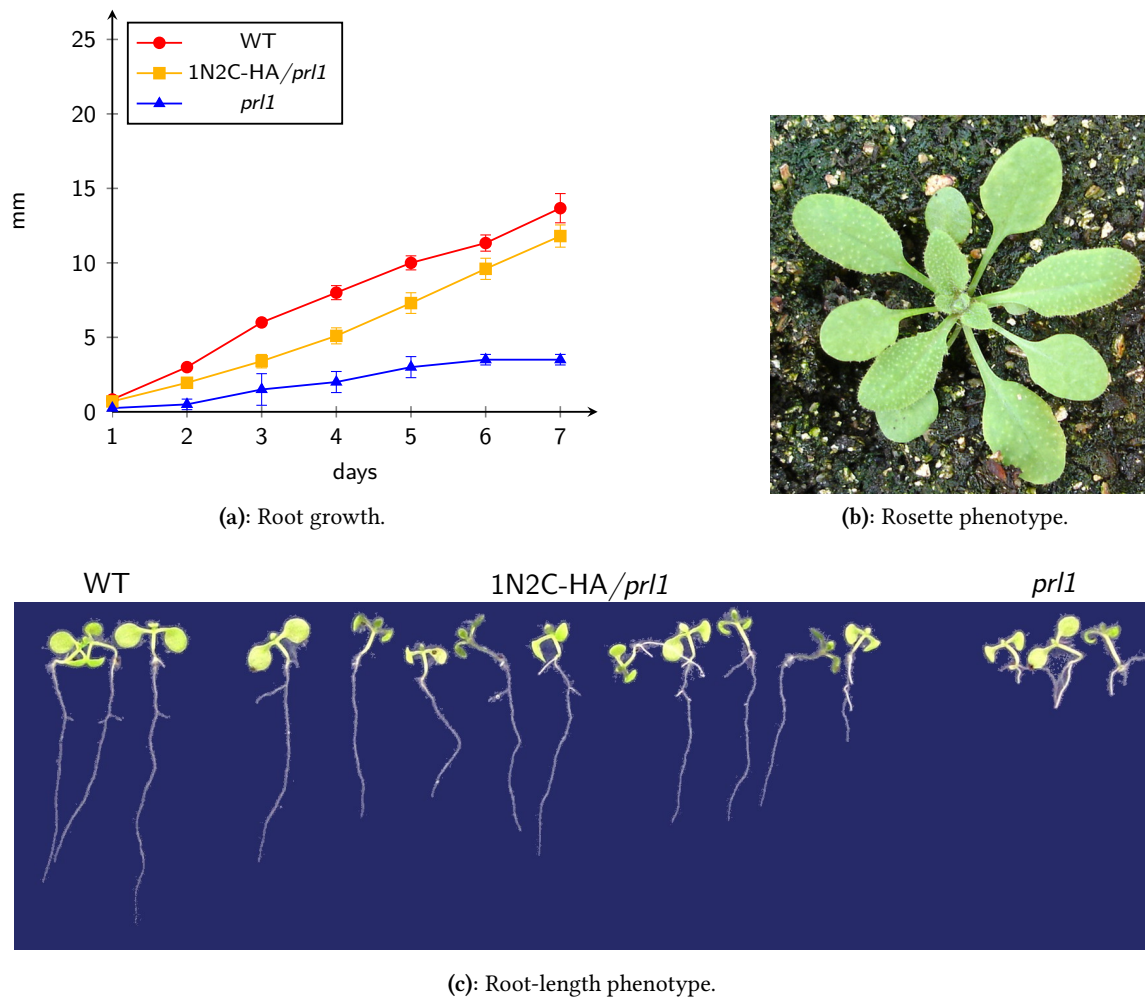


Figure 2.29: Phenotype of pPAMpat-1N2C-HA line #7-3 compared to WT and *prl1*. The measured root length (a) showed a WT phenotype (c), in addition, plants showed a WT-like rosette phenotype (b).

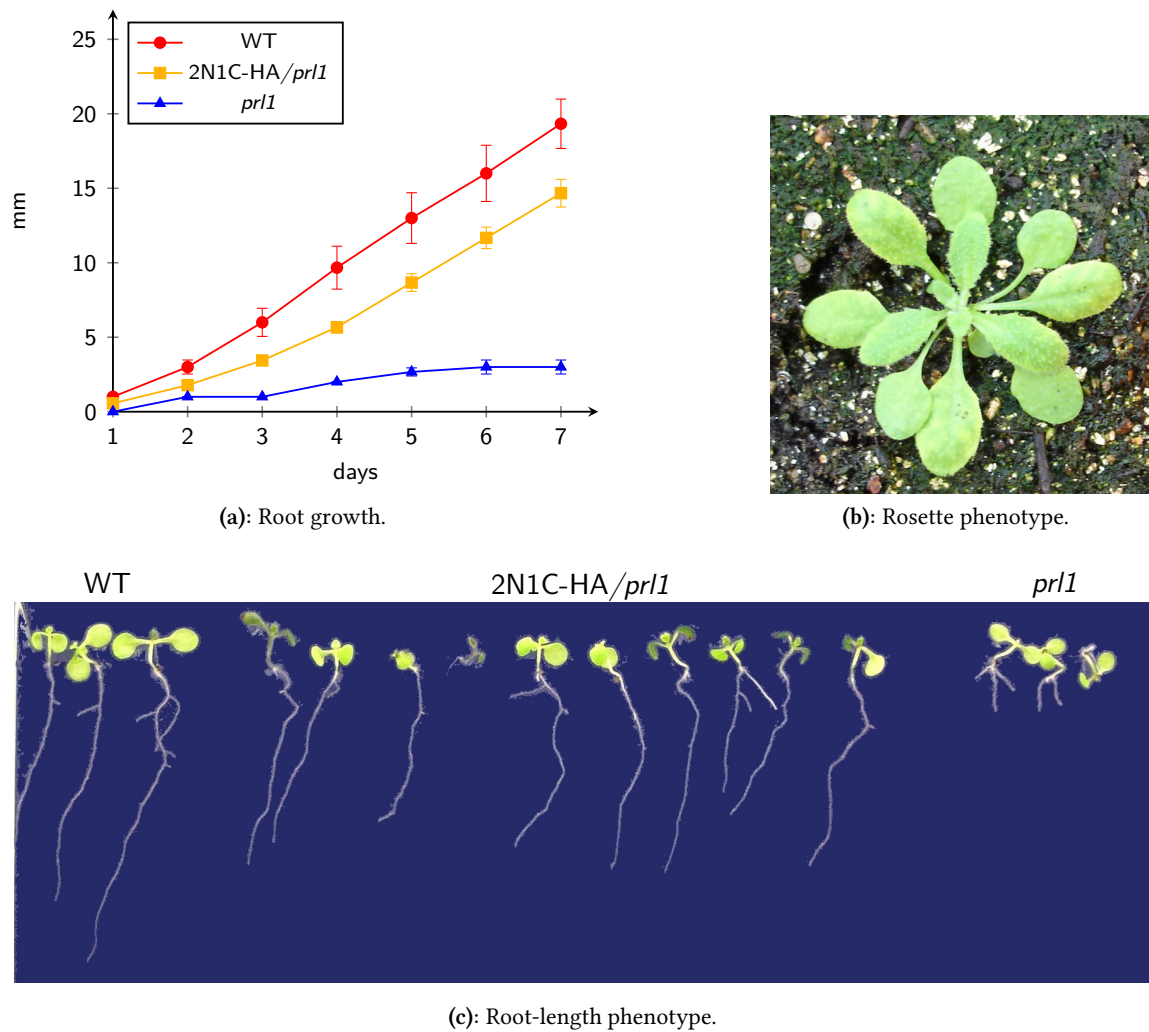


Figure 2.30: Phenotype of pPAMpat-2N1C-HA line #8-8 compared to WT and *prl1*. The measured root length (a) showed a partially-complemented phenotype (c), in addition, plants showed a WT-like rosette phenotype (b).

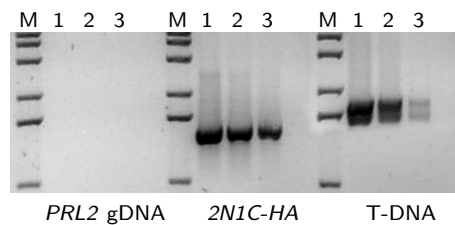


Figure 2.31: *2N1C-HA* cDNA over-expression in the *prl2* mutant (presence of band in *PRL2* gDNA PCR) allows maintenance of the T-DNA insertion (presence of band in T-DNA PCR) in a homozygous state in the *PRL2* locus..

3. Discussion

Examination of the evolutionary conservation of PRL1 orthologues in eukaryotes (section 2.1.5) indicates a remarkable conservation of PRL1 function in higher plants. So far, PRL1 functions have been implicated in the regulation of sugar signalling (Németh et al., 1998), signalling pathways in pathogenity responses (Palma et al., 2007) and constitutive activation of ROS signalling (Baruah et al., 2009). Nevertheless, the details how PRL1 performs this wide range of regulatory functions remained thus far largely elusive.

Conservation of *PRL1* orthologues in yeast, mammals and humans in conjunction with biochemical and genetic studies of the NTC complex, provided a hint that *in planta*, PRL1 may act as a subunit of the Prp19-associated spliceosome-activating complex (Potashkin et al., 1998; Ajuh et al., 2000). In fact, recent research in our laboratory confirmed the co-purification of PRL1-PIPL in native conditions from nuclear extracts, associating PRL1 with the splicing machinery (de Jong, unpublished). Recently, Monaghan et al. (2009) also confirmed the existence of a Prp19-associated complex in *Arabidopsis* with a core composition similar to the composition already observed in other species.

However, transposing orthologue functions to plants is not an easy task (Hsiao et al., 2010), especially when the N-terminal part of PRL1 in *A. thaliana* is completely different to the putative orthologues outside the plant kingdom (section 2.1.5). Therefore, it is not surprising that PRL1 has also been recently identified as a substrate receptor of a CUL4-DDB1 ubiquitin ligase complex (Lee et al., 2008).

3.1 Transcriptional regulatory effects of *prl1*

3.1.1 PRL1 function has a direct impact in gene regulation

Nuclear run-off experiments performed by Németh et al. (1998) provided an evidence that the *prl1* mutation has a direct effect on the regulation of transcription initiation or RNA elongation. Moreover, extensive RNA northern hybridization performed by Németh et al. (1998) with over 300 different gene-specific probes identified a characteristic set of stress-regulated genes. The expression of these genes shows de-repression in the *prl1* mutant.

The transcript profiling experiments performed with tiling arrays (section 2.2.1) and RNA-Seq (section 2.2.2) in this work, revealed a general alteration –specifically up-regulation– of gene transcription in the *prl1* mutant compared to wild type. The analyses of enriched GO terms were only positive for the gene-sets containing the up-regulated genes in both analyses. This enrichment analysis revealed an over-representation of genes related to biotic and abiotic stress responses. These responses include defence against bacteria and fungi, salt stress and water deprivation response, oxidative stress response, RNA metabolic processes, gene expression, transcription process, and responses to hormones, such as salicylic acid, ethylene, jasmonic acid, auxin and abscisic acid.

Furthermore, the time-course analysis performed with the conditional PRL1 complementation (ER-PRL1/*prl1* plants, section 2.2.4) provided a perspective on the early changes taking place during PRL1 depletion in a stress situation. The results revealed a genome-wide alteration in transcription control, affecting developmental processes, hormone responses, DNA and RNA-depending processes, and responses to several stress stimuli (Table C.10 on page 206 and following in the PDF version of this document).

3.1.1.1 Genes affected by the *prl1* mutation in developmental pathways

Among genes involved in floral meristem development, *PISTILLATA (PI)*, was found to be down-regulated in the tiling array analysis (2,41 fold) and in the transcription profiling with the ER-PRL1/*prl1* PRL1 depletion approach (6,19 fold) in the sucrose-limiting medium. Furthermore, *SEPALLATA3 (SEP3)* and *ULTRAPETALA 1 (ULT1)* showed similar down-regulation during the time-course. PI controls the identity of floral organs and its correct regulation is required for normal development of petals and stamens (Honma and Goto, 2000). In addition, *ULT1* has been implicated in shoot and floral meristem development (Fletcher, 2001).

The *prl1* mutant has an early flowering phenotype both under short and long days (C. Koncz, personal communication). The time-course experiment showed that *FLOWERING LOCUS T (FT)* is down-regulated (2,06 fold), in the same way as *FLOWERING LOCUS C (FLC)* in the tiling experiment (1,82 fold). *FT* has been shown to promote flowering upon activation by *CONSTANS (CO)* (Kobayashi et al., 1999) and its down-regulation would expect to delay flowering. However, down-regulation of *FT* observed in only one sample of the time-course experiment probably represents an error due to the low expression of *FT* in seedlings. In fact, other observations indicate that *FT* is expressed during short day in the *prl1* (and also *cdc5*) mutant, when no *FT* expression can be detected in wild type plants (C. Koncz, personal communication).

The flowering time-related gene *SQUAMOSA PROMOTER BINDING PROTEIN-LIKE 3 (SPL3)* was found to be up-regulated during the time-course in addition to *AGAMOUS-LIKE 24 (AGL24)*, 3,71 fold) which was also up-regulated in the RNA-Seq analysis (2,08 fold). *AGL24*, a floral meristem identity gene promoting flowering, was shown to specifically repress floral homeotic genes (Gregis et al., 2009). *SPL3* was reported to prevent early flowering due to its down-regulation by miRNA156/157 (Gandikota et al., 2007). Therefore, the co-ordinated up-regulation of these genes correlates with the early flowering phenotype of *prl1*. This is also consistent with the down-regulation of *FLC*, which is known to promote flowering.

Several genes involved in leaf development also showed an altered regulation during the time-course. For example *ARABIDOPSIS THALIANA HOMEODOMAIN BOX 1 (ATHB1)*, a transcription factor directly involved in leaf shape control, is up-regulated. Ectopic expression of *ATHB1* was

found to cause defects in leaf development (Aoyama et al., 1995). This result could reflect the leaf phenotype observed in the *prl1* mutant (Németh et al., 1998).

Root development is extremely impaired in the *prl1* mutant. This is reflected in the transcription alteration of multiple genes associated to root development. For example, *MYB77*, an interacting partner of auxin response transcription factors (Shin et al., 2007) is down-regulated 2,5–2,7-fold in *prl1* roots. As *MYB77* plays a pivotal role in the control of auxin responses, including differentiation of lateral root and control of root elongation, its altered regulation may directly be related to the root developmental defects observed in *prl1*. *ROOT HAIR DEFECTIVE 2 (RHD2)* is up-regulated in roots during the time-course (2,5 fold) whereas is down-regulated in the RNA-Seq experiment (3,1 fold). The absence of *RHD2* is reflected in a lack of root hairs due to a reduced O_2^- production (Renew et al., 2005). This different behaviour of *RHD2* in the dynamic (ER-PRL1/*prl1*) and static (*prl1*) situation could be a reflect of the adaptation changes taking place when PRL1 is depleted, whereas the down-regulation of *RHD2* in the *prl1* mutant has a direct impact in root development.

In summary, grasping complex alterations in gene regulation reflected by steady-state differences and dynamic changes in transcript levels, gives an overview to infer the different regulation of developmental processes seen in the pleiotropic phenotype of *prl1*.

3.1.1.2 Altered transcription of genes in hormone regulation

By characterizing hormonal responses of the *prl1* mutant, Németh et al. (1998) observed a hypersensitivity to cytokinins, ethylene, abscisic acid and auxin. Extensive changes in transcript levels of genes involved in these hormonal pathways have been observed by comparative transcript profiling of *prl1* and wild type seedlings, as well as during the time-course of PRL1 depletion.

For example, *CYTOKININ-RESPONSIVE GATA FACTOR 1 (CGA1)* was identified as a gene with an early light-dependent response to cytokinin signalling (Naito et al., 2007). During the time-course, *CGA1* is 2,66-fold down-regulated, suggesting an impaired mechanism of cytokinin signalling. Furthermore, *CYTOKININ OXIDASE 2 (CKX2)* is up-regulated (2,6 fold) in the RNA-Seq analysis. *CKX2* over-expression reduces the active cytokinin content, producing smaller plants (Werner et al., 2003). A lower content of active cytokinins could be the cause of the semi-dwarf phenotype of *prl1*.

Several genes related to ethylene signalling were found to be miss-regulated in the tiling array dataset. For example, *EIN3-BINDING F-BOX 1 and 2 (EBF1 and EBF2)*, were found to be up-regulated in the *prl1* mutant (4,4 and 6,2 fold, respectively). *EBF1* and *EBF2* were shown to target EIN3 to degradation, repressing ethylene action (Gagne et al., 2004). During the time course, *ACC OXIDASE 1 (ACO1)*, a key gene in ethylene production, was found to be 2,54-fold up-regulated in shoots growing in 0,1 % sucrose, whereas no change was observed in shoots growing in 3 % sucrose. This differential regulation suggest an activation of ethylene production when PRL1 is depleted, only in sucrose-limiting conditions. Contrarily, *ACC SYNTHASE 7 (ACS7)* was found to be 2-fold down-regulated in the sucrose-limiting conditions, whereas is up-regulated in the *prl1* mutant (2,07 fold in the RNA-Seq experiment). *ACS7* has been shown to have an increased expression upon treatment of GA₃, ABA or salt (Wang et al., 2005). This difference in expression reflects the adapting situation the ER-PRL1/*prl1* plants are undergoing, whereas in the static situation (*prl1* plants), the increased regulation of *ACS7* reflects a chronic stress.

Multiple responses related to abscisic acid (ABA) have been related to stress situations. *UDP-GLUCOSYL TRANSFERASE 71B6* (*UGT71B6*) encodes for an ABA glucosyl-transferase. Over-expression of *UGT71B6* was shown to produce an accumulation of glucosylated ABA (Priest et al., 2006). *UGT71B6* up-regulation in the tiling array experiment suggests that activation of this gene is a consequence of an increased ABA content or ABA signalling. This up-regulation can lead to an accumulation of glucosylated ABA in the *prl1* mutant due to an overproduction of bioactive ABA. In fact, *ABA DEFICIENT 2* (*ABA2*), a gene encoding a key enzyme in ABA biosynthesis (Léon-Kloosterziel et al., 1996), is up-regulated (2 fold) when *PRL1* content decreases. Similarly, *ABSCISIC ACID RESPONSIVE ELEMENTS-BINDING FACTOR 3* (*ABF3*) is also up-regulated during the time course. Interestingly, *ABF3* over-expression is reported to confer tolerance to stresses including low and high temperature, oxidative stress and water deficiency (Kim et al., 2004). Contrarily, *ABSCISIC ACID RESPONSIVE ELEMENTS-BINDING FACTOR 1* (*ABF1*), a bZIP transcription factor, is 4,2-fold down-regulated, suggesting an *ABA2*-independent repression of *ABF1* (Uno et al., 2000) during the time-course. These data suggest that ABA biosynthesis is constitutively activated in the *prl1* mutant. Moreover, altered regulation of these genes correlates with an enhanced ABA sensitivity of *prl1* during seed germination and seedling development (Németh et al., 1998).

Responses to auxin are also enhanced in the *prl1* mutant. Intriguingly, while *MYB77* shows down-regulation in roots during the time-course, a set of *IAA* and *ARF* factors (including *Shy2/IAA3*, *IAA6*, *IAA7*, *IAA14*, *AXR3/IAA17*, *IAA29*, *ARF10*, *ARF11*), as well as *PINOID* and *ENHANCER OF PINOID*, which act as central regulators of auxin responses, are up-regulated in shoots during the time-course. Alteration of transcript levels of genes encoding components of auxin signalling may thus correlate with the enhanced auxin sensitivity trait of *prl1*.

During the time course, *PIN-FORMED 1* and *3* (*PIN1* and *PIN3*) were found to be up-regulated in shoots growing in 0,1 % sucrose. Alteration of *PIN* expression has been shown to have effects in root growth and embryo patterning (Blilou et al., 2005). These genes do not appear as altered in the tiling or RNA-Seq analysis, indicating that the *PIN*-dependent auxin homeostasis could be differently controlled in the *prl1* mutant than in the *PRL1* depleting situation. Other example of altered expression of auxin-related genes during the time-course is *AUXIN-REGULATED GENE INVOLVED IN ORGAN SIZE* (*ARGOS*), a gene induced by auxin, which is 2,14-fold up-regulated after *PRL1* depletion. Interestingly, *ARGOS* over-expression has been related to an over-growth of *Arabidopsis* organs (Hu et al., 2003). The up-regulation of *ARGOS* after *PRL1* depletion suggests the activation of a compensatory mechanism to keep the growing rate of the ER-*PRL1/prl1* plants.

ARABIDOPSIS THALIANA HOMEODOMAIN PROTEIN 2 (*ATHB-2*) is involved in auxin perception. When auxin is applied to the *athb-2* mutant, the phenotype is restored (Steindler et al., 1999). Furthermore, *ATHB-2* expression has been shown to be repressed by rich far-red light (Carabelli et al., 1993) and involved in mediated shade-avoidance responses (Steindler et al., 1999). These results suggest a deficient auxin response in *prl1*, since *ATHB-2* is 2-fold down-regulated in the RNA-Seq sample, whereas is 3,23-fold up-regulated during the time course, which could be explained as an adaptation mechanism to control auxin homeostasis during *PRL1* depletion.

Remarkably, depletion of *PRL1* in the time-course experiment resulted in 2 to 6-fold coordinated up-regulation of transcript levels of several genes involved in the biosynthesis of tryptophan (*ANTHRANILATE SYNTHASE ALPHA SUBUNIT 1*, α and β subunits of *TRYPTOPHAN SYNTHASE TRYPTOPHAN AMINOTRANSFERASE*) and tryptophan-derived indolacetic acid derivatives, including indol-3-acetaldoxime (IAOx), a precursor of glucosynolates, such as the antifungal camalexin. In correlation with the activation of this pathway, genes encoding signalling components of

the salicylic acid-triggered camalexin-based pathogenicity responses, such as *PAD3* and *EPS1* are up-regulated during the time-course.

Jasmonic acid biosynthesis is also modified in the *prl1* mutant and this is reflected in the transcription profile. *ALLENE OXIDE CYCLASE 4 (AOC4)* and *LIPOXYGENASE 1 (LOX1)* encode for enzymes which catalyse essential steps in jasmonic acid biosynthesis (Ziegler et al., 2000). Both are up-regulated in the time-course. In addition, jasmonate signalling is also impaired in the *prl1* mutant. This is shown by the up-regulation of *JASMONATE-ZIM-DOMAIN PROTEIN 6* and *7 (JAZ6* and *JAZ7)* in the tiling arrays (1,8 and 2,3 fold, respectively). *JAZ6* has been shown to rapidly increase its expression upon wounding-induced stress (Chung et al., 2008).

Gibberellin (GA) biosynthesis is activated during the time course, this is observed in the up-regulation (2,51 fold) of *GIBBERELLIN 3-OXIDASE 1 (GA3OX1)* and the down-regulation (2,97 fold) of *GIBBERELLIN 2-OXIDASE 6 (GA2OX6)*. Both gene products have antagonistic effects in the biosynthesis of active GAs (Hedden and Kamiya, 1997), leading to an increased amount of bioactive GAs during the time-course. A similar situation was observed in the tiling results: a gibberellin 2-oxidase was found to be down-regulated (1,8 fold) in *prl1*, suggesting that gibberellin inactivation is negatively regulated in the *prl1* mutant. Gibberellin signalling could also be modified during the time-course. Genes encoding two members of the RGA-LIKE DELLA protein family, which act as redundant negative regulators of GA responses, showed a 5,5 and 1,7-fold up-regulation in shoots analysed in the time-course experiment.

The above-mentioned regulatory changes in various hormone response pathways suggest to be the cause of the observed hormone hypersensitivity traits in the *prl1* mutant. However, only genetic analysis can confirm the exact implication.

3.1.1.3 DNA and RNA-related processes are modified

In the tiling array dataset, *ARABIDOPSIS MEI2-LIKE PROTEIN 5 (AML5)* was found to be 3 fold up-regulated. *AML5* was shown to be required for a proper meiosis in *Arabidopsis* (Kaur et al., 2006). An over-expression of *AML5* in *prl1* could be an effect of a compensating mechanism targeted at maintaining DNA stability. Contrarily, *ROOT AND POLLEN ARFGAP (RPA)*, a protein that binds to single-stranded DNA at stalled replication forks, was found to be down-regulated in the RNA-Seq experiment (3,6 fold). *RPA* was shown to perform an important role during pollen development (Boavida et al., 2009), since its absence produces semi-sterility. The down-regulation of this gene in *prl1* would suggest DNA instability, and especially during pollen development. *RPA* down-regulation could be reflected in the lower seed production of *prl1*.

During PRL1 depletion, several genes related to DNA stability have an altered expression. For example, *DNA-DAMAGE REPAIR/TOLERATION 100 (DRT100)*, which was reported to increase *E. coli* tolerance to mutagenic conditions (Pang et al., 1992), is 3,4-fold up-regulated. *CYTIDINE DEAMINASE 1 (CDA1)* is 2,67-fold up-regulated during the time-course in shoots growing in presence of 0,1 % sucrose. *CDA1* was found to deaminate cytidine and deoxycytidine and shares sequence and structure homology with known prokaryotic cytidine deaminases involved in DNA repairing (Faivre-Nitschke et al., 1999). Conversely, *UV REPAIR DEFECTIVE 3 (UVR3)* is 2,58-fold down-regulated in *prl1*. *UVR3* was found to encode a photolyase that repairs the cyclobutane pyrimidine dimer caused by UV light (Nakajima et al., 1998). Together this suggests that DNA is destabilized during PRL1 depletion.

Chromatin remodelling is also affected during PRL1 depletion. *REPRESSOR OF SILENCING 1* (*ROS1*) is 1,95-fold up-regulated. *ROS1* mediates an active DNA de-methylation by removing 5-methylcytosine (Morales-Ruiz et al., 2006). This implies that during PRL1 depletion, an active de-methylation is taking place. Furthermore, *METHYLATED DNA-BINDING DOMAIN 11* (*MBD11*) is 1,73-fold up-regulated. *MBD11* belongs to the same family of *MBD7* (Scebba et al., 2003) which indirectly interacts with PRL1 via PRMT11 (Salchert, 1997; Scebba et al., 2007). Overall, these results suggest that changes in DNA methylation in a genome-wide scale are taking place during PRL1 depletion.

Interestingly, a substantial number of genes, related to DNA stability, were found in the PRL1-depleting situation, whereas less were found in the tiling and RNA-Seq experiments. This difference suggests that the transcriptional regulation of genes leading to DNA stability is compensated in the *prl1* mutant.

DNA stability could have a direct impact on RNA-dependent processes such as transcription and pre-mRNA splicing. Recent QPCR profiling of TF mRNAs revealed hundreds of regulatory genes that show differential expression in the *prl1* mutant (Baruah et al., 2009). The transcript profiling experiments presented here also indicate differential regulation of several genes involved in post-transcriptional gene silencing. Specifically, *ARGONAUTE7* (*AGO7*) is 2,73-fold up-regulated in shoots growing in 0,1 % sucrose. *AGO7* is involved in defence against virus and its transcript is up-regulated by the presence of specific viral proteins, whereas the siRNA biogenesis is reduced due to virus-dependent mechanisms (Shivaprasad et al., 2008). This up-regulation of *AGO7* suggests that during PRL1 depletion, siRNA biogenesis is constitutively activated.

Furthermore, the stability of mRNA could be affected during the time-course. *GENE WITH UNSTABLE TRANSCRIPT 15* (*GUT15*) is 1,72-fold up-regulated in the low-sucrose medium. *GUT15* was discovered as a short-lived transcript upon treatment with a transcription inhibitor (Taylor and Green, 1995). *GUT15* is actually a non-coding RNA with a mRNA structure. Alterations such the one observed for *GUT15* in non-coding RNAs have been related to responses to stress, genomic imprinting and ribozyme activity (Rymarquis et al., 2008). These results strongly suggest that DNA and RNA stability are modified during PRL1 depletion in a genome-wide scale.

3.1.1.4 Specific effects of *prl1* on biotic and abiotic stress responses

A key to further dissect PRL1 effects on regulatory genes in abiotic stress response is the down-regulation of *CBF1* and *CBF2*, as well as *DREP1A*, *2A* and *DREB2B* during the time-course. *CBF1/2* are key regulators of low temperature response pathways (Thomashow, 1999). Down-regulation of *CBF1/2* transcript levels during the time-course does not only correlate with enhanced cold sensitivity of the mutant, but also with a coordinated down-regulation in transcription of several low temperature-induced marker genes, such as *COLD REGULATED B5* (*CORB5*) and *COR47*. *DREB1A* belongs to the cold-induced CBF class of AP2 transcription factors and transcription of the *DREB2* family is stimulated by drought and osmotic stress (Shinozaki and Yamaguchi-Shinozaki, 2000). As for *CBF1/2*, down-regulation of *DREB2A/B* transcription during the time-course leads to a coordinated down-regulation of transcript levels of numerous genes involved in osmotic and drought stress responses. These genes include members of the *EARLY RESPONSIVE TO DEHYDRATION* gene family (*ERD4*, *5*, *6*, *7*, and *15*), *RESPONSIVE TO DEHYDRATION 19* (*RD19*), members of the *ARABIDOPSIS ZINC-FINGER PROTEIN TF* family (*AZF1*, *2*, and *3*), *STZ* (*SALT TOLERANCE ZINC FINGER*), *SZF1* (*SALT-INDUCIBLE ZINC FINGER 1*) and others.

However, all osmotic stress marker genes, which are positively regulated by ABA or JA are remarkably up-regulated in the *prl1* mutant. These include, members of the *RESPONSIVE TO DESICCATION* family, such as *RD2*, *RD20*, *RD22*, *RD26* and several dehydrin-encoding genes.

Activation of JA, ABA, glucosynolate, ethylene and salicylic acid-regulated pathways is indicated by the up-regulation of over hundred of known genes involved in pathogen-signalling pathways. Activation of SA biosynthesis –and signalling– during the time-course is suggested by the 2,24-fold up-regulation of *ISOCHORISMATE SYNTHASE 2 (ICS2)*, involved in SA biosynthesis (Garcion et al., 2008).

This result correlates well with the high transcription of SA-stimulated classical genes, including the *PATHOGENESIS-RELATED GENES PR1* and *PR4*, which have been previously observed also by Németh et al. (1998). Analogously, up-regulation of the JA signalling pathway is indicated by increased transcript levels of JA-induced genes, including *PDF1.2*, *PDF1.2a* and *PDF1.4*. Although not exposed to pathogen, the time-course also displays activation of several elicitor-induced genes, such as *ELICITOR-ACTIVATED GENE 3-1 (ELI3-1)* and *ELI3-2* and *AVRRPT2-INDUCED GENES (AIG1* and *AIG2)*. Activation of HR responses is indicated by an up-regulated transcription of 26 genes encoding various enzymes of phenylpropanoid pathway (including *CHALCONE SYNTHASE* and *PHYLALANINE AMMONIA LYASE* described by Németh et al, 1998) in *prl1*.

Contrarily, during the time-course, specific genes that mediate pathogen recognition are down-regulated, including *RECOGNITION OF PERONOSPORA PARASITICA 4* and *5 (RPP4* and *RPP5*, respectively) which confer resistance for downy mildew (van der Biezen et al., 2002; Parker et al., 1997, respectively). Another example is *BOTRYTIS-INDUCED KINASE1 (BIK1)*, which is up-regulated upon *Botrytis cinerea* infection, shows a 3,87-fold down-regulation during the time course.

Miss-regulation of pathogen-induced genes during PRL1 depletion could affect the expression of genes involved in responses to reactive oxygen species (ROS). Several putative peroxidases, which reduce peroxides, were found to be up-regulated in the tiling and RNA-Seq dataset, whereas none was found to be down-regulated. The time-course experiment also revealed extensive changes in ROS signalling. For example, *L-ASPARTATE OXIDASE (AO)*, is involved in the biosynthesis of NAD. The early steps of NAD biosynthesis occur in the plastid with the conversion of L-aspartate by AO (Kato et al., 2006). This result suggests that the production of NAD is highly up-regulated during PRL1 depletion. Furthermore, *RESPIRATORY BURST OXIDASE HOMOLOGUE D (RBOHD)* is also up-regulated (2,29 fold), suggesting that the pathogen- and NADP-dependent systemic signal of oxidative burst in which RBOHD is involved (Miller et al., 2009), could be up-regulated during the time-course. Interestingly, several glutaredoxins, which transfer the ROS to glutathione, are down-regulated. This suggest that the glutathion-dependent mechanism of ROS scavenging is inactivated during PRL1 depletion.

Effects of ROS can lead to cell death, and during the time-course, *ACCELERATED CELL DEATH 6 (ACD6)*, a gene involved in cell death (Dong, 2004), is highly up-regulated (2,81 fold in roots growing in the sucrose-limiting situation). Absence of *ACD6* provokes an enhanced resistance to *Pseudomonas syringae* (Rate et al., 1999) whereas its mRNA is over-expressed in uninfected tissues of infected plants by *P. syringae* (Lu et al., 2003). *ACD6* up-regulation during the time-course reinforces the hypothesis that the systemic signal against pathogen is activated during PRL1 depletion. Furthermore, *ARABIDOPSIS NAC DOMAIN CONTAINING PROTEIN 6 (ATNAC6)*, a positive regulator of senescence in leaves (Kim et al., 2009), is up-regulated not only in the sucrose-limiting conditions of the time-course, but also in the 3 % sucrose-containing medium.

Nevertheless, *SUGAR TRANSPORT PROTEIN 13 (STP13)*, whose induction has also been related to programmed cell death (Nørholm et al., 2006), is 6,73-fold down-regulated during the time-course. *STP13* could counter-act for *ACD6* and *ATNAC6* in the inactivation of the cell death programme during the time-course. These observations suggest an altered response in programmed cell death that could be reflected in the slower growth of the *prl1* mutant.

3.1.2 RNA-Seq is a powerful tool for revealing alternative splicing

3.1.2.1 Annotation-dependent

The transcript profile analysis of the RNA-Seq data, carried out with Cufflinks is able to discern expression levels of alternative-spliced isoforms from the same locus. For example, the locus *AT5G58720* shows a 3-fold over-expression in *prl1* of the third isoform exclusively, whereas isoforms one and two do not show any changes in expression. Expression of *AT5G58720* was not found to be altered in *prl1* with the transcript profiling performed using the tiling arrays.

AT5G58720 encodes a protein that has been shown to interact with the N-terminal part of PRL1 (Salchert, 1997) and it is predicted to function in DNA binding and mismatch repair. *AT5G58720* shares 44 % similarity with *SILENCING DEFECTIVE 5 (SDE5)*, a gene proposed to be involved in the transport of trans-acting short interfering RNAs (tasiRNA, Hernández-Pinzón et al., 2007). Specifically, the PAM2 motif, a motif for interaction with polyA binding proteins, is highly conserved between the two proteins. Interestingly, only the predicted product of *AT5G58720.3* contains the sequence of the last intron, whereas the last exon of the representative isoform (*AT5G58720.1*) is missing. This difference in sequences can have an impact on the function, localization, stability or interactions of *AT5G58720.3*. Moreover, the sequence of *AT5G58720* found to interact with PRL1 by Y2H (Salchert, 1997) corresponds to *AT5G58720.1*, the only isoform containing the last exon. This suggests that the isoform that interacts with PRL1 is *AT5G58720.1*, whereas the product of *AT5G58720.3*, although is up-regulated in *prl1*, could have different implications in the phenotype.

A correct evaluation of expression levels of different isoforms of the same gene model has been explored only recently. For instance, Bohnert et al. (2009) commented on quantification strategies dealing with *de novo* transcripts, whereas, Richard et al. (2010) presented a method for prediction and quantification of alternative-spliced isoforms based on exon expression levels. This last quantification method is more efficient when an accurate annotation of the different isoforms is in place.

3.1.2.2 Annotation-independent

The results presented in section 2.3.3 suggested an over-representation of exon sequences in *prl1* and *cdc5* when analysed by RNA-Seq, whereas intron sequences show a similar representation as in the WT sample. However, comparative RT-PCR analyses performed in the *prl1* and *cdc5* mutants suggest that not only the amount of retained introns is increased, but also, the alteration of splicing-related processes, including alternative splicing and alternative starting codon selection (C. Koncz, personal communication). Thus, the lack of difference in the frequency of retained introns in the RNA-Seq data remains a question.

Moreover, observing the distribution of RNA-Seq reads on genes showed that reads mapping to 3' sequences of mRNAs are higher represented than 5' sequences (Table 2.13). Conclusions concerning differences in the frequency of retained introns in *prl1* may only be made by increasing the representation of exonic and intronic reads.

An annotation-independent transcript profiling can give insights in the production of aberrant transcripts due to the alteration of splicing-related processes. Nevertheless, this analysis can only be performed with an increased coverage of the sequenced transcriptome of *prl1*. This implies that the *de novo* transcript assembly performed by Cufflinks would increase in robustness, and would be able to detect the production of non-annotated transcripts which are the result of the alteration of splicing-related processes.

3.1.3 Tiling arrays and RNA-Seq analyses provide different resolution

Both experiments were performed using the same biological samples. However, the results of these experiments did not overlap (section 2.2.3). This could be explained by the different resolution power that both technologies have in several technical and analytical aspects.

The tiling array resolution is limited to 35 bp due to its design (section 4.1.11). Moreover, the definition file used for the transcript profiling –compiled by Naouar et al. (2009)– further reduces this resolution with the condition that three consecutive probes on the array must belong to one annotated exon in order to be scored. Contrarily, the RNA-Seq sample and data analysis has 1 bp resolution, allowing a more accurate transcript measurement.

In addition, the sample preparation protocol followed for the tiling array does not allow to distinguish from which DNA strand the hybridized fragment originated. This represents a problem when both strands are transcribed. Contrarily, the protocol followed for the RNA-Seq samples is strand-aware.

Furthermore, the analysis carried out with Cufflinks for the transcript profiling relies on transcript assembly. This has the advantage, not only of a more accurate transcript measurement, but also of the measurement of different isoforms of a gene-model. Cufflinks uses differential exon coverage (Richard et al., 2010) for computing which isoform is more abundant. Contrarily, the data analysis carried out for the tiling arrays uses the mean average of the different scored exons of one gene-model –and not a transcript– for calculating the expression.

Moreover, the description file published by Naouar et al. (2009) is based on the TAIR7 release, whereas the transcript profiling performed with Cufflinks was based on the most up-to-date TAIR9 assembly and annotation release. Changes in co-ordinates between both annotation releases are extensive, having an impact in correct expression determination in transcription profile experiments.

All together, the comparison of the RNA-Seq and the tiling arrays analyses for the transcript profiling of *prl1* favours the results obtained with RNA-Seq due to its higher resolution. Nevertheless, the resolution of the tiling array technology also allows accurate transcription profile analyses with the exception of the alternative-spliced isoform analysis. However, for both technologies, not only a richer annotation, but also an accurate annotation is obligatory for a correct data analysis. Despite these advantages, both tiling and RNA-Seq methods have the great disadvantage that the transcript abundance values cannot be directly compared with results

obtained by the classical ATH1 microarrays. This problem is primarily due to the fact that the quantification process not only relies on 3' sequences of annotated genes.

As it is illustrated by this work, it is also very difficult at the moment to establish significant overlaps between RNA-Seq, tiling array and classical microarray hybridization data. This implies also that there are great difficulties in the selection of statistically-significant data, from the tiling and RNA-Seq analyses to be confirmed by QPCR assays. The microarray hybridization to 3' end-specific oligo probes can be readily reproduced in most cases by QPCR. Unfortunately, only further development of assisted-statistics and cDNA library creation approaches could resolve these discrepancies.

3.1.3.1 The case of transposable elements

The results presented in section 2.3.4 revealed a problem of consistency when comparing the transcription alteration of transposable elements between the tiling array and RNA-Seq data analyses.

This discrepancy may be related to the fact that the tiling array and RNA-Seq data analysis were based on two different genome annotation versions (TAIR7 and TAIR9, respectively). It was not until the TAIR8 release, where the transposable element category suffered a major revamp due to a mixed manual and automatic curation focused on transposable elements.

For example, in *prl1*, the annotated unit AT3G42658, a transposable element belonging to the *Sadhu* family of retro-transposons, is highly up-regulated in the tiling analysis (Table C.5), whereas in the RNA-Seq experiment, although is also up-regulated, it is just below the selected cut-off level and does not appear in the results. This reflects the differences in resolution for both technologies.

The differences in the two annotation releases are well illustrated on the example of AT3G42658. This annotated unit is located in TAIR7 between the positions 14760386 and 14761280 of chromosome 3, whereas in TAIR9 the localization shifted to positions between 14749400 and 14750294 of the same chromosome. In this case, TAIR7 and TAIR9 annotations do not overlap. This lack of overlap implies that sequences mapped in the tiling array by Naouar et al. (2009) (following the TAIR7 release) to the unit AT3G42658, do not correspond to the same co-ordinates after the TAIR9 release. In fact, a closer look to the co-ordinates annotated for TAIR7 in the TAIR9 release, revealed an empty region.

Moreover, the TAIR9 release, annotates the transcribed sequence of transposable elements as exons, suggesting that this is the reason for having a higher number of aligned sequences against the exon index in *prl1* compared to WT (Table 2.13). Nevertheless, no differences in alignment were observed for the transposable element index between WT, *prl1* and *cdc5*. This is only an apparent contradiction, since the index for transposable elements reflects the complete sequences of transposable elements, and not the transcribed sequences found in the genomic context.

3.1.4 Transposable element loci show differential expression in *prl1*

The results presented in section 2.3.4 combining the RNA-Seq and tiling arrays experiments, suggested that several units annotated as transposable elements showed differential expression in *prl1*. Transposable elements are long-known to be activated under stress situations (Grandbastien,

1998). This activation is due to a change in their methylation status (Lisch, 2009). The activation of many stress-regulated genes in *prl1* may have a relationship with the observed changes in expression of different transposon loci.

Nevertheless, mechanisms resulting in transposon silencing independent of *DDM1*, *MET1* or *CMT3* seem to be affected in *prl1*: *DDM1* and *MET1* do not show an altered transcription in *prl1*. Furthermore, *CMT3*, which is directly involved in transposon silencing (Tompa et al., 2002) and acts together with *MET1* (Kato et al., 2003), is also normally expressed in *prl1*. This result suggests an impaired gene silencing in *prl1* independent of *MET1*.

3.2 Characterization of PRL1 functions

3.2.1 *PRL1*-PIPL is expressed in native conditions

Németh et al. (1998) observed that only *PRL1* constructs carrying the whole genomic sequence complemented the *prl1* phenotype, whereas *PRL1* cDNA clones, driven by various promoters, failed to complement the phenotype. Subsequent studies of Szakonyi (2006) indicated that specifically the first two introns of *PRL1* are required for a proper *PRL1* expression. This finding was taken into account when designing the PRL1-PIPL construct. The genetic sequence containing the promoter region and the three first introns was fused in frame with the rest of the *PRL1* cDNA sequence. The expression studies performed in this work, show that PRL1-PIPL is correctly expressed in cell suspensions, and *in planta*, since a complete *prl1* complementation was observed in every identified primary transformant.

The localization of *cis*-regulatory elements in intragenic regions are not an exclusive characteristic of *PRL1*. Already Sieburth and Meyerowitz (1997) observed how *AGAMOUS* (*AG*) changed the expression pattern as expected in mutants of negative regulators of *AG*, only when the intragenic sequences were present in the reporter construct. Another example was provided by Sheldon et al. (2002), who showed that the first intron of *FLOWERING LOCUS C* (*FLC*) was required for the proper maintenance of the repression of *FLC* expression induced by vernalization. Recently, a genome-wide study performed by Rose et al. (2008) showed that in many genes, introns close to the promoter region are enriched with transcription-enhancing elements. Moreover, they observed that the enhancing signals present in introns are conserved between rice and *Arabidopsis*.

In summary, PRL1-PIPL is fully functional and is expressed in native conditions. Therefore it can be used for easily monitoring PRL1 stability, and for investigating the interactions of PRL1 in native conditions.

3.2.2 *PRL1* transcription and PRL1 accumulation are sucrose-dependent

In this work, it was shown that *PRL1* transcription –when expressed natively– is independent of sucrose concentration and shows no diurnal variations (section 2.1.2), whereas *PRL1* translation is sucrose-dependent (section 2.1.3) showing a higher protein accumulation in low-sucrose conditions. However, when *PRL1* is over-expressed, both *PRL1* transcript and protein accumulation are sucrose-dependent (section 2.2.4.2). This result confirms what was shown for the *PRL1* transcription by Németh et al. (1998). However, the changes in PRL1 accumulation do not correlate with its transcription, suggesting that post-transcriptional or post-translational mechanisms control PRL1

accumulation. Furthermore, *PRL1* stability is higher in sucrose-deprivation conditions whereas gene expression is not higher when sucrose is available.

One example of change in stability due to stress is found in *MOS4* upon pathogen attack in *Arabidopsis* where a lack of the gene product increases plant susceptibility (Palma et al., 2007). This observation suggests that *MOS4* stability and its interaction in the Prp19-associated complex (Monaghan et al., 2009) is required for signalling during the pathogen attack. The accumulation of *PRL1* in sucrose-limiting conditions could suggest a parallel requirement where *PRL1* is required for a correct sugar stress response.

The stability of *PRL1* in low-sucrose conditions could also be given by the CUL4-DDB1 complex: *PRL1* was shown to interact with the CUL4-DDB1-Ubiquitin ligase complex as a substrate receptor (Lee et al., 2008). *PRL1* mRNA level in the *cul4cs* background is similar than the levels found in WT, whereas at the protein level, *PRL1* is less abundant. This suggest that the stability of *PRL1* can also depend on its interaction with the CUL4-DDB1 complex. In this PhD work, it has been shown that *PRL1* stability, under native *PRL1* expression conditions, is higher in low-sucrose conditions than in high-sucrose conditions.

In contrast to the results when *PRL1* was expressed natively (sections 2.1.2 and 2.1.3), the ER-*PRL1/prl1* samples used for the time-course experiment in *PRL1* depletion showed a different behaviour of *PRL1* transcription and protein accumulation under the different sucrose conditions assayed. Furthermore, the transfer of the ER-*PRL1/prl1* plants from a medium with β -estradiol to a medium without β -estradiol, enabled the analysis of the *PRL1* transcript and protein stability. This was observed in the *a priori* validation (section 2.2.4.2), as well as in the comparison of *PRL1* expression in ER-*PRL1/prl1* with WT and *prl1* (section 2.2.4.4) which confirmed a higher amount of both *PRL1* transcript and protein accumulation in the sucrose-limiting medium during the inductive conditions –presence of β -estradiol–.

This observation links the efficiency in trans-gene silencing mechanisms to stress situations. Available sucrose in the medium reduces the expression of the *PRL1* trans-gene and hence its protein accumulation. Pontes et al. (2006) proposed the action of RNA-directed DNA methylation in gene silencing in *Arabidopsis*. The subsequent identification of KTF1 (KOW domain-containing transcription factor 1) showed that in its absence, the silencing of several loci is abolished, including the stress-responsive *RD29A* gene (He et al., 2009). Therefore, it could be suggested that *PRL1* pre-transcriptional silencing is impaired in sucrose-limiting conditions.

Interestingly, *PRL1* transcript and protein stability in the ER-*PRL1/prl1* samples was enhanced in the high-sucrose medium during the time-course. Although transcript content was not as high as in the sucrose-limiting conditions, transcript amount did not decrease as abruptly during the time course as in the sucrose-limiting conditions (section 2.2.4.2). This could reflect an activated post-transcriptional silencing mechanism in the sucrose-limiting conditions when the *PRL1* gene is not transcribed anymore. Differences in the biogenesis of miRNAs have been already associated to stress situations. For example, the down-regulation of *miR398* biogenesis during oxidative stress conditions allows the transcripts of two superoxide detoxification genes –*CSD1* and *CSD2*– to be stabilized and higher translated (Sunkar et al., 2006). Further studies also linked the down-regulation of *miR398* to other stress situations, including pathogen-induced stress (Jagadeeswaran et al., 2009). Contrarily, in the case of *PRL1* stability, the result suggests that the post-transcriptional silencing leading to *PRL1* degradation once the trans-gene is not transcribed anymore, is activated in sucrose-limiting conditions.

Together, this suggests that when *PRL1* is expressed in native conditions, stress conditions like sucrose deprivation stabilize PRL1. Furthermore, when *PRL1* is over-expressed, a sucrose deprivation situation enhances *PRL1* expression due to defects in pre-transcriptional gene silencing, whereas the transcript stability is highly reduced due to a constitutively activated post-transcriptional silencing mechanism.

3.2.3 PRL1 does not affect the proteasome catalytic activity

Farrás et al. (2001) showed the association of AKIN10 and AKIN11 with SKP1/ASK1, a conserved SCF ubiquitin ligase subunit, and the α 4/PAD1 proteasomal subunit. This, together with PRL1 interaction with the C-terminal domain of AKIN10/11 (Bhalerao et al., 1999) suggested that PRL1 could reduce the interaction of AKIN10/11 with SKP1/ASK1 by modifying this interaction with the proteasome. However, further studies performed by Szakonyi (2006) established that the interaction of PRL1 with the proteasome was through degradation, where PRL1 stability was enhanced by modification of the destruction box motif between residues 113–121 in transformed cell suspension or in presence of a proteasome inhibitor.

To test whether modifications in PRL1 accumulation has effects in the regulation of the proteasome activity, an activity-based proteasome profiling assay was performed (section 2.1.4). The profiling showed no change in the fluorescent probe binding to the β -catalytic subunits of the proteasome. Neither during PRL1 depletion nor PRL1 absence compared to the WT situation. However, the regulatory subunit Rpn6 was found to be more abundant in the *prl1* mutant and when PRL1 depletion was taking place.

Rpn6, a protein without ATPase activity, is located in the lid complex of the 19S regulatory subunit of the proteasome. The lid is the responsible complex of connecting the 26S proteasome in the ubiquitin-dependent protein degradation pathway (Finley, 2009) since the Rpn10 (Elsasser et al., 2004) and Rpn13 (Husnjak et al., 2008) subunits directly interact with the attached ubiquitin chain of the proteins to be degraded. The increased amount of Rpn6 in *prl1* could imply the over-representation of the 26S proteasome compared to the 20S proteasome by the interaction of the 20S particle with the abundant 19S particle. This would suggest the favouring of the ubiquitin-dependent protein degradation. Recently, Kurepa et al. (2009) linked an increased 26S proteasome biogenesis to an increased tolerance to stresses –like heat stress– that provoke misfolded proteins, whereas an increased biogenesis of the 20S proteasome increases the tolerance to oxidative stresses. This could mean a reduction in the degradation of oxidized proteins in the *prl1* mutant with a direct impact in the phenotype.

The lid complex of the 19S particle shares many similarities with the COP9 signalosome (Glickman et al., 1998; Kim et al., 2001), a protein complex involved in gene expression, cell-cycle control (Wei et al., 2008) and DNA-damage response through its interaction with cullin-RING type E3 ubiquitin ligases like the CUL4-DDB1 complex (Holmberg et al., 2005). Furthermore, studies in *Drosophila* have shown that Rpn6 interacts with a subunit of the COP9 signalosome. Taken together, the accumulation of Rpn6 in the *prl1* background could be an indirect effect of a constitutively activated DNA-damage signal in the absence of PRL1 through the CUL4-DDB1 signalling complex.

3.2.4 PRL1 could be involved in gene silencing

One hint of the exact PRL1 function in *Arabidopsis* could be given from the transcript profiling experiments performed in this work with tiling arrays and RNA-Seq. Several transposable elements from the retro-transposon class were shown to be miss-regulated (section 2.3.4). Together with an up-regulation of the majority of the differentially expressed genes in *prl1*, this indicates that the silencing mechanisms are not functional in *prl1*. This impaired silencing mechanism could be a simple explanation for having such modified responses to pathogen attack (Palma et al., 2007), ROS signalling (Baruah et al., 2009) and the overall *stressed* phenotype in the *prl1* mutant.

It is actually difficult to discern whether a stress situation elicits the expression of transposable elements, or the other way round. Similarity of promoter regions in transposable elements and *R*-genes suggest that transposable elements have *opportunistically* evolved to be easily replicated during stress situations. From the plant perspective, having genome re-arrangements during a stress situation rises the chances to be adapted to the new situation. It has been reported that genome re-arrangements of *R*-genes are enhanced during pathogen attack (Kovalchuk et al., 2003).

The idea of PRL1 involved in gene silencing was already suggested by Salchert (1997) after his studies by yeast two hybrid (Y2H) system where he found the interaction of PRL1 with AT4G29510, a protein with arginine N-methyltransferase activity, he could also map exactly this interaction to the last part of the N-terminal region of PRL1. Later studies showed the interaction of the AT4G29510 product (PRMT11) with MBD7 (Scebba et al., 2007), a protein containing a methyl-CpG-binding domain (MBD) that specifically binds to CpG methylated DNA sequences *in vitro* (Zemach and Grafi, 2003), that is localized in heterochromatic areas and interacts with DDM1 (Zemach et al., 2005).

Whether methylation-dependent gene silencing is changed in the *prl1* mutant, must still be established by further studies.

3.3 Functional comparison of PRL2 with PRL1

The alignment of the protein sequences performed by (Németh et al., 1998) and shown in Figure A.5 (page 144) revealed that the two gene products are very similar. This similarity suggests that they could have redundant or similar functions.

3.3.1 Ectopic expression of *PRL1* or *PRL2* complement mutual phenotypes

In section 2.4.7 it was shown that when overexpressed, *PRL1* can complement the *prl2* phenotype and vice-versa.

This case of mutual complementation is not the first example found in *Arabidopsis*. Already Carles et al. (2005) presented a parallel situation with *ULT1* and *ULT2*, whereby over-expression of *ULT2* complemented the *ult1-1* phenotype. Specifically, the expression patterns of *ULT1/ULT2* fully overlap during flower development, whereas for PRL1 and PRL2 the expression patterns differ considerably (section 2.4.5.2). This indicates that redundancy of function between paralogues is not an exception.

Nevertheless, only partial complementation of the root length phenotype of *prl1* can be achieved by *PRL2* over-expression and only a few lines were found where over-expression of *PRL1* complemented the *prl2* phenotype. This parallelism was also observed in the chimeric constructs (1N2C-HA and 2N1C-HA, section 2.4.8): only 1N2C-HA achieved full complementation in *prl1* background, whereas no complementing line was found for the *prl2* background. Contrarily, only 2N1C-HA could complement the *prl2* mutation and the root phenotype was only partially rescued in *prl1*. In addition, it has been shown that the expression of isolated N- or C-terminal domains of *PRL1* are not enough for genetic complementation (section 2.1.6).

These results suggest that specific sequences in the N-terminal regions of both *PRL2* and *PRL1* are required for a correct function of the proteins.

The direct comparison of the native expression of *PRL2* in the *PRL2gDNA/prl2* plants to the *PRL2-HA/prl2* plants further suggests that specific *cis*-regulatory elements are needed for a correct expression of *PRL2*. Every *PRL2gDNA/prl2* primary transformant showed a rescue of the *prl2* phenotype, whereas only a fraction of the primary transformants of *PRL2-HA/prl2* achieved the phenotype complementation. This result indicates that the proper expression pattern of *PRL2* is critical for the achievement of an efficient complementation.

Szakonyi (2006) already showed that specific *cis*-regulatory sequences present in the two first introns of *PRL1* were needed for the correct expression of the *PRL1* trans-gene. A similar situation is suggested for *PRL2*, which has a smaller promoter region than *PRL1* but longer first and second intron sequences (Figure A.3).

3.3.2 PRL1 and PRL2 are required in the nucleus

The over-expression constructs designed in this work for the localization of *PRL2* together with YFP confirmed the import of *PRL2* into the nucleus (section 2.4.5.1). Interestingly, YFP attached to the N-terminal end of *PRL2* is only localized in the nucleus, whereas the fusion protein of YFP in the C-terminal end of *PRL2* also localizes into the cytoplasm. A parallel situation was observed for *PRL1*. Hereby, the C-terminal fusion of *PRL1* to the small HA tag localized in the nucleus, whereas *PRL1* with the larger GFP tag fused to the C-terminal end of *PRL1* was also located in the cytoplasm (Szakonyi, 2006). This result indicates that the GFP protein, as opposed to the small HA tag, hinders the proper recognition of the nuclear localization signal (NLS) of *PRL1* (called SV40-type by Németh et al., 1998) located in the C-terminal end and therefore, the correct *PRL1* localization. The YFP-*PRL2* vs. *PRL2*-YFP localization result shows a similarity to the *PRL1* localization studies, suggesting that the fluorescent protein at the C-terminal end of *PRL1* –and *PRL2*– interferes with the protein localization. Furthermore, the *PRL2* sequence aligning with *PRL1* NLS is 100 % conserved (Figure A.5).

More supporting data for the requirement of *PRL1* in the nucleus comes from the constructs characterized in this work and obtained by Dr. D. Szakonyi which contain only the N- or C-terminal part of *PRL1* (section 2.1.6). For *prl1* plants transformed with those constructs, not a single primary transformant was found where the *prl1* phenotype was complemented, not even a partial rescue in the root length phenotype. The *PRL1-C-HA* construct contains the WDR domain plus the nuclear localization signal. In contrast, the *PRL1-N-HA* construct, apart from the destruction box motif found by Szakonyi (2006), has no conserved domain or known function (section 2.1.5). In the *PRL1-C-HA/prl1* plants, the construct product can very likely be imported into the nucleus, but the WDR domain alone is not enough for carrying out the *PRL1* function.

Whereas, in the *PRL1*-N-HA/*prl1* plants, the trans-gene product can not be imported into the nucleus due to the missing NLS. Although several eukaryotic orthologues of *PRL1*/*PRL2* lack the N-terminal extension found in plants, the results presented here suggest that the N-terminal domains of *PRL1* and *PRL2* are essential for the correct function of these proteins.

Previous studies on *PRL1* interactors done with the Y2H system (details in [Salchert, 1997](#)), revealed that an α -importin ([Németh et al., 1998](#)) interacted with the C-terminal end of *PRL1*. Further studies with this α -importin linked its function to defence responses. [Palma et al. \(2005\)](#) found a mutant of this AT4G02150 locus (*mos6*) as a suppressor of the autoimmune phenotype of the *snc1* mutant. Later on, the same suppression phenotype of *snc1* was reported for *mos4*. *MOS4* is shown to interact with *PRL1* through *CDC5* in the nucleus ([Palma et al., 2007](#)). These results are consistent with the suggestion that *MOS6* is specifically involved in the nuclear import of *PRL1*, which is required for its proper regulatory function.

3.3.3 Mutant phenotypes differ due to gene sub-functionalization

Although *PRL1* and *PRL2* have redundant functions, the phenotype of both mutants has no common characteristics (Figure 1.1 and 2.14, respectively). The *prl2*/*+* phenotype described in this work suggests that the function of *PRL2* is required for embryo viability, as indicated by the presence of aborted seeds in siliques of *prl2*/*+* plants and in the impossibility of obtaining homozygous *prl2/prl2* plants.

The differences in *prl1* and *prl2* phenotypes could be explained by a sub-functionalization after the gene duplication event took place. A similar example of sub-functionalization following gene duplication with impact in the phenotype can be taken from the study of [Xiao et al. \(2008\)](#) in tomato. It was shown that the *SUN* locus, which controls the elongated shape of tomato fruit, was a duplication of an existent gene which *fell* into a new genomic context with new *cis*-controlling elements. This new genomic context allows *SUN* to be highly expressed during fruit development causing the elongated tomato shape. Interestingly, it was indeed shown that the gene duplication event of *SUN* was mediated by a retro-transposition event.

Comparing the genomic sequences of the first and second introns of *PRL1* and *PRL2* could provide details on this sub-functionalization. [Szakonyi \(2006\)](#) already observed that the first and second introns of *PRL1* are needed for the proper expression of transgenic *PRL1* in order to complement the *prl1* phenotype. Interestingly, the first, but especially, the second intron of *PRL2* are longer than the *PRL1* homologues (Figure A.3 on page 140). Those added sequences to the introns could represent *cis*-regulatory regions arisen during the sub-functionalization process.

3.3.4 Induced *prl2* somatic phenotype is similar to *prl1*

The strategy followed for studying the somatic phenotype of *prl2* (section 2.4.6) revealed defects in the development of reproductive organs in *PRL2gDNA*-HS/*prl2* plants upon heat shock. As a negative control, *PRL2gDNA/prl2* plants were also heat shocked and no developmental defect could be observed. The action of the CRE recombinase was shown to have a minimal impact on *Arabidopsis* transcriptome measured by transcript profiling in a similar excision experiment ([Abdeen et al., 2010](#)). This implies that the action of CRE recombinase has no side effects than the observed phenotype in the *PRL2gDNA*-HS/*prl2* plants upon heat shock.

So far, somatic effects of *prl2* were observed in reproductive organs, and proved to be similar to the phenotype displayed by *prl1* grown in short day conditions.

3.3.5 *prl1* × *prl2*/+ suggests a partial and asymmetrical redundancy in function

The phenotype of the double *prl1* × *prl2*/+ mutant characterized in this work shows an additive interaction of *prl1* and *prl2* phenotypes with an embryo lethal phenotype of *prl1* × *prl2* seeds and a pleiotropic phenotype of *prl1* × *prl2*/+ plants. Moreover, the pleiotropic phenotype of the double mutant is more severe than the pleiotropic phenotype of *prl1* alone (section 2.4.3).

Furthermore, the RT-PCR analysis of WT plants (Figure 2.16) revealed that *PRL2* is basally expressed in vegetative organs, except in roots where was not detected. This result provides the explanation of the severe root phenotype of *prl1* due to a transcription of *PRL2* below the detection limit. Furthermore, it provides the explanation for the lack of lethality of *prl1* due to the basal expression of *PRL2* in aerial organs, as shown by the PRL1/PRL2 over-expression studies, where *PRL2* executes PRL1 function. Nevertheless, when *PRL2* is expressed under its native promoter, high expression is restricted to punctual developmental stages. This result suggests that lower expression of *PRL2* in native conditions, together with missing specific regulatory interactions of PRL1 produce the pleiotropic phenotype of *prl1*.

3.3.6 Differential expression during development reflects sub-functionalization

In section 2.4.5.2 it was shown through the GUS analysis that *PRL2* and *PRL1* transcription differ during *Arabidopsis* development. Whereas *PRL1* is present in dividing cells during most of the plant development, *PRL2* is mainly expressed during the development of masculine reproductive organs and early seed development. Although a basal *PRL2* expression during vegetative development was observed in section 2.4.4.

One overlapping point of *PRL1* and *PRL2* expression takes place during the early development of floral masculine organs (Figure 2.19). This could be the reason why the reciprocal crosses of *prl2*/+ with WT produce in both directions the same segregation ratio in the offspring for the T-DNA marker in *PRL2*. This result indicates that although *PRL2* is highly expressed in pollen development, *PRL1* expression during the micro-sporogenesis process is required for the pollen grains to be formed. Furthermore, during micro-sporogenesis until pollen grain formation, only 5 cell divisions take place. Suggesting that the accumulation of PRL1 does not go below a threshold level that would imply the abortion of gametophyte development. Nevertheless, one question to address would be the genetic stability of the sperm cells.

PRL2 expression during early seed development in the zygote and during endosperm development (Figure 2.20), suggests that in this development stage, a checkpoint in which PRL2 is involved, prevents *prl2/prl2* embryos to resume a successful development.

3.3.7 Embryo lethality of *prl2* could be linked to gene silencing

The above described differences in phenotype between *prl1* and *prl2* are striking, as *prl1* is not lethal, whereas *prl2* causes early embryonic lethality. If PRL1 function is related to gene silencing in a transcription-dependent manner, it could well be that PRL2 has the same function, but

especially, during pollen maturation and early embryo development. The function of PRL2 is specifically required during those time-framed processes, with potential implications in genetic stability for the correct development of the offspring. Recently, [Slotkin et al. \(2009\)](#) observed how genetic stability of sperm nuclei is achieved through a combined strategy of a reduction in DDM1 amount which elicits a reactivation of transposable elements (TEs) in the vegetative nucleus and in an increased siRNA biogenesis from TE-derived transcripts that reach the sperm nuclei. TE-derived siRNAs prevent the activation of TEs in the sperm nuclei. This observation rises questions about the genetic stability of sperm nuclei of *prl2* pollen grains and hence, of *prl2/prl2* zygote or *prl2/prl2* endosperm. Structures where only *PRL2* –and not *PRL1*– is expressed.

The potential involvement of PRL2 in gene silencing during micro-gametogenesis and early embryo development could be suggested by the lack of PRL2 that produces genomic instability that leads to cell death. The interaction of PRL2 with the histone deacetylase HD2A and with HOG1/SAHH (MATERNAL EFFECT EMBRYO ARREST 58) by Y2H was reported by [Breuer \(2000\)](#). HD2A is required for determining leaf polarity and its silencing results in aborted seed development ([Wu et al., 2000](#)). Mutations of *HOG1* relieve transcriptional gene silencing, methylation-dependent and homology-dependent gene silencing, and result in genome-wide demethylation which leads to zygotic embryo lethality ([Rocha et al., 2005](#)). These results strongly suggest that PRL2 performs a specific function in genome-wide control of DNA methylation and gene silencing.

Nevertheless, further experiments should be performed to clarify this hypothesis.

3.4 Final conclusions

In this work, PRL1 has been shown to be conserved across species. Nevertheless, the similarity of PRL1 with its orthologue proteins is due to the high conservation of the C-terminal domain, whereas the N-terminal domain is only conserved in plants. Due to the lack of identity observed in the N-terminal part with human and yeast models, it is suggested that PRL1 performs a function in the splicing process that is plant-specific.

The different transcript profiling experiments performed for this work support the hypothesis that the pleiotropic phenotype observed for *prl1* is due to an altered regulation of specific genes involved in stress signalling pathways. This also led to the suggestion, based on the transcript profile results, that *prl1* could be impaired in gene silencing due to the observation that most of the expression-altered genes are up-regulated and specifically several transposable elements. Already some *in vivo* data indicated this relationship of PRL1 in gene silencing, and based on orthologue systems, this function could be spliceosome-dependent. Nevertheless, *in planta* experiments are required to confirm this hypothesis.

The *prl2* mutant was shown to present a different phenotype when compared to *prl1* due to a sub-functionalization of PRL1 and PRL2 during *Arabidopsis* development. Ectopic expression of both genes complement the mutual phenotypes, supporting this hypothesis. Furthermore, PRL2, as PRL1, has been demonstrated to be localized in the nucleus. Expression pattern of the GUS reporter, driven by the *PRL2* promoter, and the phenotype of *prl2* suggest that PRL2 function is performed during pollen development, and is specifically required during early embryo development. The evolved sub-functionalization of PRL1 and PRL2, which makes both genes to have different transcription profiles during development, is the cause of observing the two different phenotypes. Nevertheless, when somatic mosaics of *prl2* are generated, the lack of expression of *PRL2* causes a *prl1*-like phenotype.

Y2H data suggest that PRL2 is linked to key regulators of genome-wide DNA methylation and gene silencing. PRL2 could play a role in these processes during micro-gametogenesis. This developmental process deserves particular attention in further studies.

4. Experimental

4.1 Materials

4.1.1 Plant material

4.1.1.1 *Arabidopsis thaliana*

Table 4.1: Accessions of *Arabidopsis thaliana* used in this work.

Genotype	Ecotype	Obtained from
Wild type	Col-0	Rédei (1992)
<i>prl1</i> KONCZ	Col-0	Németh et al. (1998)
<i>prl1</i> SALK_008466	Col-0	Alonso et al. (2003)
<i>prl2</i> GABI_228D02	Col-0	Rosso et al. (2003)
<i>prl2</i> KONCZ_16136	Col-0	Ríos et al. (2002)
<i>cdc5</i> GABI_278B09	Col-0	Rosso et al. (2003)

4.1.1.2 *Arabidopsis* cell suspensions

Experiments were performed using photosynthetic light-grown and root-derived dark-grown *Arabidopsis* Col-0 cell suspensions (Mathur and Koncz, 1998; Menges and Murray, 2002).

4.1.2 Bacterial strains

4.1.2.1 *Escherichia coli* strains

DB3.1 F⁻ *gyrA462 endA1* Δ (*sr1-recA*) *mcrB mrr hsdS20*(r_B⁻, m_B⁻) *supE44 ara14 galK2 lacY1 proA2 rpsL20*(Sm^R) *xyl5* Δ *leu mtl1* (Bernard and Couturier, 1992)

DH10B F⁻ *mcrA* Δ (*mrr-hsdRMS-mcrBC*) Δ *lacX74 deoR endA1 araD139 Δ (*ara leu*) 7697 *rpsL recA1 nupG* ϕ 80d*lacZ* Δ M15 *galU galK**

4.1.2.2 *Agrobacterium tumefaciens* strains

- GV3101** C58C1 Rif^R, pMP90 (pTiC58 *tra*^c *noc*^c ΔT-DNA) Gm^R (Koncz and Schell, 1986)
GV3101 C58C1 Rif^R, pMP90RK (pTiC58 *tra*^c *noc*^c ΔT-DNA carrying the RK2 replication and conjugation helper functions from pRK2013) Gm^R, Km^R (Koncz and Schell, 1986)
GV3101 C58C1 Rif^R, pMP90 Gm^R, pJIC Sa_RepA Tet^R (Hellens et al., 2000)

4.1.3 General consumables

Table 4.2: Chemicals and reagents used in this work.

Provider	Product
Abcam Plc., Cambridge, UK	α-H3 antibody
Applied Biosystems GmbH Darmstadt, Germany	TURBO™ DNase
Beckman Instruments Inc. Palo Alto, USA	Centrifuge tubes
Bethyl Laboratories Inc. Montgomery, USA	α-Ubiquitin antibody
BioMol GmbH, Hamburg, Germany	Secondary antibodies (Table 4.5) X-Gluc (5-Bromo-4-Chloro-3-Indolyl-1-β-D-glucuronide, CHA-salt)
Bio-Rad, München, Germany	All Blue Precision Plus Protein™ Standards Bradford Reagent iQ™SYBR® Green Supermix Secondary antibodies
Boehringer Ingelheim, Germany	RNase A
Calbiochem Corp. Darmstadt, Germany	Ethidium bromide Miracloth
Cambrex Bio Science Inc. Rockland, USA	Seakem® LE Agarose
Carl Roth GmbH Karlsruhe, Germany	dNTP solutions Filter units 0,22 μm Phenol Rotiphorese® 40 (29:1)
Corning Inc., Corning, USA	Costar® Disposable serological pipettes
Difco Laboratories, Detroit, USA	Bacto-Agar Bacto-Peptone Bacto-Tryptone Yeast Extract

continued on next page

Table 4.2 – continued from previous page

Provider	Product
Duchefa, Haarlem, The Netherlands	ATP Carbenicillin Di-sodium salt Cefotaxime sodium Phyto-agar Ticarcillin/Clavulanic acid
Enzo Life Sciences GmbH Lörrach, Germany	α -20S antibody α -Rpn6 antibody
Eppendorf AG, Hamburg, Germany	Safe-lock tubes (0,5; 1,5 and 2,0 ml) Single-use pipette tips
GE Healthcare GmbH Freiburg, Germany	ECL™ Enhanced Chemiluminescence Kit Hybond™-N nylon membrane Hyperfilm™ MP Peristaltic pump
Greiner bio-one GmbH Kremsmünster, Austria	Petri dishes Falcon tubes (15 and 50 ml)
Heirler Cenovis GmbH Radolfzell, Germany	Milk powder
Invitrogen GmbH Karlsruhe, Germany	AccuPrime™ <i>Taq</i> DNA Polymerase High Fidelity <i>Taq</i> DNA Polymerase, recombinant Dynabeads mRNA purification kit Oligonucleotides Secondary antibodies
Isogen Biosolutions BV IJsselstein, The Netherlands	Oligonucleotides
Macherey-Nagel GmbH & Co. KG. Düren, Germany	NucleoSpin® Plasmid
Merck, Darmstadt, Germany	2-propanol Chloroform Ethanol D-Glucose Glycine N,N-dimethylformamide General organic solvents
Metabion International AG Martinsried, Germany	Oligonucleotides
Millipore, Bedford, USA	Immobilon™-P (PVDF membrane)

continued on next page

Table 4.2 – continued from previous page

Provider	Product
	MF™-Membrane Filters type VSWP 0,025 µm Sterivex™ 0,22 µm filter units
Molecular Probes Europe BV Leiden, The Netherlands	Propidium iodide nucleic acid stain
New England Biolabs Frankfurt/M, Germany	1 kb DNA ladder Antarctic phosphatase Restriction endonucleases T4 DNA ligase T4 polymerase RNase-free DNase
PeqLab Biotechnologie GmbH Erlangen, Germany	E.Z.N.A.® Plasmid miniprep kit I
QIAGEN GmbH, Hilden, Germany	QIAquick® Gel Extraction Kit RNeasy® Plant Mini Kit
Roche Diagnostics GmbH Mannheim, Germany	α-HA antibody High Pure PCR Product Purification Kit Hygromycin Protector RNase Inhibitor Restriction endonucleases Transcriptor First Strand cDNA Synthesis Kit
Sartorius AG, Göttingen, Germany	Minisart 0,22 µm and 0,45 µm filter units
Serva Electrophoresis GmbH Heidelberg, Germany	Bromophenol Blue-Na-salt Ponceau S solution SDS (sodium dodecyl sulphate)
Sigma-Aldrich Co. St. Louis, USA	Acetosyringone Amino acids Antibiotics APS (ammonium per-sulphate) α-TUB antibody β-mercaptoethanol BSA (bovine serum albumin) Chloral hydrate DEPC (diethylenepyrocarbonate) DTT (dithiothreitol) Glycerol Goat α-Rat IgG, (H+L), HRP Igepal Lyticase

continued on next page

Table 4.2 – continued from previous page

Provider	Product
	MS-Basal salt mixture
	MS-Basal salt with minimal organics (MSMO)
	PIC (plant protease inhibitor cocktail)
	PMSF (phenylmethanesulphonyl fluoride)
	Secondary antibodies
	Sucrose
	TEMED (tetramethylethylenediamine)
	Triton X-100
	Tween-20
	General chemicals
TaKaRa Bio Europe S.A.S. Saint-Germain-en-Laye, France	TaKaRa LA Taq™ Polymerase
Thermo Scientific Inc., Rockford, USA	Restore™ Western Blot Stripping Buffer
Whatman, Maidstone, USA	3MM paper

4.1.4 Plasmid vectors and constructs

4.1.4.1 Plasmid vectors

Table 4.3: Plasmid vectors used in this work.

Vector	Obtained from:
pCB1	Heidstra et al. (2004)
pBluescript II SK- (pBSK)	Stratagene
pENTR11	Invitrogen
pPAMpat	gift from B. Ülker
pPCV002	Koncz et al. (1994)
pPCV812	Koncz et al. (1994)
pDONR™207	Invitrogen
pEarleyGate-GW-YFP-HA	Earley et al. (2006)
pEarleyGate-YFP-GW	Earley et al. (2006)
pBeloBAC-Kan MGL6 (contains <i>PRL2</i>)	ABRC

4.1.4.2 Plasmid constructs

Table 4.4: Plasmid constructs used or designed in this work.

Construction	Obtained from:
pGII227-HS::CRE	Heidstra et al. (2004)
pPAMpat-PRL1-HA	Dr. D. Szakonyi
pPAMpat-PRL2-HA	Dr. D. Szakonyi
pPAMpat-1N2C-HA	Dr. D. Szakonyi
pPAMpat-2N1C-HA	Dr. D. Szakonyi
pPAMpat-PRL1-N-HA	Dr. D. Szakonyi
pPAMpat-PRL1-C-HA	Dr. D. Szakonyi
pPCV002-PROM-UTR	PhD thesis D. Szakonyi (2006)
pBSK-PRL1-GAGA-cDNA-SMA1	PhD thesis D. Szakonyi (2006)
p3×tag	PhD thesis M. Horváth (2008)
pBSK-PRL1-PIPL	this work
pPCV002-PRL1::PRL1-PIPL	this work
pER8-XVE(Km)-PRL1::PRL1cDNA-HA	PhD thesis D. Szakonyi (2006)
pBSK-PRL2-PROM	Dr. D. Szakonyi
pPCV812-PRL1-PROM	PhD thesis D. Szakonyi (2006)
pPCV812-PRL1-PROM-XhoI/BmgBI	PhD thesis D. Szakonyi (2006)
pPCV812-PRL2::GUS	Dr. D. Szakonyi
pBSK-PRL2gDNA	Dr. D. Szakonyi
pBSK-PRL2-PROM	this work
pBSK-PRL2::PRL2gDNA	this work
pCB1-PRL2::PRL2gDNA	this work
pDONR TM 207-PRL2	this work
pEarlyGate-PRL2-YFP	this work
pEarlyGate-YFP-PRL2	this work

4.1.5 Oligonucleotides

The primers used in this work were provided by either Metabion (Germany) or Invitrogen (The Netherlands). Primer sequences are listed in page [151](#) and following.

4.1.6 Enzymes

Restrictions endonucleases, T4 DNA ligase and T4 DNA polymerase were purchased from New England Biolabs (NEB). All enzymatic reactions were performed following the manufacturer's instructions.

4.1.7 Antibodies

4.1.7.1 Primary antibodies

α -20S: Mixture of mouse monoclonal antibodies raised against the human 20S proteasome particle, recognizes specifically subunits α 1, α 2, α 3, α 5, α 6 and α 7 (Enzo Life Sciences GmbH). Dilution 1:1 000.

α -H3: Rabbit polyclonal antibody raised against a synthetic peptide derived from residue 100 to the end of the C-terminus of the human Histone 3 (Abcam). Dilution: 1:1 000.

α -HA: Rat monoclonal antibody (clone 3F10) to peptide YPYDVPDYA derived from the haemagglutinin protein of the human influenza virus (Roche). Dilution 1:1 000.

α -PRL1: Rabbit polyclonal antibody raised against PRL1-specific peptide VVSQPPRQPDRINEQPGPS (Németh et al., 1998). Dilution 1:1 000.

α -Rpn6: Rabbit polyclonal antibody raised against the 19S regulator non-ATPase subunit Rpn6 (ATS9) of *Arabidopsis* proteasome (Enzo Life Sciences GmbH). Dilution 1:2 000.

α -TUB: Mouse monoclonal antibody against α -tubulin purified from chick brain (clone DM 1A, Sigma). Dilution 1:1 000.

α -Ub: Rabbit antibody recognizing a peptide corresponding to amino acids 1–50 of soya bean ubiquitin (Bethyl Laboratories). Dilution 1:1 000.

4.1.7.2 Secondary antibodies

Table 4.5: Horseradish-conjugated peroxidase (HRP) and fluorescent dye-conjugated secondary antibodies used in this work.

Secondary antibody	Provider	Dilution
Goat HRP α -rabbit IgG (H+L)	Bio-Rad	1:5 000
Goat HRP α -rat IgG (H+L)	Sigma	1:5 000
Goat HRP α -mouse IgG (H+L)	Bio-Rad	1:5 000
Goat Alexa Fluor 680 α -rabbit IgG (H+L)	Invitrogen	1:5 000
Goat Alexa Fluor 680 α -rat IgG (H+L)	Invitrogen	1:20 000
Goat IRDye800 Conjugated α -rabbit IgG (H+L)	BioMol	1:20 000
Rabbit IRDye800 Conjugated α -rat IgG (H+L)	BioMol	1:5 000

4.1.8 Culture media

4.1.8.1 LB medium for *E. coli*

Bacto-Tryptone	10 g/l
Bacto-Yeast Extract	5 g/l
NaCl	10 g/l

pH was adjusted to 7,5 with NaOH and autoclaved for 20 min at 120 °C. For solid media 15 g/l Bacto-Agar was added before sterilization.

4.1.8.2 YEB medium for *A. tumefaciens*

Beef Extract	5 g/l
Bacto-Yeast Extract	1 g/l
Bacto-Peptone	1 g/l
Sucrose	5 g/l

pH was adjusted to 7,4 with NaOH and autoclaved for 20 min at 120 °C. For solid media, 15 g/l of Bacto-Agar was added before sterilization. After autoclaving, the medium was supplemented with 20 ml/l of 0,1 M MgCl₂.

4.1.8.3 Root-derived dark-grown *Arabidopsis* cell suspension medium (MS)

MS Basal Mix (Sigma)	4,3 g/l
100× B5 vitamin solution	100 ml/l
Sucrose	30 g/l

pH was adjusted to 5,8 with KOH. The medium was autoclaved at 120 °C for 20 min. After sterilization, the medium was supplemented with 1 mg/l 2,4-D (pre-adjusted pH to 5,8 with KOH).

100× B5 vitamin solution:

Nicotinic acid	1 mg/ml
Pyridoxin-HCl	1 g/ml
myo-Inositol	100 mg/ml
Thiamine-HCl	10 mg/ml

4.1.8.4 Photosynthetic light-grown *Arabidopsis* cell suspension medium (MSMO)

MSMO salts (Sigma)	4,4 g/l
Sucrose	30 g/l

pH was adjusted to 5,8 with KOH, subsequently, the medium was autoclaved at 120 °C for 20 min. Before use, the medium was supplemented with 0,5 mg/l NAA and 0,1 mg/l Kinetin. Both hormone stock solutions were pre-adjusted to pH 5,8 with KOH.

4.1.8.5 *Arabidopsis* culture solid medium (MSAR)

Prepared after (Koncz et al., 1994):

Macro-elements	25 ml/l
Micro-elements	1 ml/l
Fe-EDTA	5 ml/l
CaCl ₂ ·2H ₂ O	5,8 ml/l
KI	2,2 ml/l
Sucrose	5 g/l

Sucrose content of this medium was modified for the PRL1-PIPL protein accumulation and ER-PRL1/*prl1* transcript profiling experiments, where 1 g/l and 30 g/l sucrose concentration were respectively used. pH was adjusted to 5,8 with KOH and 7 g/l of phyto-agar was added for solidification.

Macro-elements:

NH_4NO_3	20 g/l
KNO_3	40 g/l
$\text{MgSO}_4 \cdot 7\text{H}_2\text{O}$	7,4 g/l
KH_2PO_4	3,4 g/l
$\text{Ca}(\text{H}_2\text{PO}_4)_2 \cdot \text{H}_2\text{O}$	2 g/l

Micro-elements:

H_3BO_3	6,2 g/l
$\text{MnSO}_4 \cdot 4\text{H}_2\text{O}$	16,9 g/l
$\text{ZnSO}_4 \cdot 7\text{H}_2\text{O}$	8,6 g/l
$\text{Na}_2\text{MoO}_4 \cdot 2\text{H}_2\text{O}$	0,25 g/l
$\text{CuSO}_4 \cdot 5\text{H}_2\text{O}$	0,025 mg/l
$\text{CoCl}_2 \cdot 6\text{H}_2\text{O}$	0,025 mg/l

Fe- Na_2 -EDTA:

$\text{FeSO}_4 \cdot 7\text{H}_2\text{O}$	5,56 g/l
$\text{Na}_2\text{-EDTA} \cdot 2\text{H}_2\text{O}$	7,46 g/l

KI:

KI	375 g/l
----	---------

CaCl_2 :

$\text{CaCl}_2 \cdot 2\text{H}_2\text{O}$	75 g/l
---	--------

4.1.9 Antibiotics

Table 4.6: Antibiotics and herbicides used in this work. All antibiotic solutions were filter-sterilized and stored at $-20\text{ }^{\circ}\text{C}$.

Name	Stock solution	Working concentration
Ampicillin	50 mg/ml in water	100 mg/l
Basta™	200 mg/ml	250 mg/l
Carbenicillin	50 mg/ml in water	50 mg/l
Cefotaxime	200 mg/ml in water	200–400 mg/l
DL-Phosphinothricin	10 mg/ml in water	10 mg/l
Gentamicin	25 mg/ml in water	25 mg/l
Hygromycin B	15 mg/ml in water	15 mg/l
Kanamycin	50 mg/ml in water	25 mg/l for bacteria 50 mg/l for plants
Rifampicin	25 mg/ml in methanol	100 mg/l
Spectinomycin	50 mg/ml in water	100 mg/l
Sulfadiazine	7,5 mg/ml in water	15 mg/l
Tetracycline	5 mg/ml in ethanol	12,5 mg/l
Ticarcillin + Clavulanic acid	150 mg/ml in water	150 mg/l

4.1.10 Hormones

Table 4.7: Hormones used in this work.

Name	Abbreviation	Stock solution
6-benzylaminopurine	BAP	1 mg/ml in 0,01 N NaOH
2,4-dichlorophenoxyacetic acid	2,4-D	1 mg/ml in ethanol
Kinetin	Kin	1 mg/ml in 0,01 N NaOH
1-naphtylacetic acid	NAA	1 mg/ml in 0,01 N KOH
estradiol	EST	10 mM in DMSO

4.1.11 Microarrays

GeneChip® *Arabidopsis* ATH1 Genome Array: Sequences for probe sets present in this array were selected from the re-annotated TIGR genome assembly (TIGRv2) released on 15 December, 2001 (ATH1-151201). This array contains around 22 500 probe sets, representing approximately 24 000 genes. Each probe set contains 11 pairs (perfect match/mismatch) of 25-nt oligos.

GeneChip® *Arabidopsis* Tiling 1.0R Array: Sequences used in the design of this array are based on the 5th version of the NCBI *Arabidopsis* genome assembly (TIGRv5). Mitochondrial and chloroplast sequences were selected from NCBI (Accession numbers NC_001284 and NC_000932). Pair probes (perfect match/mismatch) were tiled at an average of 35 base pair resolution, as measured from the central position of adjacent 25-nt oligos, leaving a gap of approximately 10 base pairs between probes.

4.1.12 Computational resources

4.1.12.1 Hardware

A workstation with two quad-core CPUs comprised of the Intel® Xeon® “Harpertown” core at 2,5 GHz and a total amount of 24 GB of RAM running Ubuntu GNU/Linux *Karmic Koala* was used for the diverse resource-demanding data analyses.

4.1.12.2 General software

The European Molecular Biology Open Software Suite (EMBOSS, [Rice et al., 2000](#)) was used for working with DNA, RNA and protein sequences. Shading of aligned sequences was done with `TeXStudio` ([Beitz, 2000](#)). OpenOffice.org Calc was used to tabulate the data and to perform calculations. The Leica Application Suite (v2.8.1) was used to capture microscope images.

For this PhD thesis, the pictures were edited with The GIMP (GNU Image Manipulation Program), artwork was designed with Inkscape and TikZ/PGF, whereas charts were designed using PGFPlots. References were handled with JabRef and formatted with BibTeX. This report was typeset with Linux Libertine as the roman font and the Latin Modern family for the sans-serif and monospaced fonts. The layout was completed with L^AT_EX (T_EXLive 2009 distribution) under Ubuntu GNU/Linux.

4.1.12.3 Software used in microarray analyses

The R Project (v2.10.1, [R Development Core Team, 2009](#)) with several installed Bioconductor (v2.5, [Gentleman et al., 2004](#)) packages was used to process the microarray raw data. The `affyQCReport` package was used for quality-check of the raw data. The statistical packages `limma` (v3.2.1, [Smyth et al., 2005](#)) and `RankProd` (v2.18.0, [Hong et al., 2006](#)) were used to perform the transcript profiling analyses (section 4.2.12.1). The CDF file (v1.0.1) published by [Naouar et al. \(2009\)](#), based on TAIR7, was used to analyse the *Arabidopsis* tiling arrays. The GeneSpring GX v10.0 Expression Analysis suite (Agilent Technologies, Waldbronn) was used in addition to analyse the ATH1 arrays.

Clustering of co-regulated genes from the time-course experiment involving ATH1 arrays was performed using the Bioconductor’s `Mfuzz` (v1.8.0, [Kumar and Futschik, 2007](#)) package. The metabolic pathway classification of altered transcripts was performed with Plant MetGenMAP ([Joung et al., 2009](#)) and the GO-term enrichment analysis was done with AgriGO ([Zhou and Su, 2007](#)).

4.1.12.4 RNA-Seq-specific software

Several Perl scripts were used for pre-processing the raw data. The short read aligner Bowtie (v0.12.3, [Langmead et al., 2009](#)) was used for mapping the pre-processed data to the TAIR9 *Arabidopsis thaliana* genome assembly reference. The splice junction mapper TopHat (v1.0.13, [Trapnell et al., 2009](#)) was used to map the pre-processed in a more supervised manner, taking advantage of PE-sequenced samples. Cufflinks (v0.8.0, [Trapnell et al., 2010](#)) was used to process the output data from TopHat for assembling transcripts, estimating their abundances, and testing for differential expression in the mRNA-Seq samples.

For this PhD work, Bowtie, TopHat and Cufflinks were compiled from the source code in order to take full advantage of the available hardware (section 4.1.12.1).

Visualization of processed mRNA-Seq data was performed using the Generic Genome Browser v1.70 (GBrowse) installed in the local MPIPZ network by Dr. Emiel Ver Loren van Themaat and maintained by Michael Plümer. This GBrowse set-up relies on the DBD::mysql Perl module for the annotation data storage and access in the MySQL relational database management system (<http://dev.mysql.com/>). Several Perl modules from the BioPerl project (<http://www.bioperl.org>) were used for uploading the annotation generated in this work. Annotation sketches were exported using the GD::SVG Perl module.

4.1.12.5 Public databases

AgriGO: GO Analysis Toolkit and Database for Agricultural Community (Zhou and Su, 2007) <http://bioinfo.cau.edu.cn/agriGO>

BAR: Botany Array Resource (Toufighi et al., 2005), <http://www.bar.utoronto.ca>

InterPro: Protein sequence analysis & classification (Hunter et al., 2009) <http://www.ebi.ac.uk/interpro/>

NCBI: National Center for Biotechnology Information, <http://www.ncbi.nlm.nih.gov>

Plant MetGenMAP: An Integrative Analysis System for Plant Systems Biology (Joung et al., 2009), <http://bioinfo.bti.cornell.edu/cgi-bin/MetGenMAP/home.cgi>

TAIR: *Arabidopsis* Information Resource (Swarbreck et al., 2008) <http://www.arabidopsis.org>

UniProtKB: UniProt Knowledgebase (Schneider et al., 2009), <http://www.uniprot.org>

4.2 Methods

4.2.1 Plant methods

4.2.1.1 Plant growth conditions in the greenhouse

Arabidopsis thaliana plants were grown in 7×7 cm plastic pots with soil at 22 °C day temperature and 18 °C night temperature at 70 % humidity in trays under either short day (8 h light and 16 h dark) or long day conditions (16 h light and 8 h dark) under 200 $\mu\text{E}\cdot\text{m}^{-2}\cdot\text{s}^{-1}$ to 400 $\mu\text{E}\cdot\text{m}^{-2}\cdot\text{s}^{-1}$ of irradiation energy.

4.2.1.2 Sterilization of *A. thaliana* seeds

Approximately, 200 to 500 seeds were placed in a re-used RNeasy Mini Spin column (QIAGEN), from which the silica membrane was previously removed, and only the pore plate was kept. Seeds were treated with 600 μl of 70 % ethanol for 7 min, followed by treatment with 600 μl of 96 % ethanol for 1 min. In each step, ethanol was removed by centrifugation.

4.2.1.3 *In vitro* culture of *A. thaliana* seedlings

Sterilized *Arabidopsis* seeds were germinated and grown on solid MSAR medium (Koncz et al., 1994, section 4.1.8.5), under short day conditions at 20 °C using 200 $\mu\text{E}\cdot\text{m}^{-2}\cdot\text{s}^{-1}$ to 400 $\mu\text{E}\cdot\text{m}^{-2}\cdot\text{s}^{-1}$ of irradiation energy.

4.2.1.4 Measurement of root length

For measuring the root length, sterilized *Arabidopsis* seeds were germinated in vertically-positioned squared petri dishes containing MSAR solid medium in the culture room. The germination rate was recorded and the root growth was measured by the help of a piece of grid paper every day.

4.2.1.5 Selection of *Arabidopsis* transformants

T1 seeds were sterilized in RNeasy Mini Spin columns (QIAGEN) as described in section 4.2.1.2 and germinated either on solid MSAR medium containing the appropriate antibiotics and a mixture of cefotaxime and ticarcillin to avoid *Agrobacterium* growth, or directly on soil for selection by Basta™ solution (250 mg/ml of phosphinothricin; 0,1 % Tween-20). Antibiotic-resistant transformants were transferred first onto non-selective sterile medium, and subsequently into soil.

T1 plants were cultivated in the greenhouse in order to set seeds. T2 seeds from several primary transformants were germinated in sterile conditions on MSAR medium containing appropriate antibiotics for selection. Seedlings from those T2 lines showing a 3:1 segregation of resistant:sensitive progeny were grown and screened for homozygous T3 offspring.

4.2.1.6 Crosses of *Arabidopsis* plants

To perform crosses of *Arabidopsis* plants, open flowers and siliques were removed from the selected stem after bolting. Three to four closed flowers were emasculated with a pair of tweezers by removing petals, sepals and immature anthers. Pollen from a selected mature plant was used to dust the stigma. Seed maturation was monitored regularly and fully grown siliques were collected and dried.

4.2.1.7 Sub-culture of *Arabidopsis* cell suspensions

Every 7 days, 10 ml to 15 ml of cell suspension were taken from 50 ml 7 day-old *Arabidopsis thaliana* (ecotype Col-0) cell suspension cultures and added to 35 ml to 40 ml of fresh liquid medium (Mathur and Koncz, 1998, section 4.1.8.3). Cells were grown under constant agitation with 120 rpm to 150 rpm at 18 °C to 22 °C. Photosynthetic light-grown cells suspensions were maintained under 200 $\mu\text{E}\cdot\text{m}^{-2}\cdot\text{s}^{-1}$ to 400 $\mu\text{E}\cdot\text{m}^{-2}\cdot\text{s}^{-1}$ of irradiation energy.

4.2.1.8 Histochemical assay of β -glucuronidase (*uidA*) reporter enzyme activity *in planta*

Freshly harvested seedlings or plant organs were immersed in X-Gluc solution and vacuum treated for 3 min in an desiccator, followed by incubation at 37 °C of 2 to 16 hours. The stained tissue was washed 4× in 70 % ethanol to remove chlorophylls (Jefferson et al., 1987).

X-Gluc solution:

X-Gluc (50 mg/ml in DMSO)	200 μ l/ml
Triton X-100	0,1 %
Phosphate (Na) buffer (pH 7,0)	0,1 M
K ₃ Fe(CN) ₆	0,5 mM
K ₄ Fe(CN) ₆	0,5 mM

When staining *Arabidopsis* embryos, siliques of different ages were removed from the plant, opened with a needle under a stereo-microscope. Immature seeds were isolated, fixed in acetone for 30 min on ice and subsequently washed with 0,2 M Na-phosphate buffer. Seeds were stained overnight at 37 °C submerged in X-Gluc solution. The next day, seeds were washed in 0,2 M Na-phosphate buffer, mounted on a microscope slide and cleared with freshly-prepared chloral hydrate solution on a glass slide for at least 1 h. GUS-stained embryos were inspected under the light microscope.

Chloral hydrate solution:

chloral hydrate	2,5 g
H ₂ O	0,7 ml
glycerol	0,3 ml

4.2.2 DNA handling methods

4.2.2.1 DNA extraction from plant material

Plant DNA isolation was performed using a modified method from [Koncz and Schell \(2002\)](#). Two to four leaves (50–200 mg) were ground for 3 min in presence of 750 μ l of freshly-made DNA extraction buffer in a 2 ml eppendorf tube containing 3 small steel spheres using a TissueLyser (QIAGEN) at maximal speed. The tubes were briefly centrifuged and 250 μ l of 5 M potassium acetate (pH 6,0) was added. The samples were pelleted by centrifugation for 10 min, the cleared supernatant (1 ml) was transferred to a clean eppendorf tube and 700 μ l of iso-propanol was added to precipitate the DNA for 20 min at room temperature. The DNA pellet was washed with 70 % ethanol (section 4.2.2.7) and the ethanol was completely removed. The DNA was dissolved in 400 μ l of HTE solution and incubated following by addition of 100 μ l of RNase A solution for 30 min at 37 °C. Subsequently, 100 μ l of pre-digested proteinase K solution was added and the DNA sample was incubated for 1 h at 37 °C. DNA was further purified extracting twice with 600 μ l of phenol/chloroform/iso-amyl-alcohol (25/24/1) on ice (section 4.2.2.6). Upon addition of $\frac{1}{10}$ volumes of 3 M sodium acetate (pH 6,0), DNA was precipitated with 400 μ l of iso-propanol for 30 min at 0 °C. DNA was pelleted by centrifugation for 10 min at 13 000 rpm, washed with 1 ml of 70 % ethanol and dried. Purified DNA was finally dissolved in 50 μ l of LTE solution.

DNA extraction buffer:

Tris-HCl (pH 8,5)	200 mM
EDTA	50 mM
NaCl	500 mM
β -mercaptoethanol	14 mM
SDS	1 %

HTE solution:

Tris-HCl (pH 8)	100 mM
EDTA	50 mM

LTE solution:

Tris-HCl (pH 7,5)	10 mM
EDTA	1 mM

RNase A solution (in LTE, boiled for 10 min and kept on ice until needed):

RNase A	10 mg/ml
---------	----------

Proteinase K solution (in LTE, pre-digested at 37 °C for 10 min and used immediately):

Proteinase K	2 mg/ml
--------------	---------

4.2.2.2 Plant genotyping by PCR

*TaKaRa LA Taq*TM polymerase (TaKaRa Bio Europe) was used for diagnostic amplification of plant DNA samples, in order to verify the presence of studied trans-gene or T-DNA insertion. A master mix was prepared for multiple PCR reactions, using the following components:

10× LA PCR TM Buffer II (Mg ²⁺ free)	1 μ l
25 mM MgCl ₂	1 μ l
10 mM dNTP mixture	1,6 μ l
Primer mix (10 μ M each)	2 μ l
Template DNA	1–2 μ l
TaKaRa LA Taq TM (5 U/ μ l)	0,1 μ l
Autoclaved distilled water	up to 10 μ l

A Bio-Rad DNA Engine Tetrad[®] 2 cycler was used for PCR amplification. The reactions were performed in 10 μ l final volume using the following program:

1. Denaturation: 94 °C for 5 min
 2. Denaturation: 94 °C for 30 s
 3. Extension: 68 °C for 1 min/kb
 4. End: 4 °C for ever
- ← 30× or 35×

4.2.2.3 Preparation of plasmid DNA by alkaline lysis

Isolation of plasmid DNA from *E. coli* was performed using the classical method of alkaline lysis (Birnboim and Doly, 1979). Briefly, a single bacterial colony, grown overnight on selective LB medium, was inoculated into 2–5 ml of liquid LB medium supplemented with the appropriate

antibiotics. The bacterial culture was grown overnight at 37 °C with vigorous shaking (250 rpm) and subsequently transferred into a 2 ml eppendorf tube and pelleted at maximum speed for 1 min in an eppendorf centrifuge. The supernatant was removed and the bacterial pellet was re-suspended in 280 µl of ice-cold solution I. To lyse the cells, 360 µl of freshly-prepared solution II was added to the tube and gently mixed by inversion. After 5 min of incubation, 540 µl of ice-cold solution III was added to neutralize the lysate and the mixture was incubated at 4 °C for 10 min. The cell debris was removed by centrifugation at 13 000 rpm for 10 min. One ml of supernatant was transferred into a new eppendorf tube and nucleic acids were precipitated with 500 µl of iso-propanol at -20 °C for at least 10 min.

Nucleic acids were pelleted by centrifugation at 13 000 rpm for 10 min and the supernatant was removed. The DNA pellet was re-suspended in 500 µl of 25 µg/µl RNase A solution and incubated at 37 °C for 1 h. Subsequently, DNA was precipitated by addition of 600 µl of solution IV and pelleted by centrifugation. The pellet was washed with 1 ml of 70 % ethanol and, after removing the ethanol, the purified DNA was dissolved in 50 µl of water or TE buffer.

Solution I:

Tris-HCl (pH 8,0)	50 mM
Glucose	50 mM
EDTA	10 mM

Solution II (freshly prepared):

NaOH	200 mM
SDS	1 %

Solution III:

NaOAc (pH 4,8) or KOAc (pH 6,0)	3 M
---------------------------------	-----

Solution IV:

Iso-propanol	88 %
KOAc	0,2 M

When DNA was subjected to Sanger sequencing, it was purified using the NucleoSpin[®] Plasmid kit (Macherey-Nagel) or the E.Z.N.A.[®] Plasmid miniprep kit I (PeqLab Biotechnologie) to obtain high quality samples.

4.2.2.4 DNA sequencing

Plasmids and DNA fragments were sequenced in collaboration with the Automatic DNA Isolation and Sequencing (ADIS) service at the MPIPZ. An Applied Biosystems 3730XL Genetic Analyser was used for this purpose.

4.2.2.5 Clone identification by PCR

Recombinant *Taq* DNA polymerase (Invitrogen) was used for diagnostic identification of recombinant plasmid carrying specific DNA fragments. A master mix was prepared for multiple PCR reactions from the following components on ice:

10× PCR buffer (-MgCl ₂)	2 µl
10 mM dNTP mixture	0,4 µl
50 mM MgCl ₂	0,6 µl
Primer mix (10 µM each)	1 µl
Template DNA:	
plasmid DNA	0,5 µl
colony-PCR	bacteria
Taq DNA polymerase (5 U/µl)	0,2 µl
Autoclaved distilled water	up to 20 µl

For colony-PCR screening, the DNA template was added by transferring a bacterial colony from selective medium into the PCR tube using a toothpick. The PCR amplification was performed using a Bio-Rad DNA Engine Tetrad[®] 2 cycler. The reactions were performed in a final volume of 20 µl using the following program:

1. Denaturation: 95 °C for 10 min
 2. Denaturation: 95 °C for 30 s
 3. Annealing: 58–62 °C for 30 s
(primer-pair dependent)
 4. Extension: 72 °C for 1 min/kb
 5. End: 4 °C for ever
- 25× to 30×
-

4.2.2.6 Phenol/chloroform extraction

Phenol/chloroform extraction was performed to remove contaminating proteins. DNA samples were mixed by gently vortexing with equal volume of phenol/chloroform solution (1/1) and subsequently centrifuged at 13 000 rpm for 5 min. The aqueous upper phase was collected in a new eppendorf tube and the extraction step was repeated until there was no more visible protein ring between the water and the organic solvent phases. To remove phenol traces, the sample was extracted with equal volume of chloroform/iso-amyl-alcohol (24/1) mixture on ice. Phases were separated by centrifugation and DNA from the supernatant was precipitated by adding 2 volumes of ethanol after the addition of ¹/₁₀ volumes of 3 M sodium acetate solution (pH 5,2).

4.2.2.7 DNA precipitation

DNA was precipitated using either ethanol or iso-propanol. For ethanol precipitation, ¹/₁₀ volumes of 3 M sodium acetate (pH 5,2) and 2 volumes of absolute ethanol were added and samples were incubated at -20 °C for at least 30 min. Precipitated DNA was pelleted by centrifugation at 13 000 rpm in an eppendorf centrifuge for 10 min. Pelleted DNA was washed with 70 % ethanol, centrifuged again and following the removal of ethanol, samples were dried in a desiccator. For iso-propanol precipitation, ¹/₁₀ volumes of 3 M sodium acetate (pH 5,2) and 0,7 volumes of iso-propanol were added to the samples and the DNA was precipitated by incubation on ice for at least 20 min. DNA was pelleted by centrifugation at 13 000 rpm for 10 min. The DNA pellet was washed with 1 ml of 70 % ethanol, dried and dissolved in water or LTE solution (page 109).

4.2.2.8 Agarose gel electrophoresis

Plasmids, DNA fragments and PCR products were separated by agarose gel electrophoresis. The gel agarose concentration depended on the size of the DNA fragments being analysed. Agarose was dissolved in 0,5× TBE buffer supplemented with 0,1 µg/ml of ethidium bromide and heated in a microwave oven until boiling. The agarose solution was poured into an electrophoresis tray and once gelled, submerged into a gel tank filled with 0,5× TBE buffer. DNA samples were mixed (5:1) with 6× loading dye and loaded into the gel wells. For size estimation, 5 µl of 1 kb DNA ladder (NEB) was used. Electrophoresis was performed at 50 V to 150 V. DNA was visualized using an UV light trans-illuminator. Gel images were captured using a Kodak DC-920 digital camera and processed with the Kodak Digital Science 2D v3.0.2 program.

5× TBE buffer:

Tris base	54 g/l
Boric acid	27,5 g/l
EDTA	4,65 g/l

6× loading dye:

Bromophenol blue	2,5 mg/ml
Xylene cyanol	2,5 mg/ml
Sucrose	400 mg/ml

4.2.2.9 Measurement of nucleic acid concentration

DNA concentration was determined using a Nanodrop ND-1000 spectrophotometer (PeqLab Biotechnologie). OD₂₆₀ value of 1 corresponds to 50 µg/ml of double stranded DNA or 40 µg/ml of RNA. Pure preparations should have a OD₂₆₀/OD₂₈₀ ratio between 1,8 and 2,0 ([Sambrook and Russell, 2001](#)).

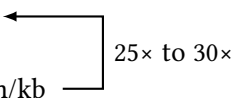
4.2.3 General cloning techniques

4.2.3.1 Reliable DNA amplification

AccuPrime™ *Taq* DNA Polymerase High Fidelity (Invitrogen) was used for cloning purposes in order to have exact copies from genomic or cDNA templates. This enzyme mix has a component that provides a proof-reading 3'→5' exonuclease activity, producing high fidelity copies. The following components were mixed in 200 µl PCR tubes:

10× AccuPrime™ PCR buffer I	5 µl
Primer mix (10 µM each)	2 µl
Template DNA	1 µl
AccuPrime™ <i>Taq</i> High Fidelity	0,2 µl
Autoclaved distilled water	up to 50 µl

After a denaturation step (94 °C for 2 min), a three-step cycling program was used:

1. Denaturation: 94 °C for 15 s
 2. Annealing: 55 °C for 30 s
 3. Extension: 68 °C for 1 min/kb
 4. End: 4 °C for ever
- 

4.2.3.2 Purification of DNA fragments from agarose gels

After gel electrophoresis, DNA fragments were excised from the agarose gel placed on an UV light trans-illuminator. DNA was extracted and purified using QIAquick® Gel Extraction Kit (QIAGEN) following the manufacturer's instructions.

4.2.3.3 Digestion with restriction endonucleases

Digestions of DNA samples were performed with restriction endonucleases according to the manufacturer's instructions. Typically, reactions were carried out in 1,5 ml eppendorf tubes in a final volume of 20 or 50 µl using 1–5 U of enzyme per µg of DNA. The duration of digestions varied from 2 h to overnight.

4.2.3.4 Blunt-end generation of digested DNA fragments

Overhanging DNA ends were blunted with T4 DNA polymerase (NEB) which can be used for removing 3'-overhanging nucleotides and fill-in 3'-recessed ends. The digested vector or isolated DNA fragment was dissolved in 1× restriction enzyme reaction NEBuffer supplemented with 100 µM dNTPs. One U of enzyme per µg of DNA was added to the reaction and incubated for 15 min at 12 °C. T4 DNA polymerase was inactivated by adding EDTA (10 mM final concentration) to the mixture followed by heating to 75 °C for 20 min.

4.2.3.5 Dephosphorylation of DNA ends

In order to prevent self-ligation of linearized vectors, digested plasmids were dephosphorylated at their 5' end with Antarctic phosphatase (NEB). As this enzyme is heat inactivated, no further purification step is necessary. Linearized vectors were purified by gel electrophoresis. $\frac{1}{10}$ volume of Antarctic phosphatase reaction buffer and 5 U of Antarctic phosphatase were added. The reaction mixture was incubated for 1 h at 37 °C followed by inactivation of the enzyme at 65 °C for 5 min to 10 min.

4.2.3.6 DNA ligation

T4 DNA ligase (NEB) was used for the ligation of linearized vectors with DNA fragments. Normally, vector and fragment were mixed at a molar ratio of 1:3. The ligase reactions were prepared by addition of 2 µl T4 DNA Ligase Reaction buffer and 1 µl of T4 DNA ligase and performed in a final volume of 20 µl with an overnight incubation at 12 °C. As a control for re-circularization of the cloning vector, a similar ligation reaction was carried out with the linearized vector.

4.2.4 Gateway® cloning

The Gateway® technology (Invitrogen) is based on the use of site-specific recombination reactions that mediate the integration and excision of the lysogenic λ phage. Integration of DNA fragments flanked by *attP* attachment sites in a carrier plasmid into a target (i.e. donor) vector harboring the suicide *ccdB* gene between the *attB* sequences is mediated by the phage encoded Integrase (Int) and bacterial IHF a/b proteins (BP Clonase). Homologous exchange recombination at the *att* sites transfers the DNA fragment into the target donor vector and converts the *attB* to *attL* sites, while the original carrier plasmid acquires the lethal *ccdB* gene flanked by *attP*-derived *attR* sequences. Using the reverse excision reaction catalysed by Int, IHF a/b and Xis (“excisionase” or LP Clonase) enzymes, the *attL*-flanked fragment can be moved from the constructed “entry” vector to any destination vector (including expression or gene fusion vectors) by exchange recombination with the *attP* sites that flank in these vectors the suicide *ccdB* marker gene (Hartley et al., 2000).

4.2.4.1 BP cloning reaction

The BP cloning reaction promotes recombination between the *attB* sites flanking a PCR product and the *attP* sites of the “donor” to create an *attL*-containing entry clone. This reaction is catalysed by the BP Clonase™ II enzyme mix (Invitrogen). The following components were mixed in a 1,5 ml eppendorf tube:

<i>attB</i> -PCR product (20 fmol to 50 fmol)	1 μ l to 7 μ l
pDONR™ vector (150 ng/ μ l)	1 μ l
TE buffer, pH 8,0	up to 8 μ l
BP Clonase™ II enzyme mix	2 μ l

Reactions were performed for 1 h at 25 °C, and stopped by addition of 1 μ l of Proteinase K solution and incubation at 37 °C for 10 min.

4.2.4.2 LR cloning reaction

The LR Clonase™ II enzyme mix (Invitrogen) facilitates the recombination reaction between the *attL*-containing entry clone and the *attR* substrate (destination vector) to create an *attB*-containing expression clone. This expression vector can be a binary vector to be transformed by *Agrobacterium* into plants. The following components were mixed in a 1,5 ml eppendorf tube:

Entry clone (50 ng to 150 ng)	1 μ l to 7 μ l
Destination vector (150 ng/ μ l)	1 μ l
TE buffer, pH 8,0	up to 8 μ l
LR Clonase™ II enzyme mix	2 μ l

Reactions were incubated for 1 h at 25 °C, stopped by addition of 2 μ l of Proteinase K solution and incubation at 37 °C for 10 min.

4.2.5 Transformation of bacteria and *Arabidopsis*

4.2.5.1 Preparation of electro-competent bacterial cells

Preparation of electro-competent *E. coli* cells was carried out according to the protocol of [Dower et al. \(1988\)](#). A single colony was inoculated in 10 ml of liquid LB and grown overnight at 37 °C with constant shaking (200 rpm). One ml of this culture was inoculated into 300 ml of liquid LB and incubated overnight at 37 °C with shaking. Subsequently, the bacterial culture was diluted to an OD₆₀₀ value of 0,1–0,2 and cells were grown at 16 °C until the OD₆₀₀ reached a value of 0,5 to 0,6. Cells were pelleted by centrifugation in Sorwall GSA tubes at 5 000 rpm for 20 min and re-suspended in 200 ml of cold water. This washing step was repeated 3 times to remove salts, then cells were re-suspended in 50 ml of water, transferred into a 50 ml falcon tube and pelleted again for 10 min at 5 000 rpm. Finally, cells were re-suspended in 800 µl of 7 % DMSO solution, aliquoted in eppendorf tubes containing 50 µl of cell suspension and immediately snap-frozen in liquid nitrogen. Aliquots were stored at –70 °C until further use.

Electro-competent *A. tumefaciens* cells were prepared using a similar protocol. *Agrobacterium* were grown in liquid YEB medium at 21 °C. After the final washing step, cells were re-suspended in 1 ml sterile 10 % glycerol solution, aliquoted, snap-frozen in liquid nitrogen and stored at –70 °C.

4.2.5.2 Electroporation of bacterial cells

An aliquot of competent *E. coli* or *A. tumefaciens* cells was thawed on ice. Cells were mixed with 0,5 µl to 3 µl of either plasmid DNA or pre-dialysed ligation mixture and transferred into pre-chilled 0,2 cm-wide electroporation cuvettes (Bio-Rad). Transformation was performed in a Bio-Rad Gene Pulser set to 2,5 kV voltage, 25 µF capacitance and 200 Ω resistance. After electroporation, bacteria were suspended in 1 ml of liquid LB or YEB medium, transferred into an eppendorf tube and incubated for 1 h at 37 °C –for *E. coli*– or 2 h at 28 °C –for *A. tumefaciens*–. After the recovery phase, *E. coli* was spread on solid LB media supplemented with antibiotics, whereas *A. tumefaciens* was plated on selective YEB medium.

4.2.5.3 *Agrobacterium*-mediated transformation of *Arabidopsis*

Agrobacterium-mediated transformation of *Arabidopsis* was performed by the flower dipping method or by co-cultivation of cell suspensions with *Agrobacterium*.

The flower dipping method ([Clough and Bent, 1998](#)) is based on genetic transformation of ovules. Five hundred ml of *Agrobacterium* cells were grown overnight in the presence of antibiotics to select for the marker of the binary vector. The *Agrobacterium* culture was pelleted at 5 000 rpm for 10 min followed by re-suspension in 300 ml of transformation medium. Open flowers and siliques were removed from bolting plants cultivated in 10 cm-diameter pots –10–12 plants per pot– and then their inflorescences were submerged in the bacterial suspension for at least 5 min. For gradual adaption to lower humidity, plants were covered with a plastic bag, which was removed 2 days later. Seeds were collected in paper bags and T1 transformants were selected on solid MSAR medium containing antibiotics corresponding to the selectable marker of the T-DNA, as well as ticarcillin and cefotaxime to avoid *Agrobacterium* growth.

Transformation medium:

MS salts	1/2
B5 vitamins	1×
Sucrose	5 %
BAP	0,044 μM
Silwet L-77	0,005 %

Arabidopsis cell suspensions were transformed with *Agrobacterium* using the protocol of Ferrando et al. (2000) with minor modifications. Briefly, *Agrobacteria* were grown in petri dishes with selective media until covering the whole plate, then, the *Agrobacterii* layer was transferred with the help of a sterile spatula into an Erlenmeyer flask containing 50 ml of 3 day-old sub-cultured cell suspension of *Arabidopsis*. Following 2 days of co-cultivation, *Agrobacterium* growth was stopped by addition of ticarcillin and cefotaxime (50 μl each). Transformed cell suspensions were sub-cultured using the 7 day-cycle, and at the 2nd sub-culture, the medium was supplemented with antibiotics to select for the T-DNA-encoded resistance marker.

4.2.6 Construction of binary vectors for transformation

4.2.6.1 pPCV002PRL1::PRL1-PIPL

The pPCV002-PRL1::PRL1-PIPL construct was designed with the help of Dr. D. Szakonyi for expression of a modified PRL1 protein in fusion with the triple PIP-L tag (see below), Strep and HiA tags under the control of the native *PRL1* promoter, and to test the functionality of this protein by genetic complementation in the *Arabidopsis prl1* mutant. D. Szakonyi has previously demonstrated that essential regulatory elements of the *PRL1* promoter are localized between the ATG codon and exon 3, whereas the 5' UTR region upstream of the ATG codon carries only enhancer elements influencing the threshold but not the tissue specificity of *PRL1* transcription (Szakonyi, 2006). A hybrid gene construct carrying a combination of the *PRL1* promoter region, including the 5' UTR and downstream sequences extending to exon 3 in the plasmid pPCV002-PROM-UTR, together with cDNA sequences containing the rest of the *PRL1* coding region from exon 3 to the translation stop codon from plasmid pBSK-PRL1-GAGA-cDNA-SMA1 was demonstrated to confer genetic complementation of the *prl1* mutation (Szakonyi, 2006). To tag this hybrid *PRL1* gene, the p3×tag construct (Horváth, 2008) was used. The p3×tag construct carries the coding region of PIP-L, Strep and HiA affinity tags.

The PIPL-tag contains the Ni/Co-binding domain of the conserved *Arabidopsis* cobalt-carrier protein PiP-L/CobW, which was originally identified by yeast two-hybrid as an interacting partner of PRL1 and as a major contaminant of His×6-tagged proteins purified from *Arabidopsis* on Ni-matrix (Horváth, 2008). The PIP-L tag has a higher Ni/Co-binding affinity than the commercial His×6 tags. To provide a second tool for highly-specific affinity chromatography, the PIP-L tag was fused to the Strep tag (Schmidt and Skerra, 1993). Additionally, the triple tag includes a C-terminal HiA-tag, which is derived from the haemagglutinin protein of human influenza virus. To avoid that potential expression of triple-tagged fusion proteins in *Agrobacterium* interferes with the analysis of tagged proteins expressed transiently in *Arabidopsis* cell suspensions, Ferrando et al. (2000) placed the intron *IV2* from the potato *ST-LS1* gene in between the coding sequence of the HA-tag.

To modify the *PRL1* coding region by replacing the stop codon with coding sequences of the triple PIP-L-Strep-HiA tag in pBSK-PRL1-PIPL, first the pBSK-PRL1-GAGA-cDNA-SMA1 construct, containing the cDNA sequence of *PRL1* between the 3rd exon and the stop codon was cut with *XbaI/SacII*. Subsequently, a PCR fragment of 400 bp was amplified with the primer pair PIPL-F and PIPL-R using the p3×tag construct as template. The PCR fragment was digested with *XbaI/SacII*, and ligated with the pBSK-PRL1-GAGA-cDNA-SMA1 construct. Clones of this intermediate construct were tested by diagnostic digestion, and the correct clones carrying the 3×tag coding region were sequenced to confirm the in-frame fusion of *PRL1* and 3×tag coding regions. From the resulting plasmid pBSK-PRL1-PIPL an *XhoI/SacII* fragment of 2,4 kb was isolated and blunt-ended with T4 DNA polymerase (NEB). This fragment was inserted into the single *SmaI* site of pPCV002-PROM-UTR. To confirm the reconstruction of the hybrid *PRL1* gene carrying the 3×tag coding sequence, *E. coli* mini-preps of the resulting plasmid were checked by diagnostic digestion with *BamHI* and *XbaI*. The final construct is depicted in Figure 4.1.

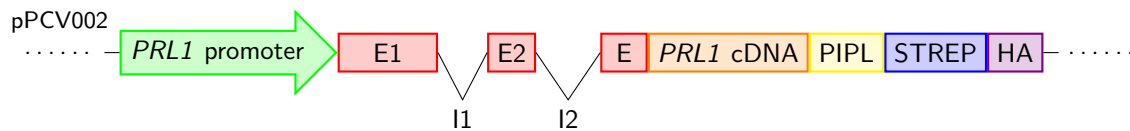


Figure 4.1: Schematic structure of the pPCV002-PRL1-PIPL construct.

4.2.6.2 Construction of pPAMpat-PRL1-HA and pPAMpat-PRL2-HA

To test the functional similarity of the N- and C-terminal domains of *PRL1* and *PRL2*, Dr. D. Szakonyi constructed a series of binary expression vectors, in which the stop codons of *PRL1* and *PRL2* cDNAs were replaced with coding sequences of the HA epitope. Coding sequences of *PRL1* and *PRL2* (both 1,4 kb-long) were amplified from the pACT2 cDNA library (Salchert, 1997) using the PRL1-F and PRL1-HA, and PRL2-F and PRL2-HA primer pairs, respectively. The PCR amplified PCR fragments were digested with *XhoI/SpeI* and inserted in between the *XhoI/SpeI* sites of the pPAMpat binary vector (B. Ülker, unpublished). Error-free PCR amplification and proper in-frame fusion of HA sequences to *PRL1* and *PRL2* coding sequences in the resulting vectors pPAMpat-PRL1-HA and pPAMpat-PRL2-HA (*PRL1-HA* and *PRL2-HA*, respectively, Figure 4.2) were verified by sequencing.

4.2.6.3 Generation of pPAMpat-PRL1-N-HA and pPAMpat-PRL1-C-HA deletion constructs

To remove the N-terminal regulatory and C-terminal WD-domains of *PRL1*, Dr. D. Szakonyi amplified by PCR the PRL1-N-HA and PRL1-C-HA fragments using the pPAMpat-PRL1-HA construct as template with the PRL1-F + PRL1-N and PRL1-C + PRL1-HA primer pairs, respectively. Subsequently, both PCR fragments were digested with *XhoI/SpeI*, ligated and cloned separately into the *XhoI/SpeI* sites of the pPAMpat vector (Figure 4.2) and verified by DNA sequencing.

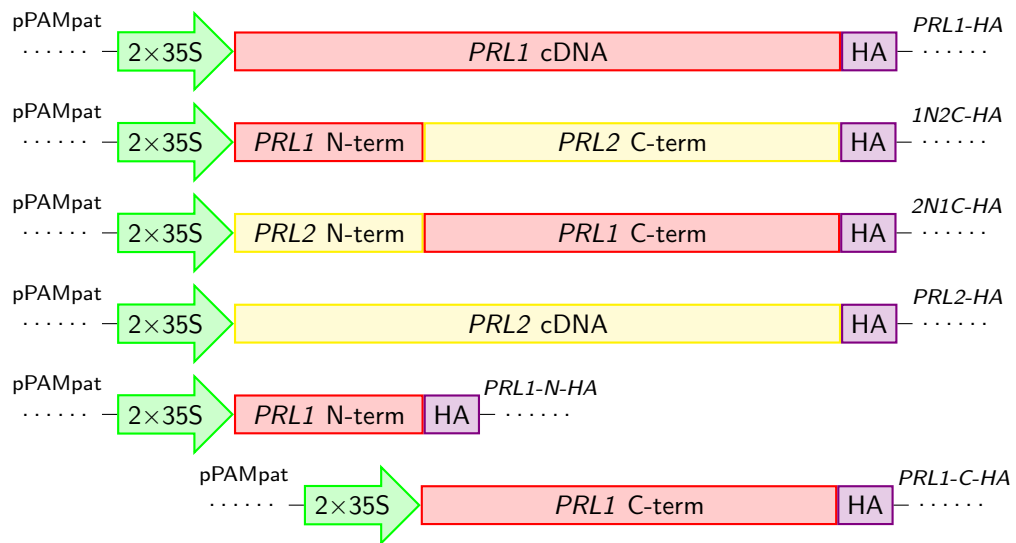


Figure 4.2: Schematic structure of the 2×35S promoter-driven *PRL1*-HA and *PRL2*-HA over-expression constructs and their deletion and sequence-swap derivatives designed by Dr. D. Szakonyi.

4.2.6.4 Generation of swapped pPAMpat-1N2C-HA and pPAMpat-2N1C-HA constructs

Sequence alignment indicated that *PRL1* and *PRL2* cDNAs carry a unique *Bgl*III site in the coding region of their first conserved WD40 domain (Figure 4.3). This unique *Bgl*III site was used to exchange the N- and C-terminal coding sequences of *PRL1* and *PRL2*, in order to express hybrid proteins carrying either the N-terminal domain of *PRL1* in fusion with the C-terminal domain of *PRL2* or vice versa. The *prl1* and *prl2* mutants were used for testing the complementary functions of these two closely related WDR proteins.

To generate these constructs, *PRL1* and *PRL2* cDNAs were amplified using pPAMpat-*PRL1*-HA and pPAMpat-*PRL2*-HA constructs (section 4.2.6.2) as templates. The PCR products were digested with *Xho*II, *Bgl*III and *Spe*I, to isolate and gel-purify the *Xho*II-*Bgl*III and *Bgl*III-*Spe*I fragments carrying the N- and C-terminal coding sequences of *PRL1* and *PRL2* CDSs, respectively. The 5' *PRL1* *Xho*II-*Bgl*III fragment of 540 bp and the 3' *PRL2* *Bgl*III-*Spe*I fragment of 1,1 kb were cloned into the *Xho*II/*Spe*I sites of the pPAMpat vector to obtain the construct pPAMpat-1N2C-HA (*1N2C*-HA). Analogously, The 5' *PRL2* *Xho*II-*Bgl*III fragment of 540 bp and the 3' *PRL1* *Bgl*III-*Spe*I fragment of 1,1 kb were cloned into the *Xho*II/*Spe*I site of pPAMpat to generate the pPAMpat-2N1C-HA construct (*2N1C*-HA, Figure 4.2). Both constructs were subsequently verified by DNA sequencing.

4.2.6.5 Construction of pEarlyGate-*PRL2*-YFP and pEarlyGate-YFP-*PRL2*

To analyse the subcellular localization of *PRL2* in cell suspension cultures of *Arabidopsis*, N- and C-terminal YFP-fused constructs with *PRL2* were generated. The *PRL2* cDNA was amplified from pPAMpat-*PRL2*-HA using a high-fidelity DNA polymerase (section 4.2.3.1 on page 112) with the *PRL2*gw-F and *PRL2*gw-R primers. The amplified *PRL2* cDNA was introduced into the pDONR™207 vector (Invitrogen) by Gateway® BP-reaction (section 4.2.4 on page 114), and the

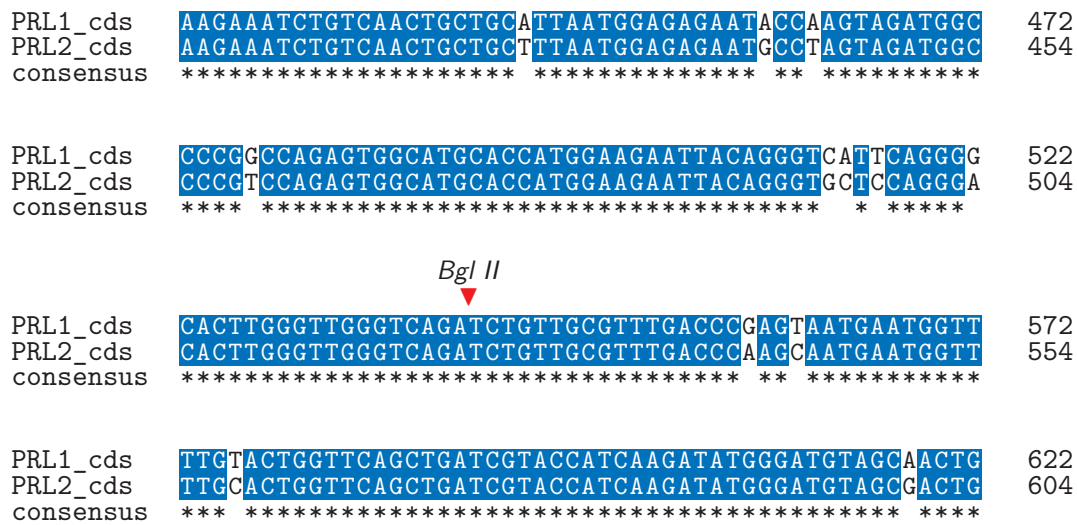


Figure 4.3: Partial nucleotide alignment of *PRL1* and *PRL2* CDSs indicating the position of the unique *Bgl*II site in the 7th exon. This *Bgl*II site was used for the generation of the sequence swap constructs. The sequence alignment was performed with the needle package from the EMBOSS suite and shaded with `TeXshade`.

resulting pDONRTM207-PRL2 construct was confirmed by sequencing using the SeLA and SeLB primers (Table A.2 on page 151). To generate the N- and C-terminal YFP fusions, pDONRTM207-PRL2 was recombined by the LR reaction with pEarleyGate-YFP-GW and pEarleyGate-GW-YFP-HA yielding pEarlyGate-YFP-PRL2 and pEarlyGate-PRL2-YFP constructs, respectively. To confirm the in-frame fusions generated by the Gateway reactions, the junctions between the PRL2 and YFP coding regions were sequenced using the PRL2-F, 2PR-R, gfp-5-junc and gfp-3-junc primers (Table A.2 on page 151), and both construct were subsequently transferred into *Agrobacterium* GV3101 (pMP90RK).

4.2.6.6 Promoter-assay construct pPCV812-PRL2::GUS

To study the tissue-specific activity of the *PRL2* promoter, D. Szakonyi generated a promoter-GUS reporter gene construct. In designing this construct, D. Szakonyi assumed that the *PRL2* promoter region extends similarly 3' downstream from the start codon, analogously to the situation observed in the case of *PRL1* (Szakonyi, 2006). The promoter region of *PRL2* is shared by the opposite-oriented *AT3G16640* unit (Figure A.2), which encodes for a member of the TCTP translationally-controlled tumor protein family.

This 5' UTR region and downstream sequences extending to exon 3 of *PRL2* (Figure A.3 in page 140) were PCR-amplified using the primer pair 2PR-F and 2PR-R and the MGL6 BAC as DNA template. The PCR fragment of 1 kb was digested with *Xba*I/*Sma*I and ligated between the *Xba*I/*Sma*I sites of the pPCV812 vector to obtain the pPCV812-PRL2::GUS construct (Figure 4.4). Subsequently, error-free amplification of the *PRL2* promoter sequences was verified by DNA sequencing using the PRL2-F and GUS-up primers and the construct was transformed into *Agrobacterium* GV3101 (pMP90RK).

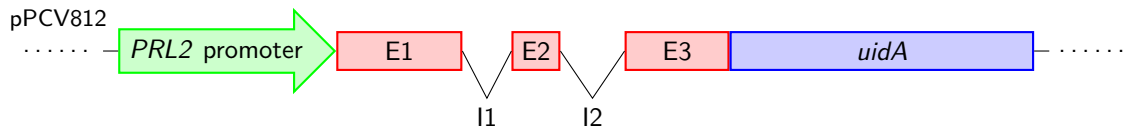


Figure 4.4: Schematic structure of the pPCV812-PRL2::GUS promoter test construct. The *uidA* reporter gene is fused in frame with the 3rd exon of *PRL2*.

4.2.6.7 Construction of pCB1-PRL2::PRL2gDNA for conditional complementation of *prl2*

To generate genetic mosaics for assessing the somatic phenotype caused by the embryo lethal *prl2* mutation, the CRE/*lox*-based conditional genetic complementation system developed by Heidstra et al. (2004) was used. This technology is based on the use of a heat inducible CRE recombinase, which precisely excises DNA sequences flanked by *lox* recognition sites. To genetically complement a lethal mutation, a wild type copy of the gene is cloned between the *lox* sites in the pCB1 binary vector, in which the *lox* sites are located between a *CaMV 35S* promoter and a gene encoding the Gal4VP16 transcription activator. Downstream of *Gal4VP16*, pCB1 carries a *GFP* reporter, the expression of which is controlled by Gal4-binding upstream activating sequences (*UAS*). pCB1 is transformed into hemizygous plants of the lethal mutation. Genetically complemented lines carrying the lethal mutation and the pCB1 construct in homozygous state are isolated. Subsequently, this line is transformed with the vector pGII227-HS::CRE, which carries the *CRE* gene under the control of a heat shock inducible *HSP18.2* promoter, and the homozygous lines for the pGII227-HS::CRE T-DNA are isolated. To visualize the phenotype conferred by the lethal mutation in vegetative or reproductive plant tissues, *CRE* expression is induced by heat-shock treatment of developing plants (or by heat treatment of local tissues), which leads to the excision of the complementing wild type gene, allowing the manifestation of the phenotype conferred by the mutation. The mutant tissue sectors are marked by the expression of the *GFP* reporter. To generate a pCB1 construct for complementation of the *prl2* mutation, the wild type *PRL2* gene was reconstructed from the promoter and coding regions cloned previously by Dr. D. Szakonyi in the pPCV812-PRL2::GUS and pBSK-PRL2gDNA constructs, respectively.

pBSK-PRL2gDNA contained the genomic sequence of *PRL2* starting from the 249th bp downstream of the ATG and extending to the end of the 3' UTR. To add the promoter and the first 249 bp, pPCV812-PRL2::GUS (section 4.2.6.6) was digested with *XbaI/XmaI* and the 1,1 kb fragment containing the promoter and the first three exons of *PRL2* was cloned into the pBluescript II SK-vector to construct pBSK-PRL2-PROM.

The resulting pBSK-PRL2-PROM construct and the pBSK-PRL2gDNA construct were then digested with *EcoRI*. Subsequently, the respective 3,5 kb and 4,1 kb fragments were ligated to obtain pBSK-PRL2::PRL2gDNA. This construct contains the *PRL2* genomic sequence together with the promoter region and the 5' and 3' UTRs. pBSK-PRL2::PRL2gDNA was subsequently digested with *XhoI/NotI*, and the resulting 4,7 kb fragment was blunted and ligated into the *NotI*-digested and end-blunted pCB1 vector generating pCB1-PRL2::PRL2gDNA (Figure 4.5).

To confirm the junctions created during the cloning procedure, pCB1-PRL2::PRL2gDNA (*PRL2*gDNA) was sequenced with the PRL2-F, PRL2-R, 2PR-F and 2PR-R primers. Clones carrying

the correct *PRL2* sequence were electroporated into *Agrobacterium* GV3101 (pMP90, pJIC) in order to transform *Arabidopsis* plants carrying the *prl2/+* GABI_228D02 allele. These plants were subsequently crossed (Figure 4.5) with a *prl2/+* GABI_228D02 line, which was previously transformed with pGII227-HS::CRE, conferring heat shock-inducible expression for the CRE recombinase (Heidstra et al., 2004).

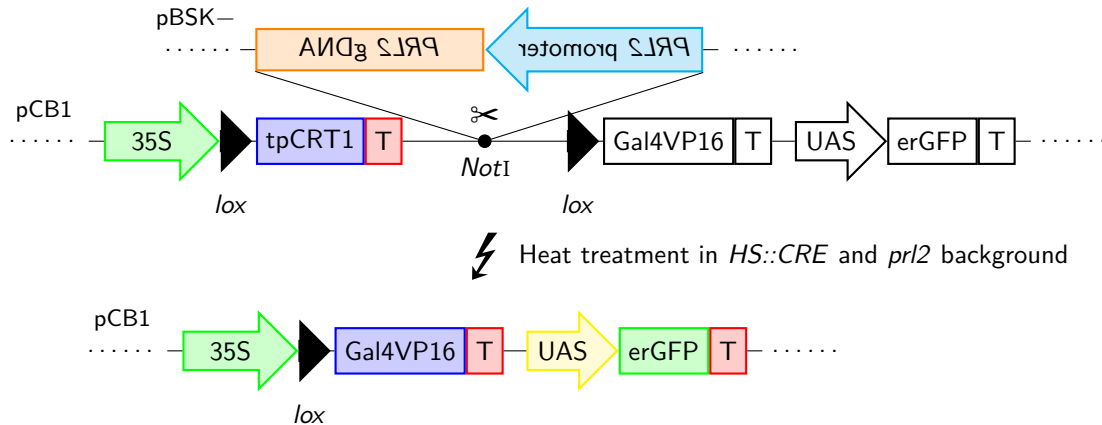


Figure 4.5: Schematic structure of the pCB1-PRL2::PRL2gDNA construct in *HS-CRE* × *prl2/prl2* background. *PRL2* is excised from the pCB1-PRL2::PRL2gDNA T-DNA upon heat shock induction of CRE and the GFP marker is expressed in cells/tissues, in which *PRL2* excision took place.

4.2.7 RNA methods

4.2.7.1 RNA extraction

From plant tissues, RNA was extracted with the QIAGEN RNeasy Plant Mini Kit (QIAGEN) according to manufacturer's instructions using 50 to 100 mg of plant material ground in either, liquid nitrogen or solid carbon dioxide.

To isolate RNA from larger amount of plant tissue, a CsCl density gradient purification protocol was used according to a modified protocol from McGookin (1984). Two to five grams of plant material was ground to powder with liquid nitrogen in a mortar, followed by addition of 8 ml of GTC buffer and 160 μ l β -mercaptoethanol while grinding. Samples were let to thaw in a fume hood, transferred to a 15 ml Falcon tube and mixed by inversion for 30 min at RT. After incubation, the supernatant was cleared by centrifugation at 4 000 rpm for 30 min in a falcon tube centrifuge. Three ml of supernatant was transferred to a 5 ml ultracentrifuge tube, on top of a 2 ml CsCl cushion and centrifuged for 16 h at 35 000 rpm at 20 °C. After carefully removing the CsCl cushion containing DNA and impurities, the pelleted RNA was dissolved in 200 μ l of DEPC-treated H₂O and then precipitated by addition of 0,1 vol of 3 M NaOAc (pH 5,2) and 2,5 vol of ethanol at -20 °C for 30 min. The RNA was pelleted by centrifugation (15 min, Eppendorf centrifuge), washed with 1 ml of 75 % ethanol, and dissolved in 100 μ l RNase-free water.

GTC solution:

Guanidiniumthiocyanate	4 M
Na-citrate	25 mM
Sarcosyl	0,5 %
DEPC-treated H ₂ O	to final volume

CsCl cushion (autoclaved):

CsCl	5,7 M
EDTA	100 mM
DEPC-treated H ₂ O	to final volume

4.2.7.2 RT-PCR

Reverse transcription-PCR was performed to synthesize cDNA from RNA template. RNA samples were treated with RNase-free DNase (NEB) for 30 min at 37 °C in order to remove DNA contamination. cDNA was prepared using the Transcriptor First Strand cDNA Synthesis Kit (Roche). A Bio-Rad DNA Engine Tetrad® 2 cycler was used for controlling the different reaction temperatures with the following components mixed in a PCR tube:

DNase-treated RNA	5 µg
oligo(dT) ₁₈ primer	1 µl
ddH ₂ O	up to 13 µl

The sample was heated to 65 °C for 10 min and cooled to 4 °C before adding the following components:

5× Transcriptor Reverse Transcriptase Reaction Buffer	4 µl
Protector RNase Inhibitor	0,5 µl
dNTP mix (10 mM each)	2 µl
Transcriptor Reverse Transcriptase	0,5 µl

The tube was gently mixed and briefly centrifuged, before performing the cDNA synthesis for 60 min at 50 °C. The enzyme was inactivated by incubating the sample at 85 °C for 5 min.

4.2.7.3 Quantitative real-time PCR

Quantitative real-time PCR (QPCR) was performed to validate the results from the transcript profiling experiments. A Bio-Rad iCycler device coupled to an iQ™5 Multicolor Real-Time PCR Detection System and controlled by the Bio-Rad iQ™5 Optical System Software (v2.0) was used. The reaction was set up using the iQ™SYBR® Green Supermix (Bio-Rad) following the manufacturer's instructions.

QPCR primers were designed in a specific manner to prevent the possible amplification of genomic DNA. The primers were designed either to span an intron in the 3' region of the target transcript or to overlap exon-exon splice junctions. T_m (i.e. melting temperature) of the primers was optimally adjusted to 60 °C. QPCR primer pairs used in this work are listed in Table A.3, on page 152 and following. The general QPCR programme included the following steps:

- | | | | |
|-------------------|--------------------|---|------------|
| 1. Denaturation: | 94 °C for 15 s | ← | 35× to 40× |
| 2. Annealing: | 60 °C for 30 s | | |
| 3. Extension: | 72 °C for 1 min/kb | | |
| 4. Measurement: | 78 °C for 20 s | | |
| 5. Melting curve: | 65 °C to 95 °C | | |

As a control, a melting curve analysis was performed with each primer combination to test for possible formation of primer dimers or unspecific amplification.

The threshold cycle (C_t), inversely correlates with the target mRNA levels, and it corresponds to the cycle number at which the SYBR[®] Green fluorescence emission increases above a fixed threshold level. Ubiquitin C_t was used to normalize and compare the abundance of different input RNA quantity across samples using the $2^{-\Delta\Delta C_t}$ method (Livak and Schmittgen, 2001), where $\Delta\Delta C_t$ is:

$$\Delta\Delta C_t = \Delta C_{t \text{ mutant}} - \Delta C_{t \text{ WT}} \quad (4.1)$$

where $\Delta C_{t \text{ mutant}}$ and $\Delta C_{t \text{ WT}}$ are calculated from:

$$\Delta C_t = \Delta C_{t \text{ query gene}} - \Delta C_{t \text{ reference gene}} \quad (4.2)$$

4.2.8 RNA-Seq methods

RNA-Seq analysis of transcripts from wild type, *prl1* and *cdc5* seedlings was performed at the Max Planck Institute for Molecular Genetics in Berlin by Dr. Tatiana Borodina in the group of Dr. Alexey Soldatov according to the protocol published by Parkhomchuk et al. (2009).

4.2.8.1 mRNA enrichment

Thirty μg of total RNA was used for polyA⁺ RNA isolation with the Dynabeads mRNA purification kit (Invitrogen) following the manufacturer's instructions. Two-step eluted mRNA was treated with TURBO[™] DNase (Applied Biosystems; 0,2 U/ μg of starting RNA) for 30 min at 37 °C.

4.2.8.2 First strand cDNA synthesis

The cDNA first strand (FS) synthesis reaction was performed in a 0,2 ml PCR tube by addition of the following components:

polyA ⁺ RNA	0,5 μg
FS-mix	4,8 μl
H ₂ O	up to 8,5 μl

Freshly prepared FS-mix:

Reverse transcription buffer (Invitrogen)	2,1×
dNTPs	1,04 mM
MgCl ₂	10,4 mM
DTT	21 mM
random primers	8,2 ng/ μl
oligo(dT) primer	5,2 μM

For better reproducibility, the reaction was performed in the PCR cyclor with the following program:

1. Denaturation: 98 °C for 1 min
2. 70 °C for 5 min
3. Primer annealing: 70 °C to 15 °C at 0,1 °C/min
4. FS-enzyme mix loading: 15 °C on hold

During hold, at 15 °C, 1,5 µl of FS-enzyme mix was loaded into the tube directly on the PCR machine. The FS-enzyme mix contains:

RNase OUT (40 U/µl, Invitrogen)	0,5 µl
SuperScript III polymerase (200 U/µl, Invitrogen)	0,5 µl
Actinomycin D solution (120 ng/µl)	0,5 µl

The incubation temperature for reverse transcription was gradually increased as a compromise among enzyme activity, primer stability and denaturation of RNA-secondary structures as follows:

5. cDNA synthesis: 0,1 °C to 25 °C at 0,1 °C/min
6. (1st step) 25 °C for 10 min
7. 25 °C to 42 °C at 0,1 °C/min
8. (2nd step) 42 °C for 45 min
9. 42 °C to 50 °C at 0,1 °C/min
10. (3rd step) 50 °C for 25 min
11. Enzyme inactivation: 75 °C for 15 min
12. End: 15 °C for ever

4.2.8.3 dNTP and primer removal

Twenty µl of 10 mM Tris-HCl (pH 8,5; Elution Buffer from QIAGEN DNeasy® Plant Mini Kit) was added to the reaction. Oligonucleotide primers and dNTPs were removed by loading the mixture on a self-made spin column containing 200 µl of Sephadex G-50 matrix, equilibrated with 1 mM Tris-HCl (pH 7,0).

4.2.8.4 Second strand synthesis

The second cDNA strand synthesis was performed substituting dTTP for dUTP. The Sephadex G-50-purified cDNA sample was transferred into a 0,5 µl eppendorf tube, supplemented with water up to 52,5 µl and mixed with 22,5 µl of freshly prepared SS-mix:

Reverse transcription buffer (from FS)	0,44×
SS buffer (Invitrogen)	3,33×
MgCl ₂	2,2 mM
DTT	4,4 mM
dUNTPs	0,89 mM
<i>E. coli</i> DNA ligase	0,22 U/µl
DNA polymerase I	0,89 U/µl
RNase H	2 U/µl

The reaction tube was incubated for 2 h at 16 °C, and the synthesized ds cDNA was purified on a QIAquick column (QIAGEN).

4.2.8.5 ds cDNA fragmentation

After spectrometric quantification of ds cDNA concentration, 200 ng to 500 ng of ds cDNA was fragmented by sonication with a Covaris S2 system (KBiosciences) to a size of 100–200 bp.

4.2.8.6 ds cDNA end repair

A mixture of T4 DNA polymerase (NEB), Klenow DNA polymerase (NEB) and T4 polynucleotide kinase (NEB) was used for repairing the ds cDNA fragments (ER-enzyme mix). For this purpose, the following components were mixed in a 0,2 ml tube:

sheared ds cDNA	50 µl
10× T4 DNA ligase buffer (NEB)	6 µl
0,25 mM dNTPs	1,5 µl
ER-enzyme mix	2,2 µl

ER-enzyme mix:

T4 DNA pol. (1,4 U/µl)	10 µl
Klenow DNA pol. (0,45 U/µl)	2 µl
T4 polynucleotide kinase (4,5 U/µl)	10 µl

The sample was incubated at 20 °C for 30 min, purified using the QIAquick-QG (QIAGEN) purification method and eluted into an eppendorf tube with 34 µl (2×18 µl) of elution buffer (10 mM Tris-HCl, pH 8,5).

4.2.8.7 A-tailing

The Klenow 3'–5' exo⁻ (NEB) enzyme was used for addition of an adenine residue to the recessed 3'-termini of the ds cDNA:

ds cDNA	34 µl
Klenow buffer	5 µl
1 mM dATP	10 µl
Klenow 3'–5' exo ⁻	0,5 µl
ddH ₂ O	up to 50 µl

The reaction was performed for 30 min at 37 °C. The sample was purified using a MinElute-QG (QIAGEN) column and eluted in 10 µl volume.

4.2.8.8 Adapter ligation

T4 DNA ligase was used to ligate the Illumina adapters (sequences on page 153) to the ds cDNA by mixing the following components:

ds cDNA (20 ng/μl)	10 μl
Adapter mix (0,9 pmol/μl)	2 μl
2× DNA ligase buffer	15 μl
T4 DNA ligase	3 μl

After 30 min of incubation at 20 °C, the sample was purified following a QIAquick-PB (QIAGEN) purification protocol and eluted in 30 μl (2×15 μl) of EB (10 mM Tris-HCl pH 8,5).

4.2.8.9 Size selection

The size of adapter-ligated ds cDNA molecules was selected by electrophoresis in a 2 % TBE agarose gel. The sample was loaded on the gel and run for 1,5 h at 120 V. A gel slice containing ds cDNA of 150–200 bp-long was cut from the gel. The ds cDNA sample was extracted from the gel slice and purified using the QIAquick-QG (QIAGEN) purification method and eluted in 50 μl (2×25 μl) of EB. Another gel slice containing the 200–300 bp fragments was also cut and reserved.

4.2.8.10 UDCase treatment of the non-amplified library

Uracil-N-glycosylase (NEB) was used to remove the uridines from the second cDNA strand in order to avoid the use of this strand as template at the library amplification step. The following components were mixed in a 0,2 ml tube:

Non-amplified library	50 μl
UDCase buffer	5,7 μl
UDCase (1 U/μl)	1 μl

The reaction was incubated for 30 min at 37 °C. No enzyme inactivation was needed.

4.2.8.11 QPCR quality test of the non-amplified library

Quantitative real-time PCR was used to determine the complexity of the library and to estimate the library quality by melting curve analysis. Thus, the number of PCR cycles to apply for large-scale PCR amplification of the library could be inferred (the complexity of the library is an estimation of the number of different cDNA molecules present).

This quality assay was performed by PCR amplification of 1 μl of non-amplified cDNA library with the PCR-2PE and PCR-1 primers (Table A.4 on page 153). The complexity C value was calculated using the formula:

$$C = \frac{\sim 0,1 \mu\text{g}}{2^A \cdot [\text{molecule size in kb}] \cdot 10^3 \cdot 2 \cdot 330 \text{ g/mol} \cdot L} = \frac{10^{11}}{2^A \cdot 0,175 \text{ kb}} \quad (4.3)$$

where L is the Avogadro constant ($6,02 \times 10^{23} \text{ mol}^{-1}$) and A is the number of cycles needed to reach the inflection point of the fluorescence measurement during amplification. Similarly, the number of cycles (N) needed for large-scale PCR amplification was calculated as:

$$N = A - \log_2 \frac{V_{\text{sample}} [\mu\text{l}] / V_{\text{reaction}} [\mu\text{l}]}{1 \mu\text{l} / 20 \mu\text{l}} \quad (4.4)$$

4.2.8.12 Library amplification and QPCR check

The library was amplified by PCR for a number of cycles as calculated above. Typically, between 10 to 13 cycles. Subsequently, the concentration of the amplified library was measured using a fluorometric method, and the cDNA library was diluted to a final concentration of 10 nM. With this diluted sample, another QPCR was performed as before in order to fine-tune the library concentration after amplification and to have an estimation of the number of clusters that will be generated later on the flow cell.

4.2.8.13 Sequencing

The amplified library was loaded into a lane of an Illumina flow cell (4 pM concentrated) and clusters were generated by PCR using the Illumina Cluster Station. Paired-end sequencing-by-synthesis was performed on an Illumina Genome Analyzer 2 using 51 cycles.

4.2.9 Microarray methods

4.2.9.1 Sample preparation

RNA was isolated from plants following the CsCl density gradient purification protocol as described in section 4.2.7.1.

Samples for the GeneChip® *Arabidopsis* ATH1 Genome Arrays were delivered to the Affymetrix CoreLab at the Westfälische Wilhelms-Universität in Münster where they were further processed following the Affymetrix GeneChip System® 3000 (Affymetrix) work-flow.

Samples for the GeneChip® *Arabidopsis* Tiling 1.0R Arrays (Affymetrix) were processed by Bruno Huettel at the Automatic DNA Isolation and Sequencing (ADIS) service of the MPIPZ, following the method described by [Laubinger et al. \(2008\)](#). Briefly, 1 µg of total RNA was used for cRNA synthesis with the MessageAmp™ II-Biotin *Enhanced* Kit (Applied Biosystems) according to the manufacturer's instructions, with the exception that the biotinylated NTP solution was replaced by a non-modified NTP solution (25 mM). Seven µg of synthesized cRNA was converted into ds cDNA using the GeneChip® WT Double-Stranded cDNA Synthesis Kit (Affymetrix) and purified using the MinElute Reaction Cleanup Kit (QIAGEN). An amount of 7,5 µg of ds cDNA was fragmented and labelled using the GeneChip® WT Double-Stranded DNA Terminal Labeling Kit (Affymetrix).

4.2.9.2 Sample hybridization and data acquisition

The GeneChip® *Arabidopsis* Tiling 1.0R Arrays (Affymetrix) were hybridized by Bruno Huettel at the Automatic DNA Isolation and Sequencing (ADIS) service of the MPIPZ. Samples were hybridized to *Arabidopsis* Tiling 1.0R arrays for 16 hours at 42 °C in a GeneChip® Fluidics Station 450 (Affymetrix), and then the arrays were washed using the wash protocol FS450_0001 in the same device.

Data from ATH1 and Tiling arrays were acquired by image scanning using a GeneChip® Scanner 3000 7 G (Affymetrix).

4.2.10 Protein analytical methods

4.2.10.1 Total plant protein extraction

Frozen plant material was ground in liquid nitrogen with a mortar and pestle. Two hundred mg of fine-powdered tissue was transferred into a centrifuge tube and 200 μ l of extraction buffer supplemented with 25 μ l/ml of plant protease inhibitor cocktail (PIC, Sigma) and 6 μ l/ml of 400 mM PMSF (Sigma) was added. The extract was thawed on ice for 30 min while the protein sample was vortexed several times. Cellular debris was removed by centrifugation at 13 000 rpm in an eppendorf centrifuge for 20 min at 4 °C. The supernatant was transferred into a clean tube.

Extraction buffer:

Tris-HCl (pH 7,5)	50 mM
Glycerol	10 %
EDTA	1 mM
NaCl	150 mM
Igepal	0,2 %

4.2.10.2 Plant nuclear protein extraction

Five grams of frozen plant material was ground in liquid nitrogen. The powder was mixed with 30 ml of nuclear isolation buffer (NIB) and:

200 mM PMSF	6 μ l/ml
PIC	1 μ l/ml
β -mercaptoethanol	1 μ l/ml
1 M ATP	2 μ l/ml

were added. The sample was incubated and further ground in the cold room on ice until the extraction buffer melted. The extract was filtered through two layers of 70 μ m and 20 μ m of nylon mesh and centrifuged at 4 000 rpm for 20 min at 4 °C in a Falcon tube centrifuge. After removing the supernatant, the nuclear pellet was gently re-suspended in 1 ml of nuclear washing buffer (NWB). The sample volume was increased to 20 ml and a mix of PMSF, PIC, β -mercaptoethanol and ATP was added as before. Nuclei were pelleted by centrifugation at 4 000 rpm for 20 min at 4 °C. The nuclear pellet was re-suspended in 200 μ l of nuclear lysis buffer (NLB), transferred to a new 1,5 ml eppendorf tube, to which 1 μ l of PMSF, PIC, β -mercaptoethanol and ATP mixture was added and the sample was vortexed for 30 s. Nuclei were disrupted in a sonication bath at 4 °C for 10 min. RNA and DNA were removed adding 20 μ l of RNase A (1 mg/ml) and 20 μ l of DNase I (1 mg/ml) to the sample by incubation for 1 h at 4 °C with gently shaking. Every 20 min, 1 μ l of PIC and PMSF was added. The sample was sonicated again for 10 min and centrifuged for 30 min at 14 000 rpm at 4 °C. The supernatant was transferred to a new eppendorf tube and the pellet was re-extracted in 50 μ l of NLB, sonicated for 10 min at 4 °C, and centrifuged for 30 min. Supernatants were pooled and protein concentration was measured using the Bradford reagent (BioRad, section 4.2.10.3).

Nuclear isolation buffer (NIB):

HEPES (NaOH) pH 7,4	50 mM
MgCl ₂	5 mM
NaCl	25 mM
Sucrose	5 %
Glycerol	30 %
Triton X-100	0,25 %

Nuclear washing buffer (3× NWB):

HEPES (NaOH) pH 7,4	50 mM
MgCl ₂	20 mM
NaCl	100 mM
Sucrose	40 %
Glycerol	40 %
Triton X-100	0,25 %

Nuclear lysis buffer (NLB):

KCl	50 mM
PIPES-KOH pH 7,5	10 mM
MgCl ₂	5 mM
Glycerol	10 %
(NH ₄) ₂ SO ₄	0,4 M

4.2.10.3 Measurement of protein concentration by Bradford assay

Protein concentration of the samples was measured by a Bradford assay (Bradford, 1976). After protein extraction, 1 µl or 2 µl of sample was mixed with 1 ml of Protein Assay Concentrated Dye Reagent (Bio-Rad), which was previously diluted 5 times in water. After 5 min of incubation at RT, OD₅₉₅ value was measured with a spectrophotometer. The protein amount was determined with the help of a standard curve previously obtained using a series of dilutions of bovine serum albumin (BSA).

4.2.10.4 SDS-polyacrylamide gel electrophoresis (SDS-PAGE)

SDS-polyacrylamide gel electrophoresis (SDS-PAGE, Laemmli, 1970) was used to separate proteins according to their size. Protein gels (1 mm thick) were poured between 10×8 cm glass plates of a Protean mini gel system (Bio-Rad). Generally, 4,5 ml of 12 % separating gel was poured first and overlaid with iso-propanol. After polymerization, the iso-propanol was removed and the surface of the gel was rinsed with water. Subsequently, a stacking gel layer was poured on top of the separating gel. This gel was cast with a 10 or 15 well comb and the glass plates were placed in a Protean mini gel electrophoresis tank filled with SDS-PAGE running buffer. Protein samples were denatured by addition of 5× SDS protein loading buffer (4:1), incubated at 95 °C for 5 min and loaded in the gel using a Hamilton syringe. Samples were run at 25 mA. The size of separated proteins was estimated using the pre-stained protein marker All Blue (Bio-Rad).

Separation gel (12 %):

ddH ₂ O	5,4 ml
29:1 acrylamide to bisacrylamide (40 %)	3,0 ml
1,5 M Tris-HCl (pH 8,8)	2,5 ml
10 % SDS	0,1 ml
20 % APS	100 µl
TEMED	10 µl

Stacking gel (4 %):

ddH ₂ O	2,4 ml
1 M Tris-HCl (pH 6,8)	1 ml
29:1 acrylamide to bisacrylamide (40 %)	0,5 ml
10 % SDS	40 µl
10 % APS	30 µl
TEMED	5 µl

SDS-running buffer:

Tris	25 mM
Glycine	192 mM
SDS	0,1 %

5× SDS protein loading buffer:

SDS	2 %
Glycerol	10 %
Tris-HCl (pH 6,8)	50 mM
β-mercaptoethanol	5 %
Bromophenol blue	0,1 %

4.2.10.5 Western blotting

To detect proteins with specific antibodies, proteins separated by SDS-PAGE were transferred and immobilized on nitrocellulose or PVDF membranes (Towbin et al., 1979). Prior to transfer, the nitrocellulose membranes were rinsed in transfer buffer for 5 min, whereas the PVDF membranes, were treated with 100 % methanol for 30 s and then submerged into transfer buffer. The stacking gel was removed from the separation SDS-PAGE gel and the gel was equilibrated in transfer buffer for 5 min. A transfer *sandwich* was assembled in the following order: a sponge layer, 3× 3MM Whatman paper sheets, SDS-PAGE gel, membrane, 3× 3MM Whatman paper sheets and a final sponge layer. This sandwich was placed in a wet blotter transfer device so that the membrane faced the anode and the gel sandwich was fully submerged in transfer buffer. Protein transfer was performed either for 1 h at 50 V or overnight at 10 V.

Transfer buffer:

Tris	50 mM
Boric acid (pH 8,0)	50 mM

To monitor successful protein transfer and to determine equal protein loading, membranes were stained in Ponceau staining solution for 1 min and the unspecific staining was washed out with water or 1× TBS solution (Hughes et al., 1988).

Ponceau staining solution:

Ponceau S	0,2 %
TCA	3 %

In order to probe with specific antibodies, the PVDF or nitrocellulose membranes were blocked in blocking solution (5 % of milk powder in TBS in case of ECL-based detection or commercial blocking solution from Licor Biosciences in the case of fluorometric quantification) for 1 h at room temperature. The primary antibody diluted in blocking solution was incubated with the membrane overnight. Next morning, the membrane was washed 3 times for 10 min with washing buffer (0,05 % of Tween-20 in TBS). Subsequently, the membrane was incubated for 1 h with the secondary antibody diluted in blocking solution. The membrane was finally washed 3 times for 10 min with washing buffer.

TBS:

NaCl	137 mM
KCl	2,7 mM
Tris-HCl (pH 7,4)	20 mM

To visualize the protein bands on the membrane, either enhanced chemiluminescence (ECL) or fluorometric detection were used.

Horseshradish peroxidase conjugated antibodies were used for the ECL detection in combination with an ECL detection kit from GE Healthcare. A freshly prepared 1:1 mixture of the two ECL reagents was applied onto the PVDF or nitrocellulose membrane. Light emission was captured on a Hyperfilm™ MP (GE Healthcare) slide and the film was developed using a Optimax X-ray Film Processor (Piotec Processor Technology).

Fluorescent dye-conjugated (IRDye or Alexa Fluor) secondary antibodies were used to quantify the amount of antibody cross-reacting proteins. In this case, the nitrocellulose membrane was blocked for 1 h with the blocking solution recommended by the provider (Licor Biosciences). Probing with the primary antibody was performed overnight in the commercial blocking solution. Subsequently, the nitrocellulose membrane was rinsed 3× in washing buffer, incubated for 1 h with the secondary antibody in darkness and rinsed again 3× in washing buffer in darkness. A last wash was performed in darkness using TBS without Tween-20. The protein bands were quantified using the Odyssey Infrared Imaging System (Licor Biosciences).

Stripping of the membrane was carried out to remove the IgGs from the first reaction and to probe the same membrane with another primary antibody. Stripping was performed either using the Ponceau staining solution since it contains TCA that can denature proteins, or using the Restore™ Western blot stripping buffer (Thermo Scientific). In the latter case, the membrane was incubated with the Restore™ Western blot stripping buffer for 10 min to 20 min at room temperature on a shaker. Subsequently, the membrane was washed 4 × for 10 min with TBS.

4.2.10.6 Measurement of proteasome activity

Proteasome activity was assayed by activity-based proteome profiling, using a fluorescent probe (MVB072, Misas-Villamil et al., in press, Figure 4.6) which derives from epoxomicin that specifically targets the *active* $\beta 1$, $\beta 2$ and $\beta 5$ subunits of 20S proteasome complex.

Fifty mg of sample was ground in liquid nitrogen, mixed with 100 μ l of ddH₂O and centrifuged in an eppendorf centrifuge for 10 min at 10 000 rpm. The supernatant was transferred into a new tube and mixed with:

L-Cys solution (2,4 mg/ml)	4 μ l
1 M NaOAc pH 7	4 μ l
Sample extract	50 μ l
MVB072 probe (1 μ M)	1,2 μ l

Sample was incubated for 2 h in darkness and the reaction was stopped adding 12 μ l of 5 \times SDS-PAGE loading buffer, boiled for 5 min and loaded on a 12 % SDS-PAGE gel.

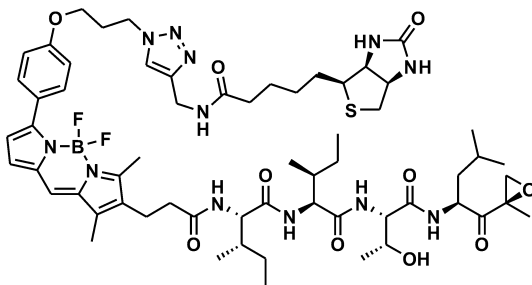


Figure 4.6: Chemical structure of MVB072. MVB072 is derived from epoxomicin and contains as prosthetic groups a fluorescent and a biotin tag. Taken from Misas-Villamil et al., (in press).

Proteins labelled with the fluorescent MVB072 probe were visualized by in-gel fluorescence scanning using a Typhoon 8600 scanner (GE Healthcare Europe GmbH). Excitation and emission wavelengths were set at 532 and 580 nm, respectively.

4.2.11 Imaging methods

4.2.11.1 Stereo microscopy

Low-magnification images were taken with a Leica MZ16FA stereo-microscope (Leica Microsystems Ltd., Switzerland) coupled to a Leica DFC Digital Camera (Leica Microsystems Ltd.) and controlled by the Leica Application Suite (v2.8.1). For GFP detection, samples were illuminated with the 480-500 nm emission line of a mercury lamp and fluorescence was recorded in the 505 nm-525 nm emission range. Images were post-processed using The GIMP.

4.2.11.2 Light microscopy

Light microscopy images were taken with a Leica DM RB microscope coupled to a Leica DFC Digital Camera controlled by the Leica Application Suite (v2.8.1). For samples cleared with chloral hydrate, an interference contrast set-up based on a Nomarski prism, was used. Images were post-processed using The GIMP.

4.2.11.3 Fluorescence microscopy

Localization of fluorescent-tagged proteins *in vivo* was visualized using a Zeiss LSM 510 META (Carl Zeiss MicroImaging GmbH, Göttingen, Germany) system, controlled by the LSM5 META software v3.2 SP2.

GFP was excited with an Argon laser at 488 nm and the emitted fluorescence was detected between 505 nm and 525 nm, YFP was excited at 514 nm and its emission was detected between 540 nm and 560 nm. Propidium iodide fluorescence and chlorophyll autofluorescence was detected between 610 nm and 720 nm. Bright-field images were simultaneously recorded by a transmission detector. Images were post-processed using The GIMP.

4.2.12 *In silico* methods

4.2.12.1 Transcript profiling analyses with tiling arrays

In case of samples hybridized to tiling arrays, where the *prl1* mutant is compared to WT, two types of analyses were performed: a fitted linear model applied to the expression data using the limma package (Smyth et al., 2005), and a non-parametric approach using the RankProd package (Hong et al., 2006) following the advice and examples of Dr. Emiel Ver Loren van Themaat and Dr. Ulrike Göbel from the MPIPZ. For both analyses, the data was first normalized with the RMA function from the affy package of R/Bioconductor.

The limma approach fits a linear model to the expression data for each gene. This approach relies on empirical Bayesian methods to share expression data between genes making the analysis more robust, even when a small number of arrays are used. Furthermore, the constraints of the classical-parametric tests do not apply. For the linear model to be specified, two matrices are needed: a *design matrix* which is a representation of the different samples and treatments, and a *contrast matrix*, where the coefficients from the design matrix are combined into contrasts of interest. The *ad hoc*-written code for this specific analysis can be found on page 155.

The RankProd approach relies on the classical non-parametric rank-product test. This test assigns a rank to the expression data of each gene. The bigger and more consistent the difference of gene expression data between control replicates and subject replicates, the higher rank the gene achieves. In this analysis, only a contrast matrix must be specified. Details and code for the analysis are written on page 156.

4.2.12.2 Transcript profiling analyses with ATH1 arrays

For the β -estradiol-dependent complementation experiment (section 2.2.4), in which the ER-PRL1/*prl1* samples were hybridized to ATH1 arrays, also two kinds of analyses were performed: a pair-wise analysis and a time-course analysis for the posterior gene clustering.

The first analysis was done with the help of Dr. Csaba Koncz, using the GeneSpring GX v10.0 Expression Analysis suite (Agilent Technologies, Waldbronn) by applying unpaired t-tests. These tests were performed pair-wise for each sucrose concentration (experimental set-up in section 2.2.4.1), and the genes showing a differential expression of 1,5 in FC (fold change) and a p-value < 0,05 were first sorted according to GO term description and then manually categorized in pathways using information from the PubMed and TAIR databases.

For the time-course analysis, data from ER-PRL1/*prl1* samples was first normalized with the *rma* function of the *affy* package and then, a linear model specific for a time-course experiment was applied using the *limma* package under R/Bioconductor (*ad hoc*-written code on page 156) for identifying transcripts showing differential regulation. Results were filtered by a p-value < 0,05 and a fold-change (FC) of at least 1,5. The contrast matrix only contains the comparisons between consecutive time-points.

4.2.12.3 Time-course clustering analysis of microarray data

Gene clustering (also known as unsupervised classification) was performed with the *Mfuzz* package (Kumar and Futschik, 2007) under R/Bioconductor. The clustering process performed by this package is the so-called *soft* clustering, which is based on fuzzy logic. *Mfuzz* clustering generates internal cluster information, assigning a fitting value in each cluster for each gene. This has the advantage that relationships between sub-groups of genes falling in the same cluster, and comparisons between the different clusters can be easily made. For the ER-PRL1/*prl1* samples, the gene classification was performed by building 9 clusters with a *fuzzification* parameter of 1,25. The written code for this analysis can be found on page 156.

4.2.12.4 Raw data processing for RNA-Seq

Base calling from raw images was performed using the Illumina RTA v1.4.15.0 pipeline followed by Bustard v1.4.0 at the Max Planck Institute for Molecular Genetics in Berlin. This data was transferred through the network to the MPIPZ and pre-processed with the computer described in section 4.1.12.1.

This pre-processing involved the conversion of Illumina-formatted files into FASTQ-formatted files with the Perl scripts developed and provided by Dr. Vyacheslav Amstislavskiy from the Max Planck Institute for Molecular Genetics in Berlin. Briefly, the **seq.txt* and **prb.txt* files from the Illumina pipeline were converted into the FASTQ format with the *sol2fastq_lite.pl* script. Subsequently, the output FASTQ file was split into two FASTQ files by the *paired2two_fq.pl* script. Each of the two FASTQ files contains only the data of one mate pair, in another words, one round of the PE sequencing.

4.2.12.5 Generation of sequence indexes for RNA-Seq

Prior to the alignment of the sequenced samples to a reference sequence, a *reference index* has to be built. The bowtie-build command from the short read aligner Bowtie (Langmead et al., 2009) was used for this purpose. In this work, 9 different indexes based on the TAIR9 assembly and annotation were created. The main index contained the whole genome sequence from the 5 chromosomes plus mtDNA and chDNA of *Arabidopsis*. Eight more indexes were created *ad hoc* with the sequence subsets for cDNA, CDS, exon, intron, 5' and 3' UTRs, transposable elements and intergenic-annotated regions of *Arabidopsis*.

4.2.12.6 RNA-Seq read alignment

Pre-processed reads were mapped with Bowtie against the reference subsets mentioned above. The fact that samples were PE-sequenced was not taken into consideration for this analysis.

For these alignments, the standard parameters of Bowtie were changed. This decision was taken after confirming that the default Bowtie parameters are not suited for the read-length of the sequenced samples, which was of 51 nt. Instead of allowing 2 mismatches in a seed-length of 28 nt, 3 mismatches were allowed in a seed-length of 35 nt.

4.2.12.7 Differential expression analysis of RNA-Seq data

When taking into account some considerations, RNA-Seq data may also be used to analyse gene transcription from a genome-wide perspective. Different tools are being developed nowadays for tackling this analysis. In this work, the TopHat (Trapnell et al., 2009) and Cufflinks (Trapnell et al., 2010) tools were used.

Pre-processed reads were mapped with TopHat against the whole *Arabidopsis* genome sequence from TAIR9. In this case, the fact that the samples were PE sequenced was taken into consideration. As parameters for TopHat, and based on the TAIR9 statistics, the minimum and maximum intron size was set to 70 bp and 10 kb, respectively. The mean inner distance between the sequence pair was set to 200 bp. TopHat mapped the reads using Bowtie and output a SAM file listing the accepted reads. In addition, TopHat also provided a wiggle file with the read coverage along the genome that was converted to the gff format and uploaded to the MySQL database using different BioPerl modules. Read coverage of the different samples was subsequently visualized with the local GBrowse setup at the MPIPZ.

The TopHat compiled file of accepted reads was post-processed with Cufflinks in order to assemble transcripts *in silico*. The parameters used with the cufflinks command were as follows: average inner distance between the sequence pair was set to 200 bp with a standard deviation for the distribution of the inner distances between sequence pairs of 50 bp. This process was supervised using the published gff file which contains the TAIR9 gene annotation.

For the differential expression analysis, the output files from TopHat, which contain the accepted reads from the *prl1*, *cdc5* and WT samples were used to run the analysis. For this, the cuffdiff command was used with the following set-up: the file containing the transcripts assembled for the WT sample with cufflinks was used as reference, the average inner distance between the sequence pair was set to 200 bp with a standard deviation of 50 bp between pairs.

Cufflinks reported the transcript abundances in Fragments Per Kilobase of exon per Million fragments mapped (FPKM), which is analogous to the “RPKM” measurement used in single read experiments. The Poisson function (f) is used by the cuffdiff command to test for differential expression:

$$f(n; \lambda) = \frac{e^{-\lambda} \lambda^n}{n!} \quad (4.5)$$

where e is the base of the natural logarithm, n is the number of observed fragments, the probability of which is given by the function, $n!$ is the factorial of n and λ is equal to the expected number of fragments.

Appendices

A. Sequences

A.1 Insertional mutants

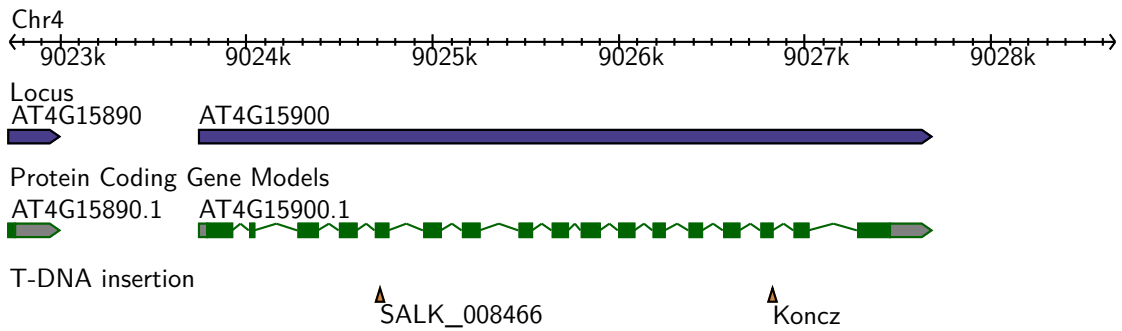


Figure A.1: Insertional mutants of *PRL1* (AT4G15900) used in this work.

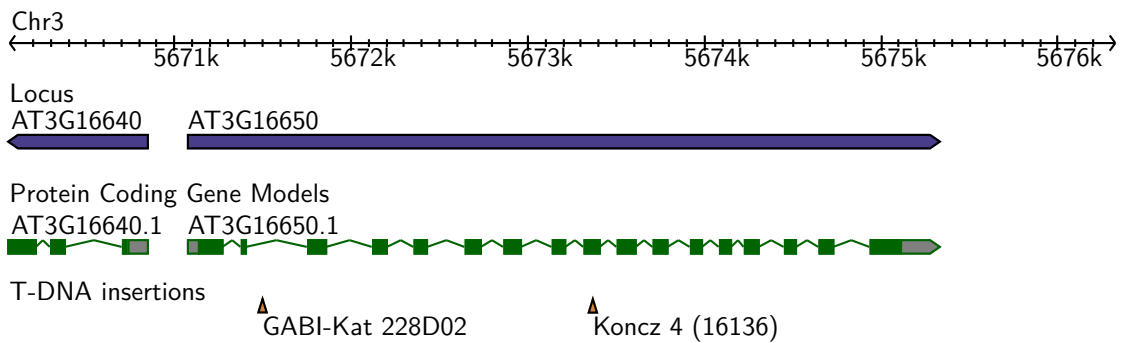
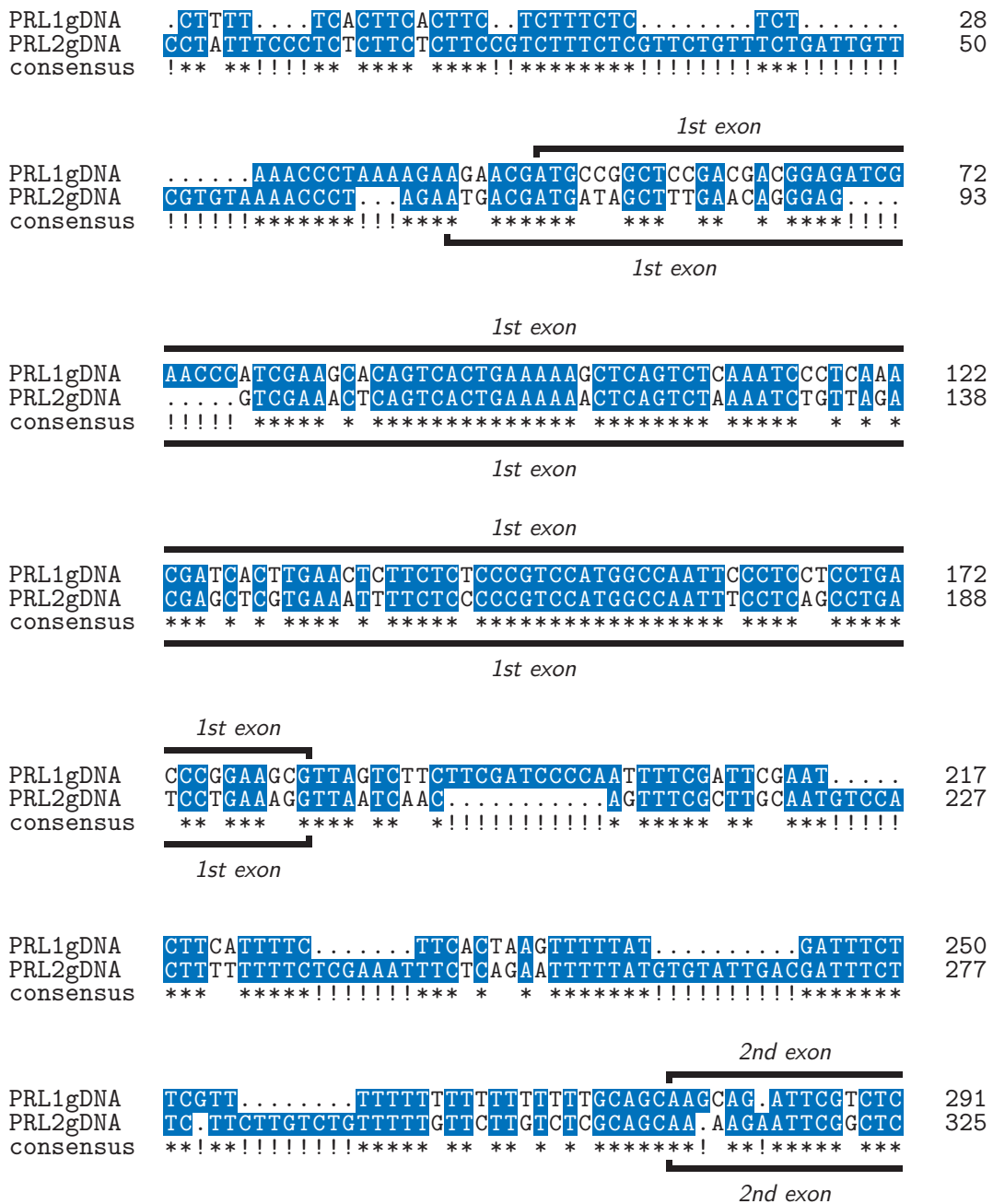


Figure A.2: Insertional mutants of *PRL2* (AT3G16650) used in this work.

A.2 Aligned sequences

Figure A.3: Nucleotide alignment of PRL1 and PRL2 genomic sequences from the beginning of the 5' UTR until the end of the third exon. Alignment was performed with the needle package, exon localization with esim4 from the EMBOSS suite and the sequence was shaded with `TeXshade`.



	<i>2nd exon</i>	
PRL1gDNA	A <u>GCCATAAGGTAA</u> <u>AACATT</u> <u>GAGTCTCTCTT</u> ..AC	323
PRL2gDNA	T <u>GCCATAAGGTAAGGGGGTTTTTCGAATATTTTTTA</u> AATTTTATCTTTGAT	375
consensus	*****!!!!!!** * * * ****!!*	
	<i>2nd exon</i>	
PRL1gDNA	C AGTC <u>TTTAGAAA</u> T <u>TTATTT</u> CAGTTATTCGCTT <u>TAA</u> TGTC <u>ATTGA</u> ..TT	372
PRL2gDNA	C ..GTG <u>TT</u> .. <u>GAAA</u> AAT..... <u>TTGTT</u> CGCTTCTTC <u>TTT</u> GTT <u>TTG</u> AGTT	415
consensus	*! ** **!!**** **!!!!!!** ***** * * * * ****!!**	
PRL1gDNA	G GATTT <u>TGG</u> <u>TTTA</u> <u>AAGCTTC</u> <u>GAAC</u> TT <u>TAG</u> TT	404
PRL2gDNA	T GATAA <u>TGG</u> ATAGCTTTATAGCAAGCTTCAGAGACGTTGAACCTGAG...	462
consensus	*** **!!!!!!*****!!!!!!*****!!!!!!** * **!!	
PRL1gDNA	T ATTCAGGT <u>TTTT</u> CCATAATTGTTCTAAATC.....T <u>TCA</u> ..GG.....	441
PRL2gDNA <u>AAAA</u> <u>TTTT</u> .. <u>ATAA</u> ..G <u>TG</u> TAAATCGAACAG <u>TCA</u> ATGGCTTATC	503
consensus	!!!!* ****!!*****!!* * *****!!!!!! ****!!*****!!!!!!	
PRL1gDNA	.. <u>TTTT</u>G <u>TTACC</u> AA <u>TAAT</u> <u>AGTAA</u> AGA.....	465
PRL2gDNA	A CTTTTATAGT <u>TTACC</u> TTT <u>TATCT</u> GGAGT.TAGATTCTTCTCATCAGCTA	552
consensus	!!*****!!!! ***** * **!!!!*****! ****!!*****!!!!!!	
PRL1gDNA	.. <u>TGG</u> TTGA. <u>TTT</u> ACTTAGACTCT..... <u>CTCTC</u> . <u>TCT</u> CTCT..	498
PRL2gDNA	C TATGTTGAGTTTGCTT..... <u>TCTAG</u> CATATTACC <u>CTC</u> ATCTTATAG	598
consensus	!!!!* ****!!*** **!!!!!!**!!!!!!** * **!!** * * !!	
PRL1gDNA	.. <u>GT</u> TGTGTA..... <u>TGTTACT</u> <u>GAT</u> TTT	519
PRL2gDNA	T AAGATGTTTAGTTTGCATCAAGCGTTTATG <u>TGA</u> ACATCAAGTAGAATAT	648
consensus	!!!* *** **!!!!!!*****!!!!!!* *** *!!!!!!***** * * *	
	<i>3rd exon</i>	
PRL1gDNA	A GAAAGTT..... <u>TTCTTT</u> GTACAGATGA <u>AAGTT</u> GC <u>TTT</u> GGA	556
PRL2gDNA	A AAAGTTAATGACTTGGACGTTACTTGTATAGATTCA <u>AAGTT</u> GA <u>TTT</u> GGA	698
consensus	* *****!!!!!!*****!!!!!!** ***** **** ***** ***** *****	
	<i>3rd exon</i>	
PRL1gDNA	G GTGTAGA <u>ACCT</u> GTTGTGAGTCA <u>ACCT</u> CCACGTC AAC <u>CTGACC</u> GCATCA	606
PRL2gDNA	G GC <u>GTAGA</u> ACC... <u>TGCA</u> AGTAAGCCTACACGTTATTG <u>CTGACC</u> ATACAG	745
consensus	** *****!!!!** *** * *** ***** ***** * **	
	<i>3rd exon</i>	
PRL1gDNA	T GAGCAGCCAGGACC. <u>TT</u> CAAATGCTCTTTCCCTCGCAGG	645
PRL2gDNA	T GAAAAGACGGCTCCATTGAAA. <u>GCC</u> CTTGCGCTTCAGG	784
consensus	*** ** * * **!!** **!!** *** * ** ****	
	<i>3rd exon</i>	

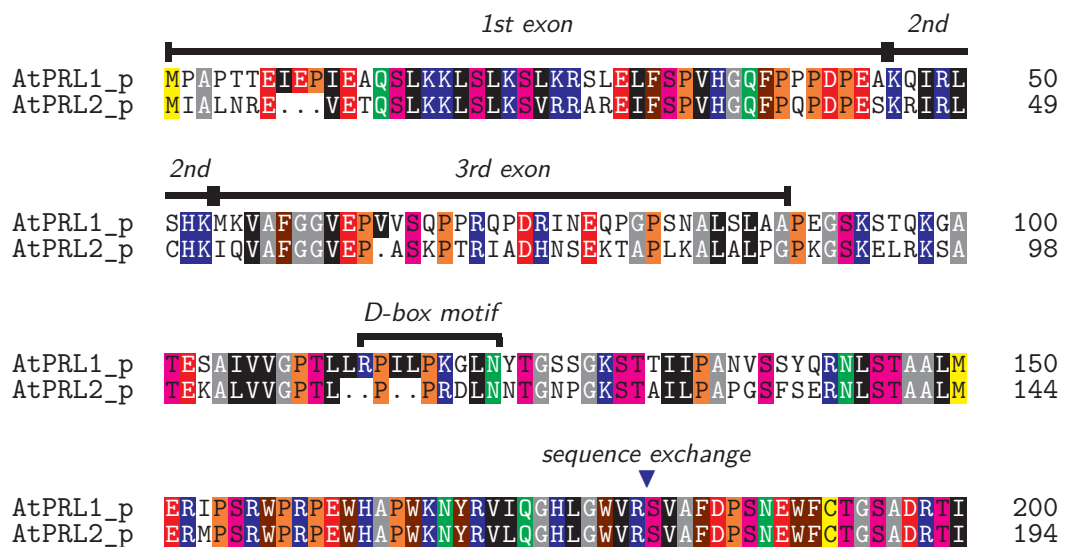
Figure A.4: Complete nucleotide alignment of *PRL1* and *PRL2* CDSs done with the needle package from the EMBOSS suite and shaded with `TeXshade`. The *Bgl*III restriction site on 7th exon was used for exchanging the *PRL1* and *PRL2* CDS sequences.

PRL1_cds	ATGCCG.....GCTCCGACGACGGAGATCGAACCCATCGAAGCACAGTC	44
PRL2_cds	ATGACGATGATAGCTTTGAACAGGGAG.....GTCGAAACTCAGTC	41
consensus	*** **!!!!!!** * * ****!!!!!!!! ***** * *****	
PRL1_cds	ACTGAAAAAGCTCAGTCTCAAATCCCTCAAACGATCACTTGAACTCTTCT	94
PRL2_cds	ACTGAAAAAATCTCAGTCTAAAATCTGTTAGACGAGCTCGTGAAATTTTCT	91
consensus	***** * ***** *	
PRL1_cds	CTCCCGTCCATGGCCAATTCCCTCCTCCTGA.CCCGGAAGCCAAAGCAG.A	142
PRL2_cds	CCCCGTCCATGGCCAATTTCCCTCAGCCTGATCCTGAAAGCAAA..AGAA	139
consensus	* ***** *	
PRL1_cds	TTCGTCTCAGCCATAAGATGAAGTTGCGTTTGGAGGTGTAGAACCCTGTT	192
PRL2_cds	TTCGGCTCTGCCATAAGATTCAGTTGCAATTTGGAGGCGTAGAACC...T	186
consensus	*** *	
PRL1_cds	GTGAGTCAAACCTCCACGTCAACCTGACCGCATCAATGAGCAGCCAGGACC	242
PRL2_cds	CAAGTAAAGCCTACACGTATTGCTGACCATAAAGTGAAGAAAGACGGCTCC	236
consensus	* *	
PRL1_cds	.TTCAAATGCTCTTTCCTCGCAGCTCCGTAAGGGTCTAAG..AGTACGC	289
PRL2_cds	ATTGAAA.GCCCTTGCGCTTCAGGTCCAAAAGGGTCAAGGAACCTTCGA	285
consensus	! *	
PRL1_cds	AAAAGGGTGCACAGAGAGTCTATTGTTGTTGGTCCAACCTTACTGCGT	339
PRL2_cds	AAAA..GCGCAACAGAGAAAGCTTTAGTTGTTGGTCCAACCTT.....	325
consensus	*****! *	
PRL1_cds	CCAATACTGCCTAAAGGCTTGAACTATACAGGT..TCCTCAGGGAAGAGC	387
PRL2_cds	...TACCGCCAAGAGACTTGAACAATACTGGTAATC..CAGGCAAAAGC	369
consensus	!!!!** *	
PRL1_cds	ACCAACATTATACCTGCAAAATGATATCTTCATATC..AAAGAAATCTGTCA	435
PRL2_cds	ACGGCATTCTTCTGCACTGGATCAT..TTCCGAAAGAAATCTGTCA	417
consensus	* *	
PRL1_cds	ACTGCTGCATTAATGGAGAGAATACCAAGTAGATGGCCCCGCCAGAGTG	485
PRL2_cds	ACTGCTGCTTTAATGGAGAGAATGCTAGTAGATGGCCCCGTCAGAGTG	467
consensus	***** *	
PRL1_cds	GCATGCACCATGGAAGAATTACAGGGTCATTGAGGGCACTTGGGTTGGG	535
PRL2_cds	GCATGCACCATGGAAGAATTACAGGGTCTCCAGGGCACTTGGGTTGGG	517
consensus	***** *	

	<i>Bgl</i> II ▼	
PRL1_cds	TCAGATCTGTTGCGTTTGACCCGAGTAATGAATGGTTTTGTACTGGTTCA	585
PRL2_cds	TCAGATCTGTTGCGTTTGACCCAAGCAATGAATGGTTTTGC ACTGGTTCA	567
consensus	***** ** *****	
PRL1_cds	GCTGATCGTACCATCAAGATATGGGATGTAGCAACTGGAGTTCTGAAGCT	635
PRL2_cds	GCTGATCGTACCATCAAGATATGGGATGTAGCAACTGGAGTTCTGAAGCT	617
consensus	***** ***** *	
PRL1_cds	AACACTTACTGGGCATATCGAGCAAGTACGAGGCCTCGCTGTAAGCAATC	685
PRL2_cds	CACACTTACTGGA CATATA GGC AAGTACGAGGCCTCGCTGTAAGCAATA	667
consensus	***** * *****	
PRL1_cds	GACATACCTATATGTTCTCTGCTGGTGATGACAAGCAAGTCAAATGCTGG	735
PRL2_cds	GACATACCTATATGTTTCTGCTGGTGATGACAAGCAAGTCAAATGCTGG	717
consensus	***** *****	
PRL1_cds	GACCTTGAGCAGAATAAGGTTATCCGATCTTATCATGGTCACTTGAGTGG	785
PRL2_cds	GACCTTGAGCAGAATAAGGTTATTCGATCTTATCATGGTCACTTG CATGG	767
consensus	***** ***** ** *	
PRL1_cds	TGTTCTATGCTTAGCTCTGCACCCAACCTTTGGATGTTTATTAACTGGGG	835
PRL2_cds	CGTTTACTGTTTAGCTCTTCATCCTACTCTTGATGTTGTACTAACCGGAG	817
consensus	* *	
PRL1_cds	GGCGAGACTCTGTCTGCAGGGTGTGGGATATTCGTACCAAGATGCAAATT	885
PRL2_cds	GGCGAGACTCTGTCTGCAGGGATGGGATATTCGTACGAAGATGCAAATT	867
consensus	***** ***** ***** *****	
PRL1_cds	TTTGC ACTCTCAGGACATGACAACACCGTTTTGTTCTGTATTACTCGTCC	935
PRL2_cds	TTTGTACTCC...ACATGACAGCGATGTTTTTTCCTGTTTGGCCCGCC	914
consensus	**** *	
PRL1_cds	AACAGACCCACAAGTTGTCACCGGATCCCATGACACGACCATTAAATTTT	985
PRL2_cds	AAC TGATCCACAAGTTATTACAGGTCTCATGACTCAACCATCAAATTTT	964
consensus	*** *	
PRL1_cds	GGGACCTTCGATATGGA AAAACAATGTCAACGCTAACACATCATAAGAAA	1035
PRL2_cds	GGGACCTTCGATATGGCAAATCGATGGCAACATAACGATCATAAGAAAG	1014
consensus	***** ***** * * * * * * * * * * * * * * * * * * *	
PRL1_cds	TCTGTCCGAGCAATGACCTCCATCCTAAAGAGAATGCC TTTGCTTCTGC	1085
PRL2_cds	ACTGTCCGAGCAATGGCTCTCCATCCGAAAGAGAATGATTTTGT TTTCTGC	1064
consensus	***** *	
PRL1_cds	ATCAGCTGACAACA CAAGAAATTTAGCCTTCCAAGGGAGAGTTCTGCC	1135
PRL2_cds	ATCAGCTGACAACATCAAGAAGTTTAGCCTTCC TAAGGGAGAGTTTGGC	1114
consensus	***** ***** ***** ***** *****	

PRL1_cds	ACAACATGCTTTCGCAACAGAAACACATAATTAATGCAATGGCTGTAAAC	1185
PRL2_cds	ACAACATGCTTTCCTCTACAGAGAACAATAATTAACGCAGTGGCTGTGAAT	1164
consensus	***** * ***** * ***** ** ***** **	
PRL1_cds	GAGGATGGTGTGATGGTCACTGGAGGTGATAATGGAAGTATATGGTTCTG	1235
PRL2_cds	GAGGATGGCGTAATGGTCACTGGAGGTGATAAAGGTGGCTTATGGTTCTG	1214
consensus	***** * ***** ***** ** * *****	
PRL1_cds	GGACTGGAAGAGTGGTCACAGTTTCCAACAGTCAGAAACTATCGTACAGC	1285
PRL2_cds	GGACTGGAAGAGTGGTCACAATTTCCAACGGCAGAAACTATTTGACAGC	1264
consensus	***** ***** * ***** *****	
PRL1_cds	CTGGTTCCTGGAGAGTGAAGCGGGTATATATGCAGCGTGTTATGATAAT	1335
PRL2_cds	CTGGTTCCTGGAGAGTGAAGCAGGTATATATGCAGCGTGTTACGATCAG	1314
consensus	***** ***** ***** ***** ** *	
PRL1_cds	ACAGGTTCAAGATGGTAACATGCGAGGCTGATAAGACGATAAAGATGTG	1385
PRL2_cds	ACGGTTCAAGGCTGGTAACGTGTGAGGAGACAAAACAATAAAGATGTG	1364
consensus	** ***** ***** ** ***** ** ** *****	
PRL1_cds	GAAAGAAGATGAGAAATGCAACTCCAGAAACTCATCCTATCAATTTCAAAC	1435
PRL2_cds	GAAAGAAGACGAGGATGCAACTCCTGAAACTCATCCTCTCAACTTTCAAAC	1414
consensus	** * ***** ** ***** ***** ***** *****	
PRL1_cds	CACCAAAGGAGATTAGGCGTTCTAA	1461
PRL2_cds	CTCCAAAGAGATCAGACGTTCTGA	1440
consensus	* * * ***** ** ***** *	

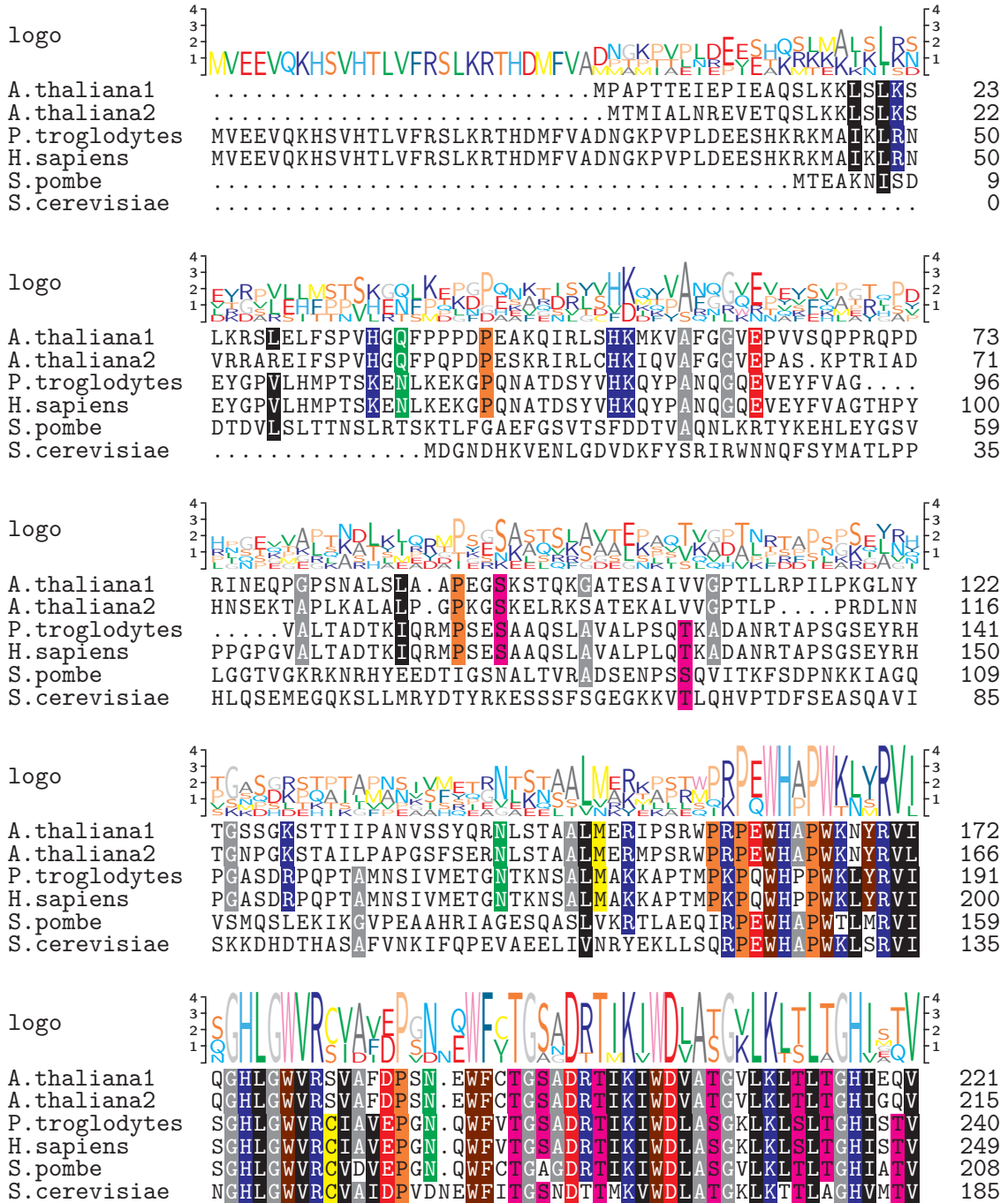
Figure A.5: Complete amino acid alignment of PRL1 and PRL2 done with the needle package from the EMBOSS suite and shaded with *Texshade*. The sequence exchange is labelled at position 180, and the NLS between positions 478 and 485 of PRL1.



AtPRL1_p	KIWDVATGVLKLTLTGHIEQVRGLAVSNRHLYMFSAGDDKQVKCWDLEQN	250
AtPRL2_p	KIWDVATGVLKLTLTGHIGQVRGLAVSNRHLYMFSAGDDKQVKCWDLEQN	244
AtPRL1_p	KVIRSYHGHLSCVYCLALHPTLDVLLTGRDSSVCRVWDIRTKMQIFALSG	300
AtPRL2_p	KVIRSYHGHLHGQVYCLALHPTLDVLLTGRDSSVCRVWDIRTKMQIFVLP.	293
AtPRL1_p	HDNTVCSVFTRPDPQVVTGSHDTTIKFWDLRYGKTMSTLTHHKKSVRAM	350
AtPRL2_p	HDSDVFSVLARPTDPQVITGSHDSTIKFWDLRYGKSMATITNHKKTVRAM	343
AtPRL1_p	TLHPKENAFASASADNTKKFSLPKGEFCHNMLSQQKTIINAMAVNEDGVM	400
AtPRL2_p	ALHPKENDEVSASADNIKKFSLPKGEFCHNMLSLQRDIINAVAVNEDGVM	393
AtPRL1_p	VTGGDNGSIWFWDWKSGHSFQQSEETIVQPGSLESEAGIYAA CYDNTGSRL	450
AtPRL2_p	VTGGDKGGLWFWDWKSGHNFQRAETIVQPGSLESEAGIYAA CYDQIGSRL	443
	NLS	
AtPRL1_p	VICEADKTIKMWKEDE NATPEHPINFKPPKEIRRF	486
AtPRL2_p	VICEGDKTIKMWKEDE DATPEHPINFKPPKEIRRF	479

X acidic (-)
X aliphatic
X aliphatic (small)
X amide
X aromatic
X basic (+)
X hydroxyl
X imino
X sulfur

Figure A.6: Alignment of *Arabidopsis* PRL1 and PRL2 orthologues performed with the emma package from the EMBOSS suite and shaded with `TeXshade`. These orthologues include genes from *Pan troglodytes*, *Homo sapiens*, *Schizosaccharomyces pombe* and *Saccharomyces cerevisiae*. The N-terminal region of *A. thaliana* PRL1 and PRL2 are very different to the rest.



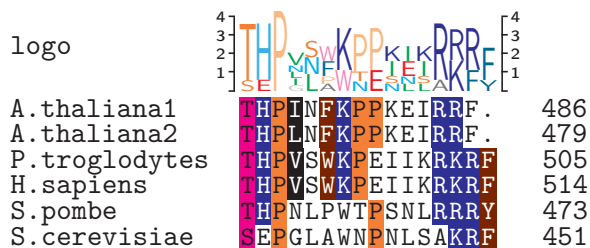
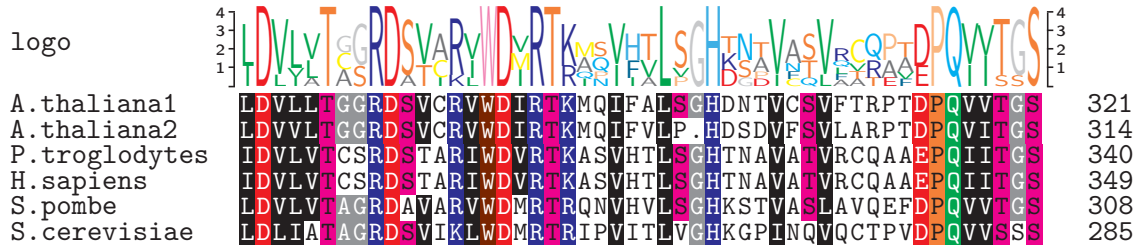
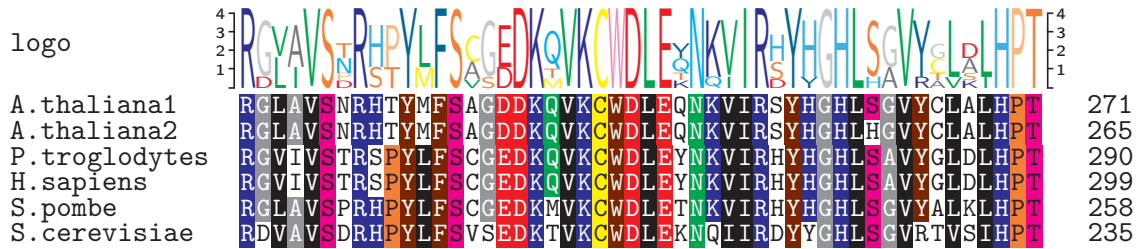
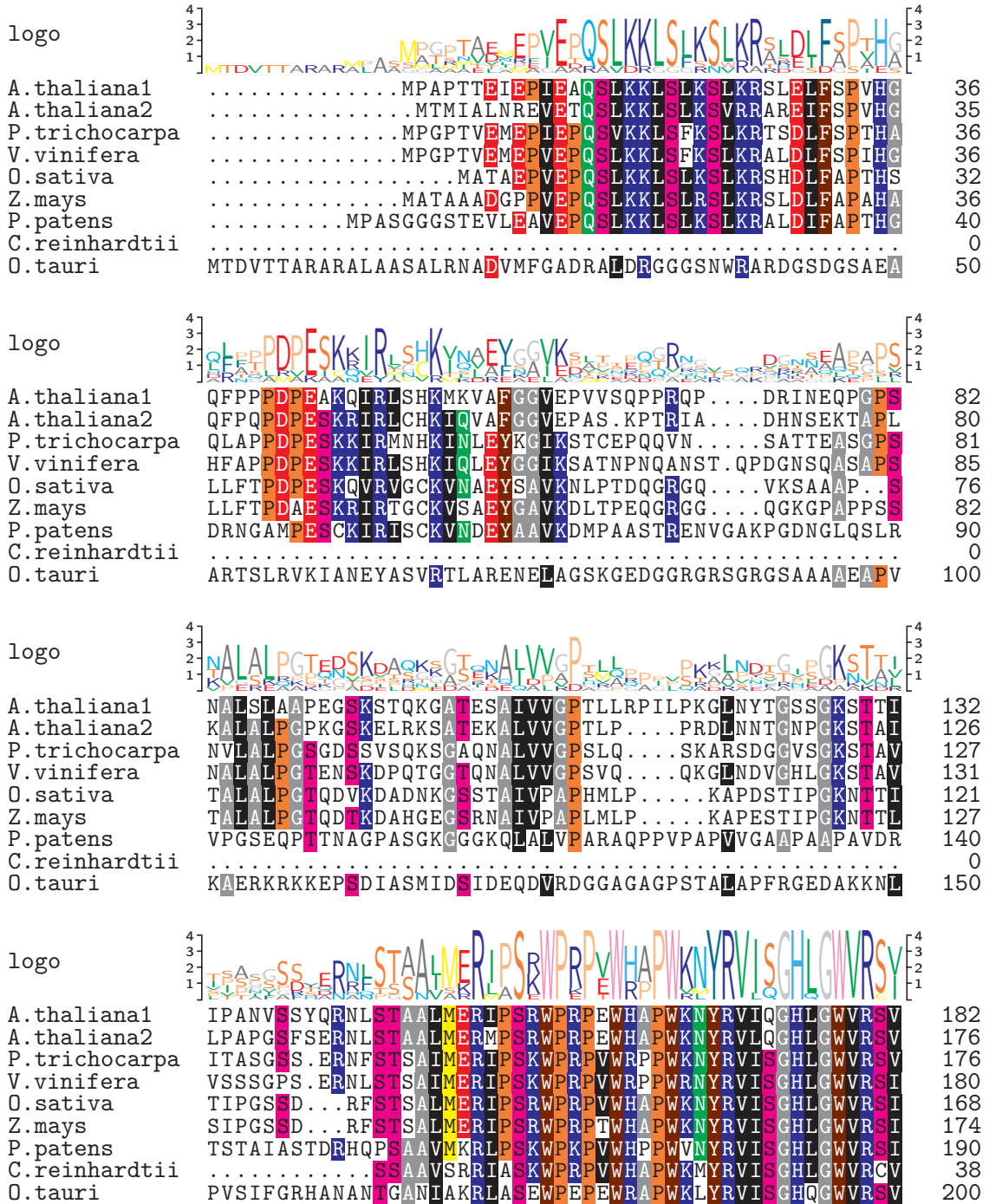


Figure A.7: Alignment of *Arabidopsis* PRL1 and PRL2 orthologues across several plant and unicellular algae species done with the emma package from the EMBOSS suite and shaded with T_Xshade. These orthologues include sequences from *Populus trichocarpa*, *Vitis vinifera*, *Oriza sativa*, *Zea mays*, *Physcomitrella patens*, *Chlamydomonas reinhardtii* and *Ostreococcus tauri*.



logo

A.thaliana1	AFDPSNEWFC TGSADRTIKIWDVATGV LKLTLTGHIEQVRGLAVSNRHTY	232
A.thaliana2	AFDPSNEWFC TGSADRTIKIWDVATGV LKLTLTGHIEQVRGLAVSNRHTY	226
P.trichocarpa	AFDPSNTWFC TGSADRTIKIWDVGSRLKLTLTGHIEQVRGLAVSQRHTY	226
V.vinifera	AFDPSNSWFC TGSADRTIKIWDVSGRLKLTLTGHIEQIRGLAVSNKHTY	230
O.sativa	AFDPSNEWFC TGSADRTIKIWDLASGTLKLTLTGHIEQIRGLAVSQRHTY	218
Z.mays	AFDPANWFC TGSADRTIKIWDLASGTLKLTLTGHIEQIRGLAVSQRHTY	224
P.patens	AFDPGNWFC TGSADRTIKIWDSGTGQLKLTLTGHIEQVRGLAVSARHPY	240
C.reinhardtii	AVDPSNEWFC TGSADRTIKIWDLASGQLKLTLTGHIEQVTGLAVSSRHPY	88
O.tauri	AVDPENKWFV TGSADRTIKVVDLASGGLKLTLTGHIEQVTGLVVS PRHPY	250

logo

A.thaliana1	MFSAGDDKQVKCWDLEQNKVIRSYHGHLSGVYCLALHPTLDVLLTGGRDS	282
A.thaliana2	MFSAGDDKQVKCWDLEQNKVIRSYHGHLSGVYCLALHPTLDVLLTGGRDS	276
P.trichocarpa	MFSAGDDKQVKCWDLEQNKAIRSYHGHLSGVYCLALHPTIDLLLTGGRDS	276
V.vinifera	MFSAGDDKQVKCWDLEQNKVIRSYHGHLSGVYCLALHPTIDILLTGGRDS	280
O.sativa	LFSAGDDKQVKCWDLEQNKVIRSYHGHLSGVYCLALHPTIDILLTGGRDS	268
Z.mays	LFSAGDDKQVKCWDLEQNKVIRSYHGHLSGVYCLALHPTIDILLTGGRDS	274
P.patens	LFSAGDDKQVKCWDLEYNKVIRSYHGHLSGVYCLALHPTLDILMTGGRDS	290
C.reinhardtii	MFSAGDDKQVKCWDLEQNKVIRSYHGHLSGVYSIALHPTLDVLLTGGRDS	138
O.tauri	MFSAGDDKQVKCWDLEYNKVIRNYHGHLSGVYSIAMHPTLDLLFTGGRDS	300

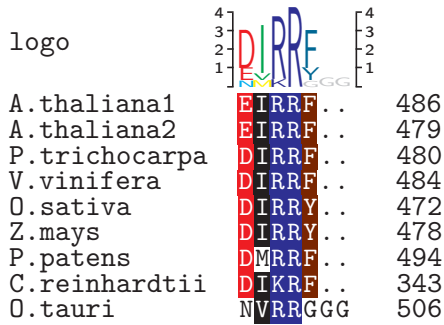
logo

A.thaliana1	VCRVMDIRTKQVYFALS GHNTVCSVFARPTDPQVVTGSHDSTIKFWDLR	332
A.thaliana2	VCRVMDIRTKMQIFVLP.HSDVFSV LARPTDPQVITGSHDSTIKFWDLR	325
P.trichocarpa	VCRVMDIRTKVQVYFALS GHNTVCSVFARPTDPQVVTGSHDSTIKFWDLR	326
V.vinifera	VCRVMDIRSKMQIHALS GHNTVCSVFARPTDPQVVTGSHDSTIKFWDLR	330
O.sativa	VCRVMDIRTKAHVSAL TGHNTVCSVFARPTDPQVVTGSHDSTIKFWDLV	318
Z.mays	VCRVMDIRTKAHVSAL TGHNTVCSVFARPTDPQVVTGSHDSTIKFWDLV	324
P.patens	VCRVMDIRTKAQVYFALS GHNTVCSVITQATDPQVVTGSHDSTIKLWDLA	340
C.reinhardtii	VVRVMDMRTKVQAMVLS GHNTVCSLLAQAPDPQVVISGSHDSTIRLWDLR	188
O.tauri	ACRVMDIRTKQVYCLTGHNTVGSILAQDENPQLVVTGSYDGTIRMWDLA	350

logo

A.thaliana1	YGKTMSTLTHHKKSVRAMALHPKENAFASASADNTKKFSLPKGEFCHNML	382
A.thaliana2	YGKSMATLTHHKKTVRAMALHPKENDFVSASADNIKKFSLPKGEFCHNML	375
P.trichocarpa	YGKTMSTLTHHKKSVRAMALHPTEHCFASASADNIKKFNLPKGEFLHNML	376
V.vinifera	YGKTMATLTHHKKSVRAMALHPKEHTFASASADNIKKFNLPKGEFLHNML	380
O.sativa	AGRTMCTLTHHKKSVRAMALHPKEKSFASASADNIKKFSLPKGEFLHNML	368
Z.mays	AGRTMCTLTHHKKSVRAMALHPKEKAFASASADNVKKFNLPKGEFLHNML	374
P.patens	AGKTMSTLTHHKKSVRALAMHPFEHTFTSASADNIKKFRLPKGDFLHNML	390
C.reinhardtii	KGKASAVLTHHKKSVIRALAMHPHEFAFASASAEIKKVALPDGDFLHNML	238
O.tauri	MGKSIINTLTHHKKGVRAMVMHKKEFVAFVSASADNIKKFSCHG.DFMHNML	399

Characterization of PRL1 and PRL2 in *A. thaliana*



- X acidic (-)
- X aliphatic
- X aliphatic (small)
- X amide
- X aromatic
- X basic (+)
- X hydroxyl
- X imino
- X sulfur

A.3 Oligonucleotides

Table A.1: Oligonucleotides used for plant genotyping.

Name	Sequence 5'→3'
FISH1	CTGGGAATGGCGAAATCAAGGCATC
FISH2	CAGTCATAGCCGAATAGCCTCTCCA
PRL1-5'	ACTTGAACTCTTCTCTCCCGTCCAT
PRL1-3'	AACCTGTATTATCATAACACGCTGC
PRL2-5'	GAACAGGGAGGTGAAACTCAGTCAC
PRL2-3'	TTCACTCTCCAGCGAACCTAACCAT
SALK-LB	TTTGGGTGATGGTTCACGTAGTGGG
Gal4VP16-R	TTCTTCTTGAGCACTTGAGCTTCTTGA

Table A.2: Oligonucleotides used in PCR-based cloning and sequencing.

Name	Sequence 5'→3'
T7	GTAATACGACTCACTATAGGGC
SP6r	ATTTAGGTGACACTATAGAAGA
SeLA	TCGCGTTAACGCTAGCATGGATCTC
SeLB	GTAACATCAGAGATTTTGAGACAC
gfp-5-junc	CCTCGCCGGACACGCTGAAC
gfp-3-junc	CTGAGCACCCAGTCCGCC
gfp-5-mid	CCCTTCAGCTCGATGCGGTTC
gfp-3-mid	GGACGACGGCAACTACAAGACCC
GUS-up	ACAGGCCGTCGAGTTTTTTGATTTTAC
2PR-F	GCTCTAGATCTGAAGTGAGGTCCCTAAGTTTGG
2PR-R	TCCCCGGGGACCTGGAAGCGCAAGGGCTTTCAATGG
PRL2-F	CCGCTCGAGATGACGATGATAGCTTTGAACAGGGAGG
PRL2-HA	CACTAGTTTAAGCATAATCTGGAACATCGTATGGATA GAAGCGTCTGATCTCTTTGGGAGG
PRL1-F	CCGCTCGAGATGCCGGCTCCGACGACGG
PRL1-N	CACTAGTTTAAGCATAATCTGGAACATCGTATGGATA CATGGTGCATGCCACTCTGGCCG
PRL1-C	CCGCTCGAGATGAAGAATTACAGGGTCATTCAGGGG
PRL1-HA	CACTAGTTTAAGCATAATCTGGAACATCGTATGGATA GAAGCGCCTAATCTCTCT
PRL2-gw-F	GGGGACAAGTTTGTACAAAAAAGCAGGCTTCATGACG ATGATAGCTTTGAACAGGG
PRL2-gw-R	GGGGACCACTTTGTACAAGAAAGCTGGGTCTGAAGCGT CTGATCTCTTTGGGAGG
PIPL-F	GCTCTAGAGGGTCATGATGATCATCACC
PIPL-R	TCCCCGGGCCTCGACAGATGACACCGC

Table A.3: Oligonucleotides used for QPCR validation of the transcript profiling data.

AGI code	Name	Sequence 5'→3'
AT1G01060	LHY-F	CAACAGCAACAACAATGCAACTAC
	LHY-R	AGAGAGCCTGAAACGCTATACGA
AT1G13280	AOC4-F	GAGCAAGATCCACCACTTCCTCCAC
	AOC4-R	CATGTTGGATCAAAAACGCAGAGACC
AT1G14350	FLP-F	GCTCGTCCCGAAAAATCCTGATG
	FLP-R	GGACTCTTTTGCAAGGGGGTGG
AT1G19180	JAZ1-F	CCGACAACAACCATGAGTTTATTCCC
	JAZ1-R	TTGGGGAGGATTGGATTGGCTC
AT1G22770	GI-F	TCTTCTTCTGCGGGCAACTGATG
	GI-R	TGAGGCGCGTGAAGAATCG
AT1G24260	SEP3-F	AGATGCCACTCCAGCTGAACCCT
	SEP3-R	CCATTCCATCTTGTGCCCCTG
AT1G49720	ABF1-F	GAATCCGCTGCTAGATCAAGGGCTC
	ABF1-R	TGACTTCACCTTCTTACCACGGACC
AT1G55020	LOX1-F	AAAACCACTGGACCTTCCTGACC
	LOX1-R	ACCAAACCTCAAGCCCATCCACTG
AT1G65480	FT-F	GATATCCCTGCTACAACCTGGAACAACC
	FT-R	TCCTCCGCAGCCACTCTCCC
AT1G69440	AGO7-F	GAAGTGGCCGTGTGCAAATCAGTAG
	AGO7-R	CTGCCTCCAATACTCATCAAAGCCC
AT1G78600	LZF-F	GCAGCAGCAGGAACAGCAGG
	LZF-R	CGCCCATGATGTCTCACCTCCC
AT2G02820	MYB88-F	GGCAACCTGATCTCCATGATTACC
	MYB88-R	CCAGTTGAGAGTAAACCACTTGTTC
AT2G06050	OPR3-F	GGAAGCAAGTTGTGGAAGCAGTTCAC
	OPR3-R	ACGTGGGAACCATCGGGCAA
AT2G21660	CCR2-F	TGGCGTCCGGTGATGTTGAG
	CCR2-R	CGCCGCTGTATCCTCCTCCA
AT2G46830	CCA1-F	CAATGCACGCCGAGTAGAATC
	CCA1-R	TTGAGTTTCCAACCGCATCCGT
AT3G02380	COL2-F	CGATGAGGATGATCGAGAGGTTGCTT
	COL2-R	AGTCACCTGCAACAAAGCCAACA
AT3G07650	COL9-F	CAATGCCTGCTCACATTAGTAACCC
	COL9-R	TGGTTGGGGTGAGAGGGTCGT
AT3G09150	HY2-F	GCGGGTTTCATGGAGCCTGAG
	HY2-R	CCCCATGGGAAAGTCTCAGCA
AT3G17609	HYH-F	CCGTGGAAGAAACCCTGTTGATAAAG
	HYH-R	CTCTTCGAGCTGGTCATTGTTGTTCTG
AT3G62250	UBQ5-F	CCAGAAGGAATCGACGCTTCATCTC
	UBQ5-R	GAGAAGGATCGATCTACCGCTACAACAG
AT4G24540	AGL24-F	GAAGAGGAATCTTCAAGAAAGCCGAT
	AGL24-R	CTCCAGCCGCTGCAACTCTTCT

continued on next page

Table A.3 — continued from previous page

AGI code	Name	Sequence 5'→3'
AT4G26150	CGA1-F	ACCACCAGCGACAGCAGCAA
	CGA1-R	ATGACCGGTGGGGATACGCC
AT4G28190	ULT1-F	GGTTATCATTGGGGCGAAAAGG
	ULT1-R	GTGAAGTCGACACAAGTCTGGCAAGT
AT4G39950	CYP79B2-F	TGCCGATGCTCACTGGACTTGA
	CYP79B2-R	ACGGCGTTTGATGGATTGTCTGG
AT5G02810	PRR7-F	TCCCCATAATCATCGCTCACA
	PRR7-R	ACTTCCACTTCCGCTTCCACTACC
AT5G15850	COL1-F	TCAACGAGTTCCAATTCTGCCCA
	COL1-R	ACAACCATGAAGCCGCCTCTGC
AT5G20240	PI-F	TGTCGAGCACGCCATTGAACA
	PI-R	CCTGAAGATTTGGCTGAATCGGTTG
AT5G20240	PI-AS-F	AGAGAACGCAAACAACAGAGTGGTGA
	PI-AS-R	GCGTGCTCGACAGCCATCAGA
AT5G39660	CDF2-F	CGGTTTAGGACGAGAAGAAGGTGATG
	CDF2-R	GCTGTTACATCGCGGACACGG
AT5G46700	TRN2-F	TGTACTTTTGGGTTGCCCTTGTCGG
	TRN2-R	ATCCACATTTTGTGGGGGCTTG
AT5G58140	PHOT2-F	GGGCAGAGGGACAGTTGGGA
	PHOT2-R	TCTTCGGGCCGCGTATTAGC
AT5G58140	PHOT2-AS-F	CCTCTACGCACGTCTGTTTGATTAC
	PHOT2-AS-R	CTAAGCAGTGAAGATATTCTAAGCCGA

Table A.4: Oligonucleotides used for preparing the Illumina library.

Name	Sequence 5'→3'
Adapter-1	TACTCTTTCCCTACACGACGCTCTCCGATCT
Adapter-2PE	p-GATCGGAAGAGCGTTTCAGCAGGAATGCCGAG*
PCR-1	AATGATACGGCGACCACCGAGATCTACTCTTTCCC TACACGACGCTCTCCGATCT
PCR-2PE	CAAGCAGAAGACGGCATACGAGATCGGTCTCGGCATT CCTGCTGAACCGCTCTCCGATCT
Seq-1	ACACTCTTTCCCTACACGACGCTCTCCGATCT
Seq-2	CGGTCTCGGCATTCTGCTGAACCGCTCTCCGATCT

B. Scripts for microarray analysis

Here follows the R code used in analysing the tiling arrays with the CDF file from [Naouar et al. \(2009\)](#). Adapted and modified from the code provided by Dr. Ulrike Göbel:

```
1 # The appropriate libraries are loaded
2 library(affy)
3 library(preprocessCore)
4 library(athtiling1.0rcdf)
5 library(limma)
6
7 # The CEL files to analyse are listed in the file targets.txt
8 targets <- readTargets("targets.txt")
9
10 # The CEL files are read
11 data <- ReadAffy(filenamees=targets$filename)
12
13 # And the description file from Naouar et al. (2009) is applied to the data
14 data@cdfName <- "athtiling1.0rcdf"
15
16 # Array data is normalized
17 eset <- rma(data)
18
19 # The linear model is designed
20 f <- factor(targets$genotype)
21 design <- cbind(Col_WT=1, pr11vsWT=targets$genotype=="pr11")
22 fit <- lmFit(eset, design)
23
24 # And the analysis is performed
25 fit <- eBayes(fit)
26
27 # The table with the results is created and saved
28 topTable(fit, coef="pr11vsWT")
29 table.out <- topTable(fit, coef="pr11vsWT", n=nrow(exprs(eset)), p.value=0.05,
30   resort.by="logFC")
31 write.table(table.out, file="missregulated_genes_p.value_0.05.txt", sep="\t")
```

Here follows the R code used for analysing the tiling arrays with RankProd, uses the CDF file from Naouar et al. (2009) and was adapted and modified using the code provided by Dr. Emiel Ver Loren van Themaat:

```

1 # The appropriate libraries are loaded
2 library(affy)
3 library(preprocessCore)
4 library(athtiling1.0rcdf)
5 library(limma)
6 library(RankProd)
7
8 # The CEL files to analyse are listed in the file targets.txt
9 targets <- readTargets("targets.txt")
10
11 # The CEL files are read
12 data <- ReadAffy(filenamees=targets$filename)
13
14 # The mapping file from Naouar et al. (2009) is applied to the data
15 data@cdfName <- "athtiling1.0rcdf"
16
17 # The annotation file from Emiel is loaded
18 load("baseAT.RData")
19
20 # Array data is normalized
21 normData <- exprs(rma(data))
22
23 # The vector that tells which slide is which for performing the
24 # statistical contrast is created. Treatment or mutant (0) and
25 # controls or WT (1).
26 contrast.c1 <- c(1,1,1,0,0,0)
27
28 # The test is run with 500 permutations
29 RP.out <- RP(normData, contrast.c1, num.perm = 500,
30   logged = TRUE, na.rm = FALSE, plot = FALSE, rand = 123)
31
32 # The topGene function shows the miss-regulated genes using (in this case) a
33 # p-value<0.05 as cutoff. The output tables are stored in tables.missregulated
34 tables.missregulated <- topGene(RP.out, cutoff = 0.05, method = "pfp",
35   logged = TRUE, logbase = 2, gene.names = RP.out$AveFC )

```

Here follows the R code used for analysing the early changes in depletion of *PRL1* in the ER-*PRL1/prl1* samples. Genes are also clustered depending on the expression profile:

```

1 # The appropriate packages for the analyses are loaded
2 library(limma)
3 library(affy)
4 library(preprocessCore)
5 library(annotate)
6 library(ath1121501.db)
7 library(Mfuzz)
8
9 # The slides to analyse are listed in the file called "targets2.txt"

```

```
10 targets <- readTargets("targets2.txt")
11
12 # The actual data is read and stored in the data object
13 data <- ReadAffy(filename=targets$filename)
14
15 # The data is normalized across the different microarrays
16 eset <- rma(data)
17
18 # The factor for the lineal model is created
19 f <- factor(targets$sample)
20
21 # and also the matrix for setting up the different comparisons
22 design <- model.matrix(~0+f)
23
24 # The levels of the factors in the design
25 colnames(design) <- levels(f)
26
27 # The data is fitted to the linear model
28 fit <- lmFit (eset, design)
29
30 # The interesting statistical contrasts are selected
31 # only for the root samples grown in 0,1 % sucrose (R01)
32 contrast.matrix.R01 <- makeContrasts (R01d4-R01d3, R01d3-R01d1, levels=design)
33 fit.R01 <- contrasts.fit (fit, contrast.matrix.R01)
34 fit.R01 <- eBayes(fit.R01)
35 table.R01 <- topTable(fit.R01, n=Inf, p.value=0.05)
36
37 exprs.R01 <- as.matrix(cbind(0,table.R01$R01d3...R01d1,table.R01$R01d4...R01d3))
38 rownames(exprs.R01) <- table.R01$ID
39 minimalSet.R01 <- new("ExpressionSet", exprs = exprs.R01)
40
41 # The data is transformed and processed for the cluster analysis
42 R01.r <- filter.NA(minimalSet.R01, thres= 0.25)
43 R01.f <- fill.NA(R01.r, mode = "mean")
44 R01.s <- standardise(R01.f)
45
46 # Nine different clusters are done
47 clusters.R01 <- mfuzz(R01.s, c=9, m=1.25)
48
49 # Clusters with genes are plotted
50 mfuzz.plot(R01.s, clusters.R01, mfrow= c(3,3))
51
52 # And the gene names are exported to reflect in which cluster they are
53 groups.R01 <- as.matrix(clusters.R01$membership)
```

C. Transcript profiling tables

In the following pages, the tables corresponding to the different transcript profiling experiments are listed. For the printed version, content of Tables C.6, C.7, C.8, C.9 and C.10 was not included due to space restrictions. The filled tables can be found in the online version of this document, available at <http://www.kups.uni-koeln.de>.

Table C.1: Enriched GO terms from the up-regulated gene-list of the tiling array experiment. The tiling array results were post-processed with AgriGO.

GO term	Ontology	Description	p-value
GO:0050896	P	response to stimulus	0,00000
GO:0042221	P	response to chemical stimulus	0,00000
GO:0006950	P	response to stress	0,00000
GO:0010033	P	response to organic substance	0,00000
GO:0009605	P	response to external stimulus	0,00000
GO:0009611	P	response to wounding	0,00000
GO:0006952	P	defense response	0,00000
GO:0009743	P	response to carbohydrate stimulus	0,00000
GO:0010200	P	response to chitin	0,00000
GO:0051707	P	response to other organism	0,00000
GO:0044249	P	cellular biosynthetic process	0,00000
GO:0009058	P	biosynthetic process	0,00000
GO:0009723	P	response to ethylene stimulus	0,00000
GO:0070887	P	cellular response to chemical stimulus	0,00000
GO:0009751	P	response to salicylic acid stimulus	0,00000
GO:0031323	P	regulation of cellular metabolic process	0,00000
GO:0045449	P	regulation of transcription	0,00000
GO:0043170	P	macromolecule metabolic process	0,00000
GO:0010556	P	regulation of macromolecule biosynthetic process	0,00000
GO:0019219	P	regulation of nucleobase, nucleoside, nucleotide and nucleic acid metabolic process	0,00000
GO:0051171	P	regulation of nitrogen compound metabolic process	0,00000
GO:0009889	P	regulation of biosynthetic process	0,00000
GO:0031326	P	regulation of cellular biosynthetic process	0,00000

continued on next page

Table C.1 – continued from previous page

GO term	Ontology	Description	p-value
GO:0080090	P	regulation of primary metabolic process	0,00000
GO:0006350	P	transcription	0,00000
GO:0019222	P	regulation of metabolic process	0,00000
GO:0016070	P	RNA metabolic process	0,00000
GO:0050789	P	regulation of biological process	0,00000
GO:0044260	P	cellular macromolecule metabolic process	0,00000
GO:0050794	P	regulation of cellular process	0,00000
GO:0010468	P	regulation of gene expression	0,00000
GO:0060255	P	regulation of macromolecule metabolic process	0,00000
GO:0006807	P	nitrogen compound metabolic process	0,00000
GO:0065007	P	biological regulation	0,00000
GO:0048583	P	regulation of response to stimulus	0,00000
GO:0009409	P	response to cold	0,00000
GO:0006979	P	response to oxidative stress	0,00000
GO:0034645	P	cellular macromolecule biosynthetic process	0,00000
GO:0009059	P	macromolecule biosynthetic process	0,00000
GO:0009266	P	response to temperature stimulus	0,00000
GO:0006139	P	nucleobase, nucleoside, nucleotide and nucleic acid metabolic process	0,00000
GO:0009719	P	response to endogenous stimulus	0,00000
GO:0009755	P	hormone-mediated signaling pathway	0,00000
GO:0032870	P	cellular response to hormone stimulus	0,00000
GO:0009873	P	ethylene mediated signaling pathway	0,00000
GO:0009628	P	response to abiotic stimulus	0,00000
GO:0009607	P	response to biotic stimulus	0,00000
GO:0010467	P	gene expression	0,00000
GO:0009651	P	response to salt stress	0,00000
GO:0000160	P	two-component signal transduction system (phosphorelay)	0,00000
GO:0009617	P	response to bacterium	0,00000
GO:0006970	P	response to osmotic stress	0,00000
GO:0006725	P	cellular aromatic compound metabolic process	0,00000
GO:0009753	P	response to jasmonic acid stimulus	0,00000
GO:0050832	P	defense response to fungus	0,00000
GO:0043687	P	post-translational protein modification	0,00000
GO:0009620	P	response to fungus	0,00000
GO:0006575	P	cellular amino acid derivative metabolic process	0,00000
GO:0032502	P	developmental process	0,00000
GO:0009664	P	plant-type cell wall organization	0,00001
GO:0042742	P	defense response to bacterium	0,00001
GO:0009725	P	response to hormone stimulus	0,00001
GO:0019538	P	protein metabolic process	0,00002
GO:0042398	P	cellular amino acid derivative biosynthetic process	0,00002
GO:0034641	P	cellular nitrogen compound metabolic process	0,00003

continued on next page

Table C.1 – continued from previous page

GO term	Ontology	Description	p-value
GO:0032501	P	multicellular organismal process	0,00003
GO:0051704	P	multi-organism process	0,00004
GO:0009698	P	phenylpropanoid metabolic process	0,00004
GO:0009056	P	catabolic process	0,00004
GO:0051716	P	cellular response to stimulus	0,00005
GO:0007275	P	multicellular organismal development	0,00008
GO:0044267	P	cellular protein metabolic process	0,00015
GO:0019438	P	aromatic compound biosynthetic process	0,00016
GO:0031347	P	regulation of defense response	0,00026
GO:0033554	P	cellular response to stress	0,00026
GO:0048856	P	anatomical structure development	0,00062
GO:0080134	P	regulation of response to stress	0,00069
GO:0006955	P	immune response	0,00091
GO:0002376	P	immune system process	0,00092
GO:0007568	P	aging	0,00092
GO:0044271	P	cellular nitrogen compound biosynthetic process	0,00110
GO:0031667	P	response to nutrient levels	0,00150
GO:0043412	P	macromolecule modification	0,00150
GO:0032787	P	monocarboxylic acid metabolic process	0,00180
GO:0019748	P	secondary metabolic process	0,00230
GO:0009991	P	response to extracellular stimulus	0,00250
GO:0006464	P	protein modification process	0,00280
GO:0009737	P	response to abscisic acid stimulus	0,00360
GO:0006355	P	regulation of transcription, DNA-dependent	0,00480
GO:0051252	P	regulation of RNA metabolic process	0,00500
GO:0006351	P	transcription, DNA-dependent	0,00760
GO:0032774	P	RNA biosynthetic process	0,00760
GO:0045087	P	innate immune response	0,01300
GO:0007242	P	intracellular signaling cascade	0,01400
GO:0006519	P	cellular amino acid and derivative metabolic process	0,04100
GO:0003700	F	transcription factor activity	0,00000
GO:0005199	F	structural constituent of cell wall	0,00000
GO:0005198	F	structural molecule activity	0,00000
GO:0043169	F	cation binding	0,00000
GO:0043167	F	ion binding	0,00000
GO:0016491	F	oxidoreductase activity	0,00000
GO:0046872	F	metal ion binding	0,00000
GO:0046914	F	transition metal ion binding	0,00000
GO:0015291	F	secondary active transmembrane transporter activity	0,00000
GO:0016740	F	transferase activity	0,00008
GO:0015297	F	antiporter activity	0,00026
GO:0050660	F	FAD binding	0,00180
GO:0016829	F	lyase activity	0,00320

continued on next page

Table C.1 – continued from previous page

GO term	Ontology	Description	p-value
GO:0009055	F	electron carrier activity	0,00550
GO:0005215	F	transporter activity	0,00570
GO:0048037	F	cofactor binding	0,02700
GO:0050662	F	coenzyme binding	0,04100
GO:0019825	F	oxygen binding	0,04500
GO:0008270	F	zinc ion binding	0,04500
GO:0005634	C	nucleus	0,00000
GO:0044464	C	cell part	0,00000
GO:0005623	C	cell	0,00000
GO:0005886	C	plasma membrane	0,00016
GO:0030312	C	external encapsulating structure	0,01500
GO:0005618	C	cell wall	0,01500
GO:0044425	C	membrane part	0,03900
GO:0009505	C	plant-type cell wall	0,04600

Table C.2: Enriched GO terms from the down-regulated gene-list of the tiling array experiment. The tiling array results were post-processed with AgriGO.

GO term	Ontology	Description	p-value
GO:0010876	P	lipid localization	0,00000
GO:0006950	P	response to stress	0,00000
GO:0006869	P	lipid transport	0,00000
GO:0033036	P	macromolecule localization	0,00000
GO:0050896	P	response to stimulus	0,00001
GO:0042221	P	response to chemical stimulus	0,00026
GO:0051234	P	establishment of localization	0,02500
GO:0006810	P	transport	0,02500
GO:0051179	P	localization	0,02700
GO:0008289	F	lipid binding	0,00000
GO:0016491	F	oxidoreductase activity	0,00710
GO:0005623	C	cell	0,00320
GO:0012505	C	endomembrane system	0,00320
GO:0044464	C	cell part	0,00320

Table C.3: Enriched GO terms from the up-regulated gene-list of the RNA-Seq experiment. The RNA-Seq results were post-processed with AgriGO.

GO term	Ontology	Description	p-value
GO:0043687	P	post-translational protein modification	0,00000
GO:0050896	P	response to stimulus	0,00000
GO:0006952	P	defense response	0,00000

continued on next page

Table C.3 – continued from previous page

GO term	Ontology	Description	p-value
GO:0006950	P	response to stress	0,00000
GO:0043170	P	macromolecule metabolic process	0,00000
GO:0051707	P	response to other organism	0,00000
GO:0044260	P	cellular macromolecule metabolic process	0,00000
GO:0019538	P	protein metabolic process	0,00000
GO:0006464	P	protein modification process	0,00000
GO:0065007	P	biological regulation	0,00000
GO:0050794	P	regulation of cellular process	0,00000
GO:0043412	P	macromolecule modification	0,00000
GO:0042221	P	response to chemical stimulus	0,00000
GO:0050789	P	regulation of biological process	0,00000
GO:0044267	P	cellular protein metabolic process	0,00000
GO:0009617	P	response to bacterium	0,00000
GO:0009058	P	biosynthetic process	0,00000
GO:0044249	P	cellular biosynthetic process	0,00000
GO:0006807	P	nitrogen compound metabolic process	0,00000
GO:0045449	P	regulation of transcription	0,00000
GO:0010556	P	regulation of macromolecule biosynthetic process	0,00000
GO:0019219	P	regulation of nucleobase, nucleoside, nucleotide and nucleic acid metabolic process	0,00000
GO:0051171	P	regulation of nitrogen compound metabolic process	0,00000
GO:0009889	P	regulation of biosynthetic process	0,00000
GO:0031326	P	regulation of cellular biosynthetic process	0,00000
GO:0010468	P	regulation of gene expression	0,00000
GO:0080090	P	regulation of primary metabolic process	0,00000
GO:0060255	P	regulation of macromolecule metabolic process	0,00000
GO:0006350	P	transcription	0,00000
GO:0031323	P	regulation of cellular metabolic process	0,00000
GO:0042742	P	defense response to bacterium	0,00000
GO:0010033	P	response to organic substance	0,00000
GO:0019222	P	regulation of metabolic process	0,00000
GO:0009607	P	response to biotic stimulus	0,00000
GO:0006139	P	nucleobase, nucleoside, nucleotide and nucleic acid metabolic process	0,00000
GO:0009408	P	response to heat	0,00000
GO:0006979	P	response to oxidative stress	0,00000
GO:0034645	P	cellular macromolecule biosynthetic process	0,00000
GO:0009059	P	macromolecule biosynthetic process	0,00000
GO:0051704	P	multi-organism process	0,00000
GO:0010467	P	gene expression	0,00000
GO:0009266	P	response to temperature stimulus	0,00000
GO:0009628	P	response to abiotic stimulus	0,00000
GO:0010200	P	response to chitin	0,00001
GO:0006633	P	fatty acid biosynthetic process	0,00001

continued on next page

Table C.3 – continued from previous page

GO term	Ontology	Description	p-value
GO:0016070	P	RNA metabolic process	0,00001
GO:0016053	P	organic acid biosynthetic process	0,00002
GO:0046394	P	carboxylic acid biosynthetic process	0,00002
GO:0010035	P	response to inorganic substance	0,00002
GO:0016265	P	death	0,00002
GO:0008219	P	cell death	0,00002
GO:0009743	P	response to carbohydrate stimulus	0,00003
GO:0009611	P	response to wounding	0,00003
GO:0050832	P	defense response to fungus	0,00003
GO:0009723	P	response to ethylene stimulus	0,00003
GO:0012501	P	programmed cell death	0,00007
GO:0009620	P	response to fungus	0,00009
GO:0070887	P	cellular response to chemical stimulus	0,00024
GO:0009605	P	response to external stimulus	0,00033
GO:0006955	P	immune response	0,00042
GO:0002376	P	immune system process	0,00043
GO:0046483	P	heterocycle metabolic process	0,00044
GO:0009056	P	catabolic process	0,00053
GO:0009414	P	response to water deprivation	0,00070
GO:0065009	P	regulation of molecular function	0,00070
GO:0045087	P	innate immune response	0,00083
GO:0006796	P	phosphate metabolic process	0,00089
GO:0006793	P	phosphorus metabolic process	0,00089
GO:0009308	P	amine metabolic process	0,00110
GO:0009755	P	hormone-mediated signaling pathway	0,00120
GO:0032870	P	cellular response to hormone stimulus	0,00120
GO:0006725	P	cellular aromatic compound metabolic process	0,00120
GO:0006468	P	protein amino acid phosphorylation	0,00120
GO:0009415	P	response to water	0,00130
GO:0006790	P	sulfur metabolic process	0,00160
GO:0044106	P	cellular amine metabolic process	0,00170
GO:0006520	P	cellular amino acid metabolic process	0,00170
GO:0006631	P	fatty acid metabolic process	0,00180
GO:0042434	P	indole derivative metabolic process	0,00220
GO:0042430	P	indole and derivative metabolic process	0,00220
GO:0006575	P	cellular amino acid derivative metabolic process	0,00230
GO:0034641	P	cellular nitrogen compound metabolic process	0,00230
GO:0008610	P	lipid biosynthetic process	0,00240
GO:0051179	P	localization	0,00280
GO:0009404	P	toxin metabolic process	0,00310
GO:0009407	P	toxin catabolic process	0,00310
GO:0019438	P	aromatic compound biosynthetic process	0,00450
GO:0016310	P	phosphorylation	0,00530
GO:0042398	P	cellular amino acid derivative biosynthetic process	0,00750

continued on next page

Table C.3 – continued from previous page

GO term	Ontology	Description	p-value
GO:0032787	P	monocarboxylic acid metabolic process	0,00810
GO:0007165	P	signal transduction	0,00930
GO:0006810	P	transport	0,00960
GO:0051234	P	establishment of localization	0,01000
GO:0033554	P	cellular response to stress	0,01100
GO:0009908	P	flower development	0,03400
GO:0032501	P	multicellular organismal process	0,04300
GO:0003700	F	transcription factor activity	0,00000
GO:0016740	F	transferase activity	0,00000
GO:0016772	F	transferase activity, transferring phosphorus-containing groups	0,00000
GO:0016301	F	kinase activity	0,00000
GO:0043169	F	cation binding	0,00000
GO:0043167	F	ion binding	0,00000
GO:0046872	F	metal ion binding	0,00000
GO:0046914	F	transition metal ion binding	0,00000
GO:0016684	F	oxidoreductase activity, acting on peroxide as acceptor	0,00000
GO:0004601	F	peroxidase activity	0,00000
GO:0060089	F	molecular transducer activity	0,00000
GO:0004871	F	signal transducer activity	0,00000
GO:0016209	F	antioxidant activity	0,00000
GO:0030554	F	adenyl nucleotide binding	0,00000
GO:0001883	F	purine nucleoside binding	0,00000
GO:0001882	F	nucleoside binding	0,00000
GO:0030246	F	carbohydrate binding	0,00000
GO:0005515	F	protein binding	0,00000
GO:0017076	F	purine nucleotide binding	0,00000
GO:0016829	F	lyase activity	0,00003
GO:0016491	F	oxidoreductase activity	0,00006
GO:0019825	F	oxygen binding	0,00007
GO:0016758	F	transferase activity, transferring hexosyl groups	0,00014
GO:0004175	F	endopeptidase activity	0,00020
GO:0016765	F	transferase activity, transferring alkyl or aryl (other than methyl) groups	0,00022
GO:0003824	F	catalytic activity	0,00023
GO:0009055	F	electron carrier activity	0,00024
GO:0005524	F	ATP binding	0,00043
GO:0032559	F	adenyl ribonucleotide binding	0,00043
GO:0004888	F	transmembrane receptor activity	0,00052
GO:0004872	F	receptor activity	0,00054
GO:0050660	F	FAD binding	0,00056
GO:0016887	F	ATPase activity	0,00110
GO:0008194	F	UDP-glycosyltransferase activity	0,00160

continued on next page

Table C.3 – continued from previous page

GO term	Ontology	Description	p-value
GO:0032555	F	purine ribonucleotide binding	0,00200
GO:0032553	F	ribonucleotide binding	0,00200
GO:0020037	F	heme binding	0,00220
GO:0005529	F	sugar binding	0,00220
GO:0008270	F	zinc ion binding	0,00320
GO:0004364	F	glutathione transferase activity	0,00430
GO:0042623	F	ATPase activity, coupled	0,00920
GO:0050662	F	coenzyme binding	0,01100
GO:0015291	F	secondary active transmembrane transporter activity	0,01300
GO:0048037	F	cofactor binding	0,01400
GO:0016773	F	phosphotransferase activity, alcohol group as acceptor	0,01800
GO:0004672	F	protein kinase activity	0,02000
GO:0004091	F	carboxylesterase activity	0,02800
GO:0004721	F	phosphoprotein phosphatase activity	0,02800
GO:0005488	F	binding	0,03200
GO:0004857	F	enzyme inhibitor activity	0,04400
GO:0044464	C	cell part	0,00000
GO:0005623	C	cell	0,00000
GO:0005634	C	nucleus	0,00000
GO:0005576	C	extracellular region	0,00002
GO:0012505	C	endomembrane system	0,00029
GO:0048046	C	apoplast	0,00061
GO:0030312	C	external encapsulating structure	0,00120
GO:0005618	C	cell wall	0,00120
GO:0044425	C	membrane part	0,00240
GO:0005773	C	vacuole	0,00350
GO:0005886	C	plasma membrane	0,02300

Table C.4: Enriched GO terms from the down-regulated gene-list of the RNA-Seq experiment. The RNA-Seq results were post-processed with AgriGO.

GO term	Ontology	Description	p-value
GO:0043170	P	macromolecule metabolic process	0,00000
GO:0044260	P	cellular macromolecule metabolic process	0,00000
GO:0050896	P	response to stimulus	0,00000
GO:0009058	P	biosynthetic process	0,00000
GO:0044249	P	cellular biosynthetic process	0,00000
GO:0006139	P	nucleobase, nucleoside, nucleotide and nucleic acid metabolic process	0,00000
GO:0006807	P	nitrogen compound metabolic process	0,00000
GO:0043687	P	post-translational protein modification	0,00000

continued on next page

Table C.4 – continued from previous page

GO term	Ontology	Description	p-value
GO:0042221	P	response to chemical stimulus	0,00000
GO:0034645	P	cellular macromolecule biosynthetic process	0,00000
GO:0019538	P	protein metabolic process	0,00000
GO:0009059	P	macromolecule biosynthetic process	0,00000
GO:0065007	P	biological regulation	0,00000
GO:0051171	P	regulation of nitrogen compound metabolic process	0,00000
GO:0050794	P	regulation of cellular process	0,00000
GO:0009889	P	regulation of biosynthetic process	0,00000
GO:0031326	P	regulation of cellular biosynthetic process	0,00000
GO:0045449	P	regulation of transcription	0,00000
GO:0031323	P	regulation of cellular metabolic process	0,00000
GO:0010556	P	regulation of macromolecule biosynthetic process	0,00000
GO:0019219	P	regulation of nucleobase, nucleoside, nucleotide and nucleic acid metabolic process	0,00000
GO:0050789	P	regulation of biological process	0,00000
GO:0080090	P	regulation of primary metabolic process	0,00000
GO:0006350	P	transcription	0,00000
GO:0010467	P	gene expression	0,00000
GO:0044267	P	cellular protein metabolic process	0,00000
GO:0019222	P	regulation of metabolic process	0,00000
GO:0010033	P	response to organic substance	0,00000
GO:0010468	P	regulation of gene expression	0,00000
GO:0060255	P	regulation of macromolecule metabolic process	0,00000
GO:0006950	P	response to stress	0,00000
GO:0006810	P	transport	0,00000
GO:0009628	P	response to abiotic stimulus	0,00000
GO:0051234	P	establishment of localization	0,00000
GO:0006464	P	protein modification process	0,00000
GO:0043412	P	macromolecule modification	0,00000
GO:0051179	P	localization	0,00000
GO:0032501	P	multicellular organismal process	0,00000
GO:0010035	P	response to inorganic substance	0,00000
GO:0016070	P	RNA metabolic process	0,00000
GO:0009733	P	response to auxin stimulus	0,00000
GO:0006091	P	generation of precursor metabolites and energy	0,00000
GO:0007275	P	multicellular organismal development	0,00001
GO:0010038	P	response to metal ion	0,00001
GO:0032502	P	developmental process	0,00001
GO:0048856	P	anatomical structure development	0,00002
GO:0055085	P	transmembrane transport	0,00002
GO:0055086	P	nucleobase, nucleoside and nucleotide metabolic process	0,00003
GO:0006952	P	defense response	0,00007
GO:0022622	P	root system development	0,00016

continued on next page

Table C.4 – continued from previous page

GO term	Ontology	Description	p-value
GO:0048364	P	root development	0,00016
GO:0044265	P	cellular macromolecule catabolic process	0,00029
GO:0030154	P	cell differentiation	0,00032
GO:0048869	P	cellular developmental process	0,00032
GO:0009653	P	anatomical structure morphogenesis	0,00120
GO:0046483	P	heterocycle metabolic process	0,00140
GO:0044262	P	cellular carbohydrate metabolic process	0,00170
GO:0030001	P	metal ion transport	0,00180
GO:0009605	P	response to external stimulus	0,00210
GO:0006412	P	translation	0,00210
GO:0006811	P	ion transport	0,00210
GO:0009639	P	response to red or far red light	0,00620
GO:0048519	P	negative regulation of biological process	0,00640
GO:0009725	P	response to hormone stimulus	0,00760
GO:0006812	P	cation transport	0,00840
GO:0033036	P	macromolecule localization	0,00840
GO:0051707	P	response to other organism	0,01100
GO:0009719	P	response to endogenous stimulus	0,01600
GO:0009056	P	catabolic process	0,04000
GO:0003700	F	transcription factor activity	0,00000
GO:0016740	F	transferase activity	0,00002
GO:0016301	F	kinase activity	0,00030
GO:0004713	F	protein tyrosine kinase activity	0,00041
GO:0016772	F	transferase activity, transferring phosphorus-containing groups	0,00041
GO:0046872	F	metal ion binding	0,00042
GO:0043167	F	ion binding	0,00042
GO:0043169	F	cation binding	0,00042
GO:0005215	F	transporter activity	0,00150
GO:0005198	F	structural molecule activity	0,00440
GO:0046914	F	transition metal ion binding	0,00570
GO:0016491	F	oxidoreductase activity	0,00650
GO:0030554	F	adenyl nucleotide binding	0,00760
GO:0001883	F	purine nucleoside binding	0,00760
GO:0001882	F	nucleoside binding	0,00760
GO:0016887	F	ATPase activity	0,00790
GO:0016829	F	lyase activity	0,00890
GO:0060089	F	molecular transducer activity	0,01200
GO:0004871	F	signal transducer activity	0,01200
GO:0005524	F	ATP binding	0,01500
GO:0032559	F	adenyl ribonucleotide binding	0,01500
GO:0008270	F	zinc ion binding	0,02500
GO:0017076	F	purine nucleotide binding	0,04900
GO:0005634	C	nucleus	0,00000

continued on next page

Table C.4 – continued from previous page

GO term	Ontology	Description	p-value
GO:0044425	C	membrane part	0,00003
GO:0044464	C	cell part	0,00003
GO:0005623	C	cell	0,00003
GO:0044422	C	organelle part	0,00010
GO:0044446	C	intracellular organelle part	0,00010
GO:0022626	C	cytosolic ribosome	0,00440
GO:0044445	C	cytosolic part	0,00480
GO:0033279	C	ribosomal subunit	0,02500
GO:0032991	C	macromolecular complex	0,03400

Table C.5: Transposable elements showing altered transcript levels in *prl1* according to the tiling array (based on TAIR7) and RNA-Seq (based on TAIR9) analyses.

AGI Code	log FC	p-value	Description
Tiling analysis			
AT3G42658	2,72	0,0015	Member of Sadhu non-coding retrotransposon family. In some natural accessions the allele is methylated and silenced.
AT1G43590	1,25	0,0348	transposable element gene; similar to unknown protein [Arabidopsis thaliana] (TAIR:AT5G34838.1); similar to hypothetical protein 24.t00017 [Brassica oleracea] (GB:ABD64939.1); contains InterPro domain Protein of unknown function DUF635; (InterPro:IPR006912)
AT4G06637	-0,99	0,0325	transposable element gene; similar to unknown protein [Arabidopsis thaliana] (TAIR:AT4G07523.1); similar to unknown protein [Arabidopsis thaliana] (TAIR:AT5G27180.1)
AT4G06505	-1,03	0,0364	transposable element gene; pseudogene, hypothetical protein
AT5G36860	-1,05	0,0483	transposable element gene; similar to Ulp1 protease family protein [Arabidopsis thaliana] (TAIR:AT2G14770.2); similar to Ulp1 protease family protein [Arabidopsis thaliana] (TAIR:AT1G27780.1); similar to Ulp1 protease family protein [Arabidopsis thaliana] (TAIR:AT1G25886.1); similar to Ulp1 protease family protein [Brassica oleracea] (GB:ABD64941.1); contains InterPro domain Peptidase C48, SUMO/Sentrin/Ubl1; (InterPro:IPR003653)
AT4G06607	-1,08	0,0147	transposable element gene; pseudogene, hypothetical protein

continued on next page

Table C.5 – continued from previous page

AGI Code	log FC	p-value	Description
AT2G04770	-1,19	0,0454	transposable element gene; CACTA-like transposase family (Ptta/En/Spm), has a 6.0e-20 P-value blast match to At5g29026.1/8-244 CACTA-like transposase family (Ptta/En/Spm) (CACTA-element) (Arabidopsis thaliana)
AT4G06511	-1,22	0,0299	transposable element gene; pseudogene, hypothetical protein
AT4G06507	-1,22	0,0433	transposable element gene; pseudogene, hypothetical protein
AT5G32473	-1,24	0,0083	transposable element gene; pseudogene, hypothetical protein
AT3G30767	-1,38	0,0449	transposable element gene; CACTA-like transposase family (Ptta/En/Spm), has a 8.3e-46 P-value blast match to At5g29026.1/8-244 CACTA-like transposase family (Ptta/En/Spm) (CACTA-element) (Arabidopsis thaliana)
RNA-Seq analysis			
AT4G20365	4,08	$6,66 \times 10^{-016}$	transposable element gene; copia-like retrotransposon family, has a 1.7e-254 P-value blast match to dbj BAA78425.1 polyprotein (Arabidopsis thaliana) (AtRE1) (Ty1_Copia-element)
AT2G03540	2,3	0	transposable element gene; similar to unknown protein [Arabidopsis thaliana] (TAIR:AT4G11710.1); similar to hypothetical protein 23.t00046 [Brassica oleracea] (GB:ABD65629.1); contains domain REVERSE TRANSCRIPTASES (PTHR19446); contains domain gb def: Hypothetical protein At2g15600 (PTHR19446:SF12)
AT3G17050	1,88	$3,75 \times 10^{-013}$	transposable element gene; pseudogene, glycine-rich protein, similar to glycine-rich protein TIGR:At1g53620.1 (Arabidopsis thaliana)
AT1G65485	1,85	0	transposable element gene; pseudogene, similar to SAE1-S9-protein, blastp match of 45% identity and 1.4e-12 P-value to GP 4760708 dbj BAA77394.1 AB012866 SAE1-S9-protein {Brassica rapa}
AT4G04410	1,47	$2,29 \times 10^{-006}$	transposable element gene; copia-like retrotransposon family, has a 1.7e-176 P-value blast match to dbj BAA78426.1 polyprotein (AtRE2-1) (Arabidopsis thaliana) (Ty1_Copia-element)
AT3G62455	1,14	0	transposable element gene; copia-like retrotransposon family, has a 7.1e-232 P-value blast match to gb AAO73529.1 gag-pol polyprotein (Glycine max) (SIRE1) (Ty1_Copia-family)

continued on next page

Table C.5 – continued from previous page

AGI Code	log FC	p-value	Description
AT2G12490	-1,06	0,01	transposable element gene; copia-like retrotransposon family, has a 0. P-value blast match to GB:CAA31653 polyprotein (Ty1_Copia-element) (Arabidopsis thaliana)
AT4G02960	-1,18	$8,77 \times 10^{-006}$	ATRE2: a copia-type retrotransposon element containing LTRs and encoding a polyprotein. This retro element exists in two loci in Landsberg erecta but only once in Columbia
AT2G04460	-1,19	0	transposable element gene; similar to unknown protein [Arabidopsis thaliana] (TAIR:AT2G10090.1); similar to pol polyprotein [Citrus x paradisi] (GB:AAK70407.1)
AT4G16020	-1,2	0,01	transposable element gene; copia-like retrotransposon family, has a $1.3e-221$ P-value blast match to GB:BAA78423 polyprotein (Ty1_Copia-element) (Arabidopsis thaliana)GB:BAA78423 polyprotein (Ty1_Copia-element) (Arabidopsis thaliana)GB:BAA78423 polyprotein (Ty1_Copia-element) (Arabidopsis thaliana)gi 4996361 dbj BAA78423.1 polyprotein (Arabidopsis thaliana) (Ty1_Copia-element)
AT2G16140	-1,6	0,01	transposable element gene; similar to DNA binding [Arabidopsis thaliana] (TAIR:AT3G47680.1); similar to hypothetical protein 24.t00018 [Brassica oleracea] (GB:ABD64940.1); contains InterPro domain Homeodomain-like; (InterPro:IPR009057)
AT5G34800	-3,1	$1,94 \times 10^{-005}$	transposable element gene; pseudogene, hypothetical protein, predicted proteins - Arabidopsis thaliana

Table C.6: Up-regulated genes in *prl1* from the tiling array analysis. The fold change (FC) cut-off is 1,5 and p-value<0,05.

AGI code	FC	p-value	Gene description
AT2G30750	19,03	0,02	CYP71A12 (CYTOCHROME P450, FAMILY 71, SUBFAMILY A, POLYPEPTIDE 12); oxygen binding
AT1G26390	15,23	0,03	FAD-binding domain-containing protein
AT1G26380	13,8	0,03	FAD-binding domain-containing protein
AT1G26410	8,63	0,03	FAD-binding domain-containing protein
AT5G38900	8,5	0,02	DSBA oxidoreductase family protein
AT5G53870	7,56	0	plastocyanin-like domain-containing protein
AT1G15125	7,18	0	S-adenosylmethionine-dependent methyltransferase
AT3G33000	6,68	0	
AT3G42658	6,58	0	
AT2G43570	6,49	0	chitinase, putative
AT3G22800	6,47	0,01	leucine-rich repeat family protein / extensin family protein
AT3G13950	6,44	0,03	similar to unknown protein [Arabidopsis thaliana] (TAIR:AT4G13266.1); similar to Ankyrin [Medicago truncatula] (GB:ABN08906.1)
AT5G25350	6,22	0,01	EBF2 (EIN3-BINDING F BOX PROTEIN 2)
AT4G24570	5,83	0	mitochondrial substrate carrier family protein
AT1G26420	5,42	0,04	FAD-binding domain-containing protein
AT3G29762	5,27	0,03	
AT2G22510	5,2	0,02	hydroxyproline-rich glycoprotein family protein
AT3G56590	5,04	0	hydroxyproline-rich glycoprotein family protein
AT1G36622	4,94	0,03	similar to unknown protein [Arabidopsis thaliana] (TAIR:AT1G36640.1)
AT1G18970	4,85	0,01	GLP4 (GERMIN-LIKE PROTEIN 4); manganese ion binding / metal ion binding / nutrient reservoir
AT5G57510	4,84	0,02	unknown protein
AT1G30160	4,57	0	similar to unknown protein [Arabidopsis thaliana] (TAIR:AT1G05540.1); contains InterPro domain Protein of unknown function DUF295 (InterPro:IPR005174)
AT5G15780	4,56	0	pollen Ole e 1 allergen and extensin family protein
AT2G45220	4,56	0,04	pectinesterase family protein
AT3G08860	4,5	0,03	alanine-glyoxylate aminotransferase, putative / beta-alanine-pyruvate aminotransferase, putative / AGT, putative
AT2G25490	4,42	0,01	EBF1 (EIN3-BINDING F BOX PROTEIN 1); ubiquitin-protein ligase
AT4G23700	4,31	0,04	ATCHX17 (CATION/H+ EXCHANGER 17); monovalent cation:proton antiporter
AT1G52890	4,23	0,03	ANAC019 (Arabidopsis NAC domain containing protein 19); transcription factor
AT3G44260	4,23	0,01	CCR4-NOT transcription complex protein, putative
AT2G27550	4,15	0	ATC (ARABIDOPSIS THALIANA CENTRORADIALIS); phosphatidylethanolamine binding
AT2G15220	4,08	0,01	secretory protein, putative
AT2G38470	4,05	0,03	WRKY33 (WRKY DNA-binding protein 33); transcription factor
AT5G64050	3,9	0	ATERS/ERS/OVA3 (OVULE ABORTION 3); glutamate-tRNA ligase
AT3G07330	3,81	0	ATCSLC06 (Cellulose synthase-like C6); transferase, transferring glycosyl groups
AT4G08770	3,77	0,03	peroxidase, putative
AT1G02930	3,71	0,02	ATGSTF6 (EARLY RESPONSIVE TO DEHYDRATION 11); glutathione transferase
AT4G16260	3,7	0,02	glycosyl hydrolase family 17 protein
AT5G25190	3,65	0	ethylene-responsive element-binding protein, putative

continued on next page

Table C.6 – continued from previous page

AGI code	FC	p-value	Gene description
AT5G13080	3,64	0,03	WRKY75 (WRKY DNA-BINDING PROTEIN 75); transcription factor
AT4G17490	3,62	0	ATERF6 (ETHYLENE RESPONSIVE ELEMENT BINDING FACTOR 6); DNA binding / transcription factor
AT5G60250	3,54	0	zinc finger (C3HC4-type RING finger) family protein
AT1G07135	3,51	0,02	glycine-rich protein
AT3G29000	3,5	0,03	calcium-binding EF hand family protein
AT5G25757	3,49	0	similar to unknown protein [Arabidopsis thaliana] (TAIR:AT5G25754.1); similar to predicted protein [Physcomitrella patens subsp. patens] (GB:EDQ51676.1); similar to unknown protein [Oryza sativa (japonica cultivar-group)] (GB:AAT77307.1); similar to predicted protein [Physcomitrella patens subsp. patens] (GB:EDQ58057.1); contains domain TPR-like (SSF48452); contains domain EUKARYOTIC TRANSLATION INITIATION FACTOR 3 (PTHR13242)
AT4G26750	3,49	0,01	hydroxyproline-rich glycoprotein family protein
AT1G02770	3,44	0,01	similar to unknown protein [Arabidopsis thaliana] (TAIR:AT1G19060.1); contains InterPro domain Protein of unknown function DUF626, Arabidopsis thaliana (InterPro:IPR006462)
AT2G38860	3,39	0,04	YLS5 (yellow-leaf-specific gene 5)
AT5G25100	3,37	0	endomembrane protein 70, putative
AT1G73220	3,36	0,04	ATOCT1 (ARABIDOPSIS THALIANA ORGANIC CATION/CARNITINE TRANSPORTER1); carbohydrate transmembrane transporter/ carnitine transporter/ transporter
AT3G55980	3,35	0,01	zinc finger (CCCH-type) family protein
AT3G28340	3,35	0,02	GATL10 (Galacturonosyltransferase-like 10); polygalacturonate 4-alpha-galacturonosyltransferase/ transferase, transferring hexosyl groups
AT3G56400	3,33	0,03	WRKY70 (WRKY DNA-binding protein 70); transcription factor
AT1G76930	3,32	0,03	AEXT4 (EXTENSIN 4)
AT1G02220	3,31	0,04	ANAC003 (Arabidopsis NAC domain containing protein 3); transcription factor
AT1G09020	3,29	0	SNF4 (Sucrose NonFermenting 4)
AT3G10930	3,28	0,03	similar to unknown protein [Arabidopsis thaliana] (TAIR:AT5G05300.1)
AT4G11650	3,26	0,01	ATOSM34 (OSMOTIN 34)
AT2G46750	3,19	0,03	FAD-binding domain-containing protein
AT5G47220	3,16	0,01	ATERF-2/ATERF2/ERF2 (ETHYLENE RESPONSE FACTOR 2); DNA binding / transcription activator/ transcription factor
AT5G24770	3,14	0,04	VSP2 (VEGETATIVE STORAGE PROTEIN 2); acid phosphatase
AT1G80840	3,12	0,02	WRKY40 (WRKY DNA-binding protein 40); transcription factor
AT3G12500	3,11	0	ATHCHIB (BASIC CHITINASE); chitinase
AT4G03292	3,09	0,01	nucleic acid binding
AT1G47510	3,04	0,02	endonuclease/exonuclease/phosphatase family protein
AT5G51190	3,04	0,01	AP2 domain-containing transcription factor, putative
AT1G02920	3,03	0,01	ATGSTF7 (GLUTATHIONE S-TRANSFERASE 11); glutathione transferase
AT2G15790	3,01	0,01	SQN (SQUINT)
AT2G39650	3	0,02	similar to unknown protein [Arabidopsis thaliana] (TAIR:AT4G14620.1); similar to unnamed protein product [Vitis vinifera] (GB:CAO69213.1); contains InterPro domain Protein of unknown function DUF506, plant (InterPro:IPR006502)
AT1G29400	3	0,01	AML5 (ARABIDOPSIS MEI2-LIKE PROTEIN 5); RNA binding
AT2G43510	3	0,02	ATT11 (ARABIDOPSIS THALIANA TRYPSIN INHIBITOR PROTEIN 1)
AT1G27730	2,99	0,01	STZ (SALT TOLERANCE ZINC FINGER); nucleic acid binding / transcription factor/ zinc ion binding
AT2G29350	2,96	0,04	SAG13 (Senescence-associated gene 13); oxidoreductase
AT3G04720	2,95	0,01	PR4 (PATHOGENESIS-RELATED 4)
AT1G74590	2,92	0,02	ATGSTU10 (Arabidopsis thaliana Glutathione S-transferase (class tau) 10); glutathione transferase

continued on next page

Table C.6 – continued from previous page

AGI code	FC	p-value	Gene description
AT3G19660	2,89	0,04	similar to unnamed protein product [<i>Vitis vinifera</i>] (GB:CAO49873.1)
AT2G15390	2,88	0,03	FUT4 (fucosyltransferase 4); fucosyltransferase/ transferase, transferring glycosyl groups
AT3G03530	2,87	0,03	NPC4 (NONSPECIFIC PHOSPHOLIPASE C4); hydrolase, acting on ester bonds
AT1G65690	2,86	0,03	harpin-induced protein-related / HIN1-related / harpin-responsive protein-related
AT2G27660	2,85	0,04	DC1 domain-containing protein
AT2G04050	2,83	0,03	MATE efflux family protein
AT3G25655	2,82	0,02	unknown protein
AT3G14840	2,76	0,02	leucine-rich repeat family protein / protein kinase family protein
AT4G19810	2,75	0,04	glycosyl hydrolase family 18 protein
AT1G22910	2,75	0,01	RNA recognition motif (RRM)-containing protein
AT1G67810	2,74	0,01	Fe-S metabolism associated domain-containing protein
AT1G36060	2,73	0,03	AP2 domain-containing transcription factor, putative
AT4G19370	2,72	0,04	similar to unknown protein [<i>Arabidopsis thaliana</i>] (TAIR:AT1G31720.1); similar to unknown [<i>Picea sitchensis</i>] (GB:ABK21519.1); similar to Os02g0703300 [<i>Oryza sativa</i> (japonica cultivar-group)] (GB:NP_001047854.1); contains InterPro domain Protein of unknown function DUF1218 (InterPro:IPR009606)
AT1G18980	2,72	0,03	germin-like protein, putative
AT2G24980	2,7	0,01	proline-rich extensin-like family protein
AT1G26250	2,7	0,03	proline-rich extensin, putative
AT4G08400	2,69	0,04	proline-rich extensin-like family protein
AT1G15530	2,69	0,01	receptor lectin kinase, putative
AT4G11280	2,69	0,01	ACS6 (1-AMINOCYCLOPROPANE-1-CARBOXYLIC ACID (ACC) SYNTHASE 6)
AT1G72920	2,68	0,02	disease resistance protein (TIR-NBS class), putative
AT5G24090	2,67	0,03	acidic endochitinase (CHIB1)
AT3G49620	2,66	0,04	DIN11 (DARK INDUCIBLE 11); oxidoreductase
AT1G67980	2,65	0,04	CCoAMT (caffeoyl-CoA 3-O-methyltransferase)
AT1G17020	2,64	0,03	SRG1 (SENESCENCE-RELATED GENE 1); oxidoreductase, acting on paired donors, with incorporation or reduction of molecular oxygen, 2-oxoglutarate as one donor, and incorporation of one atom each of oxygen into both donors
AT5G43890	2,63	0,02	SUPER1/YUCCA5 (SUPPRESSOR OF ER1); monooxygenase
AT2G12905	2,63	0,03	similar to ORF54b [<i>Pinus thunbergii</i>] (GB:NP_042462.1)
AT2G26530	2,63	0,01	AR781
AT1G17745	2,62	0,01	PGDH (3-PHOSPHOGLYCERATE DEHYDROGENASE); phosphoglycerate dehydrogenase
AT3G27940	2,62	0,01	LBD26 (LOB DOMAIN-CONTAINING PROTEIN 26)
AT2G43150	2,6	0,01	proline-rich extensin-like family protein
AT2G41480	2,58	0,02	peroxidase
AT4G08230	2,57	0,02	glycine-rich protein
AT3G22550	2,57	0,02	senescence-associated protein-related
AT5G67310	2,55	0,04	CYP81G1 (cytochrome P450, family 81, subfamily G, polypeptide 1); oxygen binding
AT5G14540	2,54	0,01	proline-rich family protein
AT5G49280	2,54	0,02	hydroxyproline-rich glycoprotein family protein
AT3G33528	2,51	0,01	similar to unknown protein [<i>Arabidopsis thaliana</i>] (TAIR:AT4G07526.3); similar to unknown protein [<i>Arabidopsis thaliana</i>] (TAIR:AT4G07526.2); similar to unknown protein [<i>Arabidopsis thaliana</i>] (TAIR:AT4G07526.1)
AT4G33050	2,5	0,04	EDA39 (embryo sac development arrest 39); calmodulin binding

continued on next page

Table C.6 – continued from previous page

AGI code	FC	p-value	Gene description
AT5G27420	2,49	0,02	zinc finger (C3HC4-type RING finger) family protein
AT2G22500	2,48	0,03	mitochondrial substrate carrier family protein
AT3G58270	2,45	0,04	meprin and TRAF homology domain-containing protein / MATH domain-containing protein
AT2G22880	2,45	0,01	VQ motif-containing protein
AT5G47230	2,44	0,04	ERF5 (ETHYLENE RESPONSIVE ELEMENT BINDING FACTOR 5); DNA binding / transcription activator/ transcription factor
AT1G76650	2,42	0,01	CML38; calcium ion binding
AT5G38910	2,42	0,04	germin-like protein, putative
AT1G28370	2,41	0	ATERF11/ERF11 (ERF domain protein 11); DNA binding / transcription factor/ transcription repressor
AT1G35910	2,4	0,02	trehalose-6-phosphate phosphatase, putative
AT4G24780	2,39	0,01	pectate lyase family protein
AT4G37370	2,39	0,04	CYP81D8 (cytochrome P450, family 81, subfamily D, polypeptide 8); oxygen binding
AT1G43590	2,38	0,03	
AT3G55890	2,37	0,01	yippee family protein
AT1G14870	2,37	0,02	Identical to Uncharacterized protein At1g14870 [Arabidopsis thaliana] (GB:Q9LQU4); similar to unknown protein [Arabidopsis thaliana] (TAIR:AT5G35525.1); similar to unnamed protein product [Vitis vinifera] (GB:CAO42338.1); contains InterPro domain Aspartic acid and asparagine hydroxylation site (InterPro:IPR000152); contains InterPro domain Protein of unknown function Cys-rich (InterPro:IPR006461)
AT4G29780	2,36	0,04	similar to unknown protein [Arabidopsis thaliana] (TAIR:AT5G12010.1); similar to unnamed protein product [Vitis vinifera] (GB:CAO43835.1); contains domain PTHR22930 (PTHR22930)
AT3G52400	2,35	0,04	SYP122 (syntaxin 122); SNAP receptor
AT2G34600	2,35	0,03	JAZ7/TIFY5B (JASMONATE-ZIM-DOMAIN PROTEIN 7)
AT5G25754	2,33	0,01	similar to unknown protein [Arabidopsis thaliana] (TAIR:AT5G25757.1); similar to predicted protein [Physcomitrella patens subsp. patens] (GB:EDQ51676.1); similar to unknown protein [Oryza sativa (japonica cultivar-group)] (GB:AAT77307.1); similar to predicted protein [Physcomitrella patens subsp. patens] (GB:EDQ58057.1); contains domain TPR-like (SSF48452); contains domain EUKARYOTIC TRANSLATION INITIATION FACTOR 3 (PTHR13242)
AT2G27690	2,33	0,02	CYP94C1 (cytochrome P450, family 94, subfamily C, polypeptide 1); oxygen binding
AT5G24060	2,32	0,01	similar to binding [Arabidopsis thaliana] (TAIR:AT3G49140.1); similar to hypothetical protein OsJ_032866 [Oryza sativa (japonica cultivar-group)] (GB:EAZ18657.1); contains domain PENTATRICOPEPTIDE REPEAT-CONTAINING PROTEIN (PTHR10483); contains domain SELENIUM-BINDING PROTEIN (PTHR10483-SF4)
AT5G53990	2,32	0,03	glycosyltransferase family protein
AT4G30460	2,32	0,01	glycine-rich protein
AT5G55560	2,32	0,01	protein kinase family protein
AT2G40140	2,31	0,02	CZF1/ZFAR1; transcription factor
AT5G17700	2,3	0,01	MATE efflux family protein
AT3G08670	2,3	0,01	similar to unknown protein [Arabidopsis thaliana] (TAIR:AT3G51540.1); similar to hypothetical protein [Vitis vinifera] (GB:CAN71240.1)
AT3G61820	2,29	0,01	aspartyl protease family protein
AT5G53590	2,29	0,03	auxin-responsive family protein
AT1G23720	2,29	0,03	proline-rich extensin-like family protein
AT5G06630	2,28	0,04	proline-rich extensin-like family protein
AT4G27280	2,26	0,03	calcium-binding EF hand family protein
AT3G04420	2,25	0,03	ANAC048 (Arabidopsis NAC domain containing protein 48); transcription factor
AT1G06350	2,25	0,01	fatty acid desaturase family protein
AT3G54950	2,25	0,02	PLA IIIA/PLP7 (Patatin-like protein 7)
AT3G61190	2,23	0,02	BAP1 (BON ASSOCIATION PROTEIN 1)

continued on next page

Table C.6 – continued from previous page

AGI code	FC	p-value	Gene description
AT1G28190	2,22	0,04	similar to unknown protein [Arabidopsis thaliana] (TAIR:AT5G12340.1); similar to unknown [Picea sitchensis] (GB:ABK21062.1)
AT2G32830	2,22	0,03	PHT5 (phosphate transporter 5); inorganic phosphate transmembrane transporter/ phosphate transmembrane transporter
AT2G16480	2,22	0,03	SWIB complex BAF60b domain-containing protein / plus-3 domain-containing protein
AT2G39710	2,21	0,04	aspartyl protease family protein
AT1G03220	2,21	0,01	extracellular dermal glycoprotein, putative / EDGP, putative
AT5G47960	2,2	0,02	SMG1 (SMALL MOLECULAR WEIGHT G-PROTEIN 1); GTP binding
AT3G21780	2,19	0,03	UGT71B6 (UDP-glucosyl transferase 71B6); UDP-glycosyltransferase/ abscisic acid glucosyltransferase/ transferase, transferring glycosyl groups
AT5G40450	2,19	0,02	similar to unknown protein [Arabidopsis thaliana] (TAIR:AT3G28770.1); similar to hypothetical protein Kpo1_1058p4 [Vanderwaltozyma polyspora DSM 70294] (GB:XP_001645325.1)
AT2G40920	2,18	0,01	F-box family protein
AT1G25400	2,17	0,03	similar to unknown protein [Arabidopsis thaliana] (TAIR:AT1G68440.1); similar to unnamed protein product [Vitis vinifera] (GB:CAO42150.1)
AT3G28550	2,16	0,01	proline-rich extensin-like family protein
AT2G30020	2,16	0,01	protein phosphatase 2C, putative / PP2C, putative
AT4G30290	2,15	0,03	ATXTH19 (XYLOGLUCAN ENDOTRANSGLUCOSYLASE/HYDROLASE 19); hydrolase, acting on glycosyl bonds
AT3G15720	2,15	0,01	glycoside hydrolase family 28 protein / polygalacturonase (pectinase) family protein
AT3G46090	2,14	0,03	ZAT7; nucleic acid binding / transcription factor/ zinc ion binding
AT3G23570	2,14	0,04	dienelactone hydrolase family protein
AT1G42990	2,13	0,03	ATBZIP60 (BASIC REGION/LEUCINE ZIPPER MOTIF 60); DNA binding / transcription factor
AT3G54590	2,13	0,01	ATHRGP1; structural constituent of cell wall
AT3G20470	2,1	0,04	
AT1G48260	2,1	0,03	CIPK17 (SNF1-RELATED PROTEIN KINASE 3.21); kinase
AT1G01670	2,08	0,01	U-box domain-containing protein
AT5G45840	2,08	0,02	leucine-rich repeat transmembrane protein kinase, putative
AT4G01720	2,07	0,03	WRKY47 (WRKY DNA-binding protein 47); transcription factor
AT5G67080	2,07	0,02	MAPKKK19 (Mitogen-activated protein kinase kinase kinase 19); kinase
AT5G06390	2,06	0,01	FLA17 (FASCICLIN-LIKE ARABINOGALACTAN PROTEIN 17 PRECURSOR)
AT4G29140	2,06	0,03	MATE efflux protein-related
AT1G60110	2,06	0,04	jacalin lectin family protein
AT5G63580	2,06	0,04	flavonol synthase, putative
AT1G33470	2,06	0,03	RNA recognition motif (RRM)-containing protein
AT1G04140	2,05	0,04	transducin family protein / WD-40 repeat family protein
AT3G19540	2,05	0,01	similar to unknown protein [Arabidopsis thaliana] (TAIR:AT1G49840.1); similar to unnamed protein product [Vitis vinifera] (GB:CAO70870.1); similar to hypothetical protein [Vitis vinifera] (GB:CAN68554.1); contains InterPro domain Protein of unknown function DUF620 (InterPro:IPR006873)
AT2G15080	2,04	0,03	disease resistance family protein
AT1G20510	2,04	0,04	OPCL1 (OPC-8:0 COA LIGASE1); 4-coumarate-CoA ligase
AT1G43910	2,04	0,03	AAA-type ATPase family protein
AT4G34740	2,04	0,01	ATASE2/ATD2 (GLN PHOSPHORIBOSYL PYROPHOSPHATE AMIDOTRANSFERASE 2); amidophosphoribosyltransferase
AT2G24580	2,04	0,02	sarcosine oxidase family protein
AT3G50340	2,04	0,01	similar to unknown protein [Arabidopsis thaliana] (TAIR:AT5G67020.1); similar to unknown protein [Oryza sativa (japonica cultivar-group)] (GB:BAD09363.1)
AT3G05690	2,03	0,02	ATHAP2B/HAP2B/UNE8 (HEME ACTIVATOR PROTEIN (YEAST) HOMOLOG 2B); transcription factor
AT4G38630	2,02	0,04	RPN10 (REGULATORY PARTICLE NON-ATPASE 10)

continued on next page

Table C.6 – continued from previous page

AGI code	FC	p-value	Gene description
AT5G26030	2,01	0,02	ferrochelatase
AT3G62680	2,01	0,03	PRP3 (PROLINE-RICH PROTEIN 3); structural constituent of cell wall
AT1G07620	2	0,04	similar to unknown protein [Arabidopsis thaliana] (TAIR:AT5G02390.1); similar to hypothetical protein [Vitis vinifera] (GB:CAN60159.1); contains InterPro domain GTP-binding protein Obg/CgtA (InterPro:IPR014100)
AT5G42650	2	0,04	AOS (ALLENE OXIDE SYNTHASE); hydro-lyase/ oxygen binding
AT3G62260	1,99	0,02	protein phosphatase 2C, putative / PP2C, putative
AT5G54730	1,99	0,03	AtATG18f (Arabidopsis thaliana homolog of yeast autophagy 18 (ATG18) f)
AT5G58860	1,99	0,02	CYP86A1 (cytochrome P450, family 86, subfamily A, polypeptide 1); oxygen binding
AT2G21060	1,99	0,03	ATGRP2B (GLYCINE-RICH PROTEIN 2B); nucleic acid binding
AT1G68620	1,98	0,04	hydrolase
AT5G54720	1,98	0,03	ankyrin repeat family protein
AT3G33004	1,98	0,03	
AT3G11910	1,98	0,03	ubiquitin-specific protease, putative
AT5G11000	1,98	0,02	similar to unknown protein [Arabidopsis thaliana] (TAIR:AT2G25200.1); similar to hypothetical protein [Vitis vinifera] (GB:CAN69699.1); contains InterPro domain Protein of unknown function DUF868, plant (InterPro:IPR008586)
AT4G38710	1,98	0,03	glycine-rich protein
AT5G64660	1,98	0,02	U-box domain-containing protein
AT3G27473	1,98	0,03	DC1 domain-containing protein
AT2G19580	1,98	0,02	TET2 (TETRASPANIN2)
AT5G02770	1,97	0,02	similar to unnamed protein product [Vitis vinifera] (GB:CAO18065.1)
AT1G62262	1,97	0,04	SLAH4 (SLAC1 HOMOLOGUE 4)
AT1G72830	1,97	0,03	HAP2C (Heme activator protein (yeast) homolog 2C); transcription factor
AT2G16570	1,97	0,02	ATASE (GLN PHOSPHORIBOSYL PYROPHOSPHATE AMIDOTRANSFERASE 1); amidophosphoribosyltransferase
AT2G19570	1,96	0,03	CDA1 (CYTIDINE DEAMINASE 1)
AT2G33550	1,96	0,02	gt-2-related
AT3G23240	1,96	0,02	ATERF1/ERF1 (ETHYLENE RESPONSE FACTOR 1); DNA binding / transcription activator/ transcription factor
AT1G54710	1,95	0,04	AtATG18h (Arabidopsis thaliana homolog of yeast autophagy 18 (ATG18) h)
AT1G69480	1,94	0,03	EXS family protein / ERD1/XPR1/SYG1 family protein
AT3G18770	1,94	0,02	similar to unknown protein [Arabidopsis thaliana] (TAIR:AT3G49590.1); similar to unknown protein [Arabidopsis thaliana] (TAIR:AT3G49590.2); similar to unnamed protein product [Vitis vinifera] (GB:CAO46479.1)
AT5G06640	1,94	0,01	proline-rich extensin-like family protein
AT4G34480	1,94	0,01	glycosyl hydrolase family 17 protein
AT1G32960	1,93	0,03	ATSBT3.3; subtilase
AT3G11580	1,93	0,03	DNA-binding protein, putative
AT5G45650	1,92	0,01	subtilase family protein
AT1G30170	1,92	0,04	similar to unknown protein [Arabidopsis thaliana] (TAIR:AT1G30160.2); contains InterPro domain Protein of unknown function DUF295 (InterPro:IPR005174)
AT5G66100	1,92	0,03	La domain-containing protein
AT1G28230	1,92	0,04	PUP1 (PURINE PERMEASE 1); purine transmembrane transporter
AT1G67870	1,92	0,02	glycine-rich protein
AT5G59550	1,92	0,01	zinc finger (C3HC4-type RING finger) family protein
AT1G73500	1,91	0,03	ATMKK9 (Arabidopsis thaliana MAP kinase kinase 9); kinase

continued on next page

Table C.6 – continued from previous page

AGI code	FC	p-value	Gene description
AT5G27840	1,91	0,03	TOPP8 (Type one serine/threonine protein phosphatase 8); protein serine/threonine phosphatase
AT3G33002	1,91	0,02	
AT2G42840	1,91	0,04	PDF1 (PROTODERMAL FACTOR 1)
AT1G10950	1,9	0,03	endomembrane protein 70, putative
AT5G64550	1,9	0,02	loricrin-related
AT2G33435	1,9	0,01	RNA recognition motif (RRM)-containing protein
AT1G20840	1,9	0,04	TMT1 (TONOPLAST MONOSACCHARIDE TRANSPORTER1); carbohydrate transmembrane transporter/ nucleoside transmembrane transporter/ sugar:hydrogen ion symporter
AT1G15130	1,89	0,03	hydroxyproline-rich glycoprotein family protein
AT4G30850	1,89	0,02	HHP2 (HEPTAHELICAL TRANSMEMBRANE PROTEIN2)
AT2G37040	1,88	0,03	PAL1 (PHE AMMONIA LYASE 1); phenylalanine ammonia-lyase
AT3G50740	1,88	0,02	UGT72E1 (UDP-glucosyl transferase 72E1); UDP-glycosyltransferase/ coniferyl-alcohol glucosyltransferase/ transferase, transferring glycosyl groups
AT2G01690	1,88	0,04	binding
AT1G69310	1,88	0,03	WRKY57 (WRKY DNA-binding protein 57); transcription factor
AT3G47600	1,87	0,02	MYB94 (myb domain protein 94); DNA binding / transcription factor
AT2G16250	1,87	0,02	leucine-rich repeat transmembrane protein kinase, putative
AT4G13390	1,87	0,03	proline-rich extensin-like family protein
AT3G14700	1,87	0,02	similar to SART-1 family protein [Arabidopsis thaliana] (TAIR:AT5G16780.1); similar to hypothetical protein OsJ_006675 [Oryza sativa (japonica cultivar-group)] (GB:EAZ23192.1); similar to Os02g0511500 [Oryza sativa (japonica cultivar-group)] (GB:NP_001046936.1); similar to hypothetical protein OsI_007241 [Oryza sativa (indica cultivar-group)] (GB:EAY86008.1); contains InterPro domain SART-1 protein (InterPro:IPR005011)
AT3G15356	1,86	0,03	legume lectin family protein
AT3G19260	1,86	0,03	LAG1 HOMOLOG 2 (LONGEVITY ASSURANCE GENE1 HOMOLOG 2)
AT1G66920	1,86	0,04	serine/threonine protein kinase, putative
AT2G20610	1,86	0,03	SUR1 (SUPERROOT 1); transaminase
AT1G07750	1,86	0,04	cupin family protein
AT4G31330	1,86	0,02	similar to unknown protein [Arabidopsis thaliana] (TAIR:AT5G10580.1); similar to hypothetical protein [Vitis vinifera] (GB:CAN79714.1); contains InterPro domain Protein of unknown function DUF599 (InterPro:IPR006747)
AT2G31110	1,85	0,03	similar to unknown protein [Arabidopsis thaliana] (TAIR:AT2G42570.1); similar to unnamed protein product [Vitis vinifera] (GB:CAO69853.1); contains InterPro domain Protein of unknown function DUF231, plant (InterPro:IPR004253)
AT5G62680	1,85	0,04	proton-dependent oligopeptide transport (POT) family protein
AT4G22390	1,85	0,03	F-box family protein-related
AT5G07920	1,84	0,02	DGK1 (DIACYLGLYCEROL KINASE 1, DIACYLGLYCEROL KINASE1); diacylglycerol kinase
AT5G27550	1,84	0,02	
AT5G57180	1,84	0,03	CIA2 (CHLOROPLAST IMPORT APPARATUS 2)
AT3G21030	1,84	0,02	
AT3G08760	1,84	0,02	ATSIK; kinase
AT5G17860	1,84	0,04	CAX7 (CALCIUM EXCHANGER 7); calcium:sodium antiporter/ cation:cation antiporter
AT4G20365	1,83	0,01	
AT3G59020	1,83	0,03	protein transporter
AT4G19120	1,82	0,04	ERD3 (EARLY-RESPONSIVE TO DEHYDRATION 3)
AT1G72450	1,82	0,02	JAZ6/TIFY11B (JASMONATE-ZIM-DOMAIN PROTEIN 6)

continued on next page

Table C.6 – continued from previous page

AGI code	FC	p-value	Gene description
AT4G14580	1,82	0,04	CIPK4 (CBL-INTERACTING PROTEIN KINASE 4); kinase
AT5G03160	1,82	0,02	DNAJ heat shock N-terminal domain-containing protein
AT5G38940	1,81	0,04	manganese ion binding / metal ion binding / nutrient reservoir
AT4G36220	1,81	0,02	FAH1 (FERULATE-5-HYDROXYLASE 1); ferulate 5-hydroxylase
AT3G04480	1,81	0,04	endoribonuclease
AT3G22142	1,81	0,03	structural constituent of cell wall
AT5G63750	1,81	0,04	IBR domain-containing protein
AT1G45201	1,81	0,03	triacylglycerol lipase
AT1G27370	1,8	0,04	squamosa promoter-binding protein-like 10 (SPL10)
AT4G33920	1,8	0,03	protein phosphatase 2C family protein / PP2C family protein
AT4G12980	1,8	0,03	auxin-responsive protein, putative
AT1G22360	1,8	0,03	UDP-glycosyltransferase
AT3G18280	1,8	0,02	protease inhibitor/seed storage/lipid transfer protein (LTP) family protein
AT1G17720	1,79	0,03	ATB BETA (Arabidopsis thaliana serine/threonine protein phosphatase 2A 55 kDa regulatory subunit B beta isoform); nucleotide binding
AT3G08040	1,79	0,04	FRD3 (FERRIC REDUCTASE DEFECTIVE 3); antiporter
AT3G42725	1,79	0,03	similar to unknown [Olimarabidopsis pumila] (GB:ABA18101.1); contains domain PROKAR_LIPOPROTEIN (PS51257)
AT5G43190	1,79	0,04	F-box family protein (FBX6)
AT5G56980	1,78	0,03	similar to unknown protein [Arabidopsis thaliana] (TAIR:AT4G26130.1); similar to unknown [Populus trichocarpa] (GB:ABK95362.1)
AT5G23190	1,78	0,03	CYP86B1 (cytochrome P450, family 86, subfamily B, polypeptide 1); oxygen binding
AT2G43590	1,77	0,02	chitinase, putative
AT1G67370	1,77	0,03	ASY1 (ASYNAPTIC 1); DNA binding
AT3G04060	1,77	0,03	ANAC046 (Arabidopsis NAC domain containing protein 46); transcription factor
AT3G16720	1,76	0,03	ATL2 (Arabidopsis T ² xicos en Levadura 2); protein binding / zinc ion binding
AT4G35800	1,76	0,02	NRPB1 (RNA POLYMERASE II LARGE SUBUNIT); DNA binding / DNA-directed RNA polymerase
AT4G38680	1,76	0,04	CSDP2/GRP2 (COLD SHOCK DOMAIN PROTEIN 2, GLYCINE RICH PROTEIN 2); nucleic acid binding
AT5G42390	1,75	0,02	metalloendopeptidase
AT3G55110	1,75	0,02	ABC transporter family protein
AT5G55896	1,75	0,03	
AT5G61520	1,74	0,03	hexose transporter, putative
AT1G13750	1,74	0,04	calcineurin-like phosphoesterase family protein
AT1G26110	1,74	0,03	similar to unknown protein [Arabidopsis thaliana] (TAIR:AT5G45330.1); similar to hypothetical protein [Glycine max] (GB:BAB41197.1); contains domain PTHR13586 (PTHR13586)
AT3G02140	1,74	0,02	TMAC2 (TWO OR MORE ABRES-CONTAINING GENE 2)
AT5G06510	1,74	0,04	CCAAT-binding transcription factor (CBF-B/NF-YA) family protein
AT2G45135	1,74	0,03	protein binding / zinc ion binding
AT5G61100	1,73	0,03	zinc ion binding
AT3G11330	1,72	0,03	leucine-rich repeat family protein
AT5G49700	1,72	0,03	DNA-binding protein-related
AT2G39720	1,72	0,03	RHC2A (RING-H2 finger C2A); protein binding / zinc ion binding
AT3G43790	1,72	0,03	ZIFL2 (ZINC INDUCED FACILITATOR-LIKE 2); carbohydrate transmembrane transporter/ sugar:hydrogen ion symporter
AT1G53790	1,72	0,04	F-box family protein

continued on next page

Table C.6 – continued from previous page

AGI code	FC	p-value	Gene description
AT3G19380	1,71	0,03	U-box domain-containing protein
AT5G24280	1,71	0,03	ATP binding
AT3G45638	1,71	0,03	
AT5G42100	1,71	0,04	ATBG_PAP/ATBG_PPAP (A. THALIANA BETA-1,3-GLUCANASE_PUTATIVE); hydrolase, hydrolyzing O-glycosyl compounds
AT3G20660	1,71	0,03	ATOCT4 (ARABIDOPSIS THALIANA ORGANIC CATION/CARNITINE TRANSPORTER4); carbohydrate transmembrane transporter/ sugar:hydrogen ion symporter
AT4G33070	1,7	0,04	pyruvate decarboxylase, putative
AT1G24430	1,7	0,02	transferase family protein
AT5G63560	1,7	0,03	transferase family protein
AT5G67420	1,7	0,04	LBD37 (LOB DOMAIN-CONTAINING PROTEIN 37)
AT4G05020	1,7	0,02	NDB2 (NAD(P)H DEHYDROGENASE B2); disulfide oxidoreductase
AT4G17550	1,7	0,03	transporter-related
AT4G25900	1,7	0,04	aldose 1-epimerase family protein
AT5G27520	1,69	0,04	mitochondrial substrate carrier family protein
AT5G49630	1,69	0,04	AAP6 (AMINO ACID PERMEASE 6); amino acid transmembrane transporter
AT1G61800	1,68	0,04	GPT2 (glucose-6-phosphate/phosphate translocator 2); antiporter/ glucose-6-phosphate transmembrane transporter
AT1G20900	1,68	0,03	ESC (ESCAROLA)
AT1G79940	1,66	0,03	heat shock protein binding / unfolded protein binding
AT5G48170	1,66	0,03	SLY2 (SLEEPY2)
AT1G22280	1,66	0,03	protein phosphatase 2C, putative / PP2C, putative
AT1G73930	1,65	0,03	similar to unnamed protein product [Vitis vinifera] (GB:CAO68016.1); similar to hypothetical protein OsJ_009810 [Oryza sativa (japonica cultivar-group)] (GB:EAZ26327.1); similar to hypothetical protein [Vitis vinifera] (GB:CAN70280.1); contains InterPro domain Protein of unknown function DUF1630 (InterPro:IPR012860)
AT1G30940	1,65	0,03	
AT4G28680	1,65	0,04	tyrosine decarboxylase, putative
AT1G48040	1,65	0,03	protein serine/threonine phosphatase
AT2G47010	1,64	0,04	similar to unknown protein [Arabidopsis thaliana] (TAIR:AT1G17030.1); similar to hypothetical protein [Vitis vinifera] (GB:CAN67131.1); similar to unnamed protein product [Vitis vinifera] (GB:CAO40236.1)
AT3G02050	1,63	0,03	KUP3 (K+ uptake permease 3); potassium ion transmembrane transporter
AT2G34490	1,63	0,04	CYP710A2 (cytochrome P450, family 710, subfamily A, polypeptide 2); C-22 sterol desaturase/ oxygen binding
AT3G11840	1,62	0,04	U-box domain-containing protein
AT3G46290	1,62	0,03	protein kinase, putative
AT3G21040	1,62	0,04	
AT3G07560	1,62	0,03	APM2/PEX13 (ABERRANT PEROXISOME MORPHOLOGY 2); protein binding
AT4G29700	1,62	0,04	type I phosphodiesterase/nucleotide pyrophosphatase family protein
AT1G29300	1,61	0,03	UNE1 (unfertilized embryo sac 1)
AT5G55920	1,61	0,03	nucleolar protein, putative
AT2G31400	1,6	0,04	pentatricopeptide (PPR) repeat-containing protein
AT1G51680	1,59	0,04	4CL1 (4-COUMARATE:COA LIGASE 1)
AT1G70370	1,59	0,03	BURP domain-containing protein / polygalacturonase, putative
AT1G68530	1,59	0,04	CUT1 (CUTICULAR 1); acyltransferase

continued on next page

Table C.6 – continued from previous page

AGI code	FC	p-value	Gene description
AT2G36850	1,58	0,04	ATGSL08 (GLUCAN SYNTHASE-LIKE 8); 1,3-beta-glucan synthase/ transferase, transferring glycosyl groups
AT3G18610	1,57	0,04	ATRANGAP1 (RAN GTPASE-ACTIVATING PROTEIN 1); nucleic acid binding
AT4G26630	1,57	0,03	GTP binding / RNA binding
AT4G26060	1,57	0,03	similar to unknown protein [Arabidopsis thaliana] (TAIR:AT5G57060.1); similar to unnamed protein product [Vitis vinifera] (GB:CAO65021.1); contains domain PTHR10052 (PTHR10052); contains domain PTHR10052:SF2 (PTHR10052:SF2)
AT2G32690	1,57	0,04	
AT1G32640	1,56	0,04	ATMYC2 (JASMONATE INSENSITIVE 1); DNA binding / transcription factor
AT5G12420	1,56	0,04	similar to unknown protein [Arabidopsis thaliana] (TAIR:AT5G16350.1); similar to unnamed protein product [Vitis vinifera] (GB:CAO48523.1); contains InterPro domain Protein of unknown function UPF0089 (InterPro:IPR004255); contains InterPro domain Protein of unknown function DUF1298 (InterPro:IPR009721)
AT3G04210	1,56	0,04	disease resistance protein (TIR-NBS class), putative
AT3G14020	1,56	0,03	CCAAT-binding transcription factor (CBF-B/NF-YA) family protein
AT5G13630	1,55	0,04	GUN5 (GENOMES UNCOUPLED 5)
AT1G28570	1,54	0,04	GDSL-motif lipase, putative
AT4G16390	1,54	0,04	chloroplastic RNA-binding protein P67, putative
AT5G14040	1,54	0,04	mitochondrial phosphate transporter
AT5G60450	1,54	0,04	ARF4 (AUXIN RESPONSE FACTOR 4); transcription factor
AT5G37020	1,53	0,04	ARF8 (AUXIN RESPONSE FACTOR 8); transcription factor
AT2G18940	1,52	0,04	pentatricopeptide (PPR) repeat-containing protein
AT1G03495	1,51	0,04	transferase

Table C.7: Down-regulated genes in *prl1* from the tiling array analysis. The fold change (FC) cut-off is -1,5 and p-value<0,05.

AGI code	FC	p-value	Gene description
AT3G01345	-11,46	0,00	Expressed protein
AT2G18050	-8,99	0,02	HIS1-3 (HISTONE H1-3); DNA binding
AT5G46900	-8,55	0,00	protease inhibitor/seed storage/lipid transfer protein (LTP) family protein
AT4G12550	-7,63	0,02	AIR1 (Auxin-Induced in Root cultures 1); lipid binding
AT2G01520	-6,38	0,01	MLP328 (MLP-LIKE PROTEIN 328)
AT1G52060	-6,09	0,01	similar to jacalin lectin family protein [Arabidopsis thaliana] (TAIR:AT1G52070.1); similar to jasmonate inducible protein [Brassica napus] (GB:CAA72271.1); contains InterPro domain Mannose-binding lectin (InterPro:IPR001229)
AT5G46890	-6,01	0,01	protease inhibitor/seed storage/lipid transfer protein (LTP) family protein
AT4G12545	-5,73	0,02	protease inhibitor/seed storage/lipid transfer protein (LTP) family protein
AT1G45015	-5,56	0,01	MD-2-related lipid recognition domain-containing protein / ML domain-containing protein
AT1G52070	-4,97	0,03	jacalin lectin family protein
AT1G19530	-3,78	0,01	similar to unnamed protein product [Vitis vinifera] (GB:CAO61141.1)
AT4G11320	-3,52	0,00	cysteine proteinase, putative
AT1G52050	-3,41	0,02	jacalin lectin family protein

continued on next page

Table C.7 – continued from previous page

AGI code	FC	p-value	Gene description
AT4G39675	-3,4	0,04	unknown protein
AT5G62340	-3,29	0,03	invertase/pectin methylesterase inhibitor family protein
AT5G51790	-3,26	0,00	basic helix-loop-helix (bHLH) family protein
AT1G66800	-3,25	0,04	cinnamyl-alcohol dehydrogenase family / CAD family
AT2G16005	-3,23	0,01	MD-2-related lipid recognition domain-containing protein / ML domain-containing protein
AT4G15990	-3,07	0,04	similar to unknown protein [Arabidopsis thaliana] (TAIR:AT4G16024.1)
AT4G11310	-2,99	0,00	cysteine proteinase, putative
AT1G77530	-2,95	0,01	O-methyltransferase family 2 protein
AT5G19970	-2,95	0,04	similar to unnamed protein product [Vitis vinifera] (GB:CAO65601.1)
AT4G22666	-2,73	0,04	similar to protease inhibitor/seed storage/lipid transfer protein (LTP) family protein [Arabidopsis thaliana] (TAIR:AT4G22630.1); contains InterPro domain Plant lipid transfer protein/seed storage/trypsin-alpha amylase inhibitor (InterPro:IPR003612); contains InterPro domain Bifunctional inhibitor/plant lipid transfer protein/seed storage (InterPro:IPR016140)
AT1G14185	-2,63	0,01	glucose-methanol-choline (GMC) oxidoreductase family protein
AT3G25930	-2,63	0,02	universal stress protein (USP) family protein
AT1G73120	-2,61	0,02	similar to hypothetical protein [Vitis vinifera] (GB:CAN69175.1)
AT1G19540	-2,61	0,01	isoflavone reductase, putative
AT3G30767	-2,6	0,04	
AT4G11190	-2,57	0,04	disease resistance-responsive family protein / dirigent family protein
AT2G01530	-2,57	0,02	MLP329 (MLP-LIKE PROTEIN 329)
AT5G54370	-2,56	0,02	late embryogenesis abundant protein-related / LEA protein-related
AT5G42590	-2,55	0,01	CYP71A16 (cytochrome P450, family 71, subfamily A, polypeptide 16); oxygen binding
AT1G12080	-2,53	0,01	contains domain PTHR22683 (PTHR22683)
AT5G38100	-2,48	0,01	methyltransferase-related
AT2G20080	-2,45	0,02	similar to unknown protein [Arabidopsis thaliana] (TAIR:AT4G28840.1); similar to unnamed protein product [Vitis vinifera] (GB:CAO65485.1)
AT2G33790	-2,45	0,04	pollen Ole e 1 allergen and extensin family protein
AT5G52070	-2,44	0,01	agenet domain-containing protein
AT5G53190	-2,43	0,02	nodulin MtN3 family protein
AT5G20240	-2,41	0,02	PI (PISTILLATA); DNA binding / transcription factor
AT2G41178	-2,38	0,01	
AT5G32473	-2,36	0,01	
AT1G14960	-2,36	0,04	major latex protein-related / MLP-related
AT5G26290	-2,36	0,01	meprin and TRAF homology domain-containing protein / MATH domain-containing protein
AT4G06511	-2,33	0,03	
AT4G06507	-2,33	0,04	
AT5G55450	-2,33	0,04	protease inhibitor/seed storage/lipid transfer protein (LTP) family protein
AT5G42580	-2,28	0,01	CYP705A12 (cytochrome P450, family 705, subfamily A, polypeptide 12); oxygen binding
AT3G14185	-2,26	0,03	
AT3G46490	-2,17	0,03	oxidoreductase, acting on paired donors, with incorporation or reduction of molecular oxygen, 2-oxoglutarate as one donor, and incorporation of one atom each of oxygen into both donors
AT4G15900	-2,15	0,02	PRL1 (PLEIOTROPIC REGULATORY LOCUS 1); nucleotide binding
AT4G35770	-2,15	0,02	SEN1 (DARK INDUCIBLE 1)

continued on next page

Table C.7 – continued from previous page

AGI code	FC	p-value	Gene description
AT4G06607	-2,12	0,01	
AT2G22630	-2,11	0,03	AGL17 (AGAMOUS-LIKE 17); transcription factor
AT1G06830	-2,11	0,04	glutaredoxin family protein
AT2G33793	-2,11	0,04	similar to unknown protein [Arabidopsis thaliana] (TAIR:AT2G46980.2); similar to unnamed protein product [Vitis vinifera] (GB:CAO63047.1)
AT3G45970	-2,11	0,03	ATEXLA1 (ARABIDOPSIS THALIANA EXPANSIN-LIKE A1)
AT5G24920	-2,09	0,03	ATGDU5 (ARABIDOPSIS THALIANA GLUTAMINE DUMPER 5)
AT5G03120	-2,08	0,04	similar to hypothetical protein [Vitis vinifera] (GB:CAN68657.1)
AT1G55240	-2,08	0,01	similar to unknown protein [Arabidopsis thaliana] (TAIR:AT1G55230.1); similar to unnamed protein product [Vitis vinifera] (GB:CAO63741.1); contains InterPro domain Protein of unknown function DUF716 (InterPro:IPR006904)
AT3G47360	-2,08	0,03	ATHSD3 (HYDROXYSTEROID DEHYDROGENASE 3); oxidoreductase
AT2G39040	-2,07	0,02	peroxidase, putative
AT4G06505	-2,05	0,04	
AT4G35160	-2,01	0,04	O-methyltransferase family 2 protein
AT5G44417	-2,01	0,03	
AT1G08530	-2	0,03	similar to unknown protein [Arabidopsis thaliana] (TAIR:AT5G09995.3); similar to unknown protein [Arabidopsis thaliana] (TAIR:AT5G09995.2); similar to unnamed protein product [Vitis vinifera] (GB:CAO70794.1)
AT5G41270	-1,99	0,04	similar to Os01g0541600 [Oryza sativa (japonica cultivar-group)] (GB:NP_001043269.1); similar to hypothetical protein OsI_002270 [Oryza sativa (indica cultivar-group)] (GB:EAY74423.1); contains InterPro domain RNase P, Rpr2/Rpp21 subunit (InterPro:IPR007175)
AT1G26665	-1,99	0,02	similar to RNA polymerase II mediator complex protein-related [Arabidopsis thaliana] (TAIR:AT5G41910.1); similar to unnamed protein product [Vitis vinifera] (GB:CAO62915.1); contains domain PTHR13345:SF2 (PTHR13345:SF2); contains domain PD331788 (PD331788); contains domain PTHR13345 (PTHR13345)
AT4G31290	-1,99	0,03	ChaC-like family protein
AT4G06637	-1,99	0,03	
AT1G70790	-1,99	0,03	C2 domain-containing protein
AT1G19900	-1,96	0,03	glyoxal oxidase-related
AT3G21950	-1,95	0,02	S-adenosyl-L-methionine:carboxyl methyltransferase family protein
AT3G23800	-1,94	0,03	selenium-binding family protein
AT4G37850	-1,94	0,04	basic helix-loop-helix (bHLH) family protein
AT2G37440	-1,93	0,04	endonuclease/exonuclease/phosphatase family protein
AT5G35940	-1,92	0,01	jacalin lectin family protein
AT3G60300	-1,92	0,03	RWD domain-containing protein
AT3G60810	-1,92	0,03	similar to unnamed protein product [Vitis vinifera] (GB:CAO24482.1); contains InterPro domain Protein of unknown function DUF1499 (InterPro:IPR010865)
AT2G25160	-1,91	0,03	CYP82F1 (cytochrome P450, family 82, subfamily F, polypeptide 1); oxygen binding
AT5G23480	-1,91	0,03	similar to SWIB complex BAF60b domain-containing protein / plus-3 domain-containing protein / GYF domain-containing protein [Arabidopsis thaliana] (TAIR:AT5G08430.1); similar to hypothetical protein [Vitis vinifera] (GB:CAN80413.1); contains InterPro domain GYF (InterPro:IPR003169)
AT1G08830	-1,9	0,04	CSD1 (copper/zinc superoxide dismutase 1)
AT3G07860	-1,9	0,02	similar to unknown protein [Arabidopsis thaliana] (TAIR:AT5G25340.1); similar to unnamed protein product [Vitis vinifera] (GB:CAO61986.1); contains domain G3DSA:3.10.20.90 (G3DSA:3.10.20.90); contains domain SSF54236 (SSF54236)
AT2G42170	-1,88	0,04	actin, putative
AT3G25710	-1,88	0,03	basic helix-loop-helix (bHLH) family protein
AT5G38140	-1,88	0,02	histone-like transcription factor (CBF/NF-Y) family protein
AT5G63280	-1,88	0,04	zinc finger (C2H2 type) family protein

continued on next page

Table C.7 – continued from previous page

AGI code	FC	p-value	Gene description
AT2G41990	-1,87	0,02	similar to unknown protein [Arabidopsis thaliana] (TAIR:AT4G35170.1); similar to hypothetical protein [Vitis vinifera] (GB:CAN73167.1)
AT2G01100	-1,86	0,02	similar to Os01g0120700 [Oryza sativa (japonica cultivar-group)] (GB:NP_001041870.1); similar to hypothetical protein OsI_000168 [Oryza sativa (indica cultivar-group)] (GB:EAY72321.1)
AT1G48950	-1,85	0,03	zinc ion binding
AT4G30570	-1,85	0,03	GDP-mannose pyrophosphorylase, putative
AT4G25500	-1,84	0,01	ATRSP35 (Arabidopsis thaliana arginine/serine-rich splicing factor 35); RNA binding
AT4G21590	-1,84	0,02	ENDO3 (ENDONUCLEASE 3); T/G mismatch-specific endonuclease/ endonuclease/ nucleic acid binding / single-stranded DNA specific endodeoxyribonuclease
AT1G74760	-1,84	0,04	
AT1G64330	-1,83	0,04	myosin heavy chain-related
AT5G10140	-1,82	0,03	FLC (FLOWERING LOCUS C); transcription factor
AT5G23990	-1,81	0,02	ATFRO5/FRO5 (FERRIC REDUCTION OXIDASE 5); ferric-chelate reductase
AT5G49400	-1,81	0,04	zinc knuckle (CCHC-type) family protein
AT3G46500	-1,81	0,02	oxidoreductase, 2OG-Fe(II) oxygenase family protein
AT1G34680	-1,81	0,04	
AT1G36460	-1,8	0,02	
AT5G27500	-1,8	0,04	
AT2G25770	-1,8	0,03	similar to unknown protein [Arabidopsis thaliana] (TAIR:AT4G32870.1); similar to hypothetical protein [Vitis vinifera] (GB:CAN83252.1); contains domain SSF55961 (SSF55961)
AT3G25440	-1,8	0,03	similar to unknown protein [Arabidopsis thaliana] (TAIR:AT2G28480.1); similar to unnamed protein product [Vitis vinifera] (GB:CAO46979.1); contains InterPro domain CRS1/YhbY (InterPro:IPR001890)
AT4G37440	-1,79	0,03	similar to unknown protein [Arabidopsis thaliana] (TAIR:AT3G59670.1); similar to unnamed protein product [Vitis vinifera] (GB:CAO46283.1)
AT5G10200	-1,79	0,04	binding
AT5G65790	-1,79	0,02	MYB68 (myb domain protein 68); DNA binding / transcription factor
AT1G61240	-1,79	0,03	similar to unknown protein [Arabidopsis thaliana] (TAIR:AT1G11170.1); similar to unknown [Picea sitchensis] (GB:ABK25584.1); contains InterPro domain Protein of unknown function DUF707 (InterPro:IPR007877)
AT1G77520	-1,78	0,03	O-methyltransferase family 2 protein
AT5G32515	-1,77	0,02	
AT4G20960	-1,77	0,03	cytidine/deoxycytidylate deaminase family protein
AT5G13770	-1,76	0,04	pentatricopeptide (PPR) repeat-containing protein
AT2G15960	-1,76	0,03	unknown protein
AT5G24410	-1,75	0,04	glucosamine/galactosamine-6-phosphate isomerase-related
AT4G14640	-1,74	0,03	CAM8 (CALMODULIN 8); calcium ion binding
AT1G05660	-1,74	0,04	polygalacturonase, putative / pectinase, putative
AT5G56590	-1,71	0,03	glycosyl hydrolase family 17 protein
AT1G62480	-1,71	0,03	vacuolar calcium-binding protein-related
AT3G20130	-1,7	0,04	CYP705A22 (cytochrome P450, family 705, subfamily A, polypeptide 22); oxygen binding
AT5G05540	-1,7	0,03	exonuclease family protein
AT2G16380	-1,7	0,04	SEC14 cytosolic factor family protein / phosphoglyceride transfer family protein
AT4G31060	-1,7	0,02	AP2 domain-containing transcription factor, putative
AT2G03913	-1,7	0,03	Encodes a defensin-like (DEFL) family protein.
AT4G01570	-1,69	0,04	pentatricopeptide (PPR) repeat-containing protein

continued on next page

Table C.7 – continued from previous page

AGI code	FC	p-value	Gene description
AT1G18450	-1,69	0,03	ATARP4 (ACTIN-RELATED PROTEIN 4); structural constituent of cytoskeleton
AT3G50560	-1,69	0,04	short-chain dehydrogenase/reductase (SDR) family protein
AT4G15290	-1,69	0,02	ATCSLB05 (Cellulose synthase-like B5); transferase/ transferase, transferring glycosyl groups
AT4G17150	-1,68	0,03	similar to unknown protein [Arabidopsis thaliana] (TAIR:AT4G14290.1); similar to unnamed protein product [Vitis vinifera] (GB:CAO23689.1); contains domain UNCHARACTERIZED (PTHR12277:SF9); contains domain no description (G3DSA:3.40.50.1820); contains domain UNCHARACTERIZED (PTHR12277); contains domain alpha/beta-Hydrolases (SSF53474)
AT5G45490	-1,66	0,03	disease resistance protein-related
AT5G57550	-1,66	0,03	XTR3 (XYLOGLUCAN ENDOTRANSGLYCOSYLASE 3); hydrolase, acting on glycosyl bonds
AT1G41723	-1,66	0,03	
AT1G78660	-1,66	0,04	ATGGH1; gamma-glutamyl hydrolase
AT1G25290	-1,66	0,04	rhomboid family protein
AT1G80190	-1,65	0,04	PSF1
AT1G21323	-1,65	0,03	unknown protein
AT1G03300	-1,65	0,03	agenet domain-containing protein
AT4G39160	-1,65	0,03	DNA binding / transcription factor
AT5G17270	-1,64	0,03	tetratricopeptide repeat (TPR)-containing protein
AT3G47690	-1,64	0,04	ATEB1A (Arabidopsis thaliana Microtubule End Binding Protein EB1A); microtubule binding
AT4G17730	-1,64	0,04	SYP23 (syntaxin 23); SNAP receptor
AT4G06621	-1,64	0,03	
AT3G33235	-1,63	0,04	
AT4G13300	-1,63	0,03	ATTPS13/TPS13 (TERPENOID SYNTHASE13); cyclase
AT1G27460	-1,63	0,03	NPGR1 (NO POLLEN GERMINATION RELATED 1); calmodulin binding
AT2G28160	-1,63	0,04	ATBHLH029/BHLH029/FIT1/FRU (FE-DEFICIENCY INDUCED TRANSCRIPTION FACTOR 1); DNA binding / transcription factor
AT1G56210	-1,63	0,03	copper chaperone (CCH)-related
AT2G39120	-1,62	0,03	similar to unknown protein [Arabidopsis thaliana] (TAIR:AT3G58520.1); similar to unnamed protein product [Vitis vinifera] (GB:CAO68916.1); contains InterPro domain Protein of unknown function DUF860, plant (InterPro:IPR008578)
AT1G80150	-1,62	0,03	pentatricopeptide (PPR) repeat-containing protein
AT4G01120	-1,62	0,04	GBF2 (G-BOX BINDING FACTOR 2); DNA binding / transcription factor
AT5G63880	-1,61	0,04	VPS20.1
AT3G18850	-1,61	0,03	LPAT5; acyltransferase
AT4G37410	-1,61	0,03	CYP81F4 (cytochrome P450, family 81, subfamily F, polypeptide 4); oxygen binding
AT4G28840	-1,6	0,04	similar to unknown protein [Arabidopsis thaliana] (TAIR:AT2G20080.1); similar to unnamed protein product [Vitis vinifera] (GB:CAO65485.1)
AT1G80620	-1,6	0,04	ribosomal protein S15 family protein
AT5G66160	-1,6	0,04	JR700 (Arabidopsis thaliana receptor homology region transmembrane domain ring H2 motif protein 1); peptidase/ protein binding / zinc ion binding
AT5G60940	-1,59	0,03	transducin family protein / WD-40 repeat family protein
AT3G24070	-1,59	0,03	zinc knuckle (CCHC-type) family protein
AT2G45250	-1,59	0,04	similar to unknown protein [Arabidopsis thaliana] (TAIR:AT4G38280.1); similar to unknown [Populus trichocarpa] (GB:ABK93717.1)
AT1G62400	-1,59	0,04	HT1 (HIGH LEAF TEMPERATURE 1); kinase/ protein serine/threonine/tyrosine kinase
AT2G39100	-1,59	0,04	zinc finger (C3HC4-type RING finger) family protein
AT3G45430	-1,58	0,04	lectin protein kinase family protein
AT4G24630	-1,58	0,04	receptor/ zinc ion binding

continued on next page

Table C.7 – continued from previous page

AGI code	FC	p-value	Gene description
AT2G23560	-1,58	0,03	hydrolase, alpha/beta fold family protein
AT3G30827	-1,58	0,04	
AT1G29930	-1,57	0,04	CAB1 (CHLOROPHYLL A/B BINDING PROTEIN 1); chlorophyll binding
AT1G35625	-1,57	0,04	protease-associated zinc finger (C3HC4-type RING finger) family protein
AT4G34140	-1,57	0,04	D111/G-patch domain-containing protein
AT4G24340	-1,56	0,03	phosphorylase family protein
AT1G50520	-1,56	0,03	CYP705A27 (cytochrome P450, family 705, subfamily A, polypeptide 27); oxygen binding
AT5G58200	-1,53	0,04	similar to unnamed protein product [<i>Vitis vinifera</i>] (GB:CAO22752.1)
AT1G04030	-1,52	0,04	similar to unknown protein [<i>Arabidopsis thaliana</i>] (TAIR:AT5G44040.1); similar to unnamed protein product [<i>Vitis vinifera</i>] (GB:CAO40580.1)
AT5G66060	-1,52	0,04	oxidoreductase, 2OG-Fe(II) oxygenase family protein
AT1G51055	-1,51	0,04	similar to unknown protein [<i>Arabidopsis thaliana</i>] (TAIR:AT5G56800.1); contains InterPro domain FBD (InterPro:IPR013596); contains InterPro domain FBD-like (InterPro:IPR006566)

Table C.8: Up-regulated genes in *prl1* from the RNA-Seq analysis. The fold change (FC) cut-off is 2 and p-value<0,05.

AGI code	FC	Gene description
AT2G47115	716198	similar to unknown protein [<i>Arabidopsis thaliana</i>] (TAIR:AT1G10660.3); similar to unknown protein [<i>Arabidopsis thaliana</i>] (TAIR:AT1G10660.1); similar to unknown protein [<i>Arabidopsis thaliana</i>] (TAIR:AT1G10660.4); similar to unnamed protein product [<i>Vitis vinifera</i>] (GB:CAO40183.1)
AT4G20365	16,91	
AT3G28899	14,52	unknown protein
AT1G14550	10,06	anionic peroxidase, putative
AT1G66600	8,22	WRKY63 (WRKY DNA-binding protein 63); transcription factor
AT5G02780	7,89	In2-1 protein, putative
AT1G51915	7,36	cryptdin protein-related
AT1G68765	7,36	IDA (INFLORESCENCE DEFICIENT IN ABSCISSION)
AT2G03505	6,77	glycosyl hydrolase family protein 17
AT3G60270	6,36	uclacyanin, putative
AT1G26240	6,32	proline-rich extensin-like family protein
AT3G02240	6,06	similar to unknown protein [<i>Arabidopsis thaliana</i>] (TAIR:AT3G02242.1)
AT2G36090	5,94	F-box family protein
AT3G02840	5,9	immediate-early fungal elicitor family protein
AT1G52620	5,82	pentatricopeptide (PPR) repeat-containing protein
AT5G06865	5,66	
AT4G12500	5,62	protease inhibitor/seed storage/lipid transfer protein (LTP) family protein
AT1G57630	5,62	disease resistance protein (TIR class), putative
AT3G25655	5,46	unknown protein
AT4G13420	5,43	HAK5 (High affinity K ⁺ transporter 5); potassium ion transmembrane transporter

continued on next page

Table C.8 – continued from previous page

AGI code	FC	Gene description
AT1G56600	5,31	ATGOLS2 (ARABIDOPSIS THALIANA GALACTINOL SYNTHASE 2); transferase, transferring glycosyl groups / transferase, transferring hexosyl groups
AT3G57260	5,28	BGL2 (PATHOGENESIS-RELATED PROTEIN 2); glucan 1,3-beta-glucosidase/ hydrolase, hydrolyzing O-glycosyl compounds
AT5G37490	4,99	U-box domain-containing protein
AT1G32350	4,99	AOX1D (ALTERNATIVE OXIDASE 1D); alternative oxidase
AT5G55150	4,96	F-box family protein
AT2G03540	4,92	
AT5G18360	4,86	disease resistance protein (TIR-NBS-LRR class), putative
AT1G49860	4,72	ATGSTF14 (Arabidopsis thaliana Glutathione S-transferase (class phi) 14); glutathione transferase
AT2G21020	4,69	
AT3G45330	4,5	lectin protein kinase family protein
AT2G17060	4,44	disease resistance protein (TIR-NBS-LRR class), putative
AT2G42060	4,38	CHP-rich zinc finger protein, putative
AT4G16600	4,29	glycogenin glucosyltransferase (glycogenin)-related
AT2G23300	4,29	leucine-rich repeat transmembrane protein kinase, putative
AT5G59680	4,29	leucine-rich repeat protein kinase, putative
AT2G31425	4,2	enzyme inhibitor/ pectinesterase
AT1G69930	4,14	ATGSTU11 (Arabidopsis thaliana Glutathione S-transferase (class tau) 11); glutathione transferase
AT2G35770	4,14	SCPL28 (serine carboxypeptidase-like 28); serine carboxypeptidase
AT4G11470	4,14	protein kinase family protein
AT2G31860	4,11	
AT3G20470	4,11	
AT4G25200	4,06	ATHSP23.6-MITO (MITOCHONDRION-LOCALIZED SMALL HEAT SHOCK PROTEIN 23.6)
AT5G19880	3,94	peroxidase, putative
AT1G51620	3,94	protein kinase family protein
AT4G11050	3,94	ATGH9C3 (ARABIDOPSIS THALIANA GLYCOSYL HYDROLASE 9C3); hydrolase, hydrolyzing O-glycosyl compounds
AT3G20360	3,94	mepirin and TRAF homology domain-containing protein / MATH domain-containing protein
AT1G53260	3,86	similar to unknown protein [Arabidopsis thaliana] (TAIR:AT3G15000.1); similar to unnamed protein product [Vitis vinifera] (GB:CAO39382.1)
AT1G64360	3,86	unknown protein
AT5G57480	3,84	AAA-type ATPase family protein
AT5G06320	3,84	NHL3 (NDR1/HIN1-like 3)
AT3G27473	3,78	DC1 domain-containing protein
AT3G21720	3,76	isocitrate lyase, putative
AT1G51913	3,73	unknown protein
AT3G48650	3,68	
AT3G17050	3,68	
AT3G46680	3,66	UDP-glucuronosyl/UDP-glucosyl transferase family protein
AT1G65500	3,63	similar to unknown protein [Arabidopsis thaliana] (TAIR:AT1G65486.1)
AT1G68390	3,61	similar to unknown protein [Arabidopsis thaliana] (TAIR:AT1G68380.1); similar to unnamed protein product [Vitis vinifera] (GB:CAO42175.1); contains InterPro domain Protein of unknown function DUF266, plant (InterPro:IPR004949)
AT1G10520	3,61	DNA polymerase lambda (POLL)
AT1G65485	3,61	

continued on next page

Table C.8 – continued from previous page

AGI code	FC	Gene description
AT2G04495	3,61	similar to unknown protein [<i>Arabidopsis thaliana</i>] (TAIR:AT2G04515.1)
AT2G19190	3,53	FRK1 (FLG22-INDUCED RECEPTOR-LIKE KINASE 1); kinase
AT5G37300	3,53	similar to unknown protein [<i>Arabidopsis thaliana</i>] (TAIR:AT2G38995.1); similar to unnamed protein product [<i>Vitis vinifera</i>] (GB:CAO48523.1); contains InterPro domain Protein of unknown function UPF0089 (InterPro:IPR004255); contains InterPro domain Protein of unknown function DUF1298 (InterPro:IPR009721)
AT2G43620	3,53	chitinase, putative
AT4G27280	3,53	calcium-binding EF hand family protein
AT2G18660	3,51	EXLB3 (EXPANSIN-LIKE B3 PRECURSOR)
AT1G26420	3,51	FAD-binding domain-containing protein
AT5G42830	3,51	transferase family protein
AT5G64401	3,48	unknown protein
AT1G30740	3,48	FAD-binding domain-containing protein
AT4G12490	3,46	protease inhibitor/seed storage/lipid transfer protein (LTP) family protein
AT4G08555	3,43	unknown protein
AT1G57590	3,43	carboxylesterase
AT5G13920	3,41	zinc knuckle (CCHC-type) family protein
AT2G20880	3,41	AP2 domain-containing transcription factor, putative
AT3G02885	3,41	GASA5 (GAST1 PROTEIN HOMOLOG 5)
AT3G07195	3,39	proline-rich family protein
AT1G74930	3,36	ORA47; DNA binding / transcription factor
AT1G68470	3,34	exostosin family protein
AT1G17090	3,32	unknown protein
AT1G47840	3,32	hexokinase, putative
AT5G44575	3,29	unknown protein
AT1G67105	3,29	
AT1G79680	3,27	wall-associated kinase, putative
AT5G55090	3,23	MAPKKK15 (Mitogen-activated protein kinase kinase kinase 15); kinase
AT1G30080	3,23	glycosyl hydrolase family 17 protein
AT4G35180	3,23	LHT7 (LYS/HIS TRANSPORTER 7); amino acid transmembrane transporter
AT4G00310	3,23	EDA8/MEE46 (EMBRYO SAC DEVELOPMENT ARREST 8)
AT1G61120	3,23	terpene synthase/cyclase family protein
AT1G65481	3,23	
AT5G57010	3,23	calmodulin-binding family protein
AT4G03270	3,23	CYCD6;1 (CYCLIN D6;1); cyclin-dependent protein kinase
AT2G39530	3,23	integral membrane protein, putative
AT4G19370	3,2	similar to unknown protein [<i>Arabidopsis thaliana</i>] (TAIR:AT1G31720.1); similar to unknown [<i>Picea sitchensis</i>] (GB:ABK21519.1); similar to Os02g0703300 [<i>Oryza sativa</i> (japonica cultivar-group)] (GB:NP_001047854.1); contains InterPro domain Protein of unknown function DUF1218 (InterPro:IPR009606)
AT2G46760	3,2	FAD-binding domain-containing protein
AT4G39830	3,2	L-ascorbate oxidase, putative
AT5G39580	3,2	peroxidase, putative
AT1G51890	3,2	leucine-rich repeat protein kinase, putative
AT1G14540	3,2	anionic peroxidase, putative

continued on next page

Table C.8 – continued from previous page

AGI code	FC	Gene description
AT1G69920	3,18	ATGSTU12 (Arabidopsis thaliana Glutathione S-transferase (class tau) 12); glutathione transferase
AT2G47110	3,16	UBQ6 (ubiquitin 6); protein binding
AT4G37370	3,16	CYP81D8 (cytochrome P450, family 81, subfamily D, polypeptide 8); oxygen binding
AT5G46080	3,16	protein kinase family protein
AT2G38830	3,14	tumor susceptibility protein-related
AT3G63380	3,14	calcium-transporting ATPase, plasma membrane-type, putative / Ca(2+)-ATPase, putative (ACA12)
AT3G50460	3,14	HR2 (HOMOLOG OF RPW8 2)
AT1G71000	3,12	DNAJ heat shock N-terminal domain-containing protein
AT5G38450	3,12	CYP735A1 (cytochrome P450, family 735, subfamily A, polypeptide 1); oxygen binding
AT5G28630	3,07	glycine-rich protein
AT4G28460	3,05	unknown protein
AT1G77010	3,05	pentatricopeptide (PPR) repeat-containing protein
AT4G37400	3,05	CYP81F3 (cytochrome P450, family 81, subfamily F, polypeptide 3); oxygen binding
AT1G47890	3,05	disease resistance family protein
AT3G13950	3,03	similar to unknown protein [Arabidopsis thaliana] (TAIR:AT4G13266.1); similar to Ankyrin [Medicago truncatula] (GB:ABN08906.1)
AT4G23215	3,03	
AT3G13435	3,01	unknown protein
AT5G58720	3,01	PRLI-interacting factor, putative
AT5G10260	3,01	AtRABH1e (Arabidopsis Rab GTPase homolog H1e); GTP binding
AT3G45130	3,01	LAS1 (Lanosterol synthase 1); lanosterol synthase
AT4G31410	2,99	similar to unknown protein [Arabidopsis thaliana] (TAIR:AT3G24740.2); similar to unknown protein [Arabidopsis thaliana] (TAIR:AT3G24740.1); similar to hypothetical protein [Vitis vinifera] (GB:CAN62770.1); contains InterPro domain Protein of unknown function DUF1644 (InterPro:IPR012866)
AT5G44585	2,99	unknown protein
AT4G33720	2,97	pathogenesis-related protein, putative
AT2G18210	2,97	similar to unknown protein [Arabidopsis thaliana] (TAIR:AT4G36500.1); similar to hypothetical protein [Thellungiella halophila] (GB:ABB45855.1)
AT4G13000	2,97	protein kinase family protein
AT1G18835	2,97	MIF3 (MINI ZINC FINGER)
AT4G33280	2,97	DNA binding / transcription factor
AT4G12740	2,97	adenine-DNA glycosylase-related / MYH-related
AT5G59930	2,97	DC1 domain-containing protein / UV-B light-insensitive protein, putative
AT1G49000	2,97	similar to unknown protein [Arabidopsis thaliana] (TAIR:AT3G18560.1); similar to hypothetical protein [Vitis vinifera] (GB:CAN78728.1); similar to unnamed protein product [Vitis vinifera] (GB:CAO68009.1)
AT5G03350	2,95	legume lectin family protein
AT2G39200	2,95	MLO12 (MILDEW RESISTANCE LOCUS O 12); calmodulin binding
AT1G36622	2,95	similar to unknown protein [Arabidopsis thaliana] (TAIR:AT1G36640.1)
AT4G37940	2,95	AGL21 (AGAMOUS-LIKE 21); transcription factor
AT3G14260	2,93	similar to unknown protein [Arabidopsis thaliana] (TAIR:AT1G53870.1); similar to unknown protein [Arabidopsis thaliana] (TAIR:AT1G53890.1); similar to unnamed protein product [Vitis vinifera] (GB:CAO62790.1); contains InterPro domain Protein of unknown function DUF567 (InterPro:IPR007612)
AT3G27940	2,93	LBD26 (LOB DOMAIN-CONTAINING PROTEIN 26)
AT1G69880	2,93	ATH8 (thioredoxin H-type 8); thiol-disulfide exchange intermediate
AT1G19610	2,91	LCR78/PDF1.4 (Low-molecular-weight cysteine-rich 78)

continued on next page

Table C.8 – continued from previous page

AGI code	FC	Gene description
AT5G12340	2,91	similar to unknown protein [Arabidopsis thaliana] (TAIR:AT1G28190.1); similar to unnamed protein product [Vitis vinifera] (GB:CAO16848.1)
AT1G75030	2,91	ATLP-3 (Arabidopsis thaumatin-like protein 3)
AT1G02920	2,89	ATGSTF7 (GLUTATHIONE S-TRANSFERASE 11); glutathione transferase
AT1G74870	2,89	protein binding / zinc ion binding
AT4G22070	2,89	WRKY31 (WRKY DNA-binding protein 31); transcription factor
AT2G30750	2,87	CYP71A12 (CYTOCHROME P450, FAMILY 71, SUBFAMILY A, POLYPEPTIDE 12); oxygen binding
AT1G07050	2,87	CONSTANS-like protein-related
AT4G39440	2,85	similar to unnamed protein product [Vitis vinifera] (GB:CAO71742.1)
AT5G36000	2,85	similar to unknown protein [Arabidopsis thaliana] (TAIR:AT3G61730.1); similar to unnamed protein product [Vitis vinifera] (GB:CAO39758.1); contains domain F-box domain (SSF81383)
AT2G39518	2,83	Identical to UPF0497 membrane protein At2g39518 [Arabidopsis Thaliana] (GB:Q56X75); similar to integral membrane protein, putative [Arabidopsis thaliana] (TAIR:AT2G39530.1); similar to hypothetical protein [Vitis vinifera] (GB:CAN64094.1); contains InterPro domain Conserved hypothetical protein CHP01569, trans-membrane plant (InterPro:IPR006459); contains InterPro domain Protein of unknown function DUF588 (InterPro:IPR006702)
AT1G13520	2,83	similar to unknown protein [Arabidopsis thaliana] (TAIR:AT1G13480.1); similar to unnamed protein product [Vitis vinifera] (GB:CAO42040.1); contains InterPro domain Protein of unknown function DUF1262 (InterPro:IPR010683)
AT2G38870	2,83	protease inhibitor, putative
AT3G04640	2,81	glycine-rich protein
AT4G28420	2,79	aminotransferase, putative
AT2G35850	2,77	similar to unknown protein [Arabidopsis thaliana] (TAIR:AT3G52360.1); similar to unnamed protein product [Vitis vinifera] (GB:CAO39911.1)
AT5G10970	2,77	zinc finger (C2H2 type) family protein
AT1G02930	2,77	ATGSTF6 (EARLY RESPONSIVE TO DEHYDRATION 11); glutathione transferase
AT4G04410	2,77	
AT4G04450	2,77	WRKY42 (WRKY DNA-binding protein 42); transcription factor
AT1G05680	2,77	UDP-glucuronosyl/UDP-glucosyl transferase family protein
AT2G40080	2,77	ELF4 (EARLY FLOWERING 4)
AT5G59260	2,75	lectin protein kinase, putative
AT1G74080	2,75	MYB122 (myb domain protein 122); DNA binding / transcription factor
AT1G22260	2,75	ZYP1a
AT4G39950	2,75	CYP79B2 (cytochrome P450, family 79, subfamily B, polypeptide 2); oxygen binding
AT4G02810	2,75	similar to unknown protein [Arabidopsis thaliana] (TAIR:AT1G03170.1); similar to hypothetical protein [Vitis vinifera] (GB:CAN75990.1)
AT4G14630	2,75	GLP9 (GERMIN-LIKE PROTEIN 9); manganese ion binding / metal ion binding / nutrient reservoir
AT5G48570	2,73	peptidyl-prolyl cis-trans isomerase, putative / FK506-binding protein, putative
AT2G21650	2,73	MEE3 (maternal effect embryo arrest 3); DNA binding / transcription factor
AT5G26690	2,73	heavy-metal-associated domain-containing protein
AT3G14630	2,73	CYP72A9 (cytochrome P450, family 72, subfamily A, polypeptide 9); oxygen binding
AT4G12735	2,71	similar to unknown protein [Arabidopsis thaliana] (TAIR:AT4G12731.1)
AT5G01550	2,71	lectin protein kinase, putative
AT5G38020	2,71	S-adenosyl-L-methionine:carboxyl methyltransferase family protein
AT2G41730	2,71	similar to unknown protein [Arabidopsis thaliana] (TAIR:AT5G24640.1); similar to unnamed protein product [Vitis vinifera] (GB:CAO14635.1)
AT3G28890	2,69	leucine-rich repeat family protein
AT1G75830	2,69	LCR67/PDF1.1 (Low-molecular-weight cysteine-rich 67)

continued on next page

Table C.8 – continued from previous page

AGI code	FC	Gene description
AT3G55900	2,68	F-box family protein
AT5G10760	2,68	aspartyl protease family protein
AT2G17740	2,64	DC1 domain-containing protein
AT4G08250	2,64	scarecrow transcription factor family protein
AT1G30700	2,64	FAD-binding domain-containing protein
AT1G47480	2,64	hydrolase
AT2G32140	2,64	transmembrane receptor
AT5G58140	2,64	PHOT2 (NON PHOTOTROPIC HYPOCOTYL 1-LIKE); kinase
AT4G15380	2,62	CYP705A4 (cytochrome P450, family 705, subfamily A, polypeptide 4); oxygen binding
AT1G51920	2,62	unknown protein
AT1G64065	2,62	similar to unknown protein [Arabidopsis thaliana] (TAIR:AT2G44000.1); similar to unnamed protein product [Vitis vinifera] (GB:CAO49537.1); contains InterPro domain Harpin-induced 1 (InterPro:IPR010847)
AT5G60900	2,62	RLK1 (RECEPTOR-LIKE PROTEIN KINASE 1); carbohydrate binding / kinase
AT1G70920	2,62	homeobox-leucine zipper protein, putative / HD-ZIP transcription factor, putative
AT5G24110	2,62	WRKY30 (WRKY DNA-binding protein 30); transcription factor
AT1G51850	2,62	leucine-rich repeat protein kinase, putative
AT4G34131	2,6	UGT73B3 (UDP-glucosyl transferase 73B3); UDP-glycosyltransferase/ abscisic acid glucosyltransferase/ transferase, transferring hexosyl groups
AT2G04070	2,6	transporter
AT1G64400	2,6	long-chain-fatty-acid-CoA ligase, putative / long-chain acyl-CoA synthetase, putative
AT3G02800	2,6	phosphoprotein phosphatase
AT5G51850	2,6	similar to unknown protein [Arabidopsis thaliana] (TAIR:AT4G25430.1); similar to unnamed protein product [Vitis vinifera] (GB:CAO17701.1)
AT5G07650	2,6	formin homology 2 domain-containing protein / FH2 domain-containing protein
AT2G19500	2,6	CKX2 (CYTOKININ OXIDASE 2); cytokinin dehydrogenase
AT4G40020	2,6	similar to unknown protein [Arabidopsis thaliana] (TAIR:AT5G16730.1); similar to hypothetical protein [Vitis vinifera] (GB:CAN70653.1); contains domain PTHR23160 (PTHR23160)
AT1G53980	2,58	polyubiquitin-related
AT2G27390	2,58	proline-rich family protein
AT4G11170	2,58	disease resistance protein (TIR-NBS-LRR class), putative
AT4G27070	2,57	TSB2 (TRYPTOPHAN SYNTHASE BETA-SUBUNIT); tryptophan synthase
AT1G73810	2,57	DNA binding
AT1G08570	2,57	thioredoxin family protein
AT3G09520	2,55	ATEXO70H4 (exocyst subunit EXO70 family protein H4); protein binding
AT4G25090	2,55	respiratory burst oxidase, putative / NADPH oxidase, putative
AT3G16530	2,55	legume lectin family protein
AT5G24230	2,55	similar to triacylglycerol lipase [Arabidopsis thaliana] (TAIR:AT5G24200.1); similar to unnamed protein product [Vitis vinifera] (GB:CAO69530.1); contains domain SSF53474 (SSF53474); contains domain G3DSA:3.40.50.1820 (G3DSA:3.40.50.1820)
AT4G31970	2,55	CYP82C2 (cytochrome P450, family 82, subfamily C, polypeptide 2); oxygen binding
AT4G20000	2,53	VQ motif-containing protein
AT5G66620	2,53	LIM domain-containing protein
AT1G73040	2,53	jacalin lectin family protein
AT3G51950	2,53	zinc finger (CCCH-type) family protein / RNA recognition motif (RRM)-containing protein

continued on next page

Table C.8 – continued from previous page

AGI code	FC	Gene description
AT4G18990	2,53	xyloglucan:xyloglucosyl transferase, putative / xyloglucan endotransglycosylase, putative / endo-xyloglucan transferase, putative
AT2G25470	2,53	leucine-rich repeat family protein
AT5G25020	2,53	similar to unknown protein [Arabidopsis thaliana] (TAIR:AT5G24990.1); similar to hypothetical protein [Vitis vinifera] (GB:CAN83078.1); contains InterPro domain Protein of unknown function DUF1336 (InterPro:IPR009769)
AT1G63520	2,53	similar to unknown protein [Arabidopsis thaliana] (TAIR:AT4G11450.1); similar to unnamed protein product [Vitis vinifera] (GB:CAO62824.1); contains InterPro domain Tubby, C-terminal (InterPro:IPR000007)
AT2G36770	2,51	UDP-glucuronosyl/UDP-glucosyl transferase family protein
AT1G21240	2,51	WAK3 (WALL ASSOCIATED KINASE 3); kinase/ protein serine/threonine kinase
AT1G73260	2,5	trypsin and protease inhibitor family protein / Kunitz family protein
AT1G52410	2,5	TSA1 (TSK-ASSOCIATING PROTEIN 1); calcium ion binding / protein binding
AT5G44050	2,5	MATE efflux family protein
AT1G76430	2,5	phosphate transporter family protein
AT2G31020	2,5	oxysterol-binding family protein
AT1G18970	2,48	GLP4 (GERMIN-LIKE PROTEIN 4); manganese ion binding / metal ion binding / nutrient reservoir
AT5G15120	2,48	similar to unknown protein [Arabidopsis thaliana] (TAIR:AT5G39890.1); similar to unnamed protein product [Vitis vinifera] (GB:CAO14912.1); contains InterPro domain Protein of unknown function DUF1637 (InterPro:IPR012864)
AT1G25280	2,48	AtTLP10 (TUBBY LIKE PROTEIN 10); phosphoric diester hydrolase/ transcription factor
AT5G60100	2,48	APRR3 (PSEUDO-RESPONSE REGULATOR 3); transcription regulator
AT3G13790	2,46	ATBFRUCT1/ATCWINV1 (ARABIDOPSIS THALIANA CELL WALL INVERTASE 1); beta-fructofuranosidase/ hydrolase, hydrolyzing O-glycosyl compounds
AT3G50930	2,46	AAA-type ATPase family protein
AT4G31950	2,45	CYP82C3 (cytochrome P450, family 82, subfamily C, polypeptide 3); oxygen binding
AT2G14620	2,45	xyloglucan:xyloglucosyl transferase, putative / xyloglucan endotransglycosylase, putative / endo-xyloglucan transferase, putative
AT5G37990	2,45	S-adenosylmethionine-dependent methyltransferase
AT4G29990	2,45	light repressible receptor protein kinase
AT2G29130	2,45	LAC2 (laccase 2); copper ion binding / oxidoreductase
AT1G07160	2,45	protein phosphatase 2C, putative / PP2C, putative
AT5G58690	2,45	phosphoinositide-specific phospholipase C family protein
AT2G44700	2,45	kelch repeat-containing F-box family protein
AT5G52320	2,45	CYP96A4 (cytochrome P450, family 96, subfamily A, polypeptide 4); oxygen binding
AT3G27950	2,45	early nodule-specific protein, putative
AT2G39330	2,45	jacalin lectin family protein
AT2G39850	2,41	subtilase
AT1G14880	2,41	similar to unknown protein [Arabidopsis thaliana] (TAIR:AT1G14870.1); similar to unnamed protein product [Vitis vinifera] (GB:CAO42338.1); similar to unnamed protein product [Vitis vinifera] (GB:CAO42335.1); contains InterPro domain Protein of unknown function Cys-rich (InterPro:IPR006461)
AT1G02390	2,41	ATGPAT2/GPAT2 (GLYCEROL-3-PHOSPHATE ACYLTRANSFERASE 2); acyltransferase
AT1G26390	2,41	FAD-binding domain-containing protein
AT5G23240	2,39	DNAJ heat shock N-terminal domain-containing protein
AT4G34510	2,39	KCS2 (3-ketoacyl-CoA synthase 2); acyltransferase
AT3G57630	2,39	exostosin family protein
AT3G04050	2,39	pyruvate kinase, putative
AT1G14680	2,39	similar to structural molecule [Arabidopsis thaliana] (TAIR:AT4G09060.1); similar to hypothetical protein [Vitis vinifera] (GB:CAN61579.1)

continued on next page

Table C.8 – continued from previous page

AGI code	FC	Gene description
AT1G01480	2,38	ACS2 (1-Amino-cyclopropane-1-carboxylate synthase 2)
AT3G25597	2,38	similar to unknown protein [Arabidopsis thaliana] (TAIR:AT1G26140.1)
AT3G51370	2,38	protein phosphatase 2C, putative / PP2C, putative
AT1G65510	2,38	similar to unknown protein [Arabidopsis thaliana] (TAIR:AT1G65490.1)
AT5G57220	2,38	CYP81F2 (cytochrome P450, family 81, subfamily F, polypeptide 2); oxygen binding
AT1G69050	2,38	unknown protein
AT1G51880	2,38	leucine-rich repeat protein kinase, putative
AT5G11210	2,36	ATGLR2.5 (Arabidopsis thaliana glutamate receptor 2.5)
AT5G07390	2,36	ATRBOHA (RESPIRATORY BURST OXIDASE HOMOLOG A); FAD binding / calcium ion binding / iron ion binding / oxidoreductase
AT3G52748	2,36	
AT2G38860	2,36	YLS5 (yellow-leaf-specific gene 5)
AT3G47780	2,36	ATATH6 (ABC2 homolog 6); ATPase, coupled to transmembrane movement of substances
AT2G32990	2,36	ATGH9B8 (ARABIDOPSIS THALIANA GLYCOSYL HYDROLASE 9B8); hydrolase, hydrolyzing O-glycosyl compounds
AT5G24090	2,35	acidic endochitinase (CHIB1)
AT1G61050	2,35	alpha 1,4-glycosyltransferase family protein / glycosyltransferase sugar-binding DXD motif-containing protein
AT2G23590	2,35	hydrolase, alpha/beta fold family protein
AT5G43580	2,35	serine-type endopeptidase inhibitor
AT2G17040	2,35	ANAC036 (Arabidopsis NAC domain containing protein 36); transcription factor
AT4G23140	2,33	CRK6 (CYSTEINE-RICH RLK 6); kinase
AT3G55150	2,33	ATEXO70H1 (exocyst subunit EXO70 family protein H1); protein binding
AT5G52760	2,33	heavy-metal-associated domain-containing protein
AT1G36640	2,33	similar to unknown protein [Arabidopsis thaliana] (TAIR:AT1G36622.1)
AT1G73120	2,33	similar to hypothetical protein [Vitis vinifera] (GB:CAN69175.1)
AT5G42930	2,33	triacylglycerol lipase
AT1G11160	2,33	nucleotide binding
AT4G15417	2,33	ribonuclease III family protein
AT3G48850	2,31	mitochondrial phosphate transporter, putative
AT4G37900	2,31	glycine-rich protein
AT5G42440	2,31	protein kinase family protein
AT1G72910	2,31	disease resistance protein (TIR-NBS class), putative
AT1G02520	2,31	PGP11 (P-GLYCOPROTEIN 11); ATPase, coupled to transmembrane movement of substances
AT4G00390	2,31	transcription regulator
AT5G40990	2,31	GLIP1 (GDSL LIPASE1); carboxylic ester hydrolase
AT1G56250	2,3	ATPP2-B14 (Phloem protein 2-B14); carbohydrate binding
AT1G17665	2,3	similar to CA-responsive protein [Brassica oleracea] (GB:ABB83615.1)
AT4G37990	2,28	ELI3-2 (ELICITOR-ACTIVATED GENE 3)
AT1G16640	2,28	transcriptional factor B3 family protein
AT4G21390	2,28	B120; protein kinase/ sugar binding
AT1G02360	2,28	chitinase, putative
AT4G01700	2,27	chitinase, putative
AT1G03220	2,27	extracellular dermal glycoprotein, putative / EDGP, putative

continued on next page

Table C.8 – continued from previous page

AGI code	FC	Gene description
AT2G05830	2,27	eukaryotic translation initiation factor 2B family protein / eIF-2B family protein
AT3G48280	2,27	CYP71A25 (cytochrome P450, family 71, subfamily A, polypeptide 25); oxygen binding
AT5G44350	2,25	ethylene-responsive nuclear protein -related
AT3G01175	2,25	similar to structural constituent of ribosome [Arabidopsis thaliana] (TAIR:AT5G39785.1); similar to structural constituent of ribosome [Arabidopsis thaliana] (TAIR:AT5G39785.2); similar to unnamed protein product [Vitis vinifera] (GB:CAO14994.1); contains InterPro domain Protein of unknown function DUF1666 (InterPro:IPR012870)
AT5G66630	2,25	LIM domain-containing protein
AT4G37170	2,25	pentatricopeptide (PPR) repeat-containing protein
AT5G51440	2,25	23.5 kDa mitochondrial small heat shock protein (HSP23.5-M)
AT2G20480	2,25	similar to unknown [Populus trichocarpa] (GB:ABK93010.1); similar to hypothetical protein OsI_030526 [Oryza sativa (indica cultivar-group)] (GB:EAZ09294.1); similar to Os09g0446000 [Oryza sativa (japonica cultivar-group)] (GB:NP_001063306.1)
AT3G13432	2,25	unknown protein
AT4G17490	2,25	ATERF6 (ETHYLENE RESPONSIVE ELEMENT BINDING FACTOR 6); DNA binding / transcription factor
AT3G63430	2,25	similar to unknown protein [Arabidopsis thaliana] (TAIR:AT1G18620.2); similar to unknown protein [Arabidopsis thaliana] (TAIR:AT1G18620.1); similar to unnamed protein product [Vitis vinifera] (GB:CAO22610.1)
AT2G47240	2,25	long-chain-fatty-acid-CoA ligase
AT2G18150	2,25	peroxidase, putative
AT2G46150	2,25	similar to unknown protein [Arabidopsis thaliana] (TAIR:AT3G54200.1); similar to plant cell wall protein SITFR88 [Lycopersicon esculentum] (GB:ABF39005.1); contains InterPro domain Harpin-induced 1 (InterPro:IPR010847)
AT5G10890	2,25	myosin heavy chain-related
AT2G43510	2,25	ATTI1 (ARABIDOPSIS THALIANA TRYPSIN INHIBITOR PROTEIN 1)
AT3G61028	2,23	similar to unknown protein [Arabidopsis thaliana] (TAIR:AT3G60940.1); similar to unnamed protein product [Vitis vinifera] (GB:CAO40196.1); contains InterPro domain Protein of unknown function DUF537 (InterPro:IPR007491)
AT5G64890	2,23	PROPEP2 (Elicitor peptide 2 precursor)
AT3G61185	2,23	
AT5G03860	2,23	malate synthase, putative
AT1G24140	2,23	matrixin family protein
AT3G04910	2,22	WNK1 (WITH NO LYSINE (K) 1); kinase
AT5G10210	2,22	similar to unknown protein [Arabidopsis thaliana] (TAIR:AT5G65030.1); similar to 80A08_18 [Brassica rapa subsp. pekinensis] (GB:AAZ67603.1); contains InterPro domain C2 calcium-dependent membrane targeting (InterPro:IPR000008)
AT1G09080	2,22	BIP3; ATP binding
AT1G47655	2,22	Dof-type zinc finger domain-containing protein
AT3G50260	2,22	ATERF#011/CEJ1 (COOPERATIVELY REGULATED BY ETHYLENE AND JASMONATE 1); DNA binding / transcription factor
AT4G04490	2,22	protein kinase family protein
AT1G30230	2,2	elongation factor 1-beta / EF-1-beta
AT3G50190	2,2	similar to unknown protein [Arabidopsis thaliana] (TAIR:AT3G50140.1); similar to unknown protein [Arabidopsis thaliana] (TAIR:AT3G50130.1); similar to unnamed protein product [Vitis vinifera] (GB:CAO71911.1); contains InterPro domain Protein of unknown function DUF247, plant (InterPro:IPR004158)
AT3G22640	2,2	cupin family protein
AT4G39580	2,2	kelch repeat-containing F-box family protein
AT3G62455	2,2	
AT3G09940	2,2	ATMDAR3/MDHAR (MONODEHYDROASCORBATE REDUCTASE); monodehydroascorbate reductase (NADH)

continued on next page

Table C.8 – continued from previous page

AGI code	FC	Gene description
AT5G16420	2,19	pentatricopeptide (PPR) repeat-containing protein
AT4G38070	2,19	bHLH family protein
AT1G14870	2,19	Identical to Uncharacterized protein At1g14870 [Arabidopsis thaliana] (GB:Q9LQU4); similar to unknown protein [Arabidopsis thaliana] (TAIR:AT5G35525.1); similar to unnamed protein product [Vitis vinifera] (GB:CAO42338.1); contains InterPro domain Aspartic acid and asparagine hydroxylation site (InterPro:IPR000152); contains InterPro domain Protein of unknown function Cys-rich (InterPro:IPR006461)
AT3G47070	2,19	similar to unknown [Populus trichocarpa] (GB:ABK95428.1)
AT5G25440	2,19	protein kinase family protein
AT1G73540	2,19	ATNUDT21 (Arabidopsis thaliana Nudix hydrolase homolog 21); hydrolase
AT3G24500	2,19	ATMBF1C/MBF1C (MULTIPROTEIN BRIDGING FACTOR 1C); DNA binding / transcription coactivator/ transcription factor
AT2G46400	2,19	WRKY46 (WRKY DNA-binding protein 46); transcription factor
AT1G68840	2,19	RAV2 (REGULATOR OF THE ATPASE OF THE VACUOLAR MEMBRANE); DNA binding / transcription factor
AT4G25020	2,19	KOW domain-containing protein / D111/G-patch domain-containing protein
AT2G14160	2,17	nucleic acid binding
AT3G25240	2,17	similar to unknown protein [Arabidopsis thaliana] (TAIR:AT3G07350.1); similar to unnamed protein product [Vitis vinifera] (GB:CAO39951.1); contains InterPro domain Protein of unknown function DUF506, plant (InterPro:IPR006502)
AT1G28480	2,17	GRX480; thiol-disulfide exchange intermediate
AT5G07780	2,17	formin homology 2 domain-containing protein / FH2 domain-containing protein
AT3G22910	2,17	calcium-transporting ATPase, plasma membrane-type, putative / Ca(2+)-ATPase, putative (ACA13)
AT4G11000	2,17	ankyrin repeat family protein
AT1G70650	2,17	zinc finger (Ran-binding) family protein
AT4G21380	2,16	ARK3 (Arabidopsis Receptor Kinase 3); kinase
AT4G23670	2,16	major latex protein-related / MLP-related
AT3G20810	2,16	transcription factor jumonji (jmjC) domain-containing protein
AT1G64170	2,16	ATCHX16 (CATION/H+ EXCHANGER 16); monovalent cation:proton antiporter
AT1G05000	2,14	tyrosine specific protein phosphatase family protein
AT1G17240	2,14	leucine-rich repeat family protein
AT2G30770	2,14	CYP71A13 (CYTOCHROME P450, FAMILY 71, SUBFAMILY A, POLYPEPTIDE 13); indoleacetaldoxime dehydratase/ oxygen binding
AT2G40120	2,14	protein kinase family protein
AT5G65670	2,14	IAA9 (indoleacetic acid-induced protein 9); transcription factor
AT2G40340	2,14	AP2 domain-containing transcription factor, putative (DRE2B)
AT2G37290	2,14	RabGAP/TBC domain-containing protein
AT4G25600	2,14	ShTK domain-containing protein
AT4G24310	2,14	similar to unknown protein [Arabidopsis thaliana] (TAIR:AT3G02430.1); similar to unnamed protein product [Vitis vinifera] (GB:CAO46970.1); contains InterPro domain Protein of unknown function DUF679 (InterPro:IPR007770)
AT1G78850	2,14	curculin-like (mannose-binding) lectin family protein
AT1G24150	2,13	ATFH4/FH4 (FORMIN HOMOLOGUE 4); actin binding / protein binding
AT1G09950	2,13	transcription factor-related
AT2G33760	2,13	pentatricopeptide (PPR) repeat-containing protein
AT5G24352	2,13	similar to unknown protein [Arabidopsis thaliana] (TAIR:AT1G64625.2); similar to expressed protein [Oryza sativa (japonica cultivar-group)] (GB:ABA96530.2); similar to hypothetical protein OsI_036304 [Oryza sativa (indica cultivar-group)] (GB:EAY82345.1); similar to unnamed protein product [Vitis vinifera] (GB:CAO70692.1); contains domain PTHR13902:SF5 (PTHR13902:SF5); contains domain PTHR13902 (PTHR13902)

continued on next page

Table C.8 – continued from previous page

AGI code	FC	Gene description
AT5G03680	2,13	PTL (PETAL LOSS); transcription factor
AT5G39020	2,13	protein kinase family protein
AT1G80120	2,13	similar to unknown protein [<i>Arabidopsis thaliana</i>] (TAIR:AT3G15810.1); similar to unknown [<i>Populus trichocarpa</i>] (GB:ABK95691.1); contains InterPro domain Protein of unknown function DUF567 (InterPro:IPR007612)
AT5G64110	2,13	peroxidase, putative
AT4G25110	2,13	ATMC2 (METACASPASE 2); caspase
AT2G24430	2,13	ANAC038/ANAC039; transcription factor
AT1G12670	2,11	
AT5G61890	2,11	AP2 domain-containing transcription factor family protein
AT5G41750	2,11	disease resistance protein (TIR-NBS-LRR class), putative
AT4G23220	2,11	protein kinase family protein
AT5G64120	2,11	peroxidase, putative
AT5G02490	2,11	heat shock cognate 70 kDa protein 2 (HSC70-2) (HSP70-2)
AT1G17147	2,1	similar to VQ motif-containing protein [<i>Arabidopsis thaliana</i>] (TAIR:AT1G78410.1); similar to Avr9/Cf-9 rapidly elicited protein 169 [<i>Nicotiana tabacum</i>] (GB:AAG43552.1); contains InterPro domain VQ (InterPro:IPR008889)
AT2G37040	2,1	PAL1 (PHE AMMONIA LYASE 1); phenylalanine ammonia-lyase
AT2G37750	2,1	unknown protein
AT4G20860	2,1	FAD-binding domain-containing protein
AT3G47220	2,1	phosphoinositide-specific phospholipase C family protein
AT1G51790	2,1	kinase
AT1G17870	2,1	ATEGY3
AT2G39210	2,08	nodulin family protein
AT4G24540	2,08	AGL24 (AGAMOUS-LIKE 24); protein binding / protein heterodimerization/ protein homodimerization/ transcription factor
AT1G72870	2,08	disease resistance protein (TIR-NBS class), putative
AT5G09800	2,08	U-box domain-containing protein
AT2G36780	2,08	UDP-glucuronosyl/UDP-glucosyl transferase family protein
AT1G78830	2,07	curculin-like (mannose-binding) lectin family protein
AT5G42330	2,07	similar to unnamed protein product [<i>Vitis vinifera</i>] (GB:CAO62026.1)
AT4G26200	2,07	ACS7 (1-Amino-cyclopropane-1-carboxylate synthase 7); 1-aminocyclopropane-1-carboxylate synthase
AT1G13480	2,07	similar to unknown protein [<i>Arabidopsis thaliana</i>] (TAIR:AT1G13520.1); similar to unnamed protein product [<i>Vitis vinifera</i>] (GB:CAO42040.1); contains InterPro domain Protein of unknown function DUF1262 (InterPro:IPR010683)
AT1G22890	2,07	unknown protein
AT1G07135	2,07	glycine-rich protein
AT1G65484	2,07	unknown protein
AT4G23190	2,07	CRK11 (CYSTEINE-RICH RLK11); kinase
AT5G61800	2,07	pentatricopeptide (PPR) repeat-containing protein
AT5G53200	2,07	TRY (TRIPTYCHON); DNA binding / transcription factor
AT5G05340	2,07	peroxidase, putative
AT2G31865	2,07	poly (ADP-ribose) glycohydrolase (PARG) family protein
AT2G31880	2,07	leucine-rich repeat transmembrane protein kinase, putative

continued on next page

Table C.8 – continued from previous page

AGI code	FC	Gene description
AT5G53110	2,06	similar to zinc finger (C3HC4-type RING finger) family protein [Arabidopsis thaliana] (TAIR:AT2G46495.1); similar to hypothetical protein [Vitis vinifera] (GB:CAN79324.1)
AT1G65845	2,06	unknown protein
AT5G52640	2,06	HSP81-1 (HEAT SHOCK PROTEIN 81-1); ATP binding / unfolded protein binding
AT4G01920	2,06	DC1 domain-containing protein
AT2G43000	2,06	ANAC042 (Arabidopsis NAC domain containing protein 42); transcription factor
AT5G14610	2,06	ATP binding / ATP-dependent helicase
AT4G14610	2,06	
AT2G42360	2,06	zinc finger (C3HC4-type RING finger) family protein
AT3G21080	2,06	ABC transporter-related
AT1G25220	2,04	ASB1 (ANTHRANILATE SYNTHASE BETA SUBUNIT 1); anthranilate synthase
AT3G11930	2,04	universal stress protein (USP) family protein
AT5G64510	2,04	similar to unnamed protein product [Vitis vinifera] (GB:CAO49799.1)
AT2G23530	2,04	similar to protein binding / zinc ion binding [Arabidopsis thaliana] (TAIR:AT4G37110.1); similar to unnamed protein product [Vitis vinifera] (GB:CAO44617.1)
AT2G19920	2,04	RNA-dependent RNA polymerase family protein
AT4G30670	2,04	contains domain PROKAR_LIPOPROTEIN (PS51257)
AT4G03460	2,04	ankyrin repeat family protein
AT5G01100	2,04	similar to unknown protein [Arabidopsis thaliana] (TAIR:AT2G37980.1); similar to unknown protein [Arabidopsis thaliana] (TAIR:AT3G54100.1); similar to unnamed protein product [Vitis vinifera] (GB:CAO15763.1); contains InterPro domain Protein of unknown function DUF246, plant (InterPro:IPR004348)
AT3G47180	2,04	zinc finger (C3HC4-type RING finger) family protein
AT4G05070	2,04	unknown protein
AT2G01830	2,04	WOL (WOODEN LEG)
AT3G51330	2,04	aspartyl protease family protein
AT4G37608	2,04	similar to hypothetical protein OsI_010192 [Oryza sativa (indica cultivar-group)] (GB:EAY88959.1); similar to hypothetical protein OsJ_009466 [Oryza sativa (japonica cultivar-group)] (GB:EAZ25983.1)
AT2G21090	2,03	pentatricopeptide (PPR) repeat-containing protein
AT1G35210	2,03	similar to unknown protein [Arabidopsis thaliana] (TAIR:AT1G22470.1); similar to hypothetical protein [Vitis vinifera] (GB:CAN82663.1)
AT1G10540	2,03	xanthine/uracil permease family protein
AT3G61280	2,03	similar to unknown protein [Arabidopsis thaliana] (TAIR:AT3G61290.1); similar to unnamed protein product [Vitis vinifera] (GB:CAO62793.1); contains InterPro domain Protein of unknown function DUF821, CAP10-like (InterPro:IPR008539); contains InterPro domain Lipopolysaccharide-modifying protein (InterPro:IPR006598)
AT5G12930	2,03	similar to unnamed protein product [Vitis vinifera] (GB:CAO21945.1); similar to hypothetical protein [Vitis vinifera] (GB:CAN80883.1)
AT1G14530	2,03	(TOM THREE HOMOLOG); virion binding
AT1G73210	2,01	similar to unknown protein [Arabidopsis thaliana] (TAIR:AT1G17830.1); similar to unnamed protein product [Vitis vinifera] (GB:CAO45300.1); contains InterPro domain Protein of unknown function DUF789 (InterPro:IPR008507)
AT5G38200	2,01	hydrolase
AT1G21120	2,01	O-methyltransferase, putative
AT5G49770	2,01	leucine-rich repeat transmembrane protein kinase, putative
AT3G29000	2	calcium-binding EF hand family protein
AT2G14100	2	CYP705A13 (cytochrome P450, family 705, subfamily A, polypeptide 13); oxygen binding
AT5G44480	2	DUR (DEFECTIVE UGE IN ROOT); catalytic
AT1G32950	2	subtilase family protein

continued on next page

Table C.8 – continued from previous page

AGI code	FC	Gene description
AT3G57540	2	remorin family protein
AT4G36988	2	CPuORF49 (Conserved peptide upstream open reading frame 49)
AT2G38823	2	similar to unknown protein [<i>Arabidopsis thaliana</i>] (TAIR:AT3G54520.1)
AT2G40850	2	phosphatidylinositol 3- and 4-kinase family protein

Table C.9: Down-regulated genes in *prl1* from the RNA-Seq analysis. The fold change (FC) cut-off is 0,5 and p-value<0,05.

AGI code	FC	Gene description
AT5G58140	0,01	PHOT2 (NON PHOTOTROPIC HYPOCOTYL 1-LIKE); kinase
AT5G64250	0,01	2-nitropropane dioxygenase family / NPD family
AT1G54410	0,01	dehydrin family protein
AT4G04640	0,02	ATPC1 (ATP synthase gamma chain 1)
AT3G02360	0,02	6-phosphogluconate dehydrogenase family protein
AT5G54940	0,03	eukaryotic translation initiation factor SUI1, putative
AT3G27380	0,03	SDH2-1 (succinate dehydrogenase 2-1)
AT3G49010	0,05	ATBBC1 (breast basic conserved 1); structural constituent of ribosome
AT2G01250	0,05	60S ribosomal protein L7 (RPL7B)
AT5G59030	0,06	COPT1 (COPPER TRANSPORTER 1); copper ion transmembrane transporter
AT3G53890	0,06	40S ribosomal protein S21 (RPS21B)
AT2G06520	0,07	PSBX (photosystem II subunit X)
AT3G58730	0,08	(VACUOLAR ATP SYNTHASE SUBUNIT D); ATPase, coupled to transmembrane movement of substances / hydrogen ion transporting ATPase, rotational mechanism
AT1G66240	0,08	ATX1; metal ion binding
AT4G15530	0,09	PPDK (PYRUVATE ORTHOPHOSPHATE DIKINASE); kinase/ pyruvate, phosphate dikinase
AT5G20710	0,1	BGAL7 (beta-galactosidase 7); beta-galactosidase
AT5G34800	0,12	
AT3G21055	0,12	PSBTN (photosystem II subunit T)
AT3G01345	0,14	Expressed protein
AT2G24360	0,16	serine/threonine/tyrosine kinase, putative
AT1G03070	0,16	glutamate binding /
AT2G37270	0,17	ATRPS5B (RIBOSOMAL PROTEIN 5B); structural constituent of ribosome
AT3G17390	0,18	MTO3 (S-adenosylmethionine synthase 3); methionine adenosyltransferase
AT5G43840	0,19	AT-HSFA6A (<i>Arabidopsis thaliana</i> heat shock transcription factor A6A); DNA binding / transcription factor
AT1G12900	0,19	GAPA-2
AT1G72610	0,19	GLP1 (GERMIN-LIKE PROTEIN 1); manganese ion binding / metal ion binding / nutrient reservoir
AT2G32700	0,2	WD-40 repeat family protein
AT3G29330	0,2	similar to hypothetical protein [<i>Vitis vinifera</i>] (GB:CAN68959.1); similar to unnamed protein product [<i>Vitis vinifera</i>] (GB:CAO15056.1)

continued on next page

Table C.9 – continued from previous page

AGI code	FC	Gene description
AT4G33170	0,21	pentatricopeptide (PPR) repeat-containing protein
AT3G10116	0,21	contains domain PD140986 (PD140986)
AT2G44910	0,21	homeobox-leucine zipper protein 4 (HB-4) / HD-ZIP protein 4
AT1G73400	0,21	pentatricopeptide (PPR) repeat-containing protein
AT1G27110	0,21	binding
AT3G50220	0,22	nucleic acid binding / pancreatic ribonuclease
AT2G45070	0,22	SEC61 BETA (suppressors of secretion-defective 61 Beta); protein transporter
AT5G08070	0,22	TCP17 (TCP domain protein 17); transcription factor
AT3G17130	0,23	invertase/pectin methylesterase inhibitor family protein
AT5G40600	0,23	similar to unknown protein [Arabidopsis thaliana] (TAIR:AT3G27420.1); similar to hypothetical protein [Vitis vinifera] (GB:CAN82033.1); similar to unnamed protein product [Vitis vinifera] (GB:CAO14664.1)
AT5G24410	0,24	glucosamine/galactosamine-6-phosphate isomerase-related
AT2G02020	0,24	proton-dependent oligopeptide transport (POT) family protein
AT1G03510	0,24	pentatricopeptide (PPR) repeat-containing protein
AT5G54370	0,24	late embryogenesis abundant protein-related / LEA protein-related
AT2G25670	0,24	similar to unknown protein [Arabidopsis thaliana] (TAIR:AT4G32610.1); similar to unnamed protein product [Vitis vinifera] (GB:CAO65578.1)
AT3G60550	0,24	CYCP3;2 (cyclin p3;2); cyclin-dependent protein kinase
AT1G16090	0,25	WAKL7 (WALL ASSOCIATED KINASE-LIKE 7)
AT1G04170	0,25	EIF2 GAMMA (eukaryotic translation initiation factor 2 gamma subunit); translation factor, nucleic acid binding
AT4G32280	0,25	IAA29 (indoleacetic acid-induced protein 29); transcription factor
AT3G47560	0,25	esterase/lipase/thioesterase family protein
AT1G29090	0,25	peptidase C1A papain family protein
AT2G20080	0,26	similar to unknown protein [Arabidopsis thaliana] (TAIR:AT4G28840.1); similar to unnamed protein product [Vitis vinifera] (GB:CAO65485.1)
AT5G50920	0,26	CLPC (HEAT SHOCK PROTEIN 93-V); ATP binding / ATPase
AT1G04840	0,26	pentatricopeptide (PPR) repeat-containing protein
AT1G75166	0,26	
AT2G22070	0,26	pentatricopeptide (PPR) repeat-containing protein
AT1G79330	0,27	AMC6/ATMC5/ATMCP2B (TYPE-II METACASPASES); caspase/ cysteine-type endopeptidase
AT1G55430	0,27	DC1 domain-containing protein
AT4G15393	0,27	CYP702A5 (cytochrome P450, family 702, subfamily A, polypeptide 5); heme binding / iron ion binding / monooxygenase
AT5G24140	0,27	SQP2 (Squalene monooxygenase 2); oxidoreductase
AT5G63240	0,27	glycosyl hydrolase family protein 17
AT1G15870	0,28	mitochondrial glycoprotein family protein / MAM33 family protein
AT3G52530	0,28	protein kinase family protein
AT2G35210	0,28	AGD10/MEE28/RPA (MATERNAL EFFECT EMBRYO ARREST 28); DNA binding
AT5G37410	0,28	binding
AT3G21950	0,28	S-adenosyl-L-methionine:carboxyl methyltransferase family protein
AT2G43290	0,29	MSS3 (MULTICOPY SUPPRESSORS OF SNF4 DEFICIENCY IN YEAST 3); calcium ion binding
AT1G01090	0,29	PDH-E1 ALPHA (PYRUVATE DEHYDROGENASE E1 ALPHA); pyruvate dehydrogenase (acetyl-transferring)
AT1G04180	0,29	flavin-containing monooxygenase family protein / FMO family protein
AT1G73965	0,29	CLE13 (CLAVATA3/ESR-RELATED 13); receptor binding

continued on next page

Table C.9 – continued from previous page

AGI code	FC	Gene description
AT1G62520	0,29	similar to unknown protein [Arabidopsis thaliana] (TAIR:AT4G22560.1); similar to AT1G62520 [Arabidopsis lyrata subsp. petraea] (GB:AAT72492.1); contains domain ADP-ribosylation (SSF56399)
AT5G35375	0,29	unknown protein
AT4G31370	0,29	FLA5 (FASCICLIN-LIKE ARABINOGALACTAN PROTEIN 5 PRECURSOR)
AT3G25590	0,29	similar to unnamed protein product [Vitis vinifera] (GB:CAO42037.1)
AT4G24110	0,29	similar to unnamed protein product [Vitis vinifera] (GB:CAO62924.1)
AT4G38390	0,3	similar to unknown protein [Arabidopsis thaliana] (TAIR:AT1G76270.1); similar to axi 1 [Nicotiana tabacum] (GB:CAA56570.1); similar to unnamed protein product [Vitis vinifera] (GB:CAO47467.1); contains InterPro domain Protein of unknown function DUF246, plant (InterPro:IPR004348)
AT5G04660	0,3	CYP77A4 (cytochrome P450, family 77, subfamily A, polypeptide 4); oxygen binding
AT2G42640	0,3	ATP binding / protein kinase/ protein serine/threonine kinase/ protein-tyrosine kinase
AT4G36925	0,3	similar to unknown protein [Arabidopsis thaliana] (TAIR:AT2G24945.1)
AT1G66810	0,3	zinc finger (CCCH-type) family protein
AT5G40290	0,3	metal-dependent phosphohydrolase HD domain-containing protein
AT1G42560	0,31	ATMLO9/MLO9 (MILDEW RESISTANCE LOCUS O 9); calmodulin binding
AT5G37180	0,31	SUS5; UDP-glycosyltransferase/ sucrose synthase
AT1G58320	0,31	similar to unknown protein [Arabidopsis thaliana] (TAIR:AT5G35525.1); similar to unnamed protein product [Vitis vinifera] (GB:CAO42113.1); contains InterPro domain Protein of unknown function Cys-rich (InterPro:IPR006461)
AT5G45540	0,31	similar to unknown protein [Arabidopsis thaliana] (TAIR:AT5G45470.1); similar to unknown protein [Arabidopsis thaliana] (TAIR:AT5G45530.1); similar to unknown protein [Arabidopsis thaliana] (TAIR:AT5G45480.1); similar to hypothetical protein [Vitis vinifera] (GB:CAN75530.1); contains InterPro domain Protein of unknown function DUF594 (InterPro:IPR007658)
AT1G10550	0,31	XTH33 (xyloglucan:xyloglucosyl transferase 33); hydrolase, acting on glycosyl bonds
AT1G79480	0,31	similar to glycosyl hydrolase family protein 17 [Arabidopsis thaliana] (TAIR:AT5G67460.1); similar to hypothetical protein [Vitis vinifera] (GB:CAN78496.1); contains InterPro domain X8 (InterPro:IPR012946)
AT3G29010	0,32	catalytic
AT3G43850	0,32	similar to unknown protein [Arabidopsis thaliana] (TAIR:AT5G21940.1); similar to unknown [Populus trichocarpa] (GB:ABK93792.1)
AT3G57670	0,32	NTT (NO TRANSMITTING TRACT); nucleic acid binding / transcription factor/ zinc ion binding
AT5G20650	0,32	COPT5 (copper transporter 5); copper ion transmembrane transporter
AT5G51060	0,32	RHD2 (ROOT HAIR DEFECTIVE 2)
AT5G61865	0,32	similar to hypothetical protein [Vitis vinifera] (GB:CAN73072.1)
AT1G70440	0,32	SRO3 (SIMILAR TO RCD ONE 3); NAD+ ADP-ribosyltransferase
AT1G28080	0,32	similar to unknown protein [Arabidopsis thaliana] (TAIR:AT5G13250.1); similar to unnamed protein product [Vitis vinifera] (GB:CAO70056.1); contains domain RING FINGER PROTEIN (PTHR10825:SF1); contains domain RING FINGER PROTEIN (PTHR10825)
AT1G70470	0,32	similar to unknown protein [Arabidopsis thaliana] (TAIR:AT1G23530.1)
AT1G31720	0,32	similar to unknown protein [Arabidopsis thaliana] (TAIR:AT4G19370.1); similar to unknown [Picea sitchensis] (GB:ABK21519.1); similar to Os02g0703300 [Oryza sativa (japonica cultivar-group)] (GB:NP_001047854.1); contains InterPro domain Protein of unknown function DUF1218 (InterPro:IPR009606)
AT1G33110	0,32	MATE efflux family protein
AT1G77700	0,33	pathogenesis-related thaumatin family protein
AT4G36530	0,33	hydrolase, alpha/beta fold family protein
AT1G48325	0,33	Expressed protein
AT2G34210	0,33	transcription initiation factor
AT1G49570	0,33	peroxidase, putative

continued on next page

Table C.9 – continued from previous page

AGI code	FC	Gene description
AT2G16140	0,33	
AT5G46900	0,33	protease inhibitor/seed storage/lipid transfer protein (LTP) family protein
AT4G23240	0,33	protein kinase family protein
AT1G54095	0,34	similar to unknown protein [Arabidopsis thaliana] (TAIR:AT1G72510.1); similar to unknown protein [Arabidopsis thaliana] (TAIR:AT1G72510.2); similar to hypothetical protein [Vitis vinifera] (GB:CAN73516.1); contains InterPro domain Protein of unknown function DUF1677, plant (InterPro:IPR012876)
AT2G45040	0,34	matrix metalloproteinase
AT4G33330	0,34	PGSIP3 (PLANT GLYCOGENIN-LIKE STARCH INITIATION PROTEIN 3); transferase, transferring glycosyl groups
AT4G15500	0,35	UGT84A4; UDP-glycosyltransferase/ sinapate 1-glycosyltransferase/ transferase, transferring glycosyl groups / transferase, transferring hexosyl groups
AT1G54630	0,35	ACP3 (ACYL CARRIER PROTEIN 3)
AT3G10740	0,35	ASD1 (ALPHA-L-ARABINOFURANOSIDASE); hydrolase, acting on glycosyl bonds
AT1G04880	0,35	high mobility group (HMG1/2) family protein / ARID/BRIGHT DNA-binding domain-containing protein
AT2G47110	0,36	UBQ6 (ubiquitin 6); protein binding
AT5G1650	0,36	CYCP4;2 (CYCLIN P4;2); cyclin-dependent protein kinase
AT1G71050	0,36	heavy-metal-associated domain-containing protein / copper chaperone (CCH)-related
AT4G03520	0,36	ATHM2 (Arabidopsis thioredoxin M-type 2); thiol-disulfide exchange intermediate
AT5G42510	0,36	disease resistance-responsive family protein
AT5G49620	0,36	AtMYB78 (myb domain protein 78); DNA binding / transcription factor
AT5G04210	0,36	RNA recognition motif (RRM)-containing protein
AT2G28160	0,36	ATBHLH029/BHLH029/FIT1/FRU (FE-DEFICIENCY INDUCED TRANSCRIPTION FACTOR 1); DNA binding / transcription factor
AT3G28510	0,36	AAA-type ATPase family protein
AT3G25795	0,36	
AT2G42260	0,36	UVI4 (UV-B-INSENSITIVE 4)
AT4G18375	0,36	KH domain-containing protein
AT4G16990	0,36	disease resistance protein (TIR-NBS class), putative
AT2G16570	0,36	ATASE (GLN PHOSPHORIBOSYL PYROPHOSPHATE AMIDOTRANSFERASE 1); amidophosphoribosyltransferase
AT5G04690	0,37	similar to unknown protein [Arabidopsis thaliana] (TAIR:AT5G04700.1); similar to unknown protein [Arabidopsis thaliana] (TAIR:AT5G04680.1); similar to unnamed protein product [Vitis vinifera] (GB:CAO64101.1); contains InterPro domain Ankyrin (InterPro:IPR002110)
AT3G18300	0,37	similar to unknown protein [Arabidopsis thaliana] (TAIR:AT1G48780.1); similar to hypothetical protein [Vitis vinifera] (GB:CAN62793.1)
AT3G25510	0,37	disease resistance protein (TIR-NBS-LRR class), putative
AT3G12345	0,37	similar to Os06g0484500 [Oryza sativa (japonica cultivar-group)] (GB:NP_001057659.1); similar to hypothetical protein OsI_022208 [Oryza sativa (indica cultivar-group)] (GB:EAZ00976.1); contains domain Chlorophyll a-b binding protein (SSF103511)
AT1G71740	0,37	similar to unknown protein [Arabidopsis thaliana] (TAIR:AT3G18560.1); similar to hypothetical protein [Vitis vinifera] (GB:CAN60388.1)
AT3G06778	0,37	heat shock protein binding / unfolded protein binding
AT4G34810	0,37	auxin-responsive family protein
AT5G16250	0,37	similar to unknown protein [Arabidopsis thaliana] (TAIR:AT3G02640.1); similar to unnamed protein product [Vitis vinifera] (GB:CAO50168.1)
AT2G22821	0,37	
AT4G14723	0,37	similar to allergen-related [Arabidopsis thaliana] (TAIR:AT3G22820.1); similar to unnamed protein product [Vitis vinifera] (GB:CAO71224.1)
AT1G20470	0,37	auxin-responsive family protein
AT3G18490	0,38	aspartyl protease family protein
AT5G61950	0,38	ubiquitin carboxyl-terminal hydrolase-related
AT1G25360	0,38	pentatricopeptide (PPR) repeat-containing protein

continued on next page

Table C.9 – continued from previous page

AGI code	FC	Gene description
AT1G21000	0,38	zinc-binding family protein
AT2G19380	0,38	RNA recognition motif (RRM)-containing protein
AT3G48550	0,39	similar to ATIDD15/SGR5 (ARABIDOPSIS THALIANA INDETERMINATE(ID)-DOMAIN 15, SHOOT GRAVITROPISM 5), nucleic acid binding / transcription factor/ zinc ion binding [Arabidopsis thaliana] (TAIR:AT2G01940.1); similar to ATIDD15/SGR5 (ARABIDOPSIS THALIANA INDETERMINATE(ID)-DOMAIN 15, SHOOT GRAVITROPISM 5), nucleic acid binding / zinc ion binding [Arabidopsis thaliana] (TAIR:AT2G01940.2); similar to ATIDD15/SGR5 (ARABIDOPSIS THALIANA INDETERMINATE(ID)-DOMAIN 15, SHOOT GRAVITROPISM 5) [Arabidopsis thaliana] (TAIR:AT2G01940.3); similar to hypothetical protein [Vitis vinifera] (GB:CAN68393.1)
AT5G55250	0,39	IAMT1 (IAA CARBOXYLMETHYLTRANSFERASE 1); S-adenosylmethionine-dependent methyltransferase
AT5G27890	0,39	similar to myosin heavy chain-related [Arabidopsis thaliana] (TAIR:AT2G15420.1)
AT5G47430	0,39	similar to unknown protein [Arabidopsis thaliana] (TAIR:AT4G17410.1); similar to hypothetical protein 31.t00039 [Brassica oleracea] (GB:ABD65123.1); similar to hypothetical protein [Vitis vinifera] (GB:CAN68806.1); similar to hypothetical protein 24.t00020 [Brassica oleracea] (GB:ABD64942.1); contains InterPro domain DWNN domain (InterPro:IPR014891); contains InterPro domain Zinc finger, RING/FYVE/PHD-type (InterPro:IPR013083)
AT2G15300	0,39	leucine-rich repeat transmembrane protein kinase, putative
AT4G15396	0,39	CYP702A6 (cytochrome P450, family 702, subfamily A, polypeptide 6); heme binding / iron ion binding / monooxygenase
AT1G52343	0,39	unknown protein
AT2G45660	0,39	AGL20 (AGAMOUS-LIKE 20); transcription factor
AT5G57320	0,39	villin, putative
AT2G05140	0,4	phosphoribosylaminoimidazole carboxylase family protein / AIR carboxylase family protein
AT1G09570	0,4	PHYA (PHYTOCHROME A); G-protein coupled photoreceptor/ signal transducer
AT2G34440	0,4	AGL29; transcription factor
AT1G78260	0,4	RNA recognition motif (RRM)-containing protein
AT5G57180	0,4	CIA2 (CHLOROPLAST IMPORT APPARATUS 2)
AT1G79220	0,4	mitochondrial transcription termination factor family protein / mTERF family protein
AT1G52570	0,41	PLDALPHA2 (PHOSPHOLIPASE D ALPHA 2); phospholipase D
AT1G53680	0,41	ATGSTU28 (Arabidopsis thaliana Glutathione S-transferase (class tau) 28); glutathione transferase
AT5G52170	0,41	HDG7 (HOMEODOMAIN GLABROUS7); DNA binding / sequence-specific DNA binding / transcription factor
AT1G55330	0,41	AGP21 (ARABINOGALACTAN PROTEIN 21)
AT2G41342	0,41	similar to unknown [Picea sitchensis] (GB:ABK27016.1)
AT1G01580	0,41	FRO2 (FERRIC REDUCTION OXIDASE 2); ferric-chelate reductase
AT1G19510	0,42	myb family transcription factor
AT3G08570	0,42	phototropic-responsive protein, putative
AT1G29610	0,42	similar to zinc finger protein-related [Arabidopsis thaliana] (TAIR:AT1G29570.1)
AT2G35945	0,42	
AT5G23320	0,42	ATSTE14 (PRENYLCYSTEINE ALPHA-CARBOXYL METHYLTRANSFERASE 14A); protein-S-isoprenylcysteine O-methyltransferase
AT4G33150	0,42	LKR (SACCHAROPINE DEHYDROGENASE)
AT2G27430	0,42	binding
AT2G16870	0,42	disease resistance protein (TIR-NBS-LRR class), putative
AT1G56130	0,42	leucine-rich repeat family protein / protein kinase family protein
AT1G02060	0,42	pentatricopeptide (PPR) repeat-containing protein
AT1G55940	0,42	CYP708A1 (cytochrome P450, family 708, subfamily A, polypeptide 1); oxygen binding
AT5G21105	0,42	L-ascorbate oxidase/ copper ion binding

continued on next page

Table C.9 – continued from previous page

AGI code	FC	Gene description
AT4G33730	0,42	pathogenesis-related protein, putative
AT3G54810	0,42	BME3/BME3-ZF (BLUE MICROPYLAR END3); transcription factor
AT2G45280	0,42	ATRAD51C (Arabidopsis thaliana Ras Associated with Diabetes protein 51C); ATP binding / damaged DNA binding
AT2G20800	0,43	NDB4 (NAD(P)H DEHYDROGENASE B4); NADH dehydrogenase
AT4G40010	0,43	SNRK2-7/SNRK2.7/SRK2F (SNF1-RELATED PROTEIN KINASE 2.7); kinase
AT4G26800	0,43	pentatricopeptide (PPR) repeat-containing protein
AT5G45830	0,43	DOG1 (DELAY OF GERMINATION 1)
AT1G63580	0,43	protein kinase-related
AT3G60140	0,43	DIN2 (DARK INDUCIBLE 2); hydrolase, hydrolyzing O-glycosyl compounds
AT1G67280	0,43	lactoylglutathione lyase, putative / glyoxalase I, putative
AT5G60730	0,44	anion-transporting ATPase family protein
AT4G30975	0,44	
AT4G33030	0,44	SQD1 (sulfoquinovosyldiacylglycerol 1); UDPsulfoquinovose synthase
AT5G56720	0,44	malate dehydrogenase, cytosolic, putative
AT2G04460	0,44	
AT4G02960	0,44	
AT3G02850	0,44	SKOR (stelar K+ outward rectifier); cyclic nucleotide binding / outward rectifier potassium channel
AT1G71930	0,44	VND7 (VASCULAR RELATED NAC-DOMAIN PROTEIN 7); transcription factor
AT4G16020	0,44	
AT5G54148	0,44	
AT5G59020	0,44	similar to unknown protein [Arabidopsis thaliana] (TAIR:AT2G29510.1); similar to hypothetical protein [Vitis vinifera] (GB:CAN70168.1); contains InterPro domain Tubby, C-terminal (InterPro:IPR000007)
AT2G46970	0,44	PIL1 (PHYTOCHROME INTERACTING FACTOR 3-LIKE 1); transcription factor
AT3G47790	0,45	ATATH7 (ABC2 homolog 7); ATPase, coupled to transmembrane movement of substances
AT1G03300	0,45	agenet domain-containing protein
AT1G30940	0,45	
AT2G13360	0,45	AGT (ALANINE:GLYOXYLATE AMINOTRANSFERASE)
AT2G06002	0,45	
AT1G63320	0,45	pentatricopeptide (PPR) repeat-containing protein
AT1G62510	0,45	protease inhibitor/seed storage/lipid transfer protein (LTP) family protein
AT5G65040	0,45	senescence-associated protein-related
AT1G78530	0,46	protein kinase family protein
AT5G44578	0,46	unknown protein
AT3G61950	0,46	basic helix-loop-helix (bHLH) family protein
AT1G11320	0,46	similar to unnamed protein product [Vitis vinifera] (GB:CAO60944.1)
AT1G48000	0,46	MYB112 (myb domain protein 112); DNA binding / transcription factor
AT5G66000	0,46	unknown protein
AT1G77870	0,46	MUB5 (MEMBRANE-ANCHORED UBIQUITIN-FOLD PROTEIN 5 PRECURSOR)
AT1G70360	0,46	F-box protein-related
AT5G59900	0,46	pentatricopeptide (PPR) repeat-containing protein
AT5G56990	0,47	similar to cysteine protease inhibitor [Arabidopsis thaliana] (TAIR:AT5G56910.1); contains InterPro domain Cystatin-related, plant (InterPro:IPR006525)

continued on next page

Table C.9 – continued from previous page

AGI code	FC	Gene description
AT5G53750	0,47	similar to CBS domain-containing protein [Arabidopsis thaliana] (TAIR:AT4G27460.1); similar to unnamed protein product [Vitis vinifera] (GB:CAO16914.1); contains InterPro domain Cystathionine beta-synthase, core (InterPro:IPR000644)
AT4G11210	0,47	disease resistance-responsive family protein / dirigent family protein
AT3G04040	0,47	similar to unknown protein [Arabidopsis thaliana] (TAIR:AT5G18250.1); similar to unnamed protein product [Vitis vinifera] (GB:CAO23501.1)
AT1G74810	0,47	BOR5; anion exchanger
AT2G25770	0,47	similar to unknown protein [Arabidopsis thaliana] (TAIR:AT4G32870.1); similar to hypothetical protein [Vitis vinifera] (GB:CAN83252.1); contains domain SSF55961 (SSF55961)
AT2G42660	0,47	myb family transcription factor
AT3G30720	0,47	unknown protein
AT1G77850	0,47	ARF17 (AUXIN RESPONSE FACTOR 17); transcription factor
AT4G02620	0,47	(VACUOLAR ATPASE SUBUNIT F); hydrogen ion transporting ATP synthase, rotational mechanism / hydrogen ion transporting ATPase, rotational mechanism
AT1G77390	0,47	CYCA1;2 (CYCLIN A1;2); cyclin-dependent protein kinase regulator
AT5G02080	0,47	DNA/panthothenate metabolism flavoprotein family protein
AT4G27290	0,47	S-locus protein kinase, putative
AT4G31180	0,48	aspartyl-tRNA synthetase, putative / aspartate-tRNA ligase, putative
AT2G19830	0,48	SNF7.2
AT5G48060	0,48	C2 domain-containing protein
AT1G74580	0,48	pentatricopeptide (PPR) repeat-containing protein
AT3G11410	0,48	AHG3/ATPP2CA (ARABIDOPSIS THALIANA PROTEIN PHOSPHATASE 2CA); protein binding / protein serine/threonine phosphatase
AT2G37320	0,48	pentatricopeptide (PPR) repeat-containing protein
AT3G26350	0,48	similar to unknown protein [Arabidopsis thaliana] (TAIR:AT1G13050.1); similar to hypothetical protein [Vitis vinifera] (GB:CAN70940.1); similar to unnamed protein product [Vitis vinifera] (GB:CAO66828.1); contains InterPro domain Harpin-induced 1 (InterPro:IPR010847)
AT2G12490	0,48	
AT3G29280	0,48	similar to unknown [Populus trichocarpa] (GB:ABK93016.1)
AT1G48780	0,48	similar to unknown protein [Arabidopsis thaliana] (TAIR:AT3G18300.1); similar to unnamed protein product [Vitis vinifera] (GB:CAO42164.1)
AT3G05240	0,48	pentatricopeptide (PPR) repeat-containing protein
AT3G62050	0,48	similar to EDA32 (embryo sac development arrest 32) [Arabidopsis thaliana] (TAIR:AT3G62210.1); similar to unnamed protein product [Vitis vinifera] (GB:CAO17351.1); contains InterPro domain Protein of unknown function DUF537 (InterPro:IPR007491)
AT5G51451	0,48	unknown protein
AT1G70410	0,48	carbonic anhydrase, putative / carbonate dehydratase, putative
AT1G19480	0,49	HhH-GPD base excision DNA repair family protein
AT5G60660	0,49	PIP2;4/PIP2F (plasma membrane intrinsic protein 2;4); water channel
AT2G41800	0,49	similar to unknown protein [Arabidopsis thaliana] (TAIR:AT2G41810.1); similar to unnamed protein product [Vitis vinifera] (GB:CAO23583.1); similar to hypothetical protein [Vitis vinifera] (GB:CAN80832.1); contains InterPro domain Protein of unknown function DUF642 (InterPro:IPR006946); contains InterPro domain Galactose-binding like (InterPro:IPR008979)
AT1G56670	0,49	GDSL-motif lipase/hydrolase family protein
AT1G04425	0,49	
AT1G79460	0,49	GA2 (GA REQUIRING 2); ent-kaurene synthase
AT4G16780	0,49	ATHB-2 (ARABIDOPSIS THALIANA HOMEBOX PROTEIN 2); DNA binding / transcription factor
AT5G66700	0,49	HB53 (homeobox-8); DNA binding / transcription factor
AT4G13990	0,49	exostosin family protein

continued on next page

Table C.9 – continued from previous page

AGI code	FC	Gene description
AT4G15210	0,49	ATBETA-AMY (BETA-AMYLASE); beta-amylase
AT4G36690	0,49	ATU2AF65A; RNA binding
AT3G13061	0,49	
AT4G28690	0,49	similar to RIN13 (RPM1 INTERACTING PROTEIN 13) [Arabidopsis thaliana] (TAIR:AT2G20310.1); similar to unnamed protein product [Vitis vinifera] (GB:CAO40534.1)
AT5G51550	0,49	phosphate-responsive 1 family protein
AT5G16600	0,49	MYB43 (myb domain protein 43); DNA binding / transcription factor
AT3G53170	0,49	pentatricopeptide (PPR) repeat-containing protein
AT4G28530	0,5	ANAC074 (Arabidopsis NAC domain containing protein 74); transcription factor
AT4G30130	0,5	similar to unknown protein [Arabidopsis thaliana] (TAIR:AT2G19090.1); similar to hypothetical protein [Vitis vinifera] (GB:CAN72045.1); contains InterPro domain Protein of unknown function DUF632 (InterPro:IPR006867); contains InterPro domain Protein of unknown function DUF630 (InterPro:IPR006868)
AT1G53500	0,5	MUM4 (MUCILAGE-MODIFIED 4); catalytic
AT1G33050	0,5	similar to unknown protein [Arabidopsis thaliana] (TAIR:AT4G10470.1)
AT3G06030	0,5	ANP3 (Arabidopsis NPK1-related protein kinase 3); kinase
AT5G18840	0,5	sugar transporter, putative
AT3G30841	0,5	2,3-biphosphoglycerate-independent phosphoglycerate mutase-related / phosphoglyceromutase-related
AT2G14580	0,5	ATPRB1 (Arabidopsis thaliana basic pathogenesis-related protein 1)
AT3G15510	0,5	ATNAC2 (Arabidopsis thaliana NAC domain containing protein 2); transcription factor
AT2G20515	0,5	similar to unnamed protein product [Vitis vinifera] (GB:CAO40634.1)
AT5G52120	0,5	ATPP2-A14 (Phloem protein 2-A14); carbohydrate binding
AT5G46800	0,5	BOU (A BOUT DE SŒUFFLE); binding

Table C.10: Pair-wise comparison of **up**- and **down**-regulated genes from the ER-PRL1/*prl1* samples. Data was generated with the GeneSpring GX v10.0 Expression Analysis suite (Agilent Technologies, Waldbronn) and the output was *manually sorted* by Dr. Csaba Koncz. Values are expressed in raw fold change.

AGI code	Gene description	0,1 % sucrose				3 % sucrose			
		root		shoot		root		shoot	
		d ₃ /d ₀	d ₄ /d ₀	d ₃ /d ₀	d ₄ /d ₀	d ₃ /d ₀	d ₄ /d ₀	d ₃ /d ₀	d ₄ /d ₀
AT4G15900	PRL1 (PLEIOTROPIC REGULATORY LOCUS 1); basal transcription repressor/ nucleotide binding / protein binding	14,19	17,97	6,83	22,66			1,93	2,14
Light regulation									
AT3G17609	HYH (HY5-HOMOLOG); DNA binding / transcription factor			1,8					2,54
AT5G58140	PHOT2 (PHOTOTROPIN 2); FMN binding / blue light photoreceptor/ kinase/ protein serine/threonine kinase				1,64				
AT1G02340	HFR1 (LONG HYPOCOTYL IN FAR-RED); DNA binding / protein binding / transcription factor				2,39				
AT4G38620	MYB4; DNA binding / transcription factor				1,64				
AT2G20180	PIL5 (PHYTOCHROME INTERACTING FACTOR 3-LIKE 5); DNA binding / phytochrome binding / transcription factor				2,06				
AT5G47800	phototropic-responsive NPH3 family protein				2,23				
AT1G03010	phototropic-responsive NPH3 family protein				2,12				
AT3G22104	phototropic-responsive NPH3 protein-related				1,52				
AT3G08660	phototropic-responsive protein, putative				1,93				
AT5G24850	CRY3 (cryptochrome 3); DNA binding / DNA photolyase/ FMN binding			2,01					
AT3G19850	phototropic-responsive NPH3 family protein				1,61				
AT1G34760	GRF11 (GENERAL REGULATORY FACTOR 11); ATPase binding / amino acid binding / protein binding / protein phosphorylated amino acid binding	2,07	1,64		2,32				
AT2G42610	LSH10 (LIGHT SENSITIVE HYPOCOTYLS 10)			1,82	10,21				
AT2G31160	LSH3 (LIGHT SENSITIVE HYPOCOTYLS 3)				3,67				
AT5G58500	LSH5 (LIGHT SENSITIVE HYPOCOTYLS 5)				1,79				
AT2G02710	PLPB (PAS/LOV PROTEIN B); signal transducer/ two-component sensor				1,91				
AT4G01120	GBF2 (G-BOX BINDING FACTOR 2); DNA binding / sequence-specific DNA binding / transcription factor	1,52							
AT3G09150	HY2 (ELONGATED HYPOCOTYL 2); phytochromobilin-ferredoxin oxidoreductase				1,56				
AT1G78600	LZF1 (LIGHT-REGULATED ZINC FINGER PROTEIN 1); transcription factor/zinc ion binding				7,79				
AT2G42870	PAR1 (PHY RAPIDLY REGULATED 1)								3,43
Circadian clock									
AT2G46830	CCA1 (CIRCADIAN CLOCK ASSOCIATED 1); DNA binding / transcription activator/ transcription factor/ transcription repressor				1,9	17,53	14,79	2,12	2,88
AT1G01060	LHY (LATE ELONGATED HYPOCOTYL); DNA binding / transcription factor				2,68			3,06	2,49

continued on next page

Table C.10 — continued from previous page

AGI code	Gene description	0,1 % sucrose				3 % sucrose				
		root		shoot		root		shoot		
		d ³ /d ₀	d ⁴ /d ₀	d ³ /d ₀	d ⁴ /d ₀	d ³ /d ₀	d ⁴ /d ₀	d ³ /d ₀	d ⁴ /d ₀	
AT5G37260	RVE2 (REVELLE 2); DNA binding / transcription factor	2,28	2,96						6,61	
AT1G72630	ELF4-L2 (ELF4-Like 2)				1,52					
AT3G22231	PCC1 (PATHOGEN AND CIRCADIAN CONTROLLED 1)			2,29	11,96					
AT4G18020	APRR2; transcription factor/ two-component response regulator				2,1					
AT5G02840	LCL1 (LHY/CCA1-like 1); DNA binding / transcription factor	1,7	1,72	1,51						
AT2G21660	CCR2 (COLD, CIRCADIAN RHYTHM, AND RNA BINDING 2); RNA binding / double-stranded DNA binding / single-stranded DNA binding				3,56				4,34	
AT5G60100	APRR3 (ARABIDOPSIS PSEUDO-RESPONSE REGULATOR 3); transcription regulator/ two-component response regulator	1,74	1,86		2,16					
AT5G24470	APRR5 (ARABIDOPSIS PSEUDO-RESPONSE REGULATOR 5); transcription regulator/ two-component response regulator		1,9	1,66	20,18				4,36	
AT5G02810	PRR7 (PSEUDO-RESPONSE REGULATOR 7); transcription regulator/ two-component response regulator				2,61					
AT2G25930	ELF3 (EARLY FLOWERING 3); protein C-terminus binding / transcription factor	1,63	1,98		1,96					
AT2G40080	ELF4 (EARLY FLOWERING 4)	3,18	2,99							
AT1G22770	GI (GIGANTEA)				2,2				2,64	
AT3G26740	CCL (CCR-LIKE)	1,87	2,75		2,39				2,95	
AT3G46640	LUX ARRHYTHMO	2,81	2,57		3,17					
Flowering time										
AT2G27550	ATC (ARABIDOPSIS THALIANA CENTRORADIALIS); phosphatidylethanolamine binding	1,98	2,04							
AT4G24540	AGL24 (AGAMOUS-LIKE 24); protein binding / protein heterodimerization/ protein homodimerization/ sequence-specific DNA binding / transcription factor				3,71					
AT5G15850	COL1 (constans-like 1); transcription factor/ zinc ion binding								2,7	
AT3G02380	COL2 (constans-like 2); transcription factor/ zinc ion binding				1,54			1,52	3,04	
AT2G24790	COL3 (CONSTANS-LIKE 3); protein binding / transcription factor/ zinc ion binding				1,89					
AT5G62430	CDF1 (CYCLING DOF FACTOR 1); DNA binding / protein binding / transcription factor								2,95	
AT5G39660	CDF2 (CYCLING DOF FACTOR 2); DNA binding / protein binding / transcription factor	1,59	1,91		1,9				2,58	
AT1G69570	Dof-type zinc finger domain-containing protein								2,19	
AT1G29160	Dof-type zinc finger domain-containing protein				1,54					
AT1G64620	Dof-type zinc finger domain-containing protein							1,62		
AT2G33810	SPL3 (SQUAMOSA PROMOTER BINDING PROTEIN-LIKE 3); DNA binding / transcription factor				3,25					
AT2G45660	AGL20 (AGAMOUS-LIKE 20); transcription factor				2,68					
AT1G65480	FT (FLOWERING LOCUS T); phosphatidylethanolamine binding / protein binding				2,06					
AT3G07650	COL9 (CONSTANS-LIKE 9); transcription factor/ zinc ion binding	1,84	1,79	2,32	2,78					
AT1G07050	CONSTANS-like protein-related			2,48	3,74					
AT3G54990	SMZ (SCHLAFMUTZE); DNA binding / transcription factor				1,92					
Meristem/flower development										

continued on next page

Table C.10 — continued from previous page

AGI code	Gene description	0,1 % sucrose				3 % sucrose			
		root		shoot		root		shoot	
		d ₃ /d ₀	d ₄ /d ₀	d ₃ /d ₀	d ₄ /d ₀	d ₃ /d ₀	d ₄ /d ₀	d ₃ /d ₀	d ₄ /d ₀
AT1G68795	CLE12 (CLAVATA3/ESR-RELATED 12); protein binding / receptor binding			1,52	1,75				
AT3G24770	CLE41 (CLAVATA3/ESR-RELATED 41); protein binding / receptor binding				2,12				
AT1G59640	ZCW32; DNA binding / transcription factor				1,88				
AT5G65700	BAM1 (BARELY ANY MERISTEM 1); ATP binding / kinase/ protein serine/threonine kinase				1,58				
AT3G49670	BAM2 (BARELY ANY MERISTEM 2); ATP binding / protein binding / protein kinase/ protein serine/threonine kinase	1,61	1,59						
AT2G02850	ARPN (PLANTACYANIN); copper ion binding / electron carrier	2,02	1,99	4,35					1,9
AT1G24260	SEP3 (SEPALATA3); DNA binding / protein binding / transcription factor				2,05				
AT5G20240	PI (PISTILLATA); DNA binding / transcription factor				6,19				
AT4G28190	ULT1 (ULTRAPETALA1); DNA binding				2,07				
AT5G02190	PCS1 (PROMOTION OF CELL SURVIVAL 1); aspartic-type endopeptidase/ peptidase				1,7				
Shoot/leaf development									
AT4G35550	WOX13 (WUSCHEL-RELATED HOMEBOX 13); DNA binding / transcription factor				1,63				
AT1G62360	STM (SHOOT MERISTEMLESS); transcription factor				1,87				
AT3G01470	ATHB-1 (ARABIDOPSIS THALIANA HOMEBOX 1); DNA binding / protein homodimerization/ sequence-specific DNA binding / transcription activator/ transcription factor				3,33				
AT3G61890	ATHB-12 (ARABIDOPSIS THALIANA HOMEBOX 12); transcription activator/ transcription factor				2,81				2,94
AT5G60690	REV (REVOLUTA); DNA binding / lipid binding / transcription factor				1,72				
AT2G45450	ZPR1 (LITTLE ZIPPER 1); protein binding				1,92				
AT1G52150	ATHB-15; DNA binding / transcription factor				1,76				
AT2G35940	BLH1 (BEL1-LIKE HOMEODOMAIN 1); DNA binding / protein heterodimerization/ protein homodimerization/ transcription factor				1,97				
AT2G26170	CYP711A1; electron carrier/ heme binding / iron ion binding / monooxygenase/ oxygen binding				2,43				
AT1G14350	FLP (FOUR LIPS); DNA binding / transcription factor				2,07				
AT2G02820	MYB88 (myb domain protein 88); DNA binding / transcription factor				1,96				
AT3G02170	LNG2 (LONGIFOLIA2)				1,77				
AT1G23380	KNAT6; DNA binding / transcription activator/ transcription factor				1,51				
AT3G01140	MYB106 (myb domain protein 106); DNA binding / transcription factor				2,75				
AT5G02030	RPL (REPLUMLESS); DNA binding / sequence-specific DNA binding / transcription factor				1,7				
AT2G19580	TET2 (TETRASPANIN2)				5				
AT5G46700	TRN2 (TORNADO 2)				1,67				
AT1G80730	ZFP1 (ZINC-FINGER PROTEIN 1); nucleic acid binding / transcription factor/ zinc ion binding	1,55	2,37						
AT2G01940	nucleic acid binding / transcription factor/ zinc ion binding				1,97				
AT2G45190	AFO (ABNORMAL FLORAL ORGANS); protein binding / transcription factor/ transcription regulator				1,96				
AT2G22840	AtGRF1 (GROWTH-REGULATING FACTOR 1); transcription activator			2,02	2,06				
AT2G36400	AtGRF3 (GROWTH-REGULATING FACTOR 3); transcription activator				2,13				

continued on next page

Table C.10 – continued from previous page

AGI code	Gene description	0,1 % sucrose				3 % sucrose			
		root		shoot		root		shoot	
		d ³ /d ₀	d ⁴ /d ₀	d ³ /d ₀	d ⁴ /d ₀	d ³ /d ₀	d ⁴ /d ₀	d ³ /d ₀	d ⁴ /d ₀
AT3G23250	MYB15 (MYB DOMAIN PROTEIN 15); DNA binding / transcription factor	1,62							
AT5G63780	SHA1 (shoot apical meristem arrest 1); protein binding / zinc ion binding			1,65	2,94				
AT2G28890	PLL4 (POLTERGEIST LIKE 4); catalytic/ protein serine/threonine phosphatase				2,24				
AT2G01850	EXGT-A3; hydrolase, acting on glycosyl bonds / xyloglucan:xyloglucosyl transferase				1,84				
Root development									
AT1G53700	WAG1 (WAG 1); kinase/ protein serine/threonine kinase							3,77	
AT3G14370	WAG2; kinase/ protein serine/threonine kinase							8,85	
AT5G48010	THAS1 (THALIANOL SYNTHASE 1); catalytic/ thalianol synthase	2,31	1,79						
AT5G48000	CYP708A2; oxygen binding / thalianol hydroxylase	1,92	1,57						
AT4G18640	MRH1 (morphogenesis of root hair 1); ATP binding / protein binding / protein kinase/ protein serine/threonine kinase/ protein tyrosine kinase							2,31	
AT2G03720	MRH6 (morphogenesis of root hair 6)	1,81	3,5						
AT1G04240	SHY2 (SHORT HYPOCOTYL 2); transcription factor							2,32	
AT5G51060	RHD2 (ROOT HAIR DEFECTIVE 2); NAD(P)H oxidase	1,54	2,5						
AT4G13195	CLE44 (CLAVATA3/ESR-RELATED 44)	1,92	2,07						
AT3G50060	MYB77; DNA binding / transcription factor	2,5	2,67						
Embryo/seed development									
AT1G28330	DYL1 (DORMANCY-ASSOCIATED PROTEIN-LIKE 1)	1,62	2		1,9				
AT5G23940	EMB3009 (embryo defective 3009); transferase/ transferase, transferring acyl groups other than amino-acyl groups							3,71	
AT1G62710	BETA-VPE (BETA VACUOLAR PROCESSING ENZYME); cysteine-type endopeptidase				1,57	4,03			
AT3G63210	MARD1					2,63			
AT5G06760	late embryogenesis abundant group 1 domain-containing protein / LEA group 1 domain-containing protein					1,66			
AT5G45830	DOG1 (DELAY OF GERMINATION 1)				1,62	3,72			
AT2G33830	dormancy/auxin associated family protein					3,92			4,29
AT1G56200	emb1303 (embryo defective 1303)		1,67						
AT2G37920	emb1513 (embryo defective 1513); copper ion transmembrane transporter					1,96			
AT3G18390	EMB1865 (embryo defective 1865); RNA binding					1,77			
AT3G29290	emb2076 (embryo defective 2076)					1,68			
AT4G04350	EMB2369 (EMBRYO DEFECTIVE 2369); ATP binding / aminoacyl-tRNA ligase/ leucine-tRNA ligase/ nucleotide binding					1,58			
AT1G05190	emb2394 (embryo defective 2394); structural constituent of ribosome		1,82			1,8			
AT1G24340	emb2421 (embryo defective 2421); monooxygenase/ oxidoreductase					1,73			
AT3G04340	emb2458 (embryo defective 2458); ATP binding / ATPase/ metalloendopeptidase/ nucleoside-triphosphatase/ nucleotide binding					1,52			
AT1G70070	EMB25 (EMBRYO DEFECTIVE 25); ATP-dependent helicase/ RNA helicase					1,82			

continued on next page

Table C.10 – continued from previous page

AGI code	Gene description	0,1 % sucrose				3 % sucrose			
		root		shoot		root		shoot	
		d ₃ /d ₀	d ₄ /d ₀	d ₃ /d ₀	d ₄ /d ₀	d ₃ /d ₀	d ₄ /d ₀	d ₃ /d ₀	d ₄ /d ₀
AT3G12080	emb2738 (embryo defective 2738); GTP binding				1,57				
AT2G01860	EMB975 (EMBRYO DEFECTIVE 975)			1,7	1,87				
AT1G62750	SCO1 (SNOWY COTYLEDON 1); ATP binding / translation elongation factor/ translation factor, nucleic acid binding				1,62				
AT5G04040	SDP1 (SUGAR-DEPENDENT1); triacylglycerol lipase				1,84				
AT3G57520	AtSIP2 (Arabidopsis thaliana seed imbibition 2); hydrolase, hydrolyzing O-glycosyl compounds	1,73			2,86				
AT2G21650	MEE3 (MATERNAL EFFECT EMBRYO ARREST 3); DNA binding / transcription factor				3,96				
AT5G45800	MEE62 (maternal effect embryo arrest 62); ATP binding / protein binding / protein kinase/ protein serine/threonine kinase/ protein tyrosine kinase				1,74				
AT2G15890	MEE14 (maternal effect embryo arrest 14)		1,76		8,49			6,71	
AT2G18650	MEE16 (maternal effect embryo arrest 16); protein binding / zinc ion binding				2,06				
AT2G34090	MEE18 (maternal effect embryo arrest 18)				2,05			2,08	
AT4G04040	MEE51 (maternal effect embryo arrest 51); diphosphate-fructose-6-phosphate 1-phosphotransferase				1,75				
AT4G37300	MEE59 (maternal effect embryo arrest 59)		1,77						
Cytokinin									
AT2G01830	WOL (WOODEN LEG); cytokinin receptor/ osmosensor/ phosphoprotein phosphatase/ protein histidine kinase				1,71				
AT3G16360	AHP4 (HPT PHOSPHOTRANSMITTER 4); histidine phosphotransfer kinase/ transferase, transferring phosphorus-containing groups				3,91				
AT4G31920	ARR10 (ARABIDOPSIS RESPONSE REGULATOR 10); transcription factor/ two-component response regulator				1,59				
AT2G40670	ARR16 (ARABIDOPSIS RESPONSE REGULATOR 16); transcription regulator/ two-component response regulator				2,83				
AT3G48100	ARR5 (ARABIDOPSIS RESPONSE REGULATOR 5); transcription regulator/ two-component response regulator				1,99				
AT5G62920	ARR6 (RESPONSE REGULATOR 6); transcription regulator/ two-component response regulator				2,05	2,17			
AT1G19050	ARR7 (RESPONSE REGULATOR 7); transcription regulator/ two-component response regulator				2,41	2,34			
AT1G74890	ARR15 (RESPONSE REGULATOR 15); transcription regulator/ two-component response regulator				1,59				
AT4G23750	CRF2 (CYTOKININ RESPONSE FACTOR 2); DNA binding / transcription factor				2,08				
AT4G26150	CGA1 (CYTOKININ-RESPONSIVE GATA FACTOR 1); transcription factor				2,04	2,66			
Ethylene									
AT2G19590	ACO1 (ACC OXIDASE 1); 1-aminocyclopropane-1-carboxylate oxidase				2,54	2,88	2,98		
AT4G08040	ACS11; 1-aminocyclopropane-1-carboxylate synthase	1,87	1,97	2,25					
AT1G01480	ACS2; 1-aminocyclopropane-1-carboxylate synthase			2,06					
AT4G11280	ACS6 (1-AMINOCYCLOPROPANE-1-CARBOXYLIC ACID (ACC) SYNTHASE 6); 1-aminocyclopropane-1-carboxylate synthase	1,79		1,62					
AT4G26200	ACS7; 1-aminocyclopropane-1-carboxylate synthase			1,73	1,92				

continued on next page

Table C.10 – continued from previous page

AGI code	Gene description	0,1 % sucrose				3 % sucrose				
		root		shoot		root		shoot		
		d ³ /d ₀	d ⁴ /d ₀	d ³ /d ₀	d ⁴ /d ₀	d ³ /d ₀	d ⁴ /d ₀	d ³ /d ₀	d ⁴ /d ₀	
ABA										
AT1G52340	ABA2 (ABA DEFICIENT 2); alcohol dehydrogenase/ oxidoreductase/ xanthoxin dehydrogenase								1,86	
AT4G34000	ABF3 (ABSCISIC ACID RESPONSIVE ELEMENTS-BINDING FACTOR 3); DNA binding / protein binding / transcription activator/ transcription factor								2,06	
AT2G46680	ATHB-7 (ARABIDOPSIS THALIANA HOMEBOX 7); transcription activator/ transcription factor								3,24	
AT1G72770	HAB1 (HOMOLOGY TO ABI1); catalytic/ protein serine/threonine phosphatase								1,67	2,04
AT1G17550	HAB2; catalytic/ protein serine/threonine phosphatase								2,18	
AT1G74660	MIF1 (MINI ZINC FINGER 1); DNA binding / transcription factor								2,28	
AT5G66400	RAB18 (RESPONSIVE TO ABA 18)								2,3	
AT2G04240	XERICO; protein binding / zinc ion binding								2,28	1,67
AT1G49720	ABF1 (ABSCISIC ACID RESPONSIVE ELEMENT-BINDING FACTOR 1); DNA binding / protein binding / transcription activator/ transcription factor	1,53	1,86						4,2	5,1
AT1G13740	AFP2 (ABI FIVE BINDING PROTEIN 2)								1,53	
AT2G46510	ATAIB (ABA-INDUCIBLE BHLH-TYPE TRANSCRIPTION FACTOR); DNA binding / transcription factor	1,74	1,62					2,28	2,15	
AT1G01720	ATAF1; transcription activator/ transcription factor								1,64	
AT1G35670	ATCDPK2 (CALCIUM-DEPENDENT PROTEIN KINASE 2); calmodulin-dependent protein kinase/ kinase								1,78	
AT5G45340	CYP707A3; (+)-abscisic acid 8'-hydroxylase/ oxygen binding					3,18	4,23			
AT2G29090	CYP707A2; (+)-abscisic acid 8'-hydroxylase/ oxygen binding						2,2			
AT5G62470	MYB96 (myb domain protein 96); DNA binding / transcription factor					2,61	2,69			
Auxin/Tryptophan biosynthesis										
AT5G60890	MYB34 (MYB DOMAIN PROTEIN 34); DNA binding / kinase/ transcription activator/ transcription factor								1,89	2,03
AT5G17990	TRP1 (tryptophan biosynthesis 1); anthranilate phosphoribosyltransferase	4,84	6,46					3,27	4,7	
AT4G31500	CYP83B1 (CYTOCHROME P450 MONOOXYGENASE 83B1); oxidoreductase, acting on paired donors, with incorporation or reduction of molecular oxygen, NADH or NADPH as one donor, and incorporation of one atom of oxygen / oxygen binding					2,16	2,38			
AT4G27070	TRYPTOPHAN SYNTHASE BETA-SUBUNIT 2	1,86	2,06							
AT2G04400	indole-3-glycerol phosphate synthase (IGPS)	2,28	2,57							
AT5G05730	ASA1 (ANTHRANILATE SYNTHASE ALPHA SUBUNIT 1); anthranilate synthase	3,08	3,66					3,13	4,81	
AT1G24807	anthranilate synthase beta subunit, putative;	2,76	2,86							
AT4G02610	tryptophan synthase, alpha subunit, putative								1,73	
AT3G54640	TSA1 (TRYPTOPHAN SYNTHASE ALPHA CHAIN); tryptophan synthase	3,2	3,75	1,64	1,59	2,26	2,95			
AT1G70560	TAA1 (TRYPTOPHAN AMINOTRANSFERASE OF ARABIDOPSIS 1); L-alanine:2-oxoglutarate aminotransferase/ L-glutamine:2-oxoglutarate aminotransferase/ L-leucine:2-oxoglutarate aminotransferase/ L-methionine:2-oxoglutarate aminotransferase/ L-phenylalanine:2-oxoglut					1,58	1,86			
AT2G23170	GH3.3; indole-3-acetic acid amido synthetase								4,51	
AT2G20610	SUR1 (SUPERROOT 1); S-alkylthiohydroximate lyase/ carbon-sulfur lyase/ transaminase	1,63	1,95	1,53	3,09					

continued on next page

Table C.10 — continued from previous page

AGI code	Gene description	0,1 % sucrose				3 % sucrose			
		root		shoot		root		shoot	
		d ³ /d ₀	d ⁴ /d ₀	d ³ /d ₀	d ⁴ /d ₀	d ³ /d ₀	d ⁴ /d ₀	d ³ /d ₀	d ⁴ /d ₀
AT3G59900	ARGOS (AUXIN-REGULATED GENE INVOLVED IN ORGAN SIZE)				2,14				
AT2G44080	ARL (ARGOS-LIKE)			1,7					
AT4G13770	CYP83A1 (CYTOCHROME P450 83A1); oxidoreductase, acting on paired donors, with incorporation or reduction of molecular oxygen, NADH or NADPH as one donor, and incorporation of one atom of oxygen / oxygen binding	1,75	2,62		3,15				
AT4G39950	CYP79B2; electron carrier/ heme binding / iron ion binding / monooxygenase/ oxygen binding	3,34	3,49	1,83	1,69	5,5	6,74		
AT2G22330	CYP79B3; electron carrier/ heme binding / iron ion binding / monooxygenase/ oxygen binding	2,06	1,98						
AT1G74100	SOT16 (SULFOTRANSFERASE 16); desulfoglucosinolate sulfotransferase/ sulfotransferase			1,69	2,41				
AT1G18590	SOT17 (SULFOTRANSFERASE 17); desulfoglucosinolate sulfotransferase/ sulfotransferase	2,22	2,48	1,62	4,19				
AT1G74090	SOT18 (DESULFO-GLUCOSINOLATE SULFOTRANSFERASE 18); 3-methylthiopropyl-desulfoglucosinolate sulfotransferase/ 4-methylthiobutyl-desulfoglucosinolate sulfotransferase/ 5-methylthiopentyl-desulfoglucosinolate sulfotransferase/ 7-methylthioheptyl-desulfoglucosinolate sulfotransferase		1,73		2,73				
AT4G16780	ATHB-2 (ARABIDOPSIS THALIANA HOMEODOMAIN PROTEIN 2); DNA binding / protein homodimerization/ sequence-specific DNA binding / transcription factor				3,23				
AT2G28350	ARF10 (AUXIN RESPONSE FACTOR 10); miRNA binding / transcription factor				1,7				
AT2G46530	ARF11 (AUXIN RESPONSE FACTOR 11); transcription factor				3,07				
AT1G04250	AXR3 (AUXIN RESISTANT 3); transcription factor				2,55				
AT1G54990	AXR4 (AUXIN RESISTANT 4)				2,26				
AT4G31820	ENP (ENHANCER OF PINOID); protein binding / signal transducer				1,97				
AT2G34650	PID (PINOID); kinase/ protein kinase/ protein serine/threonine kinase				2,74				
AT5G54490	PBP1 (PINOID-BINDING PROTEIN 1); calcium ion binding / protein binding				1,97				
AT1G73590	PIN1 (PIN-FORMED 1); transporter				1,8				
AT1G70940	PIN3 (PIN-FORMED 3); auxin:hydrogen symporter/ transporter				1,61				
AT1G76520	auxin efflux carrier family protein					3,57	5,57		
AT1G52830	IAA6 (INDOLE-3-ACETIC ACID 6); transcription factor				1,84				
AT3G23050	IAA7 (INDOLE-3-ACETIC ACID 7); transcription factor				1,86				
AT4G14550	IAA14 (INDOLE-3-ACETIC ACID INDUCIBLE 14); protein binding / transcription factor/ transcription repressor				1,6				
AT4G32280	IAA29 (INDOLE-3-ACETIC ACID INDUCIBLE 29); transcription factor				2,78				5,61
AT4G14560	IAA1 (INDOLE-3-ACETIC ACID INDUCIBLE); protein binding / transcription factor								1,68
AT3G23030	IAA2 (INDOLE-3-ACETIC ACID INDUCIBLE 2); transcription factor		1,55						1,63
AT4G05530	IBR1 (INDOLE-3-BUTYRIC ACID RESPONSE 1); binding / catalytic/ oxidoreductase				1,88				
AT4G30080	ARF16 (AUXIN RESPONSE FACTOR 16); miRNA binding / transcription factor					1,6			
AT1G44350	ILL6; IAA-amino acid conjugate hydrolase/ metalloproteinase				2,11				
AT4G27260	WES1; indole-3-acetic acid amido synthetase		1,55						
AT4G03190	GRH1 (GRR1-LIKE PROTEIN 1); auxin binding / protein binding / ubiquitin-protein ligase			1,55					
AT1G29510	SAUR68 (SMALL AUXIN UPREGULATED 68)				3,71				
AT5G53590	auxin-responsive family protein				2,01				

continued on next page

Table C.10 – continued from previous page

AGI code	Gene description	0,1 % sucrose				3 % sucrose				
		root		shoot		root		shoot		
		d ³ /d ₀	d ⁴ /d ₀	d ³ /d ₀	d ⁴ /d ₀	d ³ /d ₀	d ⁴ /d ₀	d ³ /d ₀	d ⁴ /d ₀	
AT4G34770	auxin-responsive family protein				2,91					
AT3G25290	auxin-responsive family protein			3,28	6,51					
AT1G16510	auxin-responsive family protein	1,55								
AT1G75590	auxin-responsive family protein				2,3					
AT5G18060	auxin-responsive protein, putative				3,91					
AT4G36110	auxin-responsive protein, putative				2,68					
AT3G03840	auxin-responsive protein, putative				3,16					
AT3G03830	auxin-responsive protein, putative				2,08					
AT1G29500	auxin-responsive protein, putative				2,96					
AT1G29450	auxin-responsive protein, putative				1,84					
AT2G21200	auxin-responsive protein, putative				1,53					
AT5G20820	auxin-responsive protein-related				1,66					
AT5G50760	auxin-responsive family protein				1,72	2,09	1,87			
AT5G35735	auxin-responsive family protein				3,29					
AT3G12830	auxin-responsive family protein		1,66							
AT4G12980	auxin-responsive protein, putative								1,63	
AT4G12550	AIR1; lipid binding			2,6	2,24					
Jasmonate										
AT1G13280	AOC4 (ALLENE OXIDE CYCLASE 4); allene-oxide cyclase				3,36					
AT2G06050	OPR3 (OPDA-REDUCTASE 3); 12-oxophytodieneoate reductase				1,6					
AT1G67560	lipoxygenase family protein				1,82					
AT1G55020	LOX1; lipoxygenase	5,02	7,14	2,31	2,26					
AT3G45140	LOX2 (LIPOXYGENASE 2); lipoxygenase		1,69	3,41	2,38					
AT1G52890	ANAC019 (Arabidopsis NAC domain containing protein 19); transcription factor				1,8					
AT1G72520	lipoxygenase, putative				2,59	2,77				
AT1G17420	LOX3; electron carrier / iron ion binding / lipoxygenase / metal ion binding / oxidoreductase, acting on single donors with incorporation of molecular oxygen, incorporation of two atoms of oxygen	2,07	1,85							
AT1G19670	ATCLH1 (ARABIDOPSIS THALIANA CORONATINE-INDUCED PROTEIN 1); chlorophyllase				3					
AT4G23600	CORI3 (CORONATINE INDUCED 1); cystathionine beta-lyase/ transaminase				4,54	6,29		1,76	2,18	
AT5G47220	ERF2 (ETHYLENE RESPONSIVE ELEMENT BINDING FACTOR 2); DNA binding / transcription activator/ transcription factor				1,85					
AT2G23620	MES1 (METHYL ESTERASE 1); hydrolase, acting on ester bonds / methyl indole-3-acetate esterase/ methyl jasmonate esterase/ methyl salicylate esterase				2,46					
AT3G50440	MES10 (METHYL ESTERASE 10); hydrolase/ hydrolase, acting on ester bonds / methyl jasmonate esterase				1,7	8,55				
AT1G69240	MES15 (METHYL ESTERASE 15); hydrolase		2,23							
AT4G37150	MES9 (METHYL ESTERASE 9); hydrolase, acting on ester bonds / methyl indole-3-acetate esterase/ methyl jasmonate esterase/ methyl salicylate esterase				1,57	1,75				

continued on next page

Table C.10 – continued from previous page

AGI code	Gene description	0,1 % sucrose				3 % sucrose			
		root		shoot		root		shoot	
		d_3/d_0	d_4/d_0	d_3/d_0	d_4/d_0	d_3/d_0	d_4/d_0	d_3/d_0	d_4/d_0
AT4G16690	MES16 (METHYL ESTERASE 16); catalytic/ hydrolase, acting on ester bonds / methyl indole-3-acetate esterase/ methyl jasmonate esterase				1,9				
AT3G28740	CYP81D1; electron carrier/ heme binding / iron ion binding / monooxygenase/ oxygen binding	2,53	4,3	1,9	14,73				
AT1G19180	JAZ1 (JASMONATE-ZIM-DOMAIN PROTEIN 1); protein binding				2,26				
AT1G17380	JAZ5 (JASMONATE-ZIM-DOMAIN PROTEIN 5)	1,7	1,54			2,98	2,77		
AT2G34600	JAZ7 (JASMONATE-ZIM-DOMAIN PROTEIN 7)	3,85	3,78						
AT1G30135	JAZ8 (JASMONATE-ZIM-DOMAIN PROTEIN 8)	4,86	4,98			3,5	3,53		
Gibberellin									
AT1G66350	RGL1 (RGA-LIKE 1); transcription factor				5,56				1,55
AT3G03450	RGL2 (RGA-LIKE 2); transcription factor				1,7				
AT1G78440	ATGA2OX1 (gibberellin 2-oxidase 1); gibberellin 2-beta-dioxygenase				1,75				
AT1G15550	GA3OX1 (GIBBERELLIN 3-OXIDASE 1); gibberellin 3-beta-dioxygenase/ transcription factor binding				2,51				
AT5G15230	GASA4 (GAST1 PROTEIN HOMOLOG 4)	1,75	1,81		1,73				
AT1G02400	GA2OX6 (GIBBERELLIN 2-OXIDASE 6); gibberellin 2-beta-dioxygenase			2,13	2,97				
AT2G14900	gibberellin-regulated family protein				2,49				
AT5G14920	gibberellin-regulated family protein	2,02	1,96	1,55	1,56				1,99
AT1G22690	gibberellin-responsive protein, putative				1,6				
Brassinosteroid									
AT4G34650	SQS2 (SQUALENE SYNTHASE 2); farnesyl-diphosphate farnesyltransferase				3,05				
AT4G36540	BEE2 (BR Enhanced Expression 2); DNA binding / transcription factor				1,57				
AT1G73830	BEE3 (BR ENHANCED EXPRESSION 3); DNA binding / transcription factor			1,51	2,91				2,21
AT3G30180	BR6OX2 (BRASSINOSTEROID-6-OXIDASE 2); monooxygenase/ oxygen binding		1,83	1,67	2,34				
AT2G01950	BRL2 (BRI1-LIKE 2); ATP binding / protein serine/threonine kinase/ transmembrane receptor protein serine/threonine kinase				1,54				
AT5G46570	BSK2 (BR-SIGNALING KINASE 2); ATP binding / binding / kinase/ protein kinase/ protein tyrosine kinase		1,53						
AT3G61460	BRH1 (BRASSINOSTEROID-RESPONSIVE RING-H2); protein binding / zinc ion binding				1,98				
AT2G34500	CYP710A1 (cytochrome P450, family 710, subfamily A, polypeptide 1); C-22 sterol desaturase/ oxygen binding				1,8			2,2	3,16
AT2G34490	CYP710A2 (cytochrome P450, family 710, subfamily A, polypeptide 2); C-22 sterol desaturase/ oxygen binding				1,77				
AT5G42890	SCP2 (STEROL CARRIER PROTEIN 2); oxidoreductase/ sterol carrier			1,61					
AT2G03760	ST; brassinosteroid sulfotransferase/ sulfotransferase	2,31	2,75			3	3,7		
AT1G22300	GRF10 (GENERAL REGULATORY FACTOR 10); ATP binding / protein binding / protein phosphorylated amino acid binding				1,51				
AT1G78300	GRF2 (GENERAL REGULATORY FACTOR 2); protein binding / protein phosphorylated amino acid binding				1,55				
AT4G33430	BAK1 (BRI1-ASSOCIATED RECEPTOR KINASE); kinase/ protein binding / protein heterodimerization/ protein serine/threonine kinase				1,56				

continued on next page

Table C.10 – continued from previous page

AGI code	Gene description	0,1 % sucrose				3 % sucrose			
		root		shoot		root		shoot	
		d ³ /d ₀	d ⁴ /d ₀	d ³ /d ₀	d ⁴ /d ₀	d ³ /d ₀	d ⁴ /d ₀	d ³ /d ₀	d ⁴ /d ₀
AT5G05690	CPD (CONSTITUTIVE PHOTOMORPHOGENIC DWARF); electron carrier/ heme binding / iron ion binding / monooxygenase/ oxygen binding	1,64	1,93						
AT1G17060	CYP72C1 (CYTOCHROME P450 72C1); electron carrier/ heme binding / iron ion binding / monooxygenase/ oxygen binding				2,05				
AT1G07420	SMO2-1 (STEROL 4-ALPHA-METHYL-OXIDASE 2-1); 4-alpha-methyl-delta7-sterol-4alpha-methyl oxidase/ C-4 methylsterol oxidase				2,09				1,85
AT1G76090	SMT3 (STEROL METHYLTRANSFERASE 3); S-adenosylmethionine-dependent methyltransferase/ sterol 24-C-methyltransferase				2,58				
AT1G75750	GASA1 (GAST1 PROTEIN HOMOLOG 1)	1,8	1,73		1,59				
AT5G64260	EXL2 (EXORDIUM LIKE 2)	2,3	2,23		1,83				
AT5G09440	EXL4 (EXORDIUM LIKE 4)	2,06	1,97						
AT2G17230	EXL5 (EXORDIUM LIKE 5)	2,09	2,35		1,52				
AT4G08950	EXO (EXORDIUM)	2,4	1,78						
AT1G35140	PHI-1 (PHOSPHATE-INDUCED 1)	3,79	3		7				
SA									
AT1G18870	ICS2 (ISOCHORISMATE SYNTHASE 2); isochorismate synthase				2,24				
AT5G38020	S-adenosyl-L-methionine:carboxyl methyltransferase family protein	3,11	3,46						
AT2G23590					1,75				
Sulfokine									
AT5G65870	ATPSK5 (PHYTOSULFOKINE 5 PRECURSOR); growth factor			1,52	2,18				
AT2G02220	PSKR1 (PHYTOSULFOKIN RECEPTOR 1); ATP binding / peptide receptor/ protein serine/threonine kinase				2,35				
Small RNAs									
AT1G69440	AGO7 (ARGONAUTE7); nucleic acid binding				2,73				
AT4G20910	HEN1 (HUA ENHANCER 1); RNA methyltransferase	1,68							
AT2G18440	GUT15 (GENE WITH UNSTABLE TRANSCRIPT 15); other RNA				1,72				
RNA processing									
AT5G56260	dimethylmenaquinone methyltransferase family protein				1,86				
AT5G16450	dimethylmenaquinone methyltransferase family protein				1,74				
AT3G02770	dimethylmenaquinone methyltransferase family protein				1,71				
AT1G14210	ribonuclease T2 family protein			1,61					
AT1G26820	RNS3 (RIBONUCLEASE 3); RNA binding / endoribonuclease/ ribonuclease T2				1,98				
AT1G22910	RNA recognition motif (RRM)-containing protein				1,83				
AT4G37510	ribonuclease III family protein				1,78				
AT4G39040	RNA binding				1,61				

continued on next page

Table C.10 – continued from previous page

AGI code	Gene description	0,1 % sucrose				3 % sucrose			
		root		shoot		root		shoot	
		d ₃ /d ₀	d ₄ /d ₀	d ₃ /d ₀	d ₄ /d ₀	d ₃ /d ₀	d ₄ /d ₀	d ₃ /d ₀	d ₄ /d ₀
AT3G20930	RNA recognition motif (RRM)-containing protein				1,55				
AT3G09160	RNA recognition motif (RRM)-containing protein				1,95				
AT1G76460	RNA recognition motif (RRM)-containing protein	1,84	1,68						
AT2G41500	EMB2776; nucleotide binding	1,58							
Pathogenesis									
AT1G80460	NHO1 (nonhost resistance to <i>P. s. phaseolicola</i> 1); carbohydrate kinase/ glycerol kinase				2,05				
AT3G52450	PUB22 (PLANT U-BOX 22); ubiquitin-protein ligase			1,6	5,82				
AT2G35930	PUB23 (PLANT U-BOX 23); ubiquitin-protein ligase	1,91	1,72	1,71	3,73				
AT3G11840	PUB24 (PLANT U-BOX 24); binding / ubiquitin-protein ligase			1,67					
AT4G34410	RRTF1 ((REDOX RESPONSIVE TRANSCRIPTION FACTOR 1); DNA binding / transcription factor	14,52	13,86	1,8	7,21	6,42			
AT3G61190	BAP1 (BON ASSOCIATION PROTEIN 1); phospholipid binding / protein binding	2,08	2,16						
AT2G39660	BIK1 (BOTRYTIS-INDUCED KINASE1); kinase				3,87				
AT1G29690	CAD1 (constitutively activated cell death 1)				2,02				
AT2G40000	HSPRO2 (ARABIDOPSIS ORTHOLOG OF SUGAR BEET HS1 PRO-1 2)	2,85	3,29	3,37					
AT1G22070	TGA3; DNA binding / calmodulin binding / protein binding / transcription factor								2,6
AT2G31890	RAP				1,64				
AT3G25070	RIN4 (RPM1 INTERACTING PROTEIN 4); protein binding				1,51				
AT3G07040	RPM1 (RESISTANCE TO <i>P. SYRINGAE</i> PV <i>MACULICOLA</i> 1); nucleotide binding / protein binding				1,61				
AT5G20480	EFR (EF-TU RECEPTOR); ATP binding / kinase/ protein serine/threonine kinase				2,78				
AT2G19190	FRK1 (FLG22-INDUCED RECEPTOR-LIKE KINASE 1); kinase			1,6	1,65				
AT3G50480	HR4 (HOMOLOG OF RPW8 4)				2,12				
AT1G56160	MYB72 (MYB DOMAIN PROTEIN 72); DNA binding / transcription factor	3,35	2,71						
AT2G44490	PEN2 (PENETRATION 2); hydrolase, hydrolyzing O-glycosyl compounds / thioglucosidase				1,85				
AT5G57220	CYP81F2; electron carrier/ heme binding / iron ion binding / monooxygenase/ oxygen binding	3,91	3,78	1,73	6,25	10,68	14,34		
AT4G16860	RPP4 (recognition of <i>peronospora parasitica</i> 4); LRR domain binding		2,36	3,88	1,8	1,68			
AT4G16950	RPP5 (RECOGNITION OF <i>PERONOSPORA PARASITICA</i> 5); nucleotide binding				1,92				
AT1G56510	WRR4 (WHITE RUST RESISTANCE 4); ATP binding / nucleoside-triphosphatase/ nucleotide binding / trans-membrane receptor			1,56	1,86				
AT4G31550	WRKY11; calmodulin binding / transcription factor				2,58				
AT2G23320	WRKY15; calmodulin binding / transcription factor				1,69				
AT4G31800	WRKY18; transcription factor	1,78	1,53		2,92				
AT4G01250	WRKY22; transcription factor				4,45				
AT5G07100	WRKY26; transcription factor				2,08				
AT4G18170	WRKY28; transcription factor				3,02				
AT5G24110	WRKY30; transcription factor				1,64				
AT2G38470	WRKY33; transcription factor			2,05	4,17				2,03
AT1G80840	WRKY40; transcription factor	6,62	6,53	3,4	7,01				

continued on next page

Table C.10 – continued from previous page

AGI code	Gene description	0,1 % sucrose				3 % sucrose			
		root		shoot		root		shoot	
		d ³ /d ₀	d ⁴ /d ₀	d ³ /d ₀	d ⁴ /d ₀	d ³ /d ₀	d ⁴ /d ₀	d ³ /d ₀	d ⁴ /d ₀
AT4G01720	WRKY47; transcription factor				2,12				
AT5G49520	WRKY48; transcription factor	1,69			2,63				
AT4G23810	WRKY53; DNA binding / protein binding / transcription activator/ transcription factor	2,02	1,73	4,01	8,02				
AT1G62300	WRKY6; transcription factor			1,52	3,45				
AT1G29280	WRKY65; transcription factor				1,59				
AT4G24240	WRKY7; calmodulin binding / transcription factor				3,36				
AT4G26640	WRKY20; transcription factor		1,56						
AT2G25000	WRKY60; transcription factor		1,54						
AT3G56400	WRKY70; transcription factor/ transcription repressor			2,24	4,16	10,85	11,51		
AT4G39030	EDS5 (ENHANCED DISEASE SUSCEPTIBILITY 5); antiporter/ multidrug efflux pump/ transporter				2,02				
AT3G26830	PAD3 (PHYTOALEXIN DEFICIENT 3); dihydrocamalexin acid decarboxylase/ monooxygenase/ oxygen binding	19,29	24,73	3,41			2,46	3,07	
AT5G67160	EPS1 (ENHANCED PSEUDOMONAS SUSCEPTIBILITY 1); transferase/ transferase, transferring acyl groups other than amino-acyl groups	1,92	2,15	4,13				1,99	
AT1G54040	ESP (EPITHIOSPECIFIER PROTEIN); enzyme regulator				5,02				
AT1G19250	FMO1 (FLAVIN-DEPENDENT MONOOXYGENASE 1); FAD binding / NADP or NADPH binding / electron carrier/ flavin-containing monooxygenase/ monooxygenase/ oxidoreductase	4,01	6,88			5,99	6,93		
AT2G13810	ALD1 (AGD2-LIKE DEFENSE RESPONSE PROTEIN1); catalytic/ pyridoxal phosphate binding / transaminase/ transferase, transferring nitrogenous groups					2,43	1,84		
AT5G13320	PBS3 (AVRPPHB SUSCEPTIBLE 3)					12,68	12,86		
AT5G53760	MLO11 (MILDEW RESISTANCE LOCUS O 11); calmodulin binding				1,93				
AT2G39200	MLO12 (MILDEW RESISTANCE LOCUS O 12); calmodulin binding				4,2				
AT1G42560	MLO9 (MILDEW RESISTANCE LOCUS O 9); calmodulin binding				3,55				
AT1G12280	disease resistance protein (CC-NBS-LRR class), putative				2,21				
AT1G57630	disease resistance protein (TIR class), putative	4,65	5,88			7,74	11,61		
AT3G13650	disease resistance response			2,24	5,2				
AT1G55210	disease resistance response	1,61	2,09		2,17				
AT4G23690	disease resistance-responsive family protein / dirigent family protein			1,6	1,88				
AT1G64160	disease resistance-responsive family protein / dirigent family protein	1,85	1,84						
AT2G21100	disease resistance-responsive protein-related / dirigent protein-related		1,83						
AT4G09420	disease resistance protein (TIR-NBS class), putative				3,26				
AT1G72890	disease resistance protein (TIR-NBS class), putative				1,66				
AT1G72900	disease resistance protein (TIR-NBS class), putative				2,84				
AT1G72940	disease resistance protein (TIR-NBS class), putative				1,64				
AT5G46450	disease resistance protein (TIR-NBS-LRR class), putative				2,07				
AT5G22690	disease resistance protein (TIR-NBS-LRR class), putative				1,76				
AT5G11250	disease resistance protein (TIR-NBS-LRR class), putative				2,45				
AT4G16880	disease resistance protein-related				4,51				

continued on next page

Table C.10 — continued from previous page

AGI code	Gene description	0,1 % sucrose				3 % sucrose			
		root		shoot		root		shoot	
		d ₃ /d ₀	d ₄ /d ₀	d ₃ /d ₀	d ₄ /d ₀	d ₃ /d ₀	d ₄ /d ₀	d ₃ /d ₀	d ₄ /d ₀
AT1G33590	disease resistance protein-related / LRR protein-related			1,73	1,91				
AT2G34930	disease resistance family protein	2,56	2,15						
AT3G28940	avirulence-responsive protein, putative / avirulence induced gene (AIG) protein, putative			1,64	2,55				
AT4G31310	avirulence-responsive protein-related / avirulence induced gene (AIG) protein-related				2,26				
AT3G47540	chitinase, putative	2,52	2,82		2,43				
AT1G02360	chitinase, putative			1,7	3,47	2,19	2,42		
AT2G43620	chitinase, putative		1,79	1,81	1,52				
AT2G43590	chitinase, putative	1,51	3,03						
AT2G43570	chitinase, putative	4,48	7,38			6,88	9,08		
AT3G12500	ATHCHIB (ARABIDOPSIS THALIANA BASIC CHITINASE); chitinase	2,62	3,41	2,52	5,58				
AT4G37980	ELI3-1 (ELICITOR-ACTIVATED GENE 3-1); binding / catalytic/ oxidoreductase/ zinc ion binding			1,54	2,72				
AT4G37990	ELI3-2 (ELICITOR-ACTIVATED GENE 3-2); aryl-alcohol dehydrogenase/ mannitol dehydrogenase			1,56					
AT4G18470	SNI1; transcription repressor		1,82						
AT2G14610	PR1 (PATHOGENESIS-RELATED GENE 1)				5,07				
AT3G04720	PR4 (PATHOGENESIS-RELATED 4); chitin binding	1,89	2,15	4,17	7,23				
AT1G33960	AIG1 (AVRRPT2-INDUCED GENE 1); GTP binding			1,56					
AT3G28930	AIG2 (AVRRPT2-INDUCED GENE 2)	3,23	4,41		2,12				
AT2G14560	LURP1 (LATE UPREGULATED IN RESPONSE TO HYALOPERONOSPORA PARASITICA)			1,66	8,78				
AT3G11660	NHL1				1,98				
AT5G64890	PROPEP2 (Elicitor peptide 2 precursor)	3,63	4,5						
AT5G64905	PROPEP3 (Elicitor peptide 3 precursor)	2,94	3,16						
AT5G09990	PROPEP5 (Elicitor peptide 5 precursor)				2,51				
AT1G31580	ECS1			1,7	6,19				
AT1G72260	THI2.1 (THIONIN 2.1); toxin receptor binding				5,93			2,78	3,1
AT1G66100	thionin, putative				1,56				
AT2G02130	LCR68 (LOW-MOLECULAR-WEIGHT CYSTEINE-RICH 68); peptidase inhibitor				1,86				
AT1G19610	PDF1.4; Low-molecular-weight cysteine-rich 78			1,55	3,26				
AT2G26020	PDF1.2b (plant defensin 1.2b)				8,78			2,35	4,25
AT5G44420	PDF1.2				19,76				
AT1G06160	ORA59 (OCTADECANOID-RESPONSIVE ARABIDOPSIS AP2/ERF 59); DNA binding / transcription activator/ transcription factor			1,95	2,35				
AT2G43510	ATTI1; serine-type endopeptidase inhibitor	7,46	11,29	6,59	3,03	8,44	13,67		
AT1G52030				1,66	10,45				
AT4G14060	major latex protein-related / MLP-related	3,88	5,49						
AT3G26460	major latex protein-related / MLP-related	2,76	2,47						
AT4G23680	major latex protein-related / MLP-related			3,67	5,16				
AT3G26450	major latex protein-related / MLP-related				2,03				
AT1G35260	MLP165 (MLP-LIKE PROTEIN 165)	2,02	1,97		4,4				

continued on next page

Table C.10 — continued from previous page

AGI code	Gene description	0,1 % sucrose				3 % sucrose			
		root		shoot		root		shoot	
		d ³ /d ₀	d ⁴ /d ₀	d ³ /d ₀	d ⁴ /d ₀	d ³ /d ₀	d ⁴ /d ₀	d ³ /d ₀	d ⁴ /d ₀
AT1G70830	MLP28 (MLP-LIKE PROTEIN 28)			1,77	12,97				
AT4G23670	major latex protein-related / MLP-related				3,03				
AT1G24020	MLP423 (MLP-LIKE PROTEIN 423)			1,74	4,59				
AT1G70890	MLP43 (MLP-LIKE PROTEIN 43)	1,69	2,02		3,22	2,07	2,5		
AT5G12140	ATCYS1 (A. thaliana cystatin-1); cysteine-type endopeptidase inhibitor				2,22				
AT2G31980	cysteine proteinase inhibitor-related			1,82	2,58				
AT2G23960	defense-related protein, putative	1,93	2,34						
AT3G20820	leucine-rich repeat family protein				1,93				
AT5G45000	transmembrane receptor	1,56	1,79						
AT4G11340	Toll-Interleukin-Resistance (TIR) domain-containing protein	2,68	3,36						
AT5G44920	Toll-Interleukin-Resistance (TIR) domain-containing protein				1,81				
AT1G18250	ATLP-1				2,89				
AT4G38660	thaumatin, putative				2,11				
AT4G18780	IRX1 (IRREGULAR XYLEM 1); cellulose synthase/ transferase, transferring glycosyl groups				2,28				
AT2G35960	NHL12				1,67				
AT1G20030	pathogenesis-related thaumatin family protein			1,62	4,45				
AT5G44910	Toll-Interleukin-Resistance (TIR) domain-containing protein				4,92				
AT5G06320	NHL3	1,51			2,02				
AT1G23130	Bet v I allergen family protein	1,68	2,06						
AT2G01520	MLP328 (MLP-LIKE PROTEIN 328); copper ion binding				2,15				
AT2G01530	MLP329 (MLP-LIKE PROTEIN 329); copper ion binding				3,78				
AT1G70850	MLP34 (MLP-LIKE PROTEIN 34)				2,61				
Cell death/apoptosis									
AT4G14400	ACD6 (ACCELERATED CELL DEATH 6); protein binding				3,81				
AT5G39610	ATNAC6/ORE1 (ARABIDOPSIS NAC DOMAIN CONTAINING PROTEIN 6); protein heterodimerization/ protein homodimerization/ transcription factor			2,36	2,59	2,57	3,21		
AT2G32720	CB5-B (CYTOCHROME B5 ISOFORM B); heme binding	1,84	1,99						
AT2G46650	CB5-C (CYTOCHROME B5 ISOFORM C); heme binding	2,43	3,17	1,96	5,04				
AT4G10040	CYTC-2 (cytochrome c-2); electron carrier/ heme binding / iron ion binding			1,62	1,84				
AT4G25650	ACD1-LIKE (ACD1-LIKE); 2 iron, 2 sulfur cluster binding / electron carrier/ oxidoreductase				1,78				
AT4G33300	ADR1-L1 (ADR1-like 1); ATP binding / protein binding				1,81				
AT5G26340	MSS1; carbohydrate transmembrane transporter/ hexose:hydrogen symporter/ high-affinity hydrogen:glucose symporter/ sugar:hydrogen symporter				6,73				
AT2G46240	BAG6 (BCL-2-ASSOCIATED ATHANOGENE 6); calmodulin binding / protein binding				1,76				
Cell cycle									
AT2G35190	NPSN11 (NOVEL PLANT SNARE 11); SNAP receptor/ protein transporter			1,66	2,45				

continued on next page

Table C.10 – continued from previous page

AGI code	Gene description	0,1 % sucrose				3 % sucrose			
		root		shoot		root		shoot	
		d^3/d_0	d^4/d_0	d^3/d_0	d^4/d_0	d^3/d_0	d^4/d_0	d^3/d_0	d^4/d_0
AT1G52410	TSA1 (TSK-ASSOCIATING PROTEIN 1); calcium ion binding / protein binding	1,84	1,75	2,48	8,84				
AT5G04470	SIM (SIAMESE); cyclin-dependent protein kinase inhibitor			1,53	2,18				
AT1G44110	CYCA1;1 (Cyclin A1;1); cyclin-dependent protein kinase regulator				1,58				
AT4G37490	CYCB1;1 (CYCLIN B1;1); cyclin-dependent protein kinase regulator		1,87						
AT3G63120	CYCP1;1 (cyclin p1;1); cyclin-dependent protein kinase				1,77				
AT5G61650	CYCP4;2 (CYCLIN P4;2); cyclin-dependent protein kinase	1,65	2,44						
AT5G67260	CYCD3;2 (CYCLIN D3;2); cyclin-dependent protein kinase			1,58	1,62				
AT3G50070	CYCD3;3 (CYCLIN D3;3); cyclin-dependent protein kinase				1,76				
AT3G21870	CYCP2;1 (cyclin p2;1); cyclin-dependent protein kinase				2,13				
AT1G27630	CYCT1;3 (CYCLIN T 1;3); cyclin-dependent protein kinase				1,56				
Cytoskeleton									
AT1G04820	TUA4; structural constituent of cytoskeleton				1,69				
AT1G75780	TUB1; GTP binding / GTPase/ structural molecule				3,61				
AT5G12250	TUB6 (BETA-6 TUBULIN); structural constituent of cytoskeleton				2,07				
AT2G34150	WAVE1; actin monomer binding				2,03				
AT1G01750	ADF11 (ACTIN DEPOLYMERIZING FACTOR 11); actin binding		1,79						
AT2G16700	ADF5 (ACTIN DEPOLYMERIZING FACTOR 5); actin binding			1,5					
AT4G00680	ADF8 (ACTIN DEPOLYMERIZING FACTOR 8); actin binding		2,04						
AT2G19760	PRF1 (PROFILIN 1); actin binding				1,72				
AT2G47500	ATP binding / microtubule motor				2,18				
AT4G34970	ADF9 (ACTIN DEPOLYMERIZING FACTOR 9); actin binding			1,61					
AT2G45170	AtATG8e; microtubule binding				1,63				
AT4G26700	ATFIM1; actin binding				2,06				
DNA recombination/repair									
AT3G12610	DRT100 (DNA-DAMAGE REPAIR/TOLERATION 100); nucleotide binding / protein binding				3,4				
AT3G19210	ATRAD54 (ARABIDOPSIS HOMOLOG OF RAD54); ATP binding / DNA binding / helicase/ nucleic acid binding		1,54						
AT1G11190	BFN1 (BIFUNCTIONAL NUCLEASE I); T/G mismatch-specific endonuclease/ endoribonuclease, producing 5'-phosphomonoesters / nucleic acid binding / single-stranded DNA specific endodeoxyribonuclease				2,01				
AT1G14460	DNA polymerase-related				1,63				
AT5G44680	methyladenine glycosylase family protein				1,83				
AT3G12710	methyladenine glycosylase family protein				4,13				
AT2G19570	CDA1 (CYTIDINE DEAMINASE 1); cytidine deaminase			2,06	2,67				
AT1G80420	DNA repair protein, putative (XRCC1)				1,54				
AT2G32000	DNA topoisomerase family protein				1,66				
AT3G15620	UVR3 (UV REPAIR DEFECTIVE 3); DNA (6-4) photolyase			1,96	2,58				

continued on next page

Table C.10 – continued from previous page

AGI code	Gene description	0,1 % sucrose				3 % sucrose			
		root		shoot		root		shoot	
		d ³ /d ₀	d ⁴ /d ₀	d ³ /d ₀	d ⁴ /d ₀	d ³ /d ₀	d ⁴ /d ₀	d ³ /d ₀	d ⁴ /d ₀
Response to reactive oxygen species/hypoxia									
AT5G62520	SRO5 (SIMILAR TO RCD ONE 5); NAD+ ADP-ribosyltransferase	4,01	3,67	2,26	3,1				
AT5G14760	AO (L-ASPARTATE OXIDASE); L-aspartate oxidase/ electron carrier/ oxidoreductase			1,56	3,54			1,55	2,19
AT5G47910	RBOHD (RESPIRATORY BURST OXIDASE HOMOLOGUE D); NAD(P)H oxidase				2,29				
AT5G07390	ATRBOHA (respiratory burst oxidase homolog A); calcium ion binding		1,58						
AT4G02380	SAG21 (SENESCENCE-ASSOCIATED GENE 21)				1,73				
AT5G01600	ATFER1; ferric iron binding / iron ion binding			2,07	4,38				
AT2G40300	ATFER4 (ferritin 4); binding / ferric iron binding / oxidoreductase/ transition metal ion binding				1,83				
AT1G07890	APX1 (ascorbate peroxidase 1); L-ascorbate peroxidase				1,68				
AT4G09010	APX4 (ASCORBATE PEROXIDASE 4); heme binding / peroxidase				1,66				
AT4G35970	APX5 (ASCORBATE PEROXIDASE 5); L-ascorbate peroxidase/ heme binding / peroxidase				1,86				
AT5G21100	L-ascorbate oxidase, putative				1,98				
AT4G39830	L-ascorbate oxidase, putative	2,01	2,22						
AT5G21105	L-ascorbate oxidase/ copper ion binding / oxidoreductase				1,76				
AT4G08390	SAPX (STROMAL ASCORBATE PEROXIDASE); L-ascorbate peroxidase	1,53			1,7				
AT1G17020	SRG1 (SENESCENCE-RELATED GENE 1); oxidoreductase, acting on diphenols and related substances as donors, oxygen as acceptor / oxidoreductase, acting on paired donors, with incorporation or reduction of molecular oxygen, 2-oxoglutarate as one donor, and inc			4,86	4,41				
AT3G22370	AOX1A (ALTERNATIVE OXIDASE 1A); alternative oxidase		1,66						
AT1G32350	AOX1D (alternative oxidase 1D); alternative oxidase	5,02	6,18			14,49	20,17	2,17	2,77
AT1G35720	ANNAT1 (ANNEXIN ARABIDOPSIS 1); ATP binding / calcium ion binding / calcium-dependent phospholipid binding / copper ion binding / peroxidase/ protein homodimerization				3,82				
AT5G65020	ANNAT2 (Annexin Arabidopsis 2); calcium ion binding / calcium-dependent phospholipid binding			2,17	2,25				
AT2G21640		2,52	3,35		1,69				
AT4G15440	HPL1 (HYDROPEROXIDE LYASE 1); electron carrier/ heme binding / iron ion binding / monooxygenase				2,72				
AT5G51890	peroxidase				1,67				
AT2G22420	peroxidase 17 (PER17) (P17)				2,89				
AT2G37130	peroxidase 21 (PER21) (P21) (PRXR5)			2,07	1,76				
AT5G67400	peroxidase 73 (PER73) (P73) (PRXR11)		2,38						
AT5G19880	peroxidase, putative					2,35	3,49		
AT4G36430	peroxidase, putative	2,12	2,41						
AT5G58390	peroxidase, putative			1,63	7,54				
AT5G22410	peroxidase, putative	1,59	2,35						
AT5G14130	peroxidase, putative	1,88	2,03						
AT5G06720	peroxidase, putative	1,77	2,34	2,96	1,6				
AT5G06730	peroxidase, putative	3,94	6,29						
AT5G05340	peroxidase, putative				3,25				

continued on next page

Table C.10 — continued from previous page

AGI code	Gene description	0,1 % sucrose				3 % sucrose			
		root		shoot		root		shoot	
		d_3/d_0	d_4/d_0	d_3/d_0	d_4/d_0	d_3/d_0	d_4/d_0	d_3/d_0	d_4/d_0
AT3G49960	peroxidase, putative	1,67	2,98						
AT4G30170	peroxidase, putative			11,36	6,67			2,5	3,17
AT4G26010	peroxidase, putative		2,08						
AT4G11290	peroxidase, putative				7,95				
AT4G08770	peroxidase, putative	2,39	2,99	2,28	3,56				
AT3G03670	peroxidase, putative	9,93	16,41			9,36	14,27		
AT1G68850	peroxidase, putative	1,94	2,16						
AT1G34510	peroxidase, putative	2,03	3,55						
AT4G37520				2,19					
AT2G38380		1,69	1,74						
AT4G21960	PRXR1; electron carrier/ heme binding / peroxidase			1,58	4,47				
AT1G14540	anionic peroxidase, putative	3,64	4,17		1,53				
AT1G14550	anionic peroxidase, putative	3,67	3,26						
AT1G71695	peroxidase 12 (PER12) (P12) (PRXR6)		1,69						
AT5G66390	peroxidase 72 (PER72) (P72) (PRXR8)			1,55	2,74				
AT5G24070	peroxidase family protein	1,55							
AT5G64100	peroxidase, putative			2,62	6,46				
AT5G64110	peroxidase, putative							1,64	1,56
AT5G64120	peroxidase, putative			4,13	1,69				
AT5G15180	peroxidase, putative	2,4	2,46						
AT3G28200	peroxidase, putative				1,84				
AT5G39580	peroxidase, putative	1,51	1,66	2,56	8,14				
AT4G33420	peroxidase, putative			1,72	2,12				
AT1G30870	cationic peroxidase, putative		2,14						
AT5G37940					12,61				
AT1G14870		1,58	1,62		2,87	2,74	3,19		
AT1G59730	ATH7 (thioredoxin H-type 7)	1,79	2,55						
AT1G69880	ATH8 (thioredoxin H-type 8)	4,29	11,14	6,51				3,73	3,27
AT1G21750	ATPDIL1-1 (PDI-LIKE 1-1); protein disulfide isomerase				1,53				
AT3G54960	ATPDIL1-3 (PDI-LIKE 1-3); protein disulfide isomerase				1,54				
AT1G04980	ATPDIL2-2 (PDI-LIKE 2-2); protein disulfide isomerase				1,58				
AT5G08410	FTRA2 (ferredoxin/thioredoxin reductase subunit A (variable subunit 2); catalytic/ ferredoxin reductase/ ferredoxin:thioredoxin reductase/ lipoate synthase				1,97				
AT1G11530	ATCXXS1 (C-terminal cysteine residue is changed to a serine 1); protein disulfide isomerase				2,06				
AT5G11930	glutaredoxin family protein				1,95				
AT4G33040	glutaredoxin family protein				7,9				1,61
AT2G30540	glutaredoxin family protein				2,85				
AT4G15680	glutaredoxin family protein			1,84	8,41				

continued on next page

Table C.10 — continued from previous page

AGI code	Gene description	0,1 % sucrose				3 % sucrose			
		root		shoot		root		shoot	
		d ³ /d ₀	d ⁴ /d ₀	d ³ /d ₀	d ⁴ /d ₀	d ³ /d ₀	d ⁴ /d ₀	d ³ /d ₀	d ⁴ /d ₀
AT4G15660	glutaredoxin family protein			2,03	7,11				
AT4G15690	glutaredoxin family protein			1,63	8,22				
AT4G15700	glutaredoxin family protein				6,84				
AT5G18600	glutaredoxin family protein				2,75				
AT3G62930	glutaredoxin family protein				1,87				
AT3G62950	glutaredoxin family protein				4,5				
AT1G03850	glutaredoxin family protein			1,77	2,84				
AT4G14890	ferredoxin family protein				1,66				
AT1G32550	ferredoxin family protein				1,59				
AT2G04700	ferredoxin thioredoxin reductase catalytic beta chain family protein				1,84				
AT4G32590	ferredoxin-related				1,62				
AT1G20020	FNR2 (FERREDOXIN-NADP(+)-OXIDOREDUCTASE 2); NADPH dehydrogenase/ oxidoreductase/ poly(U) binding	2,46	2,9		3,47				2,3
AT4G05390	ATRFNR1 (ROOT FNR 1); FAD binding / NADP or NADPH binding / electron carrier/ ferredoxin-NADP+ reductase/ oxidoreductase			2,14	1,98				
AT1G30510	ATRFNR2 (ROOT FNR 2); FAD binding / NADP or NADPH binding / electron carrier/ ferredoxin-NADP+ reductase/ oxidoreductase			2,02	4				
AT3G01420	DOX1; lipoxigenase	1,6	2,17	1,55		3,01	3,54	2,35	3,05
AT2G16060	AHB1 (ARABIDOPSIS HEMOGLOBIN 1); oxygen binding / oxygen transporter	1,66		3,39	4,99				
AT1G77120	ADH1 (ALCOHOL DEHYDROGENASE 1); alcohol dehydrogenase	1,9			3,43				
AT4G18360	(S)-2-hydroxy-acid oxidase, peroxisomal, putative / glycolate oxidase, putative / short chain alpha-hydroxy acid oxidase, putative	1,56	1,82	3,92	3,05			1,98	2,9
AT5G16970	AT-AER (alkenal reductase); 2-alkenal reductase				2,79				
AT1G08830	CSD1 (COPPER/ZINC SUPEROXIDE DISMUTASE 1); superoxide dismutase			1,85	1,91				
AT2G28190	CSD2 (COPPER/ZINC SUPEROXIDE DISMUTASE 2); superoxide dismutase				3,79				
AT1G20630	CAT1 (CATALASE 1); catalase				3,22				1,51
Chromatin									
AT3G15790	MBD11; DNA binding / methyl-CpG binding				1,73				
AT2G36490	DML1 (DEMETER-LIKE 1); DNA N-glycosylase/ DNA-(apurinic or apyrimidinic site) lyase/ protein binding				1,95				
AT3G48360	BT2 (BTB AND TAZ DOMAIN PROTEIN 2); protein binding / transcription factor/ transcription regulator			1,71	37,34				
AT5G67480	BT4 (BTB AND TAZ DOMAIN PROTEIN 4); protein binding / transcription regulator			1,83	2,87				
AT4G37610	BT5 (BTB AND TAZ DOMAIN PROTEIN 5); protein binding / transcription regulator				2,23				
AT5G08610	DEAD box RNA helicase (RH26)				1,52				
AT3G06980	DEAD/DEAH box helicase, putative				2,13				
AT1G59990	DEAD/DEAH box helicase, putative (RH22)							1,58	
AT5G14260	SET domain-containing protein				1,87				
AT3G07670	SET domain-containing protein				1,76				

continued on next page

Table C.10 – continued from previous page

AGI code	Gene description	0,1 % sucrose				3 % sucrose			
		root		shoot		root		shoot	
		d_3/d_0	d_4/d_0	d_3/d_0	d_4/d_0	d_3/d_0	d_4/d_0	d_3/d_0	d_4/d_0
AT1G13220	LINC2 (LITTLE NUCLEI2)				1,55				
AT1G72030	GCN5-related N-acetyltransferase (GNAT) family protein				1,57				
AT2G32020	GCN5-related N-acetyltransferase (GNAT) family protein						3,08	3,77	1,52
AT2G39030	GCN5-related N-acetyltransferase (GNAT) family protein			2,52	3,83				
AT4G28030	GCN5-related N-acetyltransferase (GNAT) family protein				1,72				
AT2G27840	HDT4; histone deacetylase			1,61	1,81				
AT4G33470	hda14 (histone deacetylase 14); histone deacetylase				2,01				
AT5G10390	histone H3				1,57				
AT2G18050	HIS1-3 (HISTONE H1-3); DNA binding / nucleosomal DNA binding	2,36	3,44						
AT2G28720	histone H2B, putative				2,52				
Response to salt, drought									
AT4G25480	DREB1A (DEHYDRATION RESPONSE ELEMENT B1A); DNA binding / transcription activator/ transcription factor			2,76	8,37				
AT5G05410	DREB2A; DNA binding / transcription activator/ transcription factor	3,62	3,66	2,25	6,86				
AT3G11020	DREB2B (DRE/CRT-BINDING PROTEIN 2B); DNA binding / transcription activator/ transcription factor				2,21				
AT5G63650	SNRK2.5 (SNF1-RELATED PROTEIN KINASE 2.5); kinase				2,13				
AT5G66880	SNRK2.3 (SUCROSE NONFERMENTING 1(SNF1)-RELATED PROTEIN KINASE 2.3); kinase/ protein kinase			1,5					
AT2G23030	SNRK2.9 (SNF1-RELATED PROTEIN KINASE 2.9); ATP binding / kinase/ protein kinase/ protein serine/threonine kinase			1,57	3,51				
AT5G14640	SK13 (SHAGGY-LIKE KINASE 13); ATP binding / protein kinase/ protein serine/threonine kinase				2,39				
AT4G30960	SIP3 (SOS3-INTERACTING PROTEIN 3); ATP binding / kinase/ protein kinase/ protein serine/threonine kinase				2,54				
AT1G74520	ATHVA22A				1,72				
AT4G24960	ATHVA22D				2,44				
AT5G03630	ATMDAR2; monodehydroascorbate reductase (NADH)				1,97				
AT4G11650	ATOSM34 (osmotin 34)	1,66	1,76	2,74	2,47				
AT2G21620	RD2				1,62				
AT5G25610	RD22; nutrient reservoir			1,55	2,44				
AT4G27410	RD26 (RESPONSIVE TO DESICCATION 26); transcription activator/ transcription factor								1,74
AT2G33380	RD20 (RESPONSIVE TO DESSICATION 20); calcium ion binding			1,68	4,3				
AT1G33170	dehydration-responsive family protein				2,45				
AT1G31850	dehydration-responsive protein, putative				1,92				
AT3G56080	dehydration-responsive protein-related				3,06				
AT3G23300	dehydration-responsive protein-related				1,56				
AT4G38410	dehydrin, putative			1,57					
AT1G69080	universal stress protein (USP) family protein				4,52				
AT1G68300	universal stress protein (USP) family protein				1,56				
AT2G47710	universal stress protein (USP) family protein				1,78				

continued on next page

Table C.10 – continued from previous page

AGI code	Gene description	0,1 % sucrose				3 % sucrose			
		root		shoot		root		shoot	
		d ³ /d ₀	d ⁴ /d ₀	d ³ /d ₀	d ⁴ /d ₀	d ³ /d ₀	d ⁴ /d ₀	d ³ /d ₀	d ⁴ /d ₀
AT3G03270	universal stress protein (USP) family protein / early nodulin ENOD18 family protein				1,93				
AT3G62550	universal stress protein (USP) family protein				3,09			1,51	3,76
AT1G20450	ERD10 (EARLY RESPONSIVE TO DEHYDRATION 10); actin binding				1,66	1,81	1,72		
AT1G76180	ERD14 (EARLY RESPONSE TO DEHYDRATION 14); calcium ion binding				2,31				
AT4G19120	ERD3 (early-responsive to dehydration 3)				2,09				
AT2G28790	osmotin-like protein, putative				1,81				
AT2G41430	ERD15 (EARLY RESPONSIVE TO DEHYDRATION 15); protein binding				1,57				1,53
AT1G30360	ERD4 (early-responsive to dehydration 4)								1,74
AT3G30775	ERD5 (EARLY RESPONSIVE TO DEHYDRATION 5); proline dehydrogenase				4,37				
AT1G08930	ERD6 (EARLY RESPONSE TO DEHYDRATION 6); carbohydrate transmembrane transporter/ sugar transmembrane transporter/ sugar:hydrogen symporter				2,18				
AT2G17840	ERD7 (EARLY-RESPONSIVE TO DEHYDRATION 7)	1,53	1,56	2,5	1,71				
AT4G39090	RD19 (RESPONSIVE TO DEHYDRATION 19); cysteine-type endopeptidase/ cysteine-type peptidase				1,59				
AT5G49480	ATCP1 (Ca ²⁺ -binding protein 1); calcium ion binding				2,89				2,58
AT5G67450	AZF1 (ARABIDOPSIS ZINC-FINGER PROTEIN 1); DNA binding / nucleic acid binding / transcription factor/ transcription repressor/ zinc ion binding				1,54				
AT3G19580	AZF2 (ARABIDOPSIS ZINC-FINGER PROTEIN 2); DNA binding / nucleic acid binding / transcription factor/ transcription repressor/ zinc ion binding	1,6	1,67						
AT5G43170	AZF3 (ARABIDOPSIS ZINC-FINGER PROTEIN 3); DNA binding / nucleic acid binding / transcription factor/ transcription repressor/ zinc ion binding			1,73	1,87				
AT1G32090	early-responsive to dehydration protein-related / ERD protein-related				2,05				
AT4G04340	early-responsive to dehydration protein-related / ERD protein-related								1,5
AT1G27730	STZ (salt tolerance zinc finger); nucleic acid binding / transcription factor/ transcription repressor/ zinc ion binding	3,16	3,05		5,51				
AT3G55980	SZF1 (SALT-INDUCIBLE ZINC FINGER 1); transcription factor	3,88	3,4	2,37	4,4				2,23
AT5G20230	ATBCB (ARABIDOPSIS BLUE-COPPER-BINDING PROTEIN); copper ion binding / electron carrier	2,27	2,25		34,11			1,56	1,86
Response to cold/mechanical									
AT4G25490	CBF1 (C-REPEAT/DRE BINDING FACTOR 1); DNA binding / transcription activator/ transcription factor	3,55	3,86	2,84	5,27				3,38
AT4G25470	CBF2 (C-REPEAT/DRE BINDING FACTOR 2); DNA binding / transcription activator/ transcription factor	4,18	5,31	2,12	9,01				
AT2G42540	COR15A (COLD-REGULATED 15A)				2,62				
AT3G05890	RCI2B (RARE-COLD-INDUCIBLE 2B)				4,78				
AT1G29395	COR414-TM1			1,79	2,77				1,93
AT2G42530	COR15B (COLD REGULATED 15B)			2,07	1,54			1,85	4,5
AT1G20440	COR47 (COLD-REGULATED 47)	1,6	1,56						
AT5G59820	RHL41 (RESPONSIVE TO HIGH LIGHT 41); nucleic acid binding / transcription factor/ zinc ion binding	2,08	2,04						
AT3G50970	LTI30 (LOW TEMPERATURE-INDUCED 30)			2,6	2,7			1,75	2,67
AT5G52310	LTI78 (LOW-TEMPERATURE-INDUCED 78)			2,78	1,73	4,24	2,74		

continued on next page

Table C.10 – continued from previous page

AGI code	Gene description	0,1 % sucrose				3 % sucrose			
		root		shoot		root		shoot	
		d ₃ /d ₀	d ₄ /d ₀	d ₃ /d ₀	d ₄ /d ₀	d ₃ /d ₀	d ₄ /d ₀	d ₃ /d ₀	d ₄ /d ₀
AT1G09070	SRC2 (SOYBEAN GENE REGULATED BY COLD-2); protein binding	1,97	1,82						
AT5G04340	ZAT6 (ZINC FINGER OF ARABIDOPSIS THALIANA 6); nucleic acid binding / transcription factor/ zinc ion binding				3,58				
AT2G40140	CZF1; transcription factor			1,69	3,06				
AT5G37770	TCH2 (TOUCH 2); calcium ion binding				1,5				
AT2G41100	TCH3 (TOUCH 3); calcium ion binding			1,56	2,27				
AT5G57560	TCH4 (Touch 4); hydrolase, acting on glycosyl bonds / xyloglucan:xyloglucosyl transferase	4,73	3,71		3,67	3,39			
Senescence									
AT1G69490	NAP (NAC-like, activated by AP3/PI); transcription factor	1,91	1,79	2,13	6,38				
AT2G29350	SAG13; alcohol dehydrogenase/ oxidoreductase	2,03	3,76	2,16	3,3	17,25	21,75		
AT3G10985	SAG20 (SENESCENCE ASSOCIATED GENE 20)			1,74					
AT5G13170	SAG29 (SENESCENCE-ASSOCIATED PROTEIN 29)			3,19	2,43				1,64
AT4G17670	senescence-associated protein-related		2,48		5,69				
AT5G65040	senescence-associated protein-related			1,51	1,64				
AT1G22160	senescence-associated protein-related				10,51				
AT3G22550	senescence-associated protein-related				2,85				1,65
AT1G78020	senescence-associated protein-related				5,21				
AT1G74940	senescence-associated protein-related				1,62	1,52	1,74		
AT2G44670	senescence-associated protein-related				2,02				
AT1G19200	senescence-associated protein-related							1,98	2,19
AT1G53885	senescence-associated protein-related				3,5				6,47
AT1G66330	senescence-associated family protein				1,73				
Dark induced									
AT3G49620	DIN11 (DARK INDUCIBLE 11); iron ion binding / oxidoreductase								1,53
AT3G60140	DIN2 (DARK INDUCIBLE 2); catalytic/ cation binding / hydrolase, hydrolyzing O-glycosyl compounds	1,95	1,79	1,64		11,25	18,51		2,21
AT5G20250	DIN10 (DARK INDUCIBLE 10); hydrolase, hydrolyzing O-glycosyl compounds				8,73				
AT3G13450	DIN4 (DARK INDUCIBLE 4); 3-methyl-2-oxobutanoate dehydrogenase (2-methylpropanoyl-transferring)/ catalytic				2,67				
AT1G67070	DIN9 (DARK INDUCIBLE 9); mannose-6-phosphate isomerase				2				
Phenylpropanoid/flavonoid/anthocyanin biosynthesis									
AT1G56650	PAP1 (PRODUCTION OF ANTHOCYANIN PIGMENT 1); DNA binding / transcription factor				1,7			2,27	2,66
AT4G29080	PAP2 (PHYTOCHROME-ASSOCIATED PROTEIN 2); transcription factor				3,63				
AT2G37040	pal1 (Phe ammonia lyase 1); phenylalanine ammonia-lyase			1,65	2,33				
AT5G04230	PAL3 (PHENYL ALANINE AMMONIA-LYASE 3); phenylalanine ammonia-lyase				1,87				
AT3G10340	PAL4 (Phenylalanine ammonia-lyase 4); ammonia ligase/ ammonia-lyase/ catalytic				2,05				

continued on next page

Table C.10 – continued from previous page

AGI code	Gene description	0,1 % sucrose				3 % sucrose			
		root		shoot		root		shoot	
		d ³ /d ₀	d ⁴ /d ₀	d ³ /d ₀	d ⁴ /d ₀	d ³ /d ₀	d ⁴ /d ₀	d ³ /d ₀	d ⁴ /d ₀
AT5G13930	TT4 (TRANSPARENT TESTA 4); naringenin-chalcone synthase	3,31	4,95	1,66	9,4				
AT3G55120	TT5 (TRANSPARENT TESTA 5); chalcone isomerase	6,17	10,43						
AT4G34230	ATCAD5 (CINNAMYL ALCOHOL DEHYDROGENASE 5); cinnamyl-alcohol dehydrogenase			1,97	2,25				
AT2G30490	C4H (CINNAMATE-4-HYDROXYLASE); trans-cinnamate 4-monooxygenase		1,52	1,67					
AT4G37970	CAD6 (CINNAMYL ALCOHOL DEHYDROGENASE 6); binding / catalytic/ oxidoreductase/ zinc ion binding				1,75				
AT4G39330	CAD9 (CINNAMYL ALCOHOL DEHYDROGENASE 9); binding / catalytic/ oxidoreductase/ zinc ion binding				1,95				
AT5G14700	cinnamoyl-CoA reductase-related	1,66	2						
AT4G30470	cinnamoyl-CoA reductase-related				2,15				2,13
AT1G72680	cinnamyl-alcohol dehydrogenase, putative					2,14	2,34		
AT1G51680	4CL1 (4-COUMARATE:COA LIGASE 1); 4-coumarate-CoA ligase			1,75	2,71				
AT3G21240	4CL2 (4-COUMARATE:COA LIGASE 2); 4-coumarate-CoA ligase			2,04	3,37				
AT1G65060	4CL3; 4-coumarate-CoA ligase	1,75	3,95						
AT3G21230	4CL5 (4-coumarate:CoA ligase 5); 4-coumarate-CoA ligase			1,76	2,37				
AT5G08640	FLS (FLAVONOL SYNTHASE); flavonol synthase	4,16	9,23		2,35				
AT5G63580	FLS2 (FLAVONOL SYNTHASE 2); flavonol synthase				7,09				
AT5G63590	FLS3 (FLAVONOL SYNTHASE 3); flavonol synthase		1,74						
AT5G63600	FLS5 (FLAVONOL SYNTHASE 5); flavonol synthase			2,19				1,83	1,71
AT3G51240	F3H (FLAVANONE 3-HYDROXYLASE); naringenin 3-dioxygenase	2,71	5,15	1,87	4,72			2,96	
AT1G75280	isoflavone reductase, putative				3,78	1,65			
AT1G75300	isoflavone reductase, putative				1,86				
AT5G05270	chalcone-flavanone isomerase family protein	2,97	3,98		3,73				
AT4G34050	caffeoyl-CoA 3-O-methyltransferase, putative			1,53	2,44				
AT1G67980	CCoAMT; caffeoyl-CoA O-methyltransferase	3,05	3,53			15,17	26,47		
AT4G36220	FAH1 (FERULIC ACID 5-HYDROXYLASE 1); ferulate 5-hydroxylase/ monooxygenase			1,54	2,16				
AT5G61160	AACT1 (anthocyanin 5-aromatic acyltransferase 1); transferase/ transferase, transferring acyl groups other than amino-acyl groups			3,14	2,94				
AT5G48930	HCT (HYDROXYCINNAMOYL-COA SHIKIMATE/QUINATE HYDROXYCINNAMOYL TRANSFERASE); quinate O-hydroxycinnamoyltransferase/ shikimate O-hydroxycinnamoyltransferase/ transferase				1,55				
AT3G28910	MYB30 (MYB DOMAIN PROTEIN 30); DNA binding / transcription factor	1,53			2,4				
Translation									
AT5G06000	EIF3G2; RNA binding / translation initiation factor	1,51	1,51						
AT4G18040	EIF4E (EUKARYOTIC TRANSLATION INITIATION FACTOR 4E); RNA binding / RNA cap binding / protein binding / translation initiation factor				1,51				
AT5G05470	EIF2 ALPHA; RNA binding / translation initiation factor		1,7						
AT3G28500	60S acidic ribosomal protein P2 (RPP2C)				2,08				
AT2G07725	60S ribosomal protein L5 (RPL5)				1,71				
AT1G36730	eukaryotic translation initiation factor 5, putative / eIF-5, putative				1,8				

continued on next page

Table C.10 – continued from previous page

AGI code	Gene description	0,1 % sucrose				3 % sucrose				
		root		shoot		root		shoot		
		d ₃ /d ₀	d ₄ /d ₀	d ₃ /d ₀	d ₄ /d ₀	d ₃ /d ₀	d ₄ /d ₀	d ₃ /d ₀	d ₄ /d ₀	
AT2G18400	ribosomal protein L6 family protein				1,7					
AT2G07675	ribosomal protein S12 mitochondrial family protein			1,99	1,57					
AT3G20260	structural constituent of ribosome				1,51					
AT4G30800	40S ribosomal protein S11 (RPS11B)	1,67	1,7							
AT3G20230	50S ribosomal protein L18 family				1,75					
AT5G54600	50S ribosomal protein L24, chloroplast (CL24)				1,56					
AT2G33450	50S ribosomal protein L28, chloroplast (CL28)				1,5					
AT1G76730	5-formyltetrahydrofolate cyclo-ligase family protein				1,52					
AT5G12110	elongation factor 1B alpha-subunit 1 (eEF1Balpha1)							1,95		
AT3G08740	elongation factor P (EF-P) family protein				2,1					
AT4G27130	eukaryotic translation initiation factor SUI1, putative					1,64	1,68			
AT1G17220	FUG1 (fu-gaeri1); translation initiation factor				1,62					
AT3G63490	ribosomal protein L1 family protein				1,6					
AT1G48350	ribosomal protein L18 family protein				1,52					
AT4G17560	ribosomal protein L19 family protein				1,64					
AT5G65220	ribosomal protein L29 family protein		1,68							
AT4G30690	translation initiation factor 3 (IF-3) family protein		1,74		2,4				2,24	
AT5G30510	RPS1 (RIBOSOMAL PROTEIN S1); RNA binding / structural constituent of ribosome				1,67					
AT4G27650	PEL1 (PELOTA); translation release factor					1,53				
AT4G17300	NS1; asparagine-tRNA ligase				1,97					
AT3G46100	ATHRS1 (HISTIDYL-TRNA SYNTHETASE 1); histidine-tRNA ligase				1,54					
AT3G58140	phenylalanyl-tRNA synthetase class IIc family protein				2,19					
AT5G49030	OVA2 (ovule abortion 2); ATP binding / aminoacyl-tRNA ligase/ catalytic/ isoleucine-tRNA ligase/ nucleotide binding				1,91					
AT1G48520	GATB (GLU-ADT SUBUNIT B); carbon-nitrogen ligase, with glutamine as amido-N-donor / glutaminyl-tRNA synthase (glutamine-hydrolyzing)/ ligase				1,83					
AT3G56020					1,56					
AT3G25920	RPL15; structural constituent of ribosome				1,5					
Protein folding										
AT4G38740	ROC1 (ROTAMASE CYP 1); peptidyl-prolyl cis-trans isomerase				3					
AT4G34870	ROC5 (ROTAMASE CYCLOPHILIN 5); peptidyl-prolyl cis-trans isomerase				2,02					
AT5G23240	DNAJ heat shock N-terminal domain-containing protein			2,17	2,6				14,58	
AT1G56300	DNAJ heat shock N-terminal domain-containing protein				12,42				11,81	
AT1G72070	DNAJ heat shock N-terminal domain-containing protein		1,59							
AT2G21510	DNAJ heat shock N-terminal domain-containing protein						1,52			
AT4G36040	DNAJ heat shock N-terminal domain-containing protein (J11)				1,5				1,53	
AT2G17880	DNAJ heat shock protein, putative		1,55							

continued on next page

Table C.10 – continued from previous page

AGI code	Gene description	0,1 % sucrose				3 % sucrose			
		root		shoot		root		shoot	
		d ³ /d ₀	d ⁴ /d ₀	d ³ /d ₀	d ⁴ /d ₀	d ³ /d ₀	d ⁴ /d ₀	d ³ /d ₀	d ⁴ /d ₀
AT4G13830	J20 (DNAJ-LIKE 20); heat shock protein binding								2,08
AT5G43260	chaperone protein dnaJ-related				2,16				
AT1G75690	chaperone protein dnaJ-related				2,18				
AT1G26230	chaperonin, putative				1,68				
AT3G12340	FK506 binding / peptidyl-prolyl cis-trans isomerase	1,51							
AT5G13410	immunophilin / FKBP-type peptidyl-prolyl cis-trans isomerase family protein				1,78				
AT3G60370	immunophilin / FKBP-type peptidyl-prolyl cis-trans isomerase family protein				2,1				
AT4G26555	immunophilin / FKBP-type peptidyl-prolyl cis-trans isomerase family protein				1,68				
AT1G20810	immunophilin / FKBP-type peptidyl-prolyl cis-trans isomerase family protein				1,62				
AT2G43560	immunophilin / FKBP-type peptidyl-prolyl cis-trans isomerase family protein				2,21				
AT4G39710	immunophilin, putative / FKBP-type peptidyl-prolyl cis-trans isomerase, putative				1,55				
AT3G10060	immunophilin, putative / FKBP-type peptidyl-prolyl cis-trans isomerase, putative				1,92				
AT5G45680	FK506-binding protein 1 (FKBP13)				1,62				
AT2G21130	peptidyl-prolyl cis-trans isomerase / cyclophilin (CYP2) / rotamase				1,8				
AT3G15520	peptidyl-prolyl cis-trans isomerase TLP38, chloroplast / thylakoid lumen PPIase of 38 kDa / cyclophilin / rotamase				1,62				
AT5G48570	peptidyl-prolyl cis-trans isomerase, putative / FK506-binding protein, putative					1,83	1,93		
AT2G38730	peptidyl-prolyl cis-trans isomerase, putative / cyclophilin, putative / rotamase, putative	1,56							
AT5G03160					3,13				
AT3G12580	HSP70 (heat shock protein 70); ATP binding				3,11			2,98	
AT5G02490	heat shock cognate 70 kDa protein 2 (HSC70-2) (HSP70-2)				2,08				
AT5G56030	HSP81-2 (HEAT SHOCK PROTEIN 81-2); ATP binding				2,05				
AT5G56000					1,86				
AT5G56500	ATP binding / protein binding				2,07				
AT1G22630	unknown protein				1,58				
AT2G34860	EDA3 (embryo sac development arrest 3); heat shock protein binding / unfolded protein binding				1,86				
AT1G80920	J8; heat shock protein binding / unfolded protein binding							2,34	
AT5G55220	trigger factor type chaperone family protein				1,55				
AT3G01480	CYP38 (cyclophilin 38); peptidyl-prolyl cis-trans isomerase				1,79				
Proteasome/Ubiquitin									
AT2G01150	RHA2B (RING-H2 FINGER PROTEIN 2B); protein binding / ubiquitin-protein ligase/ zinc ion binding				1,76				
AT5G10790	UBP22 (UBIQUITIN-SPECIFIC PROTEASE 22); ubiquitin thiolesterase/ ubiquitin-specific protease/ zinc ion binding							1,64	
AT3G61390	U-box domain-containing protein					6,06	9,01		
AT2G18290	anaphase-promoting complex, subunit 10 family / APC10 family				1,97				
AT4G36410	UBC17 (UBIQUITIN-CONJUGATING ENZYME 17); small conjugating protein ligase/ ubiquitin-protein ligase				1,96			1,84	4,09
AT1G63800	UBC5 (ubiquitin-conjugating enzyme 5); ubiquitin-protein ligase				2,04				

continued on next page

Table C.10 — continued from previous page

AGI code	Gene description	0,1 % sucrose				3 % sucrose			
		root		shoot		root		shoot	
		d ₃ /d ₀	d ₄ /d ₀	d ₃ /d ₀	d ₄ /d ₀	d ₃ /d ₀	d ₄ /d ₀	d ₃ /d ₀	d ₄ /d ₀
AT1G66160	U-box domain-containing protein				5,53				
AT4G12570	UPL5 (UBIQUITIN PROTEIN LIGASE 5); acid-amino acid ligase/ binding / ubiquitin-protein ligase		1,55						
AT4G03510	RMA1; protein binding / ubiquitin-protein ligase/ zinc ion binding								2,91
AT1G55760	BTB/POZ domain-containing protein				3,5				
AT2G30600	BTB/POZ domain-containing protein				7,12				2,69
AT2G30600	BTB/POZ domain-containing protein				6,7				2,69
AT3G19470	F-box family protein				1,66				
AT2G32560	F-box family protein				1,67				
AT5G27920	F-box family protein				3,34				
AT5G25290	F-box family protein		1,53						
AT3G23880	F-box family protein	1,8	2,16						
AT2G16365	F-box family protein							2,96	
AT1G61340	F-box family protein	2,53	2,47	3,84	5,95				
AT3G27150	kelch repeat-containing F-box family protein		1,73						
AT1G80440	kelch repeat-containing F-box family protein								2,32
AT1G23390	kelch repeat-containing F-box family protein							3,8	
AT1G63840	zinc finger (C3HC4-type RING finger) family protein			1,57	2,45				
AT5G47610	zinc finger (C3HC4-type RING finger) family protein				1,71				
AT1G20823	zinc finger (C3HC4-type RING finger) family protein				1,95				
AT5G24870	zinc finger (C3HC4-type RING finger) family protein				1,89				
AT5G41400	zinc finger (C3HC4-type RING finger) family protein				2,8				
AT1G14200	zinc finger (C3HC4-type RING finger) family protein				1,61				
AT2G15580	zinc finger (C3HC4-type RING finger) family protein				1,53				
AT3G51950	zinc finger (CCCH-type) family protein / RNA recognition motif (RRM)-containing protein				1,84				
AT1G08050	zinc finger (C3HC4-type RING finger) family protein	1,7	2,68						
AT1G14260	zinc finger (C3HC4-type RING finger) family protein	1,95	2,18						
AT1G72200	zinc finger (C3HC4-type RING finger) family protein	1,88	1,97		2,36				
AT5G42200	zinc finger (C3HC4-type RING finger) family protein	2,08	2,37						
AT3G11110	zinc finger (C3HC4-type RING finger) family protein							2,32	
AT1G49230	zinc finger (C3HC4-type RING finger) family protein	1,53	1,85	2,35	3,53				5,62
AT1G22500	zinc finger (C3HC4-type RING finger) family protein	1,85	2,12		2,27				
AT2G35910	zinc finger (C3HC4-type RING finger) family protein				1,86				
AT2G42350	zinc finger (C3HC4-type RING finger) family protein				1,91				
AT2G42360	zinc finger (C3HC4-type RING finger) family protein				1,93				
AT5G27420	zinc finger (C3HC4-type RING finger) family protein			2,26	3,71				
AT4G35480	RHA3B; protein binding / zinc ion binding			2,08	2,95				
AT5G66070	zinc finger (C3HC4-type RING finger) family protein				2,96				
AT5G59550	zinc finger (C3HC4-type RING finger) family protein	1,93	1,91						

continued on next page

Table C.10 — continued from previous page

AGI code	Gene description	0,1 % sucrose				3 % sucrose				
		root		shoot		root		shoot		
		d ³ /d ₀	d ⁴ /d ₀	d ³ /d ₀	d ⁴ /d ₀	d ³ /d ₀	d ⁴ /d ₀	d ³ /d ₀	d ⁴ /d ₀	
AT3G46620	zinc finger (C3HC4-type RING finger) family protein	1,79	1,83		1,77					
AT3G05200	ATL6; protein binding / zinc ion binding				1,74					
AT1G76410	ATL8; protein binding / zinc ion binding		1,53		1,79					
AT4G17245	zinc finger (C3HC4-type RING finger) family protein				1,97					
AT5G22920	zinc finger (C3HC4-type RING finger) family protein				3,75				3,2	
AT5G18760	zinc finger (C3HC4-type RING finger) family protein				1,55					
AT5G01520	zinc finger (C3HC4-type RING finger) family protein		1,52							
AT4G31450	zinc finger (C3HC4-type RING finger) family protein				1,86					
AT4G26400	zinc finger (C3HC4-type RING finger) family protein		1,52							
AT2G37950	zinc finger (C3HC4-type RING finger) family protein				2,01					
AT1G73760	zinc finger (C3HC4-type RING finger) family protein								1,51	
AT1G74370	zinc finger (C3HC4-type RING finger) family protein				1,64					
AT2G22680	zinc finger (C3HC4-type RING finger) family protein		1,64							
AT5G44260	zinc finger (CCCH-type) family protein								4,44	
AT3G51390	zinc finger (DHHC type) family protein				1,52					
AT5G50450	zinc finger (MYND type) family protein				5,21					
AT1G15100	RHA2A; protein binding / ubiquitin-protein ligase/ zinc ion binding				2,15				3,47	
AT4G11360	RHA1B; protein binding / zinc ion binding		1,51							
AT2G17450	RHA3A; protein binding / zinc ion binding								1,6	
AT3G18710	PUB29 (PLANT U-BOX 29); ubiquitin-protein ligase			1,59	1,69					
AT5G67340	armadillo/beta-catenin repeat family protein / U-box domain-containing protein	1,82	2,14							
AT1G60190	armadillo/beta-catenin repeat family protein / U-box domain-containing protein			1,91	2,01				4,28	
Membrane signaling										
AT5G07920	DGK1 (DIACYLGLYCEROL KINASE1); calcium ion binding / diacylglycerol kinase				1,72					
AT2G26560	PLA2A (PHOSPHOLIPASE A 2A); lipase/ nutrient reservoir	4,51	4,74		4,95	12,94	22,58	2,06	2,17	
AT2G06925	PLA2-ALPHA; phospholipase A2	1,57	1,69						1,63	
AT5G58670	PLC1 (PHOSPHOLIPASE C 1); phospholipase C			1,87	1,71					
AT3G08510	ATPLC2 (PHOSPHOLIPASE C 2); phospholipase C				1,69					
AT3G05630	PLDP2; phospholipase D					2,88	1,74			
AT1G21250	WAK1 (CELL WALL-ASSOCIATED KINASE); kinase			2,15	8,28					
Inositol/phosphoinositols										
AT5G63980	SAL1; 3'(2'),5'-bisphosphate nucleotidase/ inositol or phosphatidylinositol phosphatase	1,78	2,1		2,23					
AT5G61760	ATIPK2BETA; inositol or phosphatidylinositol kinase/ inositol trisphosphate 6-kinase				1,6					
AT1G79470	inosine-5'-monophosphate dehydrogenase	1,7	1,82							
AT4G16670	phosphoinositide binding			2,09	2,91					
AT5G58700	phosphoinositide-specific phospholipase C family protein		1,64							

continued on next page

Table C.10 – continued from previous page

AGI code	Gene description	0,1 % sucrose				3 % sucrose			
		root		shoot		root		shoot	
		d ₃ /d ₀	d ₄ /d ₀	d ₃ /d ₀	d ₄ /d ₀	d ₃ /d ₀	d ₄ /d ₀	d ₃ /d ₀	d ₄ /d ₀
AT5G45940	atnudt11 (Arabidopsis thaliana Nudix hydrolase homolog 11); hydrolase				1,93				
AT4G18010	AT5PTASE2 (MYO-INOSITOL POLYPHOSPHATE 5-PHOSPHATASE 2); inositol-polyphosphate 5-phosphatase	1,52	1,86		3,34				
AT4G13720	inosine triphosphate pyrophosphatase, putative / HAM1 family protein				1,56				
AT4G16480	INT4 (INOSITOL TRANSPORTER 4); carbohydrate transmembrane transporter/ myo-inositol:hydrogen symporter/ sugar:hydrogen symporter				1,52				
AT1G34260	phosphatidylinositol-4-phosphate 5-kinase family protein				1,61				
AT1G05470	CVP2 (COTYLEDON VASCULAR PATTERN 2); hydrolase/ inositol trisphosphate phosphatase			1,7					
AT2G01180	ATPAP1 (PHOSPHATIDIC ACID PHOSPHATASE 1); phosphatidate phosphatase				1,6				
AT1G27480	lecithin:cholesterol acyltransferase family protein / LACT family protein				2,04				
AT4G39800	MIPS1 (MYO-INOSITOL-1-PHOSPHATE SYNTHASE 1); inositol-3-phosphate synthase				3,58				
AT2G22240	MIPS2 (MYO-INOSITOL-1-PHOSPHATE SYNTHASE 2); binding / catalytic/ inositol-3-phosphate synthase			1,52	8,86				
AT2G19800	MIOX2 (MYO-INOSITOL OXYGENASE 2); inositol oxygenase				13,16				
AT4G26260	MIOX4; inositol oxygenase				7,55				
Ca/calmodulin									
AT2G38760	ANNAT3 (ANNEXIN ARABIDOPSIS 3); calcium ion binding / calcium-dependent phospholipid binding					3,39	3,54		
AT5G10230	ANNAT7 (ANNEXIN ARABIDOPSIS 7); calcium ion binding / calcium-dependent phospholipid binding						1,61		
AT3G51860	CAX3 (CATION EXCHANGER 3); calcium:cation antiporter/ calcium:hydrogen antiporter/ cation:cation antiporter	1,64	2,31	3,69	1,97				
AT5G17860	CAX7 (calcium exchanger 7); calcium:sodium antiporter/ cation:cation antiporter				1,62	2,68	3,18		
AT3G63380	calcium-transporting ATPase, plasma membrane-type, putative / Ca(2+)-ATPase, putative (ACA12)	2,84	3,13	2,29	1,63				
AT4G26470	calcium ion binding		1,55						
AT3G47480	calcium-binding EF hand family protein	2,61	3,59	1,53		9,6	11,35		
AT1G29020	calcium-binding EF hand family protein		1,93						
AT1G21550	calcium-binding protein, putative	1,86	2,83		1,72				
AT2G46600	calcium-binding protein, putative		1,65						
AT3G25600	calcium ion binding				1,9				
AT4G32060	calcium-binding EF hand family protein				1,65				
AT4G27280	calcium-binding EF hand family protein	3,02	2,69		1,54				
AT1G76650	calcium-binding EF hand family protein	4,11	4,81	2,39	8,37	5,94	3,53		
AT2G15760	calmodulin-binding protein	1,98	2,38						
AT2G41090	calmodulin-like calcium-binding protein, 22 kDa (CaBP-22)				1,64	8,25			
AT3G50770	calmodulin-related protein, putative				2,21				
AT2G38800	calmodulin-binding protein-related	1,58	1,76		1,61				
AT2G26190	calmodulin-binding family protein				1,89	2,64			
AT3G01830	calmodulin-related protein, putative	4,73	3,97	2,69	5,15				
AT1G76640	calmodulin-related protein, putative	1,66	1,77						
AT3G56690	CIP111 (CAM INTERACTING PROTEIN 111); ATPase/ calmodulin binding				1,55				

continued on next page

Table C.10 — continued from previous page

AGI code	Gene description	0,1 % sucrose				3 % sucrose			
		root		shoot		root		shoot	
		d ³ /d ₀	d ⁴ /d ₀	d ³ /d ₀	d ⁴ /d ₀	d ³ /d ₀	d ⁴ /d ₀	d ³ /d ₀	d ⁴ /d ₀
Small G-proteins									
AT1G09180	ATSARA1A (ARABIDOPSIS THALIANA SECRETION-ASSOCIATED RAS SUPER FAMILY 1); GTP binding								1,82
AT4G18430	AtRABA1e (Arabidopsis Rab GTPase homolog A1e); GTP binding	1,65	1,76						
AT5G59150	ATRABA2D (HOARABIDOPSIS RAB GTPASE HOMOLOG A2D); GTP binding								1,51
AT3G07410	AtRABA5b (Arabidopsis Rab GTPase homolog A5b); GTP binding								1,73
AT5G03530	RABC2A (RAB GTPASE HOMOLOG C2A); GTP binding / GTP-dependent protein binding / myosin XI tail binding								3,31
AT4G28950	ROP9 (RHO-RELATED PROTEIN FROM PLANTS 9); GTP binding	1,5	1,58						
AT2G45890	ROPGEF4 (RHO GUANYL-NUCLEOTIDE EXCHANGE FACTOR 4); Rho guanyl-nucleotide exchange factor		1,68						
AT5G45750	AtRABA1c (Arabidopsis Rab GTPase homolog A1c); GTP binding								1,94
AT3G15060	AtRABA1g (Arabidopsis Rab GTPase homolog A1g); GTP binding								1,94
AT1G22740	RABG3B; GTP binding	1,96	2,07						
Transcription factors									
AT1G51700	ADOF1; DNA binding / transcription factor				1,84	1,58			
AT1G02220	ANAC003 (Arabidopsis NAC domain containing protein 3); transcription factor	2,29	2,84	2,43	1,78				
AT1G32870	ANAC13 (Arabidopsis thaliana NAC domain protein 13); transcription factor	1,63	2,02						
AT5G50820	anac097 (Arabidopsis NAC domain containing protein 97); transcription factor		1,56						
AT2G43000	anac042 (Arabidopsis NAC domain containing protein 42); transcription factor	16,22	19,4			13,76	19,11		
AT2G02450	ANAC035 (Arabidopsis NAC domain containing protein 35); transcription factor			1,66	2,02				
AT3G04060	anac046 (Arabidopsis NAC domain containing protein 46); transcription factor				2,33				
AT3G04070	anac047 (Arabidopsis NAC domain containing protein 47); transcription factor			1,89	2,97				
AT5G07680	ANAC080 (ARABIDOPSIS NAC DOMAIN CONTAINING PROTEIN 80); transcription factor		1,58						
AT5G14000	anac084 (Arabidopsis NAC domain containing protein 84); transcription factor			1,51	1,54				
AT5G63790	ANAC102 (ARABIDOPSIS NAC DOMAIN CONTAINING PROTEIN 102); transcription factor				2,26				
AT2G44940	AP2 domain-containing transcription factor TINY, putative				1,67				
AT2G47520	AP2 domain-containing transcription factor, putative	2,77	3,94						
AT5G67180	AP2 domain-containing transcription factor, putative				3,13				
AT1G01250	AP2 domain-containing transcription factor, putative				1,79				
AT5G52020	AP2 domain-containing protein	4,31	3,24						
AT5G61590	AP2 domain-containing transcription factor family protein		1,89		1,88				3,74
AT1G21910	AP2 domain-containing transcription factor family protein	3,22	2,18	1,91	1,96				
AT2G33710	AP2 domain-containing transcription factor family protein			1,59	2,73				
AT5G51190	AP2 domain-containing transcription factor, putative	3,18	3,09						1,71
AT1G19210	AP2 domain-containing transcription factor, putative	6,33	6,52						
AT1G77640	AP2 domain-containing transcription factor, putative	4,38	4,49	1,56	3,04	6,51	5,39		
AT1G64380	AP2 domain-containing transcription factor, putative			5,75	7,72				

continued on next page

Table C.10 – continued from previous page

AGI code	Gene description	0,1 % sucrose				3 % sucrose			
		root		shoot		root		shoot	
		d_3/d_0	d_4/d_0	d_3/d_0	d_4/d_0	d_3/d_0	d_4/d_0	d_3/d_0	d_4/d_0
AT1G36060	AP2 domain-containing transcription factor, putative			1,57	2,27				
AT1G22810	AP2 domain-containing transcription factor, putative			2,89	3,43				
AT2G35700	ERF38 (ERF FAMILY PROTEIN 38); DNA binding / transcription factor				4,64				
AT1G53170	ERF8; DNA binding / transcription factor/ transcription repressor				1,5				
AT5G25190	ethylene-responsive element-binding protein, putative				1,65				
AT4G29100	ethylene-responsive family protein				1,71				
AT1G05710	ethylene-responsive protein, putative			1,62	1,95				
AT1G09740	ethylene-responsive protein, putative			1,7					
AT5G47230	ERF5 (ETHYLENE RESPONSIVE ELEMENT BINDING FACTOR 5); DNA binding / transcription activator/ transcription factor				2,14				
AT1G28370	ERF11 (ERF DOMAIN PROTEIN 11); DNA binding / transcription factor/ transcription repressor	1,86	2		1,77				
AT2G44840	ERF13 (ETHYLENE-RESPONSIVE ELEMENT BINDING FACTOR 13); DNA binding / transcription factor	2,83	2,94						
AT1G72360	ethylene-responsive element-binding protein, putative				1,61				
AT5G61600	ethylene-responsive element-binding family protein				2,91				
AT3G23230	ethylene-responsive factor, putative			1,64	2				
AT4G17500	ATERF-1 (ETHYLENE RESPONSIVE ELEMENT BINDING FACTOR 1); DNA binding / transcription activator/ transcription factor			2	1,56				
AT2G31230	ATERF15 (Ethylene-responsive element binding factor 15); DNA binding / transcription activator/ transcrip- tion factor				2,01				
AT4G17490	ATERF6 (ETHYLENE RESPONSIVE ELEMENT BINDING FACTOR 6); DNA binding / transcription factor	1,85	1,69	2,09	6,77				
AT1G74930	ORA47; DNA binding / transcription factor	4,99	4,69						
AT1G53910	RAP2.12; DNA binding / transcription factor				1,5				
AT1G43160	RAP2.6 (related to AP2 6); DNA binding / transcription factor			1,6					
AT5G13330	Rap2.6L (related to AP2 6L); DNA binding / transcription factor				3,27				
AT1G78080	RAP2.4 (related to AP2 4); DNA binding / transcription factor				1,78				
AT5G15830	AtbZIP3 (Arabidopsis thaliana basic leucine-zipper 3); DNA binding / transcription factor				3,26				
AT1G13600	AtbZIP58 (Arabidopsis thaliana basic leucine-zipper 58); DNA binding / protein heterodimerization/ protein homodimerization/ transcription factor				2,76				
AT1G77920	bZIP family transcription factor			1,63	1,94				
AT1G75390	AtbZIP44 (Arabidopsis thaliana basic leucine-zipper 44); DNA binding / protein heterodimerization/ transcrip- tion factor				1,56				
AT5G49450	AtbZIP1 (Arabidopsis thaliana basic leucine-zipper 1); DNA binding / protein heterodimerization/ transcrip- tion factor								2,57
AT1G08320	bZIP family transcription factor				1,57				
AT5G24800	BZIP9 (BASIC LEUCINE ZIPPER 9); DNA binding / protein heterodimerization/ transcription factor			1,98	2,5				
AT5G28770	BZO2H3; DNA binding / protein heterodimerization/ transcription factor				2,96				
AT5G47370	HAT2; DNA binding / transcription factor/ transcription repressor								2,87
AT3G60390	HAT3 (HOMEBOX-LEUCINE ZIPPER PROTEIN 3); transcription factor			2,22	1,5				

continued on next page

Table C.10 — continued from previous page

AGI code	Gene description	0,1 % sucrose				3 % sucrose			
		root		shoot		root		shoot	
		d ³ /d ₀	d ⁴ /d ₀	d ³ /d ₀	d ⁴ /d ₀	d ³ /d ₀	d ⁴ /d ₀	d ³ /d ₀	d ⁴ /d ₀
AT5G15160	bHLH family protein				1,8				1,72
AT5G46690	bHLH071 (beta HLH protein 71); DNA binding / transcription factor				2,52				
AT5G65640	bHLH093 (beta HLH protein 93); DNA binding / transcription factor			2,2	1,94	2,34	2,49		
AT1G51070	basic helix-loop-helix (bHLH) family protein				1,52				
AT1G51140	basic helix-loop-helix (bHLH) family protein				6,36				
AT5G50915	basic helix-loop-helix (bHLH) family protein			1,56					
AT5G48560	basic helix-loop-helix (bHLH) family protein			1,57	1,62				
AT3G61950	basic helix-loop-helix (bHLH) family protein				2,29				
AT4G17880	basic helix-loop-helix (bHLH) family protein				3,35				
AT4G01460	basic helix-loop-helix (bHLH) family protein				1,52				
AT1G68810	basic helix-loop-helix (bHLH) family protein	1,85	1,88						
AT2G22760	basic helix-loop-helix (bHLH) family protein					1,58	1,96		
AT2G42280	basic helix-loop-helix (bHLH) family protein				1,72				
AT3G56980	BHLH039; DNA binding / transcription factor	1,61	1,51						
AT5G04150	BHLH101; DNA binding / transcription factor	3,61	3,41						
AT1G14685	BPC2 (BASIC PENTACYSSTEINE 2); DNA binding / transcription factor				1,85				
AT2G25900	ATCTH; transcription factor				1,5				2,48
AT2G33620	DNA-binding family protein / AT-hook protein 1 (AHP1)				2,63				
AT4G14465	DNA-binding protein-related				2,71				
AT2G43140	DNA binding / transcription factor				2,97				
AT2G45850	DNA-binding family protein	1,62	1,57						
AT3G61260	DNA-binding family protein / remorin family protein	1,52							
AT5G35970	DNA-binding protein, putative				1,86				
AT2G36080	DNA-binding protein, putative				2,72				
AT2G45430	DNA-binding protein-related				1,79				
AT4G17800	DNA-binding protein-related				2,06				
AT4G40060	ATHB16 (ARABIDOPSIS THALIANA HOMEBOX PROTEIN 16); sequence-specific DNA binding / transcription activator/ transcription factor				2,13				
AT1G26960	AtHB23 (ARABIDOPSIS THALIANA HOMEBOX PROTEIN 23); DNA binding / transcription factor				2,25				
AT3G50890	AtHB28 (ARABIDOPSIS THALIANA HOMEBOX PROTEIN 28); DNA binding / transcription factor				1,98				
AT1G75240	AtHB33 (ARABIDOPSIS THALIANA HOMEBOX PROTEIN 33); DNA binding / transcription factor			1,54					
AT5G39760	AtHB23 (ARABIDOPSIS THALIANA HOMEBOX PROTEIN 23); DNA binding / transcription factor				2,09				
AT4G34680	GATA transcription factor 3, putative (GATA-3)				1,75				
AT4G36990	HSF4 (HEAT SHOCK FACTOR 4); DNA binding / transcription factor/ transcription repressor			1,54					
AT5G03720	AT-HSFA3; DNA binding / transcription factor				2,24				
AT4G18880	AT-HSFA4A; DNA binding / transcription factor	1,63	1,72	1,65	2,1				
AT1G67970	AT-HSFA8; DNA binding / transcription factor				4,18				3,87
AT5G16820	HSF3 (HEAT SHOCK FACTOR 3); DNA binding / transcription factor				1,64				

continued on next page

Table C.10 — continued from previous page

AGI code	Gene description	0,1 % sucrose				3 % sucrose			
		root		shoot		root		shoot	
		d ₃ /d ₀	d ₄ /d ₀	d ₃ /d ₀	d ₄ /d ₀	d ₃ /d ₀	d ₄ /d ₀	d ₃ /d ₀	d ₄ /d ₀
AT3G61150	HDG1 (HOMEODOMAIN GLABROUS 1); DNA binding / transcription factor				1,61				
AT3G27650	LBD25 (LOB DOMAIN-CONTAINING PROTEIN 25)				3,42				
AT3G02550	LBD41 (LOB DOMAIN-CONTAINING PROTEIN 41)				9,92			1,82	1,78
AT2G42430	LBD16 (LATERAL ORGAN BOUNDARIES-DOMAIN 16)	1,52							
AT3G11090	LBD21 (LOB DOMAIN-CONTAINING PROTEIN 21)				3,06				
AT3G49940	LBD38 (LOB DOMAIN-CONTAINING PROTEIN 38)				2,79				
AT4G37540	LBD39 (LOB DOMAIN-CONTAINING PROTEIN 39)				2,16				
AT5G07690	ATMYB29 (ARABIDOPSIS THALIANA MYB DOMAIN PROTEIN 29); DNA binding / transcription factor				4,42				
AT3G48920	AtMYB45 (myb domain protein 45); DNA binding / transcription factor			4,92	5,24				
AT4G09460	ATMYB6; DNA binding / transcription factor				1,86				
AT1G48000	MYB112 (myb domain protein 112); DNA binding / transcription factor				1,6				
AT1G74080	MYB122 (MYB DOMAIN PROTEIN 122); DNA binding / transcription factor	8,46	7,75			2,18	3,17		
AT2G31180	MYB14 (MYB DOMAIN PROTEIN 14); DNA binding / transcription factor	2,38	2,05						
AT5G61420	MYB28 (myb domain protein 28); DNA binding / transcription factor		1,58		3,49				
AT5G05790	myb family transcription factor				2,63				
AT3G09600	myb family transcription factor				4,44	1,88	1,96		3,68
AT3G04030	myb family transcription factor				1,95				
AT1G01520	myb family transcription factor				2				
AT2G40970	myb family transcription factor				1,69				
AT2G38090	myb family transcription factor				3,19				
AT5G17300	myb family transcription factor			1,53		4,26	3,25		4,35
AT3G46130	MYB111 (MYB DOMAIN PROTEIN 111); DNA binding / transcription factor	1,78	2						
AT3G24310	MYB305 (myb domain protein 305); DNA binding / transcription factor		1,7						
AT4G37260	MYB73 (MYB DOMAIN PROTEIN 73); DNA binding / transcription factor	1,53	1,7						
AT1G74430	MYB95 (myb domain protein 95); DNA binding / transcription factor			1,67					
AT1G71030	MYBL2 (ARABIDOPSIS MYB-LIKE 2); DNA binding / transcription factor		1,94		3,77				
AT5G08520	myb family transcription factor								1,82
AT1G25550	myb family transcription factor				2,73				
AT3G24120	myb family transcription factor				1,53				
AT1G13300	myb family transcription factor				4,43				
AT2G18280	AtTLP2 (TUBBY LIKE PROTEIN 2); phosphoric diester hydrolase/ transcription factor				1,52				
AT5G06510	NF-YA10 (NUCLEAR FACTOR Y, SUBUNIT A10); transcription factor				3,41				
AT3G05690	NF-YA2 (NUCLEAR FACTOR Y, SUBUNIT A2); transcription factor				2,77				
AT1G72830	NF-YA3 (NUCLEAR FACTOR Y, SUBUNIT A3); transcription factor				2,33				
AT2G34720	NF-YA4 (NUCLEAR FACTOR Y, SUBUNIT A4); specific transcriptional repressor/ transcription factor				1,92				
AT1G17590	NF-YA8 (NUCLEAR FACTOR Y, SUBUNIT A8); transcription factor				3,07				
AT1G56170	NF-YC2 (NUCLEAR FACTOR Y, SUBUNIT C2); DNA binding / transcription activator/ transcription factor				2,67				2,02
AT4G38340	RWP-RK domain-containing protein				4,14				

continued on next page

Table C.10 — continued from previous page

AGI code	Gene description	0,1 % sucrose				3 % sucrose			
		root		shoot		root		shoot	
		d ³ /d ₀	d ⁴ /d ₀	d ³ /d ₀	d ⁴ /d ₀	d ³ /d ₀	d ⁴ /d ₀	d ³ /d ₀	d ⁴ /d ₀
AT1G76350	RWP-RK domain-containing protein				1,54				
AT2G43500	RWP-RK domain-containing protein					1,59	2,64		
AT2G45160	scarecrow transcription factor family protein				1,55				
AT5G13730	SIG4 (SIGMA FACTOR 4); DNA binding / DNA-directed RNA polymerase/ sigma factor/ transcription factor				2,33				
AT1G08540	SIG2 (RNA POLYMERASE SIGMA SUBUNIT 2); DNA binding / DNA-directed RNA polymerase/ sigma factor/ transcription factor				1,66				
AT2G36990	SIGF (RNA POLYMERASE SIGMA-SUBUNIT F); DNA binding / DNA-directed RNA polymerase/ sigma factor/ transcription factor				2,07				
AT5G08330	TCP family transcription factor, putative	1,84	1,94						
AT1G69690	TCP family transcription factor, putative				2,99				
AT5G28300	trihelix DNA-binding protein, putative				1,63				
AT3G54390	transcription factor				1,92				
AT4G30410	transcription factor				2,59				
AT3G06590	transcription factor				2,23				
AT3G10040	transcription factor				1,5				
AT1G69580	transcription factor				2,18				
AT1G10585	transcription factor			2,05	2,89				
AT3G20810	transcription factor jumonji (jmjC) domain-containing protein	2,83	2,81		2,26				
AT1G29950	transcription factor/ transcription regulator				1,95				
AT2G47270	transcription factor/ transcription regulator			1,57					
AT1G24625	ZFP7 (ZINC FINGER PROTEIN 7); nucleic acid binding / transcription factor/ zinc ion binding				2,92				
AT5G13750	ZIFL1 (ZINC INDUCED FACILITATOR-like 1); tetracycline:hydrogen antiporter	2,14	2,56						
AT4G38960	zinc finger (B-box type) family protein				1,96				3,18
AT3G21890	zinc finger (B-box type) family protein								5,54
AT1G73870	zinc finger (B-box type) family protein				1,96				
AT2G21320	zinc finger (B-box type) family protein				1,67				3,13
AT4G27240	zinc finger (C2H2 type) family protein				1,87				
AT5G48250	zinc finger (B-box type) family protein			1,85	4,17				
AT4G39070	zinc finger (B-box type) family protein			2,04	4,11				
AT2G47890	zinc finger (B-box type) family protein		1,52	1,64	2,62				
AT5G22890	zinc finger (C2H2 type) family protein				1,66				
AT3G45260	zinc finger (C2H2 type) family protein				1,97				
AT2G37430	zinc finger (C2H2 type) family protein (ZAT11)			1,58	2,27				
AT5G66320	zinc finger (GATA type) family protein				1,54				
AT3G60530	zinc finger (GATA type) family protein	1,63	1,71						1,66
AT2G19810	zinc finger (CCCH-type) family protein				1,5				
AT4G29190	zinc finger (CCCH-type) family protein								3,02

continued on next page

Table C.10 – continued from previous page

AGI code	Gene description	0,1 % sucrose				3 % sucrose			
		root		shoot		root		shoot	
		d ₃ /d ₀	d ₄ /d ₀	d ₃ /d ₀	d ₄ /d ₀	d ₃ /d ₀	d ₄ /d ₀	d ₃ /d ₀	d ₄ /d ₀
Protein kinases									
AT4G21380	ARK3 (A. THALIANA RECEPTOR KINASE 3); kinase/ transmembrane receptor protein serine/threonine kinase							3,3	3,9
AT2G26290	ARSK1 (root-specific kinase 1); kinase		2,05						
AT2G26330	ER (ERECTA); transmembrane receptor protein kinase			1,59					
AT3G59700	ATHLECRK (ARABIDOPSIS THALIANA LECTIN-RECEPTOR KINASE); kinase				1,86				
AT1G01560	ATMPK11; MAP kinase/ kinase	2,69	2,72		1,54				
AT4G36450	ATMPK14 (Mitogen-activated protein kinase 14); MAP kinase/ kinase				2,41				
AT4G11330	ATMPK5 (MAP KINASE 5); MAP kinase/ kinase				1,57				
AT4G08470	MAPKKK10; ATP binding / kinase/ protein kinase/ protein serine/threonine kinase			1,63					
AT4G26070	MEK1 (MAP KINASE/ ERK KINASE 1); MAP kinase kinase/ kinase/ protein binding				1,67				
AT2G30040	MAPKKK14; ATP binding / kinase/ protein kinase/ protein serine/threonine kinase				2,46				
AT3G50310	MAPKKK20; ATP binding / kinase/ protein kinase/ protein serine/threonine kinase				4,39				
AT3G55950	CCR3 (ARABIDOPSIS THALIANA CRINKLY4 RELATED 3); kinase	1,55	1,63						
AT1G48260	CIPK17 (CBL-INTERACTING PROTEIN KINASE 17); ATP binding / kinase/ protein kinase/ protein serine/threonine kinase	1,68	2,27	1,55	2,21	3,26	5,46		
AT5G25110	CIPK25 (CBL-INTERACTING PROTEIN KINASE 25); ATP binding / kinase/ protein kinase/ protein serine/threonine kinase				3,22				
AT5G10930	CIPK5 (CBL-INTERACTING PROTEIN KINASE 5); ATP binding / kinase/ protein kinase/ protein serine/threonine kinase				6,44				2,03
AT3G23000	CIPK7 (CBL-INTERACTING PROTEIN KINASE 7); ATP binding / kinase/ protein kinase/ protein serine/threonine kinase				2,54				
AT3G17510	CIPK1 (CBL-INTERACTING PROTEIN KINASE 1); kinase/ protein binding			1,59	1,92				
AT5G45820	CIPK20 (CBL-INTERACTING PROTEIN KINASE 20); kinase/ protein serine/threonine kinase				6,9				
AT5G57630	CIPK21 (CBL-interacting protein kinase 21); ATP binding / kinase/ protein kinase/ protein serine/threonine kinase				4,36				
AT2G26980	CIPK3 (CBL-INTERACTING PROTEIN KINASE 3); kinase/ protein kinase/ protein serine/threonine kinase				2,41				
AT3G50530	CRK (CDPK-related kinase); ATP binding / calcium ion binding / calcium-dependent protein serine/threonine phosphatase/ kinase/ protein kinase/ protein serine/threonine kinase				1,52				
AT3G23340	ckl10 (Casein Kinase I-like 10); ATP binding / kinase/ protein kinase/ protein serine/threonine kinase				1,86				
AT4G23180	CRK10 (CYSTEINE-RICH RLK10); ATP binding / kinase/ protein kinase/ protein serine/threonine kinase/ protein tyrosine kinase			2,91	2,29				
AT4G23190	CRK11 (CYSTEINE-RICH RLK11); kinase/ protein kinase		1,98		2,47				
AT3G63260	ATMRK1; kinase/ protein serine/threonine/tyrosine kinase				1,51				
AT5G49780	ATP binding / kinase/ protein serine/threonine kinase	2,09	2,33						
AT1G20650	ATP binding / protein kinase/ protein serine/threonine kinase				1,65				
AT1G68690	ATP binding / protein kinase/ protein serine/threonine kinase					2,41	3,36		

continued on next page

Table C.10 — continued from previous page

AGI code	Gene description	0,1 % sucrose				3 % sucrose			
		root		shoot		root		shoot	
		d ³ /d ₀	d ⁴ /d ₀	d ³ /d ₀	d ⁴ /d ₀	d ³ /d ₀	d ⁴ /d ₀	d ³ /d ₀	d ⁴ /d ₀
AT5G65240	kinase				1,85				
AT1G18390	ATP binding / kinase/ protein kinase/ protein serine/threonine kinase/ protein tyrosine kinase				3,75				
AT5G01950	ATP binding / kinase/ protein serine/threonine kinase				2				
AT5G16810	ATP binding / protein kinase				1,89				
AT4G23260	ATP binding / protein kinase/ protein serine/threonine kinase/ protein tyrosine kinase				5,2				
AT4G08850	kinase				2,41				
AT1G51790	kinase				4,95				
AT2G28250	NCRK; kinase				1,75				
AT1G61380	SD1-29 (S-DOMAIN-1 29); carbohydrate binding / kinase/ protein kinase				2,65				
AT3G25560	NIK2 (NSP-INTERACTING KINASE 2); ATP binding / protein binding / protein kinase/ protein serine/threonine kinase				1,68				
AT1G28440	HSL1 (HAESA-Like 1); ATP binding / kinase/ protein serine/threonine kinase				1,61				
AT1G48480	RKL1; ATP binding / kinase/ protein serine/threonine kinase				1,88				
AT5G67280	RLK (Receptor-like kinase); ATP binding / kinase/ protein serine/threonine kinase				3,25				
AT2G25440	AtRLP20 (Receptor Like Protein 20); kinase/ protein binding		1,51						
AT2G32660	AtRLP22 (Receptor Like Protein 22); kinase/ protein binding			2,24	2,79				
AT3G05650	AtRLP32 (Receptor Like Protein 32); kinase/ protein binding				2,27				
AT5G40170	AtRLP54 (Receptor Like Protein 54); kinase/ protein binding				1,53				
AT1G71400	AtRLP12 (Receptor Like Protein 12); protein binding				3,34				
AT2G15080	AtRLP19 (Receptor Like Protein 19); kinase/ protein binding				2,25				
AT4G02420	lectin protein kinase, putative				1,99				
AT2G29220	lectin protein kinase, putative					3,85	3,46		
AT5G01540	LECRKA4.1 (LECTIN RECEPTOR KINASE A4.1); kinase			1,56	2,41				
AT5G60270	lectin protein kinase family protein				1,69				
AT4G02410	lectin protein kinase family protein			1,55	1,98				
AT5G65600	legume lectin family protein / protein kinase family protein	3,88	3,82		1,92				
AT1G51850	leucine-rich repeat protein kinase, putative			2,59	2,4				
AT1G51890	leucine-rich repeat protein kinase, putative	1,98	2,52	2,51					
AT1G51860	leucine-rich repeat protein kinase, putative			1,97	2,04				
AT5G56040	leucine-rich repeat protein kinase, putative				1,92				
AT1G05700	leucine-rich repeat protein kinase, putative		1,55	2,51					
AT5G67200	leucine-rich repeat transmembrane protein kinase, putative				2,17				
AT5G63410	leucine-rich repeat transmembrane protein kinase, putative	1,61	1,59		1,61				
AT5G61480	leucine-rich repeat transmembrane protein kinase, putative				1,67				
AT5G51560	leucine-rich repeat transmembrane protein kinase, putative				1,62				
AT5G51350	leucine-rich repeat transmembrane protein kinase, putative				1,63				
AT5G49770	leucine-rich repeat transmembrane protein kinase, putative	2,97	3,46			1,78	2,22		
AT5G05160	leucine-rich repeat transmembrane protein kinase, putative				1,72				

continued on next page

Table C.10 – continued from previous page

AGI code	Gene description	0,1 % sucrose				3 % sucrose			
		root		shoot		root		shoot	
		d ₃ /d ₀	d ₄ /d ₀	d ₃ /d ₀	d ₄ /d ₀	d ₃ /d ₀	d ₄ /d ₀	d ₃ /d ₀	d ₄ /d ₀
AT3G56370	leucine-rich repeat transmembrane protein kinase, putative				2,55				
AT4G39270	leucine-rich repeat transmembrane protein kinase, putative			1,51	1,65				
AT3G03770	leucine-rich repeat transmembrane protein kinase, putative				2,22				
AT2G41820	leucine-rich repeat transmembrane protein kinase, putative				2,77				
AT1G79620	leucine-rich repeat transmembrane protein kinase, putative				1,55				
AT2G23950	leucine-rich repeat family protein / protein kinase family protein				1,69				
AT2G36570	leucine-rich repeat transmembrane protein kinase, putative	1,54	2,38		5,5				
AT3G46370	leucine-rich repeat protein kinase, putative				2,32				
AT1G51800	leucine-rich repeat protein kinase, putative				5,08				
AT1G51820	leucine-rich repeat protein kinase, putative				3,61				
AT5G45840	leucine-rich repeat transmembrane protein kinase, putative			1,64	3,33				
AT1G72180	leucine-rich repeat transmembrane protein kinase, putative				1,5				
AT1G68400	leucine-rich repeat transmembrane protein kinase, putative			1,55					
AT2G31880	leucine-rich repeat transmembrane protein kinase, putative			1,65	1,57				
AT2G15300	leucine-rich repeat transmembrane protein kinase, putative	1,51							
AT5G25930	leucine-rich repeat family protein / protein kinase family protein				2,16	1,56	2		
AT5G48380	leucine-rich repeat family protein / protein kinase family protein				1,7				
AT5G10290	leucine-rich repeat family protein / protein kinase family protein				1,51				
AT1G53430	leucine-rich repeat family protein / protein kinase family protein				2,38				
AT5G01820	ATSR1 (ARABIDOPSIS THALIANA SERINE/THREONINE PROTEIN KINASE 1); ATP binding / kinase/ protein kinase/ protein serine/threonine kinase				5,06				
AT3G17420	GPK1; ATP binding / kinase/ protein kinase/ protein serine/threonine kinase		1,52		4,23				
AT5G57610	protein kinase family protein				2,42				
AT5G40380	protein kinase family protein				2,01				
AT5G39030	protein kinase family protein					1,83	2,48		
AT5G37790	protein kinase family protein				4,62				
AT4G35030	protein kinase family protein		1,7						
AT4G21230	protein kinase family protein			1,76					
AT4G10390	protein kinase family protein				2,79				
AT4G02630	protein kinase family protein				2,72				
AT1G33260	protein kinase family protein		1,84						
AT1G52290	protein kinase family protein				1,86				
AT1G07870	protein kinase family protein				1,69				
AT2G40120	protein kinase family protein				1,77				
AT1G77280	protein kinase family protein				1,97				
AT1G51170	protein kinase family protein				1,77				
AT5G50000	protein kinase, putative				1,51				
AT5G01850	protein kinase, putative				1,69				

continued on next page

Table C.10 – continued from previous page

AGI code	Gene description	0,1 % sucrose				3 % sucrose			
		root		shoot		root		shoot	
		d ³ /d ₀	d ⁴ /d ₀	d ³ /d ₀	d ⁴ /d ₀	d ³ /d ₀	d ⁴ /d ₀	d ³ /d ₀	d ⁴ /d ₀
AT1G70460	protein kinase, putative		2,33						
AT1G63580	protein kinase-related	1,77	2,07						
AT5G20050	protein kinase family protein				1,89				
AT5G25440	protein kinase family protein				2,35				
AT5G41680	protein kinase family protein				1,74				
AT5G39020	protein kinase family protein				2,35				
AT5G11410	protein kinase family protein				2,76				
AT4G38470	protein kinase family protein				3,12				
AT4G25390	protein kinase family protein				1,52				
AT4G25160	protein kinase family protein					3,56	3,46		
AT4G23270	protein kinase family protein				2,78				
AT4G23290	protein kinase family protein				4,1				
AT4G23300	protein kinase family protein				2,63				
AT4G21400	protein kinase family protein				2,24				
AT4G21410	protein kinase family protein				3,19				
AT4G11460	protein kinase family protein			1,63	1,71				
AT4G00970	protein kinase family protein			1,55	1,7				
AT1G70530	protein kinase family protein		1,5	1,57	2,69				
AT1G16260	protein kinase family protein			1,63	2,23				
AT1G67470	protein kinase family protein				1,67				
AT2G31010	protein kinase family protein				2,32				
AT1G51940	protein kinase family protein / peptidoglycan-binding LysM domain-containing protein	1,73	1,83		3,15				
AT3G57700	protein kinase, putative				2,3				
AT3G55450	protein kinase, putative				2,4				
AT3G46290	protein kinase, putative				1,58				
AT3G22750	protein kinase, putative				1,51				
AT1G61590	protein kinase, putative				1,59				
AT3G46280	protein kinase-related			2,99	3,49				
AT3G59350	serine/threonine protein kinase, putative	2,64	2,48	1,66	2				
AT4G22130	SRF8 (STRUBBELIG-RECEPTOR FAMILY 8); ATP binding / kinase/ protein binding / protein kinase/ protein serine/threonine kinase/ protein tyrosine kinase				2,23				
AT3G22420	WNK2 (WITH NO K 2); kinase/ protein kinase				1,59				
AT5G28080	WNK9; kinase/ protein kinase		1,78						
AT1G79680	wall-associated kinase, putative				2,72	3,19	4,17		
AT4G27300	S-locus protein kinase, putative				1,55				
AT1G11410	S-locus protein kinase, putative				1,61				
AT1G61500	S-locus protein kinase, putative	3,6	5,82			2,17	3,67		

continued on next page

Table C.10 – continued from previous page

AGI code	Gene description	0,1 % sucrose				3 % sucrose			
		root		shoot		root		shoot	
		d ₃ /d ₀	d ₄ /d ₀	d ₃ /d ₀	d ₄ /d ₀	d ₃ /d ₀	d ₄ /d ₀	d ₃ /d ₀	d ₄ /d ₀
Protein phosphatases									
AT3G11410	PP2CA (ARABIDOPSIS THALIANA PROTEIN PHOSPHATASE 2CA); protein binding / protein serine/threonine phosphatase								1,64
AT5G03470	ATB' ALPHA; protein phosphatase type 2A regulator		1,71					2,44	
AT3G21650	serine/threonine protein phosphatase 2A (PP2A) regulatory subunit B', putative							1,57	
AT1G67820	protein phosphatase 2C, putative / PP2C, putative							1,69	
AT5G59220	protein phosphatase 2C, putative / PP2C, putative							2,22	
AT4G32950	protein phosphatase 2C, putative / PP2C, putative		4,01						
AT3G16800	protein phosphatase 2C, putative / PP2C, putative							1,57	
AT3G05640	protein phosphatase 2C, putative / PP2C, putative							2,7	
AT2G20630	protein phosphatase 2C, putative / PP2C, putative							1,79	
AT4G27800	protein phosphatase 2C PPH1 / PP2C PPH1 (PPH1)							2,15	
AT1G07160	protein phosphatase 2C, putative / PP2C, putative				1,93			2,52	
AT3G62260	protein phosphatase 2C, putative / PP2C, putative	1,86							
AT5G26010	catalytic/ protein serine/threonine phosphatase							2,53	
AT1G03590	catalytic/ protein serine/threonine phosphatase							1,59	
SAM									
AT2G36880	MAT3 (methionine adenosyltransferase 3); copper ion binding / methionine adenosyltransferase							2,09	
AT3G23810	SAHH2 (S-ADENOSYL-L-HOMOCYSTEINE (SAH) HYDROLASE 2); adenosylhomocysteinase/ binding / catalytic	2,11	2,6					3,28	
ATP/adenylate									
AT3G09820	ADK1 (adenosine kinase 1); adenosine kinase/ copper ion binding							2,23	
AT4G22570	APT3 (ADENINE PHOSPHORIBOSYL TRANSFERASE 3); adenine phosphoribosyltransferase							1,96	
AT5G35170	adenylate kinase family protein							2,03	1,7
Starch									
AT1G10760	SEX1 (STARCH EXCESS 1); alpha-glucan, water dikinase	1,57	2,06					2,42	2,45
AT1G69830	AMY3 (ALPHA-AMYLASE-LIKE 3); alpha-amylase							3,34	3,47
AT4G18240	ATSS4; transferase, transferring glycosyl groups							2,38	
AT2G36390	SBE2.1 (starch branching enzyme 2.1); 1,4-alpha-glucan branching enzyme						3,45	2,91	
AT5G64860	DPE1 (DISPROPORTIONATING ENZYME); 4-alpha-glucanotransferase/ catalytic/ cation binding						2,04	1,71	
AT1G32900	starch synthase, putative				1,6	6,19			2,38
AT4G25000	AMY1 (ALPHA-AMYLASE-LIKE); alpha-amylase				2,2				
AT1G76130	AMY2 (ALPHA-AMYLASE-LIKE 2); alpha-amylase/ calcium ion binding / catalytic/ cation binding							2,13	
AT5G17520	RCP1 (ROOT CAP 1); maltose transmembrane transporter							1,72	

continued on next page

Table C.10 — continued from previous page

AGI code	Gene description	0,1 % sucrose				3 % sucrose				
		root		shoot		root		shoot		
		d ³ /d ₀	d ⁴ /d ₀	d ³ /d ₀	d ⁴ /d ₀	d ³ /d ₀	d ⁴ /d ₀	d ³ /d ₀	d ⁴ /d ₀	
AT3G23920	BAM1 (BETA-AMYLASE 1); beta-amylase				1,93					
AT4G15210	BAM5 (BETA-AMYLASE 5); beta-amylase				12,97			1,95	1,85	
AT5G18670	BMV3; beta-amylase/ catalytic/ cation binding							1,73	2,46	
AT5G55700	BAM4 (BETA-AMYLASE 4); beta-amylase/ catalytic/ cation binding				1,51					
AT4G39210	APL3; glucose-1-phosphate adenylyltransferase				6,41					
AT5G19220	APL1 (ADP GLUCOSE PYROPHOSPHORYLASE LARGE SUBUNIT 1); glucose-1-phosphate adenylyltransferase				1,85					
Trehalose										
AT2G22190	catalytic/ trehalose-phosphatase							1,63		
AT5G51460	ATTPPA; trehalose-phosphatase	1,99	2,01							
AT4G17770	ATTPS5; protein binding / transferase, transferring glycosyl groups / trehalose-phosphatase							3,84		
AT5G65140	trehalose-6-phosphate phosphatase, putative							1,53		
AT4G39770	trehalose-6-phosphate phosphatase, putative	1,7	1,6							
AT4G22590	trehalose-6-phosphate phosphatase, putative	1,85	2,41							
AT1G35910	trehalose-6-phosphate phosphatase, putative	2,39	3,57					2,02		
AT1G60140	ATTPS10 (trehalose phosphate synthase); transferase, transferring glycosyl groups / trehalose-phosphatase							2,33		
AT2G18700	ATTPS11; transferase, transferring glycosyl groups							3,96		
AT1G70290	ATTPS8; alpha, alpha-trehalose-phosphate synthase (UDP-forming)/ transferase, transferring glycosyl groups / trehalose-phosphatase							1,69	2,38	
AT1G23870	ATTPS9; transferase, transferring glycosyl groups / trehalose-phosphatase							2,93		
AT4G24040	TRE1 (TREHALASE 1); alpha, alpha-trehalase / trehalase							2,88		
Carbon metabolism										
AT3G52720	ACA1 (ALPHA CARBONIC ANHYDRASE 1); carbonate dehydratase/ zinc ion binding							8,13		
AT1G23730	BCA3 (BETA CARBONIC ANHYDRASE 4); carbonate dehydratase/ zinc ion binding							3,08		
AT1G71880	SUC1 (Sucrose-proton symporter 1); carbohydrate transmembrane transporter/ sucrose:hydrogen symporter/ sugar:hydrogen symporter	1,82	1,74	1,65						
AT5G54800	GPT1; antiporter/ glucose-6-phosphate transmembrane transporter							2,07		
AT1G61800	GPT2; antiporter/ glucose-6-phosphate transmembrane transporter				3,65	14,63		2,07	1,66	
AT1G11260	STP1 (SUGAR TRANSPORTER 1); carbohydrate transmembrane transporter/ sugar:hydrogen symporter							2,63		
AT3G19930	STP4 (SUGAR TRANSPORTER 4); carbohydrate transmembrane transporter/ monosaccharide transmembrane transporter/ sucrose:hydrogen symporter/ sugar:hydrogen symporter							2,31		
AT1G67300	hexose transporter, putative							1,68		
AT5G17010	sugar transporter family protein		1,66							
AT3G05400	sugar transporter, putative				1,73	3,47				
AT4G04750	carbohydrate transmembrane transporter/ sugar:hydrogen symporter							2,23		
AT5G09220	AAP2 (AMINO ACID PERMEASE 2); amino acid transmembrane transporter							3,51		

continued on next page

Table C.10 — continued from previous page

AGI code	Gene description	0,1 % sucrose				3 % sucrose				
		root		shoot		root		shoot		
		d ₃ /d ₀	d ₄ /d ₀	d ₃ /d ₀	d ₄ /d ₀	d ₃ /d ₀	d ₄ /d ₀	d ₃ /d ₀	d ₄ /d ₀	
AT5G59250	sugar transporter family protein				1,95					
AT5G18840	sugar transporter, putative	2,46	2,94	3,09	2					
AT1G77210	sugar transporter, putative				3,19					
AT2G48020	sugar transporter, putative				2,12					
AT4G36670	mannitol transporter, putative				8,52					
AT4G29130	HXK1 (HEXOKINASE 1); ATP binding / fructokinase/ glucokinase/ hexokinase				1,94					
AT1G50460	HKL1 (HEXOKINASE-LIKE 1); ATP binding / fructokinase/ glucokinase/ hexokinase				1,56					
AT1G51420	SPP1 (SUCROSE-PHOSPHATASE 1); catalytic/ magnesium ion binding / phosphatase/ sucrose-phosphatase		1,7							
AT3G52340	SPP2 (SUCROSE-6F-PHOSPHATE PHOSPHOHYDROLASE 2); catalytic/ magnesium ion binding / phosphatase/ sucrose-phosphatase				1,61					
AT1G78570	RHM1 (RHAMNOSE BIOSYNTHESIS 1); UDP-L-rhamnose synthase/ UDP-glucose 4,6-dehydratase/ catalytic				2,55					
AT1G63000	NRS/ER (NUCLEOTIDE-RHAMNOSE SYNTHASE/EPIMERASE-REDUCTASE); UDP-4-keto-6-deoxy-glucose-3,5-epimerase/ UDP-4-keto-rhamnose-4-keto-reductase/ dTDP-4-dehydrorhamnose 3,5-epimerase/ dTDP-4-dehydrorhamnose reductase				2,24					
Glycolysis/Gluconeogenesis										
AT3G43190	SUS4; UDP-glycosyltransferase/ sucrose synthase/ transferase, transferring glycosyl groups	1,7	1,71							
AT1G35580	CINV1 (cytosolic invertase 1); beta-fructofuranosidase				2,46					
AT1G43670	fructose-1,6-bisphosphatase, putative / D-fructose-1,6-bisphosphate 1-phosphohydrolase, putative / FBPase, putative				3,1					
AT5G64380	fructose-1,6-bisphosphatase family protein				2,3					
AT3G52930	fructose-bisphosphate aldolase, putative		1,58	1,67						
AT4G38970	fructose-bisphosphate aldolase, putative		2,17							
AT4G26530	fructose-bisphosphate aldolase, putative				4,36		1,92	5,46		
AT1G76550	pyrophosphate-fructose-6-phosphate 1-phosphotransferase alpha subunit, putative / pyrophosphate-dependent 6-phosphofructose-1-kinase, putative				1,6					
AT1G20950	pyrophosphate-fructose-6-phosphate 1-phosphotransferase-related / pyrophosphate-dependent 6-phosphofructose-1-kinase-related				1,51					
AT3G15020	malate dehydrogenase (NAD), mitochondrial, putative		1,89	1,85	2,67					
AT5G11110	ATSPS2F (SUCROSE PHOSPHATE SYNTHASE 2F); sucrose-phosphate synthase				2,34					
AT4G10120	ATSPS4F; sucrose-phosphate synthase/ transferase, transferring glycosyl groups				1,91					
AT1G16300	GAPCP-2; FUNCTIONS IN: NAD or NADH binding, glyceraldehyde-3-phosphate dehydrogenase (phosphorylating) activity, binding, catalytic activity, glyceraldehyde-3-phosphate dehydrogenase activity; INVOLVED IN: glycolysis, glucose metabolic process, metabolic process;			1,84	2,62					
AT3G26650	GAPA (GLYCERALDEHYDE 3-PHOSPHATE DEHYDROGENASE A SUBUNIT); glyceraldehyde-3-phosphate dehydrogenase/ protein binding		2,2							

continued on next page

Table C.10 — continued from previous page

AGI code	Gene description	0,1 % sucrose				3 % sucrose			
		root		shoot		root		shoot	
		d ³ /d ₀	d ⁴ /d ₀	d ³ /d ₀	d ⁴ /d ₀	d ³ /d ₀	d ⁴ /d ₀	d ³ /d ₀	d ⁴ /d ₀
AT1G12900	GAPA-2 (GLYCERALDEHYDE 3-PHOSPHATE DEHYDROGENASE A SUBUNIT 2); NAD or NADH binding / binding / catalytic/ glyceraldehyde-3-phosphate dehydrogenase (phosphorylating)/ glyceraldehyde-3-phosphate dehydrogenase		2,46						
AT1G42970	GAPB (GLYCERALDEHYDE-3-PHOSPHATE DEHYDROGENASE B SUBUNIT); glyceraldehyde-3-phosphate dehydrogenase (NADP+)/ glyceraldehyde-3-phosphate dehydrogenase				1,59				
AT5G14500	aldose 1-epimerase family protein								1,8
AT4G23730	aldose 1-epimerase family protein								1,63
AT5G66530	aldose 1-epimerase family protein						2,04	1,5	1,59
AT3G47800	aldose 1-epimerase family protein								3,17
AT1G74030	enolase, putative	1,61	1,85	2,33	1,83				
AT4G26270	PFK3 (PHOSPHOFRUCTOKINASE 3); 6-phosphofructokinase	1,67	2,02		1,72				
AT5G61580	PFK4 (PHOSPHOFRUCTOKINASE 4); 6-phosphofructokinase				1,55				
AT2G31390	pfkB-type carbohydrate kinase family protein			1,68	1,95				
AT3G59480	pfkB-type carbohydrate kinase family protein		1,62						
AT3G54090	pfkB-type carbohydrate kinase family protein				1,57				
AT4G27600	pfkB-type carbohydrate kinase family protein				1,63				
AT4G37870	PCK1 (PHOSPHOENOLPYRUVATE CARBOXYKINASE 1); ATP binding / phosphoenolpyruvate carboxykinase (ATP)/ phosphoenolpyruvate carboxykinase/ purine nucleotide binding				1,83				
AT1G53310	ATPPC1 (PHOSPHOENOLPYRUVATE CARBOXYLASE 1); catalytic/ phosphoenolpyruvate carboxylase				2,28				
AT5G17380	pyruvate decarboxylase family protein		1,56						
AT4G33070	pyruvate decarboxylase, putative	2,24	2,11		2,22				
AT5G54960	PDC2 (pyruvate decarboxylase-2); carboxy-lyase/ catalytic/ magnesium ion binding / pyruvate decarboxylase/ thiamin pyrophosphate binding								2,89
AT3G49160	pyruvate kinase family protein			2,03	2,04				
AT5G56350	pyruvate kinase, putative		2,08		1,5				
AT4G15530	PPDK (pyruvate orthophosphate dikinase); kinase/ pyruvate, phosphate dikinase	1,63				3,6	4,28		
AT3G06483	PDK (PYRUVATE DEHYDROGENASE KINASE); ATP binding / histidine phosphotransfer kinase/ pyruvate dehydrogenase (acetyl-transferring) kinase				1,82				
AT1G79550	PGK (PHOSPHOGLYCERATE KINASE); phosphoglycerate kinase		1,61		1,54				
AT1G78050	PGM (PHOSPHOGLYCERATE/BISPHOSPHOGLYCERATE MUTASE); catalytic/ intramolecular transferase, phosphotransferases	1,77	2,68	1,56					
AT3G08590	2,3-biphosphoglycerate-independent phosphoglycerate mutase, putative / phosphoglyceromutase, putative		1,86		1,9				
AT3G12780	PGK1 (PHOSPHOGLYCERATE KINASE 1); phosphoglycerate kinase				1,63				
AT1G23190	phosphoglucomutase, cytoplasmic, putative / glucose phosphomutase, putative			1,52	1,77				
AT1G70820	phosphoglucomutase, putative / glucose phosphomutase, putative				13,76			1,69	9,35
AT5G22620	phosphoglycerate/bisphosphoglycerate mutase family protein				1,54				
AT3G50520	phosphoglycerate/bisphosphoglycerate mutase family protein		1,56						
AT1G22170	phosphoglycerate/bisphosphoglycerate mutase family protein				1,57				

continued on next page

Table C.10 — continued from previous page

AGI code	Gene description	0,1 % sucrose				3 % sucrose			
		root		shoot		root		shoot	
		d ₃ /d ₀	d ₄ /d ₀	d ₃ /d ₀	d ₄ /d ₀	d ₃ /d ₀	d ₄ /d ₀	d ₃ /d ₀	d ₄ /d ₀
AT2G17280	phosphoglycerate/bisphosphoglycerate mutase family protein				1,65				
AT5G15490	UDP-glucose 6-dehydrogenase, putative				2,39				
AT5G39320	UDP-glucose 6-dehydrogenase, putative				2,33				
AT3G29360	UDP-glucose 6-dehydrogenase, putative				1,9				
AT2G35020	UTP-glucose-1-phosphate uridylyltransferase family protein				2,29				
AT5G13110	G6PD2 (GLUCOSE-6-PHOSPHATE DEHYDROGENASE 2); glucose-6-phosphate dehydrogenase			1,53	1,72				
AT1G24280	G6PD3 (GLUCOSE-6-PHOSPHATE DEHYDROGENASE 3); glucose-6-phosphate dehydrogenase			2,56	1,62				
AT1G09420	G6PD4 (GLUCOSE-6-PHOSPHATE DEHYDROGENASE 4); glucose-6-phosphate dehydrogenase				2,38				
AT4G30440	GAE1 (UDP-D-GLUCURONATE 4-EPIMERASE 1); UDP-glucuronate 4-epimerase/ catalytic	1,97	1,69						
AT3G23820	GAE6 (UDP-D-GLUCURONATE 4-EPIMERASE 6); UDP-glucuronate 4-epimerase/ catalytic			1,67					
AT2G47180	AtGolS1 (Arabidopsis thaliana galactinol synthase 1); transferase, transferring glycosyl groups / transferase, transferring hexosyl groups				2,36				
AT1G56600	AtGolS2 (Arabidopsis thaliana galactinol synthase 2); transferase, transferring glycosyl groups / transferase, transferring hexosyl groups				11,93				
AT1G60470	AtGolS4 (Arabidopsis thaliana galactinol synthase 4); transferase, transferring glycosyl groups / transferase, transferring hexosyl groups	1,71	2,45						
AT1G09350	AtGolS3 (Arabidopsis thaliana galactinol synthase 3); transferase, transferring glycosyl groups / transferase, transferring hexosyl groups			1,58					
AT3G13750	BGAL1 (Beta galactosidase 1); beta-galactosidase/ catalytic/ cation binding / heme binding / peroxidase/ sugar binding				2,14				
AT4G36360	BGAL3 (beta-galactosidase 3); beta-galactosidase/ catalytic/ cation binding / sugar binding				3,41				
AT1G45130	BGAL5 (beta-galactosidase 5); beta-galactosidase/ catalytic/ cation binding				2,8				
AT2G28470	BGAL8 (beta-galactosidase 8); beta-galactosidase/ catalytic/ cation binding / sugar binding				1,76				
AT5G20710	BGAL7 (beta-galactosidase 7); beta-galactosidase					6,81	8,13		
AT5G56870	BGAL4 (beta-galactosidase 4); beta-galactosidase		1,67	3,04				1,51	
AT5G63810	BGAL10 (beta-galactosidase 10); beta-galactosidase/ catalytic/ cation binding							1,81	
AT3G52840	BGAL2 (beta-galactosidase 2); beta-galactosidase/ catalytic/ cation binding				1,81				
AT3G57260	BGL2 (BETA-1,3-GLUCANASE 2); cellulase/ glucan 1,3-beta-glucosidase/ hydrolase, hydrolyzing O-glycosyl compounds				4,04				
AT1G02850	BGLU11 (BETA GLUCOSIDASE 11); catalytic/ cation binding / hydrolase, hydrolyzing O-glycosyl compounds					1,7	2,38		
AT2G44450	BGLU15 (BETA GLUCOSIDASE 15); catalytic/ cation binding / hydrolase, hydrolyzing O-glycosyl compounds		1,66	1,87	1,54				
AT2G44480	BGLU17 (BETA GLUCOSIDASE 17); catalytic/ cation binding / hydrolase, hydrolyzing O-glycosyl compounds				3,17				
AT1G52400	BGLU18 (BETA GLUCOSIDASE 18); catalytic/ cation binding / hydrolase, hydrolyzing O-glycosyl compounds			2,18	18,22			1,53	
AT3G03640	BGLU25 (BETA GLUCOSIDASE 25); catalytic/ cation binding / hydrolase, hydrolyzing O-glycosyl compounds				2,26				
AT2G44460	BGLU28 (BETA GLUCOSIDASE 28); catalytic/ cation binding / hydrolase, hydrolyzing O-glycosyl compounds				2,38			5,46	7,55
AT2G32860	BGLU33 (BETA GLUCOSIDASE 33); catalytic/ cation binding / hydrolase, hydrolyzing O-glycosyl compounds				4,63				
AT1G26560	BGLU40 (BETA GLUCOSIDASE 40); catalytic/ cation binding / hydrolase, hydrolyzing O-glycosyl compounds				3,85				

continued on next page

Table C.10 — continued from previous page

AGI code	Gene description	0,1 % sucrose				3 % sucrose			
		root		shoot		root		shoot	
		d ³ /d ₀	d ⁴ /d ₀	d ³ /d ₀	d ⁴ /d ₀	d ³ /d ₀	d ⁴ /d ₀	d ³ /d ₀	d ⁴ /d ₀
AT3G18080	BGLU44 (B-S GLUCOSIDASE 44); (R)-amygdalin beta-glucosidase/ 4-methylumbelliferyl-beta-D-glucopyranoside beta-glucosidase/ beta-gentiobiose beta-glucosidase/ cellobiose glucosidase/ esculin beta-glucosidase/ hydrolase, hydrolyzing O-glycosyl compounds								2,78
AT1G61820	BGLU46 (BETA GLUCOSIDASE 46); catalytic/ cation binding / hydrolase, hydrolyzing O-glycosyl compounds			1,65				1,55	1,5
AT4G27820	BGLU9 (BETA GLUCOSIDASE 9); catalytic/ cation binding / hydrolase, hydrolyzing O-glycosyl compounds						1,98		
AT3G60130	BGLU16 (BETA GLUCOSIDASE 16); catalytic/ cation binding / hydrolase, hydrolyzing O-glycosyl compounds						1,75		
AT5G64570	XYL4; hydrolase, hydrolyzing O-glycosyl compounds / xylan 1,4-beta-xylosidase						1,9		
AT5G57655	xylose isomerase family protein						1,53		
AT5G49360	BXL1 (BETA-XYLOSIDASE 1); hydrolase, hydrolyzing O-glycosyl compounds			1,6			2,14		
AT3G62720	XT1 (XYLOSYLTRANSFERASE 1); UDP-xylosyltransferase/ transferase/ transferase, transferring glycosyl groups / xyloglucan 6-xylosyltransferase	2,74	2,18				2,13		
AT1G12240	ATBETAFRUCT4; beta-fructofuranosidase/ hydrolase, hydrolyzing O-glycosyl compounds	2,04	2,55						
AT5G11920	AtcwINV6 (6-&1-fructan exohydrolase); hydrolase, hydrolyzing O-glycosyl compounds / inulinase/ levanase	1,52	1,55						
AT1G55120	ATFRUCT5 (BETA-FRUCTOFURANOSIDASE 5); hydrolase, hydrolyzing O-glycosyl compounds / levanase						4,65		
AT1G62660	beta-fructosidase (BFRUCT3) / beta-fructofuranosidase / invertase, vacuolar					1,73			
AT4G34860	beta-fructofuranosidase, putative / invertase, putative / saccharase, putative / beta-fructosidase, putative						1,89		
AT1G47960	C/VIF1 (CELL WALL / VACUOLAR INHIBITOR OF FRUCTOSIDASE 1); enzyme inhibitor/ pectinesterase/ pectinesterase inhibitor						2,06		
AT3G13790	ATBFRUCT1; beta-fructofuranosidase/ hydrolase, hydrolyzing O-glycosyl compounds						2,7		
AT3G06500	beta-fructofuranosidase, putative / invertase, putative / saccharase, putative / beta-fructosidase, putative						2,16		
AT5G66460	(1-4)-beta-mannan endohydrolase, putative						3,74		
AT5G54690	GAUT12 (GALACTURONOSYLTRANSFERASE 12); polygalacturonate 4-alpha-galacturonosyltransferase/ transferase, transferring glycosyl groups / transferase, transferring hexosyl groups						1,75		
AT1G05170	galactosyltransferase family protein						2,18		
AT1G65610	KOR2; catalytic/ hydrolase, hydrolyzing O-glycosyl compounds					2,42	1,73		
AT1G70710	ATGH9B1 (ARABIDOPSIS THALIANA GLYCOSYL HYDROLASE 9B1); cellulase/ hydrolase, hydrolyzing O-glycosyl compounds						2,88		
AT4G02290	AtGH9B13 (Arabidopsis thaliana glycosyl hydrolase 9B13); catalytic/ hydrolase, hydrolyzing O-glycosyl compounds						6,93		
AT1G75680	AtGH9B7 (Arabidopsis thaliana glycosyl hydrolase 9B7); catalytic/ hydrolase, hydrolyzing O-glycosyl compounds						1,63		
AT2G32990	AtGH9B8 (Arabidopsis thaliana glycosyl hydrolase 9B8); catalytic/ hydrolase, hydrolyzing O-glycosyl compounds	3,23	5,06				23,15		
AT1G48930	AtGH9C1 (Arabidopsis thaliana glycosyl hydrolase 9C1); catalytic/ hydrolase, hydrolyzing O-glycosyl compounds	1,73	2,58						
AT1G64390	AtGH9C2 (Arabidopsis thaliana glycosyl hydrolase 9C2); carbohydrate binding / catalytic/ hydrolase, hydrolyzing O-glycosyl compounds	1,85	2,24				7,63		
AT3G61490	glycoside hydrolase family 28 protein / polygalacturonase (pectinase) family protein						2,82		

continued on next page

Table C.10 – continued from previous page

AGI code	Gene description	0,1 % sucrose				3 % sucrose			
		root		shoot		root		shoot	
		d ₃ /d ₀	d ₄ /d ₀	d ₃ /d ₀	d ₄ /d ₀	d ₃ /d ₀	d ₄ /d ₀	d ₃ /d ₀	d ₄ /d ₀
AT3G16850	glycoside hydrolase family 28 protein / polygalacturonase (pectinase) family protein				1,59				
AT1G48100	glycoside hydrolase family 28 protein / polygalacturonase (pectinase) family protein				3,73				2,79
AT5G01260	glycoside hydrolase starch-binding domain-containing protein				1,66				
AT5G64790	glycosyl hydrolase family 17 protein								1,56
AT5G55180	glycosyl hydrolase family 17 protein	1,51	1,75						
AT5G42720	glycosyl hydrolase family 17 protein		1,96					3,18	
AT3G04010	glycosyl hydrolase family 17 protein			1,59					
AT4G19810	glycosyl hydrolase family 18 protein	3,09	4,94				2,37	2,84	
AT1G78060	glycosyl hydrolase family 3 protein				2,83				
AT1G02310	glycosyl hydrolase family protein 5 / cellulase family protein / (1-4)-beta-mannan endohydrolase, putative	1,52	1,59						
AT5G10560	glycosyl hydrolase family 3 protein							1,61	
AT5G13980	glycosyl hydrolase family 38 protein		1,54						
AT2G27500	glycosyl hydrolase family 17 protein							1,64	
AT2G43610	glycoside hydrolase family 19 protein							2,69	
AT3G10740	ASD1 (ALPHA-L-ARABINOFURANOSIDASE 1); alpha-N-arabinofuranosidase/ hydrolase, acting on glycosyl bonds / xylan 1,4-beta-xylosidase		1,62						
AT3G15350	glycosyltransferase family 14 protein / core-2/I-branching enzyme family protein								1,65
AT5G53990	glycosyltransferase family protein	2,49	3,12						
AT4G09500	glycosyltransferase family protein								1,77
AT2G28080	glycosyltransferase family protein								1,98
AT2G22930	glycosyltransferase family protein	2,47	3,96						
AT1G64920	glycosyltransferase family protein							1,59	
AT3G61080	fructosamine kinase family protein								1,96
AT4G34260	FUC95A; 1,2-alpha-L-fucosidase								1,99
AT2G22900	galactosyl transferase GMA12/MNN10 family protein								2,01
AT3G28340	GATL10 (Galacturonosyltransferase-like 10); polygalacturonate 4-alpha-galacturonosyltransferase/ transferase, transferring hexosyl groups	2,27	2,12						2,45
AT4G02130	GATL6; polygalacturonate 4-alpha-galacturonosyltransferase/ transferase, transferring glycosyl groups / transferase, transferring hexosyl groups								2,52
AT3G62660	GATL7 (Galacturonosyltransferase-like 7); polygalacturonate 4-alpha-galacturonosyltransferase/ transferase, transferring glycosyl groups / transferase, transferring hexosyl groups								1,69
AT5G33290	XGD1 (XYLOGALACTURONAN DEFICIENT 1); UDP-xylosyltransferase/ catalytic			2,31	1,78				
AT4G23010	UDP-galactose transporter-related			1,76					
AT4G01070	GT72B1; UDP-glucosyltransferase/ UDP-glycosyltransferase/ transferase, transferring glycosyl groups			2,1	3,29				1,85
AT5G49690	UDP-glucuronosyl/UDP-glucosyl transferase family protein					2,33	2,47		
AT3G55700	UDP-glucuronosyl/UDP-glucosyl transferase family protein		1,52						
AT3G11340	UDP-glucuronosyl/UDP-glucosyl transferase family protein				2,69				
AT1G06000	UDP-glucuronosyl/UDP-glucosyl transferase family protein	1,64	2,49		5,66				

continued on next page

Table C.10 – continued from previous page

AGI code	Gene description	0,1 % sucrose				3 % sucrose			
		root		shoot		root		shoot	
		d ³ /d ₀	d ⁴ /d ₀	d ³ /d ₀	d ⁴ /d ₀	d ³ /d ₀	d ⁴ /d ₀	d ³ /d ₀	d ⁴ /d ₀
AT1G05680	UDP-glucuronosyl/UDP-glucosyl transferase family protein	3,96	3,91			9,16	11,4	5,38	7,21
AT2G31790	UDP-glucuronosyl/UDP-glucosyl transferase family protein	2,01	2,61		2,21	1,56			
AT2G30140	UDP-glucuronosyl/UDP-glucosyl transferase family protein	1,78	2,11			4,18	5,52		
AT3G46700	UDP-glycosyltransferase/ transferase, transferring glycosyl groups	1,59	1,53	2,13	1,89				
AT3G03250	UGP (UDP-glucose pyrophosphorylase); UTP:glucose-1-phosphate uridylyltransferase/ nucleotidyltransferase								1,71
AT2G29750	UGT71C1 (UDP-GLUCOSYL TRANSFERASE 71C1); UDP-glycosyltransferase/ quercetin 3'-O-glucosyltransferase/ quercetin 7-O-glucosyltransferase/ transferase, transferring glycosyl groups								1,82
AT5G66690	UGT72E2; UDP-glycosyltransferase/ coniferyl-alcohol glucosyltransferase/ transferase, transferring glycosyl groups		1,67						
AT3G53150	UGT73D1 (UDP-glucosyl transferase 73D1); UDP-glycosyltransferase/ transferase, transferring hexosyl groups					4,08	6,25		
AT1G24100	UGT74B1 (UDP-glucosyl transferase 74B1); UDP-glycosyltransferase/ thiohydroximate beta-D-glucosyltransferase/ transferase, transferring glycosyl groups			1,83	2,98				
AT2G26480	UGT76D1 (UDP-GLUCOSYL TRANSFERASE 76D1); UDP-glycosyltransferase/ quercetin 7-O-glucosyltransferase/ transferase, transferring glycosyl groups		1,72						
AT1G30530	UGT78D1 (UDP-GLUCOSYL TRANSFERASE 78D1); UDP-glycosyltransferase/ quercetin 3-O-glucosyltransferase/ transferase, transferring glycosyl groups					6,13			
AT2G23260	UGT84B1 (UDP-glucosyl transferase 84B1); UDP-glycosyltransferase/ abscisic acid glucosyltransferase/ indole-3-acetate beta-glucosyltransferase/ quercetin 7-O-glucosyltransferase/ transferase, transferring glycosyl groups	1,8	1,95						
AT4G15490	UGT84A3; UDP-glycosyltransferase/ sinapate 1-glucosyltransferase/ transferase, transferring glycosyl groups								2,52
AT1G22400	UGT85A1; UDP-glycosyltransferase/ cis-zeatin O-beta-D-glucosyltransferase/ glucuronosyltransferase/ trans-zeatin O-beta-D-glucosyltransferase/ transferase, transferring glycosyl groups / transferase, transferring hexosyl groups								2,79
AT5G05890	UDP-glucuronosyl/UDP-glucosyl transferase family protein								1,84
AT3G46690	UDP-glucuronosyl/UDP-glucosyl transferase family protein								3,39
AT2G29740	UGT71C2 (UDP-GLUCOSYL TRANSFERASE 71C2); UDP-glycosyltransferase/ quercetin 3'-O-glucosyltransferase/ quercetin 3-O-glucosyltransferase/ quercetin 7-O-glucosyltransferase/ transferase, transferring glycosyl groups								3,99
AT3G50740	UGT72E1 (UDP-glucosyl transferase 72E1); UDP-glycosyltransferase/ coniferyl-alcohol glucosyltransferase/ transferase, transferring glycosyl groups								1,95
AT4G34138	UGT73B1 (UDP-glucosyl transferase 73B1); UDP-glycosyltransferase/ abscisic acid glucosyltransferase/ quercetin 3-O-glucosyltransferase/ quercetin 7-O-glucosyltransferase								6,34
AT2G36750	UGT73C1 (UDP-GLUCOSYL TRANSFERASE 73C1); UDP-glycosyltransferase/ UDP-glycosyltransferase/ cis-zeatin O-beta-D-glucosyltransferase/ trans-zeatin O-beta-D-glucosyltransferase/ transferase, transferring glycosyl groups								2,9
AT5G05860	UGT76C2; UDP-glycosyltransferase/ cis-zeatin O-beta-D-glucosyltransferase/ cytokinin 7-beta-glucosyltransferase/ cytokinin 9-beta-glucosyltransferase/ trans-zeatin O-beta-D-glucosyltransferase/ transferase, transferring glycosyl groups								1,8

continued on next page

Table C.10 – continued from previous page

AGI code	Gene description	0,1 % sucrose				3 % sucrose			
		root		shoot		root		shoot	
		d ₃ /d ₀	d ₄ /d ₀	d ₃ /d ₀	d ₄ /d ₀	d ₃ /d ₀	d ₄ /d ₀	d ₃ /d ₀	d ₄ /d ₀
AT2G02810	UTR1 (UDP-GALACTOSE TRANSPORTER 1); UDP-galactose transmembrane transporter/ UDP-glucose transmembrane transporter/ pyrimidine nucleotide sugar transmembrane transporter				1,59				
AT3G46970	PHS2 (ALPHA-GLUCAN PHOSPHORYLASE 2); phosphorylase/ transferase, transferring glycosyl groups	1,67	1,71		2,24				3,01
AT4G24450	PWD (PHOSPHOGLUCAN, WATER DIKINASE); ATP binding / kinase				1,93	1,91	1,81		
AT2G22990	SNG1 (SINAPOYLGLUCOSE 1); serine-type carboxypeptidase/ sinapoylglucose-malate O-sinapoyltransferase	2,35	2,9		2,68				
Pentosephosphate cycle									
AT3G02360	6-phosphogluconate dehydrogenase family protein				1,66				
AT5G41670	6-phosphogluconate dehydrogenase family protein			1,92	1,52				
AT1G32060	PRK (PHOSPHORIBULOKINASE); ATP binding / phosphoribulokinase/ protein binding	1,6	2,7						
AT5G61410	RPE; catalytic/ ribulose-phosphate 3-epimerase				1,65				
Citric acid/glyoxylate cycle									
AT5G65750	2-oxoglutarate dehydrogenase E1 component, putative / oxoglutarate decarboxylase, putative / alpha-ketoglutarate dehydrogenase, putative				1,62				
AT2G42790	CSY3 (citrate synthase 3); citrate (SI)-synthase				1,66				
AT5G03290	isocitrate dehydrogenase, putative / NAD+ isocitrate dehydrogenase, putative				1,53				
AT2G05710	aconitate hydratase, cytoplasmic, putative / citrate hydro-lyase/aconitase, putative				1,75				
AT3G09810	isocitrate dehydrogenase, putative / NAD+ isocitrate dehydrogenase, putative		1,81	1,73	1,97				
AT5G66760	SDH1-1; ATP binding / succinate dehydrogenase			1,69					
AT3G21720	ICL (ISOCITRATE LYASE); catalytic/ isocitrate lyase				1,55				
AT5G43330	malate dehydrogenase, cytosolic, putative				1,7				
Carotenoid									
AT5G52570	BETA-OHASE 2 (BETA-CAROTENE HYDROXYLASE 2); carotene beta-ring hydroxylase				1,55				
Vitamin E/tocopherol/antioxidant									
AT2G18950	HPT1 (HOMOGENTISATE PHYTYLTRANSFERASE 1); homogentisate phytyltransferase/ prenyltransferase			1,74	1,54				
AT1G64970	G-TMT (GAMMA-TOCOPHEROL METHYLTRANSFERASE); tocopherol O-methyltransferase				5,04				
Fatty acids									
AT1G77590	LACS9 (LONG CHAIN ACYL-COA SYNTHETASE 9); long-chain-fatty-acid-CoA ligase	1,52	1,53						
AT1G04220	KCS2 (3-KETOACYL-COA SYNTHASE 2); fatty acid elongase				1,66		6,37		
AT1G07720	KCS3 (3-KETOACYL-COA SYNTHASE 3); acyltransferase/ catalytic/ transferase, transferring acyl groups other than amino-acyl groups				1,53				
AT2G28630	KCS12 (3-KETOACYL-COA SYNTHASE 12); acyltransferase/ catalytic/ transferase, transferring acyl groups other than amino-acyl groups				4,4				

continued on next page

Table C.10 – continued from previous page

AGI code	Gene description	0,1 % sucrose				3 % sucrose			
		root		shoot		root		shoot	
		d ³ /d ₀	d ⁴ /d ₀	d ³ /d ₀	d ⁴ /d ₀	d ³ /d ₀	d ⁴ /d ₀	d ³ /d ₀	d ⁴ /d ₀
AT2G15090	KCS8 (3-KETOACYL-COA SYNTHASE 8); acyltransferase/ catalytic/ transferase, transferring acyl groups other than amino-acyl groups			1,71	3,74				3,52
AT5G48880	PKT2 (PEROXISOMAL 3-KETO-ACYL-COA THIOLASE 2); acetyl-CoA C-acyltransferase/ catalytic	1,89	2,69						
AT2G22780	PMDH1 (PEROXISOMAL NAD-MALATE DEHYDROGENASE 1); L-malate dehydrogenase/ binding / catalytic/ malate dehydrogenase/ oxidoreductase/ oxidoreductase, acting on the CH-OH group of donors, NAD or NADP as acceptor			1,57	1,59				
AT1G06550	enoyl-CoA hydratase/isomerase family protein	1,71	2,18		2,13				
AT2G04350	long-chain-fatty-acid-CoA ligase family protein / long-chain acyl-CoA synthetase family protein (LACS8)				1,69				
AT1G64400	long-chain-fatty-acid-CoA ligase, putative / long-chain acyl-CoA synthetase, putative				2,24				
AT1G43800	acyl-(acyl-carrier-protein) desaturase, putative / stearyl-ACP desaturase, putative			1,57	7,68	7,29	8,69		
AT2G29980	FAD3 (FATTY ACID DESATURASE 3); omega-3 fatty acid desaturase				2,61				
AT3G15850	FAD5 (FATTY ACID DESATURASE 5); 16:0 monogalactosyldiacylglycerol desaturase/ oxidoreductase				2,14				
AT4G30950	FAD6 (FATTY ACID DESATURASE 6); omega-6 fatty acid desaturase				1,61				
AT5G22500	FAR1 (FATTY ACID REDUCTASE 1); fatty acyl-CoA reductase (alcohol-forming)/ oxidoreductase, acting on the CH-CH group of donors	1,66	1,85	2,79	2,63				
AT3G44550	FAR5 (FATTY ACID REDUCTASE 5); binding / catalytic/ oxidoreductase, acting on the CH-CH group of donors	2,29	2,93						
AT1G06100	fatty acid desaturase family protein				1,78				
AT1G06080	ADS1 (DELTA 9 DESATURASE 1); oxidoreductase			4,04	3,87				
AT2G31360	ADS2 (16:0Delta9 Arabidopsis desaturase 2); oxidoreductase				3,11				2,19
AT3G06860	MFP2 (MULTIFUNCTIONAL PROTEIN 2); 3-hydroxyacyl-CoA dehydrogenase/ enoyl-CoA hydratase				1,59				
AT2G38530	LTP2 (LIPID TRANSFER PROTEIN 2); lipid binding				1,66		1,95		
AT5G59320	LTP3 (LIPID TRANSFER PROTEIN 3); lipid binding	1,96	3,05		14,26				
AT5G59310	LTP4 (LIPID TRANSFER PROTEIN 4); lipid binding				5,38				1,82
AT5G40990	GLIP1 (GDSL LIPASE1); carboxylesterase/ lipase	53,39	50,09			10,92	17,18		
AT1G31550	GDSL-motif lipase, putative				1,52		2,49		
AT1G54030	GDSL-motif lipase, putative				1,75		1,9		
AT5G55050	GDSL-motif lipase/hydrolase family protein	1,54		1,58	1,64				
AT5G45670	GDSL-motif lipase/hydrolase family protein				1,65				
AT5G45950	GDSL-motif lipase/hydrolase family protein				2,07				
AT3G48460	GDSL-motif lipase/hydrolase family protein				2,05				
AT4G30140	GDSL-motif lipase/hydrolase family protein				2,39				
AT4G28780	GDSL-motif lipase/hydrolase family protein				2,25				
AT4G26790	GDSL-motif lipase/hydrolase family protein	1,66	1,72						
AT4G18970	GDSL-motif lipase/hydrolase family protein				2,86				
AT3G14220	GDSL-motif lipase/hydrolase family protein				2,24				
AT3G16370	GDSL-motif lipase/hydrolase family protein				1,55				
AT2G23540	GDSL-motif lipase/hydrolase family protein	1,79	1,98						
AT5G33370	GDSL-motif lipase/hydrolase family protein				7,48				

continued on next page

Table C.10 — continued from previous page

AGI code	Gene description	0,1 % sucrose				3 % sucrose			
		root		shoot		root		shoot	
		d ₃ /d ₀	d ₄ /d ₀	d ₃ /d ₀	d ₄ /d ₀	d ₃ /d ₀	d ₄ /d ₀	d ₃ /d ₀	d ₄ /d ₀
AT2G04570	GDSL-motif lipase/hydrolase family protein			1,68					
AT1G28580	GDSL-motif lipase, putative							1,52	
AT5G59330	lipid binding							2,62	
AT4G33550	lipid binding							2,28	
AT1G55260	lipid binding							2,93	
AT2G44300	lipid transfer protein-related							2,88	1,82
AT2G15050	LTP; lipid binding							1,82	
AT3G08770	LTP6; lipid binding							2,89	
AT1G27950	LTPG1 (GLYCOSYLPHOSPHATIDYLINOSITOL-ANCHORED LIPID PROTEIN TRANSFER 1)	1,64	1,65						
AT5G64080	protease inhibitor/seed storage/lipid transfer protein (LTP) family protein	1,7	1,96					3,09	
AT5G55450	protease inhibitor/seed storage/lipid transfer protein (LTP) family protein							2,5	
AT5G05960	protease inhibitor/seed storage/lipid transfer protein (LTP) family protein	1,94	1,88					3,52	
AT3G58550	protease inhibitor/seed storage/lipid transfer protein (LTP) family protein	1,8	1,81						
AT3G53980	protease inhibitor/seed storage/lipid transfer protein (LTP) family protein							2,28	
AT3G43720	protease inhibitor/seed storage/lipid transfer protein (LTP) family protein	1,58	1,89						
AT4G22610	protease inhibitor/seed storage/lipid transfer protein (LTP) family protein	1,69	1,81						
AT4G22490	protease inhibitor/seed storage/lipid transfer protein (LTP) family protein							2,28	
AT4G12500	protease inhibitor/seed storage/lipid transfer protein (LTP) family protein					5,17		2,39	
AT4G12490	protease inhibitor/seed storage/lipid transfer protein (LTP) family protein			6,23					7,55 5,26
AT3G22600	protease inhibitor/seed storage/lipid transfer protein (LTP) family protein	1,5	1,72						
AT3G18280	protease inhibitor/seed storage/lipid transfer protein (LTP) family protein			1,51	1,94	2,32			
AT1G62790	protease inhibitor/seed storage/lipid transfer protein (LTP) family protein					1,87			
AT2G18370	protease inhibitor/seed storage/lipid transfer protein (LTP) family protein	1,79	1,73						
AT2G13820	protease inhibitor/seed storage/lipid transfer protein (LTP) family protein							1,9	
AT4G22470	protease inhibitor/seed storage/lipid transfer protein (LTP) family protein				3,02	4,64		3,25	2,57
AT4G12470	protease inhibitor/seed storage/lipid transfer protein (LTP) family protein			1,85		2,13			
AT1G62510	protease inhibitor/seed storage/lipid transfer protein (LTP) family protein					5,05		1,59	2,14
AT2G45180	protease inhibitor/seed storage/lipid transfer protein (LTP) family protein	2,21	2,74						
AT3G04290	LTL1 (LI-TOLERANT LIPASE 1); carboxylesterase/ hydrolase, acting on ester bonds							2,23	
AT3G62590	lipase class 3 family protein			1,87	2,26				
AT1G51440	lipase class 3 family protein							1,76	
AT2G42690	lipase, putative							1,74	
AT5G18630	lipase class 3 family protein							1,88	
AT1G02660	lipase class 3 family protein							3,65	2,29
AT1G30370	lipase class 3 family protein							1,58	
AT1G75880	family II extracellular lipase 1 (EXL1)							1,89	
AT1G28600	lipase, putative							1,64	
AT5G14180	MPL1 (MYZUS PERSICAE-INDUCED LIPASE 1); catalytic							5,41	

continued on next page

Table C.10 — continued from previous page

AGI code	Gene description	0,1 % sucrose				3 % sucrose			
		root		shoot		root		shoot	
		d ³ /d ₀	d ⁴ /d ₀	d ³ /d ₀	d ⁴ /d ₀	d ³ /d ₀	d ⁴ /d ₀	d ³ /d ₀	d ⁴ /d ₀
AT5G20410	MGD2; 1,2-diacylglycerol 3-beta-galactosyltransferase/ UDP-galactosyltransferase/ transferase, transferring glycosyl groups				2,83			2,07	2,45
AT2G11810	MGDC; 1,2-diacylglycerol 3-beta-galactosyltransferase						8,03	4,5	3,87
AT2G19450	TAG1 (TRIACYLGLYCEROL BIOSYNTHESIS DEFECT 1); diacylglycerol O-acyltransferase					1,8	2,19		
AT5G41080	glycerophosphoryl diester phosphodiesterase family protein			1,53	3,16				
AT1G74210	glycerophosphoryl diester phosphodiesterase family protein				1,71				
AT3G02040	SRG3 (senescence-related gene 3); glycerophosphodiester phosphodiesterase/ phosphoric diester hydrolase						2,11	2,16	2,66
Nitrate/NH3									
AT1G08090	ATNRT2:1 (NITRATE TRANSPORTER 2:1); nitrate transmembrane transporter	2,22	6,07						
AT2G15620	NIR1 (NITRITE REDUCTASE 1); ferredoxin-nitrate reductase/ nitrite reductase (NO-forming)			1,56					1,81
AT2G26690	nitrate transporter (NTP2)				3,95				
AT3G48450	nitrate-responsive NOI protein, putative	3	3,32						
AT1G12110	NRT1.1; nitrate transmembrane transporter/ transporter			1,82	1,97				
AT1G32450	NRT1.5 (NITRATE TRANSPORTER 1.5); nitrate transmembrane transporter/ transporter			1,59	5,12				
AT2G34470	UREG (UREASE ACCESSORY PROTEIN G); ATP binding / metal ion binding / nickel ion binding / nucleotide binding				2,31				
AT5G50200	WR3 (WOUND-RESPONSIVE 3); nitrate transmembrane transporter	1,92	1,95		2,49				
AT1G77760	NIA1 (NITRATE REDUCTASE 1); nitrate reductase			1,68	4,94				
AT1G37130	NIA2 (NITRATE REDUCTASE 2); nitrate reductase (NADH)/ nitrate reductase				1,83				
AT1G69850	ATNRT1:2 (ARABIDOPSIS THALIANA NITRATE TRANSPORTER 1:2); calcium ion binding / transporter						2,12		
AT5G56860	GNC (GATA, nitrate-inducible, carbon metabolism-involved); transcription factor			1,76					
AT4G24020	NLP7 (NIN LIKE PROTEIN 7); transcription factor				1,64				
AT1G64780	ATAMT1:2 (AMMONIUM TRANSPORTER 1:2); ammonium transmembrane transporter		1,75	2,05	3,29			2,18	
AT2G38290	ATAMT2 (AMMONIUM TRANSPORTER 2); ammonium transmembrane transporter/ high affinity secondary active ammonium transmembrane transporter				1,6				
AT3G16240	DELTA-TIP; ammonia transporter/ methylammonium transmembrane transporter/ water channel	2,05	1,93						
AT5G47450	AtTIP2:3; ammonia transporter/ methylammonium transmembrane transporter/ water channel	4,5	4,94						
Sulfate assimilation									
AT5G48850	ATSDI1 (SULPHUR DEFICIENCY-INDUCED 1); binding				17,46	6,63	5,03		
AT3G22890	APS1 (ATP SULFURYLASE 1); sulfate adenylyltransferase (ATP)		1,76		3,09				
AT1G19920	APS2; sulfate adenylyltransferase (ATP)				1,62				
AT4G14680	APS3; sulfate adenylyltransferase (ATP)	2,15	2,49		3,34				
AT1G62180	APR2 (5'ADENYLYLPHOSPHOSULFATE REDUCTASE 2); adenylyl-sulfate reductase/ phosphoadenylyl-sulfate reductase (thioredoxin)			1,63	3,08				
AT4G04610	APR1 (APS REDUCTASE 1); adenylyl-sulfate reductase	1,65	2,3	2,54	12,79				
AT4G21990	APR3 (APS REDUCTASE 3); adenylyl-sulfate reductase			1,8	5,75				

continued on next page

Table C.10 – continued from previous page

AGI code	Gene description	0,1 % sucrose				3 % sucrose			
		root		shoot		root		shoot	
		d ₃ /d ₀	d ₄ /d ₀	d ₃ /d ₀	d ₄ /d ₀	d ₃ /d ₀	d ₄ /d ₀	d ₃ /d ₀	d ₄ /d ₀
AT2G14750	APK (APS KINASE); ATP binding / adenylylsulfate kinase/ kinase/ transferase, transferring phosphorus-containing groups	1,7	1,84		3,34				
AT4G39940	AKN2 (APS-kinase 2); ATP binding / adenylylsulfate kinase/ kinase/ transferase, transferring phosphorus-containing groups	3,13	3,64		3,35				
AT3G49580	LSU1 (RESPONSE TO LOW SULFUR 1)		2,66		14,11				
AT5G24660	LSU2 (RESPONSE TO LOW SULFUR 2)			2,17	9,47				
AT5G04590	SIR; sulfite reductase (ferredoxin)/ sulfite reductase				2,12				
AT1G78000	SULTR1;2 (SULFATE TRANSPORTER 1;2); sulfate transmembrane transporter				2,09				
AT3G51895	SULTR3;1 (SULFATE TRANSPORTER 3;1); secondary active sulfate transmembrane transporter/ sulfate transmembrane transporter/ transporter			1,52	18,81				
AT3G12520	SULTR4;2; sulfate transmembrane transporter				3,37				
AT5G48370	thioesterase family protein				1,73				
AT1G35250	thioesterase family protein	2,22	2,74						
AT1G04290	thioesterase family protein		1,63						
AT1G67810	SUFE2 (SULFUR E 2); enzyme activator				1,75				
AT2G03750	sulfotransferase family protein				1,66				
AT5G10180	AST68; sulfate transmembrane transporter	2,16	3,77		1,53				
AT5G66040	STR16 (SULFURTRANSFERASE PROTEIN 16)				1,65				
AT1G77990	AST56; sulfate transmembrane transporter	2,05	2,23						
Phosphate									
AT5G13080	WRKY75; transcription factor			3,26					
AT3G23430	PHO1 (phosphate 1)				3,16				
AT2G18230	AtPPa2 (Arabidopsis thaliana pyrophosphorylase 2); inorganic diphosphatase/ pyrophosphatase				3,42				
AT2G46860	AtPPa3 (Arabidopsis thaliana pyrophosphorylase 3); inorganic diphosphatase/ pyrophosphatase	2,03	3,17						
AT4G01480	AtPPa5 (Arabidopsis thaliana pyrophosphorylase 5); inorganic diphosphatase/ pyrophosphatase			2,34	5,61				
AT5G09650	AtPPa6 (Arabidopsis thaliana pyrophosphorylase 6); inorganic diphosphatase/ pyrophosphatase	1,52	1,67						
AT3G53620	AtPPa4 (Arabidopsis thaliana pyrophosphorylase 4); inorganic diphosphatase						1,59		
AT4G35770	SEN1 (SENESCENCE 1)			5,89				1,74	
Boron									
AT2G47160	BOR1 (REQUIRES HIGH BORON 1); anion exchanger/ boron transporter				2,18				
AT4G10380	NIP5;1; arsenite transmembrane transporter/ boron transporter/ water channel			1,55	2,03				
AT1G80760	NIP6;1 (NOD26-LIKE INTRINSIC PROTEIN 6;1); boron transporter/ glycerol transmembrane transporter/ urea transmembrane transporter/ water channel/ water transporter				7,11				
Membrane transport									
AT1G31770	ABC transporter family protein				1,68				

continued on next page

Table C.10 – continued from previous page

AGI code	Gene description	0,1 % sucrose				3 % sucrose			
		root		shoot		root		shoot	
		d^3/d_0	d^4/d_0	d^3/d_0	d^4/d_0	d^3/d_0	d^4/d_0	d^3/d_0	d^4/d_0
AT5G06530	ABC transporter family protein				2,45				2,07
AT1G71960	ABC transporter family protein								2,6
AT1G51460	ABC transporter family protein				1,53				
AT3G59140	ATMRP14; ATPase, coupled to transmembrane movement of substances				1,74				
AT3G13090	ATMRP8; ATPase, coupled to transmembrane movement of substances		1,63						
AT1G67940	ATNAP3; transporter			1,59	2,31				
AT5G02270	ATNAP9; transporter		2,27						
AT3G55130	ATWBC19 (White-Brown Complex homolog 19); ATPase, coupled to transmembrane movement of substances				1,88				
AT3G21090	ABC transporter family protein			1,51	2,59				
AT2G39350	ABC transporter family protein				1,54				
AT1G32500	ATNAP6 (NON-INTRINSIC ABC PROTEIN 6); protein binding / transporter				1,51				
AT4G25450	ATNAP8; ATPase, coupled to transmembrane movement of substances / transporter				1,71				
AT1G15520	PDR12 (PLEIOTROPIC DRUG RESISTANCE 12); ATPase, coupled to transmembrane movement of substances							3,6	4,43
AT2G37280	PDR5 (PLEIOTROPIC DRUG RESISTANCE 5); ATPase, coupled to transmembrane movement of substances	1,56							
AT3G53480	PDR9 (PLEIOTROPIC DRUG RESISTANCE 9); ATPase, coupled to transmembrane movement of substances			2,45				2,21	2,65
AT2G36380	PDR6; ATPase, coupled to transmembrane movement of substances				1,91				
AT4G26760	MAP65-2				1,88				
AT5G44050	MATE efflux family protein	1,67	1,76						
AT5G38030	MATE efflux family protein			1,69	1,53				
AT3G23550	MATE efflux family protein			1,76					
AT1G71140	MATE efflux family protein					8,16	13,97		
AT1G71870	MATE efflux family protein	1,67	2,15						
AT2G04050	MATE efflux family protein	5,82	7,96			6,49	12,77		
AT1G61890	MATE efflux family protein				1,86				
AT5G52450	MATE efflux protein-related				1,73				
AT1G12950	MATE efflux family protein					1,68	1,93		
AT1G15180	MATE efflux family protein				2,41				
AT5G54250	ATCNGC4 (CYCLIC NUCLEOTIDE-GATED CATION CHANNEL 4); calmodulin binding / cation channel/ cation transmembrane transporter/ cyclic nucleotide binding				1,85				
AT4G23700	ATCHX17 (CATION/H+ EXCHANGER 17); monovalent cation:proton antiporter/ sodium:hydrogen antiporter					3,81	4,33		
AT1G64170	ATCHX16 (CATION/H+ EXCHANGER 16); monovalent cation:proton antiporter/ sodium:hydrogen antiporter				3,16				
AT1G79520	cation efflux family protein				2,27				
AT1G16310	cation efflux family protein				1,84				
AT1G51610	cation efflux family protein / metal tolerance protein, putative (MTPc4)				3,08				2,3
AT1G73220	AtOCT1 (Arabidopsis thaliana ORGANIC CATION/CARNITINE TRANSPORTER1); carbohydrate transmem- brane transporter/ carnitine transporter/ transporter	3,75	9,54		3,3				
AT1G16390	AtOCT3 (ARABIDOPSIS THALIANA ORGANIC CATION/CARNITINE TRANSPORTER 3); carbohydrate transmembrane transporter/ sugar:hydrogen symporter				2,23				

continued on next page

Table C.10 — continued from previous page

AGI code	Gene description	0,1 % sucrose				3 % sucrose			
		root		shoot		root		shoot	
		d ₃ /d ₀	d ₄ /d ₀	d ₃ /d ₀	d ₄ /d ₀	d ₃ /d ₀	d ₄ /d ₀	d ₃ /d ₀	d ₄ /d ₀
AT1G79410	AtOCT5 (Arabidopsis thaliana ORGANIC CATION/CARNITINE TRANSPORTER5); carbohydrate transmembrane transporter/ sugar:hydrogen symporter				2,22				2,37
AT5G49990	xanthine/uracil permease family protein						2,28		
AT1G49960	xanthine/uracil permease family protein			1,79					
AT3G08040	FRD3 (FERRIC REDUCTASE DEFECTIVE 3); antiporter/ transporter	1,71	1,98						
AT5G50160	FRO8 (FERRIC REDUCTION OXIDASE 8); ferric-chelate reductase/ oxidoreductase						1,96		
AT1G80830	NRAMP1 (NATURAL RESISTANCE-ASSOCIATED MACROPHAGE PROTEIN 1); inorganic anion transmembrane transporter/ manganese ion transmembrane transporter/ metal ion transmembrane transporter						1,98		
AT1G23020	FRO3; ferric-chelate reductase	1,69			2,31				
AT5G03570	ATIREG2 (IRON-REGULATED PROTEIN 2); nickel ion transmembrane transporter	1,52	1,89						
AT5G26820	ATIREG3 (IRON-REGULATED PROTEIN 3)	1,55	1,57						
AT4G19690	IRT1 (iron-regulated transporter 1); cadmium ion transmembrane transporter/ copper uptake transmembrane transporter/ iron ion transmembrane transporter/ manganese ion transmembrane transporter/ zinc ion transmembrane transporter	2,72	1,69						
Potassium									
AT4G32650	ATKC1 (ARABIDOPSIS THALIANA K ⁺ RECTIFYING CHANNEL 1); cyclic nucleotide binding / inward rectifier potassium channel			1,54	2,2				
AT2G30070	ATKT1 (POTASSIUM TRANSPORTER 1); potassium ion transmembrane transporter						1,65		
AT5G46240	KAT1 (POTASSIUM CHANNEL IN ARABIDOPSIS THALIANA 1); cyclic nucleotide binding / inward rectifier potassium channel						2,63		
Sodium									
AT4G10310	HKT1 (HIGH-AFFINITY K ⁺ TRANSPORTER 1); sodium ion transmembrane transporter								2,7
AT5G27150	NHX1 (NA ⁺ /H ⁺ EXCHANGER); protein binding / sodium ion transmembrane transporter/ sodium:hydrogen antiporter								1,69
AT3G05030	NHX2 (SODIUM HYDROGEN EXCHANGER 2); sodium ion transmembrane transporter/ sodium:hydrogen antiporter								1,74
AT4G22840	bile acid:sodium symporter family protein								2,07
AT4G12030	bile acid:sodium symporter family protein	1,96	2,74						3,3
AT3G25410	bile acid:sodium symporter family protein						1,72		
AT2G26900	bile acid:sodium symporter family protein								1,57
Zinc									
AT5G63530	ATFP3; metal ion binding / transition metal ion binding								4,01
AT3G12750	ZIP1 (ZINC TRANSPORTER 1 PRECURSOR); zinc ion transmembrane transporter	2,12	2,23						
AT1G10970	ZIP4 (ZINC TRANSPORTER 4 PRECURSOR); cation transmembrane transporter/ copper ion transmembrane transporter	1,77	1,94						

continued on next page

Table C.10 – continued from previous page

AGI code	Gene description	0,1 % sucrose				3 % sucrose			
		root		shoot		root		shoot	
		d ³ /d ₀	d ⁴ /d ₀	d ³ /d ₀	d ⁴ /d ₀	d ³ /d ₀	d ⁴ /d ₀	d ³ /d ₀	d ⁴ /d ₀
AT2G04032	ZIP7 (ZINC TRANSPORTER 7 PRECURSOR); cation transmembrane transporter/ metal ion transmembrane transporter/ zinc ion transmembrane transporter				1,56				
AT4G30110	HMA2; cadmium-transporting ATPase				4,64				
AT1G05300	ZIP5; cation transmembrane transporter/ metal ion transmembrane transporter				5,01	2,59	2,7		
AT3G58810	MTPA2 (METAL TOLERANCE PROTEIN A2); efflux transmembrane transporter/ inorganic anion transmembrane transporter/ zinc ion transmembrane transporter	2,15	1,69						
Copper									
AT5G24580	copper-binding family protein				4,97				
AT3G48970	copper-binding family protein				2,79				
AT3G24450	copper-binding family protein				2,39				
AT2G28660	copper-binding family protein								2,18
Cadmium									
AT5G44070	CAD1 (CADMIUM SENSITIVE 1); cadmium ion binding / copper ion binding / glutathione gamma-glutamylcysteinyltransferase			1,59	1,78				
Anions/Chloride									
AT3G62270	anion exchange family protein			1,64	2,16				
AT4G35440	CLC-E (CHLORIDE CHANNEL E); ion channel/ voltage-gated chloride channel				1,91				
Oligopeptides									
AT4G16370	ATOPT3 (OLIGOPEPTIDE TRANSPORTER); oligopeptide transporter							1,6	
AT3G45710	proton-dependent oligopeptide transport (POT) family protein				1,78				
AT5G2680	proton-dependent oligopeptide transport (POT) family protein			1,59	1,57				
AT4G21680	proton-dependent oligopeptide transport (POT) family protein			6,4	2,35				
AT3G01350	proton-dependent oligopeptide transport (POT) family protein				2,16				2,34
AT1G52190	proton-dependent oligopeptide transport (POT) family protein				3,51				
AT1G18880	proton-dependent oligopeptide transport (POT) family protein				3,19				
AT1G68570	proton-dependent oligopeptide transport (POT) family protein				2,44				
AT2G37900	proton-dependent oligopeptide transport (POT) family protein				1,73				
AT5G14940	proton-dependent oligopeptide transport (POT) family protein				1,74				
AT3G45680	proton-dependent oligopeptide transport (POT) family protein	2,01	2,59						
AT2G40460	proton-dependent oligopeptide transport (POT) family protein				2,44				
AT5G46050	PTR3 (PEPTIDE TRANSPORTER 3); dipeptide transporter/ transporter/ tripeptide transporter			3,55	1,91				
AT5G55930	OPT1 (OLIGOPEPTIDE TRANSPORTER 1); oligopeptide transporter				3,5				
AT4G27730	OPT6 (OLIGOPEPTIDE TRANSPORTER 1); oligopeptide transporter				1,61				
AT1G22550	proton-dependent oligopeptide transport (POT) family protein				2,11	3,03	3,06		

continued on next page

Table C.10 – continued from previous page

AGI code	Gene description	0,1 % sucrose				3 % sucrose				
		root		shoot		root		shoot		
		d ₃ /d ₀	d ₄ /d ₀	d ₃ /d ₀	d ₄ /d ₀	d ₃ /d ₀	d ₄ /d ₀	d ₃ /d ₀	d ₄ /d ₀	
AT1G22570	proton-dependent oligopeptide transport (POT) family protein								10,3	
Polyamines										
AT5G19530	ACL5 (ACAULIS 5); spermine synthase/ thermospermine synthase		1,83	1,95						
AT5G53120	SPDS3 (SPERMIDINE SYNTHASE 3); spermidine synthase/ spermine synthase								2,81	
Chloroplast										
AT5G54190	PORA; oxidoreductase/ protochlorophyllide reductase									1,75
AT4G01690	PPOX; protoporphyrinogen oxidase									1,9
AT3G22840	ELIP1 (EARLY LIGHT-INDUCIBLE PROTEIN); chlorophyll binding	3,1	4,23	2,32	4,79				4,31	1,51
AT4G14690	ELIP2 (EARLY LIGHT-INDUCIBLE PROTEIN 2); chlorophyll binding	3,86	3,59	2,12					5,38	1,76
AT2G27510	ATFD3 (ferredoxin 3); 2 iron, 2 sulfur cluster binding / electron carrier/ iron-sulfur cluster binding			1,6	1,57					
AT5G10770	chloroplast nucleoid DNA-binding protein, putative				2,68					
AT1G09750	chloroplast nucleoid DNA-binding protein-related				1,77					
AT4G17090	CT-BMY (CHLOROPLAST BETA-AMYLASE); beta-amylase									1,76
AT1G75010	ARC3 (ACCUMULATION AND REPLICATION OF CHLOROPLASTS 3)				1,84					
AT5G55280	FTSZ1-1; protein binding / structural molecule				1,57					
AT3G02450	cell division protein ftsH, putative				1,51					
AT3G01370	ATCFM2 (CRM FAMILY MEMBER 2); RNA binding				2,02					
AT1G23400	CAF2; RNA splicing factor, transesterification mechanism				2,51					
AT3G63140	CSP41A (CHLOROPLAST STEM-LOOP BINDING PROTEIN OF 41 KDA); mRNA binding / poly(U) binding				1,81					
AT5G66055	AKRP (ANKYRIN REPEAT PROTEIN); protein binding				2,02					
AT5G38660	APE1 (ACCLIMATION OF PHOTOSYNTHESIS TO ENVIRONMENT)				1,51					
AT5G46110	APE2 (ACCLIMATION OF PHOTOSYNTHESIS TO ENVIRONMENT 2); antiporter/ triose-phosphate trans-membrane transporter	1,62	2,05							
AT2G01110	APG2 (ALBINO AND PALE GREEN 2); proton motive force dependent protein transmembrane transporter				1,98					
AT3G62910	APG3 (ALBINO AND PALE GREEN); translation release factor/ translation release factor, codon specific				1,52					
AT1G03680	ATHM1; enzyme activator				1,83					
AT4G03520	ATHM2; enzyme activator				1,59					
AT1G76080	CDSP32 (CHLOROPLASTIC DROUGHT-INDUCED STRESS PROTEIN OF 32 KD)				2,09					
AT1G08520	CHLD; ATP binding / magnesium chelatase/ nucleoside-triphosphatase/ nucleotide binding				1,56					
AT4G25080	CHLM (magnesium-protoporphyrin IX methyltransferase); magnesium protoporphyrin IX methyltransferase		1,58		1,71					
AT5G51020	CRL (CRUMPLED LEAF)				1,57					
AT1G70760	CRR23 ((chlororespiratory reduction 23)				2,39					
AT2G47910	CRR6 (chlororespiratory reduction 6)				1,93					
AT1G67840	CSK (CHLOROPLAST SENSOR KINASE); ATP binding / kinase				1,66					
AT3G27160	GHS1 (GLUCOSE HYPERSENSITIVE 1); structural constituent of ribosome				1,69					

continued on next page

Table C.10 – continued from previous page

AGI code	Gene description	0,1 % sucrose				3 % sucrose			
		root		shoot		root		shoot	
		d ³ /d ₀	d ⁴ /d ₀	d ³ /d ₀	d ⁴ /d ₀	d ³ /d ₀	d ⁴ /d ₀	d ³ /d ₀	d ⁴ /d ₀
AT4G14440	HCD1 (3-HYDROXYACYL-COA DEHYDRATASE 1); carnitine racemase/ catalytic/ dodecenoyl-CoA delta-isomerase		1,51						
AT3G24430	HCF101 (HIGH-CHLOROPHYLL-FLUORESCENCE 101); ATP binding				1,63				
AT5G52440	HCF106; proton motive force dependent protein transmembrane transporter				1,51				
AT5G23120	HCF136; protein binding				2,02				
AT4G31560	HCF153				1,55				
AT4G37200	HCF164; oxidoreductase, acting on sulfur group of donors, disulfide as acceptor				1,85				
AT1G16720	HCF173 (high chlorophyll fluorescence phenotype 173); binding / catalytic/ transcription repressor				2,22				
AT5G52110	HCF208 (HIGH CHLOROPHYLL FLUORESCENCE 208)				1,99				
AT1G69740	HEMB1; catalytic/ metal ion binding / porphobilinogen synthase				1,91				
AT5G08280	HEMC (HYDROXYMETHYLBILANE SYNTHASE); hydroxymethylbilane synthase				1,61				
AT2G26540	HEMD; uroporphyrinogen-III synthase				1,53				
AT3G14930	HEME1; uroporphyrinogen decarboxylase				1,76				
AT2G40490	HEME2; uroporphyrinogen decarboxylase				1,51				
AT1G08550	NPQ1 (NON-PHOTOCHEMICAL QUENCHING 1); violaxanthin de-epoxidase				4,1			1,52	1,9
AT2G41680	NTRC (NADPH-DEPENDENT THIOREDOXIN REDUCTASE C); thioredoxin-disulfide reductase				1,71				
AT3G15840	PIFI (post-illumination chlorophyll fluorescence increase)	1,82	2,8		3,6				2,76
AT2G46820	PSI-P (PHOTOSYSTEM I P SUBUNIT); DNA binding				1,64				
AT2G38140	PSRP4 (PLASTID-SPECIFIC RIBOSOMAL PROTEIN 4); structural constituent of ribosome				1,61				
AT3G09210	PTAC13 (PLASTID TRANSCRIPTIONALLY ACTIVE13); transcription elongation regulator				1,83				
AT5G54180	PTAC15 (PLASTID TRANSCRIPTIONALLY ACTIVE15)				1,93				
AT1G80480	PTAC17 (PLASTID TRANSCRIPTIONALLY ACTIVE17)				1,54				
AT1G65260	PTAC4 (PLASTID TRANSCRIPTIONALLY ACTIVE4)				1,73				
AT4G13670	PTAC5 (PLASTID TRANSCRIPTIONALLY ACTIVE5); heat shock protein binding / unfolded protein binding				1,84				
AT1G21600	PTAC6 (PLASTID TRANSCRIPTIONALLY ACTIVE6)	1,64	1,87		1,67				
AT4G20010	PTAC9 (PLASTID TRANSCRIPTIONALLY ACTIVE 9); single-stranded DNA binding				1,66				
AT3G02150	PTF1 (PLASTID TRANSCRIPTION FACTOR 1); transcription factor				2,15				
AT1G14030	ribulose-1,5 bisphosphate carboxylase oxygenase large subunit N-methyltransferase, putative				1,6				
AT1G71500	Rieske (2Fe-2S) domain-containing protein				1,89				
AT5G52970	thylakoid lumen 15.0 kDa protein				2,15				
AT2G44920	thylakoid lumenal 15 kDa protein, chloroplast				2,3				
AT5G53490	thylakoid lumenal 17.4 kDa protein, chloroplast				2,54				
AT4G24930	thylakoid lumenal 17.9 kDa protein, chloroplast				2,23				
AT3G56650	thylakoid lumenal 20 kDa protein				1,9				
AT1G12250	thylakoid lumenal protein-related				2,01				
AT2G24820	TIC55 (TRANSLOCON AT THE INNER ENVELOPE MEMBRANE OF CHLOROPLASTS 55); 2 iron, 2 sulfur cluster binding / electron carrier/ oxidoreductase				1,68				
AT2G30950	VAR2 (VARIATED 2); ATP-dependent peptidase/ ATPase/ metallopeptidase/ zinc ion binding				1,64				

continued on next page

Table C.10 — continued from previous page

AGI code	Gene description	0,1 % sucrose				3 % sucrose			
		root		shoot		root		shoot	
		d_3/d_0	d_4/d_0	d_3/d_0	d_4/d_0	d_3/d_0	d_4/d_0	d_3/d_0	d_4/d_0
AT1G12520	ATCCS (COPPER CHAPERONE FOR SOD1); superoxide dismutase/ superoxide dismutase copper chaperone				3,04				
AT1G51110	plastid-lipid associated protein PAP / fibrillin family protein			1,59	2,64				
AT3G23400	plastid-lipid associated protein PAP / fibrillin family protein				1,57				
AT2G46910	plastid-lipid associated protein PAP / fibrillin family protein				1,74				
AT5G19940	plastid-lipid associated protein PAP-related / fibrillin-related				1,59				
AT1G58180	carbonic anhydrase family protein / carbonate dehydratase family protein				1,68				
AT1G14150	oxygen evolving enhancer 3 (PsbQ) family protein				2,44				
AT5G11450	oxygen-evolving complex-related				1,64				
AT3G55330	PPL1 (PsbP-like protein 1); calcium ion binding				1,89				
AT2G39470	PPL2 (PsbP-like protein 2); calcium ion binding				2,03				
AT1G68830	STN7 (Stt7 homolog STN7); kinase/ protein kinase				1,56				
AT3G27925	DEGP1 (DegP protease 1); serine-type endopeptidase/ serine-type peptidase				1,78				
AT4G18370	DEG5 (DEGP PROTEASE 5); catalytic/ serine-type endopeptidase/ serine-type peptidase				1,7				
AT5G39830	DEG8; peptidase/ serine-type peptidase				1,67				
AT1G50250	FTSH1 (FtsH protease 1); ATP-dependent peptidase/ ATPase/ metallopeptidase				1,73				
AT5G45390	CLPP4 (CLP PROTEASE P4); serine-type endopeptidase				1,51				
AT3G19170	ATPREP1 (PRESEQUENCE PROTEASE 1); metalloendopeptidase				2,06				
AT4G30580	ATS2; 1-acylglycerol-3-phosphate O-acyltransferase/ acyltransferase				1,7				
AT1G15980	NDF1 (NDH-DEPENDENT CYCLIC ELECTRON FLOW 1)				2,59				
AT1G64770	NDF2 (NDH-DEPENDENT CYCLIC ELECTRON FLOW 1); carbohydrate binding / catalytic				1,6				
AT1G45474	LHCA5; pigment binding				1,56				
AT1G19150	LHCA6; chlorophyll binding				1,51				
AT5G12130	PDE149 (PIGMENT DEFECTIVE 149)				1,6				
AT2G37220	29 kDa ribonucleoprotein, chloroplast, putative / RNA-binding protein cp29, putative				1,54				
AT3G15360	TRX-M4 (ARABIDOPSIS THIOREDOXIN M-TYPE 4); enzyme activator				1,94				
AT2G29650	PHT4;1; carbohydrate transmembrane transporter/ inorganic diphosphate transmembrane transporter/ inorganic phosphate transmembrane transporter/ organic anion transmembrane transporter/ sugar:hydrogen symporter				1,67				
AT1G10070	ATBCAT-2 (ARABIDOPSIS THALIANA BRANCHED-CHAIN AMINO ACID TRANSAMINASE 2); branched-chain-amino-acid transaminase/ catalytic				3,77				
AT5G57040	lactoylglutathione lyase family protein / glyoxalase I family protein				2,09				
AT1G80160	lactoylglutathione lyase family protein / glyoxalase I family protein			1,57	1,9				
AT1G15380	lactoylglutathione lyase family protein / glyoxalase I family protein				3,24				
AT5G15280	pentatricopeptide (PPR) repeat-containing protein				1,54				
AT5G04810	pentatricopeptide (PPR) repeat-containing protein				1,6				
AT3G04760	pentatricopeptide (PPR) repeat-containing protein				1,58				
AT2G17033	pentatricopeptide (PPR) repeat-containing protein				1,72				
AT1G02150	pentatricopeptide (PPR) repeat-containing protein				1,68				

continued on next page

Table C.10 – continued from previous page

AGI code	Gene description	0,1 % sucrose				3 % sucrose			
		root		shoot		root		shoot	
		d ³ /d ₀	d ⁴ /d ₀	d ³ /d ₀	d ⁴ /d ₀	d ³ /d ₀	d ⁴ /d ₀	d ³ /d ₀	d ⁴ /d ₀
AT5G10690	pentatricopeptide (PPR) repeat-containing protein / CBS domain-containing protein				2,06				
AT3G54040	photoassimilate-responsive protein-related	1,6	1,7		1,78				
AT1G05385	photosystem II 11 kDa protein-related				1,77				
AT4G02770	PSAD-1 (photosystem I subunit D-1)		2,05						
AT1G03130	PSAD-2 (photosystem I subunit D-2)								1,67
AT1G31330	PSAF (photosystem I subunit F)		1,79						
AT1G55670	PSAG (PHOTOSYSTEM I SUBUNIT G)	1,66	2,78						
AT3G16140	PSAH-1 (photosystem I subunit H-1)		1,63						
AT1G30380	PSAK (photosystem I subunit K)		2,18						
AT4G12800	PSAL (photosystem I subunit L)	1,54	2,11						
AT5G64040	PSAN; calmodulin binding		2,18						
AT1G08380	PSAO (photosystem I subunit O)	1,55	2,81						
AT4G28660	PSB28 (PHOTOSYSTEM II REACTION CENTER PSB28 PROTEIN)				1,69				
AT5G66570	PSBO1 (PS II OXYGEN-EVOLVING COMPLEX 1); oxygen evolving/ poly(U) binding	1,52	1,78						
AT3G50820	PSBO2 (PHOTOSYSTEM II SUBUNIT O-2); oxygen evolving/ poly(U) binding	1,88	2,55		1,67				
AT4G05180	PSBQ-2; calcium ion binding	1,56	1,94						
AT1G79040	PSBR (photosystem II subunit R)		1,89						
AT3G21055	PSBTN (photosystem II subunit T)	1,81	2,78						
AT2G30570	PSBW (PHOTOSYSTEM II REACTION CENTER W)		1,86						
AT5G06690	WCRKC1 (WCRKC THIOREDOXIN 1)		1,96		6,07				4,49
Photorespiration									
AT3G08860	alanine-glyoxylate aminotransferase, putative / beta-alanine-pyruvate aminotransferase, putative			1,56	13,4				
AT2G38400	AGT3 (ALANINE:GLYOXYLATE AMINOTRANSFERASE 3); alanine-glyoxylate transaminase/ catalytic/ pyridoxal phosphate binding / transaminase				3,12				
AT1G80380	phosphoribulokinase/uridine kinase-related				2,44				
Cell wall									
AT1G69530	ATEXPA1 (ARABIDOPSIS THALIANA EXPANSIN A1)	2,6	3,89						
AT1G20190	ATEXPA11 (ARABIDOPSIS THALIANA EXPANSIN 11)				4,35				
AT3G03220	ATEXPA13 (ARABIDOPSIS THALIANA EXPANSIN A13)				1,59				
AT2G03090	ATEXPA15 (ARABIDOPSIS THALIANA EXPANSIN A15)	1,73	2,4		1,78				
AT1G62980	ATEXPA18 (ARABIDOPSIS THALIANA EXPANSIN A18)	1,55	2,5						
AT2G39700	ATEXPA4 (ARABIDOPSIS THALIANA EXPANSIN A4)	1,73	2,14		2,3				
AT2G28950	ATEXPA6 (ARABIDOPSIS THALIANA EXPANSIN A6)	1,99	2,59		2,42				
AT1G12560	ATEXPA7 (ARABIDOPSIS THALIANA EXPANSIN A7)	1,66	2,18						
AT2G40610	ATEXPA8 (ARABIDOPSIS THALIANA EXPANSIN A8)	1,77	2,11	1,63	4,62				
AT2G20750	ATEXPB1 (ARABIDOPSIS THALIANA EXPANSIN B1)				6,08				

continued on next page

Table C.10 — continued from previous page

AGI code	Gene description	0,1 % sucrose				3 % sucrose			
		root		shoot		root		shoot	
		d_3/d_0	d_4/d_0	d_3/d_0	d_4/d_0	d_3/d_0	d_4/d_0	d_3/d_0	d_4/d_0
AT4G28250	ATEXPB3 (ARABIDOPSIS THALIANA EXPANSIN B3)	2,82	3,52		7,25				
AT2G37640	EXP3				5,15				
AT3G29030	EXPA5 (EXPANSIN A5)				5,87				
AT4G17030	ATEXLB1 (ARABIDOPSIS THALIANA EXPANSIN-LIKE B1)	1,72	2,11		4,01				
AT3G45970	ATEXLA1 (ARABIDOPSIS THALIANA EXPANSIN-LIKE A1)	3,49	3,01		4,08				1,55
AT3G45960	ATEXLA3 (arabidopsis thaliana expansin-like a3)	3,22	3,04						
AT1G76930	ATEXT4 (EXTENSIN 4); structural constituent of cell wall			2,03					
AT5G11210	ATGLR2.5; intracellular ligand-gated ion channel					4,85	7,07		
AT5G11180	ATGLR2.6; intracellular ligand-gated ion channel	1,58	1,51						
AT1G42540	ATGLR3.3; intracellular ligand-gated ion channel				1,86				
AT1G05200	ATGLR3.4; intracellular ligand-gated ion channel					2,71	2,31		
AT2G32390	ATGLR3.5 (GLUTAMATE RECEPTOR 3.5); intracellular ligand-gated ion channel				3,82				
AT4G38770	PRP4 (PROLINE-RICH PROTEIN 4)				3,07				
AT1G26250	proline-rich extensin, putative	3,92	5,03						
AT1G26240	proline-rich extensin-like family protein					4,6	7,11		
AT5G35190	proline-rich extensin-like family protein	1,6	3,11						
AT5G06640	proline-rich extensin-like family protein	1,73	2,23						
AT2G21140	ATPRP2 (PROLINE-RICH PROTEIN 2)				1,55				
AT1G54970	ATPRP1 (PROLINE-RICH PROTEIN 1); structural constituent of cell wall	1,75	2,92						
AT5G06630	proline-rich extensin-like family protein		2,01						
AT4G16140	proline-rich family protein				2,07				
AT2G16630	proline-rich family protein	1,73	2,06						
AT5G12880	proline-rich family protein			2,5	1,54				
AT5G07020	proline-rich family protein				2,06				
AT3G62680	PRP3 (PROLINE-RICH PROTEIN 3); structural constituent of cell wall				1,61				
AT5G55730	FLA1 (FASCICLIN-LIKE ARAB INOGALACTAN 1)				4,16				
AT5G60490	FLA12				3,23				
AT3G52370	FLA15 (FASCICLIN-LIKE ARABINOOGALACTAN PROTEIN 15 PRECURSOR)		2,11		4,45				
AT2G35860	FLA16 (FASCICLIN-LIKE ARABINOOGALACTAN PROTEIN 16 PRECURSOR)				3,72				
AT2G20520	FLA6 (FASCICLIN-LIKE ARABINOOGALACTAN 6)	1,52	2,59						
AT2G04780	FLA7 (FASCICLIN-LIKE ARABINOOGALACTAN 7)				1,96				
AT2G45470	FLA8 (FASCICLIN-LIKE ARABINOOGALACTAN PROTEIN 8)				2,08				
AT1G02205	CER1 (ECERIFERUM 1); octadecanal decarboxylase				4,8				
AT1G02205	CER1 (ECERIFERUM 1); octadecanal decarboxylase				8,08				
AT4G24510	CER2 (ECERIFERUM 2); transferase/ transferase, transferring acyl groups other than amino-acyl groups				1,59				
AT4G33790	CER4 (ECERIFERUM 4); fatty acyl-CoA reductase (alcohol-forming)/ oxidoreductase, acting on the CH-CH group of donors				4,81				
AT2G38010	ceramidase family protein				3,18				

continued on next page

Table C.10 – continued from previous page

AGI code	Gene description	0,1 % sucrose				3 % sucrose			
		root		shoot		root		shoot	
		d^3/d_0	d^4/d_0	d^3/d_0	d^4/d_0	d^3/d_0	d^4/d_0	d^3/d_0	d^4/d_0
AT5G37300	WSD1; diacylglycerol O-acyltransferase/ long-chain-alcohol O-fatty-acyltransferase				3,87				
AT2G28110	FRA8 (FRAGILE FIBER 8); glucuronosyltransferase/ transferase					1,65	1,62		2,33
AT5G17420	IRX3 (IRREGULAR XYLEM 3); cellulose synthase				1,88				
AT5G44030	CESA4 (CELLULOSE SYNTHASE A4); cellulose synthase/ transferase, transferring glycosyl groups		1,56		2,06				
AT5G09870	CESA5 (CELLULOSE SYNTHASE 5); cellulose synthase/ transferase, transferring glycosyl groups				1,82				
AT1G24070	ATCSLA10; cellulose synthase/ transferase, transferring glycosyl groups				1,74				
AT5G16190	ATCSLA11; cellulose synthase/ transferase, transferring glycosyl groups				1,54				
AT1G55850	ATCSLE1; cellulose synthase/ transferase, transferring glycosyl groups					1,9	2,48		
AT4G23990	ATCSLG3; cellulose synthase/ transferase/ transferase, transferring glycosyl groups				2,61				
AT5G22740	ATCSLA02; mannan synthase/ transferase, transferring glycosyl groups				2,56				
AT3G28180	ATCSLC04 (CELLULOSE-SYNTHASE LIKE C4); cellulose synthase/ transferase, transferring glycosyl groups	1,71			1,65				
AT4G31590	ATCSLC5 (CELLULOSE-SYNTHASE LIKE C5); cellulose synthase/ transferase, transferring glycosyl groups				2,14				
AT5G16910	CSLD2 (CELLULOSE-SYNTHASE LIKE D2); cellulose synthase/ transferase, transferring glycosyl groups				1,62				
AT3G56000	ATCSLA14; cellulose synthase/ transferase, transferring glycosyl groups				1,59				
AT2G32620	ATCSLB02; cellulose synthase/ transferase/ transferase, transferring glycosyl groups		1,54						
AT2G35650	ATCSLA07 (CELLULOSE SYNTHASE LIKE); mannan synthase/ transferase, transferring glycosyl groups				1,63				
AT5G03760	ATCSLA09; mannan synthase/ transferase, transferring glycosyl groups				5,74				
AT3G10710	pectinesterase family protein	1,66	2,41						
AT2G45220	pectinesterase family protein			4,17	2,05	2,33	2,21		
AT5G47500	pectinesterase family protein				2,33				
AT5G09760	pectinesterase family protein				2,2				
AT3G59010	pectinesterase family protein				5,46				
AT3G49220	pectinesterase family protein				2,23				
AT1G11580	PMEPCRA (METHYLESTERASE PCR A); enzyme inhibitor/ pectinesterase			1,79	3,05				
AT5G53370	PMEPCRF (PECTIN METHYLESTERASE PCR FRAGMENT F); pectinesterase				2,11				
AT4G02330	ATPMEPCRB; pectinesterase			2,04					
AT2G43050	ATPMEPCRD; enzyme inhibitor/ pectinesterase				2,4				
AT1G02810	pectinesterase family protein	2,79	2,31						
AT2G47550	pectinesterase family protein					1,68	1,71		
AT3G10720	pectinesterase, putative	1,58	1,5		2,15				
AT2G26440	pectinesterase family protein				4,2				
AT1G53840	ATPME1; pectinesterase						1,56		
AT1G67750	pectate lyase family protein				7,53				
AT5G63180	pectate lyase family protein				4,56				
AT5G48900	pectate lyase family protein				2,97				
AT3G53190	pectate lyase family protein				2,48				
AT4G24780	pectate lyase family protein	1,69	2,03		4,48				
AT3G27400	pectate lyase family protein				4,12				

continued on next page

Table C.10 — continued from previous page

AGI code	Gene description	0,1 % sucrose				3 % sucrose			
		root		shoot		root		shoot	
		d ₃ /d ₀	d ₄ /d ₀	d ₃ /d ₀	d ₄ /d ₀	d ₃ /d ₀	d ₄ /d ₀	d ₃ /d ₀	d ₄ /d ₀
AT3G07010	pectate lyase family protein				3,01				
AT1G04680	pectate lyase family protein				3,05				
AT4G19420	pectinacetyltransferase family protein			1,51	2,62				
AT3G09410	pectinacetyltransferase family protein	3,87	4,16						
AT5G04960	pectinesterase family protein		2,21						
AT1G10640	polygalacturonase				3,72				
AT1G60590	polygalacturonase, putative / pectinase, putative				3,18				
AT4G30290	XTH19 (XYLOGLUCAN ENDOTRANGLUCOSYLASE/HYDROLASE 19); hydrolase, acting on glycosyl bonds / hydrolase, hydrolyzing O-glycosyl compounds / xyloglucan:xyloglucosyl transferase				3,4				
AT1G11545	xyloglucan:xyloglucosyl transferase, putative / xyloglucan endotransglycosylase, putative / endo-xyloglucan transferase, putative				2,74				
AT2G36870	xyloglucan:xyloglucosyl transferase, putative / xyloglucan endotransglycosylase, putative / endo-xyloglucan transferase, putative				4,32				
AT4G03210	XTH9 (XYLOGLUCAN ENDOTRANGLUCOSYLASE/HYDROLASE 9); hydrolase, acting on glycosyl bonds / xyloglucan:xyloglucosyl transferase				1,69				
AT5G48070	XTH20 (XYLOGLUCAN ENDOTRANGLUCOSYLASE/HYDROLASE 20); hydrolase, acting on glycosyl bonds / hydrolase, hydrolyzing O-glycosyl compounds / xyloglucan:xyloglucosyl transferase	2,22	1,88						
AT3G48580	xyloglucan:xyloglucosyl transferase, putative / xyloglucan endotransglycosylase, putative / endo-xyloglucan transferase, putative	1,72	1,69	4,31					
AT1G10550	XTH33; hydrolase, acting on glycosyl bonds / hydrolase, hydrolyzing O-glycosyl compounds / xyloglucan:xyloglucosyl transferase				3,07				
AT3G44990	XTR8 (XYLOGLUCAN ENDO-TRANGLUCOSYLASE-RELATED 8); hydrolase, acting on glycosyl bonds / xyloglucan:xyloglucosyl transferase	2,67	3,44		4,7				
AT4G25820	XTR9 (XYLOGLUCAN ENDOTRANGLUCOSYLASE 9); hydrolase, acting on glycosyl bonds / hydrolase, hydrolyzing O-glycosyl compounds / xyloglucan:xyloglucosyl transferase				2,18				
AT5G57540	xyloglucan:xyloglucosyl transferase, putative / xyloglucan endotransglycosylase, putative / endo-xyloglucan transferase, putative				1,89				
AT4G28850	xyloglucan:xyloglucosyl transferase, putative / xyloglucan endotransglycosylase, putative / endo-xyloglucan transferase, putative				2,19	2,33	3,6		
AT1G65310	XTH17 (XYLOGLUCAN ENDOTRANGLUCOSYLASE/HYDROLASE 17); hydrolase, acting on glycosyl bonds / hydrolase, hydrolyzing O-glycosyl compounds / xyloglucan:xyloglucosyl transferase	2,68	2,21		3,36				
AT1G32170	XTR4 (XYLOGLUCAN ENDOTRANGLUCOSYLASE 4); hydrolase, acting on glycosyl bonds / hydrolase, hydrolyzing O-glycosyl compounds / xyloglucan:xyloglucosyl transferase				1,75	1,82			
AT4G25810	XTR6 (XYLOGLUCAN ENDOTRANGLUCOSYLASE 6); hydrolase, acting on glycosyl bonds / hydrolase, hydrolyzing O-glycosyl compounds / xyloglucan:xyloglucosyl transferase	2,85	1,93	2,5	3,15			2,39	2,97
AT4G14130	XTR7 (XYLOGLUCAN ENDOTRANGLUCOSYLASE 7); hydrolase, acting on glycosyl bonds / hydrolase, hydrolyzing O-glycosyl compounds / xyloglucan:xyloglucosyl transferase	2,54	2,63		3,44				1,65
AT4G30270	MER15B (meristem-5); hydrolase, acting on glycosyl bonds / xyloglucan:xyloglucosyl transferase	1,94	1,95		1,87				

continued on next page

Table C.10 — continued from previous page

AGI code	Gene description	0,1 % sucrose				3 % sucrose			
		root		shoot		root		shoot	
		d ³ /d ₀	d ⁴ /d ₀	d ³ /d ₀	d ⁴ /d ₀	d ³ /d ₀	d ⁴ /d ₀	d ³ /d ₀	d ⁴ /d ₀
AT4G30280	XTH18 (XYLOGLUCAN ENDOTRANSGLUCOSYLASE/HYDROLASE 18); hydrolase, acting on glycosyl bonds / hydrolase, hydrolyzing O-glycosyl compounds / xyloglucan:xyloglucosyl transferase				3,55				
AT5G57550	XTR3 (XYLOGLUCAN ENDOTRANSGLYCOSYLASE 3); hydrolase, acting on glycosyl bonds / xyloglucan:xyloglucosyl transferase				3,9				
Proteolysis									
AT5G07030	aspartic-type endopeptidase	2,15	2,4		4,91				
AT3G61820	aspartyl protease family protein	2,19	2,7		2,76				
AT3G12700	aspartyl protease family protein			3,95					
AT3G18490	aspartyl protease family protein				2,23				
AT4G04460	aspartyl protease family protein			1,93	1,91				
AT5G48430	aspartic-type endopeptidase	1,58	1,74		3,42				
AT5G19120	aspartic-type endopeptidase								1,68
AT4G33490	aspartic-type endopeptidase				2,14				1,77
AT3G59080	aspartyl protease family protein				2,35				
AT4G16563	aspartyl protease family protein				5,23				
AT5G37540	aspartyl protease family protein	2,48	2,42						
AT1G01300	aspartyl protease family protein							1,57	
AT2G39710	aspartyl protease family protein				1,91				
AT1G62290	aspartyl protease family protein			1,64					
AT4G01610	cathepsin B-like cysteine protease, putative			1,66	2,57				
AT1G02305	cathepsin B-like cysteine protease, putative				1,8				
AT5G43060	cysteine proteinase, putative / thiol protease, putative			1,61					
AT5G50260	cysteine proteinase, putative					2,15	2,36		
AT3G45310	cysteine proteinase, putative				1,57				
AT3G43960	cysteine proteinase, putative				2,72				
AT2G27420	cysteine proteinase, putative			1,74	3,32				
AT4G36880	CP1 (CYSTEINE PROTEINASE1); cysteine-type endopeptidase/ cysteine-type peptidase	14,09	20,03						
AT3G19390	cysteine proteinase, putative / thiol protease, putative				4,06				
AT1G70170	MMP (MATRIX METALLOPROTEINASE); metalloendopeptidase/ metallopeptidase	1,53	2,2						
AT5G51540	metalloendopeptidase				1,82				
AT5G05740	EGY2; metalloendopeptidase				1,85				
AT5G42390	metalloendopeptidase				1,77				
AT5G04200	AtMC9 (metacaspase 9); cysteine-type peptidase				2,28				
AT4G25110	AtMC2 (metacaspase 2); cysteine-type endopeptidase				2,21				
AT2G45270	glycoprotease M22 family protein				1,64				
AT5G47040	LON2 (LON PROTEASE 2); ATP binding / ATP-dependent peptidase/ nucleoside-triphosphatase/ nucleotide binding / serine-type endopeptidase/ serine-type peptidase				1,69				

continued on next page

Table C.10 — continued from previous page

AGI code	Gene description	0,1 % sucrose				3 % sucrose			
		root		shoot		root		shoot	
		d_3/d_0	d_4/d_0	d_3/d_0	d_4/d_0	d_3/d_0	d_4/d_0	d_3/d_0	d_4/d_0
AT1G13270	MAP1C (METHIONINE AMINOPEPTIDASE 1B); aminopeptidase/ metalloexopeptidase				1,53				
AT4G37040	MAP1D (METHIONINE AMINOPEPTIDASE 1D); aminopeptidase/ metalloexopeptidase				1,69				
AT2G04160	AIR3; serine-type endopeptidase			2,71					
AT4G34980	SLP2; serine-type peptidase				2,71				
AT4G12910	scpl20 (serine carboxypeptidase-like 20); serine-type carboxypeptidase				3,03				
AT3G02110	scpl25 (serine carboxypeptidase-like 25); serine-type carboxypeptidase				1,53				
AT3G07990	SCPL27 (serine carboxypeptidase-like 27); serine-type carboxypeptidase				2,12				
AT1G11080	scpl31 (serine carboxypeptidase-like 31); serine-type carboxypeptidase	2,36	4,24		3,26				
AT5G08260	scpl35 (serine carboxypeptidase-like 35); serine-type carboxypeptidase				3,81				
AT3G63470	scpl40 (serine carboxypeptidase-like 40); serine-type carboxypeptidase				1,71				
AT3G45010	scpl48 (serine carboxypeptidase-like 48); serine-type carboxypeptidase				1,96				
AT2G27920	SCPL51 (SERINE CARBOXYPEPTIDASE-LIKE 51); serine-type carboxypeptidase							1,65	
AT2G39850	identical protein binding / serine-type endopeptidase				3,51				
AT5G23210	SCPL34; serine-type carboxypeptidase	1,87	1,8						
AT2G22980	serine-type carboxypeptidase	3,49	4,01		2,49				
AT2G35780	scpl26 (serine carboxypeptidase-like 26); serine-type carboxypeptidase				1,55				
AT5G42240	scpl42 (serine carboxypeptidase-like 42); serine-type carboxypeptidase				1,71				
AT5G24260	prolyl oligopeptidase family protein				1,89				
AT1G32960	SBT3.3; identical protein binding / serine-type endopeptidase	2,34	2,41						
AT4G10510	subtilase family protein					2,72	3,47		
AT4G21326	ATSBT3.12 (SUBTILASE 3.12); identical protein binding / serine-type endopeptidase				1,88				
AT1G01900	SBTI1.1; serine-type endopeptidase				3,56				
AT5G45650	subtilase family protein				6,13				
AT5G44530	subtilase family protein				1,9				
AT4G30020	subtilase family protein				4				
AT4G21650	subtilase family protein				15,14				
AT3G14067	subtilase family protein				1,8				
AT2G05920	subtilase family protein				1,63				
AT5G51750	ATSBT1.3 (ARABIDOPSIS THALIANA SUBTILASE 1.3); identical protein binding / serine-type endopeptidase					2,24	2,21		
AT4G20430	subtilase family protein				1,53				
AT5G59090	ATSBT4.12; identical protein binding / serine-type endopeptidase				2,27				
AT4G35350	XCP1 (XYLEM CYSTEINE PEPTIDASE 1); cysteine-type endopeptidase/ cysteine-type peptidase				2,92				
AT1G20850	XCP2 (xylem cysteine peptidase 2); cysteine-type peptidase/ peptidase				2,01				
Amino acids									
AT5G49630	AAP6 (AMINO ACID PERMEASE 6); acidic amino acid transmembrane transporter/ amino acid transmembrane transporter/ neutral amino acid transmembrane transporter	1,8	2,09		3,98				2,1
AT1G77380	AAP3; amino acid transmembrane transporter				2,13				

continued on next page

Table C.10 – continued from previous page

AGI code	Gene description	0,1 % sucrose				3 % sucrose			
		root		shoot		root		shoot	
		d ³ /d ₀	d ⁴ /d ₀	d ³ /d ₀	d ⁴ /d ₀	d ³ /d ₀	d ⁴ /d ₀	d ³ /d ₀	d ⁴ /d ₀
AT5G65990	amino acid transporter family protein								1,8
AT3G56200	amino acid transporter family protein			2,07	4,17				
AT3G28960	amino acid transporter family protein				1,6				
AT1G47670	amino acid transporter family protein				1,55				
AT2G39130	amino acid transporter family protein				1,77				
AT2G41190	amino acid transporter family protein				2,4				
AT2G40420	amino acid transporter family protein				2,05				
AT5G36940	CAT3 (CATIONIC AMINO ACID TRANSPORTER 3); basic amino acid transmembrane transporter/ cationic amino acid transmembrane transporter				1,67				
AT5G04770	CAT6 (CATIONIC AMINO ACID TRANSPORTER 6); amino acid transmembrane transporter/ basic amino acid transmembrane transporter/ cationic amino acid transmembrane transporter				5,14				
AT5G40780	LHT1; amino acid transmembrane transporter			1,56	1,51				
AT4G25760	AtGDU2 (Arabidopsis thaliana GLUTAMINE DUMPER 2)				1,86				
AT2G24762	AtGDU4 (Arabidopsis thaliana GLUTAMINE DUMPER 4)				5,53				
AT3G47340	ASN1 (GLUTAMINE-DEPENDENT ASPARAGINE SYNTHASE 1); asparagine synthase (glutamine-hydrolyzing)				5,59				
AT5G65010	ASN2 (ASPARAGINE SYNTHETASE 2); asparagine synthase (glutamine-hydrolyzing)				2,26				1,81
AT2G30970	ASP1 (ASPARTATE AMINOTRANSFERASE 1); L-aspartate:2-oxoglutarate aminotransferase			1,62	1,53				
AT5G19550	ASP2 (ASPARTATE AMINOTRANSFERASE 2); L-aspartate:2-oxoglutarate aminotransferase			1,55	1,83				
AT1G62800	ASP4 (ASPARTATE AMINOTRANSFERASE 4); catalytic/ pyridoxal phosphate binding / transaminase/ transferase, transferring nitrogenous groups			1,53	8,18				
AT3G16150	L-asparaginase, putative / L-asparagine amidohydrolase, putative	1,82	1,78						
AT1G31230	AK-HSDH I (ASPARTATE KINASE-HOMOSERINE DEHYDROGENASE I); aspartate kinase/ homoserine dehydrogenase		1,8		2,15				
AT3G17820	ATGSKB6; copper ion binding / glutamate-ammonia ligase				2,68				
AT5G37600	ATGSR1; copper ion binding / glutamate-ammonia ligase			1,9	1,92				1,6
AT1G66200	ATGSR2; copper ion binding / glutamate-ammonia ligase	1,55	1,95						
AT1G65960	GAD2 (GLUTAMATE DECARBOXYLASE 2); calmodulin binding / glutamate decarboxylase				1,53				
AT2G02000	glutamate decarboxylase 3 (GAD3); FUNCTIONS IN: calmodulin binding; INVOLVED IN: carboxylic acid metabolic process, glutamate	2,61	2,29		2,67				
AT5G17330	GAD; calmodulin binding / glutamate decarboxylase			1,78					
AT5G07440	GDH2 (GLUTAMATE DEHYDROGENASE 2); ATP binding / glutamate dehydrogenase [NAD(P)+]/ glutamate dehydrogenase/ oxidoreductase			1,55	2,59			1,96	1,86
AT5G18170	GDH1 (GLUTAMATE DEHYDROGENASE 1); ATP binding / glutamate dehydrogenase [NAD(P)+]/ oxidoreductase				1,73				
AT5G04140	GLU1 (GLUTAMATE SYNTHASE 1); glutamate synthase (ferredoxin)				2,13				
AT1G15040	glutamine amidotransferase-related	1,5		1,63	5,55	3,62	4,19		
AT3G19710	BCAT4 (BRANCHED-CHAIN AMINOTRANSFERASE4); catalytic/ methionine-oxo-acid transaminase	2,48	3,75	1,53	3,72				

continued on next page

Table C.10 – continued from previous page

AGI code	Gene description	0,1 % sucrose				3 % sucrose			
		root		shoot		root		shoot	
		d^3/d_0	d^4/d_0	d^3/d_0	d^4/d_0	d^3/d_0	d^4/d_0	d^3/d_0	d^4/d_0
AT1G50110	branched-chain amino acid aminotransferase 6 / branched-chain amino acid transaminase 6 (BCAT6)				2,2				
AT1G10060	branched-chain amino acid aminotransferase 1 / branched-chain amino acid transaminase 1 (BCAT1)				2,17				1,93
AT1G11790	ADT1 (arogenate dehydratase 1); arogenate dehydratase/ prephenate dehydratase	1,52							
AT3G44720	ADT4 (arogenate dehydratase 4); arogenate dehydratase/ prephenate dehydratase	1,97	2,46						
AT5G22630	ADT5 (arogenate dehydratase 5); arogenate dehydratase/ prephenate dehydratase				2,05				
AT1G08250	ADT6 (arogenate dehydratase 6); arogenate dehydratase/ prephenate dehydratase				1,88				
AT1G64660	ATMGL (ARABIDOPSIS THALIANA METHIONINE GAMMA-LYASE); catalytic/ methionine gamma-lyase				2,17				
AT3G13110	ATSERAT2;2 (SERINE ACETYLTRANSFERASE 2;2); serine O-acetyltransferase				2,43				
AT3G59760	OASC (O-ACETYLSELINE (THIOL) LYASE ISOFORM C); ATP binding / cysteine synthase			1,64	2,6				
AT5G46180	delta-OAT; ornithine-oxo-acid transaminase				1,58				
AT5G46180	delta-OAT; ornithine-oxo-acid transaminase				1,58				
AT2G39800	P5CS: encodes a delta1-pyrroline-5-carboxylate synthase that catalyzes the rate-limiting enzyme in the biosynthesis of proline. Gene is expressed in reproductive organs and tissues under non-stress conditions but in the whole plant under water-limiting condition. Expression is also induced by abscisic acid and salt stress in a light-dependent manner. P5CS1 appears to be involved in salt stress responses related to proline accumulation, including protection from reactive oxidative species. P5CS1 appears to be present in different cells and/or different subcellular locations from P5CS2 in a tissue-dependent manner.				1,51				
AT5G38710	proline oxidase, putative / osmotic stress-responsive proline dehydrogenase, putative	2,09	2,22						
AT3G25900	HMT-1; homocysteine S-methyltransferase	1,76	1,96						
AT3G22740	HMT3; homocysteine S-methyltransferase	1,97	2,15	1,98	6,93				
AT4G14910	imidazoleglycerol-phosphate dehydratase, putative				1,51				
AT4G35630	PSAT; O-phospho-L-serine:2-oxoglutarate aminotransferase				2,12	2,35			
AT1G17745	PGDH (3-PHOSPHOGLYCERATE DEHYDROGENASE); phosphoglycerate dehydrogenase	1,87	2,17	3,65	17,59				
AT3G19480	D-3-phosphoglycerate dehydrogenase, putative / 3-PGDH, putative				2,34				
AT1G36370	SHM7 (serine hydroxymethyltransferase 7); catalytic/ glycine hydroxymethyltransferase/ pyridoxal phosphate binding				3,96			1,65	1,55
AT2G35120	glycine cleavage system H protein, mitochondrial, putative				1,89				
AT4G37930	SHM1 (SERINE TRANSHYDROXYMETHYLTRANSFERASE 1); glycine hydroxymethyltransferase/ poly(U) binding				2,27				
AT1G72810	threonine synthase, putative				2,67				
AT3G04520	THA2 (Threonine Aldolase 2); threonine aldolase			1,52	1,68				
AT1G08630	THA1 (Threonine Aldolase 1); aldehyde-lyase/ threonine aldolase				8,78				
AT2G20340	tyrosine decarboxylase, putative				1,9				
AT4G03960	tyrosine specific protein phosphatase family protein				2,69				
AT2G24850	TAT3 (TYROSINE AMINOTRANSFERASE 3); L-tyrosine:2-oxoglutarate aminotransferase/ transaminase				1,99				
AT4G34030	MCCB (3-METHYLCROTONYL-COA CARBOXYLASE); biotin carboxylase/ methylcrotonoyl-CoA carboxylase				2,32				
AT1G03090	MCCA; methylcrotonoyl-CoA carboxylase				3,74				

continued on next page

Table C.10 – continued from previous page

AGI code	Gene description	0,1 % sucrose				3 % sucrose			
		root		shoot		root		shoot	
		d ³ /d ₀	d ⁴ /d ₀	d ³ /d ₀	d ⁴ /d ₀	d ³ /d ₀	d ⁴ /d ₀	d ³ /d ₀	d ⁴ /d ₀
AT3G45300	IVD (ISOVALERYL-COA-DEHYDROGENASE); ATP binding / isovaleryl-CoA dehydrogenase				3,36				
Detoxification									
AT1G11840	ATGLX1 (GLYOXALASE I HOMOLOG); lactoylglutathione lyase/ metal ion binding			1,73	2,87				
AT5G22300	NIT4 (NITRILASE 4); 3-cyanoalanine hydratase/ cyanoalanine nitrilase/ indole-3-acetonitrile nitrilase/ nitrilase/ nitrile hydratase	2,12	2,28			3,83	5,63		
AT3G03190	ATGSTF11 (GLUTATHIONE S-TRANSFERASE F11); glutathione transferase				4,22				
AT2G30860	ATGSTF9 (GLUTATHIONE S-TRANSFERASE PHI 9); copper ion binding / glutathione binding / glutathione peroxidase/ glutathione transferase			1,61	2,26				
AT1G69920	ATGSTU12 (GLUTATHIONE S-TRANSFERASE TAU 12); glutathione transferase	6,59	5,25			7,36	10,13		
AT1G27130	ATGSTU13 (ARABIDOPSIS THALIANA GLUTATHIONE S-TRANSFERASE TAU 13); glutathione transferase				2,47				
AT1G78370	ATGSTU20 (GLUTATHIONE S-TRANSFERASE TAU 20); glutathione transferase	4,41	10,76	2,01	5,98				
AT1G78320	ATGSTU23 (GLUTATHIONE S-TRANSFERASE TAU 23); glutathione transferase				2,06				
AT1G17170	ATGSTU24 (GLUTATHIONE S-TRANSFERASE TAU 24); glutathione binding / glutathione transferase	2,02	2,31						
AT1G17180	ATGSTU25 (GLUTATHIONE S-TRANSFERASE TAU 25); glutathione transferase	4,06	5,07			4,45	6,19		
AT3G43800	ATGSTU27 (GLUTATHIONE S-TRANSFERASE TAU 27); glutathione transferase			1,58	2,23				
AT2G29460	ATGSTU4 (ARABIDOPSIS THALIANA GLUTATHIONE S-TRANSFERASE TAU 4); glutathione transferase	4,26	5,33						
AT2G29440	ATGSTU6 (ARABIDOPSIS THALIANA GLUTATHIONE S-TRANSFERASE TAU 6); glutathione transferase	1,95	2,46		2				
AT5G62480	ATGSTU9 (ARABIDOPSIS THALIANA GLUTATHIONE S-TRANSFERASE TAU 9); glutathione transferase					1,51	2,13		
AT4G23100	GSH1 (GLUTAMATE-CYSTEINE LIGASE); glutamate-cysteine ligase			1,76	1,69				
AT2G30870	GSTF10 (HALIANA GLUTATHIONE S-TRANSFERASE PHI 10); copper ion binding / glutathione binding / glutathione transferase			1,59	1,74				
AT1G74590	GSTU10 (GLUTATHIONE S-TRANSFERASE TAU 10); glutathione transferase	2,75	3,81			3,41	4,11		
AT5G17220	ATGSTF12 (ARABIDOPSIS THALIANA GLUTATHIONE S-TRANSFERASE PHI 12); glutathione transferase							1,51	1,76
AT2G29420	ATGSTU7 (ARABIDOPSIS THALIANA GLUTATHIONE S-TRANSFERASE TAU 7); glutathione transferase				1,52				
AT3G09270	ATGSTU8 (GLUTATHIONE S-TRANSFERASE TAU 8); glutathione transferase				2,01				
AT2G25080	ATGPX1 (GLUTATHIONE PEROXIDASE 1); glutathione peroxidase				1,95				
AT4G11600	ATGPX6 (GLUTATHIONE PEROXIDASE 6); glutathione peroxidase				1,72				
AT4G31870	ATGPX7 (glutathione peroxidase 7); glutathione peroxidase				2,07				
AT3G24170	ATGR1 (glutathione-disulfide reductase); FAD binding / NADP or NADPH binding / glutathione-disulfide reductase/ oxidoreductase	1,98	2,87		1,99				
P450									
AT3G20120	CYP705A21; electron carrier/ heme binding / iron ion binding / monooxygenase/ oxygen binding				1,65				
AT5G47990	CYP705A5; oxygen binding / thalian-diol desaturase	1,85	1,7						
AT1G78490	CYP708A3; electron carrier/ heme binding / iron ion binding / monooxygenase/ oxygen binding				3,16				
AT2G30750	CYP71A12 (cytochrome P450, family 71, subfamily A, polypeptide 12); electron carrier/ heme binding / iron ion binding / monooxygenase/ oxygen binding	98,17	121,33			28,5	31,94	3,28	3,68

continued on next page

Table C.10 – continued from previous page

AGI code	Gene description	0,1 % sucrose				3 % sucrose			
		root		shoot		root		shoot	
		d ₃ /d ₀	d ₄ /d ₀	d ₃ /d ₀	d ₄ /d ₀	d ₃ /d ₀	d ₄ /d ₀	d ₃ /d ₀	d ₄ /d ₀
AT2G30770	CYP71A13 (cytochrome P450, family 71, subfamily A, polypeptide 13); indoleacetaldoxime dehydratase/ oxygen binding	1,67	2,6			6,84	13,1		
AT1G13080	CYP71B2 (CYTOCHROME P450 71B2); electron carrier/ heme binding / iron ion binding / monooxygenase/ oxygen binding				1,57				
AT3G26200	CYP71B22; electron carrier/ heme binding / iron ion binding / monooxygenase/ oxygen binding				3,12				
AT1G13090	CYP71B28; electron carrier/ heme binding / iron ion binding / monooxygenase/ oxygen binding				2,35				
AT2G24180	CYP71B6 (CYTOCHROME P450 71B6); electron carrier/ heme binding / iron ion binding / monooxygenase/ oxygen binding	2,13	2,57						
AT3G14680	CYP72A14; electron carrier/ heme binding / iron ion binding / monooxygenase/ oxygen binding				1,59				
AT3G14620	CYP72A8; electron carrier/ heme binding / iron ion binding / monooxygenase/ oxygen binding	1,58	1,78			1,51	5,45	6,73	
AT3G10570	CYP77A6; electron carrier/ heme binding / iron ion binding / monooxygenase/ oxygen binding					2,54			
AT5G67310	CYP81G1; electron carrier/ heme binding / iron ion binding / monooxygenase/ oxygen binding				1,67				
AT4G37310	CYP81H1; electron carrier/ heme binding / iron ion binding / monooxygenase/ oxygen binding	1,93	2,34						
AT4G31970	CYP82C2; electron carrier/ heme binding / iron ion binding / monooxygenase/ oxygen binding	132,99	196,51	1,93		71,24	140,39		
AT1G01600	CYP86A4; fatty acid (omega-1)-hydroxylase/ oxygen binding								2,7
AT1G63710	CYP86A7; fatty acid (omega-1)-hydroxylase/ oxygen binding								1,65
AT4G39510	CYP96A12; electron carrier/ heme binding / iron ion binding / monooxygenase/ oxygen binding								3,83
AT5G52320	CYP96A4; electron carrier/ heme binding / iron ion binding / monooxygenase/ oxygen binding								7,55
AT4G39480	CYP96A9 (CYTOCHROME P450 96 A9); electron carrier/ heme binding / iron ion binding / monooxygenase/ oxygen binding								3,39
AT5G36220	CYP81D1 (CYTOCHROME P450 81D1); electron carrier/ heme binding / iron ion binding / monooxygenase/ oxygen binding				1,77	3,14	3,88		
AT4G37370	CYP81D8; electron carrier/ heme binding / iron ion binding / monooxygenase/ oxygen binding	2,38	2,69	1,72	2,43	5,3	9,18	3,1	3,9
AT3G26210	CYP71B23; electron carrier/ heme binding / iron ion binding / monooxygenase/ oxygen binding				1,5			1,84	1,93
AT4G31940	CYP82C4; electron carrier/ heme binding / iron ion binding / monooxygenase/ oxygen binding	2,23							
AT1G64900	CYP89A2 (CYTOCHROME P450 89A2); electron carrier/ heme binding / iron ion binding / monooxygenase/ oxygen binding				1,82				
AT3G03470	CYP89A9; electron carrier/ heme binding / iron ion binding / monooxygenase/ oxygen binding	1,66	2,28						
AT3G48520	CYP94B3; electron carrier/ heme binding / iron ion binding / monooxygenase/ oxygen binding	2,86	3,43	3,55	5,39				
AT1G34540	CYP94D1; electron carrier/ heme binding / iron ion binding / monooxygenase/ oxygen binding					1,51			
AT1G31800	CYP97A3 (CYTOCHROME P450-TYPE MONOOXYGENASE 97A3); carotene beta-ring hydroxylase/ oxygen binding				1,53				
AT4G15110	CYP97B3; electron carrier/ heme binding / iron ion binding / monooxygenase/ oxygen binding				1,64				
AT4G27710	CYP709B3; electron carrier/ heme binding / iron ion binding / monooxygenase/ oxygen binding		1,61		2,16				
AT3G26290	CYP71B26; electron carrier/ heme binding / iron ion binding / monooxygenase/ oxygen binding				1,57				
AT3G26320	CYP71B36; electron carrier/ heme binding / iron ion binding / monooxygenase/ oxygen binding				3,42				
AT3G26280	CYP71B4; electron carrier/ heme binding / iron ion binding / monooxygenase/ oxygen binding				1,52				
AT3G14660	CYP72A13; electron carrier/ heme binding / iron ion binding / monooxygenase/ oxygen binding	1,52	1,93		1,7				

continued on next page

Table C.10 – continued from previous page

AGI code	Gene description	0,1 % sucrose				3 % sucrose			
		root		shoot		root		shoot	
		d ³ /d ₀	d ⁴ /d ₀	d ³ /d ₀	d ⁴ /d ₀	d ³ /d ₀	d ⁴ /d ₀	d ³ /d ₀	d ⁴ /d ₀
AT3G14690	CYP72A15; electron carrier/ heme binding / iron ion binding / monooxygenase/ oxygen binding				1,59				
AT1G67110	CYP735A2; electron carrier/ heme binding / iron ion binding / monooxygenase/ oxygen binding					2,27	2,51		
AT2G45560	CYP76C1; electron carrier/ heme binding / iron ion binding / monooxygenase				3,9				
AT1G13710	CYP78A5; electron carrier/ heme binding / iron ion binding / monooxygenase/ oxygen binding			1,96	2,55				
Secondary metabolites/glucosinolates									
AT1G65860	FMO GS-OX1 (FLAVIN-MONOOXYGENASE GLUCOSINOLATE S-OXYGENASE 1); 3-methylthiopropyl glucosinolate S-oxygenase/ 4-methylthiopropyl glucosinolate S-oxygenase/ 5-methylthiopropyl glucosinolate S-oxygenase/ 6-methylthiopropyl glucosinolate S-oxygenase/ 7-methyl				4,68				
AT1G62540	FMO GS-OX2 (FLAVIN-MONOOXYGENASE GLUCOSINOLATE S-OXYGENASE 2); 3-methylthiopropyl glucosinolate S-oxygenase/ 4-methylthiopropyl glucosinolate S-oxygenase/ 5-methylthiopropyl glucosinolate S-oxygenase/ 7-methylthiopropyl glucosinolate S-oxygenase/ 8-methyl				3,86				
AT1G62560	FMO GS-OX3 (FLAVIN-MONOOXYGENASE GLUCOSINOLATE S-OXYGENASE 3); 3-methylthiopropyl glucosinolate S-oxygenase/ 4-methylthiopropyl glucosinolate S-oxygenase/ 5-methylthiopropyl glucosinolate S-oxygenase/ 6-methylthiopropyl glucosinolate S-oxygenase/ 7-methyl		1,93	2,07	10,46				
AT1G62570	FMO GS-OX4 (FLAVIN-MONOOXYGENASE GLUCOSINOLATE S-OXYGENASE 4); 4-methylthiopropyl glucosinolate S-oxygenase/ 8-methylthiopropyl glucosinolate S-oxygenase/ flavin-containing monooxygenase/ monooxygenase	1,72	2,25						
AT5G23020	IMS2 (2-ISOPROPYLMALATE SYNTHASE 2); 2-isopropylmalate synthase/ methylthioalkylmalate synthase	1,91	2,02	1,58	4,8				
Nodulins									
AT1G80530	nodulin family protein				2,14				
AT2G16660	nodulin family protein			1,58	1,86				
AT2G40900	nodulin MtN21 family protein							1,76	
AT4G08290	nodulin MtN21 family protein			1,68	2,59				
AT4G01430	nodulin MtN21 family protein			5,22	1,71				
AT4G01450	nodulin MtN21 family protein				3,31				
AT3G28130	nodulin MtN21 family protein				2,5				
AT3G28050	nodulin MtN21 family protein				1,8				
AT3G28080	nodulin MtN21 family protein				2,84				
AT3G28100	nodulin MtN21 family protein				2,22				
AT3G18200	nodulin MtN21 family protein				1,66				
AT1G21890	nodulin MtN21 family protein				2,5				
AT1G44800	nodulin MtN21 family protein			1,63	4,43				
AT1G01070	nodulin MtN21 family protein				4,24				
AT1G75500	nodulin MtN21 family protein				1,69				
AT2G37460	nodulin MtN21 family protein				2,31				
AT2G39510	nodulin MtN21 family protein	1,55	3,44		2,82				

continued on next page

Table C.10 – continued from previous page

AGI code	Gene description	0,1 % sucrose				3 % sucrose			
		root		shoot		root		shoot	
		d^3/d_0	d^4/d_0	d^3/d_0	d^4/d_0	d^3/d_0	d^4/d_0	d^3/d_0	d^4/d_0
AT5G50800	nodulin MtN3 family protein				3,5				
AT3G25190	nodulin, putative	1,75	1,59	1,53	1,96				
AT1G76800	nodulin, putative				4,53				
AT4G08300	nodulin MtN21 family protein	2,27	2,19	1,72	4,3	3,78	2,08		
AT2G37450	nodulin MtN21 family protein				1,58				
AT5G14120	nodulin family protein				4,59				
AT4G34950	nodulin family protein				2,33				
AT2G28120	nodulin family protein				2,42				
AT2G39210	nodulin family protein				2,52				
AT4G28040	nodulin MtN21 family protein				2,54				
AT3G14770	nodulin MtN3 family protein				2,42				
AT3G48740	nodulin MtN3 family protein	6,12	6,06	1,57				1,53	

Bibliography

- Abdeen, A., Schnell, J. and Miki, B. (2010). Transcriptome analysis reveals absence of unintended effects in drought-tolerant transgenic plants overexpressing the transcription factor ABF3. *BMC Genomics* 11, 69. [90](#)
- Ahmad, M., Jarillo, J. A., Klimczak, L. J., Landry, L. G., Peng, T., Last, R. L. and Cashmore, A. R. (1997). An enzyme similar to animal type II photolyases mediates photoreactivation in *Arabidopsis*. *Plant Cell* 9, 199–207. [13](#)
- Ajuh, P., Kuster, B., Panov, K., Zomerdijk, J. C., Mann, M. and Lamond, A. I. (2000). Functional analysis of the human CDC5L complex and identification of its components by mass spectrometry. *EMBO J* 19, 6569–6581. [4](#), [5](#), [6](#), [75](#)
- Albers, M., Diment, A., Muraru, M., Russell, C. S. and Beggs, J. D. (2003). Identification and characterization of Prp45p and Prp46p, essential pre-mRNA splicing factors. *RNA* 9, 138–150. [3](#)
- Alonso, J. M., Stepanova, A. N., Leisse, T. J., Kim, C. J., Chen, H., Shinn, P., Stevenson, D. K., Zimmerman, J., Barajas, P., Cheuk, R., Gadrinab, C., Heller, C., Jeske, A., Koesema, E., Meyers, C. C., Parker, H., Prednis, L., Ansari, Y., Choy, N., Deen, H., Geralt, M., Hazari, N., Hom, E., Karnes, M., Mulholland, C., Ndubaku, R., Schmidt, I., Guzman, P., Aguilar-Henonin, L., Schmid, M., Weigel, D., Carter, D. E., Marchand, T., Risseuw, E., Brogden, D., Zeko, A., Crosby, W. L., Berry, C. C. and Ecker, J. R. (2003). Genome-wide insertional mutagenesis of *Arabidopsis thaliana*. *Science* 301, 653–657. [95](#)
- Aoyama, T., Dong, C. H., Wu, Y., Carabelli, M., Sessa, G., Ruberti, I., Morelli, G. and Chua, N. H. (1995). Ectopic expression of the *Arabidopsis* transcriptional activator Athb-1 alters leaf cell fate in tobacco. *Plant Cell* 7, 1773–1785. [77](#)
- Apel, K. and Hirt, H. (2004). Reactive oxygen species: metabolism, oxidative stress, and signal transduction. *Annu Rev Plant Biol* 55, 373–399. [11](#)
- Asada, K. (2006). Production and scavenging of reactive oxygen species in chloroplasts and their functions. *Plant Physiol* 141, 391–396. [11](#)
- Baena-González, E., Rolland, F., Thevelein, J. M. and Sheen, J. (2007). A central integrator of transcription networks in plant stress and energy signalling. *Nature* 448, 938–942. [10](#)
- Baena-González, E. and Sheen, J. (2008). Convergent energy and stress signaling. *Trends Plant Sci* 13, 474–482. [8](#), [10](#)

- Barbazuk, W. B., Fu, Y. and McGinnis, K. M. (2008). Genome-wide analyses of alternative splicing in plants: opportunities and challenges. *Genome Res* **18**, 1381–1392. [7](#)
- Bartel, D. P. (2004). MicroRNAs: genomics, biogenesis, mechanism, and function. *Cell* **116**, 281–297. [17](#)
- Baruah, A., Simková, K., Hinch, D. K., Apel, K. and Laloi, C. (2009). Modulation of O-mediated retrograde signaling by the PLEIOTROPIC RESPONSE LOCUS 1 (PRL1) protein, a central integrator of stress and energy signaling. *Plant J* **60**, 22–32. [10](#), [75](#), [80](#), [88](#)
- Bayer, M., Nawy, T., Giglione, C., Galli, M., Meinnel, T. and Lukowitz, W. (2009). Paternal control of embryonic patterning in *Arabidopsis thaliana*. *Science* **323**, 1485–1488. [22](#)
- Beitz, E. (2000). TEXshade: shading and labeling of multiple sequence alignments using LATEX2 epsilon. *Bioinformatics* **16**, 135–139. [105](#)
- Bennett, C. B., Westmoreland, T. J., Snipe, J. R. and Resnick, M. A. (1996). A double-strand break within a yeast artificial chromosome (YAC) containing human DNA can result in YAC loss, deletion or cell lethality. *Mol Cell Biol* **16**, 4414–4425. [13](#)
- Bentley, D. R. (2006). Whole-genome re-sequencing. *Curr Opin Genet Dev* **16**, 545–552. [24](#)
- Berger, F. (2003). Endosperm: the crossroad of seed development. *Curr Opin Plant Biol* **6**, 42–50. [22](#), [23](#)
- Berger, F., Hamamura, Y., Ingouff, M. and Higashiyama, T. (2008). Double fertilization - caught in the act. *Trends Plant Sci* **13**, 437–443. [20](#)
- Bergink, S. and Jentsch, S. (2009). Principles of ubiquitin and SUMO modifications in DNA repair. *Nature* **458**, 461–467. [9](#)
- Bernard, P. and Couturier, M. (1992). Cell killing by the F plasmid CcdB protein involves poisoning of DNA-topoisomerase II complexes. *J Mol Biol* **226**, 735–745. [95](#)
- Bernhardt, A., Lechner, E., Hano, P., Schade, V., Dieterle, M., Anders, M., Dubin, M. J., Benvenuto, G., Bowler, C., Genschik, P. and Hellmann, H. (2006). CUL4 associates with DDB1 and DET1 and its downregulation affects diverse aspects of development in *Arabidopsis thaliana*. *Plant J* **47**, 591–603. [13](#)
- Beyer, A. L. and Osheim, Y. N. (1988). Splice site selection, rate of splicing, and alternative splicing on nascent transcripts. *Genes Dev* **2**, 754–765. [7](#)
- Bhalerao, R. P., Salchert, K., Bako, L., Okresz, L., Szabados, L., Muranaka, T., Machida, Y., Schell, J. and Koncz, C. (1999). Regulatory interaction of PRL1 WD protein with *Arabidopsis* SNF1-like protein kinases. *Proc Natl Acad Sci U S A* **96**, 5322–5327. ISSN 0027-8424 (Print). [2](#), [87](#)
- Birnboim, H. C. and Doly, J. (1979). A rapid alkaline extraction procedure for screening recombinant plasmid DNA. *Nucleic Acids Res* **7**, 1513–1523. [109](#)
- Bleuyard, J.-Y., Gallego, M. E. and White, C. I. (2006). Recent advances in understanding of the DNA double-strand break repair machinery of plants. *DNA Repair (Amst)* **5**, 1–12. [13](#)

- Blilou, I., Xu, J., Wildwater, M., Willemsen, V., Paponov, I., Friml, J., Heidstra, R., Aida, M., Palme, K. and Scheres, B. (2005). The PIN auxin efflux facilitator network controls growth and patterning in *Arabidopsis* roots. *Nature* **433**, 39–44. [78](#)
- Boavida, L. C., Shuai, B., Yu, H.-J., Pagnussat, G. C., Sundaresan, V. and McCormick, S. (2009). A collection of *Ds* insertional mutants associated with defects in male gametophyte development and function in *Arabidopsis thaliana*. *Genetics* **181**, 1369–1385. [79](#)
- Bodt, S. D., Maere, S. and de Peer, Y. V. (2005). Genome duplication and the origin of angiosperms. *Trends Ecol Evol* **20**, 591–597. [9](#)
- Bohnert, R., Behr, J. and Ratsch, G. (2009). Transcript quantification with RNA-Seq data. *BMC Bioinformatics* **10**, P5. [82](#)
- Boisnard-Lorig, C., Colon-Carmona, A., Bauch, M., Hodge, S., Doerner, P., Bancharel, E., Dumas, C., Haseloff, J. and Berger, F. (2001). Dynamic analyses of the expression of the HISTONE::YFP fusion protein in *Arabidopsis* show that syncytial endosperm is divided in mitotic domains. *Plant Cell* **13**, 495–509. [22](#)
- Bona, F. D., Ossowski, S., Schneeberger, K. and Ratsch, G. (2008). Optimal spliced alignments of short sequence reads. *Bioinformatics* **24**, i174–i180. [25](#)
- Borevitz, J. O., Liang, D., Plouffe, D., Chang, H.-S., Zhu, T., Weigel, D., Berry, C. C., Winzeler, E. and Chory, J. (2003). Large-scale identification of single-feature polymorphisms in complex genomes. *Genome Res* **13**, 513–523. [24](#)
- Bradford, M. M. (1976). A rapid and sensitive method for the quantitation of microgram quantities of protein utilizing the principle of protein-dye binding. *Anal Biochem* **72**, 248–254. [129](#)
- Bray, C. M. and West, C. E. (2005). DNA repair mechanisms in plants: crucial sensors and effectors for the maintenance of genome integrity. *New Phytol* **168**, 511–528. [13](#)
- Breuer, F. (2000). *Untersuchungen zur Funktion zweier PRL1-WD-Proteine und deren Proteininteraktionspartnern in pflanzlichen Glucose- und Streßsignaltransduktionswegen*. Ph.D. thesis, Universitätsbibliothek Köln. [92](#)
- Britt, A. B. (1996). DNA damage and repair in plants. *Annu Rev Plant Physiol Plant Mol Biol* **47**, 75–100. [13](#)
- Brodersen, P. and Voinnet, O. (2006). The diversity of RNA silencing pathways in plants. *Trends Genet* **22**, 268–280. [16](#)
- Brown, B. A., Cloix, C., Jiang, G. H., Kaiserli, E., Herzyk, P., Kliebenstein, D. J. and Jenkins, G. I. (2005). A UV-B-specific signaling component orchestrates plant UV protection. *Proc Natl Acad Sci U S A* **102**, 18225–18230. [12](#)
- Buchholz, J. T. (1920). Embryo Development and Polyembryony in Relation to the Phylogeny of Conifers. *American Journal of Botany* **7**, 125–145. ISSN 00029122. [22](#)
- Burns, C. G., Ohi, R., Krainer, A. R. and Gould, K. L. (1999). Evidence that Myb-related CDC5 proteins are required for pre-mRNA splicing. *Proc Natl Acad Sci U S A* **96**, 13789–13794. [6](#)

- Cang, Y., Zhang, J., Nicholas, S. A., Bastien, J., Li, B., Zhou, P. and Goff, S. P. (2006). Deletion of DDB1 in mouse brain and lens leads to p53-dependent elimination of proliferating cells. *Cell* 127, 929–940. [13](#)
- Carabelli, M., Sessa, G., Baima, S., Morelli, G. and Ruberti, I. (1993). The *Arabidopsis* Athb-2 and -4 genes are strongly induced by far-red-rich light. *Plant J* 4, 469–479. [78](#)
- Carles, C. C., Choffnes-Inada, D., Reville, K., Lertpiriyapong, K. and Fletcher, J. C. (2005). *ULTRAPETALA1* encodes a SAND domain putative transcriptional regulator that controls shoot and floral meristem activity in *Arabidopsis*. *Development* 132, 897–911. [88](#)
- Carmichael, J. S. and Friedman, W. E. (1995). Double Fertilization in Gnetum gnemon: The Relationship between the Cell Cycle and Sexual Reproduction. *Plant Cell* 7, 1975–1988. [20](#)
- Casacuberta, J. M. and Santiago, N. (2003). Plant LTR-retrotransposons and MITES: control of transposition and impact on the evolution of plant genes and genomes. *Gene* 311, 1–11. [15](#)
- C. elegans* Sequencing Consortium (1998). Genome sequence of the nematode *C. elegans*: a platform for investigating biology. *Science* 282, 2012–2018. [7](#)
- Chan, S.-P. and Cheng, S.-C. (2005). The Prp19-associated complex is required for specifying interactions of U5 and U6 with pre-mRNA during spliceosome activation. *J Biol Chem* 280, 31190–31199. [6](#)
- Chan, S.-P., Kao, D.-I., Tsai, W.-Y. and Cheng, S.-C. (2003). The Prp19p-associated complex in spliceosome activation. *Science* 302, 279–282. [3](#), [6](#)
- Chen, H. R., Jan, S. P., Tsao, T. Y., Sheu, Y. J., Banroques, J. and Cheng, S. C. (1998). Snt309p, a component of the Prp19p-associated complex that interacts with Prp19p and associates with the spliceosome simultaneously with or immediately after dissociation of U4 in the same manner as Prp19p. *Mol Cell Biol* 18, 2196–2204. [6](#)
- Chen, H. R., Tsao, T. Y., Chen, C. H., Tsai, W. Y., Her, L. S., Hsu, M. M. and Cheng, S. C. (1999). Snt309p modulates interactions of Prp19p with its associated components to stabilize the Prp19p-associated complex essential for pre-mRNA splicing. *Proc Natl Acad Sci U S A* 96, 5406–5411. [6](#)
- Chen, Y.-H., Li, H.-J., Shi, D.-Q., Yuan, L., Liu, J., Sreenivasan, R., Baskar, R., Grossniklaus, U. and Yang, W.-C. (2007). The central cell plays a critical role in pollen tube guidance in *Arabidopsis*. *Plant Cell* 19, 3563–3577. [20](#)
- Cheng, S. C., Tarn, W. Y., Tsao, T. Y. and Abelson, J. (1993). PRP19: a novel spliceosomal component. *Mol Cell Biol* 13, 1876–1882. [6](#)
- Chevreur, B., Pfisterer, T., Drescher, B., Driesel, A. J., Müller, W. E. G., Wetter, T. and Suhai, S. (2004). Using the miraEST assembler for reliable and automated mRNA transcript assembly and SNP detection in sequenced ESTs. *Genome Res* 14, 1147–1159. [25](#)
- Chinnusamy, V. and Zhu, J.-K. (2009). Epigenetic regulation of stress responses in plants. *Curr Opin Plant Biol* 12, 133–139. [10](#)

- Chung, H. S., Koo, A. J. K., Gao, X., Jayanty, S., Thines, B., Jones, A. D. and Howe, G. A. (2008). Regulation and function of *Arabidopsis* JASMONATE ZIM-domain genes in response to wounding and herbivory. *Plant Physiol* **146**, 952–964. [79](#)
- Ciechanover, A. (2005). Intracellular protein degradation: from a vague idea, through the lysosome and the ubiquitin-proteasome system, and onto human diseases and drug targeting (Nobel lecture). *Angew Chem Int Ed Engl* **44**, 5944–5967. [8](#)
- Clough, S. J. and Bent, A. F. (1998). Floral dip: a simplified method for *Agrobacterium*-mediated transformation of *Arabidopsis thaliana*. *Plant J* **16**, 735–743. [115](#)
- Collins, L. and Penny, D. (2005). Complex spliceosomal organization ancestral to extant eukaryotes. *Mol Biol Evol* **22**, 1053–1066. [4](#)
- Creissen, Firmin, Fryer, Kular, Leyland, Reynolds, Pastori, Wellburn, Baker, Wellburn and Mullineaux (1999). Elevated glutathione biosynthetic capacity in the chloroplasts of transgenic tobacco plants paradoxically causes increased oxidative stress. *Plant Cell* **11**, 1277–1292. [11](#)
- Córdoba-Cañero, D., Morales-Ruiz, T., Roldán-Arjona, T. and Ariza, R. R. (2009). Single-nucleotide and long-patch base excision repair of DNA damage in plants. *Plant J* **60**, 716–728. [13](#)
- Dalmay, T., Hamilton, A., Rudd, S., Angell, S. and Baulcombe, D. C. (2000). An RNA-dependent RNA polymerase gene in *Arabidopsis* is required for posttranscriptional gene silencing mediated by a transgene but not by a virus. *Cell* **101**, 543–553. [17](#)
- Dayyeh, B. K. A. A., Quan, T. K., Castro, M. and Ruby, S. W. (2002). Probing interactions between the U2 small nuclear ribonucleoprotein and the DEAD-box protein, Prp5. *J Biol Chem* **277**, 20221–20233. [3](#)
- Denoëud, F., Aury, J.-M., Silva, C. D., Noel, B., Rogier, O., Delledonne, M., Morgante, M., Valle, G., Wincker, P., Scarpelli, C., Jaillon, O. and Artiguenave, F. (2008). Annotating genomes with massive-scale RNA sequencing. *Genome Biol* **9**, R175. [23](#)
- Doke, N. (1985). NADPH-dependent O₂-generation in membrane fractions isolated from wounded potato tubers inoculated with *Phytophthora infestans*. *Physiological Plant Pathology* **27**, 311–322. [11](#)
- Dong, X. (2004). The role of membrane-bound ankyrin-repeat protein ACD6 in programmed cell death and plant defense. *Sci STKE* **2004**, pe6. [81](#)
- Dower, W. J., Miller, J. F. and Ragsdale, C. W. (1988). High efficiency transformation of *E. coli* by high voltage electroporation. *Nucleic Acids Res* **16**, 6127–6145. [115](#)
- Dresselhaus, T. and Márton, M. L. (2009). Micropylar pollen tube guidance and burst: adapted from defense mechanisms? *Curr Opin Plant Biol* **12**, 773–780. [20](#)
- Earley, K. W., Haag, J. R., Pontes, O., Opper, K., Juehne, T., Song, K. and Pikaard, C. S. (2006). Gateway-compatible vectors for plant functional genomics and proteomics. *Plant J* **45**, 616–629. [99](#)
- Elsasser, S., Chandler-Militello, D., Müller, B., Hanna, J. and Finley, D. (2004). Rad23 and Rpn10 serve as alternative ubiquitin receptors for the proteasome. *J Biol Chem* **279**, 26817–26822. [87](#)

- Erilova, A., Brownfield, L., Exner, V., Rosa, M., Twell, D., Scheid, O. M., Hennig, L. and Köhler, C. (2009). Imprinting of the polycomb group gene *MEDEA* serves as a ploidy sensor in *Arabidopsis*. *PLoS Genet* 5, e1000663. [22](#)
- Faivre-Nitschke, S. E., Grienemberger, J. M. and Gualberto, J. M. (1999). A prokaryotic-type cytidine deaminase from *Arabidopsis thaliana* gene expression and functional characterization. *Eur J Biochem* 263, 896–903. [79](#)
- Farrás, R., Ferrando, A., Jásik, J., Kleinow, T., Ökrész, L., Tiburcio, A., Salchert, K., del Pozo, C., Schell, J. and Koncz, C. (2001). SKP1-SnRK protein kinase interactions mediate proteasomal binding of a plant SCF ubiquitin ligase. *EMBO J* 20, 2742–2756. [2](#), [8](#), [31](#), [87](#)
- Faure, J.-E., Rotman, N., Fortuné, P. and Dumas, C. (2002). Fertilization in *Arabidopsis thaliana* wild type: developmental stages and time course. *Plant J* 30, 481–488. [20](#)
- Fedurco, M., Romieu, A., Williams, S., Lawrence, I. and Turcatti, G. (2006). BTA, a novel reagent for DNA attachment on glass and efficient generation of solid-phase amplified DNA colonies. *Nucleic Acids Res* 34, e22. [24](#)
- Ferrando, A., Farrás, R., Jásik, J., Schell, J. and Koncz, C. (2000). Intron-tagged epitope: a tool for facile detection and purification of proteins expressed in *Agrobacterium*-transformed plant cells. *Plant J* 22, 553–560. [116](#)
- Feschotte, C., Jiang, N. and Wessler, S. R. (2002). Plant transposable elements: where genetics meets genomics. *Nat Rev Genet* 3, 329–341. [14](#)
- Feschotte, C. and Pritham, E. J. (2007). DNA transposons and the evolution of eukaryotic genomes. *Annu Rev Genet* 41, 331–368. [14](#)
- Finley, D. (2009). Recognition and processing of ubiquitin-protein conjugates by the proteasome. *Annu Rev Biochem* 78, 477–513. [87](#)
- Flagel, L. E. and Wendel, J. F. (2009). Gene duplication and evolutionary novelty in plants. *New Phytol* 183, 557–564. [9](#), [10](#)
- Fletcher, J. C. (2001). The *ULTRAPETALA* gene controls shoot and floral meristem size in *Arabidopsis*. *Development* 128, 1323–1333. [76](#)
- Fong, Y. W. and Zhou, Q. (2001). Stimulatory effect of splicing factors on transcriptional elongation. *Nature* 414, 929–933. [7](#)
- Fortschegger, K., Wagner, B., Voglauer, R., Katinger, H., Sibilina, M. and Grillari, J. (2007). Early embryonic lethality of mice lacking the essential protein SNEV. *Mol Cell Biol* 27, 3123–3130. [6](#)
- Friedman, A. R. and Baker, B. J. (2007). The evolution of resistance genes in multi-protein plant resistance systems. *Curr Opin Genet Dev* 17, 493–499. [11](#)
- Friedman, W. E. (2001). Developmental and evolutionary hypotheses for the origin of double fertilization and endosperm. *C R Acad Sci III* 324, 559–567. [20](#)
- Friml, J., Vieten, A., Sauer, M., Weijers, D., Schwarz, H., Hamann, T., Offringa, R. and Jürgens, G. (2003). Efflux-dependent auxin gradients establish the apical-basal axis of *Arabidopsis*. *Nature* 426, 147–153. [21](#)

- Gagne, J. M., Smalle, J., Gingerich, D. J., Walker, J. M., Yoo, S.-D., Yanagisawa, S. and Vierstra, R. D. (2004). *Arabidopsis* EIN3-binding F-box 1 and 2 form ubiquitin-protein ligases that repress ethylene action and promote growth by directing EIN3 degradation. *Proc Natl Acad Sci U S A* **101**, 6803–6808. [77](#)
- Gandikota, M., Birkenbihl, R. P., Höhmann, S., Cardon, G. H., Saedler, H. and Huijser, P. (2007). The *miRNA156/157* recognition element in the 3' UTR of the *Arabidopsis* SBP box gene *SPL3* prevents early flowering by translational inhibition in seedlings. *Plant J* **49**, 683–693. [76](#)
- Garcion, C., Lohmann, A., Lamodièrre, E., Catinot, J., Buchala, A., Doermann, P. and Métraux, J.-P. (2008). Characterization and biological function of the *ISOCHORISMATE SYNTHASE2* gene of *Arabidopsis*. *Plant Physiol* **147**, 1279–1287. [81](#)
- Gautier, L., Irizarry, R., Cope, L. and Bolstad, B. (2003). Textual description of affy. *Vignette available at the Bioconductor website <http://www.bioconductor.org>*. [25](#)
- Gehring, M., Bubb, K. L. and Henikoff, S. (2009). Extensive demethylation of repetitive elements during seed development underlies gene imprinting. *Science* **324**, 1447–1451. [22](#)
- Gehring, M., Choi, Y. and Fischer, R. L. (2004). Imprinting and seed development. *Plant Cell* **16** Suppl, S203–S213. [22](#)
- Gentleman, R. C., Carey, V. J., Bates, D. M., Bolstad, B., Dettling, M., Dudoit, S., Ellis, B., Gautier, L., Ge, Y., Gentry, J., Hornik, K., Hothorn, T., Huber, W., Iacus, S., Irizarry, R., Leisch, F., Li, C., Maechler, M., Rossini, A. J., Sawitzki, G., Smith, C., Smyth, G., Tierney, L., Yang, J. Y. H. and Zhang, J. (2004). Bioconductor: open software development for computational biology and bioinformatics. *Genome Biol* **5**, R80. [25](#), [105](#)
- Glickman, M. H., Rubin, D. M., Coux, O., Wefes, I., Pfeifer, G., Cjeka, Z., Baumeister, W., Fried, V. A. and Finley, D. (1998). A subcomplex of the proteasome regulatory particle required for ubiquitin-conjugate degradation and related to the COP9-signalosome and eIF3. *Cell* **94**, 615–623. [8](#), [87](#)
- Glickman, M. H., Rubin, D. M., Fu, H., Larsen, C. N., Coux, O., Wefes, I., Pfeifer, G., Cjeka, Z., Vierstra, R., Baumeister, W., Fried, V. and Finley, D. (1999). Functional analysis of the proteasome regulatory particle. *Mol Biol Rep* **26**, 21–28. [8](#)
- Grandbastien, M. (1998). Activation of plant retrotransposons under stress conditions. *Trends in plant science* **3**, 181–187. [15](#), [84](#)
- Grandbastien, M. A., Lucas, H., Morel, J. B., Mhiri, C., Vernhettes, S. and Casacuberta, J. M. (1997). The expression of the tobacco *Tnt1* retrotransposon is linked to plant defense responses. *Genetica* **100**, 241–252. [15](#)
- Gregis, V., Sessa, A., Dorca-Fornell, C. and Kater, M. M. (2009). The *Arabidopsis* floral meristem identity genes *AP1*, *AGL24* and *SVP* directly repress class B and C floral homeotic genes. *Plant J* **60**, 626–637. [76](#)
- Grey, M., Düsterhöft, A., Henriques, J. A. and Brendel, M. (1996). Allelism of *PSO4* and *PRP19* links pre-mRNA processing with recombination and error-prone DNA repair in *Saccharomyces cerevisiae*. *Nucleic Acids Res* **24**, 4009–4014. [6](#)

- Grillari, J., Ajuh, P., Stadler, G., Löscher, M., Voglauer, R., Ernst, W., Chusainow, J., Eisenhaber, F., Pokar, M., Fortschegger, K., Grey, M., Lamond, A. I. and Katinger, H. (2005). SNEV is an evolutionarily conserved splicing factor whose oligomerization is necessary for spliceosome assembly. *Nucleic Acids Res* 33, 6868–6883. [6](#)
- Grote, M., Wolf, E., Will, C. L., Lemm, I., Agafonov, D. E., Schomburg, A., Fischle, W., Urlaub, H. and Lührmann, R. (2010). The Molecular Architecture of the Human Prp19/CDC5L Complex. *Mol Cell Biol*. [6](#)
- Harris, T. D., Buzby, P. R., Babcock, H., Beer, E., Bowers, J., Braslavsky, I., Causey, M., Colonell, J., Dimeo, J., Efcavitch, J. W., Giladi, E., Gill, J., Healy, J., Jarosz, M., Lapen, D., Moulton, K., Quake, S. R., Steinmann, K., Thayer, E., Tyurina, A., Ward, R., Weiss, H. and Xie, Z. (2008). Single-molecule DNA sequencing of a viral genome. *Science* 320, 106–109. [24](#)
- Hartley, J. L., Temple, G. F. and Brasch, M. A. (2000). DNA cloning using *in vitro* site-specific recombination. *Genome Res* 10, 1788–1795. [114](#)
- Havecker, E. R., Gao, X. and Voytas, D. F. (2004). The diversity of LTR retrotransposons. *Genome Biol* 5, 225. [15](#)
- He, X.-J., Hsu, Y.-F., Zhu, S., Wierzbicki, A. T., Pontes, O., Pikaard, C. S., Liu, H.-L., Wang, C.-S., Jin, H. and Zhu, J.-K. (2009). An effector of RNA-directed DNA methylation in *Arabidopsis* is an ARGONAUTE 4- and RNA-binding protein. *Cell* 137, 498–508. [86](#)
- Hedden, P. and Kamiya, Y. (1997). GIBBERELLIN BIOSYNTHESIS: Enzymes, Genes and Their Regulation. *Annu Rev Plant Physiol Plant Mol Biol* 48, 431–460. [79](#)
- Heidstra, R., Welch, D. and Scheres, B. (2004). Mosaic analyses using marked activation and deletion clones dissect *Arabidopsis* SCARECROW action in asymmetric cell division. *Genes Dev* 18, 1964–1969. [61](#), [99](#), [100](#), [120](#), [121](#)
- Hellens, R. P., Edwards, E. A., Leyland, N. R., Bean, S. and Mullineaux, P. M. (2000). pGreen: a versatile and flexible binary Ti vector for *Agrobacterium*-mediated plant transformation. *Plant Mol Biol* 42, 819–832. [96](#)
- Hennig, L., Menges, M., Murray, J. A. H. and Grissem, W. (2003). *Arabidopsis* transcript profiling on Affymetrix GeneChip arrays. *Plant Mol Biol* 53, 457–465. [24](#)
- Henriques, J. A., Vicente, E. J., da Silva, K. V. L. and Schenberg, A. C. (1989). PSO4: a novel gene involved in error-prone repair in *Saccharomyces cerevisiae*. *Mutat Res* 218, 111–124. [6](#), [13](#)
- Hernández-Pinzón, I., Yelina, N. E., Schwach, F., Studholme, D. J., Baulcombe, D. and Dalmay, T. (2007). *SDE5*, the putative homologue of a human mRNA export factor, is required for transgene silencing and accumulation of trans-acting endogenous siRNA. *Plant J* 50, 140–148. [82](#)
- Hershko, A. and Ciechanover, A. (1998). The ubiquitin system. *Annu Rev Biochem* 67, 425–479. [9](#)
- Hideg, E., Kálai, T., Hideg, K. and Vass, I. (1998). Photoinhibition of photosynthesis *in vivo* results in singlet oxygen production detection via nitroxide-induced fluorescence quenching in broad bean leaves. *Biochemistry* 37, 11405–11411. [11](#)

- Hirayama, T. and Shinozaki, K. (1996). A cdc5+ homolog of a higher plant, *Arabidopsis thaliana*. *Proc Natl Acad Sci U S A* **93**, 13371–13376. [6](#)
- Hochstrasser, M. (2004). Ubiquitin signalling: what's in a chain? *Nat Cell Biol* **6**, 571–572. [9](#)
- Holley, S. R., Yalamanchili, R. D., Moura, D. S., Ryan, C. A. and Stratmann, J. W. (2003). Convergence of signaling pathways induced by systemin, oligosaccharide elicitors, and ultraviolet-B radiation at the level of mitogen-activated protein kinases in *Lycopersicon peruvianum* suspension-cultured cells. *Plant Physiol* **132**, 1728–1738. [12](#)
- Hollister, J. D. and Gaut, B. S. (2007). Population and evolutionary dynamics of Helitron transposable elements in *Arabidopsis thaliana*. *Mol Biol Evol* **24**, 2515–2524. [14](#)
- Holmberg, C., Fleck, O., Hansen, H. A., Liu, C., Slaaby, R., Carr, A. M. and Nielsen, O. (2005). Ddb1 controls genome stability and meiosis in fission yeast. *Genes Dev* **19**, 853–862. [87](#)
- Homer, N., Merriman, B. and Nelson, S. F. (2009). BFAST: an alignment tool for large scale genome resequencing. *PLoS One* **4**, e7767. [25](#)
- Hong, F., Breitling, R., McEntee, C. W., Wittner, B. S., Nemhauser, J. L. and Chory, J. (2006). RankProd: a bioconductor package for detecting differentially expressed genes in meta-analysis. *Bioinformatics* **22**, 2825–2827. [37](#), [105](#), [133](#)
- Honma, T. and Goto, K. (2000). The *Arabidopsis* floral homeotic gene *PISTILLATA* is regulated by discrete cis-elements responsive to induction and maintenance signals. *Development* **127**, 2021–2030. [76](#)
- Horváth, M. (2008). *Arabidopsis* AMP-activated protein kinases in proteasomal complexes and their role in cell signaling. Ph.D. thesis, Universitätsbibliothek Köln. [27](#), [100](#), [116](#)
- Hsiao, T.-L., Revelles, O., Chen, L., Sauer, U. and Vitkup, D. (2010). Automatic policing of biochemical annotations using genomic correlations. *Nat Chem Biol* **6**, 34–40. [23](#), [75](#)
- Hu, J., McCall, C. M., Ohta, T. and Xiong, Y. (2004). Targeted ubiquitination of CDT1 by the DDB1-CUL4A-ROC1 ligase in response to DNA damage. *Nat Cell Biol* **6**, 1003–1009. [13](#)
- Hu, Y., Xie, Q. and Chua, N.-H. (2003). The *Arabidopsis* auxin-inducible gene *ARGOS* controls lateral organ size. *Plant Cell* **15**, 1951–1961. [78](#)
- Hughes, J. H., Mack, K. and Hamparian, V. V. (1988). India ink staining of proteins on nylon and hydrophobic membranes. *Anal Biochem* **173**, 18–25. [131](#)
- Human Genome Sequencing Consortium (2004). Finishing the euchromatic sequence of the human genome. *Nature* **431**, 931–945. [7](#)
- Hunter, S., Apweiler, R., Attwood, T. K., Bairoch, A., Bateman, A., Binns, D., Bork, P., Das, U., Daugherty, L., Duquenne, L., Finn, R. D., Gough, J., Haft, D., Hulo, N., Kahn, D., Kelly, E., Laugraud, A., Letunic, I., Lonsdale, D., Lopez, R., Madera, M., Maslen, J., McAnulla, C., McDowall, J., Mistry, J., Mitchell, A., Mulder, N., Natale, D., Orengo, C., Quinn, A. F., Selengut, J. D., Sigrist, C. J. A., Thimma, M., Thomas, P. D., Valentin, F., Wilson, D., Wu, C. H. and Yeats, C. (2009). InterPro: the integrative protein signature database. *Nucleic Acids Res* **37**, D211–D215. [106](#)

- Husnjak, K., Elsasser, S., Zhang, N., Chen, X., Randles, L., Shi, Y., Hofmann, K., Walters, K. J., Finley, D. and Dikic, I. (2008). Proteasome subunit Rpn13 is a novel ubiquitin receptor. *Nature* **453**, 481–488. [87](#)
- Ihaka, R. and Gentleman, R. (1996). R: A language for data analysis and graphics. *Journal of computational and graphical statistics* **5**, 299–314. [25](#)
- Ingouff, M., Hamamura, Y., Gourgues, M., Higashiyama, T. and Berger, F. (2007). Distinct dynamics of HISTONE3 variants between the two fertilization products in plants. *Curr Biol* **17**, 1032–1037. [20](#)
- Ingouff, M., Sakata, T., Li, J., Sprunck, S., Dresselhaus, T. and Berger, F. (2009). The two male gametes share equal ability to fertilize the egg cell in *Arabidopsis thaliana*. *Curr Biol* **19**, R19–R20. [20](#)
- Irizarry, R., Gautier, L. and Cope, L. (2003a). *The Analysis of Gene Expression Data: Methods and Software*, chapter An R package for analyses of Affymetrix oligonucleotide arrays. Parmigiani, G., Garrett, E.S., Irizarry, R.A. and Zeger, S.L (eds), Springer, pages 102–119. [25](#)
- Irizarry, R. A., Bolstad, B. M., Collin, F., Cope, L. M., Hobbs, B. and Speed, T. P. (2003b). Summaries of Affymetrix GeneChip probe level data. *Nucleic Acids Res* **31**, e15. [25](#)
- Jagadeeswaran, G., Saini, A. and Sunkar, R. (2009). Biotic and abiotic stress down-regulate miR398 expression in *Arabidopsis*. *Planta* **229**, 1009–1014. [86](#)
- Jawad, Z. and Paoli, M. (2002). Novel sequences propel familiar folds. *Structure* **10**, 447–454. [4](#)
- Jeddeloh, J. A., Bender, J. and Richards, E. J. (1998). The DNA methylation locus DDM1 is required for maintenance of gene silencing in *Arabidopsis*. *Genes Dev* **12**, 1714–1725. [16](#)
- Jefferson, R. A., Kavanagh, T. A. and Bevan, M. W. (1987). GUS fusions: beta-glucuronidase as a sensitive and versatile gene fusion marker in higher plants. *EMBO J* **6**, 3901–3907. [108](#)
- Jones, J. D. G. and Dangl, J. L. (2006). The plant immune system. *Nature* **444**, 323–329. [11](#)
- Jones-Rhoades, M. W. and Bartel, D. P. (2004). Computational identification of plant microRNAs and their targets, including a stress-induced miRNA. *Mol Cell* **14**, 787–799. [17](#)
- Jones-Rhoades, M. W., Borevitz, J. O. and Preuss, D. (2007). Genome-wide expression profiling of the *Arabidopsis* female gametophyte identifies families of small, secreted proteins. *PLoS Genet* **3**, 1848–1861. [24](#)
- Joung, J.-G., Corbett, A. M., Fellman, S. M., Tieman, D. M., Klee, H. J., Giovannoni, J. J. and Fei, Z. (2009). Plant MetGenMAP: an integrative analysis system for plant systems biology. *Plant Physiol* **151**, 1758–1768. [105](#), [106](#)
- Jurica, M. S. and Moore, M. J. (2003). Pre-mRNA splicing: awash in a sea of proteins. *Mol Cell* **12**, 5–14. [5](#)
- Jürgens, G., Mayer, U., Ramon A., T. R., Berleth, T. and Miséra, S. (1991). Genetic analysis of pattern formation in the *Arabidopsis* embryo. *Development* **113**, 27–38. [21](#)
- Kaiser, G., Kleiner, O., Beisswenger, C. and Batschauer, A. (2009). Increased DNA repair in *Arabidopsis* plants overexpressing CPD photolyase. *Planta* **230**, 505–515. [13](#)

- Kang, I.-H., Steffen, J. G., Portereiko, M. F., Lloyd, A. and Drews, G. N. (2008). The AGL62 MADS domain protein regulates cellularization during endosperm development in *Arabidopsis*. *Plant Cell* **20**, 635–647. [22](#)
- Kankel, M. W., Ramsey, D. E., Stokes, T. L., Flowers, S. K., Haag, J. R., Jeddloh, J. A., Riddle, N. C., Verbsky, M. L. and Richards, E. J. (2003). *Arabidopsis* MET1 cytosine methyltransferase mutants. *Genetics* **163**, 1109–1122. [16](#)
- Kapitonov, V. V. and Jurka, J. (2001). Rolling-circle transposons in eukaryotes. *Proc Natl Acad Sci U S A* **98**, 8714–8719. [14](#)
- Kasianowicz, J. J., Brandin, E., Branton, D. and Deamer, D. W. (1996). Characterization of individual polynucleotide molecules using a membrane channel. *Proc Natl Acad Sci U S A* **93**, 13770–13773. [24](#)
- Kato, M., Miura, A., Bender, J., Jacobsen, S. E. and Kakutani, T. (2003). Role of CG and non-CG methylation in immobilization of transposons in *Arabidopsis*. *Curr Biol* **13**, 421–426. [85](#)
- Katoh, A., Uenohara, K., Akita, M. and Hashimoto, T. (2006). Early steps in the biosynthesis of NAD in *Arabidopsis* start with aspartate and occur in the plastid. *Plant Physiol* **141**, 851–857. [81](#)
- Kaur, J., Sebastian, J. and Siddiqi, I. (2006). The *Arabidopsis*-*mei2*-like genes play a role in meiosis and vegetative growth in *Arabidopsis*. *Plant Cell* **18**, 545–559. [79](#)
- Kazan, K. (2003). Alternative splicing and proteome diversity in plants: the tip of the iceberg has just emerged. *Trends Plant Sci* **8**, 468–471. [7](#)
- Kim, J.-B., Kang, J.-Y. and Kim, S. Y. (2004). Over-expression of a transcription factor regulating ABA-responsive gene expression confers multiple stress tolerance. *Plant Biotechnol J* **2**, 459–466. [78](#)
- Kim, J. H., Woo, H. R., Kim, J., Lim, P. O., Lee, I. C., Choi, S. H., Hwang, D. and Nam, H. G. (2009). Trifurcate feed-forward regulation of age-dependent cell death involving *miR164* in *Arabidopsis*. *Science* **323**, 1053–1057. [81](#)
- Kim, T., Hofmann, K., von Arnim, A. G. and Chamovitz, D. A. (2001). PCI complexes: pretty complex interactions in diverse signaling pathways. *Trends Plant Sci* **6**, 379–386. [87](#)
- Kimura, S., Tahira, Y., Ishibashi, T., Mori, Y., Mori, T., Hashimoto, J. and Sakaguchi, K. (2004). DNA repair in higher plants; photoreactivation is the major DNA repair pathway in non-proliferating cells while excision repair (nucleotide excision repair and base excision repair) is active in proliferating cells. *Nucleic Acids Res* **32**, 2760–2767. [13](#)
- Kleinridders, A., Pogoda, H.-M., Irlenbusch, S., Smyth, N., Koncz, C., Hammerschmidt, M. and Brünig, J. C. (2009). PLRG1 is an essential regulator of cell proliferation and apoptosis during vertebrate development and tissue homeostasis. *Mol Cell Biol* **29**, 3173–3185. [4](#)
- Kobayashi, Y., Kaya, H., Goto, K., Iwabuchi, M. and Araki, T. (1999). A pair of related genes with antagonistic roles in mediating flowering signals. *Science* **286**, 1960–1962. [76](#)
- Koncz, C., Martini, N., Szabados, L., Hrouda, M., Bachmair, A. and Schell, J. (1994). *Plant Molecular Biology Manual*, chapter Specialized vectors for gene tagging and expression studies. Gelvin S. and Schilperoort B. (eds.), Kluwer Academic Publisher, Dordrecht, The Netherlands, pages 1–22. [99](#), [102](#), [107](#)

- Koncz, C. and Schell, J. (1986). The promoter of TL-DNA gene 5 controls the tissue-specific expression of chimaeric genes carried by a novel type of *Agrobacterium* binary vector. *Molecular and General Genetics MGG* **204**, 383–396. [96](#)
- Koncz, C. and Schell, J. (2002). *Molecular Plant Biology (Volume One): A Practical Approach*, chapter T-DNA tagging. Gilmartin P. M. and Bowler C. (eds.), Oxford University Press Inc., New York, United States, pages 33–51. [108](#)
- Koonin, E. V. (2005). Orthologs, paralogs, and evolutionary genomics. *Annu Rev Genet* **39**, 309–338. [9](#)
- Kovalchuk, I., Kovalchuk, O., Kalck, V., Boyko, V., Filkowski, J., Heinlein, M. and Hohn, B. (2003). Pathogen-induced systemic plant signal triggers DNA rearrangements. *Nature* **423**, 760–762. [11](#), [88](#)
- Kumar, A. and Bennetzen, J. L. (1999). Plant retrotransposons. *Annu Rev Genet* **33**, 479–532. [15](#)
- Kumar, L. and Futschik, M. E. (2007). Mfuzz: A software package for soft clustering of microarray data. *Bioinformatics* **2**, 5–7. [46](#), [105](#), [134](#)
- Kurepa, J., Wang, S., Li, Y. and Smalle, J. (2009). Proteasome regulation, plant growth and stress tolerance. *Plant Signal Behav* **4**, 924–927. [87](#)
- Kwon, C. S. and Wagner, D. (2007). Unwinding chromatin for development and growth: a few genes at a time. *Trends Genet* **23**, 403–412. [16](#)
- Laemmli, U. K. (1970). Cleavage of structural proteins during the assembly of the head of bacteriophage T4. *Nature* **227**, 680–685. [129](#)
- Langmead, B., Trapnell, C., Pop, M. and Salzberg, S. L. (2009). Ultrafast and memory-efficient alignment of short DNA sequences to the human genome. *Genome Biol* **10**, R25. [25](#), [105](#), [135](#)
- Larsen, N. A. and Harrison, S. C. (2004). Crystal structure of the spindle assembly checkpoint protein Bub3. *J Mol Biol* **344**, 885–892. [4](#)
- Laubinger, S., Zeller, G., Henz, S. R., Sachsenberg, T., Widmer, C. K., Naouar, N., Vuylsteke, M., Schölkopf, B., Rätsch, G. and Weigel, D. (2008). At-TAX: a whole genome tiling array resource for developmental expression analysis and transcript identification in *Arabidopsis thaliana*. *Genome Biol* **9**, R112. [127](#)
- Lee, J.-H., Terzaghi, W., Gusmaroli, G., Charron, J.-B. F., Yoon, H.-J., Chen, H., He, Y. J., Xiong, Y. and Deng, X. W. (2008). Characterization of *Arabidopsis* and rice DWD proteins and their roles as substrate receptors for CUL4-RING E3 ubiquitin ligases. *Plant Cell* **20**, 152–167. [13](#), [75](#), [86](#)
- Li, H. and Durbin, R. (2010). Fast and accurate long-read alignment with Burrows-Wheeler transform. *Bioinformatics* **26**, 589–595. [25](#)
- Lim, P. O., Kim, H. J. and Nam, H. G. (2007). Leaf senescence. *Annu Rev Plant Biol* **58**, 115–136. [12](#)
- Lipshutz, R. J., Fodor, S. P., Gingeras, T. R. and Lockhart, D. J. (1999). High density synthetic oligonucleotide arrays. *Nat Genet* **21**, 20–24. [23](#)

- Lipshutz, R. J., Morris, D., Chee, M., Hubbell, E., Kozal, M. J., Shah, N., Shen, N., Yang, R. and Fodor, S. P. (1995). Using oligonucleotide probe arrays to access genetic diversity. *Biotechniques* 19, 442–447. 23
- Lisch, D. (2009). Epigenetic regulation of transposable elements in plants. *Annu Rev Plant Biol* 60, 43–66. 85
- Lister, R., Gregory, B. D. and Ecker, J. R. (2009). Next is now: new technologies for sequencing of genomes, transcriptomes, and beyond. *Curr Opin Plant Biol* 12, 107–118. 1
- Lister, R., O'Malley, R. C., Tonti-Filippini, J., Gregory, B. D., Berry, C. C., Millar, A. H. and Ecker, J. R. (2008). Highly integrated single-base resolution maps of the epigenome in *Arabidopsis*. *Cell* 133, 523–536. 16
- Liu, Y., Ren, D., Pike, S., Pallardy, S., Gassmann, W. and Zhang, S. (2007). Chloroplast-generated reactive oxygen species are involved in hypersensitive response-like cell death mediated by a mitogen-activated protein kinase cascade. *Plant J* 51, 941–954. 12
- Livak, K. J. and Schmittgen, T. D. (2001). Analysis of relative gene expression data using real-time quantitative PCR and the 2⁻(Delta Delta C(T)) Method. *Methods* 25, 402–408. 123
- Lu, C.-A., Lin, C.-C., Lee, K.-W., Chen, J.-L., Huang, L.-F., Ho, S.-L., Liu, H.-J., Hsing, Y.-I. and Yu, S.-M. (2007). The SnRK1A protein kinase plays a key role in sugar signaling during germination and seedling growth of rice. *Plant Cell* 19, 2484–2499. 11
- Lu, H., Rate, D. N., Song, J. T. and Greenberg, J. T. (2003). ACD6, a novel ankyrin protein, is a regulator and an effector of salicylic acid signaling in the *Arabidopsis* defense response. *Plant Cell* 15, 2408–2420. 81
- Lu, X. and Legerski, R. J. (2007). The Prp19/Pso4 core complex undergoes ubiquitylation and structural alterations in response to DNA damage. *Biochem Biophys Res Commun* 354, 968–974. 13
- Léon-Kloosterziel, K. M., Gil, M. A., Ruijs, G. J., Jacobsen, S. E., Olszewski, N. E., Schwartz, S. H., Zeevaart, J. A. and Koornneef, M. (1996). Isolation and characterization of abscisic acid-deficient *Arabidopsis* mutants at two new loci. *Plant J* 10, 655–661. 78
- Margulies, M., Egholm, M., Altman, W. E., Attiya, S., Bader, J. S., Bemben, L. A., Berka, J., Braverman, M. S., Chen, Y.-J., Chen, Z., Dewell, S. B., Du, L., Fierro, J. M., Gomes, X. V., Godwin, B. C., He, W., Helgesen, S., Ho, C. H., Ho, C. H., Irzyk, G. P., Jando, S. C., Alenquer, M. L. I., Jarvie, T. P., Jirage, K. B., Kim, J.-B., Knight, J. R., Lanza, J. R., Leamon, J. H., Lefkowitz, S. M., Lei, M., Li, J., Lohman, K. L., Lu, H., Makhijani, V. B., McDade, K. E., McKenna, M. P., Myers, E. W., Nickerson, E., Nobile, J. R., Plant, R., Puc, B. P., Ronan, M. T., Roth, G. T., Sarkis, G. J., Simons, J. F., Simpson, J. W., Srinivasan, M., Tartaro, K. R., Tomasz, A., Vogt, K. A., Volkmer, G. A., Wang, S. H., Wang, Y., Weiner, M. P., Yu, P., Begley, R. F. and Rothberg, J. M. (2005). Genome sequencing in microfabricated high-density picolitre reactors. *Nature* 437, 376–380. 24
- Mathur, J. and Koncz, C. (1998). Establishment and maintenance of cell suspension cultures. *Methods Mol Biol* 82, 27–30. 95, 107

- Matsukura, S., Mizoi, J., Yoshida, T., Todaka, D., Ito, Y., Maruyama, K., Shinozaki, K. and Yamaguchi-Shinozaki, K. (2010). Comprehensive analysis of rice *DREB2*-type genes that encode transcription factors involved in the expression of abiotic stress-responsive genes. *Mol Genet Genomics* **283**, 185–196. [7](#)
- Maumus, F., Allen, A. E., Mhiri, C., Hu, H., Jabbari, K., Vardi, A., Grandbastien, M.-A. and Bowler, C. (2009). Potential impact of stress activated retrotransposons on genome evolution in a marine diatom. *BMC Genomics* **10**, 624. [15](#)
- Mayer, U., Ruiz, R., Berleth, T., Miseéra, S. and Juürgens, G. (1991). Mutations affecting body organization in the *Arabidopsis* embryo. *Nature* **353**, 402–407. [21](#)
- McClintock, B. (1950). The origin and behavior of mutable loci in maize. *Proc Natl Acad Sci U S A* **36**, 344–355. [1](#), [13](#), [15](#)
- McCormick, S. (1993). Male Gametophyte Development. *Plant Cell* **5**, 1265–1275. [18](#)
- McCormick, S. (2004). Control of male gametophyte development. *Plant Cell* **16 Suppl**, S142–S153. [18](#)
- McGookin, R. (1984). *Methods in Molecular Biology, Volume 2, Nucleic Acids*, chapter RNA Extraction by the Guanidine Thiocyanate Procedure. Walker J. M. (ed.), Humana Press Inc., pages 113–116. [121](#)
- Meinke, D. W., Cherry, J. M., Dean, C., Rounsley, S. D. and Koornneef, M. (1998). *Arabidopsis thaliana*: a model plant for genome analysis. *Science* **282**, 662, 679–662, 682. [19](#)
- Menges, M. and Murray, J. A. H. (2002). Synchronous *Arabidopsis* suspension cultures for analysis of cell-cycle gene activity. *Plant J* **30**, 203–212. [95](#)
- Meyers, B. C., Tingey, S. V. and Morgante, M. (2001). Abundance, distribution, and transcriptional activity of repetitive elements in the maize genome. *Genome Res* **11**, 1660–1676. [16](#)
- Miller, G., Schlauch, K., Tam, R., Cortes, D., Torres, M. A., Shulaev, V., Dangl, J. L. and Mittler, R. (2009). The plant NADPH oxidase RBOHD mediates rapid systemic signaling in response to diverse stimuli. *Sci Signal* **2**, ra45. [81](#)
- Miller, J. R., Koren, S. and Sutton, G. (2010). Assembly algorithms for next-generation sequencing data. *Genomics*. [25](#)
- Mirouze, M., Reinders, J., Bucher, E., Nishimura, T., Schneeberger, K., Ossowski, S., Cao, J., Weigel, D., Paszkowski, J. and Mathieu, O. (2009). Selective epigenetic control of retrotransposition in *Arabidopsis*. *Nature* **461**, 427–430. [16](#)
- Miura, A., Yonebayashi, S., Watanabe, K., Toyama, T., Shimada, H. and Kakutani, T. (2001). Mobilization of transposons by a mutation abolishing full DNA methylation in *Arabidopsis*. *Nature* **411**, 212–214. [16](#)
- Molinier, J., Lechner, E., Dumbliuskas, E. and Genschik, P. (2008). Regulation and role of *Arabidopsis* CUL4-DDB1A-DDB2 in maintaining genome integrity upon UV stress. *PLoS Genet* **4**, e1000093. [13](#)

- Monaghan, J., Xu, F., Gao, M., Zhao, Q., Palma, K., Long, C., Chen, S., Zhang, Y. and Li, X. (2009). Two Prp19-like U-box proteins in the MOS4-associated complex play redundant roles in plant innate immunity. *PLoS Pathog* 5, e1000526. 6, 42, 75, 86
- Moore, M. J., Schwartzfarb, E. M., Silver, P. A. and Yu, M. C. (2006). Differential recruitment of the splicing machinery during transcription predicts genome-wide patterns of mRNA splicing. *Mol Cell* 24, 903–915. 7
- Morales-Ruiz, T., Ortega-Galisteo, A. P., Ponferrada-Marín, M. I., Martínez-Macías, M. I., Ariza, R. R. and Roldán-Arjona, T. (2006). *DEMETER* and *REPRESSOR OF SILENCING 1* encode 5-methylcytosine DNA glycosylases. *Proc Natl Acad Sci U S A* 103, 6853–6858. 80
- Morgante, M., Brunner, S., Pea, G., Fengler, K., Zuccolo, A. and Rafalski, A. (2005). Gene duplication and exon shuffling by helitron-like transposons generate intraspecies diversity in maize. *Nat Genet* 37, 997–1002. 9
- Mourrain, P., Béclin, C., Elmayan, T., Feuerbach, F., Godon, C., Morel, J. B., Jouette, D., Lacombe, A. M., Nikic, S., Picault, N., Ré moué, K., Sanial, M., Vo, T. A. and Vaucheret, H. (2000). *Arabidopsis* *SGS2* and *SGS3* genes are required for posttranscriptional gene silencing and natural virus resistance. *Cell* 101, 533–542. 17
- Murata, S., Yashiroda, H. and Tanaka, K. (2009). Molecular mechanisms of proteasome assembly. *Nat Rev Mol Cell Biol* 10, 104–115. 8
- Myers, E. W., Sutton, G. G., Delcher, A. L., Dew, I. M., Fasulo, D. P., Flanigan, M. J., Kravitz, S. A., Mobarry, C. M., Reinert, K. H., Remington, K. A., Anson, E. L., Bolanos, R. A., Chou, H. H., Jordan, C. M., Halpern, A. L., Lonardi, S., Beasley, E. M., Brandon, R. C., Chen, L., Dunn, P. J., Lai, Z., Liang, Y., Nusskern, D. R., Zhan, M., Zhang, Q., Zheng, X., Rubin, G. M., Adams, M. D. and Venter, J. C. (2000). A whole-genome assembly of *Drosophila*. *Science* 287, 2196–2204. 25
- Möller, B. and Weijers, D. (2009). Auxin control of embryo patterning. *Cold Spring Harb Perspect Biol* 1, a001545. 21
- Naito, T., Kiba, T., Koizumi, N., Yamashino, T. and Mizuno, T. (2007). Characterization of a unique GATA family gene that responds to both light and cytokinin in *Arabidopsis thaliana*. *Biosci Biotechnol Biochem* 71, 1557–1560. 77
- Nakajima, S., Sugiyama, M., Iwai, S., Hitomi, K., Otsoshi, E., Kim, S. T., Jiang, C. Z., Todo, T., Britt, A. B. and Yamamoto, K. (1998). Cloning and characterization of a gene (*UVR3*) required for photorepair of 6-4 photoproducts in *Arabidopsis thaliana*. *Nucleic Acids Res* 26, 638–644. 79
- Naouar, N., Vandepoele, K., Lammens, T., Casneuf, T., Zeller, G., van Hummelen, P., Weigel, D., Rätsch, G., Inzé, D., Kuiper, M., Veylder, L. D. and Vuylsteke, M. (2009). Quantitative RNA expression analysis with Affymetrix Tiling 1.0R arrays identifies new E2F target genes. *Plant J* 57, 184–194. 24, 37, 43, 83, 84, 105, 155, 156
- Nawy, T., Lukowitz, W. and Bayer, M. (2008). Talk global, act local-patterning the *Arabidopsis* embryo. *Curr Opin Plant Biol* 11, 28–33. 20
- Neer, E. J., Schmidt, C. J., Nambudripad, R. and Smith, T. F. (1994). The ancient regulatory-protein family of WD-repeat proteins. *Nature* 371, 297–300. 4

- Németh, K., Salchert, K., Putnoky, P., Bhalerao, R., Koncz-Kálmán, Z., Stankovic-Stangeland, B., Bakó, L., Mathur, J., Ókrész, L., Stabel, S., Geigenberger, P., Stitt, M., Rédei, G. P., Schell, J. and Koncz, C. (1998). Pleiotropic control of glucose and hormone responses by PRL1, a nuclear WD protein, in *Arabidopsis*. *Genes Dev* 12, 3059–3073. ISSN 0890-9369 (Print). 2, 28, 29, 33, 34, 54, 58, 75, 77, 78, 81, 85, 88, 89, 90, 95, 101
- Neugebauer, K. M. (2002). On the importance of being co-transcriptional. *J Cell Sci* 115, 3865–3871. 7
- Nielsen, C. B., Cantor, M., Dubchak, I., Gordon, D. and Wang, T. (2010). Visualizing genomes: techniques and challenges. *Nat Methods* 7, S5–S15. 25
- Nørholm, M. H. H., Nour-Eldin, H. H., Brodersen, P., Mundy, J. and Halkier, B. A. (2006). Expression of the *Arabidopsis* high-affinity hexose transporter *STP13* correlates with programmed cell death. *FEBS Lett* 580, 2381–2387. 82
- Nowack, M. K., Ungru, A., Bjerkan, K. N., Grini, P. E. and Schnittger, A. (2010). Reproductive cross-talk: seed development in flowering plants. *Biochem Soc Trans* 38, 604–612. 23
- Ohi, M. D. and Gould, K. L. (2002). Characterization of interactions among the Cef1p-Prp19p-associated splicing complex. *RNA* 8, 798–815. ISSN 1355-8382 (Print). 3, 5, 6
- Ohi, M. D., Kooi, C. W. V., Rosenberg, J. A., Ren, L., Hirsch, J. P., Chazin, W. J., Walz, T. and Gould, K. L. (2005). Structural and functional analysis of essential pre-mRNA splicing factor Prp19p. *Mol Cell Biol* 25, 451–460. 6
- Ohi, M. D., Link, A. J., Ren, L., Jennings, J. L., McDonald, W. H. and Gould, K. L. (2002). Proteomics analysis reveals stable multiprotein complexes in both fission and budding yeasts containing Myb-related Cdc5p/Cef1p, novel pre-mRNA splicing factors, and snRNAs. *Mol Cell Biol* 22, 2011–2024. 5
- Ohi, R., Feoktistova, A., McCann, S., Valentine, V., Look, A. T., Lipsick, J. S. and Gould, K. L. (1998). Myb-related *Schizosaccharomyces pombe* cdc5p is structurally and functionally conserved in eukaryotes. *Mol Cell Biol* 18, 4097–4108. 6
- Ohi, R., McCollum, D., Hirani, B., Haese, G. J. D., Zhang, X., Burke, J. D., Turner, K. and Gould, K. L. (1994). The *Schizosaccharomyces pombe* cdc5+ gene encodes an essential protein with homology to c-Myb. *EMBO J* 13, 471–483. 6
- Ossowski, S., Schneeberger, K., Clark, R. M., Lanz, C., Warthmann, N. and Weigel, D. (2008). Sequencing of natural strains of *Arabidopsis thaliana* with short reads. *Genome Res* 18, 2024–2033. 25
- Palma, K., Zhang, Y. and Li, X. (2005). An importin alpha homolog, MOS6, plays an important role in plant innate immunity. *Curr Biol* 15, 1129–1135. 90
- Palma, K., Zhao, Q., Cheng, Y. T., Bi, D., Monaghan, J., Cheng, W., Zhang, Y. and Li, X. (2007). Regulation of plant innate immunity by three proteins in a complex conserved across the plant and animal kingdoms. *Genes Dev* 21, 1484–1493. 6, 42, 75, 86, 88, 90
- Pang, Q., Hays, J. B. and Rajagopal, I. (1992). A plant cDNA that partially complements *Escherichia coli* recA mutations predicts a polypeptide not strongly homologous to RecA proteins. *Proc Natl Acad Sci U S A* 89, 8073–8077. 79

- Parker, J. E., Coleman, M. J., Szabò, V., Frost, L. N., Schmidt, R., van der Biezen, E. A., Moores, T., Dean, C., Daniels, M. J. and Jones, J. D. (1997). The *Arabidopsis* downy mildew resistance gene *RPP5* shares similarity to the toll and interleukin-1 receptors with N and L6. *Plant Cell* **9**, 879–894. [81](#)
- Parkhomchuk, D., Borodina, T., Amstislavskiy, V., Banaru, M., Hallen, L., Krobitch, S., Lehrach, H. and Soldatov, A. (2009). Transcriptome analysis by strand-specific sequencing of complementary DNA. *Nucleic Acids Res* **37**, e123. [123](#)
- Peng, H. and Ling, X. S. (2009). Reverse DNA translocation through a solid-state nanopore by magnetic tweezers. *Nanotechnology* **20**, 185101. [24](#)
- Pontes, O., Li, C. F., Nunes, P. C., Haag, J., Ream, T., Vitins, A., Jacobsen, S. E. and Pikaard, C. S. (2006). The *Arabidopsis* chromatin-modifying nuclear siRNA pathway involves a nucleolar RNA processing center. *Cell* **126**, 79–92. [86](#)
- Pop, M. and Salzberg, S. L. (2008). Bioinformatics challenges of new sequencing technology. *Trends Genet* **24**, 142–149. [25](#)
- Potashkin, J., Kim, D., Fons, M., Humphrey, T. and Frendewey, D. (1998). Cell-division-cycle defects associated with fission yeast pre-mRNA splicing mutants. *Curr Genet* **34**, 153–163. [3](#), [75](#)
- Priest, D. M., Ambrose, S. J., Vaistij, F. E., Elias, L., Higgins, G. S., Ross, A. R. S., Abrams, S. R. and Bowles, D. J. (2006). Use of the glucosyltransferase UGT71B6 to disturb abscisic acid homeostasis in *Arabidopsis thaliana*. *Plant J* **46**, 492–502. [78](#)
- Pruitt, R. and Hülskamp, M. (1994). *Arabidopsis*, chapter From pollination to fertilization in *Arabidopsis*. Somerville, C.R. and Meyerowitz, E.M. (eds.), Cold Spring Harbor Laboratory Pr, pages 467–483. [20](#)
- Pühler, G., Leffers, H., Gropp, F., Palm, P., Klenk, H. P., Lottspeich, F., Garrett, R. A. and Zillig, W. (1989). Archaeobacterial DNA-dependent RNA polymerases testify to the evolution of the eukaryotic nuclear genome. *Proc Natl Acad Sci U S A* **86**, 4569–4573. [10](#)
- R Development Core Team (2009). *R: A Language and Environment for Statistical Computing*. R Foundation for Statistical Computing, Vienna, Austria. ISBN 3-900051-07-0. [105](#)
- Rate, D. N., Cuenca, J. V., Bowman, G. R., Guttman, D. S. and Greenberg, J. T. (1999). The gain-of-function *Arabidopsis acd6* mutant reveals novel regulation and function of the salicylic acid signaling pathway in controlling cell death, defenses, and cell growth. *Plant Cell* **11**, 1695–1708. [81](#)
- Reape, T. J., Molony, E. M. and McCabe, P. F. (2008). Programmed cell death in plants: distinguishing between different modes. *J Exp Bot* **59**, 435–444. [12](#)
- Redman, J. C., Haas, B. J., Tanimoto, G. and Town, C. D. (2004). Development and evaluation of an *Arabidopsis* whole genome Affymetrix probe array. *Plant J* **38**, 545–561. [24](#)
- Rehauer, H., Aquino, C., Grissem, W., Henz, S. R., Hilson, P., Laubinger, S., Naouar, N., Patrignani, A., Rombauts, S., Shu, H., de Peer, Y. V., Vuylsteke, M., Weigel, D., Zeller, G. and Hennig, L. (2010). AGRONOMICS1: a new resource for *Arabidopsis* transcriptome profiling. *Plant Physiol* **152**, 487–499. [24](#)

- Ren, B., Robert, F., Wyrick, J. J., Aparicio, O., Jennings, E. G., Simon, I., Zeitlinger, J., Schreiber, J., Hannett, N., Kanin, E., Volkert, T. L., Wilson, C. J., Bell, S. P. and Young, R. A. (2000). Genome-wide location and function of DNA binding proteins. *Science* **290**, 2306–2309. [24](#)
- Renew, S., Heyno, E., Schopfer, P. and Liskay, A. (2005). Sensitive detection and localization of hydroxyl radical production in cucumber roots and *Arabidopsis* seedlings by spin trapping electron paramagnetic resonance spectroscopy. *Plant J* **44**, 342–347. [77](#)
- Rice, P., Longden, I. and Bleasby, A. (2000). EMBOSS: the European Molecular Biology Open Software Suite. *Trends Genet* **16**, 276–277. [105](#)
- Richard, H., Schulz, M. H., Sultan, M., Nürnbergger, A., Schrunner, S., Balzereit, D., Dagand, E., Rasche, A., Lehrach, H., Vingron, M., Haas, S. A. and Yaspo, M.-L. (2010). Prediction of alternative isoforms from exon expression levels in RNA-Seq experiments. *Nucleic Acids Res.* **38**, 82, [83](#)
- Richter, B. G. and Sexton, D. P. (2009). Managing and analyzing next-generation sequence data. *PLoS Comput Biol* **5**, e1000369. [25](#)
- Robinson-Beers, K., Pruitt, R. E. and Gasser, C. S. (1992). Ovule Development in Wild-Type *Arabidopsis* and Two Female-Sterile Mutants. *Plant Cell* **4**, 1237–1249. [19](#)
- Rocha, P. S. C. F., Sheikh, M., Melchiorre, R., Fagard, M., Boutet, S., Loach, R., Moffatt, B., Wagner, C., Vaucheret, H. and Furner, I. (2005). The *Arabidopsis* HOMOLOGY-DEPENDENT GENE SILENCING1 gene codes for an S-adenosyl-L-homocysteine hydrolase required for DNA methylation-dependent gene silencing. *Plant Cell* **17**, 404–417. [92](#)
- Ronaghi, M., Uhlén, M. and Nyrén, P. (1998). DNA SEQUENCING: A Sequencing Method Based on Real-Time Pyrophosphate. *Science* **281**, 363–365. [24](#)
- Rose, A. B., Elfersi, T., Parra, G. and Korf, I. (2008). Promoter-proximal introns in *Arabidopsis thaliana* are enriched in dispersed signals that elevate gene expression. *Plant Cell* **20**, 543–551. [85](#)
- Rosso, M. G., Li, Y., Strizhov, N., Reiss, B., Dekker, K. and Weisshaar, B. (2003). An *Arabidopsis thaliana* T-DNA mutagenized population (GABI-Kat) for flanking sequence tag-based reverse genetics. *Plant Mol Biol* **53**, 247–259. [56](#), [95](#)
- Rymarquis, L. A., Kastenmayer, J. P., Hüttenhofer, A. G. and Green, P. J. (2008). Diamonds in the rough: mRNA-like non-coding RNAs. *Trends Plant Sci* **13**, 329–334. [80](#)
- Rédei, G. P. (1992). *Methods in Arabidopsis Research*, chapter A heuristic glance at the past of *Arabidopsis* genetics. Koncz C., Chua N. H. and Schell J. (eds.), World Scientific, Singapore, pages 1–15. [95](#)
- Ríos, G., Lossow, A., Hertel, B., Breuer, F., Schaefer, S., Broich, M., Kleinow, T., Jásik, J., Winter, J., Ferrando, A., Farrás, R., Panicot, M., Henriques, R., Mariaux, J.-B., Oberschall, A., Molnár, G., Berendzen, K., Shukla, V., Lafos, M., Koncz, Z., Rédei, G. P., Schell, J. and Koncz, C. (2002). Rapid identification of *Arabidopsis* insertion mutants by non-radioactive detection of T-DNA tagged genes. *Plant J* **32**, 243–253. [2](#), [56](#), [95](#)

- Salchert, K. (1997). *Untersuchungen zur Funktion von PRL1 durch Identifizierung und Charakterisierung von PRL1-interagierenden-Proteinen*. Ph.D. thesis, Universitätsbibliothek Köln. 80, 82, 88, 90, 117
- Sambrook, J. and Russell, D. (2001). *Molecular Cloning: a Laboratory Manual, 3rd Edition*. Cold Spring Harbor Laboratory Press. 112
- Sanger, F., Coulson, A. R., Friedmann, T., Air, G. M., Barrell, B. G., Brown, N. L., Fiddes, J. C., Hutchison, C. A., Slocombe, P. M. and Smith, M. (1978). The nucleotide sequence of bacteriophage ϕ X174. *Journal of Molecular Biology* 125, 225–246. 23
- Scebba, F., Bastiani, M. D., Bernacchia, G., Andreucci, A., Galli, A. and Pitto, L. (2007). PRMT11: a new *Arabidopsis* MBD7 protein partner with arginine methyltransferase activity. *Plant J* 52, 210–222. 80, 88
- Scebba, F., Bernacchia, G., Bastiani, M. D., Evangelista, M., Cantoni, R. M., Cella, R., Locci, M. T. and Pitto, L. (2003). *Arabidopsis* MBD proteins show different binding specificities and nuclear localization. *Plant Mol Biol* 53, 715–731. 80
- Schena, M., Shalon, D., Davis, R. W. and Brown, P. O. (1995). Quantitative monitoring of gene expression patterns with a complementary DNA microarray. *Science* 270, 467–470. 23
- Schmidt, T. G. and Skerra, A. (1993). The random peptide library-assisted engineering of a C-terminal affinity peptide, useful for the detection and purification of a functional Ig Fv fragment. *Protein Eng* 6, 109–122. 116
- Schneider, M., Lane, L., Boutet, E., Lieberherr, D., Tognolli, M., Bougueleret, L. and Bairoch, A. (2009). The UniProtKB/Swiss-Prot knowledgebase and its Plant Proteome Annotation Program. *J Proteomics* 72, 567–573. 106
- Schwartz, S., Meshorer, E. and Ast, G. (2009). Chromatin organization marks exon-intron structure. *Nat Struct Mol Biol* 16, 990–995. 7
- Schweikert, G., Zien, A., Zeller, G., Behr, J., Dieterich, C., Ong, C. S., Philips, P., Bona, F. D., Hartmann, L., Bohlen, A., Krüger, N., Sonnenburg, S. and Rättsch, G. (2009). mGene: accurate SVM-based gene finding with an application to nematode genomes. *Genome Res* 19, 2133–2143. 25
- Scott, R. J. and Spielman, M. (2006). Genomic imprinting in plants and mammals: how life history constrains convergence. *Cytogenet Genome Res* 113, 53–67. 22
- Sheldon, C. C., Conn, A. B., Dennis, E. S. and Peacock, W. J. (2002). Different regulatory regions are required for the vernalization-induced repression of *FLOWERING LOCUS C* and for the epigenetic maintenance of repression. *Plant Cell* 14, 2527–2537. 85
- Shendure, J. and Ji, H. (2008). Next-generation DNA sequencing. *Nat Biotechnol* 26, 1135–1145. 24
- Shendure, J., Porreca, G. J., Reppas, N. B., Lin, X., McCutcheon, J. P., Rosenbaum, A. M., Wang, M. D., Zhang, K., Mitra, R. D. and Church, G. M. (2005). Accurate multiplex polony sequencing of an evolved bacterial genome. *Science* 309, 1728–1732. 24

- Shin, R., Burch, A. Y., Huppert, K. A., Tiwari, S. B., Murphy, A. S., Guilfoyle, T. J. and Schachtman, D. P. (2007). The Arabidopsis transcription factor MYB77 modulates auxin signal transduction. *Plant Cell* **19**, 2440–2453. [77](#)
- Shinozaki, K. and Yamaguchi-Shinozaki, K. (2000). Molecular responses to dehydration and low temperature: differences and cross-talk between two stress signaling pathways. *Curr Opin Plant Biol* **3**, 217–223. [80](#)
- Shivaprasad, P. V., Rajeswaran, R., Blevins, T., Schoelz, J., Meins, F., Hohn, T. and Pooggin, M. M. (2008). The CaMV transactivator/viroplasm interferes with RDR6-dependent transacting and secondary siRNA pathways in *Arabidopsis*. *Nucleic Acids Res* **36**, 5896–5909. [80](#)
- Shoemaker, D. D., Schadt, E. E., Armour, C. D., He, Y. D., Garrett-Engle, P., McDonagh, P. D., Loerch, P. M., Leonardson, A., Lum, P. Y., Cavet, G., Wu, L. F., Altschuler, S. J., Edwards, S., King, J., Tsang, J. S., Schimmack, G., Schelter, J. M., Koch, J., Ziman, M., Marton, M. J., Li, B., Cundiff, P., Ward, T., Castle, J., Krolewski, M., Meyer, M. R., Mao, M., Burchard, J., Kidd, M. J., Dai, H., Phillips, J. W., Linsley, P. S., Stoughton, R., Scherer, S. and Boguski, M. S. (2001). Experimental annotation of the human genome using microarray technology. *Nature* **409**, 922–927. [24](#)
- Shumway, M., Cochrane, G. and Sugawara, H. (2010). Archiving next generation sequencing data. *Nucleic Acids Res* **38**, D870–D871. [25](#)
- Sieburth, L. E. and Meyerowitz, E. M. (1997). Molecular dissection of the *AGAMOUS* control region shows that cis elements for spatial regulation are located intragenically. *Plant Cell* **9**, 355–365. [85](#)
- Sihn, C.-R., Cho, S. Y., Lee, J. H., Lee, T. R. and Kim, S. H. (2007). Mouse homologue of yeast Prp19 interacts with mouse SUG1, the regulatory subunit of 26S proteasome. *Biochem Biophys Res Commun* **356**, 175–180. [6](#)
- Sikder, D., Johnston, S. A. and Kodadek, T. (2006). Widespread, but non-identical, association of proteasomal 19 and 20 S proteins with yeast chromatin. *J Biol Chem* **281**, 27346–27355. [8](#)
- Slotkin, R. K., Vaughn, M., Borges, F., Tanurdzić, M., Becker, J. D., Feijó, J. A. and Martienssen, R. A. (2009). Epigenetic reprogramming and small RNA silencing of transposable elements in pollen. *Cell* **136**, 461–472. [18](#), [92](#)
- Smyth, D. R., Bowman, J. L. and Meyerowitz, E. M. (1990). Early flower development in *Arabidopsis*. *Plant Cell* **2**, 755–767. [17](#), [19](#)
- Smyth, G. K., Michaud, J. and Scott, H. S. (2005). Use of within-array replicate spots for assessing differential expression in microarray experiments. *Bioinformatics* **21**, 2067–2075. [37](#), [46](#), [105](#), [133](#)
- Steindler, C., Matteucci, A., Sessa, G., Weimar, T., Ohgishi, M., Aoyama, T., Morelli, G. and Ruberti, I. (1999). Shade avoidance responses are mediated by the ATHB-2 HD-zip protein, a negative regulator of gene expression. *Development* **126**, 4235–4245. [78](#)
- Sun, L. and Chen, Z. J. (2004). The novel functions of ubiquitination in signaling. *Current Opinion in Cell Biology* **16**, 119 – 126. ISSN 0955-0674. [9](#)

- Sunkar, R., Kapoor, A. and Zhu, J.-K. (2006). Posttranscriptional induction of two Cu/Zn superoxide dismutase genes in *Arabidopsis* is mediated by downregulation of *miR398* and important for oxidative stress tolerance. *Plant Cell* **18**, 2051–2065. [86](#)
- Swarbreck, D., Wilks, C., Lamesch, P., Berardini, T. Z., Garcia-Hernandez, M., Foerster, H., Li, D., Meyer, T., Muller, R., Ploetz, L., Radenbaugh, A., Singh, S., Swing, V., Tissier, C., Zhang, P. and Huala, E. (2008). The Arabidopsis Information Resource (TAIR): gene structure and function annotation. *Nucleic Acids Res* **36**, D1009–D1014. [7](#), [106](#)
- Szakonyi, D. (2006). *Genetic dissection of regulatory domains and signalling interactions of PRL1 WD-protein in Arabidopsis*. Ph.D. thesis, Universitätsbibliothek Köln. [2](#), [31](#), [32](#), [43](#), [56](#), [61](#), [85](#), [87](#), [89](#), [90](#), [100](#), [116](#), [119](#)
- Tardiff, D. F., Lacadie, S. A. and Rosbash, M. (2006). A genome-wide analysis indicates that yeast pre-mRNA splicing is predominantly posttranscriptional. *Mol Cell* **24**, 917–929. [7](#)
- Tarn, W. Y., Hsu, C. H., Huang, K. T., Chen, H. R., Kao, H. Y., Lee, K. R. and Cheng, S. C. (1994). Functional association of essential splicing factor(s) with PRP19 in a protein complex. *EMBO J* **13**, 2421–2431. [6](#)
- Taylor, C. B. and Green, P. J. (1995). Identification and characterization of genes with unstable transcripts (*GUTs*) in tobacco. *Plant Mol Biol* **28**, 27–38. [80](#)
- Tena, G., Asai, T., Chiu, W. L. and Sheen, J. (2001). Plant mitogen-activated protein kinase signaling cascades. *Curr Opin Plant Biol* **4**, 392–400. [12](#)
- Tennyson, C. N., Klamut, H. J. and Worton, R. G. (1995). The *human dystrophin* gene requires 16 hours to be transcribed and is cotranscriptionally spliced. *Nat Genet* **9**, 184–190. [7](#)
- Thomashow, M. F. (1999). PLANT COLD ACCLIMATION: Freezing Tolerance Genes and Regulatory Mechanisms. *Annu Rev Plant Physiol Plant Mol Biol* **50**, 571–599. [80](#)
- Tiwari, B. S., Belenghi, B. and Levine, A. (2002). Oxidative stress increased respiration and generation of reactive oxygen species, resulting in ATP depletion, opening of mitochondrial permeability transition, and programmed cell death. *Plant Physiol* **128**, 1271–1281. [12](#)
- Tompa, R., McCallum, C. M., Delrow, J., Henikoff, J. G., van Steensel, B. and Henikoff, S. (2002). Genome-wide profiling of DNA methylation reveals transposon targets of CHROMOMETHYLASE3. *Curr Biol* **12**, 65–68. [85](#)
- Toufighi, K., Brady, S. M., Austin, R., Ly, E. and Provart, N. J. (2005). The Botany Array Resource: e-Northerns, Expression Angling, and promoter analyses. *Plant J* **43**, 153–163. [106](#)
- Towbin, H., Staehelin, T. and Gordon, J. (1979). Electrophoretic transfer of proteins from polyacrylamide gels to nitrocellulose sheets: procedure and some applications. *Proc Natl Acad Sci U S A* **76**, 4350–4354. [130](#)
- Trapnell, C., Pachter, L. and Salzberg, S. L. (2009). TopHat: discovering splice junctions with RNA-Seq. *Bioinformatics* **25**, 1105–1111. [25](#), [105](#), [135](#)
- Trapnell, C., Williams, B. A., Pertea, G., Mortazavi, A., Kwan, G., van Baren, M. J., Salzberg, S. L., Wold, B. J. and Pachter, L. (2010). Transcript assembly and quantification by rna-seq reveals unannotated transcripts and isoform switching during cell differentiation. *Nat Biotechnol* **28**, 511–515. [105](#), [135](#)

- Turcatti, G., Romieu, A., Fedurco, M. and Tairi, A.-P. (2008). A new class of cleavable fluorescent nucleotides: synthesis and optimization as reversible terminators for DNA sequencing by synthesis. *Nucleic Acids Res* **36**, e25. [24](#)
- Ulm, R., Ichimura, K., Mizoguchi, T., Peck, S. C., Zhu, T., Wang, X., Shinozaki, K. and Paszkowski, J. (2002). Distinct regulation of salinity and genotoxic stress responses by *Arabidopsis* MAP kinase phosphatase 1. *EMBO J* **21**, 6483–6493. [12](#)
- Ulm, R., Revenkova, E., di Sansebastiano, G. P., Bechtold, N. and Paszkowski, J. (2001). Mitogen-activated protein kinase phosphatase is required for genotoxic stress relief in *Arabidopsis*. *Genes Dev* **15**, 699–709. [12](#)
- Ungu, A., Nowack, M. K., Reymond, M., Shirzadi, R., Kumar, M., Biewers, S., Grini, P. E. and Schnittger, A. (2008). Natural variation in the degree of autonomous endosperm formation reveals independence and constraints of embryo growth during seed development in *Arabidopsis thaliana*. *Genetics* **179**, 829–841. [23](#)
- Uno, Y., Furihata, T., Abe, H., Yoshida, R., Shinozaki, K. and Yamaguchi-Shinozaki, K. (2000). *Arabidopsis* basic leucine zipper transcription factors involved in an abscisic acid-dependent signal transduction pathway under drought and high-salinity conditions. *Proc Natl Acad Sci U S A* **97**, 11632–11637. [78](#)
- van der Biezen, E. A., Freddie, C. T., Kahn, K., Parker, J. E. and Jones, J. D. G. (2002). *Arabidopsis* RPP4 is a member of the RPP5 multigene family of TIR-NB-LRR genes and confers downy mildew resistance through multiple signalling components. *Plant J* **29**, 439–451. [81](#)
- van Nocker, S. and Ludwig, P. (2003). The WD-repeat protein superfamily in *Arabidopsis*: conservation and divergence in structure and function. *BMC Genomics* **4**, 50. [4](#)
- Venter, J. C. (2010). Multiple personal genomes await. *Nature* **464**, 676–677. [23](#)
- Vernhettes, S., Grandbastien, M. A. and Casacuberta, J. M. (1997). *In vivo* characterization of transcriptional regulatory sequences involved in the defence-associated expression of the tobacco retrotransposon *Tnt1*. *Plant Mol Biol* **35**, 673–679. [15](#)
- Vongs, A., Kakutani, T., Martienssen, R. A. and Richards, E. J. (1993). *Arabidopsis thaliana* DNA methylation mutants. *Science* **260**, 1926–1928. [16](#)
- Wahl, M. C., Will, C. L. and Lührmann, R. (2009). The spliceosome: design principles of a dynamic RNP machine. *Cell* **136**, 701–718. [5](#)
- Walbot, V. (1985). On the life strategies of plants and animals. *Trends in Genetics* **1**, 165–169. [17](#)
- Wang, B.-B. and Brendel, V. (2004). The ASRG database: identification and survey of *Arabidopsis thaliana* genes involved in pre-mRNA splicing. *Genome Biol* **5**, R102. [9](#)
- Wang, B.-B. and Brendel, V. (2006). Molecular characterization and phylogeny of U2AF35 homologs in plants. *Plant Physiol* **140**, 624–636. [10](#)
- Wang, N. N., Shih, M.-C. and Li, N. (2005). The GUS reporter-aided analysis of the promoter activities of *Arabidopsis* ACC synthase genes *AtACS4*, *AtACS5*, and *AtACS7* induced by hormones and stresses. *J Exp Bot* **56**, 909–920. [77](#)

- Wei, N., Serino, G. and Deng, X.-W. (2008). The COP9 signalosome: more than a protease. *Trends Biochem Sci* **33**, 592–600. [87](#)
- Werner, T., Motyka, V., Laucou, V., Smets, R., Onckelen, H. V. and Schmülling, T. (2003). Cytokinin-deficient transgenic *Arabidopsis* plants show multiple developmental alterations indicating opposite functions of cytokinins in the regulation of shoot and root meristem activity. *Plant Cell* **15**, 2532–2550. [77](#)
- Wicker, T., Sabot, F., Hua-Van, A., Bennetzen, J. L., Capy, P., Chalhoub, B., Flavell, A., Leroy, P., Morgante, M., Panaud, O., Paux, E., SanMiguel, P. and Schulman, A. H. (2007). A unified classification system for eukaryotic transposable elements. *Nat Rev Genet* **8**, 973–982. [14](#)
- Wilkinson, K. D. (1997). Regulation of ubiquitin-dependent processes by deubiquitinating enzymes. *FASEB J* **11**, 1245–1256. [9](#)
- Wu, K., Tian, L., Malik, K., Brown, D. and Miki, B. (2000). Functional analysis of HD2 histone deacetylase homologues in *Arabidopsis thaliana*. *Plant J* **22**, 19–27. [92](#)
- Xiao, H., Jiang, N., Schaffner, E., Stockinger, E. J. and van der Knaap, E. (2008). A retrotransposon-mediated gene duplication underlies morphological variation of tomato fruit. *Science* **319**, 1527–1530. [90](#)
- Yadegari, R. and Drews, G. N. (2004). Female gametophyte development. *Plant Cell* **16 Suppl**, S133–S141. [18](#)
- Yang, P., Fu, H., Walker, J., Papa, C. M., Smalle, J., Ju, Y.-M. and Vierstra, R. D. (2004). Purification of the *Arabidopsis* 26 S proteasome: biochemical and molecular analyses revealed the presence of multiple isoforms. *J Biol Chem* **279**, 6401–6413. [8](#)
- Zemach, A. and Grafi, G. (2003). Characterization of *Arabidopsis thaliana* methyl-CpG-binding domain (MBD) proteins. *Plant J* **34**, 565–572. [88](#)
- Zemach, A., Li, Y., Wayburn, B., Ben-Meir, H., Kiss, V., Avivi, Y., Kalchenko, V., Jacobsen, S. E. and Grafi, G. (2005). DDM1 binds *Arabidopsis* methyl-CpG binding domain proteins and affects their subnuclear localization. *Plant Cell* **17**, 1549–1558. [88](#)
- Zerbino, D. R. and Birney, E. (2008). Velvet: algorithms for de novo short read assembly using de Bruijn graphs. *Genome Res* **18**, 821–829. [25](#)
- Zerbino, D. R., McEwen, G. K., Margulies, E. H. and Birney, E. (2009). Pebble and rock band: heuristic resolution of repeats and scaffolding in the velvet short-read *de novo* assembler. *PLoS One* **4**, e8407. [25](#)
- Zhang, J. (2003). Evolution by gene duplication: an update. *Trends in Ecology & Evolution* **18**, 292–298. [9](#)
- Zhang, N., Kaur, R., Lu, X., Shen, X., Li, L. and Legerski, R. J. (2005). The Pso4 mRNA splicing and DNA repair complex interacts with WRN for processing of DNA interstrand cross-links. *J Biol Chem* **280**, 40559–40567. [13](#)
- Zhou, X. and Su, Z. (2007). EasyGO: Gene Ontology-based annotation and functional enrichment analysis tool for agronomical species. *BMC Genomics* **8**, 246. [105](#), [106](#)

- Zhu, T. and Wang, X. (2000). Large-scale profiling of the *Arabidopsis* transcriptome. *Plant Physiol* 124, 1472–1476. [24](#)
- Ziegler, J., Stenzel, I., Hause, B., Maucher, H., Hamberg, M., Grimm, R., Ganal, M. and Wasternack, C. (2000). Molecular cloning of allene oxide cyclase. The enzyme establishing the stereochemistry of octadecanoids and jasmonates. *J Biol Chem* 275, 19132–19138. [79](#)

Agradecimientos

This project wouldn't been possible with the help of many people, from whom I've learnt a lot during these years, not only from the scientific perspective, but also from the personal perspective. These last words are addressed to them.

First of all, I would like to thank my supervisor, Dr. Csaba Koncz for choosing me to be one of the two *ADONIS* students, for his patience teaching me, for understanding me and for making my PhD time an unforgettable experience that has positively influenced my personal development.

I thank Prof. George Coupland for being my *Doktorvater* and supporting my work in his department, especially for the funding during the extension time. I would like to thank Prof. Wolfgang Werr for agreeing so quick in being my second supervisor, Prof. Flügge for being my *Vorsitzender* and Dr. Heiko Schoof my *Beisitzer*.

I would like to thank all the present and past people I've met in the Koncz group, especially Mohsen for his calmness, Claudia for the bench-talks, Sabine for her prompt help and organization, Zsuzsa for her comments, Farshad for his GUS experience, Mihály for sharing his opinions, Gergő for giving me another perspective of Hungarians and Hasnain for the way he looks at life.

Two post-docs in the group have especially guided me through all this project, Dr. Dóra Szakonyi introduced me to an exciting project and had a lot of material for me to characterize: You taught me a lot about molecular biology and how to work independently. Dr. Femke de Jong took my hand during the last year of this project. Femke, ik wil je bedanken voor je geduld, de discussies, je advies, voor het delen van je mening, voor het duidelijk formuleren van dingen en, bovenal, omdat je het voorelkaar hebt gekregen deze thesis te vormen in iets waar ik trots op ben. Zonder jou hulp was het onmogelijk geweest dit punt te bereiken.

A qui voldria agrair també molt especialment és a la Marta: per les conversacions, per les estones junts al laboratori, pels nostres intercanvis d'*opinions*, pels dinars compartits; per tot això han sigut aquests darrers anys al laboratori molt més agradables. Quin encert va ser que el nostre cap es decidís per tu!

The interactions of the Koncz group inside Coupland's department made my work easier. I would like to thank Dr. Renier van der Hoorn for providing me with the proteasome probe and la dulce Johana por enseñarme tan pacientemente los detalles del protocolo. I also include here many colleagues in the Coupland's group who contributed during my time here not only to loads of feedback, but also towards a great atmosphere.

Two people taught me how to make pictures, one was Dr. Elmon Schmelzer whose help with the different microscopes was invaluable, and the other one was Maret-Linda Kalda, whose photos reflected what I wanted from my plants. Plants that couldn't be in better conditions thanks to Ingrid Reinsch: Thank you very much for taking care of them and for harvesting my seeds!

I've learnt a lot from two real bioinformaticians who have helped me with advices during this project. Dr. Ulrike Göbel, who proved to me that one can jump from the biological perspective to the bioinformatics one. And, I would like to especially thank Dr. Emiel Ver Loren van Themaat not only for his help, suggestions and support in the technical aspects, but also for understanding *newbie's* questions.

This project also included the collaboration of many people outside the MPIPZ, I would like to thank, from the Max Planck Institute for Molecular Genetics in Berlin, Dr. Alexey Soldatov, for teaching me the RNA-Seq protocol and for sequencing my samples for free, Dr. Tatiana Borodina and Alexey Davydov for processing them, and Dr. Vyacheslav Amstislavskiy for his advices and Perl code for the data pre-processing.

I never miss an opportunity to advocate supporting Open Source software: I have to thank countless people in the Open Software community who contribute with outstanding software, not only for the analysis of biological data, but also for everyday uses: This PhD project was carried out using Open Source software in a 98 %.

The fact that this project was framed in a European Excellence Network made me to get in touch with the *elite* of the plant research in Europe: Fabio, Michaël, Belmiro, Anna, Sonja, Andrea, Imma, Niels, Izabela, Michał, Jean-Baptiste, Sisi, Ola, Florina, Barbara, Subhash, and Ceylan. You made me understand what *excellence* really means. I will miss all the personal and scientific *discussions* we had during our different meetings around Europe. I've learnt a lot from you!

Afortunadamente, que el MPIPZ tenga una comunidad hispana tan numerosa me ha ayudado a aprender a escuchar y compartir opiniones en mi lengua materna. Voy a echar de menos las comidas de los viernes donde ponerme al día de las últimas *noticias* del instituto. Gracias Sara, Fernando, Maida, y Amaury (*l'adopté*) por darme la perspectiva del *piso de arriba*. Voy a echar especialmente de menos en las comidas a Eva y a María: El contraste norte-sur que nos traíamos me ha hecho reír mucho. Tampoco me puedo olvidar de los que ya no están aquí, Jose y mi familia mejicana favorita: ¡No veo la hora de ir a visitaros!

I would like to thank very specially Karo –and also Martin– for letting me join her during the writing process of our respective thesis. Thank you for making me realize that help must be always welcomed and accepted, no matter where it comes from. It's a pleasure for me to be a friend of the best German couple ever. You've taught me how close our cultures are. I don't want to forget Kerstin, my favourite north-German girl: Du bist die beste Nachbarin in der Dasselstraße !

Los primeros en entender a lo que me afrontaba al iniciar esta aventura fueron mis compañeros de Fisiología Vegetal de la Universidad de Oviedo: Vosotros me hicisteis darme cuenta de que todo iba a cambiar. La desventaja de tener que irme es que echo mucho de menos nuestras salidas de *vinoteo*. Cande, Estre y Rebe: ¡Cómo echo de menos los rajes en el cubículo con vosotras!

Esta tesis está dedicada a mis padres, que junto con mi hermano siempre me han apoyado en todas mis decisiones –empezando por la aventura de irme a otro país–. Siempre me habéis hecho pensar que mi decisiones eran las correctas. Todo lo que soy os lo debo a vosotros, ¡gracias por apoyarme y entenderme!

Ich möchte ganz besonders einem Menschen danken, der mich immer auf den Boden der Tatsachen zurückgeholt hat: Marcus, als ich mich entschied nach Deutschland zu gehen, hätte ich nicht erwartet, jemanden wie dich zu treffen. Vielen lieben Dank! Du hast mir gezeigt, dass es neben der Wissenschaft auch ganz andere wichtige Dinge im Leben gibt. Danke auch dafür, dass du mir dieses Land näher gebracht hast und mich jeden Tag von Neuem unterstützt hast. Ich bin auch der Meinung, dass wir das allerbeste Team sind, du mit deiner spanisch-deutschen Art und ich mit meiner deutsch-spanischen Art. Dies ist erst der Anfang von vielen weiteren gemeinsamen Unternehmungen in unserem Leben.

Erklärung

Ich versichere, dass ich die von mir vorgelegte Dissertation selbständig angefertigt, die benutzten Quellen und Hilfsmittel vollständig angegeben und die Stellen der Arbeit – einschließlich Tabellen, Karten und Abbildungen –, die anderen Werken im Wortlaut oder dem Sinn nach entnommen sind, in jedem Einzelfall als Entlehnung kenntlich gemacht habe; dass diese Dissertation noch keiner anderen Fakultät oder Universität zur Prüfung vorgelegen hat; dass sie – abgesehen von unten angegebenen Teilpublikationen – noch nicht veröffentlicht worden ist sowie, dass ich eine solche Veröffentlichung vor Abschluss des Promotionsverfahrens nicht vornehmen werde. Die Bestimmungen der Promotionsordnung sind mir bekannt. Die von mir vorgelegte Dissertation ist von Prof. Dr. George Coupland betreut worden.

Köln, den 31. Mai 2011

Nicolas F. Villacorta

Lebenslauf

Persönliche Angaben

Name, Vorname: Fernández Villacorta, Nicolás
Adresse: Dasselstr. 68, 50674, Köln
Geburtsdatum: 19. Januar 1980
Geburtsort: Oviedo, Spanien
Staatsangehörigkeit: Spanisch

Ausbildung

- 2006–2010 Doktorand am Max-Planck-Institut für Züchtungsforschung in Köln unter der Leitung von Dr. Csaba Koncz. Mitglied des Marie-Curie-Exzellenz-Netzwerkes ADONIS. Fachrichtungen: Genetik, Molekularbiologie, Bioinformatik
- 2005–2006 *Post-graduate advanced research* am *Departamento de Biología de Organismos y Sistemas* der *Universidad de Oviedo* in Spanien unter der Leitung von Prof. Sánchez-Tamés. Fachrichtungen: Pflanzenphysiologie und Chromatographie
- 2003–2005 MSc in Pflanzenphysiologie: „Plant growth regulators in growth and floral development of hops (*Humulus lupulus* L.)“ am *Departamento de Biología de Organismos y Sistemas* der *Universidad de Oviedo* in Spanien unter der Leitung von Dr. M^a Ángeles Revilla. Fachrichtungen: Pflanzenbiotechnologie und -physiologie
- 1998–2003 Grund- und Hauptstudium der Biologie an der *Universidad de Oviedo* in Spanien. Fachrichtungen: Biochemie, Genetik, Molekularbiologie und Botanik

Schulbildung

- 1994–1998 Gymnasium *Pérez de Ayala*, Oviedo, Spanien. Abschluss mit Hochschulreife
- 1985–1994 Grundschule *Amor Misericordioso*, Colloto, Spanien

Publikationen

Nicolás F. Villacorta, Helena Fernández, Els Prinsen, Pablo L. Bernad, M. Ángeles Revilla. 2008. Endogenous hormonal profiles in hop development. *J. Plant Growth Regul.* 27(1): 93–98. DOI 10.1007/s00344-007-9028-1

V. Menéndez, N. F. Villacorta, M. A. Revilla, V. Gotor, P. Bernard, H. Fernández. 2006. Exogenous and endogenous growth regulators on apogamy in *Dryopteris affinis* (Lowe) Fraser-Jenkins sp. *affinis*. *Plant Cell Rep.* 25(2): 85–91. DOI 10.1007/s00299-005-0041-1